Impacts of volcanic ash on surface transportation networks: considerations for Auckland City, New Zealand

A thesis submitted in partial fulfilment of the requirements for the degree of

Doctor of Philosophy in Disaster Risk and Resilience

by

Daniel Mark Blake

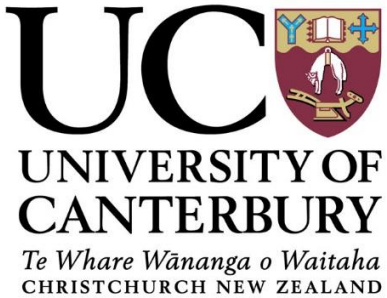

University of Canterbury

2016

~

During volcanic eruptions, fragile transportation networks can have grave consequences for local populations. They also delay the effective potential for those affected to help themselves and impede relief provided by local authorities or from abroad.

Developing the resilience of transportation networks is crucial to substantially reduce damage and service disruption.

~

Text: *adapted from the Sendai Framework for Disaster Risk Reduction 2015-2030 (UNISDR 2015), and World Risk Report 2016 (UNU-EHS 2016).*

Photo: *Auckland City, New Zealand, with Harbour Bridge in the background, taken from Mt. Eden, one of the volcanic cones in the Auckland Volcanic Field (Daniel Blake 2014).*

ABSTRACT

Volcanic eruptions can cause a variety of impacts on critical infrastructure through a multitude of accompanying hazards. Impacts from volcanic ash can be highly disruptive, widespread and long-lasting, with substantial consequences for society. With a growing worldwide population and associated expansion of complex critical infrastructure networks in volcanically active areas, volcanic risk assessments are more important than ever. However, there are many challenges, particularly as research developments in the discipline are relatively recent; many opportunities for improved understanding remain. Transportation is arguably the most crucial type of critical infrastructure during volcanic eruptions as it may be required for a variety of response and recovery activities, including the maintenance and restoration of all other critical infrastructure. In long-lasting eruptions, people may live with volcanic ash for months to years and use transportation networks affected by ash on a daily basis. Although there are many observations of surface transportation impacts following previous eruptions, vulnerability data has been largely qualitative and there has been a lack of reliable quantitative data, particularly to assess network functionality. Advancing our understanding of volcanic ash vulnerability will enhance management strategies and improve the resilience of transportation networks.

This thesis provides quantitative empirical results for vulnerability assessments of volcanic ash impacts on surface transportation, primarily through laboratory experimentation under controlled conditions that investigate three key impact types: 1) skid resistance on ash-covered roads and airfields, 2) road marking coverage by volcanic ash, and 3) visibility in airborne volcanic ash. Surface transportation functionality for thin (mm-cm) ash deposits forms the primary focus of this research due to limited existing knowledge, and as thin deposits often cover extensive areas and are readily re-suspended with potential repeated disruption. Various ash characteristics (e.g. thickness, particle size, soluble components, and ash wetness) are investigated in laboratory studies to assess the implications of different hazard intensity metrics on surface transportation functionality, with a focus on the transportation network in Auckland, New Zealand. Laboratory findings are used to identify thresholds for particular impacts, which are subsequently used to refine existing, and propose new, fragility functions for surface transportation and volcanic ash. Recommendations for clean-up and other mitigation measures to deal with volcanic ash on surface transportation networks are also suggested. Finally, new and previous impact findings are applied to a scenario focused on a hypothetical eruption in the Auckland Volcanic Field, New Zealand. Here, *Level-of-Service* metrics are developed to describe the disruption encountered by transportation end-users when networks are affected by volcanic ash, effectively providing a measure of transportation vulnerability. Overall, the findings of the thesis allow improvements to future volcanic impact and risk assessments and guide the development of resilient transportation infrastructure in volcanically active areas.

ACKNOWLEDGEMENTS

This thesis would not have been possible without the support and advice of many people, to whom I express my sincere thanks. Many are acknowledged individually within the separate chapters of this thesis, but some require special thanks.

First, I wish to thank my senior supervisor, Assoc. Prof. Tom Wilson – your enthusiasm and contribution to the volcanic risk and resilience discipline is inspiring. I am extremely grateful for all the time, advice, and encouragement you gave me over the past three years. I especially appreciate all of the support towards national and international travel to attend workshops and conferences, share findings, and to collaborate with other worldwide experts in the field; I feel that this benefitted the research tremendously and has opened many future opportunities.

Thank you also to my co-supervisors:

- Assoc. Prof. Jan Lindsay – I really appreciate your support, including that to help initiate the research project during my time in Auckland, assistance to secure funding and for making me feel welcome into PhD-life. Your expert knowledge throughout, especially on all things geology and Auckland Volcanic Field related was of great help too.
- Dr. Natalia Deligne – thank you for your dedication and commitment to the many components of the research that you were involved with. Your support, and professional and detailed advice throughout was amazing, and I appreciate the time you spent to travel and have meetings at UC, and host me at GNS Science.
- Prof. Jim Cole – thanks especially for your regular morning office visits, frequent support and advice to help the research run smoothly, and incredibly quick manuscript and report reviews!

I acknowledge financial support from the following sources, which made this research possible: the Earthquake Commission (EQC), Determining Volcanic Risk in Auckland (DeVoRA) Project, University of Canterbury's Mason Trust Fund and Department of Geological Sciences Capital Expenditure budget, the University of Auckland's Postgraduate Research Student Support (PReSS), the Ministry of Business, Innovation and Employment's (MBIE) Natural Hazard Research Platform (NHRP) support, Geoscience Society of New Zealand's (GSNZ) Young Researcher Travel Grant, and Chartered Institute of Logistics and Transport's (CILT) Transport Research and Educational Trust Fund.

Thanks to the various natural hazard and risk researchers that I met and collaborated with, fellow postgraduate students and fantastic friends and officemates; it was great being able to informally discuss research matters with you as well as having the odd social bash!

Finally, I owe my deepest heartfelt gratitude to my partner and family. In addition to the occasional editing, formatting and technical assistance, this PhD would not have been possible without your support, extreme patience and commitment, so thank you.

CO-AUTHORSHIP FORMS

Deputy Vice-Chancellor's Office

Postgraduate Office

UNIVERSITY OF CANTERBURY
Te Whare Wānanga o Waitaha
CHRISTCHURCH NEW ZEALAND

Co-Authorship Form

Chapter 3: Impact of volcanic ash on road and airfield surface skid resistance

Submitted to: Journal of Transportation Research Part D: Transport and Environment

The submitted manuscript was compiled and written by Daniel M Blake, who also devised the research objectives, conducted laboratory analysis and interpreted the results. The concept of the manuscript was developed through discussions between Daniel M Blake, Thomas M Wilson, Jan M Lindsay and Natalia I Deligne. Thomas M Wilson contributed to refining and developing the manuscript. All co-authors reviewed draft versions of the manuscript before it was edited for submission by Daniel M Blake.

Certification by Co-authors:

If there is more than one co-author then a single co-author can sign on behalf of all

The undersigned certifies that:

- The above statement correctly reflects the nature and extent of the PhD candidate's contribution to this co-authored work
- In cases where the candidate was the lead author of the co-authored work he or she wrote the text

Name:	Dr. Thomas Wilson
Signature:	
Date:	08 November 2016

Deputy Vice-Chancellor's Office

Postgraduate Office

UNIVERSITY OF CANTERBURY
Te Whare Wānanga o Waitaha
CHRISTCHURCH NEW ZEALAND

Co-Authorship Form

Chapter 4: Road marking coverage by volcanic ash: an experimental approach

Published by: Environmental Earth Sciences (2016, 75:20, pp.1-12)

The published manuscript was compiled and written by Daniel M Blake, who also devised the research objectives, conducted laboratory analysis and interpreted the results. The concept of the manuscript was developed through discussions between Daniel M Blake and Thomas M Wilson. Christopher Gomez provided advice on the analytical approaches used for the study. Thomas M Wilson contributed to refining and developing the manuscript. All co-authors reviewed draft versions of the manuscript before it was edited for submission by Daniel M Blake.

Certification by Co-authors:

If there is more than one co-author then a single co-author can sign on behalf of all

The undersigned certifies that:

- The above statement correctly reflects the nature and extent of the PhD candidate's contribution to this co-authored work
- In cases where the candidate was the lead author of the co-authored work he or she wrote the text

Name:	Dr. Thomas Wilson
Signature:	
Date:	08 November 2016

Deputy Vice-Chancellor's Office

Postgraduate Office

UNIVERSITY OF CANTERBURY
Te Whare Wānanga o Waitaha
CHRISTCHURCH NEW ZEALAND

Co-Authorship Form

Chapter 5: Visibility in airborne volcanic ash: considerations for surface transportation using a laboratory-based method

Submitted to: Natural Hazards

The submitted manuscript was compiled and written by Daniel M Blake, who also devised the research objectives, conducted laboratory analysis and interpreted the results. The concept of the manuscript was developed through discussions between Daniel M Blake and Thomas M Wilson. Thomas M Wilson and Carol Stewart contributed to refining and developing the manuscript. All co-authors reviewed draft versions of the manuscript before it was edited for submission by Daniel M Blake.

Certification by Co-authors:

If there is more than one co-author then a single co-author can sign on behalf of all

The undersigned certifies that:

- The above statement correctly reflects the nature and extent of the PhD candidate's contribution to this co-authored work
- In cases where the candidate was the lead author of the co-authored work he or she wrote the text

Name:	Dr. Thomas Wilson
Signature:	
Date:	08 November 2016

Deputy Vice-Chancellor's Office

Postgraduate Office

UNIVERSITY OF CANTERBURY
Te Whare Wānanga o Waitaha
CHRISTCHURCH NEW ZEALAND

Co-Authorship Form

Chapter 6: Improving volcanic ash fragility functions through laboratory studies: example of surface transportation networks

Submitted to: Journal of Applied Volcanology

Daniel M Blake planned, coordinated and led all the laboratory experimental work mentioned in this manuscript. The submitted manuscript was also compiled and written by Daniel M Blake including the development of new methodologies. Natalia I Deligne and Thomas M Wilson provided advice throughout the methodological development process and the compilation of the manuscript. Natalia I Deligne and Thomas M Wilson also provided thorough reviews of draft versions of the manuscript. Grant Wilson assisted by providing the initial methodologies on which the research is based, and a brief review of a draft version of the manuscript before submission by Daniel M Blake.

Certification by Co-authors:

If there is more than one co-author then a single co-author can sign on behalf of all

The undersigned certifies that:

- The above statement correctly reflects the nature and extent of the PhD candidate's contribution to this co-authored work
- In cases where the candidate was the lead author of the co-authored work he or she wrote the text

Name:	Dr. Thomas Wilson
Signature:	
Date:	08 November 2016

Deputy Vice-Chancellor's Office

Postgraduate Office

UNIVERSITY OF CANTERBURY
Te Whare Wānanga o Waitaha
CHRISTCHURCH NEW ZEALAND

Co-Authorship Form

Chapter 7: Investigating the consequences of urban volcanism using a scenario approach: insights into transportation network damage and functionality

Submitted to: Journal of Volcanology and Geothermal Research

The submitted manuscript was compiled and written by Daniel M Blake. Conceptual approaches of the manuscript were developed by Daniel M Blake, involving discussions with Natalia I Deligne, Thomas M Wilson and Jan M Lindsay. Daniel M Blake conducted the analytical and interpretive work with guidance from Natalia I Deligne, Thomas M Wilson and Richard Woods. All co-authors reviewed draft versions of the manuscript before submission by Daniel M Blake.

Certification by Co-authors:

If there is more than one co-author then a single co-author can sign on behalf of all

The undersigned certifies that:

- The above statement correctly reflects the nature and extent of the PhD candidate's contribution to this co-authored work
- In cases where the candidate was the lead author of the co-authored work he or she wrote the text

Name:	Dr. Thomas Wilson
Signature:	
Date:	08 November 2016

Deputy Vice-Chancellor's Office

Postgraduate Office

UNIVERSITY OF CANTERBURY
Te Whare Wānanga o Waitaha
CHRISTCHURCH NEW ZEALAND

Co-Authorship Form

Appendix A: The 2014 eruption of Kelud volcano, Indonesia: impacts on infrastructure, utilities, agriculture and health

Published by: GNS Science, Report No 2015/15, November 2015.

Daniel M Blake was lead author – he coordinated and compiled the majority of the report and heavily contributed to field data collection. Daniel M Blake edited the entire report following reviews of draft sections from co-authors. Other co-authors (G. Wilson, C. Stewart, H.M. Craig, J.L Hayes, S.F. Jenkins, T.M. Wilson, C.J. Horwell, S. Andreastuti, R. Daniswara, D. Ferdiwijaya, G.S. Leonard, M. Hendrasto, S. Cronin) contributed to field data collection, and writing and reviewing sections of the report where their area of expertise most suited.

Certification by Co-authors:

If there is more than one co-author then a single co-author can sign on behalf of all

The undersigned certifies that:

- The above statement correctly reflects the nature and extent of the PhD candidate's contribution to this co-authored work
- In cases where the candidate was the lead author of the co-authored work he or she wrote the text

Name:	Dr. Thomas Wilson
Signature:	
Date:	08 November 2016

Deputy Vice-Chancellor's Office

Postgraduate Office

UNIVERSITY OF CANTERBURY
Te Whare Wānanga o Waitaha
CHRISTCHURCH NEW ZEALAND

Co-Authorship Form

Appendix D: Framework for developing volcanic fragility and vulnerability functions for critical infrastructure

Submitted to: Journal of Applied Volcanology

Daniel M Blake was the second author and contributed to the development of fragility functions for surface transportation networks based on post-eruption impact data. Grant Wilson was the lead author and wrote the majority of the report, devised the majority of methodologies and implemented most of the approaches discussed. Thomas M Wilson and Natalia I Deligne provided advice to Grant Wilson during the conceptual development and support with writing the manuscript. Jim Cole provided reviews of draft versions of the manuscript and all other co-authors reviewed and edited the manuscript before submission.

Certification by Co-authors:

If there is more than one co-author then a single co-author can sign on behalf of all

The undersigned certifies that:

- The above statement correctly reflects the nature and extent of the PhD candidate's contribution to this co-authored work
- In cases where the candidate was the lead author of the co-authored work he or she wrote the text

Name:	Dr. Thomas Wilson
Signature:	
Date:	08 November 2016

Deputy Vice-Chancellor's Office

Postgraduate Office

UNIVERSITY OF CANTERBURY
Te Whare Wānanga o Waitaha
CHRISTCHURCH NEW ZEALAND

Co-Authorship Form

Appendix E1: Investigating the consequences of urban volcanism using a scenario approach I: development and application of a hypothetical eruption in the Auckland Volcanic Field, New Zealand

Submitted to: Journal of Volcanology and Geothermal Research

Daniel M Blake was the third author and contributed to initial impact scenario development in particular. He also made contributions to the evacuation section and made edits to the manuscript. Natalia I Deligne coordinated, wrote and edited the manuscript – she also led much of the scenario development and application which appears in this manuscript. Rebecca Fitzgerald contributed to much of the initial hazard scenario, on which this manuscript evolves from. Thomas M Wilson, Ranella Carneiro and Scott Muspratt were heavily involved with the electricity component in particular. Richard Woods made suggestions regarding operational activities throughout. All co-authors made revisions and edits to the final manuscript before submission by Natalia I Deligne.

Certification by Co-authors:

If there is more than one co-author then a single co-author can sign on behalf of all

The undersigned certifies that:

- The above statement correctly reflects the nature and extent of the PhD candidate's contribution to this co-authored work
- In cases where the candidate was the lead author of the co-authored work he or she wrote the text

Name:	Dr. Thomas Wilson
Signature:	
Date:	08 November 2016

Deputy Vice-Chancellor's Office

Postgraduate Office

UNIVERSITY OF CANTERBURY
Te Whare Wānanga o Waitaha
CHRISTCHURCH NEW ZEALAND

Co-Authorship Form

Appendix E2: Economics of Resilient Infrastructure Auckland Volcanic Field scenario

Published by: GNS Science, Report No 2015/03, October 2015

Daniel M Blake was the second author – he coordinated a preliminary version of the report (unpublished internal EQC workshop scenario), was the lead on the road and rail sections and contributed to the evacuation section. He also edited much of the final version of the report and attended sector meetings. Natalia I Deligne coordinated this report, adapted the original scenario, created hazard layers, was the lead for many of the infrastructure sections, edited the final report, and attended sector meetings. Between them, Alistair J Davies, Josh Hayes, Carol Stewart, and Emily S Grace led some of the report sections and attended some sector meetings. Thomas M Wilson coordinated the overall UC contributions, contributed to the electricity section, attended a sector meeting, and edited the final report. Grant Wilson and Sally Potter undertook preliminary work on some of the report sections.

Certification by Co-authors:

If there is more than one co-author then a single co-author can sign on behalf of all

The undersigned certifies that:

- The above statement correctly reflects the nature and extent of the PhD candidate's contribution to this co-authored work
- In cases where the candidate was the lead author of the co-authored work he or she wrote the text

Name:	Dr. Thomas Wilson
Signature:	
Date:	08 November 2016

CONTENTS

LIST OF FIGURES

LIST OF TABLES

1. INTRODUCTION AND BACKGROUND

1.1 Disaster Risk Reduction (DRR)

Risk information provides a critical foundation for managing disasters (GFDRR 2014). Insurance, government and infrastructure groups, as well as the end-users of systems, all require disaster risk assessments to determine the nature and extent of risk (UNDP 2010) and inform decisions and strategies that ultimately reduce impacts from adverse events. Despite substantial international efforts to reduce impacts in recent years however, economic losses from disasters are rising – from US$50 billion per annum in the 1980s, to around US$200 billion per annum in the last decade (World Bank and GFDRR 2013, GFDRR 2014). The recently established Sendai Framework for Disaster Risk Reduction (2015-2030) sets out to "substantially reduce disaster risk and losses in lives, livelihoods and health and in the economic, physical, social, cultural and environmental assets of persons, businesses, communities and countries" (UNISDR 2015, p.36).

Risk can be expressed qualitatively and/or quantitatively where it is derived as a combination of the likelihood / magnitude of the hazard and its consequences (UNISDR 2009). For the purpose of disaster risk assessments, risk is typically broken down into three principal components:

1. **Hazard** – potentially damaging phenomena that may cause loss of life or injury, property damage, social and economic disruption, or environmental degradation.
2. **Exposure** – elements at risk such as people, land and infrastructure.
3. **Vulnerability** – the susceptibilities and capacities of the elements impacted by hazards (Crichton 1999, UNISDR 2004, Bouchon 2006).

In order to achieve the goal of DRR, integrated and inter-disciplinary measures that prevent and reduce hazard exposure and vulnerability to disaster, increase preparedness for response and recovery, and strengthen *resilience*[1] should be implemented at all levels (UNISDR 2015, Few and Barclay 2016, Stewart et al. 2016). The research documented in this thesis investigates the impacts of volcanic ash on surface transportation networks. It helps inform DRR measures, specifically contributing to the following global target of the Sendai Framework for DRR (2015-2030) in relation to volcanic risk assessment:

[1] There are various definitions of resilience. The definition provided by the United Nations Office for Disaster Risk Reduction is used for the purpose of this thesis: "The ability of a system, community or society exposed to hazards to resist, absorb, accommodate to and recover from the effects of a hazard in a timely and efficient manner, including through the preservation and restoration of its essential basic structures and functions" (UNISDR 2009).

"To substantially reduce disaster damage to critical infrastructure and disruption of basic services through developing their resilience" (UNISDR 2015, p.12).

This, in turn, helps to reduce the number of people affected by volcanic hazards and associated economic loss. The broad framework for this thesis, illustrating how the components are integrated with risk management and DRR, is shown in Figure 1.1.

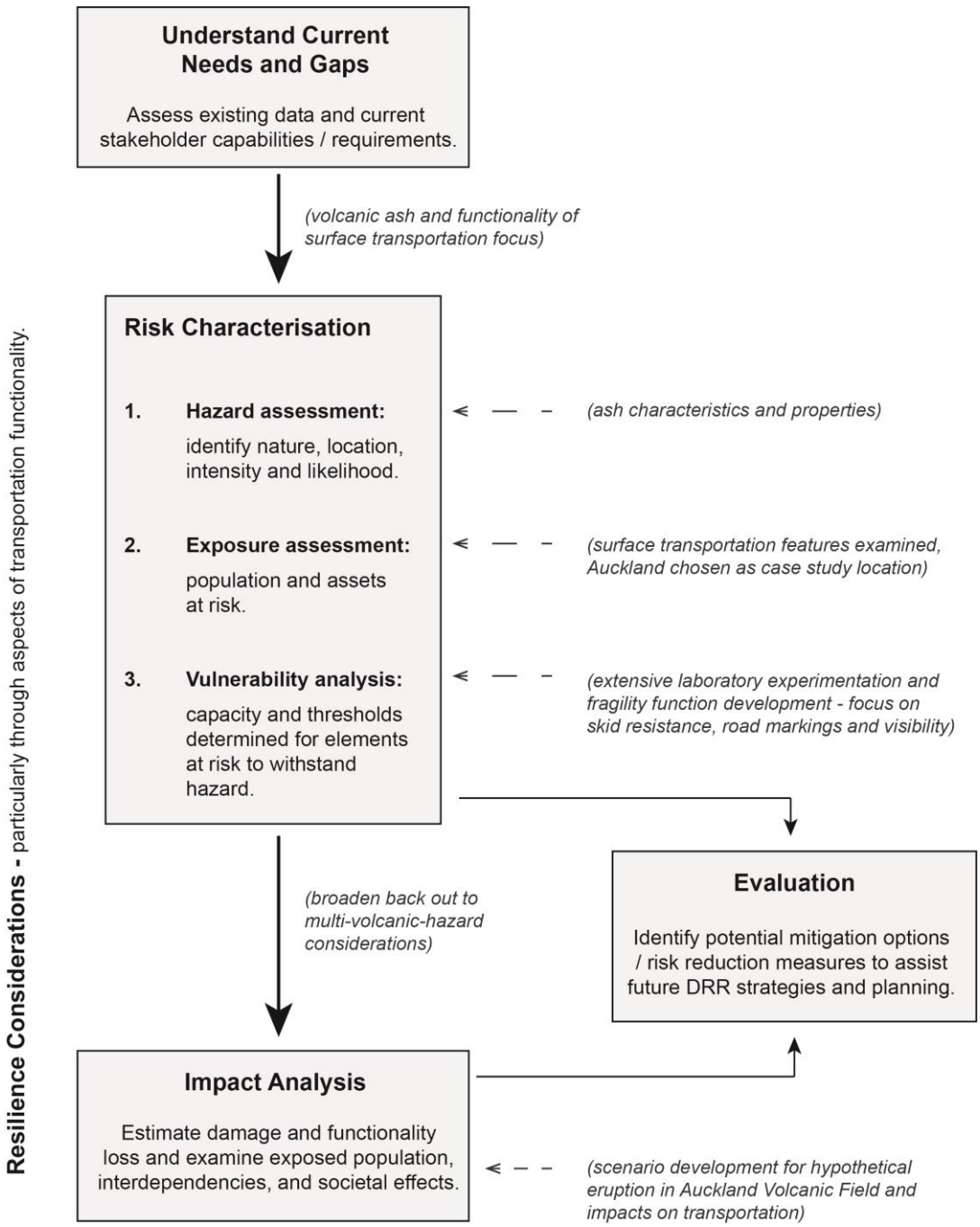

Figure 1.1 Conceptual framework for the thesis (adapted from UNDP 2010). Italicised text indicates how this thesis contributes to volcanic risk management for surface transportation.

1.2 Risk Assessment Considerations

Risk assessments are fundamental for effective DRR policies and practices, as they determine the nature and extent of risk, by considering hazard, exposure, and vulnerability in combination; they analyse hazard characteristics and evaluate existing conditions of vulnerability that together could potentially harm exposed people, property, services, livelihoods and the environment on which they depend (UNDP 2010, UNISDR 2015). Risk assessments provide opportunities before disaster events to estimate deaths, damages, disruption, and losses (direct and indirect) that will result. They can also assess the value of actions to reduce impacts on individuals, communities and governments (GFDRR 2014). Once the risk has been assessed, it can be used to inform management strategies before, during and/or following disasters, such as exclusion zones, hazard/risk maps and signs, land-use planning (e.g. Fitzgerald et al. 2016), and advice to end-users of *critical infrastructure*[2]. Therefore, risk assessments are used by many stakeholders and, because of their importance, have been developed over a number of years. The Global Facility for Disaster Reduction and Recovery highlight that the earliest records of risk assessments relate to practices of minimising financial risk from shipping, and the origins of property insurance practices can be traced back nearly 350 years (GFDRR 2014). More recently, technological advances such as increased computational power and resources have led to the rapid development of modern risk assessments which link exposure and vulnerability data with hazard models (GFDRR 2014). Substantial progress on each element of the risk assessment process has been made since, including during the timeframe of the Hyogo Framework for Action (2005-2015), and tools and models for identifying, analysing, and managing risk have grown in number and utility (GFDRR 2014).

Risk assessments are not the conclusion of the process however; rather they provide a foundation for long-term engagement focused on the use of risk information (GFDRR 2014). Many of the responses to new information derived from risk assessments, such as developing new emergency management policies and engineering-focused improvements to infrastructure, are effectively a form of increasing resilience. Indeed, reducing risk, in terms of the ability of people or assets to withstand a disruptive scenario (reducing vulnerability) and to recover (increasing recoverability), can also be achieved as a result of developing resilience (Barker and Ramirez-Marquez 2016). As such, resilience is an important and compatible component of DRR, as it means targeted systems are able to absorb unexpected and potentially high consequence shocks and stresses, and adapt to adverse events (NAS 2012, Linkov et al. 2016, Palma-Oliveira and Trump 2016).

Despite their advantages, some risk assessments today still adopt relatively traditional approaches, especially in that they strive for systems that are completely fail-safe in nature by focusing on short-

[2] Critical infrastructure is defined here as “infrastructure so vital that its incapacitation or destruction would have a debilitating impact on defence or economic security” (Moteff et al. 2003). In some countries, critical infrastructure may also be referred to as *critical utilities* or *lifelines.*

term system hardness and physical damage that occurs during adverse events (Linkov et al. 2016). However, this approach is often too rigid, inflexible, data-intensive, and expensive, especially given the increasing interconnectedness of systems (GFDRR 2016a, Linkov et al. 2016, Palma-Oliveira and Trump 2016). Risk assessments also need to consider events that could cause long-lasting and widespread damage to society, such as through the loss of functionality of systems. This is particularly true for events where there has been a lack of focus by previous risk assessments, and for high uncertainty or low probability events. For example, volcanic eruptions have often been ignored in reinsurance and other global risk assessment models because of low risk awareness, insufficient resources, and/or a perceived low priority compared to other events. This is despite the potentially catastrophic consequences for society should an eruption occur (NAS 2012, Merz et al. 2009, Park et al. 2013, Linkov et al. 2016, Palma-Oliveira and Trump 2016, Stewart et al. 2016). Integrating resilience into risk assessments is an appropriate solution as it encompasses dynamic properties such as the temporal components of adaptation, response and recovery and regards risk management as a socially constructed process (Lalonde and Boiral 2012, Vugrin 2016). Resilience strategies enable effective preparatory measures for the disruption of critical infrastructure services such as energy and transportation (Linkov et al. 2016).

Rarely do countries or communities face potential risks from only one hazard. Our complex and interconnected systems, which rely on novel technologies, are such that multiple hazards with cascading risks are of increasing importance (Lalonde and Boiral 2012). Despite this understanding, many risk assessments currently adopt a single hazard approach, often with a particular focus on a hazard which has substantial existing (or newly discovered) knowledge of likely impacts. Subsequently, some policies, guidelines and codes have little consideration for lesser-known or emergent hazards and, in many cases, it is not possible to account for all threats to all critical infrastructure all of the time (Vugrin 2016). However, individual hazards should not be discounted altogether, and adopting a multi-hazard risk approach leads to better land-use planning, better response capacity, greater risk awareness, and increased ability to set priorities for mitigation actions. Indeed, failure to consider the full hazard environment can lead to maladaptation (GFDRR 2014). Indeed, many governments recognise the importance of a multi-hazard risk approach. For example, the US government highlights this through Presidential Directive 21 (White House 2013) which states that critical infrastructure “must be secure and able to withstand and rapidly recover from all hazards” (Barker and Ramirez-Marquez 2016). Combining community observations and knowledge with scientific expertise can assist the development of multi-hazard risk assessments. Successful critical infrastructure resilience activities should focus on the ability to continue providing goods and services, even in uncertain and multi-hazard environments (Vugrin 2016). Considering the needs of infrastructure users and overall impacts and consequences to the system is therefore paramount.

Although an important component of risk assessments, vulnerability data related to some hazards remains scarce, particularly for volcanic hazards. This is in part due to often infrequent occurrence of volcanic eruptions and associated impacts in the past (Wilson et al. 2012), particularly in the

developed world, and also the labour- and resource-intensive nature of data collection, which often focuses on vulnerability types specific to a certain country or region (Jenkins et al. 2014a). Furthermore, the multiple hazards that occur during most eruptions and multi-faceted nature of individual volcanic hazards themselves (Stewart et al. 2016) (e.g. different volcanic ash characteristics and dynamic pressure variations within PDCs), mean that the overall vulnerability can be difficult to decipher. As such, most vulnerability assessments are often simplified, focusing on one hazard in particular and physical damage from that hazard, sometimes dismissing functional loss considerations altogether. However, with an increasing focus on DRR globally, and following recent high-profile eruptions, such as the Eyjafjallajökull (2010) eruption in Iceland, and their impacts, attitudes to vulnerability assessment are changing. The somewhat challenging components of vulnerability form major themes of this thesis. There is a strong focus on volcanic ash, including considering the vulnerability resulting from different ash characteristics, but a broader multi-volcanic hazard approach is undertaken in the form of a scenario to demonstrate new findings.

1.3 Resilience of Critical Infrastructure during Disasters

Critical infrastructure is of particular relevance to DRR; it is of such vital importance in both a societal and economic context that its failure or degradation can result in sustained supply shortages, significant disruption of public safety and security, and/or other dramatic consequences (BBK 2016, UN-EHS 2016). However, some infrastructure and services are extremely fragile in the face of unanticipated shocks (Hughes and Healy 2014), and can themselves become a driver of risk (Bach et al. 2013, Kadri et al. 2014, UN-EHS 2016). Internationally, there is thus a growing demand to improve the resilience of critical infrastructure. For example, in the USA following the 11 September 2001 terrorist attacks in New York and devastation wrought by Hurricane Katrina in 2005, resilience emerged as a complimentary goal to the previous prevention-focused activities (Vugrin 2016). In New Zealand, the 2010-11 Canterbury earthquake sequence caused extensive critical infrastructure damage and disruption in Christchurch; liquefaction and ground deformation severely affected power, water, wastewater, and transportation networks (CCC 2011, Giovinazzi et al. 2011, Seville et al. 2014). The core vision of the most recent New Zealand Treasury National Infrastructure Plan is that *"by 2045 New Zealand's infrastructure is resilient and coordinated and contributes to a strong economy and high living standards"* (NIU 2015). As Godschalk (2002) suggest, there are two key reasons behind the importance of resilient critical infrastructure:

1. The vulnerability of technological, natural and social systems cannot always be predicted. Therefore, the ability to accommodate change without catastrophic failure in times of disaster is critical.
2. People and infrastructure fare better in resilient cities when struck by disasters – fewer buildings collapse, fewer power outages occur, fewer businesses are put at risk, and fewer deaths and injuries occur (Godschalk 2002).

During disasters, critical infrastructure is often in high demand and existing resources may be disrupted. For example, in the 1994 Northridge earthquake in Los Angeles, Gordon et al. (1998) estimated that around 25% of business interruption losses could be attributed to the failure of highway bridges (Chang et al. 2014). Hence, a system's ability to perform without immediate maintenance or repair would be a desirable resilient feature (Vugrin 2016). However, in assessing resilience, it is necessary to define the critical function/s of a system, and stakeholders play a key role in this process (Linkov et al. 2016). Vulnerabilities and resilience to disasters must be characterised to allow the prioritisation of mitigation efforts to improve resilience (Burby et al. 1999, Mileti 1999, Chang et al. 2014). There have been various suggestions for the most appropriate way to measure critical infrastructure resilience (Ayyub 2014) including:

- Developing metrics which describe expected degradation in the quality of the infrastructure by quantifying robustness, redundancy, resourcefulness, and time to recovery (Bruneau and Reinhorn 2007).
- Calculating the percentage of infrastructure network links and nodes damaged versus the network performance (Garbin and Shortle 2007).
- Assessing the functionality of an infrastructure system after an external shock including the time it takes to return to its initial level of performance (i.e. expected recovery time) (Tierney and Bruneau 2007).

For the purpose of this thesis, measuring resilience particularly utilises the last approach, with a strong focus on critical infrastructure functionality, particularly in relation to end-user needs. Additionally however, an understanding of impact thresholds is required to forecast whether a system is able to absorb a shock, and to provide knowledge on alternative functional regimes following disruption (Linkov et al. 2016). Although such thresholds have previously been determined for infrastructural components when they encounter select natural hazards (e.g. bridge failure from seismic shaking; power line damage from high winds), they remain unexplored for other hazards such as volcanic ashfall. The work in this thesis strives to determine thresholds that characterise the impacts on surface transportation functionality during volcanic hazards, particularly ashfall – a previously under-researched topic. In order to achieve this, the key vulnerable components of surface transportation networks must first be derived to allow detailed quantitative studies to be conducted in the relevant areas. Such work will improve the resilience of surface transportation (and indeed other critical infrastructure through interdependent properties) by enabling more suitable and targeted risk management practices to deal with volcanic eruptions – it is also likely that this will improve resilience in the face of other shocks.

1.4 Volcanic Eruptions

Volcanoes are commonly associated with catastrophe and devastation (Scarth 1994). However, the effects of volcanic eruptions on society are not always as explicit – a result of the multiple and

distinctive but complex hazards associated with such phenomena. Hazards include those that generally occur in areas close to the vent, such as lava flows and pyroclastic density currents (PDCs), through to widespread tephra fall (Magill and Blong 2005) (Figure 1.2), which can disperse hundreds to thousands of kilometres from the source (Wilson et al. 2012). A range of secondary hazards such as earthquakes, tsunami, lahars, fire and drought can also be triggered by an eruption, or at least associated with increased volcanic unrest. Proximal volcanic hazards generally cause relatively severe and direct damage. Volcanic ash however (i.e. tephra particles with a diameter <2 mm), although not necessarily as damaging, can lead to widespread and complex disruption through interactions with infrastructure components (Blong 1984, Johnston 1997, Wilson et al. 2012, Wilson et al. 2014). Ash can originate from different eruption styles; it can be produced by explosive activity in eruption columns and PDCs, as well as by effusive eruptions in lofting plumes associated with dome collapse or basaltic fire-fountaining (Figure 1.2) (Lindsay and Peace 2005). Volcanic ash can also lead to major concerns for human and agricultural health (Horwell and Baxter 2006, Stewart et al. 2013), as well as accidents and injuries in ash-laden environments (e.g. ICAO 2007, Jenkins et al. 2013, Tamaki and Tatano 2014). The widespread and wide-ranging effects of ash on utilities, infrastructure, and health were observed during the infamous Mount St. Helens (1980) eruption, with many impacts to transportation networks in particular (Blong 1984).

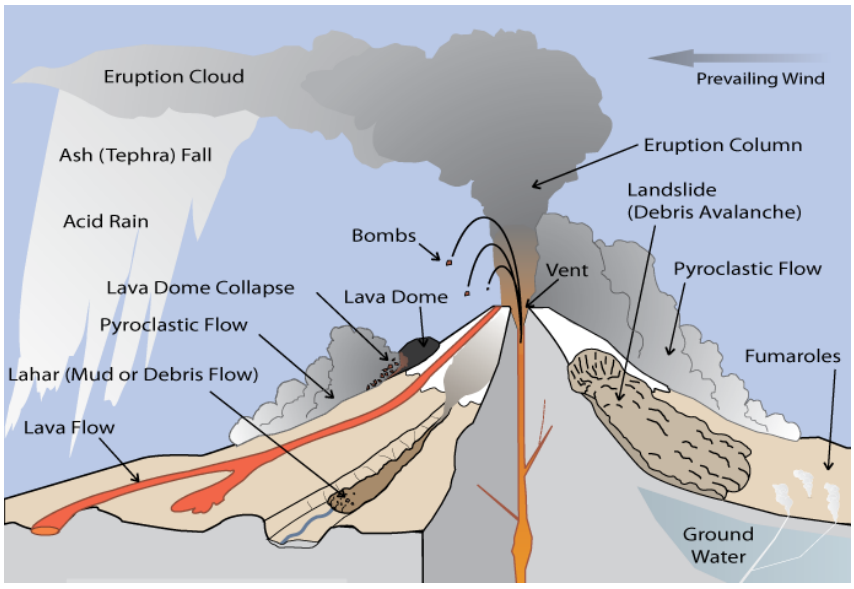

Figure 1.2 Potential volcanic hazards that can damage or harm assets and people (adapted from USGS 2010).

During the last 500 years over 250,000 people have been killed either directly by eruptions or by some of the indirect hazards they produce (Alexander 2002, Auker et al. 2013, Loughlin et al. 2015). In terms of loss-of-life, one of the worst examples of a volcanic disaster in the last 200 years occurred in 1902 when the town of St Pierre on the Island of Martinique, Caribbean, was hit by PDCs from Mount Pelée. The eruption killed 28,000 people, including all but two of the town's inhabitants

(Boudon and Gourgaud 1989, Alexander 2002). Many cities around the world are vulnerable to the potentially devastating effects of volcanic hazards (e.g. Auckland City, New Zealand; Mexico City, Mexico; Naples, Italy; Yogyakarta, Indonesia; Kagoshima, Japan) due to their close proximity to active volcanoes (Figure 1.3). The cities are often particularly vulnerable to the effects of ashfall, which can disperse tens to hundreds of kilometres from vents. An increasing number of people inhabit such areas as the world's population grows (Woo 2009) and urbanisation continues (UN 2014). Development associated with such growth, and technological advances in recent years, has led to the increasing exposure of complex critical infrastructure networks such as transportation. The Global Volcano Model (GVM) Network estimate that 800 million people in 86 countries currently live within 100 km of a volcano that could potentially erupt (Loughlin et al. 2015). The infrastructure networks associated with such populations are understandably extensive. Furthermore, volcanic ashfall is associated with increasingly large economic impacts (Loughlin et al. 2015). Such substantial economic effects were demonstrated by the relatively modest eruption of Eyjafjallajökull, Iceland, in 2010 which caused serious disruption to air traffic across Europe and resulted in cumulative global economic losses of around US$5 billion (Ragona et al. 2011).

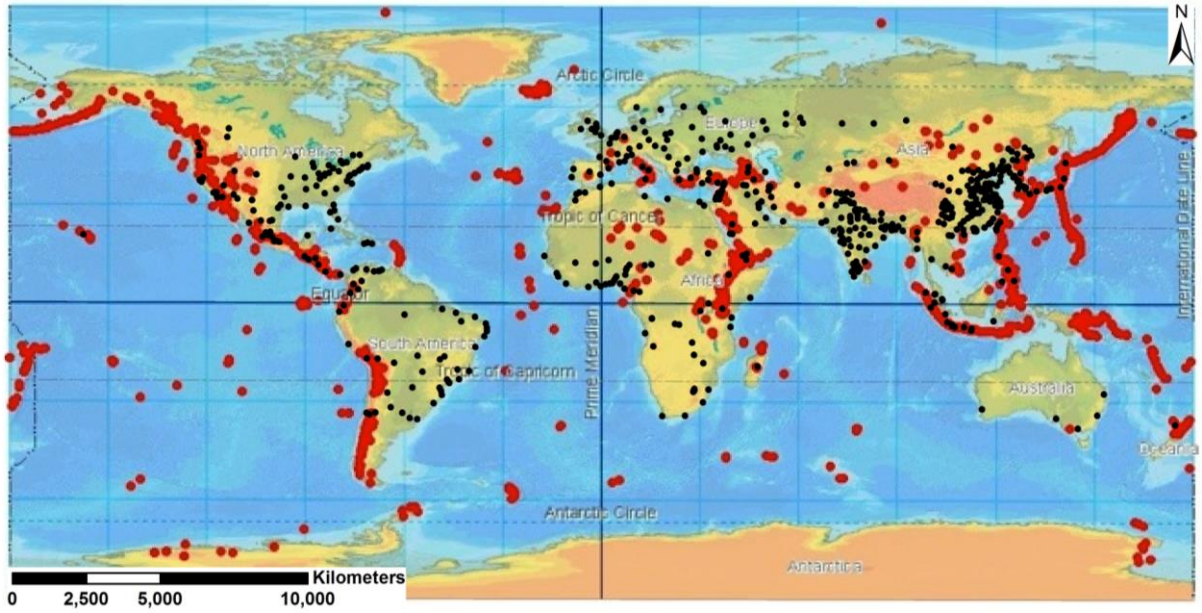

Figure 1.3 Volcanically active areas (red) and cities with more than 750,000 people (black) worldwide. [City data sourced from the UN population division (UN 2007) via Nordpil (2010). Volcano data sourced from Cccarto (2016)].

In recent years, there has been an increasing number of studies on the impacts of volcanic hazards on society, including those which focus on the effects of tephra fall, particularly ash, which can cause especially complex interactions with the built environment (e.g. Blong 1984, Wilson et al. 2009, Barnard et al. 2009, Wardman et al. 2012a, Weber et al. 2013, Wilson et al. 2012, Wilson et al. 2014, Hampton et al. 2015, Zorn and Walter 2016). Many of these ash-focused studies have demonstrated

that although ashfall rarely endangers human life directly, threats to public health and disruption to critical infrastructure can lead to significant societal impacts (Wilson et al. 2012). The properties of volcanic ash and environmental conditions at the time of, and following, ashfall will determine whether there are significant impacts (Wilson et al. 2011). Even relatively small eruptions can cause widespread disruption, damage and economic loss. For example, the 1995/96 eruptions of Ruapehu volcano in New Zealand were relatively small (VEI 3) but still covered over 20,000 km^2 of agricultural land with volcanic ash and caused significant disruption and damage to critical infrastructure (Cronin et al. 1998, Johnston et al. 2000). Thick tephra deposits are often constrained to proximal vent areas because coarse-grained material quickly settles out of the atmosphere under the force of gravity. Conversely, thin deposits often cover wide swathes of land because fine-grained ash disperses further, and this is thus the most likely volcanic hazard to affect critical infrastructure networks. However, previous studies have often focussed on very large eruptions and impacts associated with ash falls >10 mm thick, rarely reporting on the effects from ashfall <2 mm thick (Wilson et al. 2012). This presents a source of uncertainty for emergency management planning and risk assessments (Wilson et al. 2012). Furthermore, the relatively fresh state of volcanic impact research means that, while some topics have seen considerable advancements in knowledge (e.g. impacts of ash on electricity distribution networks and roof structure loading), others remain relatively understudied with opportunities for improved knowledge that will inform DRR. This includes the impacts of ash on surface transportation networks, particularly in relation to functionality, on which this thesis is based.

1.4.1 Contemporary volcanic risk assessment

In this subsection, the core components for assessing risk, as outlined in the conceptual framework (Figure 1.1), are covered in detail in relation to volcanic eruptions.

Determining the characteristics of volcanic hazards (including the probability of occurrence, degree of warning, and extent, duration and intensity of impacts; Bouchon 2006) has traditionally been the dominant focus of risk assessments in the past. However, volcanic risk assessments that also fully consider the exposure of assets and populations, as well as their vulnerability in the face of all hazards (not just those that cause severe damage or complete destruction), are important to fulfil stakeholder needs. Such contemporary risk assessments more appropriately account for critical infrastructure end-users than traditional approaches, and are more compatible with the goal of increasing resilience through striving for optimum system functionality. Probabilistic assessments best incorporate uncertainty, both in terms of the physical processes and the current state of scientific knowledge, and there is a growing expectation to incorporate probabilistic approaches when assessing volcanic risk (Woo 2009, Magill et al. 2006, Hurst and Smith 2010, Jenkins et al. 2012). However, it is impossible to eliminate uncertainty altogether in models and is thus essential for uncertainties to be conceptually integrated into the framework of volcanic risk assessments and consequently into estimates of damage and functional loss (GFDRR 2014).

A variety of data sources is ideal for compiling contemporary volcanic risk assessments, and, in most cases, a combination of quantitative and qualitative data types is optimal. The most fundamental is

post-eruption empirical data that defines historical events (e.g. Baxter et al. 2005, Jenkins et al. 2014a), in particular the date, geographical location and extent, and maximum intensity (GFDRR 2014, GFDRR 2016a). Such data may be applied in a deterministic or probabilistic sense, either assessing the impact of past events given current exposure, or estimating the probability of a hazard occurring at a given site with a specific intensity. Sometimes, the lack of observational data (due to inaccessibility and relatively low frequency of volcanic hazards impacting urban areas), means that a combination of theoretical and other empirical knowledge is required to inform the components of risk assessments (e.g. Petrazzuoli and Zuccaro 2004, Jenkins et al. 2014a). Such data can be derived from laboratory experimentation (e.g. Zuccaro and Gregorio 2013) or expert judgment (e.g. Chang et al. 2014), and both of these data types strongly inform the work in this thesis.

The information used to develop exposure datasets can be derived at various resolutions, depending on the risk that is being considered:

- Local – councils and local governments, Non-Governmental Organisations (NGOs), household surveys, aerial photos.
- Regional – state-based agencies, NGOs, statistical offices, census data, GIS data.
- National – statistical agencies, census data, global databases, NGOs, remote sensing (GFDRR 2014, GFDRR 2016a).

Exposure to volcanic hazards is commonly dynamic and characteristics change over time; they may change slowly as a result of development (Alexander 2000) but may also change very quickly due to a sudden disaster (Bouchon 2006). It is also important to consider population and demography characteristics due to the potential temporal variation in exposure. For example, the population and movement of people and goods within cities are often very different in the day compared to at night (Tomsen et al. 2014), and substantial variations in impacts from adverse events can occur as a result.

Vulnerability information is typically described in terms of damage and/or loss, assessed using functions that relate to hazard intensity. In the past, vulnerability analyses for volcanic eruptions have sometimes simply discounted distal areas and assumed high impact to any people residing within proximal areas to vents, whether rich or poor, landowner or landless farm labourer, man or woman, young or old (Blaikie et al. 2000). However, beyond areas of any total destruction, vulnerability forms a crucial factor in determining risk. Vulnerability assessment varies greatly depending upon the type of exposure being considered (e.g. people, infrastructure), the resolution of exposure (e.g. local, regional, national), and the information available. Vulnerability data is usually derived in three ways: empirically (from post-eruption observations and experimental studies), analytically, and/or using expert judgment (GFDRR 2016a). However, opportunities are often missed in the collection of damage and functional loss data following volcanic eruptions – information that is critical to assessing vulnerability (GFDRR 2014). Furthermore, as with exposure, vulnerability is dynamic and evolves over time. A good example worldwide is the general shift of populations towards cities (GFDRR 2016a); by 2050, 66% of the world's population is expected to reside in cities, an increase of around 12% from 2014 (UN 2014). Many cities have evolved in locations with favourable economic conditions such as

near coasts and fertile volcanic soils, but these often correlate with hazard-prone areas (Bilham 2009). An awareness of current vulnerability through continued data collection is thus essential to allow risk assessments that relate to such dynamic changes in environments. This in turn supports policies that promote resilient societies in urban settings (GFDRR 2014, GFDRR 2016b).

1.4.2 Application of volcanic risk information

Risk information can be used by a variety of stakeholders to inform preparedness and mitigation activities. It may help facilitate effective communication between stakeholders during times of crisis, which enables the implementation of successful response and recovery strategies (Jolly and Cronin 2014, Stewart et al. 2016).

Preparedness and mitigation activities include the implementation of warning systems, installation of protective shelters, evacuation planning, emergency response strategies and training exercises, and land-use planning (Fitzgerald et al. 2016). Many activities can be conducted well in advance of volcanic eruptions, during times of heightened volcanic activity, or indeed during and following an eruption itself. Such processes may also act as sources of risk information to many people (e.g. through the transfer of advice in publically available evacuation and emergency management plans and signage). Hazard/risk maps are another source of risk information, displaying spatial extents of volcanic hazard, exposure, vulnerability and risk through geological evidence and/or modelling (Sparks et al. 2013, Fitzgerald et al. 2016). Such maps are often one of the most widely accessed resources for warnings and emergency response (Leonard et al. 2014).

Scenario development based on previous or analogous eruptions is a common risk management activity. Although scenarios may not capture all possible future events with the risk information available (Wilson 2015), they present an opportunity to study the effects of multiple volcanic hazards on critical infrastructure networks and cascading effects for society, particularly when they integrate both spatial and temporal components of risk. Once a range of possible scenarios is established, stochastic models can be developed to find a sub-set of permutations and combinations of possible effects (Zuccaro et al. 2008).

1.5 Transportation Networks and Impacts from Volcanic Hazards

Transportation systems comprise physical man-made infrastructure in geographic and socio-economic contexts, which interact with the surrounding social, economic, financial, political, manufactured, and ecological environment. They have evolved over time into a patchwork of physical networks consisting of varied links and modes (World Bank 2015). Functional transportation networks are critical for society, both in normal operating conditions and emergencies. They enable commerce, and the movement of people and goods. Strong links between road, rail, shipping and aviation are often vital for moving people and freight around and between nations (NIU 2015). In urban

environments in particular, enhancing the resilience of transportation networks is imperative for two primary reasons:

1. They provide critical support to every socio-economic activity and are themselves one of the most important economic sectors.
2. The paths that convey people and services are the same paths through which risks are propagated (Bellini et al. 2016).

During adverse conditions, the ability of transportation networks to function, and then quickly recover to acceptable levels-of-service is therefore imperative to the wellbeing of communities (Hughes and Healy 2014).

Transportation that occurs on the surface of Earth (henceforth named *surface transportation*) is the primary focus of this thesis – that is road, rail and maritime transportation, as well as ground transportation at airports. Transportation by airborne aircraft is highlighted in places within but not investigated in detail; the reader is referred to other sources for further information on this subject, including Ajtai et al. (2010), Gislason (2011), Dunn (2012) and Harris (2014). Generic impact models for surface transportation group impacts by their principal effect along with some of their causal relationships. In general, surface transportation impacts can:

- compromise the quality of the surface
- block or damage infrastructure
- compromise end-user visibility
- compromise mobility, and / or
- create a temporary obstacle (Cover and Conger 2003).

However, transportation vulnerability is not uniform across people, vehicles, traffic flow, infrastructure or the environment. Vulnerability is a complex combination of end-user vulnerability, the potential for an incident to decrease the serviceability of the transportation system, and overall network reliability.

Use of surface transportation routes and facilities contaminated by pyroclastic material including ash may be required a) if evacuations are necessary, b) if an eruption continues for a prolonged period of time, c) to allow re-entry, and d) to allow immediate and long-term recovery of the impacted area. This can result in potentially large populations being exposed to volcanic hazards, especially in urban locations. Historical eruptions, including recent activity at Etna, Italy (2013); Sakurajima, Japan (2013); Kelud, Indonesia (2014); Culbuco, Chile (2015), and Sinabung, Indonesia (2014-16), have demonstrated that there are several issues associated with volcanic hazards and surface transportation (Figure 1.4).

The resilience of transportation networks to volcanic ashfall is poorly understood; there is limited knowledge of thresholds for when functional loss occurs. Furthermore, although transportation functionality investigations and modelling have been conducted for other natural hazards (e.g. earthquakes, dust storms, fog), volcanic hazards have many unique properties, which can result in

substantially different impacts. For example, PDCs exhibit varying dynamic pressures (Jenkins et al. 2014a), and volcanic ash, unlike mineral dust from most wind-blown soils, often has particularly abrasive properties (Langmann 2013). Therefore, a thorough understanding of all components for volcanic risk management (including the spatio-temporal hazard, vulnerability, capacity and exposure characteristics associated with critical infrastructure functionality loss) is urgently required for DRR policies and practices associated with transportation to be successful, and for achieving more resilient transportation networks (UNISDR 2015).

Moteff et al. (2003) show that not all components of transportation networks are equally critical. They highlight that, although congestion on surface transportation routes is common in urban areas, redundancy in networks means that there are usually alternative transportation routes or facilities available. There are few instances where this is not the case and these are perhaps the true “critical” pieces of transportation infrastructure (Moteff et al. 2003). Such critical infrastructure locations are often termed *pinchpoints* (Opus 2007, AELG 2014, NIU 2014, NIU 2015) to indicate converging networks and particularly heightened utility service disruption. However, surface transportation vulnerability is often not consistent over time; networks may be extended or upgraded with improved connections, and new components such as electric or autonomous vehicles may be introduced, sometimes over relatively short timeframes. Subsequent cascading effects for transportation may include intelligent transportation system improvements from big data collection on travel patterns, and different accident rates across the network leading to variations in the number of casualties and fatalities (NIU 2015, UN-EHS 2016). Static transportation infrastructure may also change in response to such new components. For example, road markings may be better maintained, and different traffic signals may be installed so that they can be seen by autonomous vehicle sensors. A consideration of resilience, which considers potential dynamic spatio-temporal shifts in functionality, is thus important for volcanic risk assessments on surface transportation, and investigations must clearly specify the state of transportation networks under consideration.

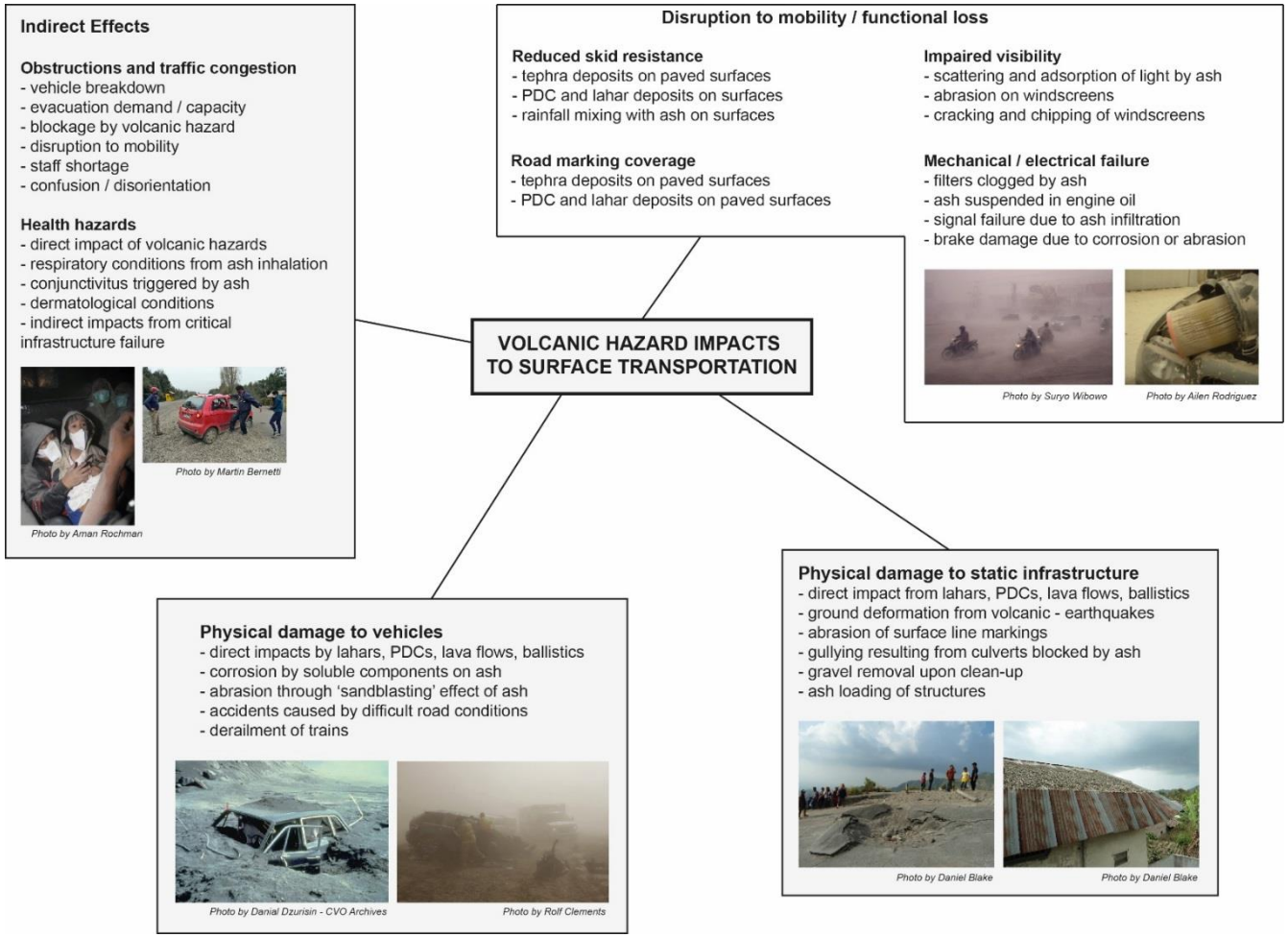

Figure 1.4 Examples of known volcanic hazard impacts to surface transportation (information from: Warwick 1981, Blong 1984, Johnston 1997, Nakada 1999, Durand et al. 2001, Nairn 2002, Barnard 2004, Cole and Blumenthal 2004, Cole et al. 2005, Horwell and Baxter 2006, Leonard et al. 2006, Wilson et al. 2007, Barnard 2009, Wilson et al. 2011, Barsotti et al. 2010, Sword-Daniels et al. 2011, Wardman et al. 2012b, Magill et al. 2013, Wilson et al. 2012, Wilson et al. 2013, Wilson et al. 2014). Health hazards are included because of the effects on transportation personnel.

In the following subsections, the key volcanic impacts to each surface transportation mode considered in this thesis (i.e. roads, rail, and transportation at airports and at sea) are highlighted, largely drawing from post-eruption observations.

1.5.1 Volcanic hazards and roads

Impacts to road transportation from volcanic hazards are relatively common around the world. Proximal hazards such as lahars, lava flows and pyroclastic density currents often cause severe damage or closure (Blong 1984, Johnston 1997, Nairn 2002, Wilson et al. 2014). However, the impact of volcanic ash on roads is frequently disruptive and widespread (Blong 1984, Barnard 2009, Wilson et al. 2014). Most records of volcanic tephra impacts to road transportation occur post-1980, probably a result of the high profile impacts from the 1980 Mount St Helens eruption triggering further observations and studies, but also in part likely attributable to growing worldwide populations and associated increased exposure to volcanic hazards. The majority of tephra effects are associated with widespread distal deposits, which usually comprise relatively thin (mm-cm) layers of low-density (pumiceous) silicic ash (Nairn 2002). Vehicle drivers can be affected by reduced visibility during volcanic ashfall; occasionally, “near-total darkness” is reported (e.g. Blong 1982, Wilson et al. 2012), although there have been no investigations to date to quantify the impacts of airborne ash on visual range. Indirect visibility effects may also occur from damage to vehicle windscreens. Ash caught between windscreens and wiper blades will scratch and permanently mark the windscreen glass when the wipers are used (e.g. Johnston and Neall 1995, Johnston 1997, Leonard et al. 2006) and vehicles may experience cracking of windscreens from the impact of lapilli and blocks ejected from the vent (e.g. Magill et al. 2013).

Ash deposits can cover road markings and reportedly reduce skid resistance, reducing braking ability and handling, and increasing stopping distances and accident rates (Barnard 2009, Wilson et al. 2012). Despite these potentially severe consequences for road transportation functionality, there have been no detailed studies that attempt to quantify the ash characteristics responsible for such impacts. As such, risk assessments may take a very precautionary approach at present, and road closures may be enforced in the absence of specific vulnerability information. For example, state highways were closed multiple times following light ashfall during the Ruapehu 1995-96 eruption, New Zealand, partly due to concerns of slippery surfaces (Johnston 1997). Closure effectively results in no service and severe consequences for end-users, even through routes may be traversable if they were open. Further studies are clearly required to improve our knowledge of road transportation functionality in ashfall and to minimise functionality loss, but must simultaneously account for variations in accident rate and life-safety considerations.

If ash accumulates to sufficient thicknesses, roads can become physically impassable. For example, during the Rabaul eruption in 1994, up to 1 meter of ash fall caused some roads to be impassable, even for four-wheel drive vehicles (Stammers 2000). Road vehicles themselves are also vulnerable to volcanic ash. Ash can clog filters and brake systems, thicken oil and abrade moving parts and seals within engines. However, severe mechanical impacts to vehicles can often be prevented through the frequent changing or cleaning of filters and other affected components.

Unconsolidated dry ash is readily remobilised by wind and fluvial processes, vehicle movement or other human activities, affecting areas further from the source than the original deposits, even after the eruption itself has ceased. This often makes clean-up of ash from roads logistically challenging and costly (Wilson et al. 2012, Hayes et al. 2015), with particular problems arising in on-going eruptions and substantial remobilisation events. Improved knowledge of thresholds for when clean-up is required, in order to maintain surface transportation functionality but minimise unnecessary clean-up efforts and expenses, would be highly beneficial to emergency and transportation management authorities.

1.5.2 Volcanic hazards and rail

There have been several reports of impacts to rail as a result of proximal volcanic hazards, particularly lahars and lava flows, such as the Tangiwai 1953 rail disaster (Ruapehu, New Zealand, 1945), and blockage of the Circumvesuvian Railway (Vesuvius, Italy, 1906 and 1944; Blong 1984). Rail track displacement by ground deformation has also occurred (e.g. Usu, Japan, 1944, and Kīlauea, U.S.A, 1968; Blong 1984). In contrast to roads however, there have been few recorded ash impacts to rail during historical eruptions, likely in part due to the less extensive (or absence of) rail networks in volcanically active areas. Despite few records, the impacts of ash on signaling and potential train-to-track communication disruption for electric rail may be particularly problematic. For example, following the 2011 Shinmoedake eruption at the Kirishima volcanic complex in Japan, trace quantities of both wet and dry ash led to the mechanical failure of switches due to loss of electrical contact between trains and track, stopping services on the network (Magill et al. 2013). As such, electric rail infrastructure appears vulnerable to volcanic ash, and any impact to electricity networks could also have cascading effects on rail systems in the absence of alternative diesel-powered fleet or back-up power supplies. Like roads, for tephra impact to rail, there appear to be minimal pre-1980 records. In fact, only one was identified in a literature search – that of derailment following the eruption of La Soufrière, Saint Vincent in 1902 (Blong 1984). However, the derailment was on a tram network, and these typically have different construction and operating features to conventional rail.

1.5.3 Volcanic hazards and airports

Volcanic ash is extremely hazardous to aircraft, particularly those with jet engines, due to potential for engine failure and/or damage (ICAO 2012, Prata and Rose 2015). Since 1953, there have been ~100 confirmed encounters with volcanic ash by in-flight aircraft, at least 80 of which incurred airframe or engine damage (e.g. Guffanti et al. 2009). The International Civil Aviation Authority advises that aircraft should avoid volcanic ash encounters altogether (ICAO 2012).

On the ground, which is the primary focus of this thesis for aviation, airports have been directly and indirectly impacted by volcanic hazards (Guffanti et al. 2009). The mere threat of an eruption can impact airport operations; aircraft may be redistributed and physical modifications at the airport may be undertaken. For example, before the 1979 Karkar and 1983 Tavurvur eruptions in Papua New Guinea, nearby airport runways were extended due to potential evacuation requirements (Blong 1984). The 1979 Karkar impact was the only pre-1980 tephra-related impact to airports identified through literature analysis. As with other transportation modes, proximal hazards often cause severe

damage to airports. For example, the abandonment of airports has occurred following ground displacement near Iwo-jima, Japan, 1957 (Corwin and Foster 1959, Guffanti et al. 2009), and pyroclastic density currents from Soufrière Hills, Caribbean, 1997 (Guffanti et al. 2009). Lava flows shortened the runway of an airport near Nyiragongo, Democratic Republic of Congo, 2002 (Guffanti et al. 2009). Even if airports are not abandoned, it is likely that no, or minimal, operations (i.e. no level-of-service) will occur given proximal impacts until the immediate threat has diminished and material is cleared from airfield surfaces.

Direct tephra impacts from ash span from ~1 mm thick ash, which must be removed from airport surfaces to avoid reduced runway friction and visibility impairment (ICAO 2001), to ash accumulations up to several meters thick, which can result in the abandonment or relocation of airports (Blong 1984). However, the ~1 mm threshold is often used quite loosely in aviation policy and, like for roads, there appears to be little information regarding the degree of functional loss (e.g. thresholds for reduced skid resistance or road marking coverage) should airfields remain operational when thicknesses are <1 mm; additional empirical data could help to fill these gaps in knowledge. Indirect impacts are usually temporary airport closure due to closed airspace over the airport, sometimes with no ash accumulation on the ground itself (Guffanti et al. 2009), as occurred at many north western European airports during the 2010 Eyjafjallajökull eruption, Iceland and associated ash plumes (Bolic and Sivcev 2011, Weber et al. 2012).

1.5.4 Volcanic hazards and maritime transportation

There have been several recorded impacts to maritime transportation, particularly from highly explosive eruptions since the 17th century. These impacts have predominantly consisted of pumice rafts following explosive eruptions causing obstruction to navigation (e.g. Sakurajima, Japan, 1779; Blong 1984, Tambora, Indonesia, 1815; Oppenheimer 2003, Chaitén, Chile, 2008; Wilson et al. 2012). There have also been some cases of tephra sedimentation in channels reducing navigability (Mount St Helens, U.S.A, 1980; Blong 1984, Hudson, Chile, 1991; Wilson et al. 2011), and extensive accumulation of tephra on ships, which required removal to avoid excessive loading (e.g. Krakatau, Indonesia, 1883, and Vesuvius, Italy, 1944; Blong 1984). If ports themselves are severely impacted, they will not be able to fulfil their primary role of sending and receiving goods, and are effectively closed.

1.5.5 Interdependencies

Transportation networks are arguably the most important type of critical infrastructure in emergencies because of their vital role in the provision of access for restoration of all other infrastructure (Cova and Conger 2003). Emergency managers must route personnel to an accident site, restore services, relocate threatened populations, and provide relief, all of which rely on transportation. Transportation in emergencies is of high importance for such reasons. However, it should be noted that transportation also depends on other infrastructure for its optimum functionality, and is thus more than a simple aggregation of its individual components. Typically as large sets of components are brought together and interact with one another, synergies emerge. They exhibit interdependent properties and can be seen as systems of interacting agents (Bouchon 2006). An understanding of how each infrastructure

type is connected with others is therefore critical for fully addressing problems (Sword-Daniels et al. 2015). Indeed, many complex interdependencies between modern infrastructure networks exist, with multiple failure modes, all of which can affect infrastructure functionality (Hughes and Healy 2014). Complex, interconnected systems create benefits and efficiencies during times of normal operation, yet can bring vulnerabilities and operational challenges, especially when natural hazards are encountered (Hughes and Healy 2014). Therefore, in addition to being 'at risk', each critical infrastructure contributes a degree of risk itself, since its partial or complete disruption constitutes a potential impact for other infrastructure and society (Bouchon 2006). For example, the banking and finance industry may be severely impacted by transportation disruption as the ability of staff to travel to their place of work is reduced. Systemic risks such as these may spread further from the original hazard source (IRGC 2006), and widely affect different infrastructure and systems that society depends on. Many relationships are bidirectional in nature. For example, the electricity network may rely on transportation for the supply of fuel for generators, but transportation may rely on continuous electricity for traffic signals to function (Rinaldi et al. 2001).

1.6 Transportation Vulnerability to Volcanic Hazards: Requirements

For transportation, as with all critical infrastructure, operators strive to ensure that assets and services are resilient in that they function continually and safely in the face of a range of existing and emerging hazards (Hughes and Healy 2014). Vulnerability assessments are key for volcanic risk modelling for transportation as they provide descriptions of impacts to individual components or the broader network for different hazard intensities. They differ from vulnerability assessments conducted for conventional buildings and structures in that transportation networks consist of spatially distributed components which are physically and functionally connected (Stergiou and Kiremidjian 2010). The following subsections outline some of the key considerations required for the assessment of surface transportation vulnerability to volcanic hazards.

1.6.1 Multi-hazard

For volcanic activity, challenges for vulnerability assessments may arise due to the multi-hazard component. Some areas of the network may experience multiple impacts of different intensities and with various hazard and infrastructure characteristics responsible for damage or disruption. For example, dynamic pressures from PDCs may cause damage to bridge structures, with further damage possible from loading by thick tephra or ballistic impact. However, few studies have been conducted to assess the vulnerability of surface transportation networks to volcanic ashfall, let alone to consider the effect of multiple hazards, which is important for DRR strategies (UNISDR 2015).

1.6.2 Functionality

The impact on surface transportation functionality during eruption crises has not been well constrained by existing vulnerability models, particularly in distal areas affected by ashfall. For example, it is often unknown how much transportation end-users will be affected by slippery roads or impaired visibility

following ashfall. Few impact thresholds exist to inform emergency and transportation management decisions during such conditions or indeed planning activities beforehand. In contrast, operational decisions in areas affected by proximal volcanic hazards are often relatively straightforward. For example, emergency management officials may simply make the call to completely close routes due to life-safety implications. A better understanding of surface transportation functionality in areas affected by volcanic ashfall is required for future vulnerability assessments and to inform operational decisions.

1.6.3 Fragility function development

Sometimes, simple vulnerability assessments in the form of qualitative descriptions of infrastructure vulnerability based on hazard intensity thresholds, or indeed the mere existence of a hazard (Wilson 2015), are sufficient for certain applications. However, fragility functions are presently the crux of more complex vulnerability assessments – they are probabilistic vulnerability models that describe the chances of damage or functional states being reached or exceeded for given hazard intensities (Singhal and Kiremidjian 1996, Choi et al. 2004, Rossetto et al. 2013, Tarbotton et al. 2015). Fragility functions thus allow the quantification of risk and provide a basis for improving mitigation strategies and strengthening resilience in many applications (Jenkins et al. 2014b, Wilson et al. 2014). They may relate to relatively local conditions and specific characteristics, but such detail must be recognised and highlighted for the appropriate determination of measures to reduce disaster risk (UNISDR 2015). Recent studies, including those by Wilson (2015) have made considerable progress at developing a framework for volcanic fragility functions for critical infrastructure including surface transportation networks. However, due to the somewhat coarse approach taken (necessary in order to cover the vast number of infrastructure types considered), previous research has generally focused on physical damage. Some aspects of infrastructure functionality have also been developed but many opportunities remain to progress this work further, and this forms one of the key goals of this thesis.

1.6.4 Vulnerability data: post-eruption impact assessment and experimental approaches

In the context of surface transportation impacts, there have been many observations (including anecdotal, qualitative and semi-quantitative) following previous eruptions, particularly through critical infrastructure impact assessment studies which have involved specialists travelling to specific locations (e.g. Tungurahua, Ecuador, 1999-2010 – Sword-Daniels et al. 2011; Merapi, Indonesia, 2006 – Wilson et al. 2007; Pacaya, Guatemala, 2010 – Wardman et al. 2012b; Shinmoedake, Japan, 2011 – Magill et al. 2013). In addition to direct field observations, data is frequently collected through interviews with staff at emergency management and critical infrastructure authorities during such studies – hence, involving a degree of expert judgment and inherent limitations associated with data derived from interviews (Opdenakker 2006). Such field studies and interviews have allowed the extensive development of impact data in a variety of worldwide locations over the past 20 years or so. Opportunities to obtain data from new impact assessment trips should certainly not be overlooked as new impacts may be discovered and larger qualitative datasets can complement and support

quantitative data that is used to inform risk assessments. Chapter 2 summarises the findings from new field studies and interviews conducted near Kelud volcano, Indonesia.

Data from field studies and interviews is mostly in qualitative form and there have been few targeted experimental studies to investigate such impacts quantitatively and systematically in detail. Conducting detailed quantitative studies using high specification equipment is a logical next step in advancing vulnerability assessments for surface transportation affected by volcanic ashfall. Such studies could occur during and after eruptions, but there are many difficulties associated with conducting work in the field, including equipment set-up requirements/practicalities and life-safety considerations. Undertaking experimental studies in controlled laboratory environments solves many of these difficulties and is possible during times of volcanic quiescence. Experimental studies have proved successful in other natural hazard disciplines including earthquake engineering (e.g. Mehrabi et al. 1996, Sims 1999, Ricles et al. 2002) and flood risk management (e.g. De Sutter et al. 2001, Jackson et al. 2008), as well as for other critical infrastructure types affected by volcanic ash (e.g. jet engines – Drexler et al. 2011; electricity - Wardman et al. 2012a; roof loading – Hampton et al. 2015). Data from such studies for surface transportation would inform fragility functions, and thus vulnerability assessments, through the consideration of specific infrastructure features at different hazard intensities and in different locations. Additionally, a more extensive and reliable quantitative data set for transportation impacts allows for advanced numerical modelling, and existing models can also be verified using experimental data (Maqsood et al. 2014). Additionally, previously unknown impacts, or properties attributable to such impacts, can be discovered and understood. Much of this thesis focuses on laboratory experimentation to expand quantitative data associated with surface transportation functionality and assist future vulnerability assessments.

1.7 Auckland, New Zealand Context

Auckland, New Zealand is selected as a case study for much of the work in this thesis. Laboratory studies are based on the city's surface transportation network and environmental properties, and some aspects of the locational setting are carried through to fragility function development, although most functions are applicable across the developed world. The scenario used to test and demonstrate the findings is also based in Auckland, and thus the volcanic eruption styles, geographical features, and societal characteristics of the city are important to consider. In this section, key background material is introduced, outlining aspects of volcanic risk in Auckland associated with both proximal volcanic hazards and distal sources of ashfall.

1.7.1 Auckland geography and volcanic risk

Auckland is located in the North Island of New Zealand with a regional population of ~1.6 million (and increasing), accounting for ~34% of the national population (Statistics New Zealand 2015a). Auckland City is built directly on top of a basaltic volcanic field (the Auckland Volcanic Field; AVF); it is exposed to future eruptions within the AVF itself (Section 1.7.2), as well as from tephra originating from elsewhere in New Zealand (Section 1.7.3) (Figure 1.5).

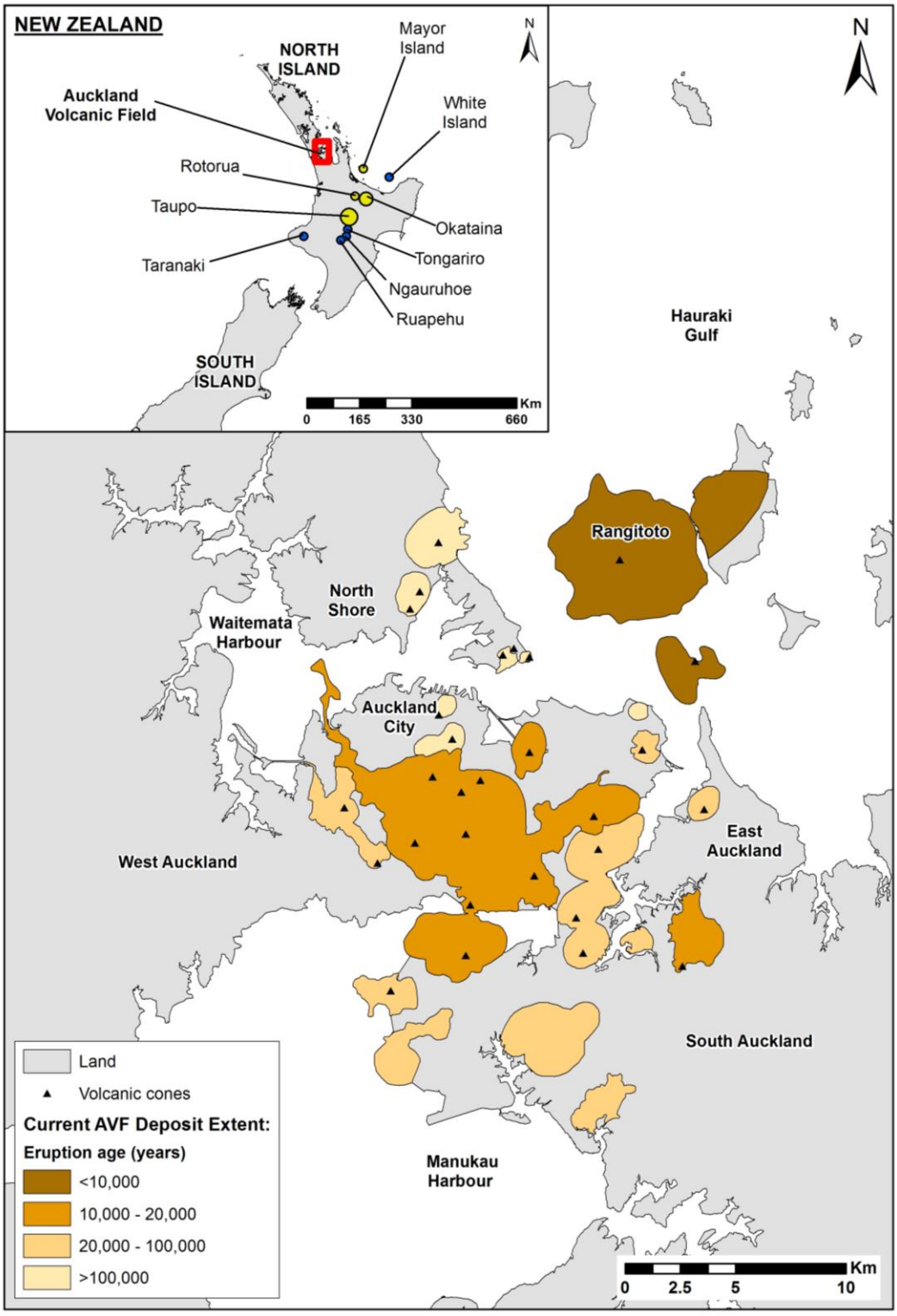

Figure 1.5 Auckland Volcanic Field (AVF) and potential distal sources of ash in New Zealand (inset). Andesitic stratovolcanoes are shown in blue and rhyolitic calderas in yellow. (Data provided by Auckland Regional Council, 2009).

Although the likelihood of eruptions is relatively low, the potential consequences of an AVF eruption or very large eruption elsewhere in New Zealand are considered major-to-catastrophic for the country

(DPMC 2011; Figure 1.6). The continued functionality of critical infrastructure is paramount in such events, and therefore, many national policies and acts (e.g. New Zealand's Civil Defence and Emergency Management Act (2002)) specify transportation as one of the critical infrastructure sectors. Managers of transportation organisations in New Zealand have a direct interest in understanding and developing resilience to hazards, with a desire to enable transportation networks to function at their fullest possible level-of-service (Hughes and Healy 2014).

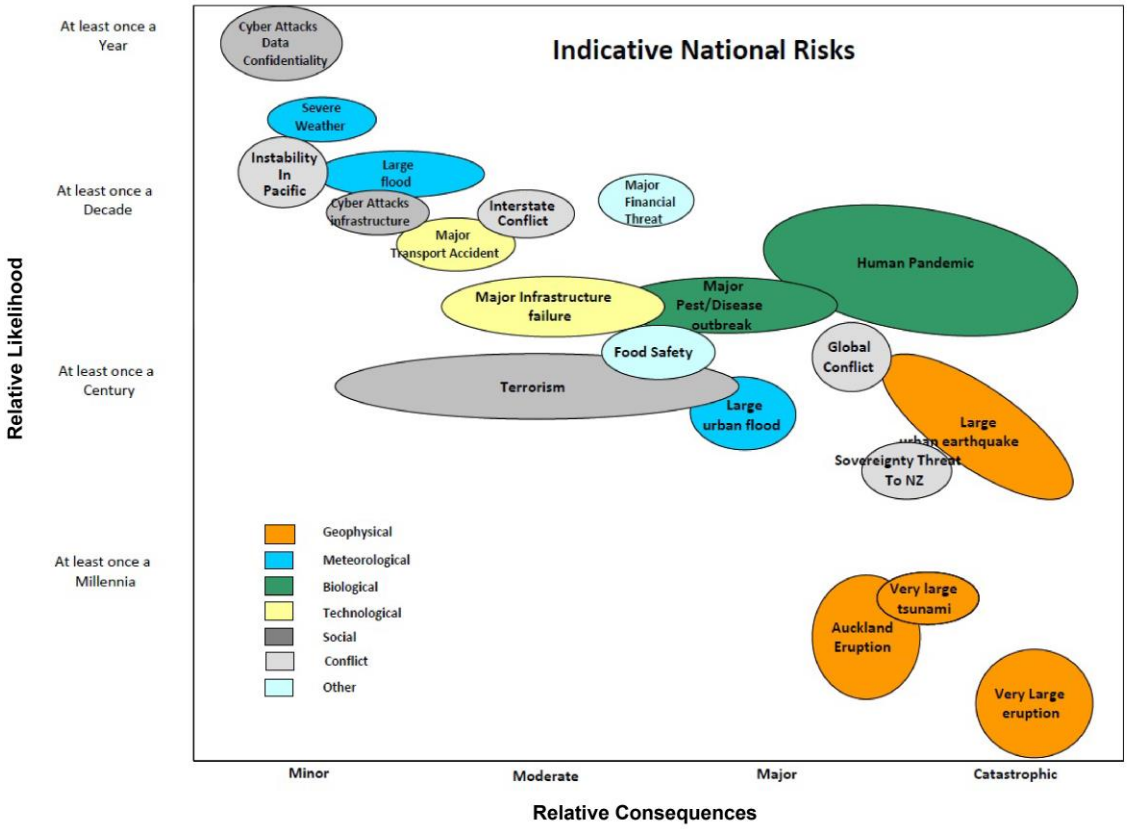

Figure 1.6 Indicative risks in New Zealand from a national security perspective (adapted from DPMC 2011).

The Lloyd's City Risk Index (2015), which analyses the economic exposure from 18 threats over ten years from 2015, ranks a volcanic eruption as the fourth largest threat to Auckland City, with an estimated US$ 0.54 billion GDP at risk. In Auckland, the latest emergency management group plan available at the time of writing (Auckland CDEM 2011), assigns a distant source volcanic eruption a risk ranking of 'very high' (the highest possible category) and a local AVF eruption a risk ranking of 'high' (the second-highest category) in its comparitive analysis of likelihood and consequence for 36 individual hazards in Auckland. Various societal challenges stem from both an increasing population and the geographical constraints of the area: the Waitemata and Manukau Harbours (to the north-east and south-west of the city respectively; Figure 1.5), restrict all land-based infrastructure through two isthmuses and limit evacuation routes (Auckland CDEM 2015). The southern isthmus is just ~2 km wide at its narrowest point and in order to enter or leave the city on the state highway network, one of

two key motorway bridges must be traversed in the area (Tomsen et al. 2014). This presents many challenges for transportation, and congestion across the road network is becoming more frequent (Edbrooke et al. 2003). Substantial transportation improvement projects are underway and planned for the city, including the NZ$1.4 billion Waterview Connection linking two key state highways (due: 2017), Auckland Manukau Eastern Transport Initiative (AMETI) (partially complete), and NZ$2.5 billion City Rail Link (under construction) (Auckland Transport 2016a, Auckland Transport 2016b, NZTA 2016). With alterations in network redundancy as a result of such projects, vulnerability is highly dynamic. However, with potentially heightened current exposure to volcanic hazards (through inward population flux), and major transportation network and geographical challenges with consequences for eruption vulnerability, understanding the expected impacts of volcanic hazards on transportation is more important than ever to increase preparedness, response and recovery efforts, and thus strengthen resilience.

1.7.2 Auckland Volcanic Field (AVF)

With more than 50 volcanoes in and around the city, the Auckland Volcanic Field (AVF) (Figure 1.5) forms many distinctive landmarks in Auckland. Cones, maars and other surficial features created by ~200,000 years of past volcanic activity (Kermode 1992, Shane and Sandiford 2003, Lindsay and Leonard 2009, Molloy et al. 2009, Lindsay et al. 2011, Le Corvec et al. 2013) dot the Auckland landscape, covering around 360 km^2. The geologically recent eruption of Rangitoto (~550 years ago; Needham et al. 2011), comparison with lifespans of analogue volcanic fields, and the presence of a mantle anomaly at depths of about 70–90 km beneath Auckland that has been interpreted as a zone of partial melting (Horspool et al. 2006), all suggest the field will erupt again (Lindsay 2010).

Before an eruption in the AVF, volcanic-induced earthquakes (up to around MM6) present the most danger to infrastructure (Smith and Allen 1993). Earthquakes of this intensity would be felt by the majority of the population but likely only cause little to minor damage close to the epicentres (Sherburn et al. 2007), especially on ground with low strength. Eruptions in Auckland typically start with an explosive phreatomagmatic phase (~83% in the past; Kereszturi et al. 2014) resulting from the fragmentation of magma due to interaction with water. Given that the AVF now encompasses an area that is either below seawater or with a high water table in soft sediments, the potential for phreatomagmatic activity is very high (Németh et al. 2012, Agustín-Flores et al. 2014). At high water to magma ratios (≥ 0.3; Wohletz 1983), phreatomagmatic eruptions are dominated by the formation of explosion craters and vertical eruption columns of lithic rock fragments and ash with pyroclastic surges. If groundwater and surface water become excluded from the active vent and the magma supply is sufficient for continuation, then activity becomes wholly magmatic and can include fire-fountaining and tephra fall, forming scoria cones (Allen and Smith 1994, Kereszturi et al. 2014). The latter stages of some Auckland eruptions are characterised by extensive lava flows (e.g. Rangitoto, Three Kings and Mt. Eden). Individual vents often display several different eruption styles (Allen and Smith 1994, Houghton et al. 1996, Kereszturi et al. 2014) but Auckland eruptions have tended to be small in volume, typically producing 0.1 to 1.0 km^3 of ejecta and lava (Johnston 1997).

Despite considerable research efforts, especially in the past 20 years or so, no conclusive spatial or temporal patterns in AVF eruptive activity have been identified. Previous activity across the entire field has generally been random but sometimes episodic (Molloy et al. 2009, Bebbington and Cronin 2010) and is simply constrained by outer geological boundaries such as the uplifted greywacke basement rocks to the east of Rangitoto (Allen and Smith 1994). Repose periods vary from around 500 to 20,000 years, although >2,000 is more characteristic of the field (Allen and Smith 1994, Molloy et al. 2009, Hurst and Smith 2010) Evidence suggests that the AVF is generally monogenetic (Allen and Smith 1994, Sherburn et al. 2007, Kereszturi et al. 2013), with most eruptions lasting a few months, possibly a few years. However, eruptions at other volcanic fields (e.g. Jorollo and Parícutin volcanoes in the Michoacan Guanajuato volcanic field, Mexico; Fries 1953, Luhr and Simkin 1993, Rowland et al. 2009, De la Cruz-Reyna and Yokoyama 2011) suggest that single eruptions could continue for around a decade (Sherburn et al. 2007). Additionally, episodic eruptions from individual volcanic vents may occasionally occur (e.g. Crater Hill; Houghton et al. 1999, Motokorea; McGee et al. 2012, Rangitoto; Needham et al. 2011, Shane et al. 2013, Linnell et al. 2016), although some of this behaviour may be attributed to intermittent water-magma interaction, changes in magma supply rate and/or degassing, with no hiatuses in activity, and is therefore not all considered truly polygenetic (Houghton et al. 1999, Spargo et al. 2007, Hopkins et al. 2015). This does however have major implications for hazard assessment, such that when a future eruption occurs in the AVF, it will be necessary to consider the conduit a possible pathway for another eruption for up to several decades afterwards following a period of quiescence (Lindsay 2010, Needham et al. 2011).

1.7.3 Tephra fall in Auckland from distal eruptions

There are two main volcano types in the central North Island that may affect Auckland (Figure 1.5):

1. **Andesitic stratovolcanoes** including Taranaki, the Tongariro complex (including Ngauruhoe), Ruapehu and White Island. Eruptions at these volcanoes occur on average every 50 to 300 years from approximately the same vent area, and are typically characterized by a succession of small to moderate-sized eruptive episodes over a long period of time (weeks to months or even years) (Wilson et al. 1995, AELG 2001, Lindsay and Peace 2005).

2. **Rhyolitic calderas** including Taupo, Okataina, Rotorua and Mayor Island. Activity at caldera volcanoes is characterised by far less frequent (on average every 1,000 to 2,000 years) moderate to large-sized eruptions, which generate huge quantities of tephra (Lindsay and Peace 2005).

Tephra ejected from any of the vents can be distributed over areas extending many hundreds of kilometres. The extent and severity of tephra fall in Auckland will depend on wind directions and speeds during eruptive episodes, as well as the magnitude and duration of eruptions and eruption column height (Lindsay and Peace 2005, Shane 2007).

Drill coring at several sites in Auckland has revealed around 40 ash layers that have erupted over the past 27,000 years originating from five distal North Island volcanoes (Sandiford et al. 2001, Shane and Hoverd 2002, Shane 2005, Lindsay and Peace 2005, Molloy et al. 2009, Zawalna-Geer et al. 2016).

Molloy et al. (2009) determine the average fallout frequency of ash in Auckland from ~80,000 years of data. They found 52 Egmont events at one per 1.5 ka; 21 Taupo volcanic zone rhyolite (Okataina and Taupo) events at one per 3.8 ka; 24 AVF events at one per 3.5 ka; seven Tongariro events at one per 11.4 ka; and two Mayor Island events at one per 40 ka. More recently, Zawalna-Geer et al. (2016) analyse the combined macro- and crypto-tephra record from Pupuke sediment for the Holocene epoch. They determined that the Taupo Volcanic Centre is the most frequent contributor of tephra to Auckland (one event per ~1.3 ka), followed by Tongariro (one per ~2.2 ka), Okataina, Egmont and AVF (one each every ~3.0 ka) and Mayor Island (one tephra event in the Holocene). This suggests that Auckland has been inundated by tephra at least once every 424 years on average (Zawalna-Geer et al. 2016). Zwalana-Geer et al.'s (2016) fallout frequencies are likely more representative of current predominant wind directions and profiles than those reported by Molloy et al. (2009), although a less complete eruptive record was considered. Any calculated recurrence rates (and probabilities) must be considered with caution as not all eruptions will be preserved in the geologic ash record, and certainly not all eruptions will be represented by ash at specific coring sites. For example, the 1995-96 eruption of Ruapehu caused light ash fall, resulting in the closure of Auckland International Airport on 18 June 1996, but no record of ash fall was preserved from this particular eruption (Lindsay and Peace 2005).

1.7.4 Volcanic risk assessment for transportation in Auckland

Volcanic risk assessments are actively used to inform emergency management and planning in Auckland. For example, the Auckland Evacuation Plan (Auckland CDEM 2014) presents an all-hazards approach for conducting evacuations around, out of, and into Auckland, and the AVF Contingency Plan (Auckland CDEM 2015) sets out the planning arrangements specifically for the management of an eruption within the AVF. However, previous volcanic risk assessments for Auckland have largely focussed on building structures and loss of human life. In Magill and Blong's (2005) risk ranking for Auckland, tephra produces the highest risk by an order of magnitude in terms of physical infrastructure damage, followed by lava flows and pyroclastic surge. Pyroclastic surges with high dynamic pressures are seen to present the highest risk in terms of loss-of-life in the AVF (Magill and Blong 2005, Sherburn et al. 2007, Brand et al. 2014). Houghton et al. (2006) suggest that rapid cone growth during future eruptions will define a region of some 30 to 100 ha where complete destruction will occur. The cost of such destruction was calculated at between NZ$ 200 million and NZ$ 1.4 billion (Houghton et al. 2006). Magill et al. (2006) place the loss due to structural damage at NZ$ 1 billion at an average recurrence interval of around 35,000 years (taking the AVF and five other volcanic centres into consideration). The Auckland Lifelines Group (ALG) recognise that an eruption in the AVF is likely to have severe infrastructure impacts within a few kilometres from the eruption vent, stating that "ash will hamper movement on road networks, with particular issues for the movement of people for evacuation as well as access for lifelines to critical infrastructure for repairs and maintenance" (AELG 2014).

In Auckland, it is unlikely that volcanic ashfall alone will require large-scale evacuations. However, other hazards associated with the eruption, and coincident unrelated hazards such as storms, tsunami or fire, may require evacuations using transportation networks compromised by ash. As part of an initial risk assessment following a change in seismicity in the AVF, Auckland Civil Defence and

Emergency Management (CDEM) use radial distances from an identified vent zone to inform primary (0-3 km) and secondary (3-5 km) evacuation zones (Auckland CDEM 2015). Due to the lack of viable transportation alternatives, the primary method of evacuation over large distances in New Zealand is likely to be by road (Cole et al. 2005, Cole and Blumenthal 2004), particularly as many people have easy access to a vehicle. According to the most recent census data from March 2013, 92% of households in New Zealand have access to at least one motor vehicle (Statistics New Zealand 2015b). Recent modelling of the Auckland road network suggests evacuation clearance times of one to thirteen hours at best, based on evacuating a 5 km radius area in the central city and assuming no direct impacts to transportation infrastructure from volcanic hazards (Tomsen 2010, Baker and Cox 2014). With transportation networks affected by ashfall, evacuation and recovery efforts could be severely disrupted and damage to other critical infrastructure or cascading effects may slow the efforts further (Wilson et al. 2012). For example, many issues were encountered during the evacuation for Hurricane Katrina in 2005 when cars ran out of fuel or had other mechanical problems (Litman 2006). Besides evacuation, surface transportation will be required for emergency service access and maintenance / repair of key facilities and networks by critical infrastructure staff. Additionally, during recurring or prolonged eruptions in the AVF, or indeed ashfall from distal eruptions with potential repetitive effects due to ash remobilisation, normal societal activities may be conducted on compromised transportation networks. Therefore, it is crucial to improve risk assessments by better understanding the impacts of volcanic ash on such networks, particularly with regards to the topics outlined in Section 1.6.

1.8 Thesis Objectives

The fundamental goal of this thesis is to improve volcanic risk assessments through investigating and quantifying the impacts of volcanic ash on surface transportation; Auckland City is used as a case study throughout. Impacts on surface transportation have frequently been observed and reported following previous eruptions worldwide. However, information to date has been largely qualitative and there is currently a lack of quantitative empirical data to describe transportation functionality. The primary objectives of this thesis are to:

1. **Identify and address key unknown or uncertain consequences of volcanic ash impacts on surface transportation following a synthesis of existing information.**
   The initial objective involves the analysis of known consequences for surface transportation network damage and functionality during and after all volcanic hazards. Any gaps in knowledge that would likely aid the strengthening of transportation resilience when filled, will be addressed primarily through extensive laboratory experimentation, adopting novel approaches to investigate specific impact types.

2. **Improve existing thresholds for transportation functional loss (for ash thickness) and identify new thresholds for alternative hazard intensity metrics.**
   This will be achieved by applying the results of laboratory experiments and through considering new observations of volcanic ash impacts to transportation (objective 1). The

relative importance of hazard intensity metrics to surface transportation will also be considered.

3. **Assess the vulnerability of Auckland City's transportation infrastructure to volcanic hazards and consider international applicability.**
   Here, the research will focus on the vulnerability of transportation networks in Auckland to functionality disruption and damage as determined in objectives 1 and 2. This will be achieved through the development of a volcanic hazard scenario in the AVF that can be used to assess risk to multiple critical infrastructure types. Although all stakeholders will be considered, addressing end-user needs in particular will form an important part of this objective.

1.9 Thesis Structure and Declarations

The subsequent content of this thesis forms six core chapters comprising published scientific report content or submitted manuscripts to academic journals. One manuscript was published at the time of writing this thesis.

- Chapter 2 summarises key findings from post-eruption impact assessment studies conducted following the February 2014 eruption of Kelud volcano, Indonesia. The full findings, published as a GNS Science Report, can be found in Appendix A, but considerations for transportation have been extracted and compiled in Chapter 2 to address objective one and demonstrate the breadth of research undertaken. Three of the key impacts to surface transportation observed during eruptions such as Kelud, where volcanic ash deposits occur, are reduced skid resistance on paved surfaces, road marking coverage, and visibility impairment during the initial ashfall and re-suspended ash. These impacts, and investigation of associated hazard intensity thresholds, form the focus of the next three chapters in the thesis.

- Chapter 3 contains a version of a submitted manuscript that investigates the impact of volcanic ash on road and airfield surface skid resistance. An experimental approach, using the standardised British pendulum test, is adopted to test the skid resistance on paved surfaces covered by ash with a variety of characteristics. Recommendations for road safety and effective road cleaning techniques are also discussed.

- Chapter 4 comprises a version of a separate manuscript (recently published), which adopts another experimental approach, in this case with the addition of digital image analysis, to investigate road marking coverage by volcanic ash. Risk management measures are also suggested based on the key findings.

- Chapter 5 consists of a version of the third and final manuscript related to laboratory experimentation, on the topic of visibility in airborne volcanic ash. Here, a novel set-up is used to reproduce potential ash-settling rates and other characteristics for Auckland City to calculate expected visual ranges. Potential implications for surface transportation disruption are discussed, particularly in relation to transportation and emergency management planning.

- Chapter 6 illustrates how the findings of the laboratory experiments (outlined in Chapters 3-5) can be applied to improve volcanic ash fragility functions, thus fulfilling objective two of the thesis. The chapter comprises a submitted manuscript, which is heavily based on initial fragility functions that were recently developed for surface transportation (and other infrastructure), and which is outlined in Appendix D. Existing transportation fragility functions for volcanic ash thickness are refined in Chapter 6, and new fragility functions with ash-settling rate as the core measure of hazard intensity (based on the work in Chapter 5) are proposed. The chapter particularly highlights the importance of considering different hazard intensity metrics besides ash thickness when assessing disruption to surface transportation.

- The final core section of this thesis, Chapter 7, uses a scenario approach to provide insights for transportation network damage and functionality during volcanic eruptions, covering all volcanic hazards that could occur given an AVF eruption. This chapter is the second in a series of submitted manuscripts based on the hypothetical "Māngere Bridge" eruption in South Auckland, New Zealand. The first manuscript of the series outlines the geophysical hazard sequence of the scenario and is included in Appendix E1. The studies largely stem from initial work developed for both an internal workshop held by the EQC, and the Economics of Resilient Infrastructure (ERI) Programme. A published report on the latter is included in Appendix E2. A key component of Chapter 7 is the development of Level-of-Service (LoS) metrics that consider transportation network end-users, which highlight the importance of considering end-user needs in volcanic impact and risk assessments in the future. Interdependencies with transportation are briefly considered within. The work in this chapter successfully fulfils objective three of the thesis.

- The final chapter of the thesis (Chapter 8) concludes by summarising the key findings in relation to the original thesis aims. It also outlines recommendations for future work, which largely stem from the recent contributions to the discipline covered in this thesis.

The content of all chapters in this thesis directly result from my own research and studies. Co-authors made invaluable contributions and their associated inputs are declared in the signed co-authorship forms at the beginning of each chapter. Others who assisted with the work are acknowledged in the acknowledgement sections of the individual chapters. I am the co-author of Appendix D, E1 and E2, and am the lead author of all other appendices in this thesis including the GNS Science Report (Appendix A); my contribution to the content of each is outlined accordingly in signed co-authorship forms which accompany each Appendix.

1.10 References

AELG (2001) Volcanic ash review, part 1: impacts on lifelines services and collection/disposal issues, Auckland Regional Council Technical Publication 144, Auckland Engineering Lifelines Group, 50 p.

AELG (2014) Auckland Engineering Lifelines project: stage 2. Auckland Engineering Lifelines Group, Auckland, New Zealand.

Agustín-Flores, J. Németh, K. Cronin, S.J. Lindsay, J.M. Kereszturi, G., Brand, B.D., Smith, I.E.M. (2014) Phreatomagmatic eruptions through unconsolidated coastal plain sequences, Maungataketake, Auckland Volcanic Field (New Zealand). Journal of Volcanology and Geothermal Research, 276, 46–63.

Ajtai, N. Ştefănie, H.I. Stoian, L.C. Oprea, M.G. (2010) The volcanic ash and its impact on European air transport industry. A case study on the detection and impact of the Eyjafjallajökull volcanic ash plume over North-Western Europe between 14th and 21st April 2010, 2:1, pp.57–68.

Alexander, D. (2002) Natural Disasters. Routledge, London.

Allen, S.R. Smith, I.E.M. (1994) Eruption styles and volcanic hazard in the Auckland Volcanic Field, New Zealand. Geoscience Reports of Shizuoka University, 20, 5–14.

Auckland CDEM (2011) Auckland Civil Defence and Emergency Management Group Plan: 2011-2016. http://www.aucklandcivildefence.org.nz/media/45880/AC-0162-CDEM-Group-Plan_WEB.PDF, Auckland, New Zealand. Accessed 31 August 2016.

Auckland CDEM (2014) Auckland Evacuation Plan. http://www.aucklandcivildefence.org.nz/media/48200/BC3598-Auckland-Evacuation-Plan_WEB-spreads-.pdf, Auckland, New Zealand. Accessed 19 September 2016.

Auckland CDEM (2015) Auckland Volcanic Field Contingency Plan. http://www.aucklandcivildefence.org.nz/media/48896/2015-03-27-Auckland-Volcanic-Field-Contingency-Plan-Version-2-.pdf, Auckland, New Zealand. Accessed 19 September 2016.

Auckland Transport (2016a) Auckland Manukau Eastern Transport Initiative (AMETI). Auckland Transport. https://at.govt.nz/projects-roadworks/ameti/, Accessed 27 September 2016.

Auckland Transport (2016b) City Rail Link: project overview. Auckland Transport. https://at.govt.nz/projects-roadworks/city-rail-link/, Accessed 01 August 2016.

Auker, M.R. Sparks, R.S.J. Siebert, L. Crosweller, H.S. Ewert, J. (2013) A statistical analysis of the global historical volcanic fatalities record. Journal of Applied Volcanology, 2, pp.1-24.

Ayyub, B.M. (2014) Systems resilience for multihazard environments: definition, metrics, and valuation for decision making. Risk Analysis, 34:2, pp.340–55.

Bach, C. Gupta, A.K. Nair, S.S. Birkmann, J. (2013) Critical infrastructures and disaster risk reduction. New Delhi National Institute of Disaster Management and Deutsche Gesellschaft für Internationale Zusammernarbeit GmbH.

Baker, C. Cox, J. (2014) Modelling an emergency evacuation in Auckland. Presentation at Determining Volcanic Risk in Auckland Forum, November 2014 (given by Blake, D.M.), University of Auckland, Auckland, New Zealand.

Barker, K. Ramirez-Marquez, J.E. (2016) Infrastructure network resilience. IN: IRGC (2016) Resource guide on resilience. EPFL International Risk Governance Centre. V29-07-2016. http://www.irgc.org/risk-governance/resilience/, Accessed 20 September 2016.

Barnard, S. (2004) Results of a reconnaissance trip to Mt. Etna, Italy: the effects of the 2002 eruption of Etna on the province of Catania. Bulletin of the New Zealand Society for Earthquake Engineering, 37:2, pp.47–61.

Barnard, S.T. (2009) The vulnerability of New Zealand lifelines infrastructure to ashfall. PhD Thesis, Department of Geological Sciences, University of Canterbury, New Zealand.

Barsotti, S. Andronico, D. Neri, A. Del Carlo, P. Baxter, P. J. Aspinall, W. P. Hincks, T. (2010) Quantitative assessment of volcanic ash hazards for health and infrastructure at Mt. Etna (Italy) by numerical simulation. Journal of Volcanology and Geothermal Research, 192, pp.85–96.

Baxter, P.J. Boyle, R. Cole, P. Neri, A. Spence, R. Zuccaro, G. (2005) The impacts of pyroclastic surges on buildings at the eruption of the Soufrière Hills volcano, Montserrat. Bulletin of Volcanology, 67:4, pp.292–313.

BBK (2016) Kritische Infrastrukturen. Bundesamt für Bevölkerungsschutz und Katastrophenhilfe [Federal Office of Civil Protection and Disaster Assistance]. http://www.bbk.bund.de/DE/Home/home_node.html, Accessed 19 September 2016.

Bebbington, M. Cronin, S. (2010) Spatio-temporal hazard estimation in the Auckland Volcanic Field, New Zealand, with a new event-order model. Bulletin of Volcanology, pp.1–18.

Bellini, E. Nesi, P. Ferreira, P. (2016) Operationalize data-driven resilience in urban transport systems. IN: IRGC (2016) Resource guide on resilience. EPFL International Risk Governance Centre. V29-07-2016. http://www.irgc.org/risk-governance/resilience/, Accessed 20 September 2016.

Bilham, R. (2009) The seismic future of cities. Bulletin of Earthquake Engineering, 7:4, pp.839–87.

Blaikie, P.M. Cannon, T. Davis, I. Wisner, B. (2000) At risk: natural hazards, people's vulnerability and disasters. Routledge, London.

Blong, R.J. (1982) The time of darkness: local legends and volcanic reality in Papua New Guinea. Australian National University Press, Canberra, Australia, 257 p.

Blong, R.J. (1984) Volcanic hazards: a sourcebook on the effects of eruptions. Academic Press, Sydney, Australia, 424 p.

Bolic, T. Sivcev, Z. (2011) Eruption of Eyjafjallajökull in Iceland: experience of European air traffic management. Transportation Research Record, 2214, pp.136-143.

Bouchon, S. (2006) The Vulnerability of interdependent critical infrastructures systems : Epistemological and conceptual state-of-the-art. European Commission Directorate-General Joint Research Centre, Institute for the Protection and Security of the Citizen, Italy.

Boudon, G. Gourgaud, A. (1989) Mount Pelée. Journal of Volcanology and Geothermal Research. 38, pp.1-213.

Bruneau, M. Reinhorn, A. (2007) Exploring the concept of seismic resilience for acute care facilities. Earthquake Spectra, 23:1, pp.41–62.

Burby, R.J. Beatley, T. Berke, P.R. Deyle, R.E. French, S.P. Godschalk, D.R. Kaiser, E.J. Kartez, J.D. May, P.J. Olshansky, R. Paterson, R.G. Platt, R.H. (1999) Unleashing the power of planning in creating disaster-resilient communities. Journal of the American Planning Association, 65:3, pp.247–258.

CCC (2011) Christchurch earthquake response: liquefaction, frequently asked questions. Christchurch, New Zealand. http://canterburyearthquake.files.wordpress.com/2011/03/liquefaction-factsheet- 20110316.pdf, Accessed 12 December 2014.

Cccarto (2016) Volcanoes of the world. http://www.cccarto.com/, Accessed 30 September 2016.

Chang, S.E. McDaniels, T. Fox, J. Dhariwal, R. Longstaff, H. (2014) Toward disaster-resilient cities: characterizing resilience of infrastructure systems with expert judgments. Risk Analysis, 34:3, pp.416–34.

Choi, E. DesRoches, R. Nielson, B. (2004) Seismic fragility of typical bridges in moderate seismic zones. Engineering Structures, 26, pp.187-199.

Cole, J. Blumenthal, E. (2004) Evacuate! what an evacuation order given because of a pending volcanic eruption could mean to residents of the Bay of Plenty. Tephra, June 2004, Natural Hazards Research Centre, University of Canterbury.

Cole, J.W. Sabel, C.E. Blumenthal, E. Finnis, K. Dantas, A. Barnard, B. Johnston, D.M. (2005) GIS-based emergency and evacuation planning for volcanic hazards in New Zealand. Bulletin of the New Zealand Society for Earthquake Engineering. 38:2, pp.149-164.

Corwin, G. Foster, H.L. (1959) The 1957 explosive eruption on Iwo Jima, Volcano Islands. American Journal of Science, 257, pp.161–171.

Cova, T.J. Conger, S. (2003) Transportation hazards, IN: Kutz, M. (Ed.) Handbook of Transportation Engineering, McGraw-Hill Handbook.

Crichton, D. (1999) The risk triangle. IN: Ingleton, J. (Ed.) Natural Disaster Management. Tudor Rose, London.

Cronin, S.J. Hedley, M.J. Neall, V.E. Smith, G. (1998) Agronomic impact of tephra fallout from 1995 and 1996 Ruapehu volcano eruptions, New Zealand. Environmental Geology, 34, pp.21–30.

De la Cruz-Reyna, S. Yokoyama, I. (2011) A geophysical characterization of monogenetic volcanism. Geofisica Internacional, 50:4, pp.465–484.

De Sutter, R. Verhoeven, R. Krein, A. (2001) Simulation of sediment transport during flood events: laboratory work and field experiments. Hydrological Sciences Journal, 46:4.

DPMC (2011) New Zealand's National Security System. Department of the Prime Minister and Cabinet. http://www.dpmc.govt.nz/sites/all/files/publications/national-security-system.pdf, Wellington, New Zealand. Accessed 02 September 2016.

Drexler, J.M. Gledhill, A.D. Shinoda, K. Vasiliev, A.L. Reddy, K.M. Sampath, S. Padture, N.P. (2011) Jet engine coatings for resisting volcanic ash damage. Advanced Materials, 23:21, pp. 2419-2424.

Dunn, M.G. (2012) Operation of gas turbine engines in an environment contaminated with volcanic ash. Journal of Turbomachinery, 134:5.

Durand, M. Gordon, K. Johnston, D. Lorden, R. Poirot, T. Scott, J. Shephard, B. (2001) Impacts and responses to ashfall in Kagoshima from Sakurajima Volcano: lessons for New Zealand. GNS Science Report 2001/30, 53 p.

Edbrooke, S.W. Mazengarb, C. Stephenson, W. (2003) Geology and geological hazards of the Auckland urban area, New Zealand. Quaternary International, 103:1, pp.3–21.

Few, R. Barclay, J. (2011) Societal impacts of natural hazards: a review of international research funding. May 2011, UK Collaborative on Development Sciences, London, UK.

http://www.ukcds.org.uk/sites/default/files/content/resources/Disasters%20001%20SOCIETAL%20IMPACTS%20OF%20NATURAL%20HAZARDS%20130611final.pdf, Accessed 03 October 2016.

Fitzgerald, R.H. Kennedy, B.M. Wilson, T.M. Leonard, G.S. Tsunematsu, K. Keys, H. (2016) The communication and risk management of volcanic ballistic hazards. IN: Fearnley, C. Bird, D. Jolly, G. Haynes, K. McGuire, B. (Eds.) Observing the volcano world: volcano crisis communication. Advances in Volcanology. Springer International Publishing.

Fries, Jr. C. (1953) Volumes and weights of pyroclastic material, lava, and water erupted by Parícutin volcano, Michoacan, Mexico. Transactions – American Geophysical Union, 34, pp.603-616.

Garbin, D.A. Shortle, J.F. (2007) Measuring resilience in network-based infrastructures. IN: McCarthy, J.A. (Ed.) Critical thinking: moving from infrastructure protection to infrastructure resiliency. George Mason University, Virginia, U.S.

GFDRR (2014) Understanding risk in an evolving world: emerging best practices in natural disaster risk assessment. Global Facility for Disaster Reduction and Recovery, The World Bank, Washington. https://www.gfdrr.org/sites/gfdrr/files/publication/Understanding_Risk-Web_Version-rev_1.8.0.pdf, Accessed 23 September 2016.

GFDRR (2016a) Solving the puzzle: innovating to reduce disaster risk. Global Facility for Disaster Reduction and Recovery, The World Bank, Washington. https://www.gfdrr.org/solving-the-puzzle-report, Accessed 27 September 2016.

GFDRR (2016b) Managing disaster risk for a resilient future: a work plan for the Global Facility for Disaster Reduction and Recovery, 2016-2018. Global Facility for Disaster Reduction and Recovery, The World Bank, Washington. https://www.gfdrr.org/sites/default/files/publication/GFDRR_Work_Plan_2016-18.pdf, Accessed 21 September 2016.

Giovinazzi, S. Wilson, T. Davis, C. Bristow, D. Gallagher, M. Schofield, A. Tang, A. (2011) Lifelines performance and management following the 22 February 2011 Christchurch earthquake, New Zealand: highlights of resilience. Bulletin of the New Zealand Society for Earthquake Engineering, 44:4, pp.402–417.

Gislason, S.R. Hassenkam, T. Nedel, S. Bovet, N. Eiriksdottir, E.S. Alfredsson, H.A. Hem, C.P. Balogh, Z.I. Dideriksen, K. Oskarsson, N. Sigfusson, B. Larsen, G. Stipp, S.L.S. (2011) Characterization of Eyjafjallajökull volcanic ash particles and a protocol for rapid risk assessment. Proceedings of the National Academy of Sciences of the United States of America, 108:18, pp.7307–12.

Godschalk, D.R. (2002) Urban hazard mitigation: creating resilient cities. Urban Hazards Forum, January 2002, John Jay College, City University of New York.

Gordon, P. Richardson, H.W. Davis, B. (1998) Transport-related impacts of the Northridge earthquake. Journal of Transportation and Statistics, 1:2, pp.21–36.

Guffanti, M. Mayberry, G.C. Casadevall, T.J. Wanderman, R. (2009) Volcanic hazards to airports. Natural Hazards, 51, pp.287-302.

Hampton, S.J. Cole, J.W. Wilson, G. Wilson, T.M. Broom, S. (2015) Volcanic ashfall accumulation and loading on gutters and pitched roofs from laboratory empirical experiments: Implications for risk assessment. Journal of Volcanology and Geothermal Research, 304, pp.237–252.

Harris, S. (2014) On-board device helps prevent volcanic ash damage to aircraft. The Engineer, October 2014. http://www.theengineer.co.uk/aerospace/news/on-board-device-helps-prevent-volcanic-ash-damage-to-aircraft/1019299.article, Accessed 27 September 2016.

Hayes, J. L. Wilson, T. M. Magill, C. (2015) Tephra fall clean-up in urban environments. Journal of Volcanology and Geothermal Research, 304, pp.359–377.

Hopkins, J.L. Millet, M.-A. Timm, C. Wilson, C.J.N. Leonard, G.S. Palin, J.M. Neil, H. (2015) Tools and techniques for developing tephra stratigraphies in lake cores: a case study from the basaltic Auckland Volcanic Field, New Zealand. Quaternary Science Reviews, 123, pp.58–75.

Horspool, N.A. Savage, M.K. Bannister, S. (2006) Implications for intraplate volcanism and back-arc deformation in northwestern New Zealand, from joint inversion of receiver functions and surface waves. Geophysical Journal International, 166, pp.1466–1483.

Horwell, C.J. Baxter, P.J. (2006) The respiratory health hazards of volcanic ash: a review for volcanic risk mitigation. Bulletin of Volcanology, 69:1, pp.1–24.

Houghton, B.F. Wilson, C.J.N. Rosenberg, M.D. Smith, I.E.M. Parker, R.J. (1996) Mixed deposits of complex magmatic and phreatomagmatic volcanism: an example from Crater Hill, Auckland, New Zealand. Bulletin of Volcanology, 58, pp.59–66.

Houghton, B.F. Wilson, C.J.N. Smith, I.E.M. (1999) Shallow-seated controls on styles of explosive basaltic volcanism: a case study from New Zealand. Journal of Volcanology and Geothermal Research, 91:1–2, pp.97–120.

Houghton, B.F. Bonadonna, C. Gregg, C.E. Johnston, D.M. Cousins, W.J. Cole, J.W. Del Carlo, P. (2006) Proximal tephra hazards: recent eruption studies applied to volcanic risk in the Auckland volcanic field, New Zealand. Journal of Volcanology and Geothermal Research, 155, pp.138–149.

Hughes, J.F. Healy, K. (2014) Measuring the resilience of transport infrastructure, February 2014. New Zealand Transport Agency Research Report 546, Wellington, New Zealand, 82 p.

Hurst, A.W. Smith, W.D. (2010) Volcanic ashfall in New Zealand: probabilistic hazard modelling for multiple sources. New Zealand Journal of Geology and Geophysics, 53, pp.1–14.

ICAO (2001) Manual on volcanic ash, radioactive material and toxic chemical clouds. International Civil Aviation Organisation. http://www3.alpa.org/portals/alpa/volcanicash/12_Doc9691ManualICAOVolAshRadioactiveMaterial.pdf, Accessed 16 June 2016.

ICAO (2012) Flight safety and volcanic ash: risk management of flight operations with known or forecast volcanic ash contamination. International Civil Aviation Organisation. http://www.icao.int/publications/Documents/9974_en.pdf, Accessed 16 June 2016.

IRGC (2006) White paper on risk governance: towards an integrative approach. International Risk Governance Council, Geneva, Switzerland.

Jackson, B.M. Wheater, H.S. Mcintyre, N.R. Chell, J. Francis, O.J. Frogbrook, Z. Marshall, M. Reynolds, B. Solloway, I. (2008) The impact of upland land management on flooding: insights from a multiscale experimental and modelling programme. Journal of Flood Risk Management, 1:2, pp.71-80.

Jenkins, S. Magill, C. McAneney, J. Blong, R. (2012) Regional ash fall hazard I: a probabilistic assessment methodology. Bulletin of Volcanology, 74:7, pp.1699-1712.

Jenkins, S. Komorowski, J.-C. Baxter, P.J. Spence, R. Picquout, A. Lavigne, F. (2013) The Merapi 2010 eruption: An interdisciplinary impact assessment methodology for studying pyroclastic density current dynamics. Journal of Volcanology and Geothermal Research, 261, pp.316–329.

Jenkins, S.F. Spence, R.J.S. Fonseca, J.F.B.D. Solidum, R.U. Wilson, T.M. (2014a) Volcanic risk assessment: quantifying physical vulnerability in the built environment. Journal of Volcanology and Geothermal Research, 276, pp.105-120.

Jenkins, S.F. Wilson, T.M. Magill, C.R. Miller, V. Stewart, C. (2014b) Volcanic ash fall hazard and risk. Technical background paper for the UN-ISDR Global Assessment Report on Disaster Risk Reduction, May 2014, Global Assessment Report on Disaster Risk Reduction, Global Volcano Model and IAVCEI. www.preventionweb.net/english/hyogo/gar, Accessed 03 October 2016.

Johnston, D.M. (1997) Physical and social impacts of past and future volcanic eruptions in New Zealand. PhD Thesis. Earth Science, Massey University, Palmerston North, New Zealand.

Johnston, D.M. Neall, V.E. (1995) Ruapehu awakens: the 1945 eruption of Ruapehu. The Science Centre and Manawatu Museum Scientific Monograph, 1, 28 p.

Johnston, D.M. Houghton, B.F. Neall, V.E. Ronan, K.R. Paton, D. (2000) Impacts of the 1945 and 1995–1996 Ruapehu eruptions, New Zealand: an example of increasing societal vulnerability. Geological Society of America Bulletin, 112, pp.720–726.

Jolly, A.D. Cronin, S.J. (2014) From eruption to end-user; bridging the science-mangement interface during the 2012 Te Maari eruption, Tongariro Volcano, New Zealand. Journal of Volcanology and Geothermal Research, 286, 183p.

Kadri, F. Birregah, B.C. Châtelet, E. (2014) The impact of natural disasters on critical infrastructures: a domino effect-based study. Journal of Homeland Security and Emergency Management, 11:2, pp.217-241.

Kereszturi, G. Németh, K. Cronin, S.J. Agustín-Flores, J. Smith, I.E.M. Lindsay, J. (2013) A model for calculating eruptive volumes for monogenetic volcanoes - implication for the Quaternary Auckland Volcanic Field, New Zealand. Journal of Volcanology and Geothermal Research, 266, pp.16–33.

Kereszturi, G. Németh, K. Cronin, S.J. Procter, J. Agustín-Flores, J. (2014) Influences on the variability of eruption sequences and style transitions in the Auckland Volcanic Field, New Zealand. Journal of Volcanology and Geothermal Research, 286, pp.101–115.

Kermode, L.O. (1992) Geology of the Auckland Urban Area. Institute of Geological & Nuclear Sciences Geological Map and Booklet. Lower Hutt, New Zealand, 63 p.

Lalonde, C. Boiral, O. (2012) Managing risks through ISO 31000: a critical analysis. Risk Management, 14:4, pp.272-300.

Langmann, B. (2013) Volcanic ash versus mineral dust: atmospheric processing and environmental and climate impacts. Atmospheric Sciences. Hindawi Publishing Corporation. https://www.hindawi.com/journals/isrn/2013/245076/, Accessed 30 August 2014.

Le Corvec, N. Bebbington, M.S. Lindsay, J.M. McGee, L.E. (2013) Age, distance, and geochemical evolution within a monogenetic volcanic field: analysing patterns in the Auckland Volcanic Field eruption sequence. Geochemistry, Geophysics, Geosystems, 14:9, pp.3648–3665.

Leonard, G.S. Johnston, D.M. Williams, S. Cole, J.W. Finnis, K. Barnard, S. (2006) Impacts and management of recent volcanic eruptions in Ecuador: lessons for New Zealand. GNS Science Report 2005/20, 52p.

Leonard, G.S. Stewart, C. Wilson, T.M. Procter, J.N. Scott, B.J. Keys, H.J. Jolly, G.E. Wardman, J.B. Cronin, S.J. McBride, S.K. (2014) Integrating multidisciplinary science, modelling and impact data into evolving, syn-event volcanic hazard mapping and communication: a case study from the 2012 Tongariro eruption crisis, New Zealand. Journal of Volcanology and Geothermal Research, 286, pp.208–232.

Linkov, I. Trump, B.D. Fox-Lent, C. (2016) Resilience: approaches to risk analysis and governance. IN: IRGC (2016) Resource guide on resilience. EPFL International Risk Governance Centre. V29-07-2016. http://www.irgc.org/risk-governance/resilience/, Accessed 20 September 2016.

Lindsay, J.M. (2010) Volcanoes in the big smoke: A review of hazard and risk in the Auckland Volcanic Field. IN: Williams, A.L. Pinches, G.M. Chin, C.Y. McMorran, T.Y. Massey, C.I. (Eds.) Geologically Active. Taylor and Francis Group, London.

Lindsay, J. M. Peace, C. (2005) Project AELG-7: health and safety issues in a volcanic ash environment. Auckland Regional Council Technical Publication 290, Auckland Engineering Lifelines Group, 55 p.

Lindsay, J. M. Leonard, G. (2009) Age of the Auckland Volcanic Field. IESE Report 1-2009.02, June 2009, Institute of Earth Science and Engineering, Auckland, New Zealand.

Lindsay, J.M. Leonard, G.S. Smid, E.R. Hayward, B.W. (2011) Age of the Auckland Volcanic Field : a review of existing data. New Zealand Journal of Geology & Geophysics, 54:4, pp.379–401.

Linnell, T. Shane, P. Smith, I. Augustinus, P. Cronin, S. Lindsay, J. Maas, R. (2016) Long-lived shield volcanism within a monogenetic basaltic field: the conundrum of Rangitoto volcano, New Zealand. Geological Society of America Bulletin, B31392.1.

Litman, T. (2006) Lessons from Katrina and Rita: what major disasters can teach transportation planners. Journal of Transportation Engineering, 132, pp.11–18.

Lloyds City Risk Index (2015) Lloyds City Risk Index 2015-2025: Auckland, New Zealand. http://www.lloyds.com/cityriskindex/locations/fact_sheet/auckland. Accessed 31 August 2016.

Loughlin, S.C. Sparks, S. Brown, S.K. Jenkins, S.F. Vye-Brown, C. (2015) Global Volcanic Hazards and Risk. Global Volcano Model Network. http://globalvolcanomodel.org/wp-content/uploads/2015/08/Global-Volcanic-Hazards-and-Risk-Full-book-low-res.pdf, Accessed 19 September 2016.

Luhr, J.F. Simkin, T. (1993) Parícutin: the volcano born in a Mexican cornfield. Smithsonian Institution, Geoscience Press, Arizona, U.S.A.

Magill, C. Blong, R. (2005). Volcanic risk ranking for Auckland, New Zealand. II: hazard consequences and risk calculation. Bulletin of Volcanology, 67, pp.340-349.

Magill, C.R. Hurst, A.W. Hunter, L.J. Blong, R.J. (2006) Probabilistic tephra fall simulation for the Auckland Region, New Zealand. Journal of Volcanology and Geothermal Research. 153, pp.370–386.

Magill, C. Wilson, T. Okada, T. (2013) Observations of tephra fall impacts from the 2011 Shinmoedake eruption, Japan. Earths Planets and Space, 65, pp.677-698.

Maqsood, T. Wehner, M. Ryu, H. Edwards, M. Dale, K. Miller, V. (2014) GAR15 regional vulnerability functions. Reporting on the UNISDR/GA SE Asian Regional Workshop on Structural Vulnerability Models for the GAR Global Risk Assessment. 11-14 November 2013, Geoscience Australia Record 2014/38, 614p.

McGee, L.E. Millet, M-A. Smith, I.E.M. Németh, K. Lindsay, J.M. (2012) The inception and progression of melting in a monogenetic eruption: Motukorea Volcano, the Auckland Volcanic Field, New Zealand. Lithos, 155, pp.360–374.

Mehrabi, A. Benson Shing, P. Schuller, M. Noland, J. (1996) Experimental evaluation of masonry-infilled RC frames. Journal of Structural Engineering, 122:3, pp.228-237.

Merz, B. Elmer, F. Theiken, A.H. (2009) Significance of high probability/low damage versus low probability/high damage flood events. Natural Hazards and Earth System Science, 9:3, pp.1033-1046.

Mileti, D.S. (1999) Disasters by design: a reassessment of natural hazards in the US. National Academy Press, Washington DC.

Molloy, C. Shane, P. Augustinus, P. (2009) Eruption recurrence rates in a basaltic volcanic field based on tephra layers in maar sediments: implications for hazards in the Auckland volcanic field. Geological Society of America Bulletin, 121:11-12, pp.1666–1677.

Moteff, J. Copeland, C. Fischer, J. (2003) Critical infrastructures: what makes an infrastructure critical, Report for Congress, 29 January 2003, The Library of Congress, U.S.A.

Nakada, S. (1999) Overview of the 1990 – 1995 eruption at Unzen Volcano. Journal of Volcanology and Geothermal Research, 89, pp.1–22.

Nairn, I.A. (2002) The effects of volcanic ash fall (tephra) on road and airport surfaces. GNS Science Report 2002/13, 32p.

NAS (2012) Disaster resilience: a national imperative. Committee on Increasing National Resilience to Hazards and Disasters, Committee on Science, Engineering, and Public Policy, The National Academy of Sciences. The National Academies Press, Washington D.C.

Needham, A.J. Lindsay, J.M. Smith, I.E.M. Augustinus, P. Shane, P.A. (2011) Sequential eruption of alkaline and sub-alkaline magmas from a small monogenetic volcano in the Auckland Volcanic Field, New Zealand. Journal of Volcanology and Geothermal Research, 201:1–4, pp.126–142.

Németh, K. Cronin, S.J. Smith, I.E.M. Agustin Flores, J. (2012) Amplified hazard of small-volume monogenetic eruptions due to environmental controls, Orakei Basin, Auckland Volcanic Field, New Zealand. Bulletin of Volcanology, pp.1–17.

NIU (2014) Infrastructure update: occasional newsletter from the National Infrastructure Unit, Issue 16, October 2014. National Infrastructure Unit, The Treasury, Wellington, New Zealand. http://www.infrastructure.govt.nz/plan/newsletters/pdfs/niu-news-2014-16.pdf, Accessed 19 September 2016.

NIU (2015) The Thirty Year New Zealand Infrastructure Plan 2015. National Infrastructure Unit, The Treasury, Wellington, New Zealand. http://www.infrastructure.govt.nz/plan/2015/nip-aug15.pdf, Accessed 19 September 2016.

Nordpil (2010) World database of large urban area, 1950-2050: version 1.1, 01 March 2010. https://nordpil.com/resources/world-database-of-large-cities/, Accessed 30 September 2016.

NZTA (2016) Waterview Connection: project overview. New Zealand Transport Agency. http://www.nzta.govt.nz/projects/the-western-ring-route/waterview-connection/, Accessed 01 August 2016.

Opdenakker, R. (2006) Advantages and disadvantages of four interview techniques in qualitative research. Qualitative Social Research, 7:4, September 2006.

Oppenheimer, C. (2003) Climatic, environmental and human consequences of the largest known historic eruption: Tambora volcano (Indonesia) 1815. Progress in Physical Geography. 27:2, pp.230–259.

Opus (2007) Project AELG-3; Auckland engineering lifelines, assessment of infrastructure hotspots in the Auckland region. Opus International Consultants Ltd., Auckland Engineering Lifelines Group, Auckland, New Zealand.

Palma-Oliveira, J.M. Trump, B.D. (2016) Modern resilience: moving without movement. IN: IRGC (2016) Resource guide on resilience. EPFL International Risk Governance Centre. V29-07-2016. http://www.irgc.org/risk-governance/resilience/, Accessed 20 September 2016.

Park, J.T. Seager, P. Rao, P.S.C. Convertino, M. Linkov, I. (2013) Integrating risk and resilience approaches to catastophe management in engineering systems. Risk Analysis, 33:3, pp.356-367.

Petrazzuoli, S.M. Zuccaro, G. (2004) Structural resistance of reinforced concrete buildings under pyroclastic flows: a study of the Vesuvian area. Journal of Volcanology and Geothermal Research, 133:1–4, pp.353–367.

Prata, F. Rose, B. (2015) Volcanic ash hazards to aviation, IN: Sigurdsson, H. Houghton, B. McNutt, S. Rymer, H. Stix, J. (Eds.) The Encyclopedia of Volcanoes, 2nd Edition. Academic Press, Amsterdam, pp.911–934.

Ragona, M. Hannstein, F. Mazzocchi, M. (2011) The impact of volcanic ash crisis on the European airline industry. IN: Alemannio, A. (Ed.) Governing disasters: the challenges of emergency risk regulations. Edward Elgar Publishing.

Ricles, J.M. Sause, R. Peng, S.W. Lu, L.W. (2002) Experimental evaluation of earthquake resistant posttensioned steel connections. Journal of Structural Engineering, 128:7, pp.850-859.

Rinaldi, B.S.M. Peerenboom, J.P. Kelly, T.K. (2001) Complex networks: identifying, understanding, and analyzing critical infrastructure interdependencies. IEEE Control Systems Magazine, U.S.A., December 2001, pp11–25.

Rossetto, T. Ioannou, I. Grant, D.N. (2013) Existing empirical vulnerability and fragility functions: compendium and guide for selection. GEM Technical Report 2013-X, GEM Foundation, Pavia, Italy.

Rowland, S.K. Jurado-Chichay, Z. Ernst, G. Walker, G.P.L. (2009) Pyroclastic deposits and lava flows from the 1759-1774 eruption of El Jorullo, México: aspects of “violent Strombolian” activity and comparison with Parícutin. Special Publications of IAVCEI, 2, pp.105–128.

Sandiford, A. Alloway, B.V. Shane, P. (2001) A 28,000–6,600 cal yr record of local and distal volcanism preserved in a paleolake, Auckland, New Zealand. New Zealand Journal of Geology and Geophysics, 44:2, pp.323–336.

Scarth, A. (1994) Volcanoes: an introduction. UCL Press, University College London, London, UK.

Seville, E. Giovinazzi, S. Stevenson, J. Vargo, J. Brown, C. (2014) Disruption and resilience: how organisations coped with the Canterbury earthquakes. ERI Research Report 2014/002, December 2014, 28p.

Sherburn, S. Scott, B.J. Olsen, J. Miller, C. (2007) Monitoring seismic precursors to an eruption from the Auckland Volcanic Field, New Zealand. New Zealand Journal of Geology and Geophysics, 50, pp.1–11.

Shane, P. (2005) Towards a comprehensive distal andesitic tephrostratigraphic framework for New Zealand based on eruptions from Egmont volcano. Journal of Quaternary Science, 20, pp.45–57.

Shane, P. (2007) Comment on: Probabilistic tephra fall simulation for the Auckland region, New Zealand by Magill et al. (2006). Journal of Volcanology and Geothermal Research, 159, pp.421–422.

Shane, P. Hoverd, J. (2002) Distal record of multi-sourced tephra in Onepoto Basin, Auckland, New Zealand: implications for volcanic chronology, frequency and hazards. Bulletin of Volcanology, 64:7, pp.441–454.

Shane, P. Sandiford, A. (2003) Paleovegetation of marine isotope stages 4 and 3 in northern New Zealand and the age of the widespread Rotoehu Tephra. Quaternary Research, 59, pp.420–429.

Shane, P. Gehrels, M. Zawalna-Geer, A. Augustinus, P. Lindsay, J. Chaillou, I. (2013) Longevity of a small shield volcano revealed by crypto-tephra studies (Rangitoto volcano, New Zealand): Change in eruptive behavior of a basaltic field. Journal of Volcanology and Geothermal Research, 257, pp.174–183.

Singhal, A. Kiremidjian, A.S. (1996) Method for probabilistic evaluation of seismic structural damage. Journal of Structural Engineering, 122, pp.1459–1467.

Sims, B. (1999) Testing in an earthquake-engineering laboratory. Social Studies of Science, 29:4, pp.483-518.

Smith, I.E.M. Allen, S.R. (1993) Volcanic hazards at the Auckland volcanic field. Volcanic hazards information series. Ministry of Civil Defence and Emergency Management, Wellington, 5, 34p.

Spargo, S.R. Smith, I.E. Wilson, C.J. (2007) How 'monogenetic' is the Auckland Volcanic Field? Eos Transactions AGU, 88:23.

Stammers, S.A.A. (2000) The effects of major eruptions of Mt Pinatubo, Philippines and Rabaul Caldera, Papua New Guinea, and the subsequent social disruption and urban recovery: lessons for the future. University of Canterbury, New Zealand.

Statistics New Zealand (2015a) Subnational population estimates. http://nzdotstat.stats.govt.nz/wbos/Index.aspx?DataSetCode=TABLECODE7502. Accessed 31 August 2016.

Statistics New Zealand (2015b) 2013 Census quickstats about transport and communications. http://www.stats.govt.nz/Census/2013-census/profile-and-summary-reports/quickstats-transport-comms/number-motor-vehicles.aspx Accessed 19 September 2016.

Stergiou, E.C. Kiremidjian, A.S. (2010) Risk assessment of transportation systems with network functionality losses. Structure and Infrastructure Engineering, 6:1–2, pp.111–125.

Stewart, C. Horwell, C. Plumlee, G. Cronin, S. Delmelle, P. Baxter, P. Calkins, J. Damby, D. Mormon, S. Oppenheimer, C. (2013) Protocol for analysis of volcanic ash samples for assessment of hazards from leachable elements. IAVCEI, IVHHN, Cities on Volcanoes Commission, USGS, GNS Science.

Stewart, C. Wilson, T.M. Sword-Daniels, V. Wallace, K. Magill, C. Horwell, C.J. Leonard, G.S. Baxter, P.J. (2016) Communication demands of volcanic ashfall events. IN: Fearnley, C. Bird, D. Jolly, G. Haynes, K. McGuire, B. (Eds.) Observing the volcano world: volcano crisis communication. Advances in Volcanology. Springer International Publishing.

Sword-Daniels, V. Stewart, C. Johnston, D. Wardman, J. Wilson, T. Rossetto, T. (2011) Infrastructure impacts, management and adaptations to eruptions at Volcán Tungurahua, Ecuador, 1999-2010. GNS Science Report 2011/24, 73 p.

Sword-Daniels, V.L. Rossetto, T. Wilson, T.M. Sargeant, S. (2015) Interdependence and dynamics of essential services in an extensive risk context: a case study in Montserrat, West Indies. Natural Hazards Earth Systems Science, 15, pp.947-961.

Tamaki, T. Tatano, H. (2014) Evaluation method of restoration process for road networks after volcanic eruption. IEEE International Conference on Systems, Man and Cybernetics, October 5-8, 2014. San Diego, U.S.A., pp.2693–2698.

Tarbotton, C. Dall'Osso, F. Dominey-Howes, D. Goff, J. (2015) The use of empirical vulnerability functions to assess the response of buildings to tsunami impact: comparative review and summary of best practice. Earth-Science Reviews, 142, pp.120-134.

Tierney, K. Bruneau, M. (2007) Conceptualizing and measuring resilience. Transportation Research News, May-June 2007, 250, pp.14–17. http://onlinepubs.trb.org/onlinepubs/trnews/trnews250_p14-17.pdf, Accessed 03 October 2016.

Tomsen, E. (2010) GIS-based mass evacuation planning for the Auckland Volcanic Field. Masters Thesis, Department of Geography, The University of Auckland, Auckland, New Zealand.

Tomsen, E. Lindsay, J. Gahegan, M. Wilson, T. Blake, D.M. (2014) Auckland Volcanic Field evacuation planning: a spatio-temporal approach for emergency management and transportation network decisions. Journal of Applied Volcanology, 3:6.

UN (2016) Population division. Department of Economic and Social Affairs, United Nations. http://www.un.org/en/development/desa/population/, Accessed 01 October 2016.

UN (2014) World urbanization prospects: the 2014 revision. Department of Economic and Social Affairs, United Nations, New York, USA. https://esa.un.org/unpd/wup/Publications/Files/WUP2014-Highlights.pdf, Accessed 22 September 2016.

UNDP (2010) Disaster risk assessment. Bureau for Crisis Prevention and Recovery, United Nations Development Programme, New York, USA. www.undp.org/cpr/we_do/disaster_global_risk_id.shtml, Accessed 20 September 2016.

UN-EHS (2016) World Risk Report 2016. Bündnis Entwicklung Hilft and Institute for Environment and Human Security, United Nations University. http://collections.unu.edu/view/UNU:5763#viewAttachments, Accessed 17 September 2016.

UNISDR (2004) Living with risk: a global review of disaster reduction initiatives. United Nations International Strategy for Disaster Reduction, Geneva, Switzerland, 429 p. http://www.unisdr.org/we/inform/publications/657, Accessed 10 September 2016.

UNISDR (2009) UNISDR terminology on disaster risk reduction. United Nations International Strategy for Disaster Reduction, Geneva, Switzerland. http://www.unisdr.org/files/7817_UNISDRTerminologyEnglish.pdf, Accessed 21 April 2016.

UNISDR (2015) Sendai Framework for Disaster Risk Reduction (2015-2030). United Nations International Strategy for Disaster Reduction, Geneva, Switzerland. http://www.unisdr.org/we/coordinate/sendai-framework, Accessed 15 June 2016.

USGS (2010) What are volcano hazards? U.S. Geological Survey Fact Sheet 002-97. August 2010. http://pubs.usgs.gov/fs/fs002-97/, Accessed 01 October 2016.

Vugrin, E.D. (2016) Critical infrastructure resilience. IN: IRGC (2016) Resource guide on resilience. EPFL International Risk Governance Centre. V29-07-2016. http://www.irgc.org/risk-governance/resilience/, Accessed 20 September 2016.

Wardman, J.B. Wilson, T.M. Bodger, P.S. Cole, J.W. Johnston, D.M. (2012a) Investigating the electrical conductivity of volcanic ash and its effect on HV power systems. Physics and Chemistry of the Earth, 45–46, pp.128–145.

Wardman, J. Sword-Daniels, V. Stewart, C. Wilson, T. (2012b) Impact assessment of the May 2010 eruption of Pacaya volcano, Guatemala. GNS Science Report 2012/09, 90p.

Warrick, R.A. (1981). Four communities under ash. Institute of Behavioural Science, University of Colorado, Boulder, U.S.

Weber, K. Eliasson, J. Vogel, A. Fischer, C. Pohl, T. van Haren, G. Meier, M. Grobéty, B. Dahmann, D. (2012) Airborne in-situ investigations of the Eyjafjallajökull volcanic ash plume on Iceland and over north-western Germany with light aircrafts and optical particle counters. Atmospheric Environment, 48, pp.9–21.

Weber, K. Fischer, C. Vogel, A. Pohl, T. Böhlke, C. (2013). First results of an airborne release of volcanic ash for testing of volcanic ash plume measurement instruments. Proceedings of Energy and Environment, pp.169-172.

White House (2013). Presidential Policy Directive 21 – critical infrastructure security and resilience. Office of the Press Secretary. The White House, Washington, DC.

Wilson, C.J.N. Houghton, B.F. McWilliams, M.O. Lanphere, M.A. Weaver, S.D. Briggs, R.M. (1995) Volcanic and structural evolution of the Taupo Volcanic Zone, New Zealand: a review. Journal of Volcanology and Geothermal Research, 68, pp.1-28.

Wilson, G. Wilson, T.M. Deligne, N.I. Cole, J.W. (2014) Volcanic hazard impacts to critical infrastructure: a review. Journal of Volcanology and Geothermal Research, 286, pp.148–182.

Wilson, G. (2015) Vulnerability of critical infrastructure to volcanic hazards. PhD Thesis. Hazards and Disaster Management, Department of Geological Sciences, University of Canterbury, Christchurch, New Zealand.

Wilson, T. Kaye, G. Stewart, C. Cole, J. (2007) Impacts of the 2006 eruption of Merapi volcano, Indonesia, on agriculture and infrastructure. GNS Science Report 2007/07, 69 p.

Wilson, T. M. Daly, M. Johnston, D. (2009) Project AELG-19: Review of impacts of volcanic ash on electricity distribution systems, broadcasting and communication networks. Auckland Regional Council Technical Report 51, Auckland Engineering Lifelines Group, Auckland, New Zealand.

Wilson, T.W. Stewart, C. Cole, J.W. Dewar, D.J. Johnston, D.M. Cronin, S.J. (2011) The 1991 eruption of Volcán Hudson, Chile: impacts on agriculture and rural communities and long-term recovery. GNS Science Report 2009/66, 99 p.

Wilson, T.M. Stewart, C. Sword-Daniels, V. Leonard, G.S. Johnston, D.M. Cole, J.W. Wardman, J. Wilson, G. Barnard, S. (2012) Volcanic ash impacts on critical infrastructure. Physics and Chemistry of the Earth, 45–46, pp.5–23.

Wilson, T. Outes, V. Stewart, C. Villarosa, G. Bickerton, H. Rovere, E. Baxter, P. (2013) Impacts of the June 2011 Puyehue-Cordón Caulle volcanic complex eruption on urban infrastructure , agriculture and public health. GNS Science Report 2012/20, 88 p.

Wohletz, K.H. (1983) Mechanisms of hydrovolcanic pyroclast formation: grain-size, scanning electron microscopy, and experimental studies. Journal of Volcanology and Geothermal Research, 17, pp.31–63.

Woo, G. (2008) Probabilistic criteria for volcano evacuation decisions. Natural Hazards, 45, pp.87-97.

World Bank and GFDRR (2013) Building resilience: integrating climate and disaster risk into development. The World Bank, Global Facility for Disaster Reduction and Recovery. http://documents.worldbank.org/curated/en/762871468148506173/pdf/826480WP0v10Bu0130Box37986200OUO090.pdf, Accessed 25 August 2016.

World Bank (2015) Disaster risk management in the transport sector: a review of concepts and international case studies, June 2015. The World Bank Group. http://documents.worldbank.org/curated/en/524081468188378328/pdf/98202-WP-P126896-Box391506B-PUBLIC-DRM-Final.pdf, Accessed 19 September 2016.

Zawalna-Geer, A. (2016). Towards a tephra framework for the Auckland maar lake sediments and the potential of applying cryptotephra techniques. PhD Thesis, Geology, The University of Auckland, Auckland, New Zealand.

Zorn, E. Walter, T.R. (2016) Influence of volcanic tephra on photovoltaic (PV)-modules: an experimental study with application to the 2010 Eyjafjallajökull eruption, Iceland. Journal of Applied Volcanology, 5:2, pp.1-14.

Zuccaro, G. Cacace, F. Spence, R.J.S. Baxter, P.J. (2008) Impact of explosive eruption scenarios at Vesuvius. Journal of Volcanology and Geothermal Research, 178:3, 416-453.

Zuccaro, G. Gregorio, D. (2013) Time and space dependency in impact damage evaluation of a sub-Plinian eruption at Mount Vesuvius. Natural Hazards, 68:3, 1399–1423.

2. THE 2014 ERUPTION OF KELUD VOLCANO, INDONESIA: TRANSPORTATION IMPACTS AND IMPLICATIONS FOR RISK ASSESSMENT

2.1 Abstract

The February 2014 eruption of Kelud volcano in East Java, Indonesia, produced multiple and extensive impacts to critical infrastructure including transportation networks. It provided opportunities to increase the understanding of critical infrastructure vulnerability to volcanic hazards, including that related to surface transportation functionality following volcanic ashfall – a feature where current knowledge gaps hinder the development of contemporary volcanic risk assessments.

Physical damage and functionality loss in the proximal areas to the volcanic vent (i.e. the Kelud flanks extending ~30 km radially) and the distal locations (with a particular focus on Yogyakarta Special Region Province in Central Java, ~220 km west of Kelud) are considered in this study. In the proximal areas, impacts were severe with a range of hazards including ballistics, pyroclastic density currents, lahars, and heavy tephra fall responsible for the destruction of bridges and ~3 km of road. These impacts disrupted access to the crater and created knock-on societal consequences for communities in nearby villages. In the distal areas, widespread reduction in transportation functionality resulted from government advice to stay off roads, along with reduced skid resistance and impaired visibility encountered by those who travelled on ash-covered routes. Other distal consequences from ash included disruption to bus services and aviation, and some impacts were prolonged following ash remobilisation. The diesel rail network demonstrated resilience to volcanic ash, with the network's capacity even increasing at times in response to the increase in rail demand resulting from the negative effects on other transportation.

The study allows the identification of differences and similarities between proximal and distal impacts, and highlights potential hazard intensity metrics for ash (e.g. thickness, particle size) responsible for impacts. The range of effects from different hazards demonstrates the importance of adopting multi-hazard approaches for volcanic risk assessments. Additionally, the study highlights how volcanic ash can cause long-lasting and multi-faceted impacts to transportation, particularly in the form of functionality reduction. Complex interactions between different infrastructure and societal effects are also discussed, including considerations of the level-of-service encountered by transportation end-users, which are increasingly important for transportation and emergency management planning.

2.2 Introduction

Contemporary volcanic risk assessments require a thorough understanding of impacts to society, specifically through knowledge of exposure and vulnerability to multiple hazards (Crichton 1999, UNISDR 2009). Volcanic hazards can occur both close to the vent (e.g. pyroclastic density currents, lava flows, lahars) or extend much further afield, particularly in the form of ashfall (Magill and Blong

2005, Wilson et al. 2012). With the widespread nature of ashfall, and often disruptive consequences for critical infrastructure, urban areas are more likely to be affected by ash than any of the other volcanic hazards. As such, it is especially important to have detailed information on the likely impacts of volcanic ash on critical infrastructure, which can allow for improved DRR strategies before, during, and following future eruptions.

Post-eruption data is the most fundamental information to compile volcanic risk assessments (Baxter et al. 2005, Jenkins et al. 2014). Impact assessment trips allow the collection of such data and have been a common approach adopted in recent years (e.g. Barnard 2004, Leonard et al. 2005, Sword-Daniels et al. 2011, Wilson et al. 2011, Wardman et al. 2012, Jenkins et al. 2013, Wilson et al. 2013). They enable improved knowledge on the exposure of infrastructure including surface transportation to volcanic hazards, as well as on components of vulnerability and resilience that influence the overall impact. Despite the frequency of recent impact assessment studies, vulnerability data for volcanic hazards remains relatively sparse and new eruptions present opportunities to add to the global knowledge base (Magill et al. 2013). Furthermore, many previous studies have focussed on physical damage to critical infrastructure, sometimes with little regard for the overall functionality of networks and implications for end-users. New impact assessment trips can help fill such knowledge gaps and also provide insights into previously unidentified impacts.

The 2014 eruption of Kelud volcano, Indonesia, provided a prime opportunity to observe proximal and distal impacts from a short-lived, explosive (VEI 4) volcanic eruption on society. This thesis chapter presents findings from an impact assessment trip to Central and East Java, Indonesia (Figure 2.1), which investigated the impacts from the 2014 Kelud eruption. Impacts to transportation networks from the Kelud 2014 eruption form the primary focus of this chapter, although impacts to all critical infrastructure can be found in Appendix A – the full GNS Science Report, from which the content in this chapter has been extracted and modified. The impact assessment focuses on two distinct locations – proximal areas to the volcano up to ~30 km radially from the vent, and a distal location ~220 km from the vent where ashfall was the only volcanic hazard to affect infrastructure and society. As such, the impacts of ashfall on transportation network damage and functionality are spatially compared, allowing analysis of vulnerable components and identification of potential hazard intensity metrics (HIMs) responsible for such impacts.

2.2.1 Study areas

Both the proximal and distal areas to Kelud contain high populations; the population density in Yogyakarta Special Region Province (Figure 2.1) is ~2,000/km^2, and the mean population density in the three regencies surrounding Kelud is ~1,000/km^2 (BPS 2010). Proximal and distal areas contain many infrastructure similarities with multiple transportation modes (road, rail and airports) in both. There are also multiple risk management strategies in both locations associated with adjacent volcanoes (Merapi volcano is located approximately 28 km to the north of Yogyakarta City; (Figure 2.1). For example, hazard maps and land use plans covering areas potentially affected by proximal hazards provide a way to manage development and minimise disaster risk in both areas (Mulyana et al. 2004, Sagala 2009), and there are active monitoring and warning systems in place on the flanks of

both volcanoes, as well as physical mitigation strategies such as sabo dams and ‘sand mining’ in river beds to minimise the impact of lahars (De Bélizal 2014).

Eruptions at Merapi, occur more frequently than those at Kelud (recently every ~2-3 years as opposed to every ~20 years; Fadeli 2012, GVP 2014 a,b). Therefore, the communities on the flanks of Merapi have been more frequently exposed to volcanic hazards, but may not be as familiar with the distal effects of ashfall. There were few complications introduced by hazards from other eruptions (such as from Merapi volcano) at the time of the Kelud impact assessment trip. The last major eruption at Kelud was ~24 years earlier, and the last at Merapi was in 2010. Additionally, the short-lived eruption of Kelud in 2014 allows the study of impacts that can be easily assigned to discrete volcanic hazards. Despite the short timeframe for direct hazards during the Kelud eruption, there were various cases of people travelling on affected transportation networks, which allows substantial investigation into the impacts (both functionality and physical damage), including the vulnerability of infrastructure and risk management strategies that were implemented.

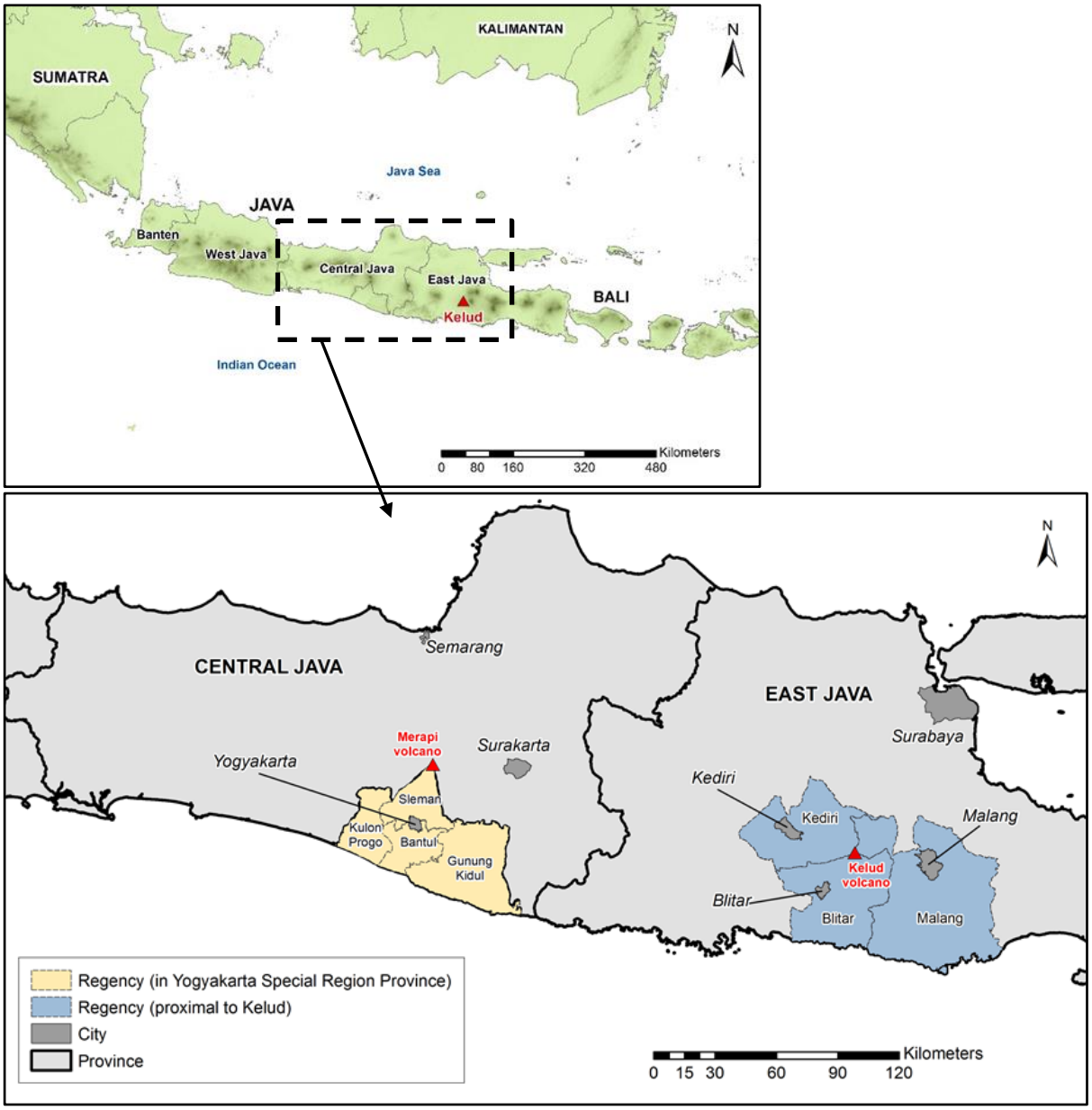

Figure 2.1 Location of East and Central Java in Indonesia and the regencies in proximal (blue) and distal (yellow) areas to Kelud where the field visits occurred. Also shown are cities and locations in Central and East Java of importance to the chapter, and location of Merapi volcano. (Data sourced from diva-gis.org (2014) rtwilson.com (2014))

2.2.2 Transportation in Java

The road, rail and domestic airline network (Figure 2.2) are used extensively throughout Java, with key shipping ports for connections to other Indonesian islands located mainly on the northern coast. A wide variety of vehicles are used for road transport. Buses operate within and between the larger cities with minibuses servicing many of the smaller towns. Motorbikes are by far the most popular vehicle in Java (71% of motor vehicles in 2003; World Bank 2013) with many adapted to transport a variety of goods in addition to passengers (Figure 2.3). Taxis and cycle rickshaws, called *becak* are common in

most cities. Private cars are becoming more popular, especially with the increasing purchasing power of Indonesians and liberalisation of import motor vehicle rules. However, vehicle growth outpaces the construction of new roads and congestion is common, particularly on the major roads through cities (World Bank 2013).

There are two major rail lines running the length of the island in addition to several minor lines. Air transport serves as an important way to connect the thousands of Indonesian islands and cities with passenger and flight numbers having increased drastically over the past two decades (Picquout et al. 2013), particularly since the advent of low-cost flights.

Figure 2.2 Major transportation routes of Java (Mau Ke Mana 2014).

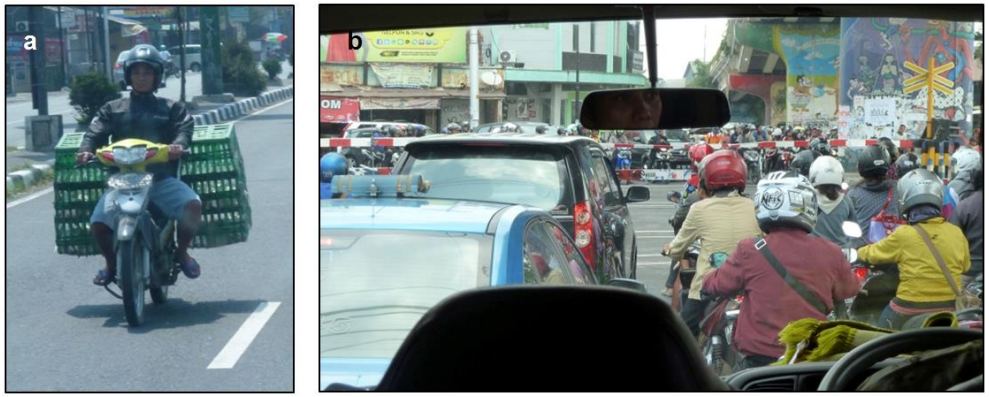

Figure 2.3 Motorbikes in Java (a) Motorbike adapted for transporting poultry. (b) Motorbikes and other traffic waiting at a railway crossing in Yogyakarta.

2.2.3 Volcanic risk management at Kelud

The information in this subsection provides a brief summary of risk management strategies at Kelud, which can influence impacts to transportation. Specifically, it relates to decisions that affect evacuations and transportation use. Various organisations, which are mentioned throughout the chapter, are also introduced. More detailed information on emergency management activities can be found in Appendix A.

During volcanic eruptions and other crises, risk assessments at a national level in Indonesia are primarily achieved through a Presidential Decree. The decree requires the analysis of certain indicators such as the number of victims, loss of properties, destruction of infrastructure, area affected, and socio-economic impacts. The impact of volcanic hazards on transportation thus forms a critical component of the assessment process. Different administrative divisions and groups (which operate in the regencies bordering the Kelud vent – Figure 2.4, and further afield) have key risk management roles during heightened volcanic activity at Kelud volcano, including:

- The Kelud Volcano Observatory (KVO) located 7.5 km west of the crater (Figure 2.5) who make regular visual observations of the volcanic activity (CVGHM 2014a) and send reports to the CVGHM (Centre for Volcanology and Geological Hazard Mitigation)[3] and surrounding chiefs of settlement (De Bélizal et al. 2012).
- The CVGHM who analyse information received and provide advice to BPBDs (Badan Penanggulangan Bencana Daerah – the provincial Disaster Management Agencies) and BNPB (Badan Nasional Penanggulangan Bencana – the National Agency for Disaster Management).
- The BNPB and BPBDs who issue information about the status of alerts and implement measures including evacuation zoning.
- Various community groups who contribute to volcanic risk management at Kelud. For example, JANGKAR Kelud (Jangkane Kawula Redi Kelud), which is a platform of representatives from the community, teachers and local government in the three regencies surrounding Kelud, directly assist with evacuations and the communication of information between villages.

A hazard map is used to communicate some of the hazard and risk information at Kelud (Appendix A). However, there are some concerns that the map does not accurately depict the true threat from some hazards (Indonesian Session 2014), suggesting that new risk assessment data may be beneficial. Transportation network impact information, such as that outlined in this chapter, could assist future risk assessments and hazard map development.

[3] The CVGHM is also known by its Indonesian name, PVMBG (Pusat Vulkanologi dan Mitigasi Bencana Geologi).

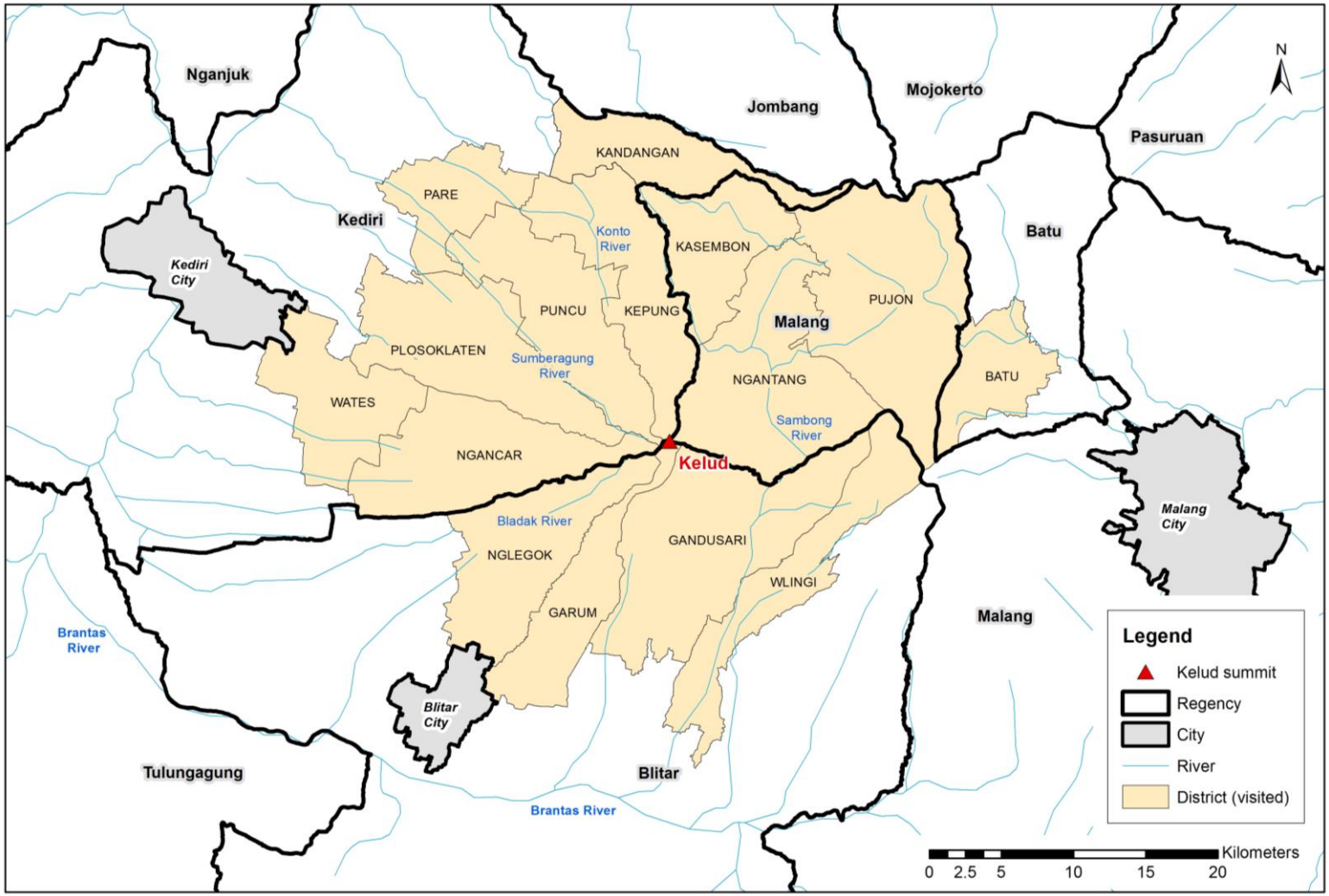

Figure 2.4 The three regencies (Malang, Kediri and Blitar) surrounding Kelud's summit and neighbouring regencies. Also shown (in yellow) are the districts on the flanks of Kelud where field studies, observations and/or interviews were conducted. (Data sourced from diva-gis.org (2014) and rtwilson.com (2014)).

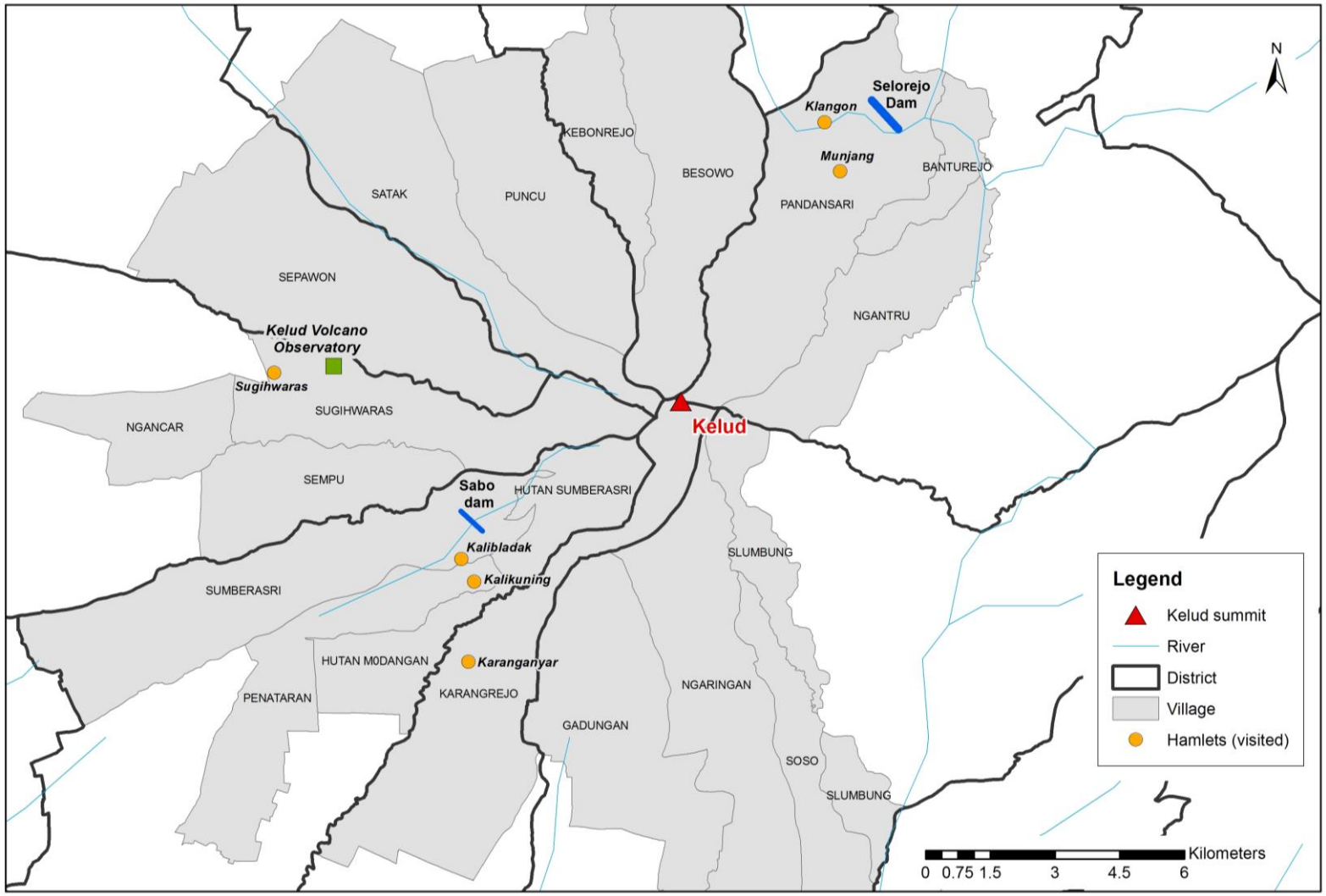

Figure 2.5 Location of villages (grey areas) surrounding the Kelud summit and the hamlets (orange points) within, which were visited during the impact assessment trip. The two dams and KVO shown on the map were also visited. (Data sourced from diva-gis.org (2014) and rtwilson.com (2014)).

2.2.4 Kelud 2014 eruption chronology

A chronology of the February 2014 eruption of Kelud volcano including unrest episodes, volcanic hazards, and key emergency management activity is provided in Table 2.1.

Table 2.1 Chronology of the February 2014 Kelud eruption. (Data sourced from BPBD Blitar Regency 2014a, BPBD DIY 2014a*, BPBD DIY 2014b, CVGHM 2014a, CVGHM 2014b, CVGHM 2014c, CVGHM 2014d, CVGHM 2014e, GVP 2014c, GVP 2014d, Indonesian Session 2014, Irvine-Brown 2014, Kalikuning 2014*, KVO 2014*, Munjang 2014a*, Muryanto & Susanto 2014, Sunstar 2014).

Date	Time (WIB)	Event
June 2009 - 2 February 2014	-	Alert Level 1 ('Normal') status
10 September 2013 - 9 February 2014	-	Crater lake water temperature increase
1 January 2014 - 2 February 2014	-	Shallow volcanic (VB) and deep volcanic (VA) earthquakes increase
2 February 2014	14:00	Alert status raised to Level 2 ('Advisory')
3-10 February 2014	-	Deep and shallow volcanic earthquakes increase (some 3 km below summit)
10 February 2014	-	Inflation detected at one tiltmeter station, crater lake temperature decrease
10 February 2014	16:00	Alert status raised to Level 3 ('Watch'). 5 km radius exclusion zone
10 February 2014	16:00	Some residents evacuate area up to 10 km from vent
13 February 2014	00:00-22:49	Increase in number of VB, VA and low frequency (LF) earthquakes
13 February 2014	21:15	Alert status raised to Level 4 ('Warning'). 10 km radius exclusion zone
13 February 2014	21:15	Evacuations within 10 km of crater in response to new alert status
13 February 2014	**22:46**	**Start of Eruption**
13 February 2014	22:50	Evacuation of some Pandansari residents in response to eruption
13 February 2014	23:30	Large explosion at vent, three seismic stations destroyed (one remaining)
14 February 2014	~03:00	Ash fall starts in Yogyakarta (220 km west of Kelud)
14 February 2014	**~03:00**	**Volcanic acitivity at vent decreases**
14 February 2014	(morning)	Military evacuate some Pandansari residents who sheltered overnight
14-15 February 2014	(daytime)	Some farmers returning in exclusion zone to check on properties, crops and livestock
15-20 February 2014	-	Amplitude of tremors decreased and white plumes (rather than grey) from vent
16 February 2014	-	End of ash fall in Yogyakarta (some may have been from substantial remobilisation)
17 February 2014	(daytime)	Many farmers returning to check on properties, crops and livestock
19 February 2014	-	Concern from KVO over future lahar threat
20 February 2014	11:00	Alert status lowered to Level 3 ('Watch'). 5 km radius exclusion zone
20-28 February 2014	-	Further reduction in tremor amplitude
28 February 2014	16:30	Alert status lowered to Level 2 ('Advisory'). 3 km exclusion zone advised
7 August 2014	12:00	Alert status lowered to Level 1 ('Normal')

2.3 Research Methods

Data collection was conducted using several approaches. At the time of the eruption, collection and analysis of online emergency management and other official reports, maps, news and media articles was undertaken. Care was taken to verify these resources, especially the media reports, either by cross-checking or subsequent follow up. Where this was not possible, resources were excluded from analysis. A reconnaissance trip to observe primary impacts immediately after the eruption to collect perishable observational data was proposed, but was postponed due to difficulties finding appropriate local Indonesian collaborators, which is a key recommendation by volcanic crises best practice guidelines (e.g. IAVCEI 1999). The field visit was deferred by 7 months until the immediate crisis period had subsided, when it was possible to partner with Muhammad Hendrasto, the Head of CVGHM, and his team. This assessment trip was undertaken between 08 September and 23 September 2014 following University of Canterbury Human Ethics Committee approval, to two areas: "proximal" which extended ~30 km radially from the vent (Figure 2.4) and "distal" which was focused on Yogyakarta Special Region Province (Figure 2.1). Field data collection consisted of direct observations by researchers and interviews with staff at organisations involved with the response and/or early recovery. Most interviews were pre-arranged and semi-structured, largely conducted in Bahasa Indonesia through experienced English speaking translators from Java, Indonesia. Discussions with residents and other stakeholders were also held in the field on a more ad-hoc basis when appropriate opportunities arose, taking care to observe cultural and contextual sensitivities. These discussions provided additional qualitative and semi-quantitative data on the impacts of volcanic hazards, particularly on the vulnerability and capacity of critical infrastructure and agriculture. All interviewees that inform the research in this chapter of the thesis are shown in Table 2.2, unless they requested to remain anonymous.

Table 2.2 Interviewees who provided information that informs this chapter of the thesis. The column titled 'citation' indicates how the material is subsequently referred to. All information sourced from interviews and discussions is cited with an asterisk symbol herein.

Agency/ Business	Location	Citation
Badan Penanggulangan Bencana Daerah Kabupaten Blitar (the disaster management agency of Blitar Regency)	Wlingi, East Java	BPBD Blitar Regency 2014b*
Badan Penanggulangan Bencana Daerah Istimewa Yogyakarta (The disaster management agency of Yogyakarta Special Region Province)	Yogyakarta Special Region Province	BPBD DIY 2014a*
Disaster Research, Education and Management (DREAM) Centre, Universitas Pembangunan Nasional (UPN) Veteran Yogyakarta (National Development University, Yogyakarta)	Sleman Regency, Yogyakarta Special Region Province	Daniswara (pers comm, 2014)*
Dawet vendor - drinks stand near BPBD DIY Office	Yogyakarta Special Region Province	Dawet (pers comm, 2014)*
Direktorat Jenderal Perhubungan Darat (Directorate General of Land Transportation) and Direktorat Jenderal Perhubungan Laut (Directorate General of Sea Transportation), Kementerian Perhubungan (Ministry of Transportation)	Yogyakarta Special Region Province	DJPD & DJPL 2014*
Direktorat Jenderal Perhubungan Udara (Directorate	Yogyakarta Special Region	DJPU 2014*

General of Civil Aviation), Kementerian Perhubungan (Ministry of Transportation)	Province	
Kalikuning Village residents / farmers	Blitar Regency, East Java Province	Kalikuning 2014*
Karanganyar Village residents	Blitar Regency, East Java Province	Karanganyar 2014*
Sand miner in Sambong River next to Kalngon Hamlet	Pandansari Village, Ngantang District, Malang Regency, East Java Province	Klangon 2014*
Warung owners next to Konto River bridge	near Kandangan, East Java Province	Konto 2014*
Kelud Volcano Observatory (KVO)	Sugihwaras Village, Ngancar District, Kediri Regency, East Java Province	KVO 2014*
Luwakmas Family Café and Restro	Sugihwaras Village, Ngancar District, Kediri Regency, East Java Province	Luwakmas Café 2014*
Kakadu Tour and Travel (tour manager)	Yogyakarta Special Region Province	Mahjum (pers comm, 2014)*
Dinas Kesehatan Provinsi Daerah Istimewa Yogyakarta, Republik Indonesia (the provincial Health Agency)	Yogyakarta Special Region Province	Health Agency DIY 2014*
Farmer / Munjang resident in fields to south of Munjang Hamlet	Pandansari Village, Ngantang District, Malang Regency, East Java Province	Munjang 2014a*
Residents at a house being renovated in Munjang Hamlet	Pandansari Village, Ngantang District, Malang Regency, East Java Province	Munjang 2014b*
PT. Jogja Tugu Trans (the Trans Jogja Bus Transport Company)	Yogyakarta Special Region Province	PT-JTT 2014*
Kakadu Tour and Travel (translator and guide)	Yogyakarta Special Region Province	Purwana (pers comm, 2014)*
Sand miner in Sambong River, below Selorejo dam	Pandansari Village, Ngantang District, Malang Regency, East Java Province	Selorejo 2014*
Universitas Pembangunan Nasional (UPN) Veteran Yogyakarta, (National Development University, Yogyakarta)	Sleman Regency, Yogyakarta Special Region Province	UPN 2014*

2.4 Findings: Post-Eruption Observations of Volcanic Hazards

2.4.1 Proximal hazards

The VEI 4 eruption of Kelud on 13-14 February 2014, which started around 90 minutes after the highest alert status (‘Warning’) was issued, caused multiple proximal hazards. The initial eruption left a large crater around 400 m in diameter and destroyed the lava dome which emerged in 2007-2008, along with the parking area and part of Crater Road (Figure 2.6) that previously extended up to the summit (GVP 2014c). Around 1.5 hours after the start of the eruption, there were reports of an explosion that was heard over 200 km away, including in Surabaya, Surakarta and Yogyakarta (ABC News 2014a, BPBD DIY 2014b, Irvine-Brown 2014, SMH 2014). During the explosive eruption, PDCs extended up to ~2 km from the vent, particularly to the south and south west, destroying previously forested areas (Figure 2.6).

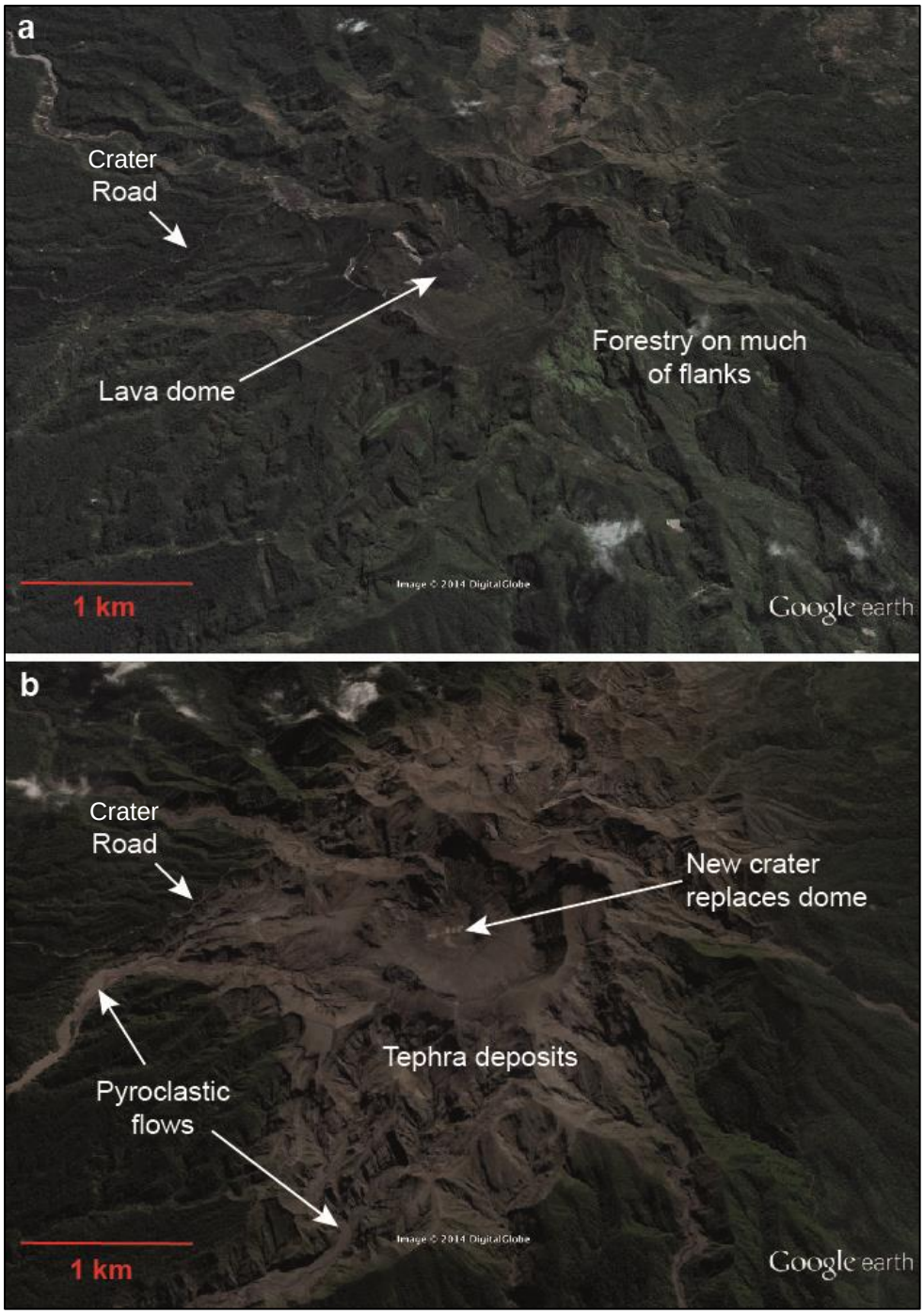

Figure 2.6 Images from the south of Kelud crater area (a) before (23 August 2012), and (b) after (19 May 2014) the 13 February eruption (GoogleEarth 2014). The lava dome was removed by the explosive eruption leaving a ~400 m diameter crater. In the second photo, PDC deposits can be seen, which extend over 2 km from the vent, particularly to the south. Thick tephra deposits are also visible, particularly extending to the north east towards Pandansari Village.

Many ballistic bombs were ejected from the vent with some measuring up to 600 mm in length falling up to 3 km away (BPBD Blitar Regency 2014a, KVO 2014*). Lapilli and blocks which fell in the heavily

impacted area of Pandansari Village (extending 7 km from the vent; Figure 2.5) had maximum sizes of 50-80 mm in diameter (Baku-APA 2014). Pumice clast sizes of around 50 mm were reported to the west of the crater, up to ~8 km from the vent, with clasts up to 80 mm found at the KVO, 7.5 km west of the crater.

Within ~2-3 km of the crater, tephra accumulated up to a metre thick (Volcano Discovery 2014). Areas to the north east of the volcano in the Malang Regency (Figure 2.4) were heavily impacted by tephra fall, and thicknesses were likely up to 500 mm (but more widely 200 mm) in parts of the Ngantang District, including Pandansari Village, 7 km away from the vent (Baku-APA 2014, KVO 2014*, Munjang 2014b*). In September 2014, PDC and thick tephra deposits were still evident extending ~2 km from the vent with little primary vegetation recolonising the area. There was evidence of landsliding and gullying due to the newly exposed and unstable conditions.

Around 6-8 km to the south and west from the vent, in the Blitar and Kediri regencies (Figure 2.4), some sites experienced depths of ~100 mm. Overall tephra here was generally coarser than what fell in the Malang Regency, mainly consisting of lapilli - (often referred to as 'coarse sand') sized pumice clasts (BPBD DIY 2014a*, Health Agency DIY 2014*, KVO 2014*, Purwana (pers comm, 2014)*). Some individual clasts were up to ~80 mm in diameter in these locations (Kalikuning 2014*, Karanganyar 2014*, KVO 2014*, Luwakmas Café 2014*). However, further to the south, including Wlingi in the Blitar Regency, residents experienced no tephra fall despite the sky darkening overhead at times (BPBD Blitar Regency 2014b*). This may have been a result of low altitude winds blowing from the south and ash remaining in suspension in the plume at higher altitudes.

Heavy rain, particularly torrential downpours from 16 February 2014 onwards (Pitaloka 2014), mixed with the fresh pyroclastic deposits on the ground to form lahars. Lahars on Tuesday 18 February 2014 followed the courses of rivers in all three proximal regencies, causing damage to buildings, bridges and agricultural land (BNPB 2014). These included lahars in the Konto (Kediri Regency, 35 km N) and Bladak (Blitar Regency, 20 km SW) rivers (GVP 2014c; Figure 2.5).

2.4.2 Distal ashfall

In distal areas, such as Yogyakarta, the ashfall from the Kelud eruption came as a surprise to both residents and officials as they did not expect that ash originating from so far away would impact these areas. No warning of potential ashfall was received in these areas and the fact that the eruption occurred at night, with ash beginning to fall at around 03:00 on 14 February, also added to the surprise with many people awaking to unexpected ashfall outside (BPBD DIY 2014a*, Irvine-Brown 2014, Daniswara (pers comm, 2014)*).

2.4.2.1 Ash dispersion

Ground reports indicate that ash plumes rose to an altitude of 17-20 km above sea level forming an umbrella cloud as wide as ~200 km across (CVGHM 2014a, Nakada 2014). Ash fell in areas NE, NW, and W of the vent, with many reports from as far as Yogyakarta (220 km WSW; Figure 2.1),

Banjarnegara (320 km WNW), and Banyuwangi (228 km E) (BOM 2014, Dawet (pers comm, 2014)*, KVO 2014*). Trace quantities of ash even fell in Bandung, the capital of West Java 550 km away, and there were concerns that the ash would fall in the Indonesian capital of Jakarta 650 km away (Laia 2014, Jakarta Globe 2014). Analysis by the Darwin Volcanic Ash Advisory Centre (VAAC) determined that the ash cloud reached 85,000 ft (25.9 km) with the majority of the cloud at 57,000 feet (17.4 km) (BOM 2014).

2.4.2.2 Ash accumulation and characteristics

Figure 2.7 shows the approximate tephra thickness in different locations. This map includes lapilli (2-64 mm diameter) and ash (<2 mm diameter) sized tephra; volcanic bombs or ballistic clasts (>64 mm diameter) are not accounted for in the thicknesses. The total estimated tephra volume from the eruption is likely around 105 million m^3 (EDSM 2014), but potentially up to 160 million m^3 (Jakarta Post 2014a).

In Yogyakarta, fine-grained tephra accumulated to average depths of 20-30 mm, and up to 50 mm in places (BPBD DIY 2014a*, BPBD DIY 2014b, DJPD & DJPL 2014*, Volcano Discovery 2014). Ash from the Kelud eruption was said to be more of a problem than that from the Merapi (2010) eruption in Yogyakarta as it covered a much larger area (BPBD DIY 2014a*, Daniswara (pers comm, 2014)*, Mahjum (pers comm, 2014)*). Merapi ash was mostly directed to the west in 2010. Due to the fine nature of the Kelud ash in distal locations, remobilisation by wind, traffic and other human activities was a particular issue. As a result, ash was prevalent in Yogyakarta for over one month (BPBD DIY 2014a*) and some ash remained on the ground and other surfaces over 7 months after the eruption at the time of our field visit. There was light rainfall in Yogyakarta on 14 February, although this was not enough to prevent further remobilisation by re-suspension in the atmosphere. No major remobilisation issues were reported in the proximal areas where the ash was coarser and not as readily re-suspended. Ash from Kelud that fell farther afield in Java, particularly to the north west of Yogyakarta also accumulated to measurable depths. At Borobudur temple, around 25 km north-west of Yogyakarta City, 3-5 mm of ash accumulated (Antara News 2014a).

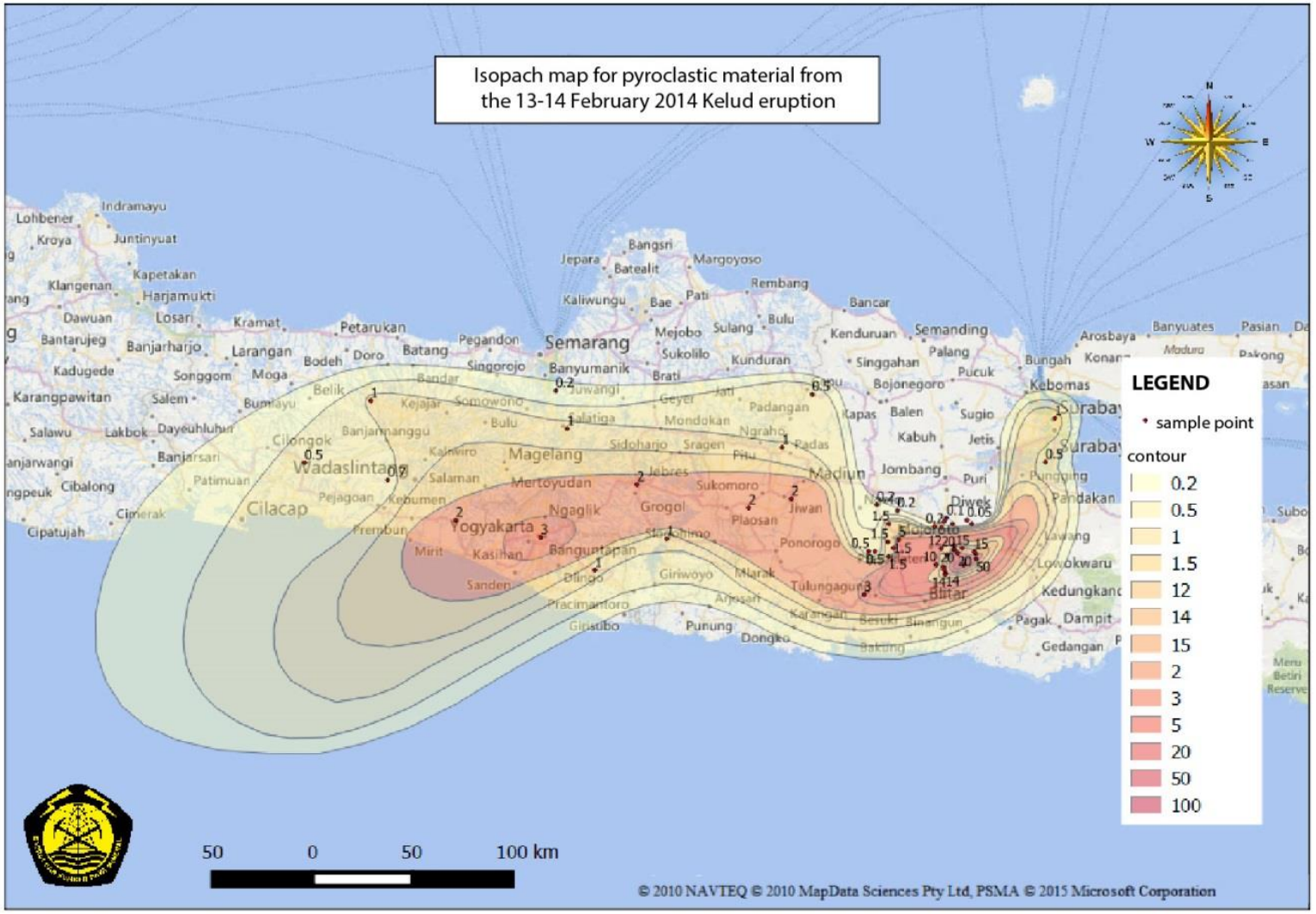

Figure 2.7 Isopach map for tephra thickness (in mm) produced by the Feburary 2014 eruption (Andreastuti et al. 2015)

2.5 Findings: Impacts on Transportation Networks

Transportation networks are frequently impacted following volcanic eruptions, often in both proximal and distal locations from the vent (Section 1.5). The February 2014 Kelud eruption was no exception and there were effects on all transportation modes to some degree on the flanks of Kelud and in distal cities over 200 km away. The estimated cost of damage and losses associated with transportation was Rp 76,500,000 (~NZ$ 1,597,000) in the Blitar Regency alone (BPBD Blitar Regency 2014a). However, this only represents a small percentage of the overall loss, particularly as no major airports operate within this regency and ash thickness in this regency was relatively low.

Transportation was used extensively during the evacuations on 10 February 2014 (officially excluding residents from a 5 km radius of the crater) and 13 February 2014 (with a 10 km radius exclusion zone implemented) (CVGHM 2014c, GVP 2014c, IFRC 2014). Most residents evacuated using their own transport, particularly motorbikes, but some by car and on foot. Evacuations were reportedly undertaken in a very calm manner with no major traffic problems and JANGKAR Kelud members appeared to be very effective for helping disseminate information from village to village and assisting with evacuations. As of 14 February 2014, the number of internally displaced persons was said to stand at 100,248 (IFRC 2014).

2.5.1 Aviation

The Volcanic Ash Advisory Centre (VAAC) in Darwin, Australia issued a series of advisories in response to the Kelud eruption, some key points of which are summarised below:

- The initial volcanic ash advisory (IDD41295) (VAAC 2014) was issued at 17:21 UTC, 13 February 2014 (00:21, 14 February 2014 Indonesia Western Time / WIB). This summarised that a high level eruption with Aviation Colour Code red had occurred.

- The next advisory was issued around half an hour later and estimated that the plume had risen to Flight Level 450 (45,000 feet / 13.7 km nominal altitude) and extended 50 nautical miles (93 km) to the west of the crater at 16:32 UTC, 13 Feb (23:32 WIB, 14 Feb). This was based on the temperature from the MTSAT-2 IR satellite (available hourly) and the Surabaya 12:00 UTC atmospheric profile (BOM 2014, GVP 2014c).

- By 20:32 UTC, 13 Feb (03:32 WIB, 14 Feb), this plume had extended 240 nautical miles (444 km) west of the active vent and details emerged relating to the plume also spreading at Flight Level 200 (20,000 feet / 6.1 km nominal altitude) and extending 80 nautical miles (148 km) to the north east (VAAC 2014).

- The upper plume had reached Flight Level 650 (65,000 feet / 19.8 km nominal altitude)[4] to the west at 16:32 UTC (23:32 WIB), 14 Feb (VAAC 2014).

Shortly before 05:00 local time (WIB) on 14 February 2014, a Jetstar Airbus A320 aircraft carrying passengers from Perth, Australia to Jakarta, Indonesia entered the Kelud volcanic ash cloud. It was reported that the flight crew suddenly heard unusual faint noises with the captain observing green sparks outside the cockpit about 30 seconds later. A faint sulphuric smell and light haze also began forming in the flight deck (Foo and Tan 2014). The flight crew donned oxygen masks and changed direction after diagnosing that the plane had probably flown through volcanic ash (Foo and Tan 2014). They landed safely at Jakarta at 05:50. Reports soon after estimated that the cost of replacing the two damaged engines could be ~US$ 20 million (~NZ$ 25.8 million) (Thomas 2014). At the time of writing, the circumstances surrounding this incident were still under investigation and no International Civil Aviation Organisation incident report (ICAO ANNEX 13) was available (Goodwin (pers comm, 2014), EASA 2014).

As ash began to blanket parts of Central and East Java provinces, operations at seven airports (four international in Yogyakarta, Surakarta, Surabaya and Semarang, and three domestic in Bandung, Malang and Cilacap) were disrupted by closures that were ordered by the Department of Transportation (Figure 2.8) (BPBD DIY 2014b). Military air bases at some of the above airports and at Iswahyudi airfield in the Madiun Regency were also closed. It appears that these closures were ordered in response to the ashfall as few warnings prior to this were received in the distal areas from Kelud. Cancellations and delays affected many airlines in Indonesia and further afield including Australia (Australian 2014, Gough 2014). There were many impacts considered at airports including concerns of reduced skid resistance for aircraft landing, damage to aircraft engines and reduced visibility (Australian 2014, DJPD & DJPL 2014, Gough 2014, Sunstar 2014), all of which are common volcanic hazard impact types (Guffanti et al. 2009). Clean air announcements from Darwin VAAC were required before airports could reopen (DJPU 2014*) but there were also many issues associated with ash on the ground. Four airports (those at Surabaya, Malang, Semarang and Cilacap) resumed normal operation late on Saturday 15 February (3News 2014) (~2 days after the eruption started) (Figure 2.8). Estimated losses at the airport in Surabaya alone were said to have totalled around Rp 3 billion (~ NZ$ 315,000) (Boediwardhana and Harsaputra 2014). Flights at Bandung resumed on Sunday 16 February (Gough 2014) (~3 days after the eruption started) and the international airports in Yogyakarta and Surakarta reopened on Wednesday 19 February (~6 days after) (BPBD DIY 2014a*, DJPU 2014*, KVO 2014*) and Thursday 20 February (~7 days after) respectively (Figure 2.8) (Muryanto & Susanto 2014). As operations re-commenced at some of the affected airports, there were still some on-going issues due to the challenges of scheduling and plane supply with other airports still closed (DJPU 2014*).

[4] Post-event analysis by Darwin VAAC indicated that the ash in fact reached a maximum height of 85,000 feet / 25.9 km (BOM 2014).

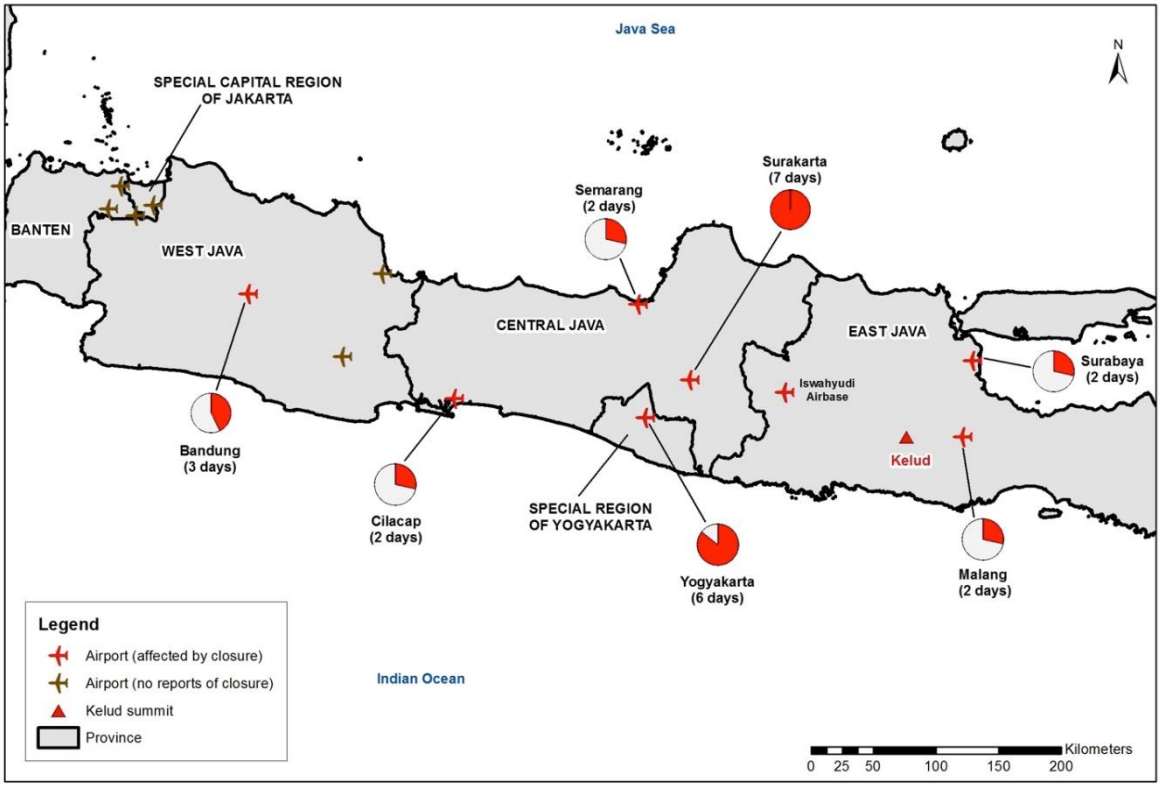

Figure 2.8 Total airport closure times after the eruption (indicated by coloured portion of circles, with totally coloured circle representing 7 days closure) where known.

Adisucipto International Airport (AIA), Yogyakarta case study

It was estimated that 20-50 mm of ash fell at AIA following the eruption of Kelud (DJPU 2014, Jakarta Post 2014a). As the ash started falling at ~03:00 WIB and the normal opening time of the airport is at 04:00 WIB, the decision was made to not open AIA to passengers at all on 14 February. People arriving at the airport were told that it was closed which led to traffic congestion in the area (DJPU 2014*). The airport is used for both civilian and military purposes with a taxiway for each. Military planes are kept in hangers and did not come into contact with ash. At least two commercial planes however, were outside for the night of the 13 February (e.g.* Figure 2.9*) and ash infiltrated into the engines of the stationary planes despite being covered by plastic sheeting at some stage. Subsequently, the engines required dismantling, deep-cleaning and complete oil changes – a very expensive process which required specialist technicians (DJPU 2014*). The Directorate General of Civil Aviation reported that there were no indications of any damage to paintwork on the two stranded planes or to airfield surface line markings resulting from the ash.*

The closure of AIA following the Merapi 2010 eruption was largely due to airborne ash and there was little accumulation at the airport as occurred in February 2014 from the Kelud eruption (DJPU 2014). The fine-grained ash from Kelud at Yogyakarta meant that the ash was readily remobilised by wind and efforts to reopen the airport were hampered by this (Section 2.5.5.2). Over the course of AIA's*

closure in February 2014 (based on the loss of five average operating days; DJPU 2014) it is estimated that as many as 600 domestic, 750 military (including training flights) and 20 international flights were cancelled. The transportation of cargo was also affected as this is normally carried on the above flights.*

Figure 2.9 ***Aircraft covered in ash on 14 February 2014 at Adisucipto International Airport, Yogyakarta*** *(ABC News 2014b).*

2.5.2 Roads

2.5.2.1 Proximal

Severe impacts occurred to ~3 km of asphalt concrete road (within ~2 km radius of the vent) immediately following the eruption, particularly from ballistics, PDCs and landslides (Figure 2.10 a-e). The largest ballistic impact crater on roads visible in this region was around 3.6 m in diameter (Figure 2.10 a) and some ballistics completely penetrated bridges with subsequent holes to the ground below up to 1.1 m in diameter (Figure 2.10 b). Around 1 km of road was completely destroyed by these volcanic hazards with the remainder buried by tephra to a depth of ~1 m in places. At the time of observation, 7 months after the eruption, these sections of road remain closed to everyday traffic and repair work had not commenced, presumably in part due to the continued instability of the land. Some asphalt concrete road surfaces within ~10 km of the crater (particularly to the north east) were damaged by vehicles driving over the roads that were covered in lapilli and ash (Munjang 2014b*). This is perhaps due to an increased attrition rate caused by the direct impact of tephra on asphalt concrete and subsequent layer remaining on the road surface, which could lead to increased fluvial erosion and pothole formation.

Figure 2.10 Road and bridge impacts within ~2 km of the crater (taken 20 September 2014). (a) large ballistic impact crater in asphalt concrete road surface (3.6 m along the longest axis). (b) holes in asphalt concrete and reinforced concrete bridge (now covered in wood) after being penetrated by ballistics. (c) ballistics embedded within bridge surface and damage to edge of bridge. (d) bridge structure and railing damage. (e) remaining section of the road near the crater, now cleared of ash.

Around 9 km NE of the Kelud crater, at least two bridges crossing the Sambong River were destroyed by a lahar. This lahar may have occurred as soon as 18 February 2014 (BNPB 2014) four days after the eruption, immediately forcing the closure of some roads (Pitaloka 2014). The bridge to the north east of Munjang Hamlet, which was frequently used by its residents and also used in the evacuation,

was ~10 m long and was of standard concrete and metal construction with an asphalt concrete deck. Seven months after the eruption, this had yet to be rebuilt and vehicles were driving on the now wider and aggraded riverbed to cross the river here (Figure 2.11). The bridge, of similar construction style, adjacent to Klangon Village was ~35 m long (Selorejo 2014*). Within ~2 weeks of being destroyed by a lahar, it was replaced by a small bamboo bridge (Figure 2.12 a) allowing residents to cross the river either by foot or motorbike. This was subsequently replaced by a more substantial bridge on loan from the Indonesian Army (Figure 2.12 b) which took 6-7 months to install, enabling easy access for all vehicles to Klangon. This larger bridge will be replaced with a new permanent bridge when the government has funds (Klangon 2014*).

Figure 2.11 Kostrad TNI-AD (the Strategic Reserve Command of the Indonesian Army) help vehicles cross the Sambong River at site of old bridge between Munjang Hamlet and Selorejo Dam on Wednesday 19 February 2014 following a lahar (Haryanti 2014). The bridge at this site had yet to be rebuilt as of 21 September 2014.

Figure 2.12 Sambong River crossing near Klangon Hamlet, Pandansari Village. (a) Temporary bamboo bridge over the Sambong River built ~2 weeks after the lahar and improving access for pedestrians and motorbikes to Klangon Hamlet (Adonai 2014). (b) Larger temporary army- bridge built nearby ~6-7 months after the lahar (photo taken on 21 September 2014).

The Sambong River (Figure 2.12) is a tributary of the larger Konto River, which was also affected by at least one lahar. On the western side of Kandangan (~20 km north of the crater), the lahar was said

to arrive very slowly and rose gradually until the surface came to ~0.5 m of the road deck (Konto 2014*) on the major bridge carrying the main road between Pare and Kandangan. A roadside *warung* and many houses lie just above the level of this bridge close to the riverbanks. It is unclear when this lahar arrived but according to *warung* owners nearby, police closed the bridge for 2 hours (18:00-20:00) on 14 February due to the possibility of structural damage. In fact, there was little damage to this bridge apart from scour damage to the upstream side of the central support at the base and some subsidence and erosion of the surrounding stone and concrete riverbank structures, although it cannot be confirmed that these were a result of lahars alone.

Some residents, particularly in the Pandansari area to the north east of the crater evacuated as ash was falling, and they experienced very low visibility (with a visual range of just a few meters; Gough 2014), which made driving difficult. There were no reports of direct impacts to vehicles on the flanks of Kelud because most were either taken during evacuations or stored under shelters before the tephra fall arrived, as occurred in Kalikuning (Kalikuning 2014*). Some areas, such as the road to the west of the KVO were mainly affected by light pumice, which was not dense enough to cause any substantial vehicle damage (Luwakmas Café 2014*).

When residents returned to areas affected by ashfall around Kelud volcano, tephra had accumulated to depths of around 50-500 mm at 5-35 km from the crater across the north west to north east segment of the flanks (KVO 2014*). Although traffic was reported to be light in some areas such as Kediri City (Irvine-Brown 2014), there were several accidents due to slippery roads in proximal areas, particularly involving residents on motorbikes which had increased stopping distances and skidded into one another (KVO 2014*). In some instances, including in Selorejo, this resulted in personal injury. It was reported that most vehicle accidents occurred between residents on the first day of return, although this cannot be backed-up with accident data. The visual range in Kediri upon return may have been around 1000 m (Baku-APA 2014), adding to the driving difficulties. There were no reports of engine or other mechanical damage to vehicles in this area, perhaps due to the grain size of ash being relatively large.

2.5.2.2 Distal

In Yogyakarta, the government advised people to stay off roads and to only drive or go outside when absolutely necessary and to turn their lights on if they had to drive (BPBD DIY 2014a*, Mahjum (pers comm, 2014)*). Most people obeyed this advice and many were reluctant to drive in their vehicles anyway because of concerns about vehicle damage including scratched windows and engine problems, difficulties driving in ash and impacts on breathing and health (DJPD & DJPL 2014*). Some cars were covered in plastic sheeting as a protective measure (Figure 2.13) (BPBD DIY 2014b). As a result, the roads in Yogyakarta were relatively quiet for up to a week after the eruption (DJPD & DJPL 2014*, Irvine-Brown 2014, Mahjum (pers comm, 2014)*), although police were out helping to manage traffic flow (BPBD DIY 2014a*). Visibility in Yogyakarta was reduced to a visual range of just 1-3 m at times (BPBD DIY 2014a*, BPBD DIY 2014b, DJPD & DJPL 2014*). This was largely due to remobilisation from vehicles and worsened in areas where ash was thicker, making it difficult to drive

(Figure 2.14) (DJPD & DJPL 2014*). Outside of the city, visibility was also very low with a visual range of ~7 m near Borobudur Temple reported (Antara News 2014a).

Figure 2.13 Cars at Castle Bridge, Yogyakarta covered in plastic protective sheeting (BPBD DIY 2014b).

Figure 2.14 Motorbikes driving through ash in Yogyakarta (Washington Post 2014). Remobilisation of fine ash in the city meant that visual range was ~3 m at times.

Another complication was from ash covering the solar panels of traffic lights. These solar panels are used to power the traffic lights and are near horizontal in the tropics so collect ash easily. When covered, the batteries only last for ~1.5 days before needing to be recharged (DJPD & DJPL 2014*). The Directorate General of Land Transportation took two key mitigative measures to prevent traffic lights from failing:

1. Near-discharged batteries were replaced with recharged ones.

2. Solar panels were cleaned every day for ~5 days to prevent ash accumulation.

This prevented further traffic congestion at intersections. Visibility of functional traffic lights was not affected as the cover over each light prevented ash accumulation in front of the lights, stopping them from being obscured. There is no evidence that ash stuck to and obscured road signs.

Despite lower traffic volumes and many people driving more slowly than usual within the city (DJPD & DJPL 2014*), there were several traffic accidents, often from motorbikes skidding and colliding on the slippery roads (BPBD DIY 2014a*, Mahjum (pers comm, 2014)*). This appears to have been due to increased stopping distances rather than sliding on corners, and the failure to see the brake lights of motorbikes through the suspended ash (DJPD & DJPL 2014*). The Directorate General of Land Transportation reported that some cars experienced braking problems due to brake disks becoming scratched. According to hospital figures that were retrieved from the Health Agency of Yogyakarta Special Region Province, there were at least 50 injuries as a result of 'accidents' (likely traffic-related) in Yogyakarta Special Region Province within one month of the eruption (Health Agency DIY 2014*). It was also reported that there were at least 12 injuries within 2 days of the eruption at Panembahan Senopati hospital in Bantul, in the south of Yogyakarta (Susanto 2014).

Water rather than wipers was used to clean vehicle windows as previous experience suggested that the use of wipers can result in scratched windows (DJPD & DJPL 2014*). Following the Kelud ashfall, water was sourced largely from existing stocks of bottled water and from irrigation channels using buckets. Many people took a collaborative approach, cleaning their vehicles at the same time and helping one another. Discussions with the Directorate General of Land Transportation indicated that the cleaning of vehicles and related increase of water on roads may have led to a 'sludge' of ash forming on some road sections resulting in further nose-to-tail motorbike collisions. However, people reacted to this and cleaned roads of wet ash.

There was rainfall in Yogyakarta within three days of the eruption but this was not enough to wash ash from roads and may have made surfaces more slippery (BPBD DIY 2014a*). After one week, there was heavy rainfall in Yogyakarta and there were fewer accidents following this. In the weeks following the eruption, engine air filters became clogged and required cleaning or changing (DJPD & DJPL 2014*).

Trans Jogja Bus Company, Yogyakarta case study

The decision was made by the Trans Jogja Bus Company not to operate its fleet of 74 buses in the ashy environment and the two buses that were out were called back to the depot during the eruption. The decision to stop bus operations was based on concerns about 'the sharp nature of volcanic ash compared to usual road dirt' and previous experience that the company chairman had gained working for the National Bus Company during the Merapi (2010) eruption (PT-JTT 2014). No Trans Jogja buses operated for four days after the Kelud eruption.*

From days 4 to 10 following the eruption, only 50% of buses operated at one time with the other 50% being cleaned and serviced by technicians and equipment supplied by PT Jogja Tugu Trans. There was also a corresponding ~50% loss of income for the company during this time. There was ~30-40 mm of ash at the sides of the roads at the start of this operational period and bus drivers travelled nearer the middle of the roads where possible to avoid thicker ash. Some bus drivers wore masks due to health concerns. There were reportedly no major problems related to reduced skid resistance, window abrasion or route diversions during this time (PT-JTT 2014).*

A total of 20 technicians were employed following the eruption to help clean and maintain Trans Jogja buses with each technician responsible for three buses (PT-JTT 2014). It took around one hour to clean three buses. As part of the regular servicing, windows were washed and air filters (both engine and air conditioning) were cleaned with compressed air. Some air filters were replaced because they were blocked. Air conditioning filters needed particular attention as the units are located on the top of buses and therefore susceptible to ash. Vacuums were used to remove ash from the bottom of engine bays and radiator systems where it was prone to accumulation. Brakes were also vacuumed via a hole in the system due to concerns about ash sticking to brake components where it could then thicken and solidify (PT-JTT 2014*).*

Bus operations returned to normal ~10 days after the eruption following the heavy rain in Yogyakarta. However, in the months following the eruption, maintenance of buses by Trans Jogja was increased to once per two months (usually once per four months). The two buses that were out when the initial ashfall occurred experienced engine and turbo-pressure issues around two months after the eruption which the staff attributed to driving through the ashfall.

There were indications that national bus services were also disrupted by ashfall for a time with only the routes to East Java from Yogyakarta operating on the first day after the eruption (BPBD DIY 2014b).

2.5.3 Rail

Diesel trains run on all areas of the rail network that were impacted by ash from Kelud (the only electric trains in Java are found in Jakarta) (DJPD & DJPL 2014*). Although there was evidence of rail tracks becoming thinly covered in ash from the Kelud eruption (Figure 2.15), there were no reports of rail services being delayed or cancelled specifically due to ash impacts. This is difficult to monitor in Java as delays and cancellations are relatively frequent, especially to the economy class services. However, rail appears to have been the least affected transportation mode with BPBD DIY staff claiming that it was ‘the only transportation sector able to penetrate volcanic ash disruption’.

After interviewing the Directorate General of Land Transportation, it appears that the level-of-service on the rail network actually increased at times with extra trains running and some trains lengthened with extra cars in certain areas including Yogyakarta Special Region Province. This was a result of higher demand caused by cancelled flights, and buses and trains were full with passengers despite

the increased capacity (DJPD & DJPL 2014*). A similar approach was taken during the Merapi (2010) eruption where train numbers on certain routes were increased and all trains were lengthened by two cars, although this was in anticipation of an exodus of people living on the slopes and in Yogyakarta (Picquout et al. 2013). Some train cars are air conditioned but there were no reported problems to these systems due to ash from the Kelud eruption.

Figure 2.15 Surabaya to Bandung train passing through ash deposited at Kalimenur, Yogyakarta Special Region Province on 16 February 2014, over two days after the eruption (Habibie 2014).

The apparent resilient nature of the diesel rail system to ashfall coincides with the lack of reported impacts on similar networks worldwide following other eruptions, with the key exception of the 1980 Mt. St Helens event (Blong 1984). This contrasts with electric rail systems which appear more vulnerable to small ash accumulations (e.g. following the Shinmoedake 2011 eruption, and Sakurajima eruptions in Japan in recent years (Magill et al. 2013)).

2.5.4 Ports

There were no major shipping ports that were impacted by heavy ashfall from the Kelud eruption, with the nearest (Tanjung Perak, Surabaya) located over 90 km to the north east. However, there are plans for a new port on the south Java coast near Yogyakarta (Daniswara (pers comm, 2014)*) which, given the same wind directions as those on 13-14 February 2014 could be exposed to future ashfall.

2.5.5 Transportation network clean-up

Previous studies of tephra-impacted cities have identified efficient clean-up operations as a way to mitigate infrastructure impacts and as a fundamental aspect of post tephra fall recovery efforts and restoration of economic activities (Wilson et al. 2012).

2.5.5.1 Proximal

In the Kediri Regency alone, approximately 2,500 military and police personnel assisted the community with clean-up using whatever suitable tools were available (Antara News 2014b, KVO 2014*). As occurred in some areas of Yogyakarta, it appears that a coordinated approach was adopted with many clean-up activities in proximal areas occurring at the same time and involving many people (Figure 2.16). By 04:00 on 14 February (around 5 hours after the eruption), tephra had been moved to the sides of some roads in the Ngancar District including the road leading to the KVO from Sugihwaras Village (KVO 2014*). This was largely achieved using *ongsrok*, a wooden implement similar in design to a rake but with a wooden plank instead of metal teeth (Figure 2.17). Tephra was taken from roadsides to be sold for construction material, which essentially offset the cost of clean-up (KVO 2014*). The coarser properties of tephra in proximal areas meant that it was more suitable for construction purposes than that in distal regions (Purwana (pers comm, 2014)*).

Figure 2.16 A coordinated approach to clean-up was adopted in many areas. (a) Residents cleaning a street together in the Kediri Regency (Irvine-Brown 2014). (b) TNI staff help to clear streets in Pandansari Village, Ngantang District, Malang Regency (Washington Post 2014).

Figure 2.17 Clean-up using *ongsrok*, a common tool used for clean-up of ash consisting of a wooden pole and small plank of wood (Tempo.co 2014).

2.5.5.2 Distal

On Friday 14 February around 20-30 mm (up to 50 mm in places) of fine-grained tephra fell on Yogyakarta from the eruption of Kelud (BPBD DIY 2014a*, BPBD DIY 2014b, DJPD & DJPL 2014*). Official clean-up operations, under the control of BPBD DIY, did not begin until the morning of Saturday 15 February 2014. BPBD DIY and the Governor asked all parts of the community to join government workers to assist with clean-up operations (BPBD DIY 2014a*, BPBD DIY 2014b). Two thousand military and police personnel were allocated to assist with clean-up efforts in the city and at AIA, Yogyakarta (Muryanto 2014). It was reported that tephra was still falling when the clean-up began, although this could have been tephra remobilising out of trees (BPBD DIY 2014a*). A major clean-up effort was conducted at the end of the weekend on Sunday 16 February. The clean-up was prioritised to remove ash from critical infrastructure facilities (BPBD DIY 2014a*, DJPD & DJPL 2014*).

At AIA, The runway, along with all airport buildings had to be completely cleaned before the airport could re-open (DJPU 2014*). Clean-up operations began on 15 February and it was hoped that the airport would re-open on Tuesday 18 February, but clean-up operations took longer than expected and re-opening was delayed until Wednesday 19 February (Muryanto & Susanto 2014). In an effort to remove ash from the runway as quickly as possible, it was initially swept into drainage channels on the first day of clean-up, largely using *ongsrok* tools (Figure 2.17). The following day, ash was removed from the drainage channels and placed into bags, which BPBD DIY then collected for disposal. Shovels were used to remove the bulk of the ash, before brooms were used for the last few millimetres (DJPU 2014*). Seven water cannons were sourced from the Yogyakarta Fire Department. These were only used for the clean-up at night as they were required for other purposes elsewhere during the day. The water cannon belonging to AIA was not used for clean-up purposes as it was thought to be too powerful, potentially damaging paved surfaces. Water for cleaning AIA was extracted from two nearby rivers using the Fire Department's water pump (DJPU 2014*).

BPBD DIY instructed those cleaning up in the city that ash should not be swept into drainage networks because it could clog them. They also advised to keep water use to a minimum for the same reason and also to prevent surfaces becoming slippery. In Yogyakarta, ash was mainly collected using manual tools such as brooms and shovels, and placed into 50 kg sacks. The full bags were then collected from the roadside by more than 50 BPBD DIY trucks along with many trucks provided by military, the Provincial Public Works Agency, and private operators, and driven to temporary storage sites. Clean-up in Yogyakarta came to a total cost of around Rp 3 billion (NZ$ 315,000) with around Rp 1 billion (NZ$ 105,000) coming from the nation.

2.5.5.3 Clean-up challenges

The clean-up in Yogyakarta was initially very difficult because the fine-grained tephra meant it was easily remobilised by vehicles (DJPD & DJPL 2014*). This necessitated the spraying of tephra with water from hoses and water cannons to consolidate it before it was collected and removed in bags

(BPBD DIY 2014a*, BPBD DIY 2014b). However, difficulties were experienced when too much water was added causing tephra to become cemented and stick to paved surfaces (UPN 2014*). Light rainfall (~2-8 mm per day) until 17 February may have added to these difficulties. Ash adhered to the leaves of trees and was later dislodged and remobilised by wind, settling onto previously cleaned roads (BPBD DIY 2014a*, DJPD & DJPL 2014*). As such, the clean-up was easier in Yogyakarta than in the surrounding villages because there are fewer trees for ash to accumulate on in the urban area (DJPD & DJPL 2014*). Overall clean-up was aided by the heavy rain (~15 mm) which arrived on Tuesday 18 February in Yogyakarta, causing most remaining ash in trees and on roofs to fall to the ground (BPBD DIY 2014a*, DJPD & DJPL 2014*, UPN 2014*). If this rain had arrived earlier in the clean-up process, before the majority of ash had been removed, it may well have led to blocked drains and flooding. Heavy rain arrived earlier (~11 mm on 15 February) in Semarang, located ~230 km NW of Kelud. However, as only light ashfall occurred in the city, the rain helped to clean ash from the streets without any flooding problems reported (Suherdjoko & Ayuningtyas 2014).

2.6 Discussion

A variety of data is ideal for compiling contemporary volcanic risk assessments. The post-eruption impact assessment following the Kelud 2014 eruption has provided contributions in the form of qualitative and semi-quantitative empirical vulnerability data in particular. Volcanic tephra fall was clearly a key hazard responsible for much of the critical infrastructure damage and disruption. Despite the eruption being very short-lived, disruption from ashfall was long-lasting and widespread, especially in the distal study area. This emphasises the advantages of considering multiple hazards for risk assessments, as incorporating impacts from ashfall, in addition to impacts from proximal volcanic hazards, is important for improving DRR strategies (UNISDR 2015) and reducing economic loss.

The importance of transportation functionality and consequences for society during volcanic eruptions has been one of the crucial factors highlighted by this post-eruption study. In particular, low visibility and reduced skid resistance on ash-covered roads was an issue in several locations and attributed to increased accident rates. However, surface transportation networks continued to operate in many areas outside of exclusion zones, albeit with a reduced level-of-service in some cases. This indicates the importance of incorporating indicators of functionality reduction in future risk assessments to account for areas of transportation networks that are disrupted, but not necessarily physically damaged or closed. Such indicators are especially relevant in locations such as Java where there has traditionally been a strong focus on infrastructure destruction (rather than disruption). Additionally, the impacts on functionality, along with the unexpected ashfall impacts in distal locations, suggests that operational advice could be useful to mitigate impacts in future eruptions. For example, HIM thresholds to represent functionality reduction could act as useful prompts for the initiation of mitigation measures by transport operators including speed restrictions and clean-up activities.

The study has demonstrated the potential influence of particle size as well as ash thickness on critical infrastructure functionality. For example, accidents due to slippery road surfaces appeared to be more commonplace in proximal areas where the ash was coarse, and visibility impairment was frequently reported in distal areas where the fine-grained ash was readily remobilised. However, the hazard intensity thresholds (in terms of precise ash thickness and particle size distribution for example) attributed to such impacts remain unclear. Such information would enable a better understanding of the capacity of infrastructure elements to withstand hazards, strengthening resilience in the future (Tierney and Bruneau 2007, Ayyub 2014, UNISDR 2015). A system's ability to perform without immediate maintenance or repair is a desirable resilient feature (Vugrin 2016). From the post-eruption study, diesel rail transportation networks appear particularly resilient when they encounter light ashfall, suggesting that diesel rail could be a less vulnerable transportation mode during future eruptions.

Effective communication between different groups was evident from the post-eruption studies, an important concept to aid risk management. Various risk management successes were demonstrated through the mitigation strategies implemented before, during and after the eruption, such as the widely obeyed advice by motorists to not travel unless absolutely necessary and coordinated and collaborative approach to clean-up. However, the clean-up was clearly very labour and resource intensive which is another important consideration for recovery planning during future eruptions.

2.7 Summary and Conclusions

Post-eruption impact assessment studies enable a better understanding of the components of risk – hazard, exposure, and particularly vulnerability. They allow better risk assessments in the future through more appropriate estimations of consequences for society, including damage and disruption to critical infrastructure. The improved risk assessments can inform management strategies before, during and/or following volcanic eruptions, increase preparedness for response and recovery, and strengthen resilience (UNISDR 2015).

The short-lived VEI 4 eruption of Kelud on 13-14 February 2014 produced many volcanic hazards including PDCs, ballistics, landslides and lahars close to the volcano itself, in addition to tephra, with volcanic ash dispersed by winds up to 600 km from the vent. Relatively thick tephra accumulated in proximal areas ~0-10 km to the north east and in a zone ~200-250 km west of the vent. Tephra accumulations of 200-500 mm in some proximal areas led to severe consequences for agriculture and critical infrastructure including surface transportation. However, impacts to transportation networks, particularly in terms of reduced functionality, were extensive in distal areas including Yogyakarta, located ~220 km to the west of the vent. The total economic impact of the eruption is difficult to calculate, although soon after the eruption, the PMI estimated it could be in the region of Rp 1.2 trillion (~NZ$ 122 million) (IFRC 2014).

In proximal areas, the already established and strong relationships between staff at organisations such as the three BPBDs, KVO and community groups (including representatives of the risk reduction platform, JANGKAR Kelud), appear to have aided the rapid dissemination of consistent warnings and information. Much of the general population reacted quickly upon receiving official advice, not hesitating to evacuate. However, not all hamlets in the proximal areas received warning messages in advance of the eruption with some evacuating as soon as the eruption began, utilising transportation routes affected by fresh volcanic hazards. In Yogyakarta, little to no warning of the Kelud eruption and potential impacts was received or disseminated until ash fell, around four hours following the eruption. Distal volcanoes to Yogyakarta such as Kelud perhaps receive less focus in terms of preparedness measures as they are out-of-sight and often more 'out-of-mind' than nearby Merapi volcano. However, ash from the 2014 Kelud eruption caused more problems in Yogyakarta than that from the 2010 Merapi eruption, particularly as it was more widespread and of finer grain size (hence readily remobilised). A state of emergency for Yogyakarta Special Region Province was declared in the day following the Kelud eruption. Interviews and discussions with staff at various organisations and members of the public in distal areas revealed that the Kelud ashfall and associated impacts came as a huge surprise to most.

Impacts to transportation infrastructure in the three regencies on the flanks of Kelud varied spatially and with hazard intensity. There was complete destruction to parts of the network from the immediate proximal hazards, particularly ballistics, PDCs and landslides. Lahars in the days following the eruption caused further destruction, completely destroying some bridges. Some surface flooding due to blocked drains occurred in village centres. Severe impacts occurred in many of the hamlets within ~7-10 km of the vent with tephra causing reduced visibility and skid resistance as it fell, and accumulations of up to ~500 mm requiring extensive clean-up. In Yogyakarta, there was substantial disruption to the road network in the city, particularly due to reduced skid resistance and impaired visibility, making it difficult to drive. Risk management strategies included the cancellation of bus services and communication of government advice for people to stay off the roads. Despite fewer vehicles however, the number of accidents increased. Effects to aviation were global as four of the seven Indonesian airports that were closed usually service international flights. The closure (some for up to a week) caused flight cancellations and disruption throughout Java and further afield including Australia. One aircraft flew through the Kelud ash cloud around six hours after the eruption and sustained heavy repair costs as a result. Resilience to ashfall was evident in the diesel rail system where the number of train services and capacity was increased to cater for the higher number of passengers resulting from aviation and road transportation disruption.

Following return of residents, a proactive and collaborative approach was largely taken for tephra clean-up and recovery. Various people including workers and staff from the BPBDs, Provincial Public Works Agency, military, police, fire brigades, volunteers and many residents worked together to clean vehicles, public and residential buildings, trees and streets. Spraying fine-grained ash with water and clearing immediately after was deemed effective for minimising ash remobilisation. Some recovery

processes were temporary, such as the replacement of bridges with river crossings or military-built structures until funds permit more permanent structures to be built.

The impact assessment trip following the Kelud 2014 eruption has highlighted several important considerations for future volcanic risk assessments that cover the vulnerability of transportation networks:

- Multi-hazard vulnerability and resilience is key for thorough risk assessments. Qualitative and semi-qualitative post-eruption findings demonstrated the importance and widespread and long-lasting effects of volcanic ash, in addition to proximal hazards, on transportation impacts.

- Functionality of surface transportation, particularly road networks, can have substantial consequences for society. Although routes may remain operational when affected by volcanic ash, level-of-service may be reduced through less skid resistance and impaired visibility and associated increases in accident rates. Disruption from volcanic ash could be extensive, whereas destruction or severe damage from hazards such as PDCs and ballistics is often confined to a smaller areas proximal to vents.

- Further work is required to determine hazard intensity thresholds responsible for transportation impacts. The Kelud study has indicated approximate ash thicknesses that may be attributable for specific impacts but further quantitative data is required to refine thickness thresholds. In addition to informing impact states, such thresholds would be desirable to inform volcanic deposit clean-up strategies. The study has also highlighted that other HIMs (besides ash thickness – particularly ash particle size) may also play important roles on the level of impact that occurs, so further work should also assess the relevance of such alternative HIMs.

- Many of the risk mitigation strategies implemented at Kelud and in affected areas appeared highly successful. For example, the clean-up of transportation routes was conducted in a coordinated and collaborative manner, effectively reducing volcanic risk. This was likely a result of the effective communication between various stakeholders before, during and after the time of crisis, which should be encouraged in other volcanically active areas.

The following chapters of this thesis consider all of these points, contributing further to future volcanic risk assessments.

2.8 Acknowledgments

We thank the University of Canterbury Mason Trust scheme, Natural Hazards Research Platform (contract C05X0804), New Zealand Earthquake Commission (EQC) and Determining Volcanic Risk in

Auckland (DEVORA) project for their financial support towards the field trip to Indonesia, both directly and through the provision of funding for the researchers involved in the study.

We express sincere thanks for the support of the many people in Indonesia involved in the work whose help was vital to the success of this report. In particular we wish to thank Muhammad Hendrasto, chief of the CVGHM, and his team in Bandung for granting permission for our work in Indonesia to take place. The interpreters, drivers and field support provided by Kakadu Tour and Travel and UPN in Yogyakarta were outstanding. They included Mahjum, Purwana (aka. Luna), Riswanda Daniswara (aka. Dadan), 'Bruno', and Djoni Ferdiwijaya, an independent consultant at the time of our visit. The findings would not have been possible without the participation of the organisations, residents and workers with whom we held thirty-three interviews and formal discussions in Yogyakarta and closer to Kelud. We express our particular thanks to staff from BPBD Blitar Regency, BPBD DIY, DJPD, DJPL, DJPU, KVO, PMI, PT-JTT and UPN. Daniel Blake would also like to thank Edouard De Bélizal (Université Paris-Est), Ian Goodwin (Airbus), Cyndee Seals (Darwin VAAC) and Luna (Kakadu Tour and Travel, Yogyakarta) for the provision of additional information.

The team was supported in New Zealand by Professor Jim Cole of the University of Canterbury who made edits to the GNS Science report (Appendix A) from which this thesis section is derived. We also thank our peer reviewers, Nico Fournier and Bradley Scott of GNS Science for their comments and suggestions following thorough reviews of the initial report.

2.9 References

3News (2014) Cleanup begins after Mt Kelud eruption, 3News. http://www.3news.co.nz/world/cleanup-begins-after-mt-kelud-eruption-2014021707, Accessed 07 October 2014.

ABC News (2014a) Mount Kelud, Java Island erupts, ABC News. http://abcnews.go.com/International/wireStory/indonesias-mount-kelud-java-island-erupts-22502220, Accessed 05 March 2014.

ABC News (2014b) Plane in Yogyakarta covered in ash from Mt Kelud eruption. http://www.abc.net.au/news/2014-02-15/plane-in-yogyakarta-covered-in-ash-from-mt-kelud-eruption/5262122, Accessed 15 October 2014.

Adonai (2014) Eruption of Mt. Kelut disrupted fresh water supply in districts around the volcano, The Watchers. http://thewatchers.adorraeli.com/2014/03/07/eruption-of-mt-kelut-disrupts-fresh-water-supply-in-districts-around-the-volcano/, Accessed 25 October 2014.

Andreastuti, S. Budianto, A. Heriwaseso, A. Gunawan, H. Prianto, B. (2015) The 2014 eruption of Kelud volcano: An example of typical short duration and large plinian eruption. Prosiding Pertemuan Imiah Tahunan Ikatan Ahli Bencana Indonesia (Proceeding of Annual Meeting of Indonesian Disaster Expert Association), Yogyakarta, May 2015.

Antara News (2014a) Tourists, local people join hands in Borobudur local cleanup, Antara News. http://www.antaranews.com/en/news/92820/tourists-local-people-join-hands-in-borobudur-temple-cleanup, Accessed 24 October 2014.

Antara News (2014b) 2,500 personnel to clean up volcanic ashes, Antara News. http://www.antarajatim.com/lihat/berita/127204/2500-personnel-to-clean-up-volcanic-ashes, Accessed 28 October 2014.

Australian (2014) Flights hit as Indonesian volcano erupts, spewing ash into atmosphere, The Australian. http://www.theaustralian.com.au/news/world/flights-hit-as-indonesian-volcano-erupts-spewing-ash-into-the-atmosphere/story-e6frg6so-1226827133251, Accessed 07 November 2014.

Ayyub, B.M. (2014) Systems resilience for multihazard environments: definition, metrics, and valuation for decision making. Risk Analysis, 34:2, pp.340–55.

Baku-APA (2014) Death toll rises to four in Indonesian volcano eruption, Baku-APA. http://en.apa.az/news/207168, Accessed 31 October 2014.

Barnard, S. (2004) Results of a reconnaissance trip to Mt. Etna, Italy: the effects of the 2002 eruption of Etna on the province of Catania. Bulletin of the New Zealand Society for Earthquake Engineering, 37:2, pp.47–61.

Baxter, P.J. Boyle, R. Cole, P. Neri, A. Spence, R. Zuccaro, G. (2005) The impacts of pyroclastic surges on buildings at the eruption of the Soufrière Hills volcano, Montserrat. Bulletin of Volcanology, 67:4, pp.292–313.

Blong, R.J. (1984) Volcanic hazards: a sourcebook on the effects of eruptions. Academic Press, New South Wales, Australia.

BNPB (2009) Indonesian National Disaster Management Plan 2010-2014, Badan Nasional Penanggulangan Bencana. http://www.preventionweb.net/english/professional/policies/v.php?id=26349, Accessed 20 October 2014.

BNPB (2014) 50 juta meter kubik ancam lahar dingin lereng Kelud (50 million cubic meters of cold lava threaten slopes of Kelud), Badan Nasional Penanggulangan Bencana. http://bnpb.go.id/berita/1930/50-juta-meter-kubik-ancam-lahar-dingin-lereng-kelud, Accessed 07 October 2014.

Boediwardhana, W. Harsaputra (2014) Kelud causes billions in losses, The Jakarta Post. http://www.thejakartapost.com/news/2014/02/17/kelud-causes-billions-losses.html. Accessed 07 October 2014.

BOM (2014) Kelut: 13/02/2014. Darwin Volcanic Ash Advisory Centre, Bureau of Meteorology, Australia.

BPBD Blitar Regency (2014a) Foto dokumentasi erupsi Gunung Kelud (photo documentation of the Kelud eruption). BPBD Kabupaten Blitar (BPBD Blitar Regency), East Java, Indonesia.

BPBD Blitar Regency (2014b) Interview with staff at Badan Penanggulangan Bencana Daerah Kabupaten Blitar (Disaster Management Agency of Blitar Regency), Wlingi, East Java, Indonesia. Conducted on 22 September 2014.

BPBD DIY (2014a) Interview with staff at Badan Penanggulangan Bencana Daerah Istimewa Yogyakarta (The disaster management agency of Yogyakarta Special Region Province), Yogyakarta, Indonesia. Conducted on 15 September 2014.

BPBD DIY (2014b) BPBD DIY report on the Kelud 2014 eruption. BPBD Yogyakarta, Yogyakarta Special Region Province, Indonesia.

BPS (2010) Population. Badan Pusat Statistik; Statistics Indonesia. http://www.bps.go.id/Subjek/view/id/12#subjekViewTab3|accordion-daftar-subjek1, Accessed 01 November 2016.

Crichton, D. (1999) The risk triangle. IN: Ingleton, J. (Ed.) Natural Disaster Management. Tudor Rose, London.

CVGHM (2014a) Penurunan Status G. Kelud Dari Awas (level iv) Menjadi Siaga (level iii), 20 Februari 2014, The Indonesian Centre for Volcanology and Geological Hazard Mitigation. http://www.vsi.esdm.go.id/index.php/gunungapi/aktivitas-gunungapi/326-penurunan-status-g-kelud-dari-awas-level-iv-menjadi-siaga-level-iii-20-februari-2014, Accessed 03 March 2014.

CVGHM (2014b) Penurunan Status G. Kelud Dari Siaga (level iii) Menjadi Waspada (level ii), 28 Februari 2014, The Indonesian Centre for Volcanology and Geological Hazard Mitigation. http://www.vsi.esdm.go.id/index.php/gunungapi/aktivitas-gunungapi/353-penurunan-status-g-kelud-dari-siaga-level-iii-menjadi-waspada-level-ii-28-februari-2014-, Accessed 03 March 2014.

CVGHM (2014c) Peningkatan Status G. Kelud Dari Siaga (level iii) Menjadi Awas (level iv), 13 Februari 2014, The Indonesian Centre for Volcanology and Geological Hazard Mitigation. http://www.vsi.esdm.go.id/index.php/gunungapi/aktivitas-gunungapi/319-peningkatan-status-g-kelud-dari-siaga-level-iii-menjadi-awas-level-iv-13-februari-2014-, Accessed 20 February 2014.

CVGHM (2014d) Penurunan Status Aktivitas G. Kelud Dari Waspada (level ii) Menjadi Normal (level i), The Indonesian Centre for Volcanology and Geological Hazard Mitigation. http://www.vsi.esdm.go.id/index.php/gunungapi/aktivitas-gunungapi/603-penurunan-status-aktivitas-g-kelud-dari-waspada-level-ii-menjadi-normal-level-i, Accessed 06 November 2014.

CVGHM (2014e) Perkembangan Aktivitas G. Kelud Status Siaga (level iii) Tanggal 21 Februari 2014 Hingga Pukul 06:00 Wib, The Indonesian Centre for Volcanology and Geological Hazard Mitigation. http://www.vsi.esdm.go.id/index.php/gunungapi/aktivitas-gunungapi/345-perkembangan-aktivitas-g-kelud-status-siaga-level-iii-tanggal-21-februari-2014-hingga-pukul-0600-wib, Accessed 03 March 2014.

Daniswara, R. (personal communication, September 2014). Student at Disaster Research, Education and Management (DREAM) Centre, Universitas Pembangunan Nasional (UPN) Veteran Yogyakarta (National Development University, Yogyakarta), Sleman Regency, Yogyakarta, Indonesia.

Dawet vendor (personal communication, 18 September 2014). Drinks seller near BPBD DIY Office, Yogyakarta, Indonesia.

De Bélizal, E. Lavigne, F. Gaillard, J.C. Grancher, D. Pratomo, I. Komorowski, J-C. (2012) The 2007 eruption of Kelut volcano (East Java, Indonesia): Phenomenology, crisis management and social response. Geomorphology, 136, pp.165-175.

De Bélizal, E. (2014) Resource, vulnerability, resilience and risk at Merapi volcano: is sand mining a sustainable livelihood? Presentation at the Cities on Volcanoes 8 Conference, Iniversitas Gadjah Mada, Yogyakarta, Indonesia. Conducted on 13 September 2014.

divagis.org (2014) Free spatial data: Indonesia. http://www.diva-gis.org/Data, Accessed 01 March 2014.

DJPD, DJPL (2014) Interview with staff at the Direktorat Jenderal Perhubungan Darat (Directorate General of Land Transportation) and Direktorat Jenderal Perhubungan Laut (Directorate General of Sea Transportation), Kementerian Perhubungan (Ministry of Transportation), Yogyakarta, Indonesia. Conducted on 17 September 2014.

DJPU (2014) Interview with staff at the Direktorat Jenderal Perhubungan Udara (Directorate General of Civil Aviation), Kementerian Perhubungan (Ministry of Transportation), Yogyakarta, Indonesia. Conducted on 17 September 2014.

EASA (2014) Volcanic ash ingestion in turbine engines: Explanatory note to ED decision 2014/027/R and comment-response document 2012-21. European Aviation Safety Agency, Rulemaking Directorate. http://easa.europa.eu/system/files/dfu/Explanatory%20Note%20to%20ED%20Decision%202014-027-R%20and%20CRD%202012-21.pdf, Accessed 07 October 2014.

EDSM (2014) Activity of Kelud volcano. Kementerian Energi Dan Sumber Daya Mineral (Ministry of Energy and Mineral Resources), Indonesia. https://docs.unocha.org/sites/dms/ROAP/Indonesia/Documents/BriefingSheetKelud_23022014_English.pdf, Accessed 25 February 2015.

Fadeli, A. (2012) Volcanic earthquakes at Merapi (Central Java) during the lava dome building beginning in October 1986. IN: Gasparini, P. Scarpa, R. Aki, K. (Eds.) Volcanic Seismology, Science.

Foo, A. Tan, L. (2014) Volcanic Ash and Aviation Safety: The Leading Edge, Civil Aviation Authority of Singapore. http://www.caas.gov.sg/caas/en/About_CAAS/Our_Publications/EDM/2014/may2014/theLEADINGedge_issue2_2014.pdf, Accessed 07 October 2014.

GoogleEarth (2014) 7°56'32.16"S 112°18'19.25"E. Kelud Volcano, East Java Province, Indonesia 19 May 2014 and 23 August 2012. Retrieved 28 December 2014.

Goodwin, I. (personal communication, 05 December 2014) Head of product safety enhancement, Airbus, Toulouse, France. Email correspondence.

Gough, D. (2014) Ash from 'most dangerous' volcano delays more flights. The Traveller. http://www.traveller.com.au/ash-from-most-dangerous-volcano-delays-more-flights-32s9i, Accessed 07 October 2014.

Guffanti, M. Mayberry, G.C. Casadevall, T.J. Wunderman, R. (2009) Volcanic hazards to airports. Natural Hazards, 51, pp.287-302.

GVP (2014a) Kelut: Background, Smithsonian Institution Global Volcanism Program. http://www.volcano.si.edu/volcano.cfm?vn=263280, Accessed 14 October 2014.

GVP (2014b) Kelut: Eruptive history, Smithsonian Institution Global Volcanism Program. http://www.volcano.si.edu/volcano.cfm?vn=263280, Accessed 13 October 2014.

GVP (2014c) Kelut (Kelud), Java, Indonesia, Smithsonian Institution Global Volcanism Program. http://www.volcano.si.edu/volcanoes/region06/java/kelut/3902Kelut.pdf, Accessed 07 October 2014.

GVP (2014d) Kelut: Bulletin reports, Smithsonian Institution Global Volcanism Program. http://www.volcano.si.edu/volcano.cfm?vn=263280, Accessed 18 October 2014.

Habibie, R. (2014) Running with dust, Flickr. http://www.flickr.com/photos/bieb/12560914674/, Accessed 15 October 2014.

Haryanti, D. (2014) KOSTRAD TNI-AD: TNI membantu warga menyeberangi Kali Sambong di Desa Pandansari, Ngantang, Jawa TImur, Rabu (19/2). http://www.flickr.com/photos/110095122@N02/12630241045/, Accessed 15 October 2014.

Health Agency DIY (2014) Interview with staff at Dinas Kesehatan Provinsi Daerah Istimewa Yogyakarta, Republik Indonesia (Health Agency of Yogyakarta Special Region Province), Yogyakarta, Indonesia. Conducted on 16 September 2014.

IAVCEI (1999) Professional conduct of scientists during volcanic crises. Bulletin of Volcanology, 60, pp.323-334.

IFRC (2014) Emergency plan of action (EPoA) Indonesia: Volcanic eruption - Mt Kelud. International Federation of Red Cross and Red Crescent Societies. http://reliefweb.int/report/indonesia/indonesia-volcanic-eruption-mt-kelud-emergency-plan-action-epoa-operation-n, Accessed 07 July 2014.

Indonesian Session (2014) Indonesian session: Community speaks. Cities on Volcanoes 8 Conference, Universitas Gadjah Mada, Yogyakarta, Indonesia. Conducted on 13 September 2014.

Irvine-Brown, R. (2014) Java volcano: Reactions from Kediri to Bandung, BBC News. http://www.bbc.com/news/world-asia-pacific-26193586, Accessed 09 October 2014.

Jakarta Globe (2014) Mount Kelud ash expected to fall on Jakarta, The Jakarta Globe. http://thejakartaglobe.beritasatu.com/news/mount-kelud-ash-expected-to-fall-on-jakarta/, Accessed 06 November 2014.

Jakarta Post (2014a) Mt. Kelud eruption paralyzes Java, The Jakarta Post. http://www.thejakartapost.com/news/2014/02/15/mt-kelud-eruption-paralyzes-java.html, Accessed 28 November 2014.

Jakarta Post (2014b) Farmers receive post-eruption aid, The Jakarta Post. http://www.thejakartapost.com/news/2014/03/05/farmers-receive-post-eruption-aid.html, Accessed 20 October 2014.

Jakarta Post (2014c) Mt. Kelud death toll revised down to 4, The Jakarta Post. http://www.thejakartapost.com/news/2014/02/16/mt-kelud-death-toll-revised-down-4.html, Accessed 31 October 2014.

Jenkins, S. Komorowski, J.C. Baxter, P. Spence, R. Picquout, A. Lavigne, F. Surono (2013) The Merapi 2010 eruption: An interdisciplinary impact assessment methodology for studying pyroclastic density current dynamics. Journal of Volcanology and Geothermal Research, 261, pp.316-329.

Jenkins, S.F. Spence, R.J.S. Fonseca, J.F.B.D. Solidum, R.U. Wilson, T.M. (2014) Volcanic risk assessment: quantifying physical vulnerability in the built environment. Journal of Volcanology and Geothermal Research, 276, pp.105-120.

Kalikuning (2014) Interview with Kalikuning Village residents / farmers, Blitar Regency, East Java Province, Indonesia. Conducted on 22 September 2014.

Karanganyar (2014) Interview with Karanganyar Village residents, Blitar Regency, East Java Province, Indonesia. Conducted on 22 September 2014.

Klangon (2014) Interview with sand miner in Sambong River, next to Kalngon Hamlet, Pandansari Village, Ngantang District, Malang Regency, East Java Province, Indonesia. Conducted on 21 September 2014.

Konto (2014) Interview with w*arung* owners next to Konto River bridge, near Kandangan, East Java Province, Indonesia. Conducted on 20 September 2014.

KVO (2014) Interview with staff at the Kelud Volcano Observatory, Sugihwaras Village, Ngancar District, Kediri Regency, East Java Province, Indonesia. Conducted on 20 September 2014.

Laia, K.C. (2014) Power of Kelud's eruption explains ash cloud's reach, The Jakarta Globe. http://thejakartaglobe.beritasatu.com/news/power-of-keluds-eruption-explains-ash-clouds-reach/, Accessed 06 November 2014.

Leonard, G.S. Johnston, D.M. Williams, S. Cole, J.W. Finnis, K. Barnard, S. (2006) Impacts and management of recent volcanic eruptions in Ecuador: lessons for New Zealand. GNS Science Report 2005/20, 52p.

Luwakmas Café (2014) Interview with staff at Luwakmas Family Café and Restro, Sugihwaras Village, Ngancar District, Kediri Regency, East Java Province, Indonesia. Conducted on 20 September 2014.

Magill, C. Blong, R. (2005). Volcanic risk ranking for Auckland, New Zealand. II: hazard consequences and risk calculation. Bulletin of Volcanology, 67, pp.340-349.

Magill, C. Wilson, T. Okada, T. (2013) Observations of tephra fall impacts from the 2011 Shinmoedake eruption, Japan. Earth, Planets and Space, 65, pp.677-698.

Mahjum (personal communication, September 2014). Tour Manager, Kakadu Tour and Travel, Yogyakarta, Indonesia.

Mau Ke Mana (2014) Helping you to see more of Indonesia: Indonesian Train Timetable and Map. http://flights.indonesiamatters.com/train-timetable-indonesia/, Accessed 15 October 2014.

Mulyana, A.R. Nasution, A. Martono, A. Sumpena, A.D. Purwoto. Santoso, M.S. (2004) Peta Kawasan Rawan Bencana Gunungapi Kelud, Propinsi Jawa Timur (Volcanic hazards map of Kelud Volcano, East Java Province. Direktorat Vulkanologi Dan Mitigasi Bencana Geologi (Centre of Volcanology and Geological Hazard Mitigation, CVGHM), Indonesia

Munjang (2014a) Interview with farmer / Munjang resident in fields to south of Munjang Hamlet, Pandansari Village, Ngantang District, Malang Regency, East Java Province, Indonesia. Conducted on 21 September 2014.

Munjang (2014b) Interview with residents at a house being renovated in Munjang Hamlet, Pandansari Village, Ngantang District, Malang Regency, East Java Province, Indonesia. Conducted on 21 September 2014.

Muryanto (2014) Volcanic ash slows down airport cleanup, The Jakarta Post. http://www.thejakartapost.com/news/2014/02/15/volcanic-ash-slows-down-airport-cleanup.html, Accessed 24 October 2014.

Muryanto, B. Susanto, S. (2014) Airport, temples reopen but Mt. Kelud high alert remains, The Jakarta Post. http://www.thejakartapost.com/news/2014/02/20/airport-temples-reopen-mt-kelud-high-alert-remains.html, Accessed 07 October 2014.

Nakada, S. (2014) Recent eruptions in Japan and Indonesia and related research. Keynote Speech. Cities on Volcanoes 8 Conference, Universitas Gadjah Mada, Yogyakarta, Indonesia. Conducted on 09 September 2014.

Nania, J. Bruya, T.E. (1982) In the wake of Mt St Helens. Annals of Emergency Medicine, 11:4, pp.184-191.

Picquout, A. Lavigne, F. Mei, E.T.W. Grancher, D. Noer, C. Vidal, C.M. Hadmoko, D.S. (2013) Air traffic disturbance due to the 2010 Merapi volcano eruption. Journal of Volcanology and Geothermal Research, 261, pp.366-375.

Pitaloka, D.A. (2014) Torrential rain worsens Kelud misery, The Jakarta Globe. http://thejakartaglobe.beritasatu.com/news/torrential-rain-worsens-kelud-misery/?doing_wp_cron=1396750361.2484030723571777343750, Accessed 09 October 2014.

PT-JTT (2014) Interview with staff at PT. Jogja Tugu Trans (the Trans Jogja Bus Transport Company), Yogyakarta, Indonesia. Conducted on 16 September 2014.

Purwana (personal communication, September 2014). Translator and Guide, Kakadu Tour and Travel, Yogyakarta, Indonesia.

Rossetto, T. Ioannou, I. Grant, D.N. (2013) Existing empirical vulnerability and fragility functions: compendium and guide for selection. GEM Technical Report 2013-X, GEM Foundation, Pavia, Italy.

rtwilson.com (2014) Free GIS Data. http://freegisdata.rtwilson.com/#home, Accessed 01 March 2014.

Sagala, S. (2009) Implementable land use plan in volcano prone area in Indonesia: challenges and opportunities. Conference Proceedings: International Conference on Urban and Regional Planning: “Positioning Planning in Global Crises”. Institute of Technology Bandung, Bandung, Indonesia, 12-13 November 2009.

Selorejo (2014) Interview with sand miner in Sambong River, below Selorejo dam, Pandansari Village, Ngantang District, Malang Regency, East Java Province, Indonesia. Conducted on 21 September 2014.

SMH (2014) Volcano eruption cancels Bali Phuket flights and closes Indonesian airports, The Sydney Morning Herald. http://www.smh.com.au/travel/travel-incidents/volcano-eruption-cancels-bali-phuket-flights-and-closes-indonesian-airports-20140214-32qd8.html, Accessed 05 March 2014.

Suherdjoko. Ayuningtyas, K. (2014) Rain rinses Semarang, residents hand in hand to clean up Surakarta, The Jakarta Post. http://www.thejakartapost.com/news/2014/02/15/rain-rinses-semarang-residents-hand-hand-clean-surakarta.html, Accessed 24 October 2014.

Sunstar (2014) Indonesian volcano eruption a 'blessing' to some, Sunstar. http://www.sunstar.com.ph/breaking-news/2014/02/16/indonesian-volcano-eruption-blessing-some-328619, Accessed 20 October 2014.

Susanto, S. (2014) Dozens treated as a result of volcanic ash, The Jakarta Post. http://www.thejakartapost.com/news/2014/02/15/dozens-treated-a-result-volcanic-ash.html, Accessed 09 October 2014.

Sword-Daniels, V. Stewart, C. Johnston, D. Wardman, J. Wilson, T. Rossetto, T. (2011) Infrastructure impacts, management and adaptations to eruptions at Volcán Tungurahua, Ecuador, 1999-2010. GNS Science Report 2011/24, 73 p.

Tempo.co (2014) Firemen help to clean Kelud ash, Tempo.co. http://en.tempo.co/read/news/2014/02/16/055554688/Firemen-Help-to-Clean-Kelud-Ash, Accessed 24 October 2014.

Thomas, G. (2014) $20m Ash cloud damage bill, The West Australian. https://au.news.yahoo.com/thewest/a/21618743/20m-ash-cloud-damage-bill/, Accessed 08 October 2014.

Tierney, K. Bruneau, M. (2007) Conceptualizing and measuring resilience. Transportation Research News, May-June 2007, 250, pp.14–17. http://onlinepubs.trb.org/onlinepubs/trnews/trnews250_p14-17.pdf, Accessed 03 October 2016.

UNISDR (2009) UNISDR terminology on disaster risk reduction. United Nations International Strategy for Disaster Reduction, Geneva, Switzerland. http://www.unisdr.org/files/7817_UNISDRTerminologyEnglish.pdf, Accessed 21 April 2016.

UNISDR (2015) Sendai Framework for Disaster Risk Reduction (2015-2030). United Nations International Strategy for Disaster Reduction, Geneva, Switzerland. http://www.unisdr.org/we/coordinate/sendai-framework, Accessed 15 June 2016.

UPN (2014) Interview with staff at Universitas Pembangunan Nasional (UPN) Veteran Yogyakarta, (National Development University, Yogyakarta), Sleman Regency, Yogyakarta, Indonesia. Conducted on 18 September 2014.

VAAC (2014) VAAC Advisories (13-14 February 2014), Volcanic Ash Advisory Centre, Bureau of Meteorology, Australia. ftp://ftp.bom.gov.au/anon/gen/vaac/2014/. Accessed 07 October 2014.

Volcano Discovery (2014) The sub-plinan eruption of Mt Kelut volcano on 13 Feb 2014. http://www.volcanodiscovery.com/kelut/eruptions/13feb2014plinian-explosion.html, Accessed 31 October 2016.

Vugrin, E.D. (2016) Critical infrastructure resilience. IN: IRGC (2016) Resource guide on resilience. EPFL International Risk Governance Centre. V29-07-2016. http://www.irgc.org/risk-governance/resilience/, Accessed 20 September 2016.

Wardman, J. Sword-Daniels, V. Stewart, C. Wilson, T. (2012b) Impact assessment of the May 2010 eruption of Pacaya volcano, Guatemala. GNS Science Report 2012/09, 90p.

Washington Post (2014) Mount Kelud erupts in Indonesia, The Washington Post. http://www.washingtonpost.com/world/mount-kelud-erupts-in-indonesia/2014/02/14/de8c2e24-957c-11e3-afce-3e7c922ef31e_gallery.html#item0, Accessed 15 October 2014.

Wilson, T. Kaye, G. Stewart, C. Cole, J. (2007) Impacts of the 2006 eruption of Merapi volcano, Indonesia, on agriculture and infrastructure. GNS Science Report 2007/07, Lower Hutt, Wellington, New Zealand.

Wilson, T.M. Cole, J.W. Johnston, D.M. Stewart, C. Dewar, D.J. Cronin, S.J. (2011) The 1991 eruption of Volcán Hudson, Chile: Impacts on agriculture and rural communities and long term recovery. GNS Science Report 2009/66, Lower Hutt, Wellington, New Zealand.

Wilson, T.M. Stewart, C. Sword-Daniels, V. Leonard, G. Johnston, D.M. Cole, J.W. Wardman, J. Wilson, G. Barnard, S. (2012) Volcanic ash impacts on critical infrastructure. Physics and Chemistry of the Earth, 45, pp.5-23.

Wilson, T. Outes, V. Stewart, C. Villarosa, G. Bickerton, H. Rovere, E. Baxter, P. (2013) Impacts of the June 2011 Puyehue-Cordón Caulle volcanic complex eruption on urban infrastructure , agriculture and public health. GNS Science Report 2012/20, 88 p.

World Bank (2013) Transport in Indonesia, The World Bank. http://web.worldbank.org/WBSITE/EXTERNAL/COUNTRIES/EASTASIAPACIFICEXT/EXTEAPREGTOPTRANSPORT/0,,contentMDK:20458729~menuPK:2066318~pagePK:34004173~piPK:34003707~theSitePK:574066,00.html, Accessed 23 October 2014.

3. IMPACT OF VOLCANIC ASH ON ROAD AND AIRFIELD SURFACE SKID RESISTANCE

Daniel M Blake[1], Thomas M Wilson[1], Jim W Cole[1], Natalia I Deligne[2], Jan M Lindsay[3]

[1] Department of Geological Sciences, University of Canterbury, Private Bag 4800, Christchurch, New Zealand

[2] GNS Science, 1 Fairway Drive, Avalon 5010, PO Box 30-368, Lower Hutt 5040, New Zealand

[3] School of Environment, The University of Auckland, Private Bag 92019, Auckland, New Zealand

Journal: Transportation Research Part D: Transport and Environment

Received: 01 February 2016

Current Status: In Review

3.1 Abstract

Volcanic ash deposited on paved surfaces during volcanic eruptions compromises skid resistance, which is a major component of road and airfield safety. This can result in increased stopping distances for vehicles and higher accident rates. Impacts can be widespread and long lasting, particularly during eruptions that continue for weeks to months and where ash is readily dispersed or remobilised by wind, vehicles or other human activity. Despite numerous anecdotal observations to this effect, few detailed studies have quantified the impacts of volcanic ash on skid resistance. It is important to fill this knowledge gap, as the effects of thin ash deposits in particular present a source of uncertainty for impact and loss assessment models. We adopt the British pendulum test method in laboratory conditions to investigate the skid resistance of road asphalt and airfield concrete surfaces covered by ash sourced from various locations in New Zealand. Controlled variations in ash characteristics include type (rhyolite and basalt), depth (up to 9 mm thick), wetness, particle size and soluble components. We use Stone Mastic Asphalt (SMA) for most road surface tests. However, we also test porous asphalt and line-painted road surfaces, and a roller screed concrete mix used for airfields. Due to their importance for skid resistance, SMA surface macrotexture and microtexture are analysed with semi-quantitative image analysis, microscopy and a standardised sand patch volumetric test, which enables determination of the relative effectiveness of different cleaning techniques. We find that SMA surfaces covered by thin deposits (~1 mm) of ash result in skid resistance values slightly lower than those observed on wet uncontaminated surfaces. At these depths, a higher relative soluble content for low-crystalline ash and a coarser particle size results in lower skid resistance. Skid resistance results for relatively thicker deposits (3-5 mm) of non-vesiculated basaltic ash are similar to those for thin deposits. Although there is initially little difference in skid resistance between surfaces covered in dry or wet ash, testing indicates that surfaces covered by wet ash remain slippery for longer. There are similarities between road asphalt and airfield concrete, although there is little difference in skid resistance between bare airfield surfaces and airfield surfaces covered by 1 mm of ash. Based on our findings, we provide recommendations for maintaining road safety in a volcanic ash environment and suggest effective road cleaning techniques.

3.2 Introduction

Functional transport networks are critical for society both under normal operating conditions and in emergencies. During volcanic eruptions, transport networks may be required for the evacuation of residents, to allow sufficient access for emergency services or military personnel to enter affected areas and for regular societal activities. Once direct threats have subsided, transport networks are crucial for both immediate and long-term recovery, including the clean-up and disposal of pyroclastic material, and restoration of services and commerce. Thus, it is imperative that effective and realistic transport management strategies are incorporated into volcanic contingency planning in areas where

society and infrastructure are at risk (e.g., Auckland, New Zealand; Kagoshima, Japan; Mexico City, Mexico; Naples, Italy; Yogyakarta, Indonesia).

Volcanic eruptions produce many hazards. Damage to transport from proximal hazards such as lava flows, pyroclastic density currents and lahars is often severe, leaving ground routes impassable and facilities such as airports closed or inoperable. Volcanic ash (ejected material with particle sizes <2 mm in diameter) is widely dispersed and, although not necessarily damaging to static transport infrastructure, is generally the most disruptive of all volcanic hazards (Johnston and Daly 1997, Wilson et al. 2014). Even relatively small eruptions are capable of widespread disruption on surface transport and aviation, which may continue for months due to the remobilisation and secondary deposition of ash by wind, traffic or other human activities, even after an eruption has subsided.

To date studies on the impacts of volcanic hazards to society have focussed on the effects of ash (e.g. Guffanti et al. 2009, Wilson et al. 2009, Horwell et al. 2010, Wilson et al. 2011, Dunn 2012, Wardman et al. 2012a, Wilson et al. 2012a, Stewart et al. 2013, Wilson et al. 2014). These studies and reports suggest four frequently occurring types of volcanic ash impacts on surface transport:

1. Reduction of skid resistance on roads and runways covered by volcanic ash.
2. Coverage of road and airfield markings by ash.
3. Reduction in visibility during initial ashfall and any ash re-suspension.
4. Blockage of engine air intake filters which can lead to engine failure.

Despite much anecdotal evidence, there has been little work to quantify the impact of ash on surface transport including roads and airfields. Quantitative, empirical evidence could inform management strategies in syn-eruptive and post-ashfall environments such as evacuation planning, safe travel advice in the recovery phase and recommended clean-up operations.

Existing studies of exposed critical infrastructure have generally focussed on very large eruptions and ashfall deposits >10 mm thick, rarely reporting the effects from ashfall <10 mm thick (Wilson et al. 2012a). This presents a source of uncertainty for emergency management planning and loss assessment models, which is important, as thin deposits are more frequent and often cover larger areas (Pyle 1989). Some notable eruptions that have led to reported reduced skid resistance on roads in the past are highlighted in Table 3.1. Wilson et al. (2014) suggest that impacts start at ~2-3 mm ash thickness, although there have been few studies that have quantified such impacts in detail. Indeed, the limited quantitative data available from historic observations generally relates impacts to approximate depths of ash, which may not be the best metric: ash characteristics such as particle size, ash type, degree of soluble components and wetness, may influence or even control the level of skid resistance. We investigate the importance of these alternative characteristics in this paper.

Here, we present experimental methods and results from the University of Canterbury's Volcanic Ash Testing Laboratory (VAT Lab) on the reduction of skid resistance on surfaces covered by volcanic ash. We test the skid resistance on road and airfield surfaces using the British Pendulum Tester

(BPT), a standard instrument used by road engineers for surface friction testing since its development in the 1950s (Wilson 2006), and still used in many countries, particularly at problematic road sites. Despite the widespread and frequent use of the BPT by road engineers, we are unaware of other studies that have utilised the instrument on ash-covered surfaces.

Table 3.1 Historical reports of reduced skid resistance following volcanic eruptions. There may be other instances described as 'general impacts to transportation' or which have not been recorded in the literature.

Volcano and country	Year	Ash thickness (mm)	Observations related to skid resistance
St Helens, United States of America	1980	17	Ash became slick when wet[1,2,3]
Hudson, Chile	1991	*not specified*	Traction problems from ash on road[4]
Tavurvur and Vulcan, Papua New Guinea	1994	1000	Vehicles sunk and stuck in deep ash, although passable if hardened[5,6,7]
Sakurajima, Japan	1995	>1	Roads slippery[6,8]
Ruapehu, New Zealand	1995-96	"thin"	Slippery sludge from ash-rain mix (roads closed)[6,9]
Soufrière Hills, United Kingdom (overseas territory)	1997	*not specified*	Rain can turn particles into a slurry of slippery mud[10]
Etna, Italy	2002	2-20	Traction problems, although damp and compacted ash easier to drive on[6]
Reventador, Ecuador	2002	2-5	Vehicles banned due to slippery surfaces[6,11]
Chaitén, Chile	2008	*not specified*	Reduced traction caused dam access problems[12,13]
Merapi, Indonesia	2010	*not specified*	Slippery roads caused accidents (Figure 2) and increased journey times[14]
Pacaya, Guatemala	2010	20-30	Slippery roads with coarse ash[15]
Puyehue-Cordón Caulle, Chile	2011	>100	2WDs experienced traction problems (wet conditions)[16]
Shinmoedake, Japan	2011	*not specified*	Ladders very slippery[17]
Sinabung, Indonesia	2014	80-100	Road travel impracticable in wet muddy ash[18]

Information from [1]Warrick 1981, [9]Johnston 1997, [7]Stammers 2000, [8]Durand et al. 2001, [5]Nairn 2002, [2]Cole and Blumenthal 2004, [3]Cole et al. 2005, [11]Leonard et al. 2006, [13]Wilson (2009 unpublished field notes), [6]Barnard 2009, [10]USGS 2009, [14]Jamaludin 2010, [4]Wilson et al. 2011, [17]Wilson (2011 unpublished field notes), [15]Wardman et al. 2012a, [12]Wilson et al. 2012b, [16]Wilson et al. 2013, [18]Volcano Discovery 2014.

3.3 Skid Resistance

Skid resistance (i.e. the force developed when a tyre that is prevented from rotating slides along a pavement surface (Highway Research Board 1972)) is a fundamental component of road safety and should be managed so that it is adequate to enable safe operation (Dookeeram et al. 2014). Skid resistance is also essential for airfields to enable sufficient acceleration, deceleration and change in direction of aircraft on the surface (ICAO 2013). It has become particularly important since the advent of turbojet aircraft with their greater weight and high landing speeds (FAA 1997, Blastrac 2015). Skid resistance is essentially a measure of the Coefficient of Friction (CoF) obtained under standardised conditions in which the many variables are controlled so that the effects of surface characteristics can be isolated (Wilson and Chan 2013).

Skid resistance of surfaces changes over time, typically increasing in the first two years following pavement construction for roads due to the wearing by traffic, and rough aggregate surfaces becoming exposed, then decreasing over the remaining pavement life as aggregates become polished (Asi 2007).

3.3.1 Surface macrotexture and microtexture

Surface friction is primarily a result of the macrotexture and microtexture of road and airfield pavements; these are thus intrinsically linked to skid resistance. As defined by the World Road Association-PIARC (1987):

- Macrotexture defines the amplitude of pavement surface deviations with wavelengths from 0.5 to 50 mm.
- Microtexture is the amplitude of pavement surface deviations from the plane with wavelengths less than or equal to 0.5 mm, measured at the micron scale (Ergun et al. 2005).

Microtexture, a property of each individual aggregate chip, contributes to skid resistance for vehicles at low speed (i.e. the tyre rubber locally bonds to the surface through adhesion). Microtexture varies from harsh to polished. When a pavement is newly constructed, microtexture is particularly rough; however, once in service, microtexture changes due to the effects of traffic and weather conditions (Ergun et al. 2005). Macrotexture, the coarse texture of pavement surface aggregates, helps to reduce the potential for aquaplaning and provides skid resistance at high speeds through the effect of hysteresis (caused by the surface projections deforming the tyre) (Wilson and Chan 2013, Dookeeram et al. 2014). Typically, if the surface binder and aggregate chips have been appropriately applied, macrotexture levels should gradually and linearly decrease over time as the aggregate surface slowly abrades (Wilson 2006).

3.3.2 Road skid resistance

The minimum recommended values of skid resistance and calculated corresponding CoFs for different sites on road networks that are measured with the BPT under typical wet conditions are shown in Table 3.2 and are reported in various literature sources internationally (e.g. British Pendulum Manual 2000, Asi 2007, Impact 2010).

Table 3.2 Minimum recommended Skid Resistance Values for different road network sites, under wet conditions and measured using the British Pendulum Tester (British Pendulum Manual 2000, Asi 2007, Impact 2010).

Type of site	Minimum recommended Skid Resistance Value	Corresponding Coefficient of Friction
Difficult sites such as: (a) Roundabouts (b) Bends with radius less than 150 m on unrestricted roads c) Gradients, 1 in 20 or steeper, of lengths >100 m	65.0	0.74

d) Approaches to traffic lights on unrestricted roads		
Motorways and heavily trafficked roads in urban areas (with >2000 vehicles per day)	55.0	0.60
All other sites	45.0	0.47

Rain, snow and ice are common hazards that compromise the quality of road surfaces (Benedetto 2002, Andrey 1990, Cova and Conger 2003) by interfering with surface macrotexture and microtexture. Bennis and De Wit (2003) and Persson et al. (2005) quantified how surface friction varies with time during a short rain shower following a reasonable period of no rain (Figure 3.1). The measured skid resistance significantly reduces immediately after rainfall and then recovers to a more typical wet skid resistance. However, the effect of individual contaminants, such as vehicle residues and atmospheric dust, on surface friction is poorly understood (Wilson 2006).

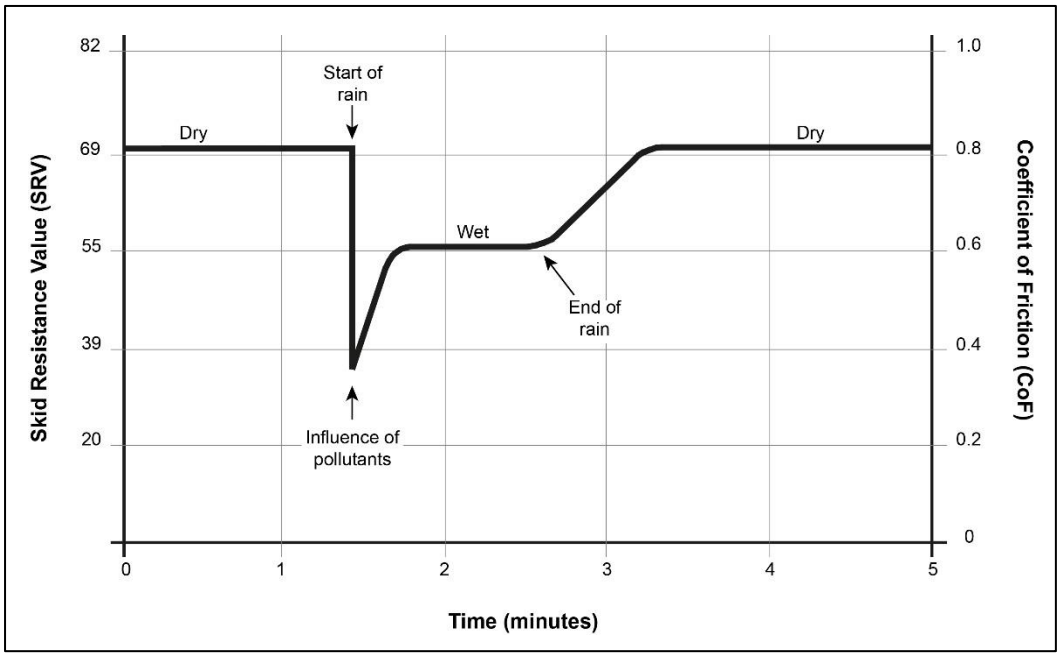

Figure 3.1 Variation in CoF during a rain event (after Bennis and De Wit 2003, Persson et al. 2005, Wilson 2006, Do et al. 2014).

Many studies have focused on snow- and rain-related crashes in northern states of the U.S. (e.g., Qin et al. 2006, Khattak and Knapp 2001, Oh et al. 2009; Abdel-Aty et al. 2011). We propose that parallels may be drawn between such hazards and the hazard presented by ashfall on roads. Following a review of the literature, Aström and Wallman (2001) summarise typical CoFs for different road conditions (Table 3.3). The effect of hazards such as ice and snow can be substantial with most

Skid Resistance Values (SRVs) under such conditions falling below the minimum recommended levels (Table 3.2). Skid resistance is very limited under black ice conditions.

Table 3.3 Skid Resistance Values and calculated corresponding CoFs for different road conditions (adapted from Aström and Wallman 2001). The two measures of friction are related by the equation: CoF = (3 x SRV) / (330 – SRV) (Lester 2014).

Type of Site	Typical Skid Resistance Value	Corresponding Coefficient of Friction
Dry, bare surface	69.5-82.5	0.8-1.0
Wet, bare surface	62.4-69.5	0.7-0.8
Packed snow	20.6-30.0	0.20-0.30
Loose snow / slush	20.6-47.1 (higher value when tyres in contact with pavement)	0.20-0.50
Black ice	15.7-30.0	0.15-0.30
Loose snow on black ice	15.7-25.4	0.15-0.25
Wet black ice	5.4-10.6	0.05-0.10

3.3.3 Airfield skid resistance

In addition to the contaminants mentioned in Section 3.3.2, a common and important contaminant on airport runway surfaces is tyre rubber. With repeated aircraft landings, rubber from tyres can cover the entire surface of landing areas, filling the surface voids and reducing macrotexture and microtexture, resulting in loss of aircraft braking capacity and directional control, especially when runways are wet (FAA 1997, Blastrac 2015). The extent of rubber tyre contaminant accumulation on runways is dependent on the volume and type of aircraft which use the airport (FAA 1997).

Unfortunately, there is no common index for ground friction measurements on airfields. Currently, individual airport operating authorities are responsible for providing any take-off and landing performance data as a function of a braking coefficient with ground speed, and relating this data to a friction index measured by a ground device (EASA 2010). CoF values measured by Continuous Friction Measuring Equipment (CFME) can be used as guidelines for evaluating friction deterioration of runway pavements (FAA 1997). The CoFs for three classification levels for FAA qualified CFME operated at 65 and 95 km/h test speeds are shown in Table 3.4. There are no airfield guideline thresholds for the BPT as it only provides spot friction measurements of the surface (and is not classified as CFME). However, BPTs are sometimes used on runways and we thus summarise BPT results for airfield concrete surfaces in Section 3.5

Table 3.4 Guideline friction values for three classification levels for FAA qualified CFME operated at 65 and 95 km/h test speeds (FAA 1997). Note that there are no airfield guideline thresholds for the BPT which is not CFME and only provides spot friction measurements.

	65 km/h			95 km/h		
	Minimum	Maintenance Planning	New Design/ Construction	Minimum	Maintenance Planning	New Design/ Construction
Mu Meter	.42	.52	.72	.26	.38	.66
Dynatest Consulting, Inc. Runway Friction Tester	.50	.60	.82	.41	.54	.72
Airport Equipment Co. Skiddometer	.50	.60	.82	.34	.47	.74
Airport Surface Friction Tester	.50	.60	.82	.34	.47	.74
Airport Technology USA Safegate Friction Tester	.50	.60	.82	.34	.47	.74
Findlay, Irvine, Ltd. Griptester Friction Meter	.43	.53	.74	.24	.36	.64
Tatra Friction Tester	.48	.57	.76	.42	.52	.67
Norsemeter RUNAR (operated at fixed 16% slip)	.45	.52	.69	.32	.42	.63

3.3.4 Volcanic ash and skid resistance

Due to its rapid formation, volcanic ash particles comprise various proportions of vitric (glassy, non-crystalline), crystalline or lithic (non-magmatic) particles (Wilson et al. 2012a) which are usually hard and highly angular. Volcanic ash properties are influenced by various factors, including the magma source type, distance from the vent, weather conditions and time since the eruption. Important volcanic ash properties include:

- Particle size and surface area
- Composition and degree of soluble components
- Hardness and vesicularity
- Angularity and abrasiveness
- Wetness.

Since coarser and denser particles are deposited close to the source, fine glass and pumice shards are relatively enriched in ash fall deposits at distal locations (Sarna-Wojcicki et al. 1981). Newly erupted ash has coatings of soluble components (Matsumoto et al. 1988, Delmelle et al. 2005) resulting from interactions with volcanic gases and their new surfaces. Mineral fragment composition is dependent on the chemistry of the magma from which it was erupted, with the most explosive eruptions dispersing high silica rhyolite rich in hard quartz fragments (Heiken and Wohletz 1985, Wardman et al. 2012b). Volcanic ash is very abrasive (Blong 1984, Labadie 1994, Heiken et al. 1995,

Johnston 1997, Miller and Casadevall 2000, Gordon et al. 2005) with the degree of abrasiveness dependent on the hardness of the material forming the particles and their shape; high angularity leads to greater abrasiveness (Wilson et al. 2012a). Most abrasion occurs from particles <500 μm in diameter, with a sharp increase in the abrasion rate from 5 to 100 μm (Gordon et al. 2005).

Skid resistance from volcanic ash may be different to that expected from other contaminants due to cementitious and vesicular properties of the ash. There is also potential for large thicknesses to develop on ground surfaces or contamination to reoccur once cleaned due to re-suspension and re-deposition. There have been several instances where road line markings have become obscured by settled volcanic ash (e.g. Mt Reventador 2002, Leonard et al. 2006; Mt Hudson 1991, Wilson et al. 2011). An ash thickness of only ~0.1 mm can lead to road marking coverage in some cases (Blake et al. in review). Drivers can unintentionally drive over road markings, which may have different skid resistance properties to unmarked road surfaces. Additionally, with ash accumulation, the vibrations that drivers receive from rumble strips incorporated in some markings will likely be subdued or even eliminated, decreasing road safety further. Vehicle accidents during or after ashfall (e.g. Figure 3.2) are a particular concern where no road closures occur, due to decreased braking ability and increased stopping distances caused by low skid resistance.

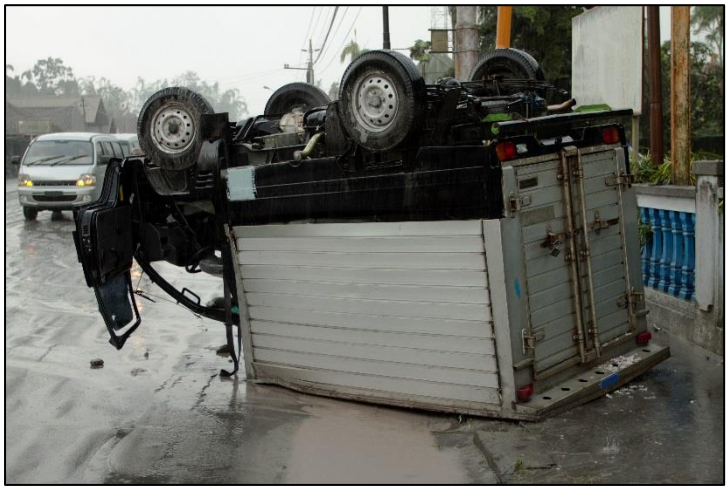

Figure 3.2 Vehicle accident attributed to reduced skid resistance after ashfall from Merapi volcano, Indonesia (2010) (Anderson 2010).

At airports, ash accumulation above trace amounts usually requires closure and the removal of ash from airfields before full operations can resume, both of which incur considerable expense (Guffanti et al. 2009). For example, the eruption of Mt. Redoubt volcano in Alaska in 1989 resulted in a minimum loss of US $21 million at Anchorage International airport (Tuck et al. 1992). Many airports face closure even before ash settles on the airfield due to potential damage to aircraft by airborne ash, or solely the threat of ash in the vicinity. As such, there are limited observations of ash resulting in reduced skid

resistance on airfields, although Guffanti et al. (2009) note that slippery runways are one of the primary hazards to airports from volcanic eruptions.

3.4 Methods

3.4.1 Sample preparation

3.4.1.1 Volcanic ash

Volcanic ash samples derived from four different volcanic sources in New Zealand were used in this study to investigate two volcanic ash types (basalt and rhyolite) and to span a range of hardness and mineral components. The locations and ash types are shown in Table 3.5. Compositions and characteristics were selected as they are representative of ash likely to be encountered in the future in New Zealand, but are also common worldwide. For logistical and supply reasons, experimentation on basaltic ash was focussed on a proxy ash sourced from locally abundant basaltic lava blocks from the Lyttelton Volcanic Group at Gollans Bay Quarry in the Port Hills of Christchurch, New Zealand. Ash was physically produced from the blocks by splitting, crushing and pulverisation as described by Broom (2010) and Wilson et al. (2012), a method generally found to provide good correlations with real volcanic ash grain sizes. Some of the proxy Lyttelton basaltic ash produced was pulverised and sieved to 1000 μm and some to 106 μm to investigate the effect of grain size on skid resistance. In addition, further basaltic ash was sourced from deposits originating from the Pupuke eruption in the Auckland Volcanic Field and Punatekahi eruptions in the Taupo Volcanic Zone. Rhyolitic ash was sourced from deposits from the Hatepe eruption in the Taupo Volcanic Zone. These three samples were pulverised (splitting and crushing was not necessary due to their smaller original sizes) and sieved to 1000 μm (Table 3.5). The grain size distributions for all samples are shown in Figure 3.3.

Table 3.5 Ash samples prepared for testing. RCL = Ruapehu Crater Lake, WICL = White Island Crater Lake.

Ash Source	Ash Type	Sieve Size (μm)	Soluble Components Added	Sample ID
Lyttelton Volcanic Group	Hard Basalt	1000	No	LYT-BAS1
			Yes (RCL)	LYT-BAS2
			Yes (WICL)	LYT-BAS3
		106	No	LYT-BAS4
Punatekahi cone, Taupo	Scoriaceous Basalt	1000	No	PUN-BAS1
			Yes (RCL)	PUN-BAS2
			Yes (WICL)	PUN-BAS3
Hatepe ash, Taupo	Pumiceous Rhyolite	1000	No	HAT-RHY
Pupuke, Auckland Volcanic Field	Scoriaceous Basalt	1000	No	PUP-BAS1
			Yes (WICL)	PUP-BAS3

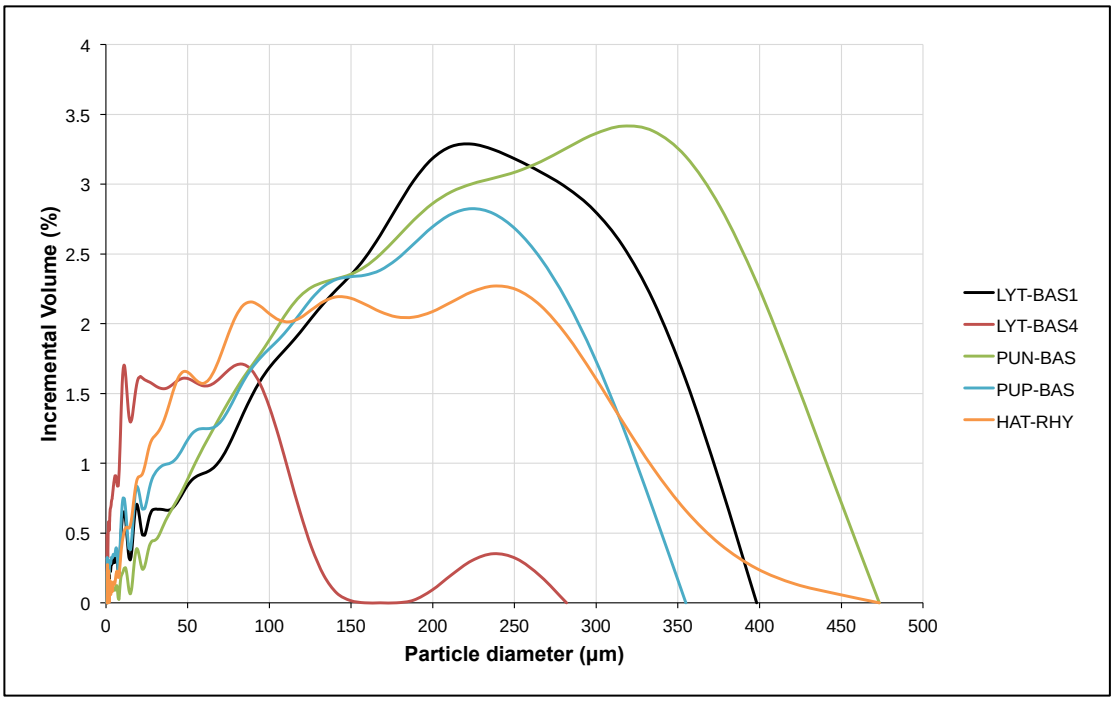

Figure 3.3 Mean particle size distribution analysed using a Micromeritics Saturn DigiSizer II Laser-Sizer (3x runs per sample). Note that the maximum particle sizes for the four samples that were sieved to 1000 µm are in fact <500 µm, likely due to the pulverisation process. Some particles for the LYT-BAS4 sample (sieved to 106 µm) exceed 106 µm due to the often-tabular nature of volcanic ash particles and their ability to pass through the sieve mesh when vertically orientated.

As fresh ash contains adhered soluble components, we dosed a portion of our ash samples with fluid from volcanic crater lakes to mimic the volatile adsorption processes which occur in volcanic plumes, thus enabling the effects of soluble components on skid resistance to be studied. A dosing method using fluids from the crater lakes of Ruapehu and White Island volcanoes, New Zealand, described by Broom (2010) and Wilson et al. (2012), was used for a portion of the 1000 µm Lyttelton and Punatekahi basaltic ash samples for road testing, and Pupuke basaltic ash sample for airfield testing. The following dosing solutions were used as work by Broom (2010) and Wilson et al. (2012) established that they produce samples representative of real fresh volcanic ash:

- 100% strength Ruapehu Crater Lake fluid (Appendix B1), i.e. no dilution, mixed at a ratio of 1:1 (ash to dosing agent)
- 20% strength White Island Crater Lake fluid (Appendix B1), i.e. 4 parts de-ionised water to 1 part White Island Crater Lake fluid, mixed at a ratio of 4:1 (ash to dosing agent)

We undertook a water leachate test using the method outlined by Stewart et al. (2013) to measure the concentration of dissolved material in solution for all of the samples used and verify the effectiveness of dosing. Both 1:20 and 1:100 ratios of ash (g) to de-ionised water (ml) were used. The water leachate test findings (Appendix B2) revealed that the soluble components in the samples we dosed (LYT-BAS2, LYT-BAS3, PUN-BAS2, PUN-BAS3, PUP-BAS3) were considerably higher than those that were not dosed and confirms that the samples used provide a suitable means of testing the

effects of this characteristic on skid resistance. Additionally, the lowest pH values were generally recorded for the dosed samples.

3.4.1.2 Test surfaces

Stone Mastic Asphalt (SMA) surfaces are commonly used on modern motorways, such as in parts of the UK and on the Auckland State Highway Network in New Zealand (Boyle 2005). However, concerns have been raised about its use, as initial skid resistance may be low until the thick binder film is worn down: it sometimes takes up to two years for the material to offer an acceptable level of skid resistance (Bastow et al. 2004, BBC 2005, Daily Telegraph 2008). The desire to have good macrotexture led to the development of Open Graded Porous Asphalt (OGPA; Boyle 2005).

For this study, we focus mainly on tests of skid resistance for SMA surfaces using 300 x 300 x 45 mm slabs, newly constructed by the Road Science Laboratory in Tauranga, New Zealand. We also conducted some comparative tests on OGPA also constructed by the Road Science Laboratory, and on concrete surfaces constructed as 220 x 220 x 40 mm slabs by Firth Concrete. The concrete mix was compiled with the same specifications as used for placement via manual labour and a roller screed on the airfield (i.e. runways, taxiways and hardstand areas) at Auckland Airport, although we note that airfield surfaces vary between countries and airports. However, unless otherwise specified, we refer to SMA surfaces in this paper.

3.4.1.3 Painted road markings

Under typical conditions, road markings reduce accident rates (NZRF 2005) as they provide continuous visual guidance of features such as road edges and centres. However, when non-mechanical markings such as paint and thermoplastics are applied, the microtexture of the road surface changes and, with thicker non-mechanical markings, the macrotexture also alters as voids in the asphalt become filled. Consequently, localised skid resistance can be substantially reduced. The skid resistance of the markings is generally lower than that for the bare pavement, although the addition of retroreflective glass beads to the surface can increase skid resistance to more acceptable levels (NZRF 2005). As little as 0.1 mm of volcanic ash may obscure road markings (Blake et al. in review), meaning that drivers may unintentionally travel over marked road surfaces (e.g. such as crossing centre lines). Further accumulation may inhibit the effectiveness of rumble strips which normally cause vibrations within the vehicle.

Paint is the most common form of road marking material used in many countries, including New Zealand, and is typically applied by spraying in dry film with thicknesses varying from 70 µm to 500 µm (NZRF 2009). In New Zealand, retroreflective glass beads are often applied to longitudinal centre line paint but not to paint on the road margins (Howard Jamison, Roading Supervisor, personal communication, 2014). Road lines are usually re-painted once or twice a year to account for abrasion, with skid resistance decreasing as the paint fills more voids in the asphalt surface. With a typical asphalt lifespan of ~10 years, marking paint accumulation can be substantial in places (Howard

Jamison, Roading Supervisor, personal communication, 2014). In this study we test skid resistance on SMA slabs, machine painted by Downer Group with a typical road paint (Damar Bead Lock oil-based paint containing 63% solids), in four forms:

- 1x application (180-200 µm thick) without retroreflective glass beads
- 1x application (180-200 µm thick) with retroreflective glass beads
- 4x applications (720-800 µm thick) without retroreflective glass beads
- 4x applications (720-800 µm thick) with retroreflective glass beads.

The asphalt with one application of paint is used to replicate markings that have been heavily abraded, whereas that with four applications mimics typical marking thickness found on New Zealand roads (Howard Jamison, Roading Supervisor, personal communication, 2014).

3.4.2 Skid Resistance Testing

The test procedure for the BPT (Figure 3.4) is standardised in the ASTM E303 (2013) method. It is a dynamic pendulum impact type test, based on the energy loss occurring when a rubber slider edge is propelled across the test surface. The method is intended to correlate with the performance of a vehicle with patterned tyres braking with locked wheels on a wet road at 50 km/h (Impact 2010). Since the BPT is designed to test the skid resistance of extensive surfaces in-situ, care was taken to ensure that the instrument was stable and slabs were aligned before conducting our testing in the laboratory environment. Both 3” rubber mounted TRL (55) sliders (used for road testing) and 3” CEN sliders (used for airfield testing), purchased from Cooper Technology UK, were used in our study.

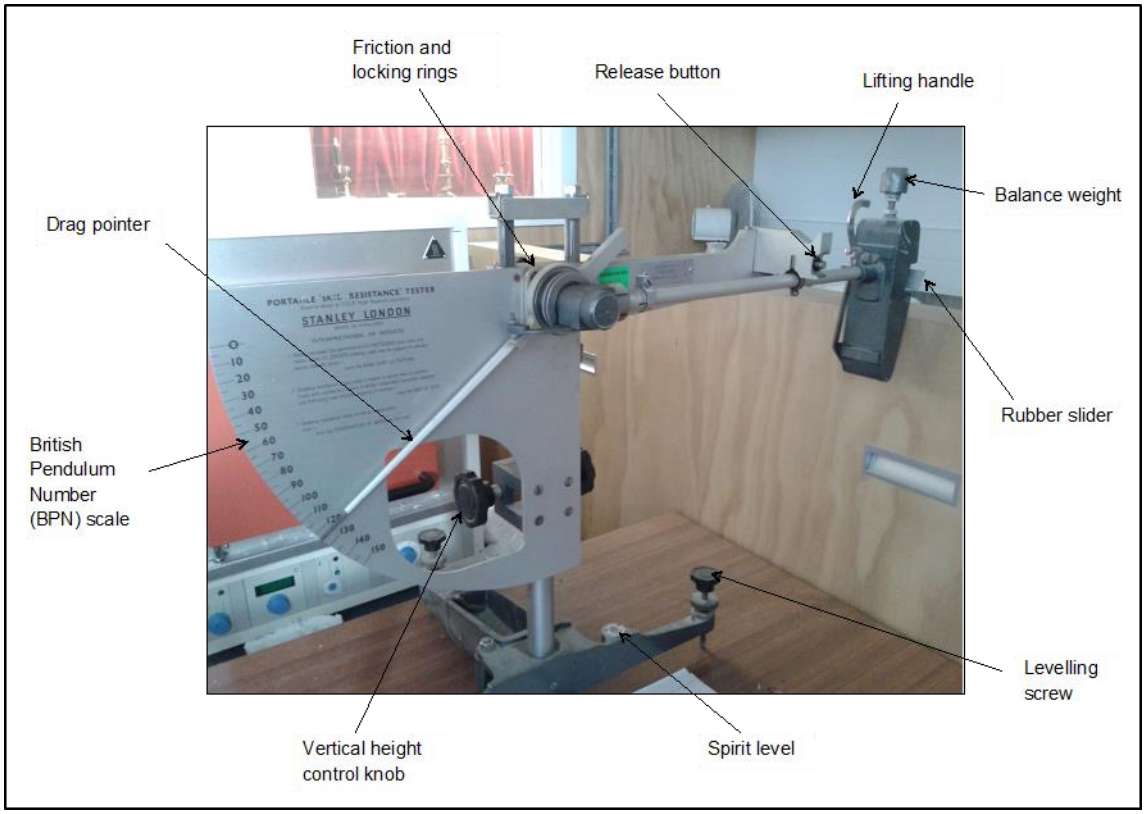

Figure 3.4 British Pendulum Tester (BPT) used for surface friction testing.

3.4.2.1 Surfaces not covered by ash

As the ASTM E303 (2013) method states, the direct values are measured as British Pendulum (Tester) Numbers (BPNs). Typically, tests using the BPT are conducted on wet surfaces. However, as we are also investigating the effects of dry volcanic ash on skid resistance, we also ran the experiments under dry conditions. For surfaces not covered in ash, we adopted the same technique as used by the New Zealand Transport Agency (NZTA) (TNZ 2003), whereby for each test surface area, results of a minimum of five successive swings which do not differ by more than 3 BPNs are recorded. The mean of the 5 BPNs is then calculated to give a value representing skid resistance (i.e. the Skid Resistance Value (SRV)). The tests were conducted on every side of each slab to retrieve four SRVs (later averaged) for each condition. CoFs for each mean SRV are calculated using the equation provided by Lester (2014):

$$CoF = (3 \times SRV) / (330 - SRV) \quad (1)$$

3.4.2.2 Surfaces covered by ash

The ash characteristics analysed during experimentation and production techniques are summarised in Appendix B3. For the surfaces covered in ash, we use two test methods to replicate different ash settling conditions in combination with vehicle movement effects:

1. A similar procedure as adopted by the NZTA (TNZ 2003) whereby five successive swings are recorded, which do not differ by more than 3 BPNs and the SRV calculated. Between each swing, ash which has been displaced by the pendulum movement is replenished with new ash of the same type (and re-wetted if applicable) to maintain a consistent depth (and wetness). This test method mimics to some degree the effect of vehicles driving during ash fall, with ash settling on a road surface and filling any voids left by vehicle tyres before the next vehicle passes. A mean SRV is calculated by repeating the test on all four sides of each asphalt slab.

2. Eight successive swings of the pendulum are taken over each ash-covered test surface area but ash is not replenished between each swing. For each swing, the BPN is taken to be the SRV, allowing the change in skid resistance to be observed through analysis of the individual results. If the original surface has been wetted, further water is applied between each swing. To some degree, this method represents vehicle movement over an ash-covered surface in dry or wet conditions, where ashfall onto the road surface has ceased. A mean SRV is calculated for each successive swing by repeating the test on all four sides of each asphalt slab where possible.

In dry field conditions, the impact of remobilised ash might be more substantial than captured in the laboratory tests. However, some remobilisation during experimentation is achieved as a result of the pendulum arm movement and associated ash disturbance.

3.4.2.3 Cleaning

Following testing, the ash was cleaned from the asphalt concrete slabs by brushing and using compressed air if dry, or a combination of compressed air, water and light scrubbing if wet. Wetted slabs were then left to air-dry for 3-4 days before any further dry tests were conducted.

3.4.3 Macrotexture

3.4.3.1 Sand patch method

This volumetric technique is standardised in the ASTM E965 (2006) method and summarised in Appendix B4. It involves a procedure for determining the average depth of pavement macrotexture by careful application of a known volume of spherical glass beads on the surface and subsequent measurement of the total area covered. The average pavement macrotexture depth is calculated using the following equation:

$$MTD = 4V / \pi D^2 \qquad (2)$$

where MTD = mean texture depth of pavement macrotexture (mm), V = sample volume (mm^3) and D = average diameter of the area covered by the material (mm).

We use this approach to determine the macrotexture of new non-contaminated SMA surfaces and SMA surfaces that were contaminated by ash but have undergone testing (10x BPT swings) and cleaning (Section 3.4.2.3). The method is not suitable for the airfield concrete slabs due to there being considerably fewer voids at the macrotexture scale and thus a much larger area would be required to conduct the test.

3.4.3.2 Image analysis

In addition to the ASTM sand patch method, a visual technique involving digital photography and image analysis was adopted to distinguish between ash and asphalt at a macrotextural level on the SMA slabs. This provides a proxy for surface macrotexture and allows the relative success of cleaning techniques in relation to ash removal and skid resistance reduction to be quantitatively assessed through the calculation of remaining ash coverage. The light-coloured rhyolitic volcanic ash (sample ID: HAT-RHY) was used to allow easy visual interpretation between the ash and dark-coloured asphalt concrete.

- White paint was marked on the edge of the slabs in order to identify the same segment of the slab between each testing round.
- A Fuji Finepix S100 (FS) digital SLR camera (with settings: Manual, ISO 800, F6.4, 10-second timer) was mounted on a tripod directly above the asphalt slab.
- Halogen tripod worklights were used to illuminate the surface of the slab and all ambient light was blocked out using black sheeting before images were taken to keep lighting levels consistent between photos.
- Images were analysed for percentage coverage of ash by means of ‘training’ and ‘segmentation’ using ‘Ilastik’ and ‘Photoshop’ software.

3.4.3 Microtexture – microscopy

A Meiji EMZ-8TRD (0.7-4.5 zoom) stereomicroscope and Lumenera Infinity 1 digital camera were used to capture images of 10 x 10 mm areas on the asphalt slabs and thus enable visual identification of remaining ash particles at a microtextural level. The microscope was mounted directly above the slab and Leica CLS 100 LED fibre-optic lighting was used to illuminate the section of interest, with all ambient light blocked using black sheeting. A portable (300 x 300 mm internal dimension) grid (with 10 mm squares) was constructed to fit securely over the slab and allow easy identification of specific segments between each testing round (Appendix B5).

3.5 Results and Discussion

3.5.1 Consistent depth

When ash was replenished between each swing, the skid resistance remained relatively constant with time, permitting calculation of a mean SRV for each condition. The mean SRVs and corresponding CoFs for the non-contaminated SMA (new and cleaned) and for the SMA covered by three samples sieved to 1000 µm are shown in Figure 3.5. Similarly, the SRVs and CoFs for the airfield concrete, both clean and covered by two samples sieved to 1000 µm are shown in Figure 3.6. The Pupuke volcano sample (PUP-BAS1) was found to have very similar values to the Punatekahi (PUN-BAS1) sample. This was expected as they are both scoriaceous basalt. Due to limitations in available ash and time constraints, full testing was only conducted with one of the scoriaceous samples on the SMA and airfield concrete.

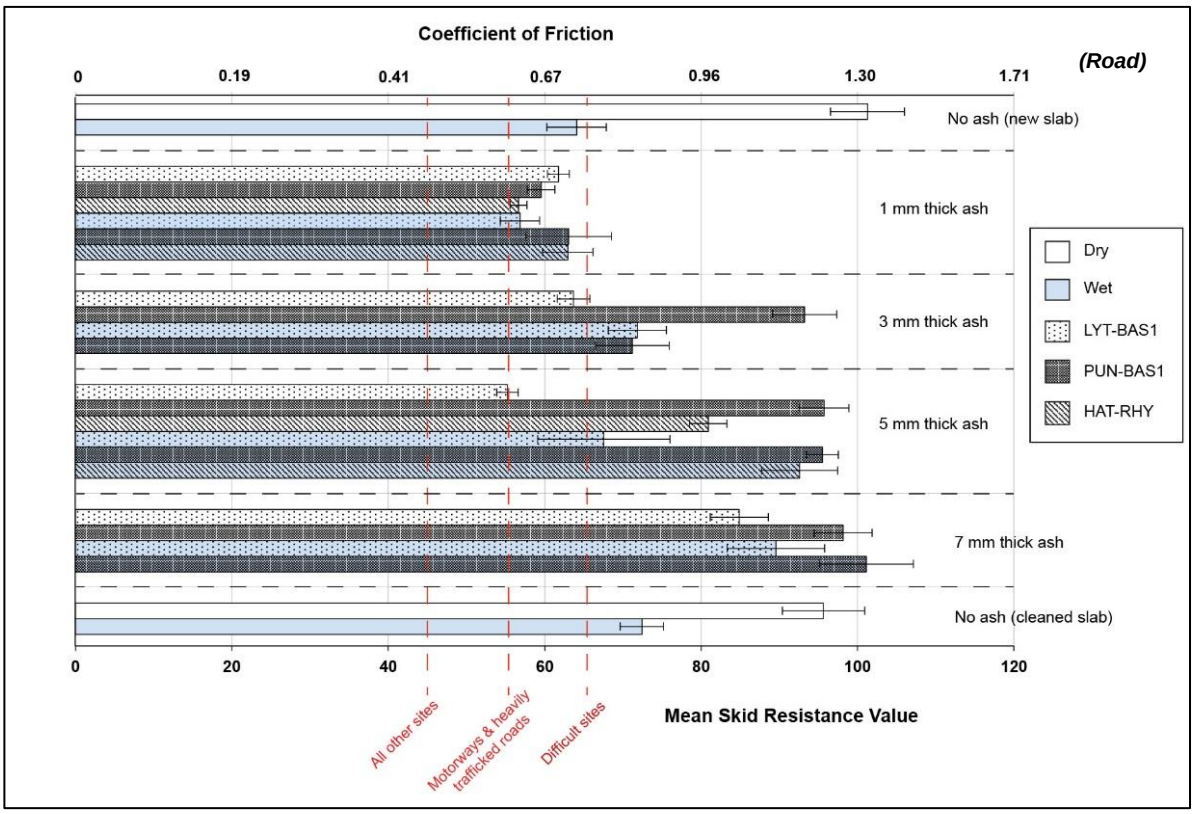

Figure 3.5 Mean SRVs and CoFs for the non-contaminated SMA and SMA covered in the three ash types sieved to 1000 µm. Wet and dry samples at 1, 3, 5 and 7 mm thicknesses are shown although limitations in the quantity of rhyolite (HAT-RHY) meant that testing was only conducted at 1 and 5 mm thickness for this ash type. The error bars represent the standard deviation for each data set. Also displayed (as red dashed lines) are the minimum recommended SRVs for different road network sites (Table 3.2).

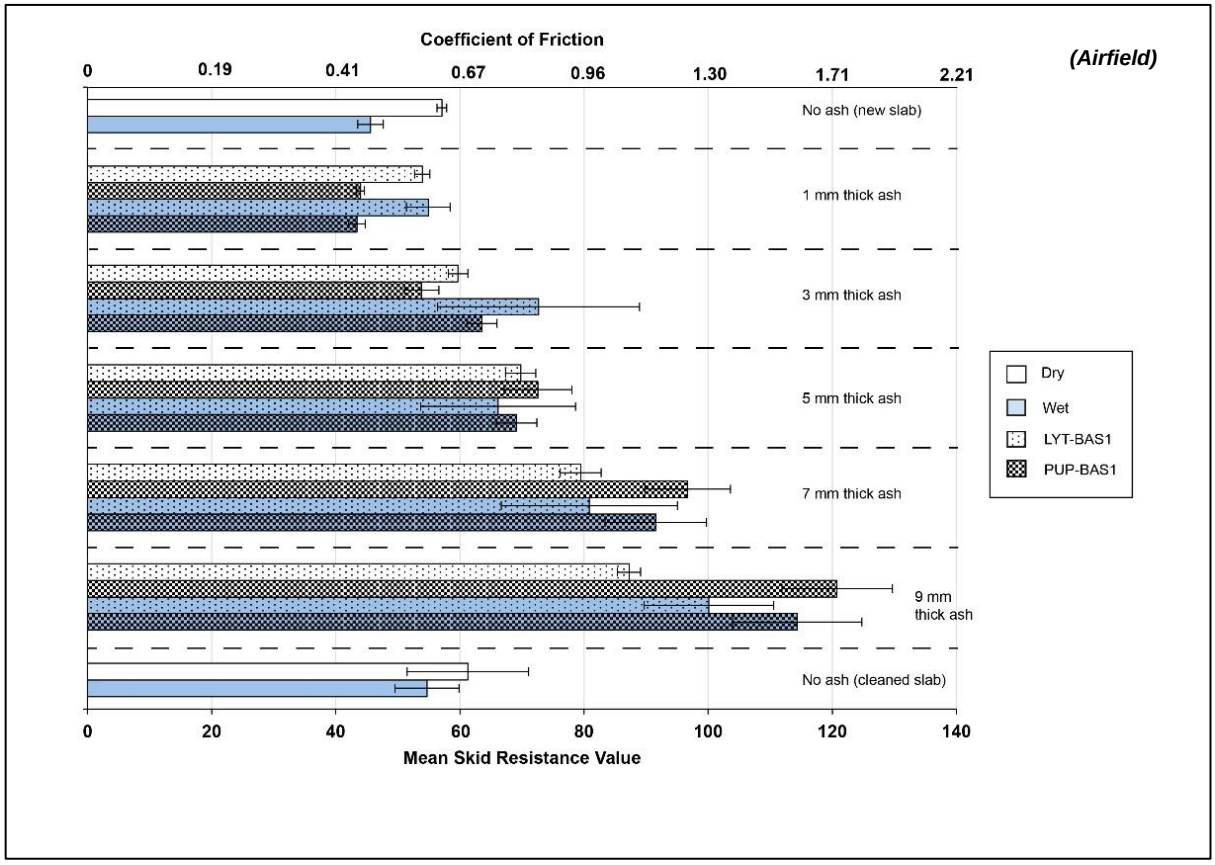

Figure 3.6 Mean SRVs and COFs for the non-contaminated airfield concrete and airfield concrete covered in the two ash types sieved to 1000 µm. Wet and dry samples at 1, 3, 5, 7 and 9 mm thicknesses are shown. The error bars represent the standard deviation for each data set.

3.5.1.1 Ash type and wetness

Anecdotal observations during historical eruptions suggest that skid resistance on roads is reduced following dry unconsolidated ash accumulation. This is consistent with our results, which also reveal that reduced SRVs are particularly pronounced under dry conditions for a 1 mm thick ash layer on asphalt (Figure 3.5). Mean SRVs for all 1 mm thick ash types fall below the minimum recommended SRV for difficult sites (an SRV of 65). Wet 1 mm ash-covered surfaces are not necessarily more slippery than dry 1 mm ash-covered surfaces and the wet surfaces covered in 1 mm thick ash are only slightly more slippery than the wet asphalt without ash contamination.

For the 3 and 5 mm thick ash-covered asphalt surfaces, we observe different trends. The LYT-BAS1 sample has similar SRVs to the 1 mm thick ash layer and the mean SRV for 5 mm is near the recommended minimum SRV for motorways (SRV 55). Samples PUN-BAS1 and HAT-RHY however, have greater SRVs than those for 1 mm of ash, suggesting that these ash types are perhaps less slippery when thicker, especially sample PUN-BAS1. The wetted PUN-BAS1 and HAT-RHY >1 mm samples have increasing SRVs as thickness increases. SRV values exceed those for bare wet asphalt surfaces and are similar to those for dry bare asphalt surfaces when ash is >5 mm thick. The

vesicular nature of these two samples may play a role in increasing SRVs with the individual particles perhaps able to effectively interlock with one another and with the asphalt aggregate beneath. The pumiceous HAT-RHY sample is more friable than the PUN-BAS1 sample, which may explain the slight difference in SRVs between the two. We note that the pendulum arm may be slowed upon initial impact with the thicker deposits, producing higher than true representative SRVs. However, the comparatively low SRVs for the 5 mm thick LYT-BAS1 sample suggest that other ash characteristics are also important.

Compared to asphalt, there is less difference between SRVs for bare airfield concrete surfaces and those covered by 1 mm of ash (Figure 3.6), perhaps due to the initially smooth surface when bare. However, as with the asphalt, results suggest little difference in slipperiness between wet and dry surfaces with 1 mm of ash deposition. The scoriaceous and vesicular sample PUP-BAS1 exhibits especially large SRVs as thickness is increased, reinforcing our hypothesis that ash of this type is less slippery when thicker. Following the addition of ash, the apparent increase in SRVs to values greater than those for bare surfaces may be a function of the pendulum arm slowing upon contact.

3.5.1.2 Soluble components

There are no clear differences in SRVs observed between non-dosed and dosed LYT-BAS ash at 1 mm thick (Figure 3.7). However, the highly crystalline properties of this ash type may reduce the impact that dosing has on SRVs. SRVs for the dosed scoriaceous PUN-BAS ash used on road asphalt (Figure 3.7) and dosed scoriaceous PUP-BAS ash used on airfield concrete (Figure 3.8) are generally less than those which are not dosed. For all ash thicknesses, the PUN-BAS3 sample (i.e. that dosed in WICL fluid) produce lower SRVs than the PUN-BAS2 sample (i.e. that dosed in RCL fluid), suggesting that the skid resistance of non-crystalline ash-covered road surfaces decreases if the soluble component of the ash increases. This corresponds with Persson et al's (2005) findings from other road contaminants, demonstrating a friction drop at the transition between no rain and rain due to the high-viscosity mix of rain water and road debris. As such, only WICL fluid was used to dose the PUP-BAS sample (used for airfield concrete) to assess results representative of a 'likely worse-case' SRV scenario.

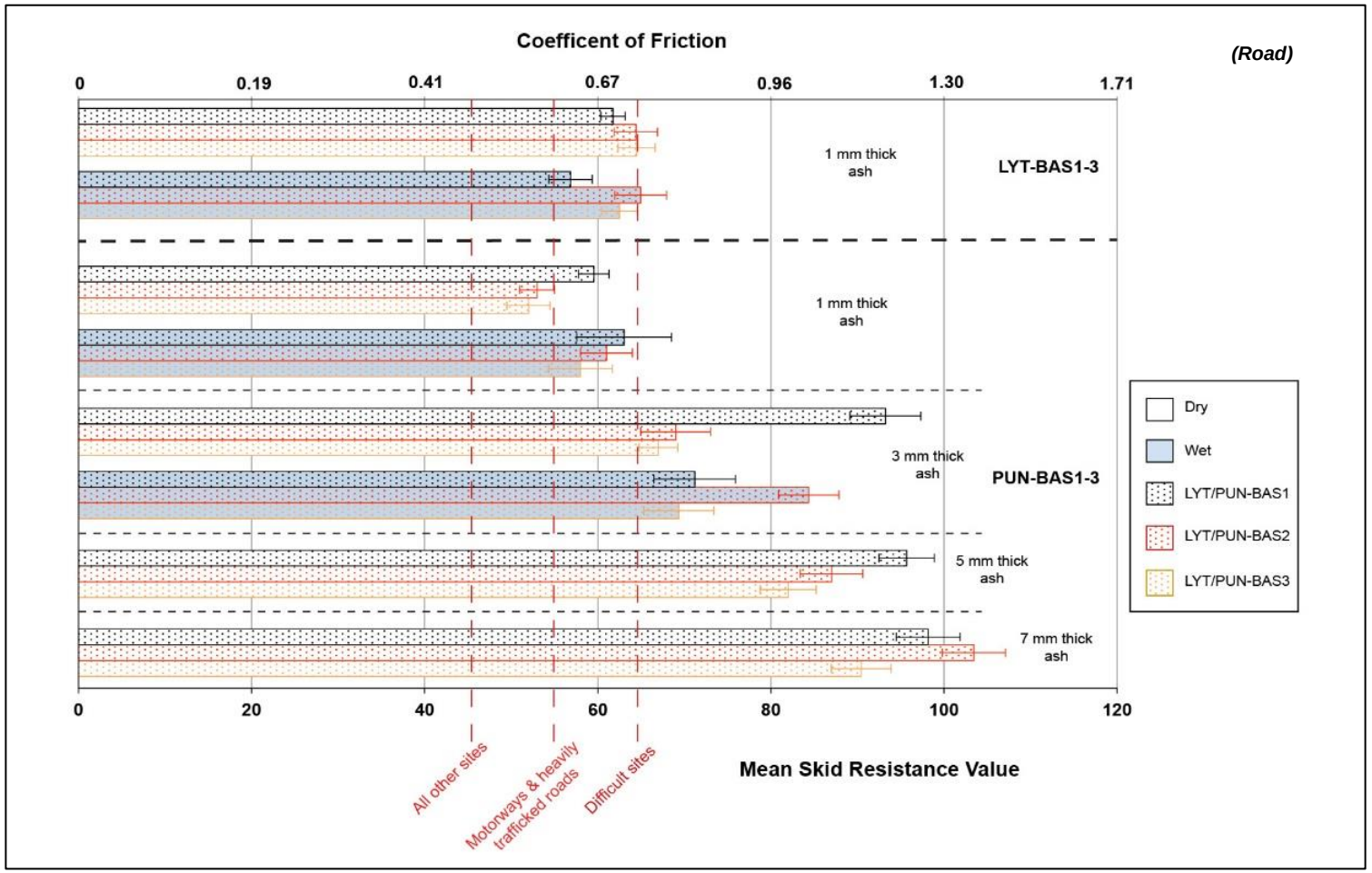

Figure 3.7 Mean SRVs and CoFs for the road asphalt covered in non-dosed and dosed LYT-BAS and PUN-BAS ash sieved to 1000 µm. Both samples dosed in RCL and WICL fluid under dry and wet conditions are displayed. Due to limitations in dosing fluids and possible interference caused by the crystalline characteristics of the LYT-BAS samples, most testing was undertaken using the PUN-BAS samples. Large quantities of freshly dosed ash samples were required for each thick ash test under wet conditions, hence only dry conditions were analysed for the 5 and 7 mm thick testing rounds. Also displayed (as red dashed lines) are the minimum recommended SRVs for different road network sites (Table 3.2).

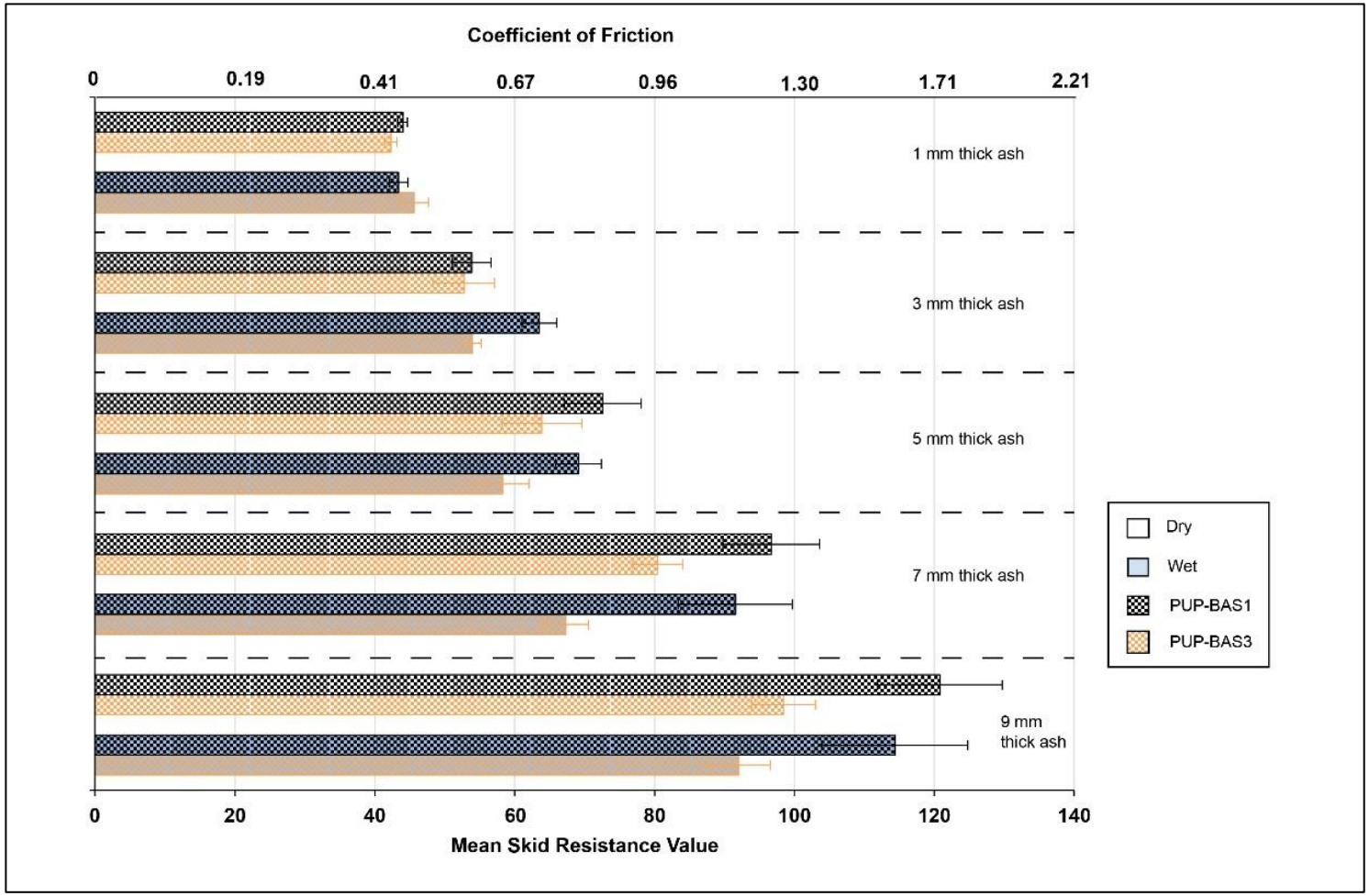

Figure 3.8 Mean SRVs and CoFs for the airfield concrete covered in non-dosed and dosed PUP-BAS ash sieved to 1000 µm. The samples dosed in WICL fluid under both dry and wet conditions are displayed.

3.5.1.3 Ash particle size

The mean SRVs for fine-grained basaltic ash (LYT-BAS4) are slightly higher than those for the coarse-grained ash of the same type (LYT-BAS1) when at 1 mm thickness on roads, with mean values for both wet and dry samples above the minimum recommended SRVs for difficult sites (Figure 3.9). This concurs with field observations made by the Kagoshima City Office staff following frequent volcanic ash deposition on roads from the multiple eruptions of Sakurajima volcano, Japan (since 1955). Reports suggest that the finer ash from the recent eruptions at the Showa crater resulted in less slippery roads than the generally coarser-grained ash produced during past eruptions from the Minami-daki summit area (Kagoshima City Office, personal communication, 08 June 2015). We hypothesise that this is due to the finer particles being more easily mobilised and displaced at the tyre-asphalt interface, allowing improved contact between the tyre and asphalt. However, no clear correlations exist between the fine- and coarse-grained ash when at 5 mm thick, perhaps due to both types covering the asphalt surface when the tyre makes contact.

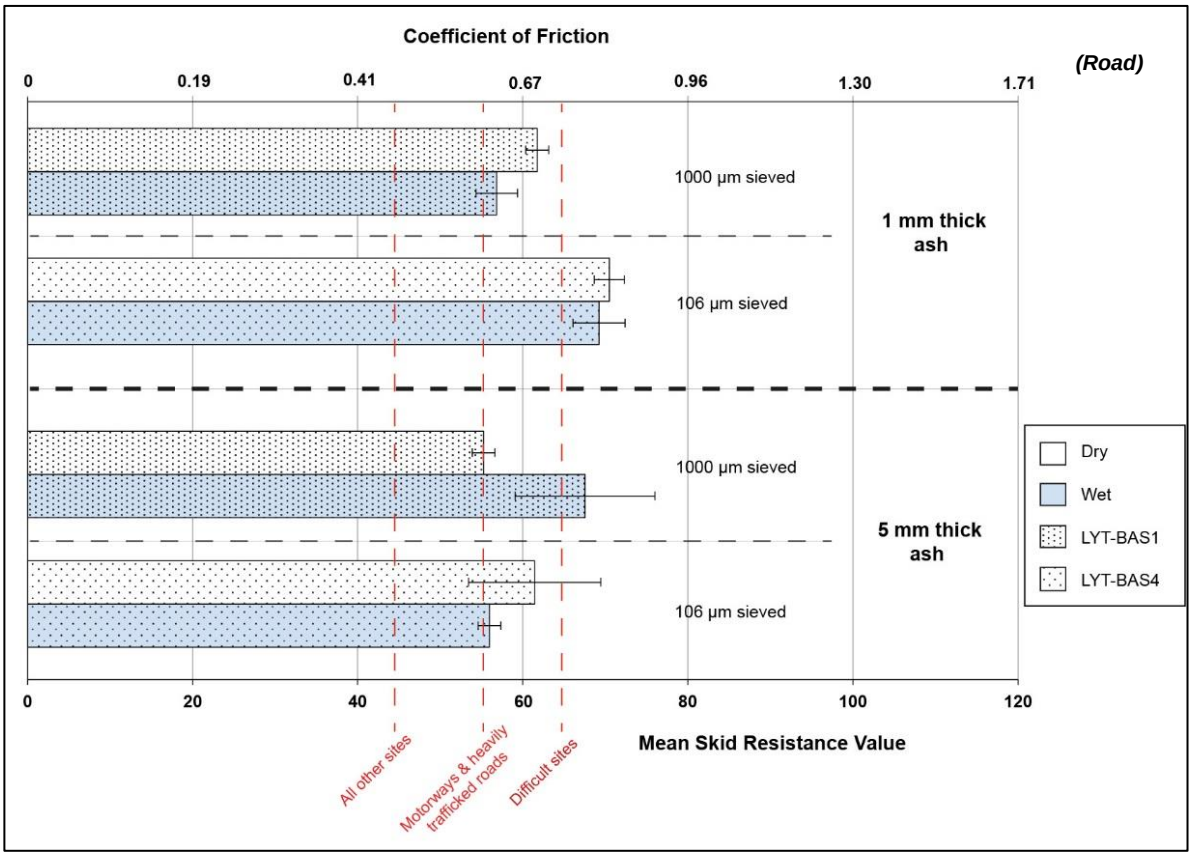

Figure 3.9 Mean SRVs and CoFs for the asphalt covered in coarse-grained (i.e. LYT-BAS1, 1000 µm sieved) and fine-grained (i.e. LYT-BAS4, 106 µm sieved) samples at 1 mm and 5 mm ash thickness under both dry and wet conditions. Also displayed (as red dashed lines) are the minimum recommended SRVs for different road network sites (Table 3.2).

3.5.1.4 Line-painted asphalt surfaces

SRVs can be reduced substantially as a result of road markings, although the addition of retroreflective glass beads can increase values to more acceptable levels (NZRF 2005). This is demonstrated in our findings for wet conditions, in which BPT analysis is typically conducted, with mean SRVs on line-painted asphalt surfaces with no beads and no ash the lowest of all our results. SRVs for these wet surfaces range from 40 to 46, and lie below the minimum recommended skid resistance for 'all other sites' when 4x coats of line paint have been applied (Figure 3.10). The addition of glass beads does increase SRVs (by around 5), although values are still relatively low. SRVs for 'clean' and dry line-painted asphalt surfaces are very high, but as with non-painted surfaces, the addition of a 1 mm ash layer decreases SRVs substantially. Conversely, the SRVs for wet asphalt concrete increase with a 1 mm ash layer to similar levels as for dry conditions. With the thicker (5 mm) ash layer on top of line-painted surfaces, SRVs increase further by around 20 (Figure 3.10).

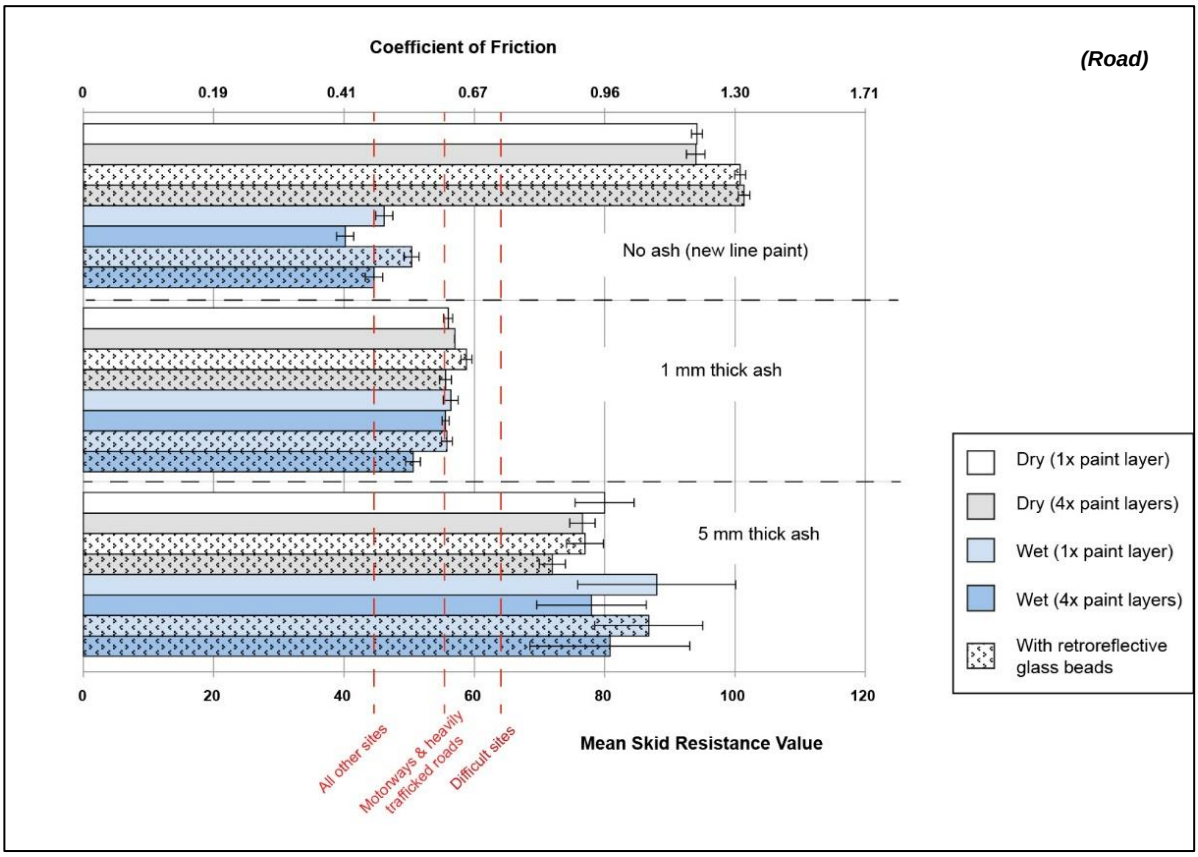

Figure 3.10 Mean SRVs and CoFs for the road asphalt with line-painted surfaces. Conditions of no ash, 1 mm thick ash, and 5 mm thick ash (using the LYT-BAS1 ash type) were analysed under both wet and dry conditions. Also displayed (as red dashed lines) are the minimum recommended SRVs for different road network sites (Table 3.2).

3.5.1.5 Asphalt comparison

Because of increased macrotexture of the surface, higher SRVs (~5) were measured on the bare OGPA than the SMA slabs when wet. Similar differences in SRVs existed between the two asphalt types covered by wet volcanic ash (both at 1 mm and 5 mm depths). However, no major differences in SRVs were observed between the two asphalt types when dry, whether surfaces were covered by ash or not.

3.5.2 Inconsistent depth

Where ash was not replenished between each swing, SRVs represent those expected for surfaces where ashfall has ceased but where there is some traffic movement.

3.5.2.1 Ash types and wetness

SRV results obtained for the samples sieved to 1000 μm (at 1mm and 5 mm ash thickness) and deposited on road asphalt are shown in Figure 3.11. Note that tests of other thicknesses (3, 7 and 9 mm) were also conducted but these have been omitted from the figure for clarity. Despite the large standard deviations, the 5 mm thick PUN-BAS1 and HAT-RHY samples initially produced high SRVs. However, the SRVs recorded for the first 2-3 swings of the pendulum over 5 mm thick ash should be interpreted with caution. This is due to possible interference of the thicker deposit when the pendulum slider first impacts the surface; similar circumstances may occur in the field when initial vehicles are driven into thicker ash deposits. When wet however, the SRVs are higher than the mean recorded on the bare asphalt surface, particularly for the PUN-BAS1 sample, suggesting that thicker layers of vesiculated (and especially harder) volcanic ash are perhaps initially less slippery than thin layers of ash of those ash types. Observations during our experimentation revealed that the wet 5 mm thick vesiculated deposits (PUN-BAS1 and HAT-RHY) consolidated, thus resisting major ash displacement more than for dry ash (Figure 3.12), even following several swings of the pendulum arm. The consolidated deposits were very firm to touch and, although further work is required to test this, it is suggested that light vehicles would be able to drive over the surface without sinking substantially.

Very similar patterns in skid resistance were observed for the airfield concrete surfaces where ash was not replenished between swings. The main difference was that the initially high SRVs for the scoriaceous sample (PUP-BAS) decreased more quickly with pendulum swings, most likely due to the ash being more easily displaced from the smoother concrete surface than for asphalt.

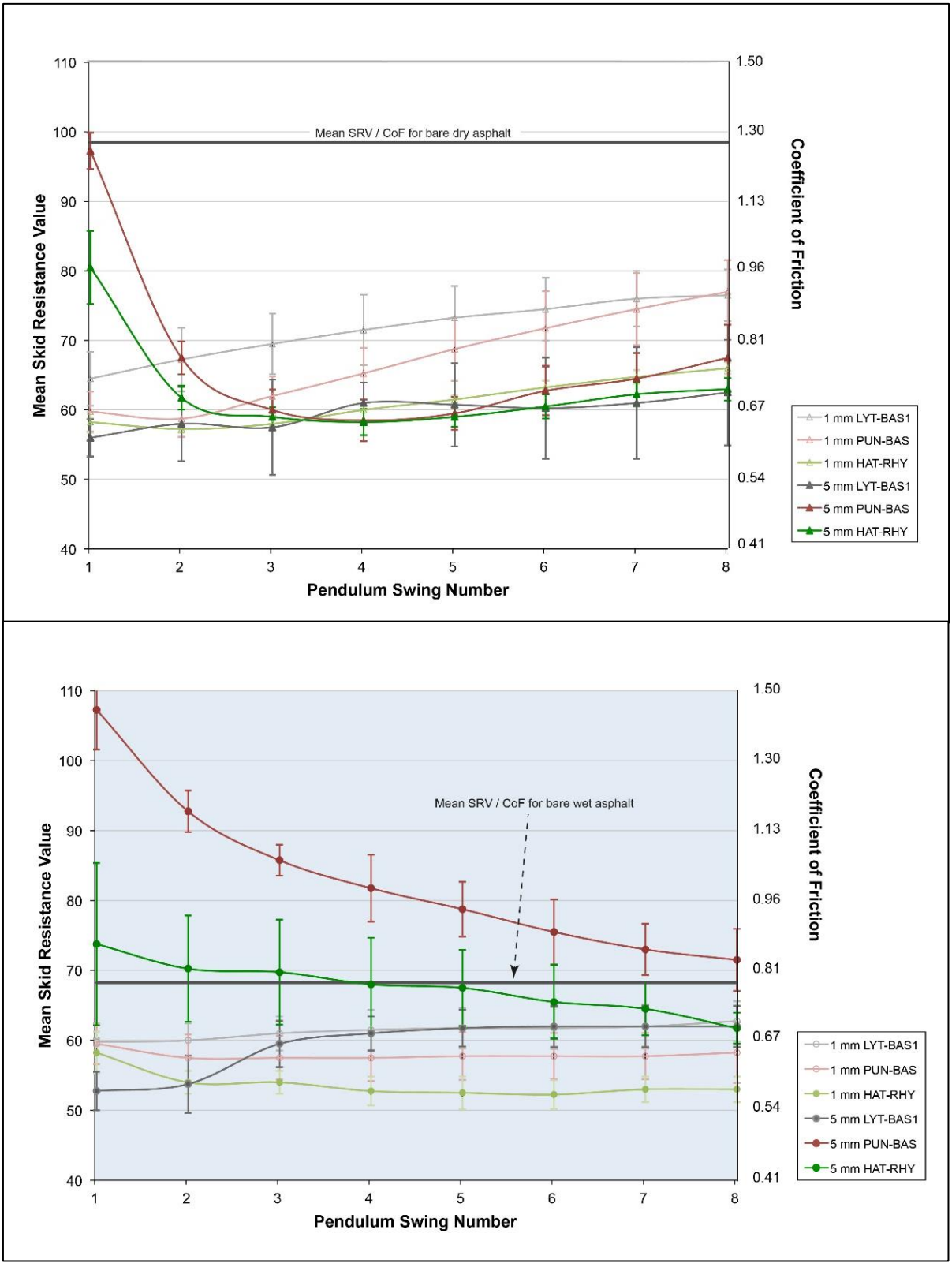

Figure 3.11 SRVs and corresponding CoFs on asphalt covered by ash sieved to 1000 µm, under (A) dry and (B) wet conditions. Also shown are the mean SRVs for bare asphalt, taken from Section 3.5.1. Error bars display the standard deviations for each pendulum swing number for the different sample types. Note that the first 2-3 swings over 5 mm deposits should be interpreted with caution due to possible impacts on SRVs caused by the initial contact between the pendulum slider and surface.

Figure 3.12 Dry ash displacement from the BPT slider-surface interface after 8x swings of the pendulum arm for (a) SMA, and (b) airfield concrete. Dry ash was displaced from the surface more readily than wet ash.

3.5.2.2 Ash particle size

No major changes were observed for the fine-grained basaltic ash samples (LYT-BAS4) over the course of the eight pendulum swings on asphalt, other than a gradual increase in SRVs over time, particularly for the dry ash at 1 mm thickness as observed for the coarse-grained samples (Figure 3.11a). As with the testing where ash was replenished, SRVs for the fine-grained ash samples were generally slightly higher than those for coarse-grained samples, suggesting that fine-grained ash is a little less slippery than coarser material.

3.5.2.3 Soluble components

The testing involving non-replenished dosed ash confirmed the key finding already discussed during replenished testing (Section 3.5.1.2): non-crystalline ash containing a higher soluble component content generally produces lower SRVs than undosed ash. However, with an increasing number of swings of the pendulum, this trend becomes less pronounced, particularly under wet conditions where the effect of adding water between each test leaches the samples, thus reducing the soluble component content of the ash.

3.5.2.4 Line-painted asphalt surfaces

Line-painted asphalt surfaces covered in ash produce relatively low SRVs (Figure 3.13). Although the first 2-3 swings involving 5 mm thick ash are not considered, it is evident that wet painted surfaces are generally slightly more slippery than painted dry surfaces. The trend of quick SRV recovery (as seen in Section 3.5.2.1) is also evident under dry line-painted conditions, when compared to wet conditions which remain slippery for longer. Under dry conditions, the addition of retroreflective glass in the line-paint appears to aid the recovery of skid resistance over time (as shown by the rising green and orange lines for the latter swings in Figure 3.13a). However, this trend is not evident for wet conditions.

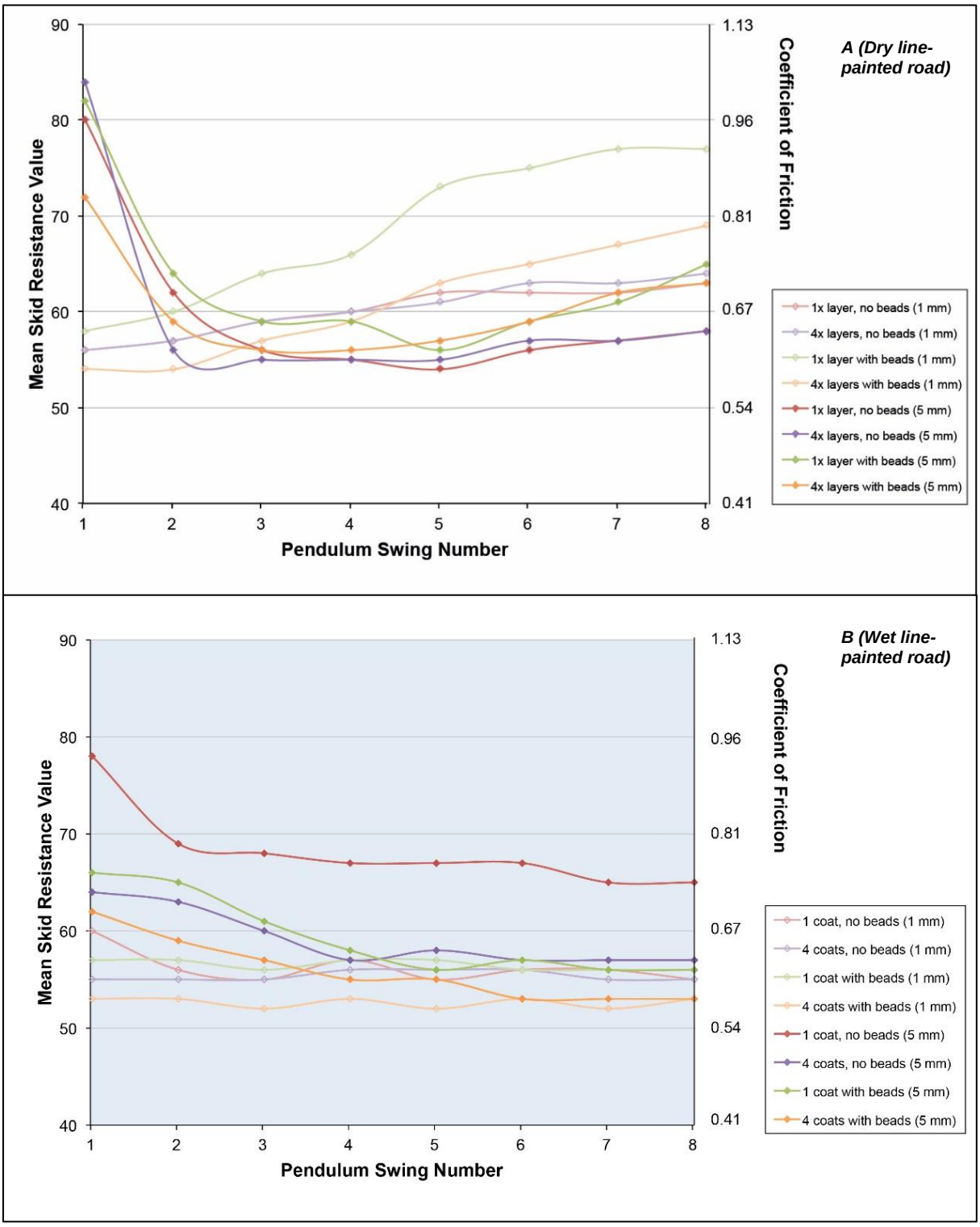

Figure 3.13 SRVs and corresponding CoFs for line-painted asphalt surfaces covered in 1 mm or 5 mm thick LYT-BAS1, under (A) dry, and (B) wet conditions. Only one test was conducted on each surface type due to the availability of line-painted slabs. Therefore, no standard deviations were calculated and the results should be treated with some caution. Note that the initial 2-3 swings over the 5 mm deposits should be treated with particular caution.

3.5.3 Surface macro and microtexture

3.5.3.1 Ash displacement and removal

The results for mean macrotexture depth calculated using the sand patch method for the bare, clean, new asphalt surface and the asphalt surface following dry testing and brushing, and cleaning with compressed air after contamination are shown in Table 3.6.

Table 3.6 Mean macrotexture depth of asphalt slab before and after testing/cleaning, calculated using the ASTM sand patch method, and percentage ash surface coverage.

Asphalt Concrete Slab Condition	Mean Macrotexture Depth (mm)	Ash surface coverage (%)
Bare, clean and new	1.37	0
Ashed, 10x BPT swings	-	81
Ashed, 10x BPT swings and brushed (10x strokes)	0.99	40
Cleaned with compressed air	1.29	<1

The results for the new slab and pre-contaminated slab after cleaning with compressed air suggest that there is little difference in macrotexture depth after cleaning using this method. However, cleaning using only brush strokes shows a mean macrotexture depth reduction of 0.38 mm, 28% less depth than the original new surface. This suggests that cleaning of dry road surfaces using only brushes may not be entirely effective and that alternative methods should be considered where possible. To confirm this, after brushing and 10x swings of the BPT, some HAT-RHY ash remains - as shown in the digital photography macrotexture image sequence (Figure 3.14) and semi-quantitative analysis of these images using 'Ilastik' and 'Adobe Photoshop' gives results of surface coverage (Table 3.6).

Cleaning using high-pressure water spraying and brushing was more effective than brushing alone at removing ash (<1% surface ash coverage afterwards). However, this approach requires large quantities of water and the microscope imagery revealed that some small particles of ash remain on the surface, which would perhaps still reduce skid resistance somewhat. Field observations from Kagoshima, Japan, where high quantities of only low-pressure water are used to clean road surfaces indicates that some ash remains on the road surfaces even immediately after cleaning (Kagoshima City Office, personal communication, 08 June 2015). Furthermore, clearing ash from roads using water may cause some drainage systems to become blocked (Barnard 2009), potentially resulting in surface water flooding.

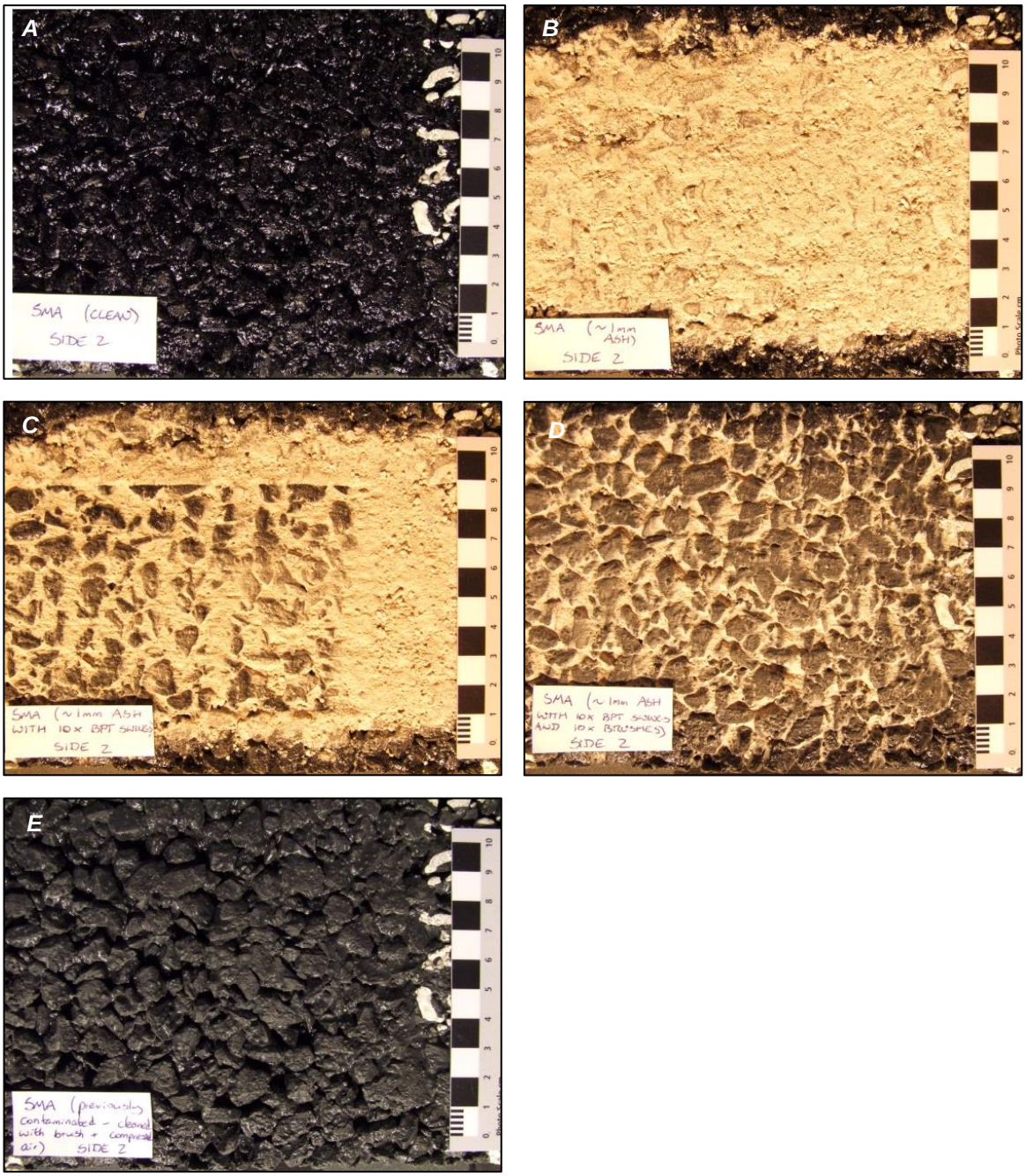

Figure 3.14 Macrotexture image sequence for asphalt. (A) Clean new slab, (B) covered with 1 mm rhyolitic ash (100% surface coverage), (C) after 10x BPT swings (81% surface ash coverage), (D) after cleaning with 10x brush strokes (40% surface ash coverage), (E) after cleaning with compressed air (<1% surface ash coverage). The macrotexture of the surface is visibly affected in images b-d with much ash remaining between the asphalt's aggregate pore spaces, even after 10x BPT swings and cleaning using a brush.

3.5.3.2 Temporal change of skid resistance on bare asphalt surfaces

In normal conditions, the skid resistance of bare asphalt surfaces changes over time. Typically, during the first two years following construction it increases as the surface is worn by traffic and rough

aggregate surfaces become exposed, and then decreases over time as the aggregates become more polished (Asi 2007). The initial trend of increasing skid resistance was confirmed during our testing of the bare wet asphalt and concrete slabs before and after contamination with ash (but following cleaning), particularly so for the asphalt (Figure 3.5). We suggest that the abrasive properties of volcanic ash accelerates these processes, especially for our testing as all ash particles were <500 µm in diameter. Following testing, the SRV of bare wet asphalt had increased by around 5. The microscopy imagery showed that the lustrous film on the new asphalt slabs had been removed during BPT experimentation (Figure 3.15).

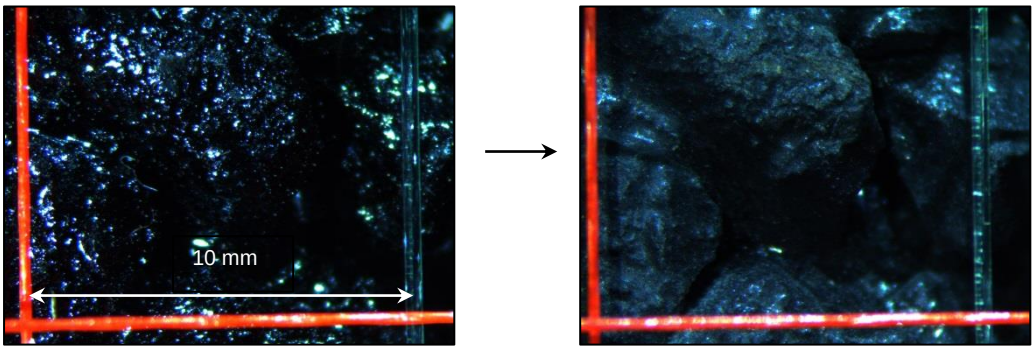

Figure 3.15 Microscope images on the same segment of asphalt, (A) on the new slab and (B) after contamination with volcanic ash and cleaning with compressed air. Much of the shiny film visible on the surface of the new asphalt has been removed. Note that lighting conditions and microscope settings were consistent for both images.

3.6 Conclusions

3.6.1 Key findings

Our experiments suggest that the following lead to particularly reduced skid resistance on asphalt road surfaces and can thus lead to slippery surfaces following volcanic ashfall:

- Thin (~1 mm deep) layers of relatively coarse-grained ash, with ash type having little effect at this depth (average SRVs of 55-65).
- Thicker (~ 5 mm deep) layers of hard, non-vesiculated ash (average SRVs of 55-60).
- Ash of low crystallinity or containing a high degree of soluble components (average SRVs ~5 lower than for ash that has undergone substantial leaching).
- Line-painted surfaces that are either dry or wet but covered by thin layers of ash, particularly when paint does not incorporate retroreflective glass beads (average SRVs of ~55).

Importantly, the largest change in skid resistance for surfaces that became covered by ash occurs during dry conditions, where SRVs fall to levels just below those for wet non-contaminated surfaces, with similar SRVs as the wet contaminated surfaces. This large reduction in skid resistance may not

be expected by motorists who may consequently not adjust driving, potentially resulting in high accident rates. As time goes on, wet ash deposits on roads are most likely to lead to reduced skid resistance, particularly for thicker deposits as these remain slippery for longer (typical SRVs of around 55).

Similarities exist for airfield surfaces and the second and third bullet points above are especially true for the concrete surface type. The following additional key findings are also drawn:

- There is little difference in skid resistance between bare airfield surfaces and those covered by ~1 mm of ash.
- Low crystalline ash containing high soluble components may result in SRVs of up to 20 less than non-dosed samples, particularly if the ash is thicker (~7-9 mm depth).
- Ash is more readily displaced on smoother airfield concrete than road asphalt causing SRVs to recover to 'typical non-contaminated' values at a faster rate with consistent traffic flow.

3.6.2 Recommendations for road safety

Based on skid resistance analysis, we make the following recommendations to increase road safety in areas with volcanic ashfall exposure of ≤ 5 mm depth:

- During initial ash fall, vehicle speed (or advisory speed) should immediately be reduced to levels below those advised for driving in very wet conditions on that road, whether the surface is wet or dry. Wet ash is not necessarily more slippery than dry ash, at least initially.
- Fresh ash contains more soluble components, which results in lower SRVs than for leached ash. Therefore, it is important to advise motorists promptly of any restrictions.
- Particular caution should be taken on dry surfaces that become covered by coarse-grained ash, as skid resistance will reduce substantially from what occurs on dry non-contaminated surfaces. The slipperiness of dry surfaces with such contamination may not be expected by motorists (SRVs will be similar as for wet fresh ash and slightly less than for wet non-contaminated conditions).
- Road markings may be hidden from view, impacting road safety through lack of visual and audio guidance of road features. Areas of road that are line-painted and covered in thin ash are especially slippery. Motorcyclists and cyclists in particular should take extreme care.

It is unlikely that road closures will be necessary for thin ash accumulations based on loss of skid resistance alone. SRVs rarely fall below the minimum recommended threshold for motorways and heavily trafficked roads (i.e. SRV 55) although many values fall between this and the threshold for minimum recommended skid resistance for difficult sites (i.e. SRV 65). These results are conservative however, because of the typical reduction in skid resistance over the later stages of the pavement life. Based on observations from previous eruptions along with work by Barnard (2009), physical obstruction to road vehicles may occur once ash deposits exceed ~100 mm, and road closures may be necessary. It should be stressed however, that all recommendations given ignore other impacts

from volcanic ashfall such as visibility impairment, local road authority decisions, breakdowns and driver behaviour which often introduce further complexities associated with driving in volcanic ashfall. For example, lower thresholds for road closures and lower speed restrictions may be required where visibility is reduced.

3.6.3 Airport safety

We do not make any specific recommendations for airport safety related to concrete airfield surfaces, although it is highlighted that extensive efforts may be required to clean airfield surfaces as has occurred following historical eruptions (e.g. Chaitén 2008 (Wilson 2009 unpublished field notes), Kelud 2014 (Blake et al. 2015)). It is likely that airports will remain closed until all ash has been cleared from runways due to other potential impacts such as damage to aircraft turbine engines. Our results suggest that residual ash of minimal depths on concrete airfield surfaces is likely to have little effect on skid resistance. However, airport managers should be aware that freshly erupted ash or ash that has not been leached (i.e. containing higher soluble components) will likely be more slippery than that which has persisted in the environment for some time. As with road asphalt, wet ash is not necessarily more slippery than dry ash on airfield concrete and any restrictions implemented should thus be in place for both conditions.

3.6.4 Recommendations for cleaning

The following advice for road cleaning is given based on our studies of macrotexture and microtexture and from the observations during small-scale cleaning conducted on our slabs between skid resistance tests:

- Brushing alone will not restore surfaces to their original condition in terms of skid resistance. Following simple brushing practices on asphalt roads, the macrotexture depth may be around one third less than the original depth and ~40% ash coverage may occur on the surface.
- If surfaces are dry and contaminated with dry ash, air blasting combined with suction and capture of loosened ash, is an effective way to remove ash from macrotextural pores. Minor quantities of ash may remain at the microtextural level although this is deemed too low to substantially affect skid resistance.
- If surfaces are wet, a combination of water spraying and brushing and/or air blasting (with suction and ash capture) is an effective way to remove most ash and restore surface skid resistance. However, large quantities of water are required and some ash will remain in the asphalt pore spaces, especially if low-pressure water is used. Care should be taken if using water for ash removal due to the potential for blockage of some drainage systems.

Ash remobilisation should be carefully considered prior to cleaning. Extensive (and often expensive) cleaning efforts may be useless if ash continues to fall or is remobilised from elsewhere and deposited onto roads and airfields.

3.7 Acknowledgements

We thank the University of Canterbury Mason Trust scheme, New Zealand Earthquake Commission (EQC) and Determining Volcanic Risk in Auckland (DEVORA) project for their support towards the study through the provision of funding. We also express thanks to the organisations and people who helped source equipment that was vital to the project. In particular, we would like to thank Alan Nicholson and John Kooloos of the Civil and Natural Resources Engineering department at the University of Canterbury for the loan of the BPT, and Janet Jackson, Howard Jamison and the wider laboratory and road teams at Downer Group for their support towards coordinating the construction and line-painting of asphalt slabs and for providing Daniel Blake with BPT training. We thank Roy Robertson (Auckland Airport) and Robert McKinnon (Firth Concrete) for their advice on airfield surfaces and for providing the airfield concrete slabs used in this study. Particular thanks also go to the people who provided support with the laboratory set-up at various stages, including technician support from Rob Spiers, Matt Cockcroft, Chris Grimshaw and Sacha Baldwin-Cunningham. We also thank researchers Emily Lambie, Rinze Schuurmans, Alec Wild and Alistair Davies for their assistance with sample preparation and skid resistance testing.

3.8 References

Abdel-Aty, M. Ekram, A-A. Huang, H. Choi, K. (2011) A study on crashes related to visibility obstruction due to fog and smoke. Accident Analysis and Prevention, 43:5, pp.1730-1737.

Andersen, O. (2010) Van traffic accident on slippery road. iStock Photograph 14892158. http://www.istockphoto.com/photo/van-traffic-accident-on-slippery-road-gm183542417-14892158?st=a141548, Accessed 01 February 2016.

Andrey, J. (1990) Relationships between weather and traffic safety: past, present and future directions. Climatological Bulletin, 24, pp.124-136.

Asi, I. (2007) Evaluating skid resistance of different asphalt concrete mixes. Building and Environment, 42:1, pp.325-329.

ASTM E303 (2013) Standard test method for measuring surface frictional properties using the British Pendulum Tester. ASTM E303-93 (Reapproved 2013).

ASTM E965 (2006) Standard test method for measuring pavement macrotexture depth using a volumetric technique. ASTM E965-96 (Reapproved 2006).

Aström, H. Wallman, C. (2001) Friction measurement methods and the correlation between road friction and traffic safety: a literature review. Swedish National Road and Transport Research Institute (VTI), Linkōping, Sweden.

Barnard, S. (2009) The vulnerability of New Zealand lifelines infrastructure to ashfall. PhD Thesis, Hazard and Disaster Management, University of Canterbury, Christchurch, New Zealand.

Bastow, R. Webb, M. Roy, M. Mitchell, J. (2004) An investigation of the skid resistance of stone mastic asphalt laid on a rural English county road network. Transit New Zealand, pp.1-16. http://www.nzta.govt.nz/resources/surface-friction-conference-2005/7/docs/investigation-skid-resistance-stone-mastic-asphalt-laid-rural-english-county-road-network.pdf, Accessed 16 June 2015.

BBC (2005) 'Hidden menace' on UK's roads. BBC News. http://news.bbc.co.uk/2/hi/programmes/file_on_4/4278419.stm, Accessed 12 February 2015.

Benedetto, J. (2002) A decision support system for the safety of airport runways: the case of heavy rainstorms. Transportation Research Part A: Policy and Practice, 8, pp.665-682.

Bennis, T.A. De Wit, L.B. (2003) PIARC State-of-the-art on Friction and IFI. Paper presented at the 1st Annual Australian Runway and Roads Friction Testing Workshop. Sydney, Australia.

Blake, D.M. Wilson, G. Stewart, C. Craig, H.M. Hayes, J.L. Jenkins, S.F. Wilson, T.M. Horwell, C.J. Andreastuti, S. Daniswara, R. Ferdiwijaya, D. Leonard, G.S. Hendrasto, M. Cronin, S. (2015) The 2014 eruption of Kelud volcano, Indonesia: impacts on infrastructure, utilities, agriculture and health. GNS Science Report 2015/15, 139p. *[CHAPTER 2 OF THIS THESIS]*

Blake, D.M. Wilson, T.M. Gomez, C. (in review) Road marking coverage by volcanic ash. Environmental Earth Sciences. *[CHAPTER 4 OF THIS THESIS]*

Blastrac (2015) Airport runways: skid resistance and rubber removal. Blastrac, The Netherlands. www.theairportshow.com/Portal/assets/.../BrochureAirport_LR.pdf.aspx, Accessed 05 October 2015.

Blong, R.J. (1984) Volcanic hazards: a sourcebook on the effects of eruptions. New South Wales, Australia.

Boyle, T. (2005) Skid resistance management on the Auckland State Highway Network. Transit New Zealand. http://www.nzta.govt.nz/resources/surface-friction-conference-2005/8/docs/skid-resistance-management-auckland-state-highway-network.pdf, Accessed 16 June 2015.

British Pendulum Manual (2000) Operation manual of the British Pendulum Skid Resistance Tester. Wessex Engineering Ltd., United Kingdom.

Broom, S.J. (2010) Characterisation of "pseudo-ash" for quantitative testing of critical infrastructure components with a focus on roofing fragility. BSc Thesis, University of Canterbury, Christchurch, New Zealand.

Cole, J. Blumenthal, E. (2004) Evacuate! what an evacuation order given because of a pending volcanic eruption could mean to residents of the Bay of Plenty. Tephra, June 2004, Natural Hazards Research Centre, University of Canterbury.

Cole, J.W. Sabel, C.E. Blumenthal, E. Finnis, K. Dantas, A. Barnard, B. Johnston, D.M. (2005) GIS-based emergency and evacuation planning for volcanic hazards in New Zealand. Bulletin of the New Zealand Society for Earthquake Engineering. 38:2, pp.149-164.

Cova, T. Conger, S. (2003) Transportation hazards. In: Transportation Engineers' Handbook, Kutz, M. (Ed.) Centre for Natural and Technological Hazards, University of Utah.

Daily Telegraph (2008) Get a grip: Motorcycle road safety. Daily Telegraph. http://www.telegraph.co.uk/motoring/motorbikes/2750422/Motorcycle-road-safety-Get-a-grip.html, Accessed 12 February 2015.

Delmelle, P. Villiéras, F. Pelletier, M. (2005) Surface area, porosity and water adsorption properties of fine volcanic ash particles. Bulletin of Volcanology, 67, pp.160-169.

Do, M.T. Cerezo, V. Zahouani, H. (2014) Laboratory test to evaluate the effect of contaminants on road skid resistance. Proceedings of the Institution of Mechanical Engineers, Part J: Journal of Engineering Tribology, 228:11, pp.1276-1284.

Dookeeram, V. Nataadmadja, A.D. Wilson, D.J. Black, P.M. (2014) The skid resistance performance of different New Zealand aggregate types. IPENZ Transportation Group Conference 23-26 March 2014, Shed 6, Wellington, New Zealand.

Dunn, M.G. (2012) Operation of gas turbine engines in an environment contaminated with volcanic ash. Journal of Turbomachinery, 134:5, 18p.

Durand, M. Gordon, K. Johnston, D. Lorden, R. Poirot, T. Scott, J. Shephard, B. (2001) Impacts and responses to ashfall in Kagoshima from Sakurajima Volcano: lessons for New Zealand. GNS Science Report 2001/30, 53p.

EASA (2010) RuFAB – Runway friction characteristics measurement and aircraft braking: volume 3, functional friction. European Aviation Safety Agency, Research Project EASA 2008/4, BMT Fleet Technology Limited, Kanata, Ontario, Canada. https://easa.europa.eu/system/files/dfu/Report%20Volume%203%20-%20Functional%20friction.pdf, Accessed 05 October 2015.

Ergun, M. Iyinam, S. Iyinam, F. (2005) Prediction of road surface friction coefficient using only macro- and microtexture measurements. Journal of Transportation Engineering, 131, pp.311-319.

FAA (1997) Measurement, construction and maintenance of skid-resistant airport pavement surfaces. Advisory Circular 150/5320-12C, U.S. Department of Transportation, Federal Aviation Administration. http://www.faa.gov/documentLibrary/media/advisory_circular/150-5320-12C/150_5320_12c.PDF, Accessed 03 October 2015.

Gordon, K.D. Cole, J.W. Rosenberg, M.D. Johnston, D.M. (2005) Effects of volcanic ash on computers and electronic equipment. Natural Hazards, 34, pp.231-262.

Guffanti, M. Mayberry, G.C. Casadevall, T.J. Wunderman, R. (2009) Volcanic hazards to airports. Natural Hazards, 51, pp.287-302.

Heiken, G. Wohletz, K. (1985) Volcanic ash. University of California Press, Berkeley.

Heiken, G. Murphy, M. Hackett, W. Scott, W. (1995) Volcanic hazards to energy infrastructure-ash fallout hazards and their mitigation. World Geothermal Congress, Florence, Italy, pp.2795-2798.

Highway Research Board (1972) National Cooperative Highway Research Program Synthesis of Highway Practice 14: skid resistance. Highway Research Board, National Academy of Sciences, Washington D.C.

Hill, D.J. (2014) Filtering out the ash: mitigating volcanic ash ingestion for generator sets. Masters Thesis, Hazard and Disaster Management, University of Canterbury, Christchurch, New Zealand.

Horwell, C.J. Baxter, P.J. Hillman, S.E. Damby, D.E. Delmelle, P. Donaldson, K. Dunster, C. Calkins, J.A. Fubini, B. Hoskuldsson, A. Kelly, F.J. Larsen, G. Le Blond, J.S. Livi, K.J.T. Mendis, B. Murphy, F. Sweeney, S. Tetley, T.D. Thordarson, T. Tomatis, M. (2010) Respiratory health hazard assessment of ash from the 2010 eruption of Eyjafjallajökull volcano, Iceland: a summary of initial findings from a multi-centre laboratory study. IVHHN and Durham University, Durham, UK.

ICAO (2013) Industry best practices manual for timely and accurate reporting of runway surface conditions by ATS/AIS to flight crew. International Civil Aviation Organisation, Regional Aviation Safety Group (Asian and Pacific Region). http://www.icao.int/APAC/Documents/edocs/FS-07IBP%20Manual%20on%20Reporting%20of%20Runway%20Surface%20Condition.pdf, Accessed 02 October 2015.

Impact (2010) Skid tester: AG190. Impact Test Equipment Ltd. http://www.impact-test.co.uk/docs/AG190_HB.pdf, Accessed 04 November 2014.

Jamaludin, D. (2010) BORDA respond to Merapi disaster. Bremen Overseas Research and Development Association, South East Asia. http://www.borda-sea.org/news/borda-sea-news/article/borda-respond-to-merapi-disaster.html, Accessed 20 October 2015.

Johnston, D.M. (1997) Physical and social impacts of past and future volcanic eruptions in New Zealand. PhD Thesis, Earth Science, Massey University, Palmerston North, New Zealand.

Johnston, D.M. Daly, M. (1997) Auckland erupts!! New Zealand Science Monthly, 8:10, pp.6-7.

Khattak, A.J. Knapp, K.K. (2001) Interstate highway crash injuries during winter snow and non-snow events. Transportation Research Board, 1746, pp.30-36.

Labadie, J. R. (1994) Volcanic ash effects and mitigation. Adapted from a report prepared in 1983 for the Air Force Office of Scientific Research and the Defence Advanced Research Projects Agency.

Leonard, G.S. Johnston, D.M. Williams, S. Cole, J.W. Finnis, K. Barnard, S. (2006) Impacts and management of recent volcanic eruptions in Ecuador: lessons for New Zealand. GNS Science Report 2005/20.

Lester, T. (2014) Pedestrian slip resistance testing: AS/NZS 3661.1:1993. Opus International Consultants Ltd. Lower Hut, Wellington, New Zealand.

Matsumoto, H. Okabyashi, T. Mochihara, M. (1988) Influence of eruptions from Mt. Sakurajima on the deterioration of materials. In: Proceedings Kagoshima International Conference on Volcanoes, pp.732-735.

Miller, T.P. Casadevall, T.J. (2000) Volcanic ash hazards to aviation. In: Sigurdsson et al. (eds), Encyclopedia of Volcanoes, Academic Press, San Diego, CA, United States, pp.915-930.

Nairn, I.A. (2002) The effects of volcanic ash fall (tephra) on road and airport surfaces. GNS Science Report 2002/13, 32p.

NZRF (2005) Road marking IS road safety, Potters Asia Pacific. New Zealand Road Marking Federation Inc. 2005 Conference.

NZRF (2009) NZRF Roadmarking materials guide. New Zealand Roadmarkers Federation Inc. Auckland, New Zealand.

Oh, S. Chung, K. Ragland, D.R. Chan, C. (2009) Analysis of wet weather related collision concentration locations: empirical assessment of continuous risk profile. In: Proceedings of the 88th Annual Meeting of the Transportation Research Board, Transportation Research Board, Washington D.C, U.S.

Persson, B.N.J. Tartaglino, U. Albohr, O. (2005) Rubber friction on wet and dry road surfaces: the sealing effect. Physical Review B, 71.

Pyle, D.M. (1989) The thickness, volume and grainsize of tephra fall deposits. Bullentin of Volcanology, 51, pp.1-15.

Qin, X. Noyce, D. Lee, C. Kinar, J.R. (2006) Snowstorm event-based crash analysis. Transportation Research Record, 1948, pp.135-141.

Sarna-Wojcicki, A.M. Shipley, S. Waitt, R.B. Dzurisin, D. Wood, S.H. (1981) Areal distribution, thickness, mass, volume, and grain size of air-fall ash from the six major eruptions of 1980. The 1980 Eruptions of Mount Saint Helens, Washington, pp.577-600.

Stammers, S.A.A. (2000) The effects of major eruptions of Mt Pinatubo, Philippines and Rabaul Caldera, Papua New Guinea, and the subsequent social disruption and urban recovery: lessons for the future. University of Canterbury, New Zealand.

Stewart, C. Horwell, C. Plumlee, G. Cronin, S. Delmelle, P. Baxter, P. Calkins, J. Damby, D. Mormon, S. Oppenheimer, C. (2013) Protocol for analysis of volcanic ash samples for assessment of hazards from leachable elements. IAVCEI, IVHHN, Cities on Volcanoes Commission, USGS, GNS Science.

TNZ (2003) Standard test procedure for measurement of skid resistance using the British Pendulum Tester, Report TNZ T/2:2003. Transit New Zealand, New Zealand.

Tuck, B.H. Huskey, L. Talbot, L. (1992) The economic consequences of the 1989-90 Mt. Redoubt eruptions. Institute of Social and Economic Research, University of Alaska, Anchorage.

USGS (2009) Small explosion produces light ash fall at Soufriere Hills volcano, Montserrat. United States Geological Survey. https://volcanoes.usgs.gov/ash/ashfall.html#eyewitness, Accessed 20 October 2015.

Volcano Discovery (2014) Sinabung eruption update: 13 January 2014. Volcano Discovery. http://www.volcanodiscovery.com/sinabung-eruptions.html, Accessed 16 January 2014.

Wardman, J. Sword-Daniels, V. Stewart, C. Wilson, T. (2012a) Impact assessment of the May 2010 eruption of Pacaya volcano, Guatemala. GNS Science Report 2012/09.

Wardman, J.B. Wilson, T.M. Bodger, P.S. Cole, J.W. Johnston, D.M. (2012b) Investigating the electrical conductivity of volcanic ash and its effect on HV power systems. Physics and Chemistry of the Earth, 45-46, pp.128-145.

Warrick, R.A. (1981). *Four communities under ash.* Institute of Behavioural Science, University of Colorado, Boulder, U.S.

Wilson, D.J. (2006) An analysis of the seasonal and short-term variation of road pavement skid resistance. PhD Thesis, Department of Civil and Environmental Engineering, University of Auckland, Auckland, New Zealand.

Wilson, D.J. Chan, W. (2013) The effects of road roughness (and test speed) on GripTester measurements. NZ Transport Agency Research Report 523, Clearway Consulting Ltd., Auckland, New Zealand.

Wilson, G. Wilson, T. Cole, J. Oze, C. (2012) Vulnerability of laptop computers to volcanic ash and gas. Natural Hazards, 63, pp.711-736.

Wilson, G. Wilson, T.M. Deligne, N.I. Cole, J.W. (2014) Volcanic hazard impacts to critical infrastructure: a review. Journal of Volcanology and Geothermal Research, 286, pp.148-182.

Wilson, T. Daly, M. Johnston, D. (2009) Review of impacts of volcanic ash on electricity distribution systems, broadcasting and communication networks. Auckland Engineering Lifelines Group, Auckland Regional Council Technical Publication No. 051.

Wilson, T.M. Stewart, C. Cole, J.W. Dewar, D.J. Johnston, D.M. Cronin, S.J. (2011) The 1991 eruption of Volcan Hudson, Chile: impacts on agriculture and rural communities and long-term recovery. GNS Science Report 2009/66, 99p.

Wilson, T.M. Stewart, C. Sword-Daniels, V. Leonard, G.S. Johnston, D.M. Cole, J.W. Wardman, J. Wilson, G. Barnard, S.T. (2012a) Volcanic ash impacts to critical infrastructure. Physics and Chemistry of the Earth, 45-46, pp.5-23.

Wilson, T.M. Cole, J. Johnston, D. Cronin, S. Stewart, C. Dantas, A. (2012b) Short- and long-term evacuation of people and livestock during a volcanic crisis: lessons from the 1991 eruption of Volcán Hudson, Chile. Journal of Applied Volcanology, 1:1, pp.1-11.

Wilson, T. Outes, V. Stewart, C. Villarosa, G. Bickerton, H. Rovere, E. Baxter, P. (2013) Impacts of the June 2011 Puyehue-Cordón Caulle volcanic complex eruption on urban infrastructure , agriculture and public health. GNS Science Report 2012/20, 88p.

World Road Association-PIARC (1987) “Technical committee report on road surface characteristics”, Permanent International Association of Road Congress. Proceedings of the 18th World Congress, Brussels, Belgium.

4. ROAD MARKING COVERAGE BY VOLCANIC ASH: AN EXPERIMENTAL APPROACH

Daniel M Blake[1], Thomas M Wilson[1], Christopher Gomez[2]

[1] Department of Geological Sciences, University of Canterbury, Private Bag 4800, Christchurch, New Zealand

[2] Department of Geography, University of Canterbury, Private Bag 4800, Christchurch, New Zealand

Journal: Environmental Earth Sciences

Received: 09 February 2016

Edits Received: 13 June 2016

Accepted: 02 October 2016

Published: 13 October 2016 *(details: 75:20, pp.1-12)*

Also available from: http://rdcu.be/kVAy

4.1 Abstract

Coverage of road markings by volcanic ash is one of the most commonly reported impacts to surface transportation networks during volcanic ashfall. Even minimal accumulation can obscure markings, leading to driver disorientation, diminished flow capacity and an increase in accidents. Such impacts may recur due to repeated direct ashfall (i.e. during prolonged eruptions) and/or due to the re-suspension of ash by wind, water, traffic or other human activities, and subsequent secondary deposition on the road surface. Cleaning is thus required to restore and maintain road network functionality. Previous studies have not constrained ash accumulation measurements to inform road cleaning initiation or plans for safe road operations in environments containing ash. This study uses a laboratory approach with digital image analysis to quantify the percentage of white road marking coverage by three types of volcanic ash with coarse, medium and fine particle size distributions. We find that very small accumulations of ash are responsible for road marking coverage and suggest that around 8% visible white paint or less would result in the road markings being hidden. Road markings are more easily covered by fine-grained ash, with ash area densities of ~30 g m^{-2} (estimated at less than 0.1 mm surface thickness) potentially causing markings to be obscured. For the coarse ash in our study, road marking coverage occurs at area densities of ~1,000 – 2,200 g m^{-2} (~1.0 – 2.5 mm depth) with ash colour and line paint characteristics causing some of the variation. We suggest that risk management measures such as vehicle speed reduction and the initiation of road cleaning activities, should be taken at or before the lower thresholds as our experiments are conducted at a relatively short horizontal distance and the ability to observe road markings when driving will be comparatively reduced.

4.2 Introduction

As populations grow worldwide, more people are residing in volcanically active areas, generally with associated development and expansion of infrastructure including transportation networks (Loughlin et al. 2015). Volcanic ash is the most widely dispersed of all volcanic hazards, often affecting road transport potentially hundreds to thousands of kilometers from its source. Common impacts include reduced skid resistance and visual range, and engine air filter blockage (Wilson et al. 2014). However, perhaps the most frequent and greatest impact during initial ash accumulation is the coverage of road markings. Road marking coverage is also recognised as a substantial impact in areas affected by duststorms, as experienced for example in parts of the Middle East (Aljassar et al. 2006) and North America (ADOT 2011). It is of concern, as much of the visual information needed by a driver to navigate roads safely is provided by continuous road markings (Gibbons et al. 2004). Coverage can lead to driver disorientation (Durand et al. 2001, T.Wilson et al. 2012, USGS 2013) and cascading effects on vehicle movement across the road network, such as diminished flow capacity and an increase in traffic accidents (Wolshon 2009, Blake et al. 2016). For example, the Automobile Association in Australia estimate that if ‘average standard’ road markings are maintained, the

percentage of crash rates is reduced by between 10 and 40%, depending on the crash type (Carnaby 2005).

Road marking coverage by volcanic ash is by no means transient. Impacts may recur due to repeated ashfall (i.e. during prolonged eruptions) and/or due to the re-suspension of ash by wind, water, traffic or other human activities, and subsequent secondary deposition on the road surface. Road cleaning may thus be required to restore and maintain road network functionality. Some authorities (e.g. Kagoshima City Office near Sakurajima volcano, Japan) use road marking coverage as a prompt to mobilise road sweepers and commence ash removal. In 2014 alone when there were 450 eruptions, this led to the removal of 1,274 m^3 of ash from the region's roads (Kagoshima City Office, personal communication, June 08 2015).

Road marking coverage by volcanic ash has been recorded on road networks following a number of eruptions, such as Mt St Helens, USA (1980), Hudson, Chile (1991), Ruapehu, New Zealand (1995-96), Reventador, Ecuador (2002), and during the many ashfall events on Kagoshima City (Japan) from Sakurajima volcano (1955-2015) (Becker et al. 2001, Cole et al. 2005, Leonard et al. 2005, Barnard 2009, Wilson et al. 2011, Magill et al. 2013). However, a review of available sources reveals only limited estimates of volcanic ash thickness that have caused complete coverage, ranging from trace amounts to 5 mm. We suggest that other characteristics, such as the size of ash particles, colour of ash and road surface texture may account for the range to some extent. At such small accumulations however, depths of ash are difficult to measure accurately and other measurements such as the area density of ash may be more appropriate.

In this study at the University of Canterbury's Volcanic Ash Testing Laboratory (VATLab), we adopt a method to replicate volcanic ash deposition on road surfaces by using asphalt slabs painted with two thicknesses of line paint. We employ image classification and segmentation techniques to quantify the extent of road marking coverage by ash and to determine ash depth and surface area density when markings are visually obscured. Based on our findings, suggestions to maintain road safety are made, particularly thresholds for road cleaning initiation.

4.3 Methods

4.3.1 Ash and road surface type

Stone Mastic Asphalt (SMA), constructed as 300 x 300 x 45 mm slabs (with aggregate particle size <13.2 mm and a bitumen content of 5.9 %) by the Road Science Laboratory in Tauranga, New Zealand, were placed directly beneath an ash delivery system (Section 4.3.2). Three ash types (a basalt of dark colouration, an andesite of medium colouration, and a rhyolite of light colouration) were sourced from different ash deposits in New Zealand (Table 4.1) to provide a means of contrast comparison (Blake et al. 2016). As the un-modified samples contained coarse material (some up to 20 mm diameter), all material was dried and then processed using a rock pulveriser and/or sieving to

achieve three distinct clusters of particle size distributions (Figure 4.1). Spatial distributions of particle sizes from ashfall events are often complex. However, ash particle sizes are typically larger closer to the vent with smaller particles carried further downwind (Jenkins et al. 2014).

Particle sizes (Figure 4.1) were determined using a Micrometrics Saturn DigiSizer II Laser-Sizer (three runs per sample). We note that the maximum particle sizes for some samples are substantially less than the size of the disc measure used for pulverisation or sieve mesh aperture. For example, the Pupuke basalt sample in the medium particle size group (Table 4.1) was pulverised with a disc spacing of 990 µm and sieved with a mesh aperture of 1000 µm, but all resulting particles are <500 µm in diameter (Figure 4.1). This is likely due to the process of pulversiation and mechanism of breakage. Conversely, the maximum particle sizes for some samples are greater than the size of the sieve mesh aperture used (e.g. the fine-grained rhyolite sample, which was sieved at 54 µm but contains a fraction of particles up to 280 µm in diameter). This is due to the tabulate form of some ash particles and their orientation when passing through the sieve.

Table 4.1 Ash samples used for testing and their characteristics following processing. There is no coarse particle group for the Hatepe rhyolite ash type due to the smaller particle sizes of the raw field sample.

	Pupuke, Auckland Volcanic Field			**Poutu, Tongariro**			**Hatepe, Taupo**	
Time of eruption	~200,000 years BP			~11,000 - 12,000 BP			~1,770 years BP	
Ash type	Basalt			Andesite			Rhyolite	
Colour (determined from Munsell Rock Colour Chart)	N4: Medium Dark Grey			5Y 6/1: Light Olive Grey (with a small 10YR 6/6 Dark Yellowish Orange component when coarse)			5Y 8/1: Yellowish Grey	
SiO_2 content (determined by Philips PW2400 XRF analysis)	44% (mafic)			52% (intermediate)			70% (felsic)	
Dominant minerals (determined by Philips XRD analysis)	Diopside, Forsterite, Anorthite			Albite, Augite			Sanidine, Quartz	
Particle size group	coarse	medium	fine	coarse	medium	fine	medium	fine
Modal particle size (µm) (Figure 4.1)	680	220	40	540	200	40	180	35
Dry bulk density ($g\ cm^{-3}$)	1.1	1.5	1.1	1.3	1.2	0.9	0.9	0.7

Mafic ash such as the Pupuke samples, along with intermediate ash such as Poutu, is relatively common from eruptions globally. Eruptions of felsic ash such as Hatepe, are less common (Wicander and Monroe 2006), but the high concentration and quantity of lighter elements, high explosivity and

generally high eruption columns, means that the ash can be dispersed up to hundreds of kilometers from the vent (Woo 2009).

Paint is the most common and widespread form of road marking material in most countries worldwide. In this study, Downer Group applied a Damar Beadlock paint, which contains 63% solids, using a standard machine on the asphalt concrete slabs. The side of one slab was painted with a single coat 180-200 µm thick, and the other side with four coats (720-800 µm thick in total) to replicate markings that have been exposed to different abrasion or multiple paint applications. The other slab was painted with the same thickness lines but with retroreflective glass beads incorporated in the paint mix.

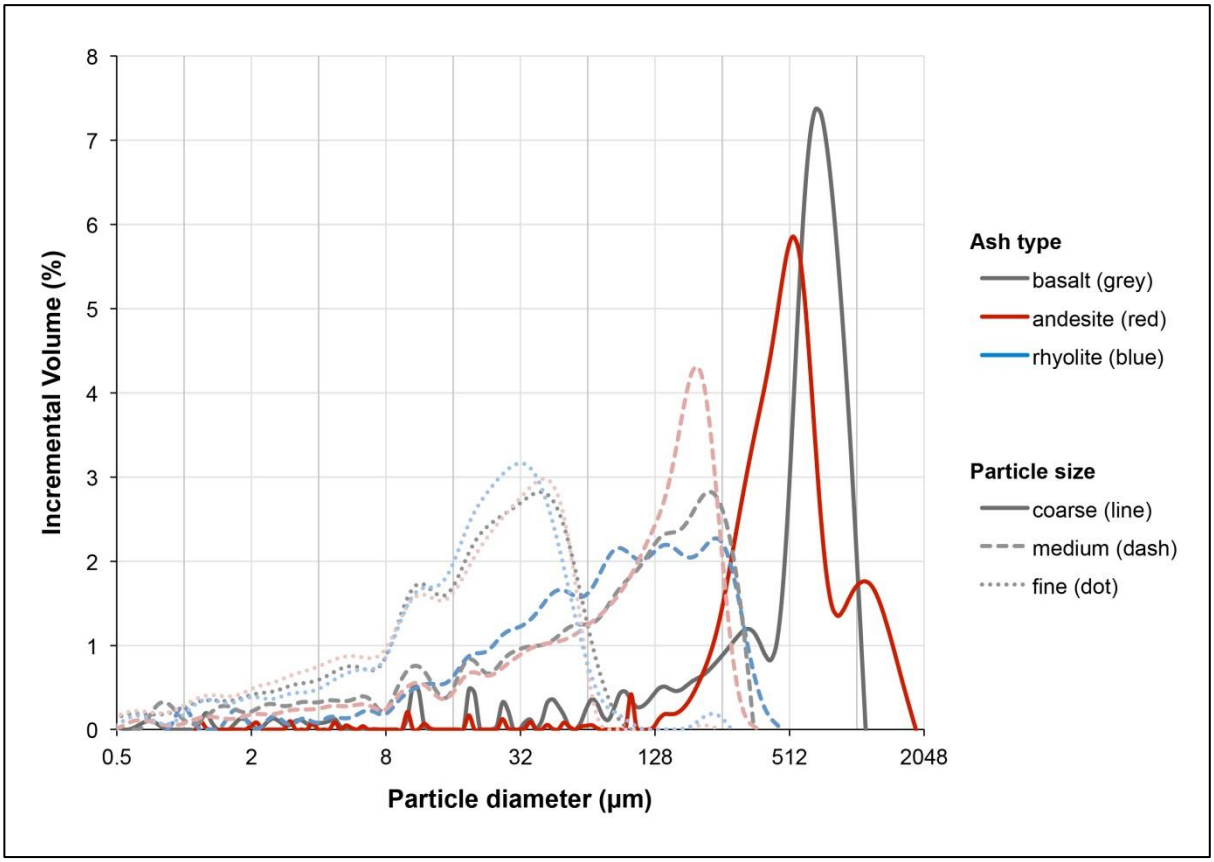

Figure 4.1 Mean particle size distributions of samples used in experimentation and their designated classification discussed in this article (i.e. coarse, medium and fine).

4.3.2 Ash application and measurement

The ash delivery system used comprises of a 400 x 400 x 100 mm sieve box with an adaptable mesh base (of 1 mm, 500 µm or 125 µm aperture depending on the particle size distribution of the ash) and manual-striking hammer which causes ash to fall through when struck. The set-up has been used in previous experiments including by G.Wilson et al. (2012) and Hill (2014). The ash delivery system produces ash in a consistent and repeatable manner and is calibrated to replicate ash settling

velocities and accumulation rates that would be expected from real ashfalls. The delivery system has been designed using formulas derived from Bonadonna et al. (1998) (equations 1-3) to ensure that the majority of ash particles dispensed from the sieve box reach terminal velocity well before ground level (Hill 2014):

$$V_t \approx (3.1\, g\, \rho\, d / \sigma)^{1/2} \quad (1)$$

$$V_t \approx (g\, \rho\, d^2 / 18\, \mu) \quad (2)$$

$$Vt \approx d\, (4\rho^2\, g^2 / 225\, \mu\, \sigma)^{1/3} \quad (3)$$

where V_t is the terminal velocity, g is the acceleration due to gravity (9.81 m s^{-2}), ρ is the density of the particles, d is the particle diameter, σ is the density of the air and μ is the dynamic viscosity of the medium (Bonadonna et al. 1998, Hill 2014).

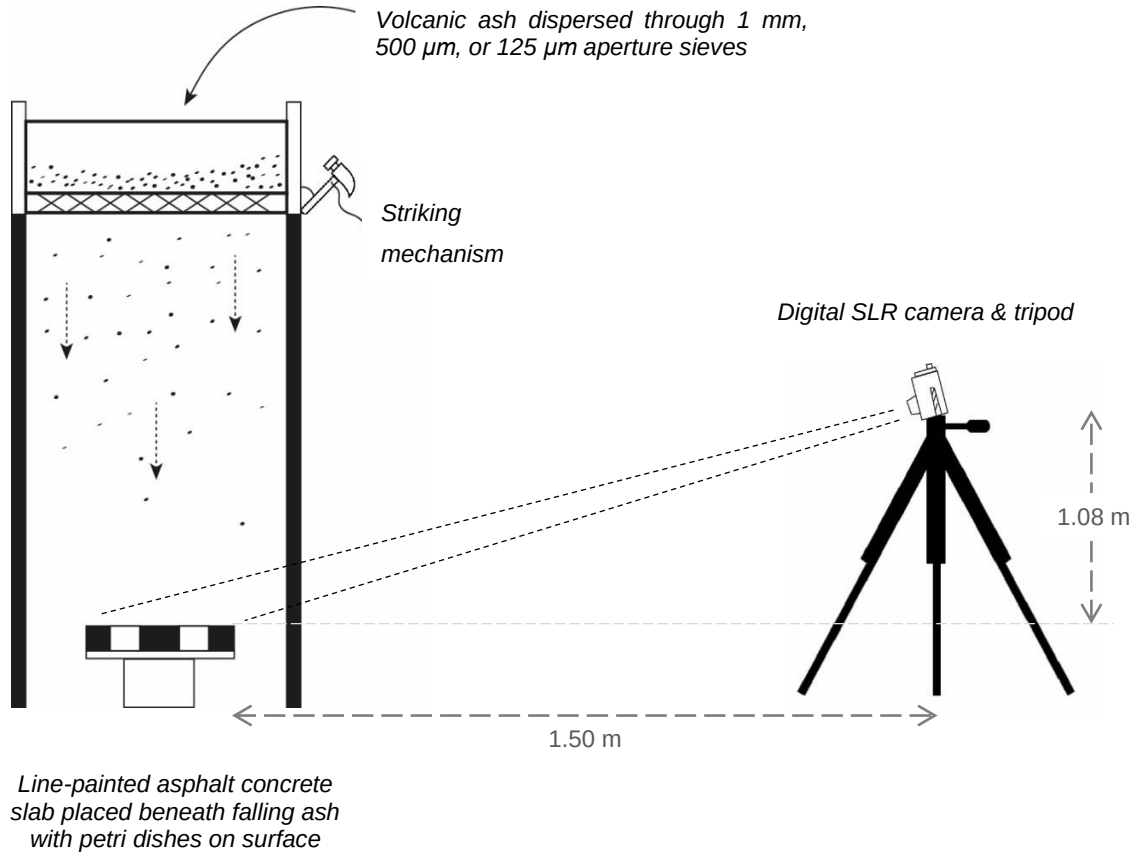

Figure 4.2 Experimental set-up for road marking visibility testing (adapted from Blake et al. 2016).

In this study, we incorporate the ash delivery system to investigate failure thresholds (i.e. when road markings become obscured by ash). Petri dishes (85 mm in diameter) were placed on the asphalt

surface at the end of each road marking line to enable measurements of ash thickness from a flat surface (using a calliper). Ash thicknesses within asphalt aggregate pores of both average and distinctively large depth, and from the top of aggregate grains were also recorded (averaged from 5 measurements for each). Furthermore, the mass of ash collected in the petri dishes was measured at each stage in order to calculate the area density throughout experimentation. This was conducted to allow a more accurate measure of ash deposition, particularly as the thickness of ash at low accumulations is difficult to measure, and also the quantity of ash released by the delivery system experiences slight variations between ash types and as the experiment progresses and sieve mesh becomes clogged.

4.3.3 Image collection

A Fuji Finepix S100 (FS) digital SLR camera was mounted on a tripod 1.5 m horizontally and 1.08 m vertically away from the slab (Figure 4.2), 1.08 m being the height of the driver's eye above the road in measuring stopping sight distances (Fambro et al. 1997, Blake et al. 2016). A digital photograph was taken at a focal length of 200 mm (under consistent camera and light conditions) and observations were noted following strikes of the ash delivery system after the ash had settled. This was conducted until five photos after the ash visually appeared to the observer to completely cover the markings. The number of strikes between each photo was varied depending how readily the ash sample passed through the sieve mesh. The mean depths of ash in the asphalt pores and on the surfaces of both the asphalt slab and petri dishes, along with the mass of petri dishes containing ash were measured and recorded in conjunction with each photo.

Other research involving road marking visibility has been conducted in the past, often involving participant drivers in simulated driving conditions (e.g. Brooks et al. 2011) or on the road at specialised road research facilities (e.g. Gibbons et al. 2004, Gibbons and Williams 2012). Specialised technical equipment has also been developed to measure the retroreflective luminance of markings (e.g. Carlson and Miles 2011). Most previous experiments have assessed the effectiveness of road markings where atmospheric conditions such as rainfall and fog present a hazard to driving. In these experiments, the distance between participants or equipment from road markings is often in the order of tens of meters. Our experimental set-up enables precise analysis of ash accumulation on the road surface and detailed measurements under controlled conditions. We investigate road markings at close range (1.5 m horizontal distance) and, due to spatial laboratory constraints, do not directly account for viewing road markings >1.5 m away. Additionally, we do not account for visibility interference due to airborne volcanic ash, which requires separate investigation. Therefore, our results for road marking coverage are conservative, and at greater viewing distances or where the atmosphere contains ash, road marking visibility will likely be even less than portrayed.

4.3.4 Image analysis

Each image file was opened using Ilastik version 0.5.12 software (Sommer et al. 2011) to conduct supervised segmentation by pixel colour; one class was created for the white paint, and another class

for ash or asphalt (Figure 4.3) (Blake et al. 2016). After segmentation (which displayed the white paint as red, and asphalt and ash as green), image registration was achieved in Adobe Photoshop version CS6, ensuring that each image was cropped automatically without the geometry of objects changing between images. The photographs were intentionally not nadir, and the images were not orthorectified as the viewing angle and associated properties of visibility were of particular interest in the study. The mean pixel resolution was 1 pixel to 0.088 mm for the cropped area of the photographs. A fuzziness setting of 200 was selected to account for the range of colours in the ash, asphalt and line paint. This selects all pixels that are the exact same colour as the pixels clicked on, as well as all pixels that are within 200 brightness values lighter or darker. The 'histogram' function was then used to observe and record the pixel count for the white paint (red pixels). The number of pixels for the ash/asphalt was then calculated by subtracting the number for the white paint from the total pixel count. A total of 142 photographs (i.e. 284 cropped line images) were analysed with a mean of nine images analysed for each sample of specific particle size distribution and ash type.

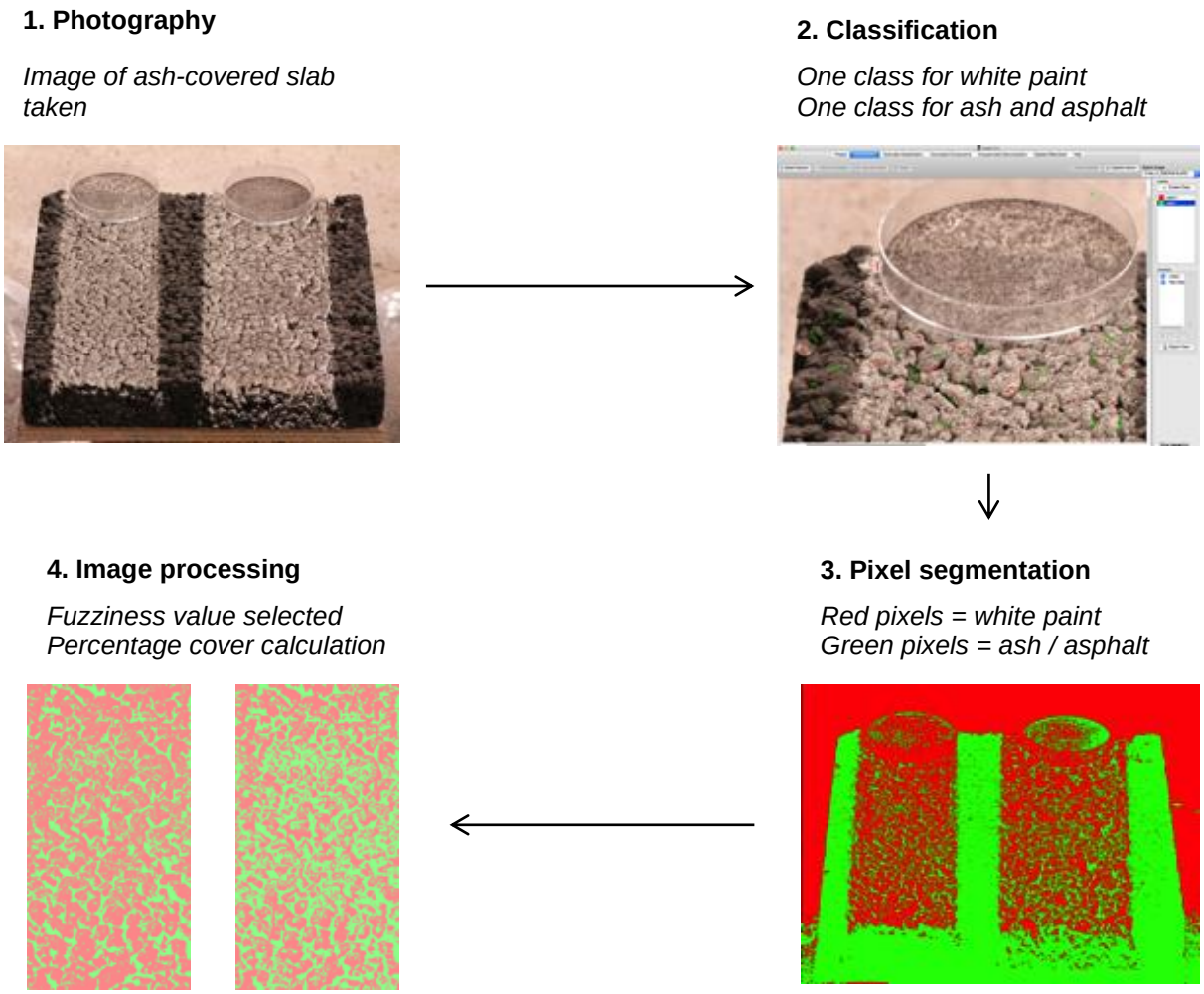

Figure 4.3 Generalised steps for the image analysis process.

4.4 Results and Discussion

After the sieve box had been struck 5 times, the subsequent dispersal of ash through the delivery system and accumulation on the slabs led to a substantial decrease in the percentage of pixels representing white road marking paint for all of our samples (Figure 4.4). This suggests that only very small ash accumulations are required for an impact on road marking visibility reduction (Blake et al. 2016). With further ash accumulation, the road markings continue to become obscured but at a decreasing rate. Through physical visual observations in the laboratory and comparisons with raw and analysed images (Section 4.3.4), it was decided that when 8% white line paint or less is visible that it would be unlikely that drivers could effectively view road markings when driving (Blake et al. 2016). Therefore, the measurements of ash area density and depth at this threshold are of interest. It appeared particularly difficult to delineate the edges of the markings around this value, although we note that the 8% threshold is somewhat subjective and that there are few comparative studies; most others adopt instruments such as retroreflectometers, which are used over several tens of meters (e.g. Dravitzki et al. 2003, Babic et al. 2014).

The 8% threshold of pixels for white paint (i.e. 92% pixels for ash/asphalt) was evident through image analysis at ash area densities of between 30 g m^{-2} and 2,150 g m^{-2} for all ash samples used in experimentation (Table 4.2). This equates to ash depths of between trace amounts (taken to be <0.1 mm in our study) and 2.2 mm, measured from the surface of the asphalt aggregate. The large range in measurements is largely due to the influence of particle size, but also ash type and road paint characteristics to some degree (Sections 4.4.1 – 4.4.3).

Our findings correspond well with the ash characteristics and observations of road marking coverage at Sakurajima volcano in Kyushu, Japan. In June 2015, the Kagoshima City Office reported that area densities were ~300-400 g m^{-2} when road markings could not be seen and cleaning was required (Kagoshima City Office, personal communication, June 08 2015). The ash is typically of andesitic type, typically with a SiO_2 content of ~59%, and mode particle sizes of 150-200 μm at this distance (4-5 km) for recent eruptions from the Showa crater (Yamanoi et al. 2008, Matsumoto et al. 2013, Nanayama et al. 2013, Miwa et al. 2015). Our summarised results (Table 4.2) suggest that ash depths on the roads, measured from the surface of the asphalt aggregate, would have been approximately 0.5 mm at the time.

We highlight the importance of outlining the specifics for depth type measured on road surfaces for ash accumulations less than ~10 mm. Depths within the asphalt aggregate voids were found to be over five times greater than those measured from the surface of the aggregate in some cases (e.g. for the coarse andesite, ash depths within voids were ~7.5 mm when surface depths were ~1.4 mm).

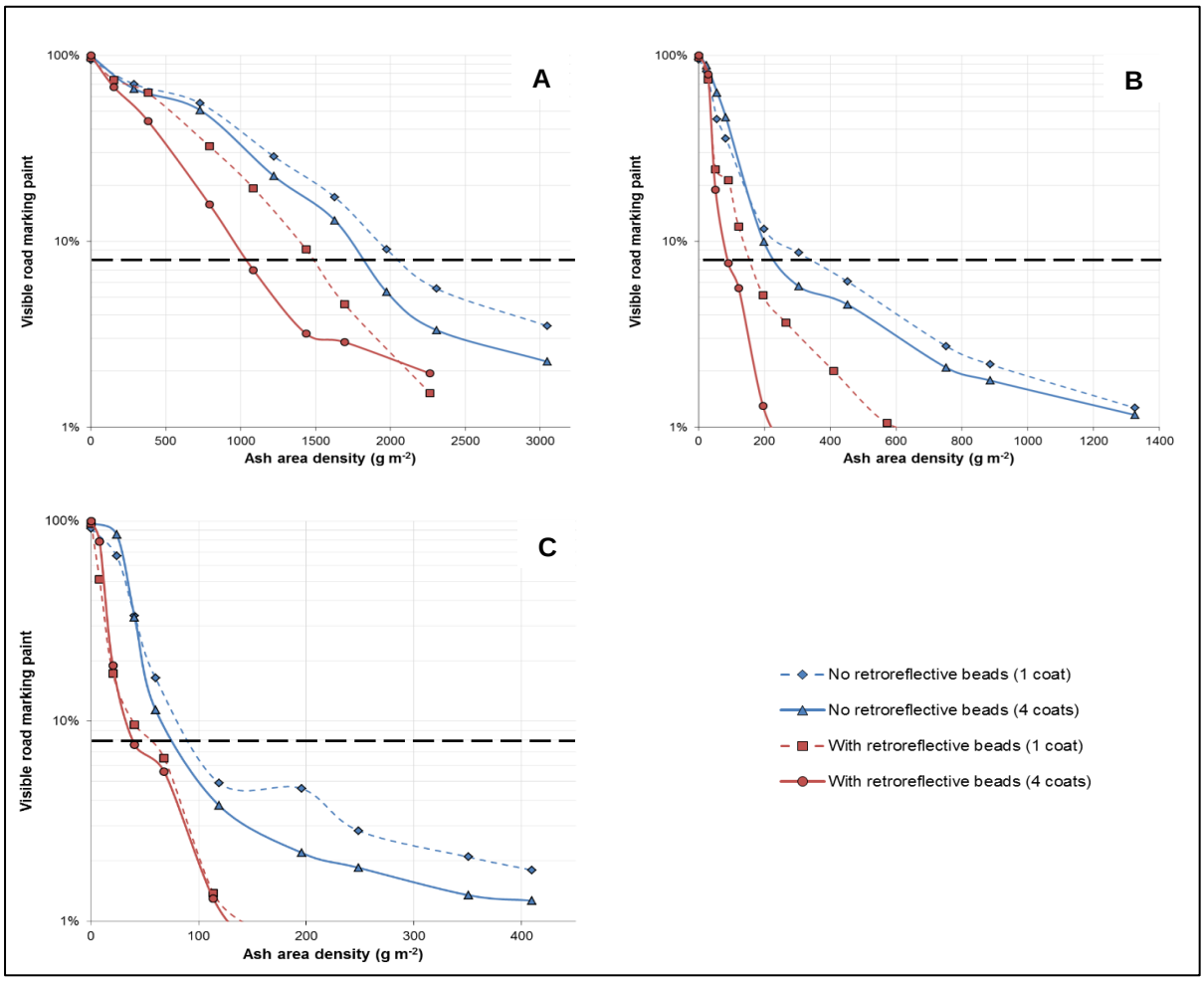

Figure 4.4 Percentage of white road marking paint visible and ash area densities for the andesite sample with mode particle size of a) 600 µm, b) 200 µm, and c) 40 µm. The results for asphalt slabs covered by one and four coats of paint with and without retroreflective glass beads incorporated in the paint mix are shown. Also displayed are the thresholds for 8% visible road marking paint (horizontal black dashed lines). We suggest that it would be difficult for drivers to view road markings at or below this threshold.

Table 4.2 Measurements of ash area density and depths when it would be difficult for drivers to see road markings (i.e. when 8% white line marking paint was visible), determined through image analysis for all of the ash samples tested. The range of values is largely due to differences in paint thickness (i.e. number of coats) and retroreflective bead content of the paint (see Section 4.4.3), as well as unavoidable but natural variations in surface texture across the asphalt slabs.

		ASH TYPE		
		Basalt	**Andesite**	**Rhyolite**
MODE PARTICLE SIZE DISTRIBUTION	**Coarse (600 – 700 µm)**	Area density: 1350 – 2150 g m^{-2} Depth on surface: 1.0 – 2.2 mm Depth in voids: 3.3 – 7.5 mm	Area density: 1050 – 2100 g m^{-2} Depth on surface: 1.0 – 1.4 mm Depth in voids: 3.2 – 7.5 mm	*(No data as sample not possible at this particle size)*
	Intermediate (200 – 260 µm)	Area density: 240 – 450 g m^{-2} Depth on surface: 0.3 – 0.8 mm Depth in voids: 0.9 – 1.5 mm	Area density: 80 – 350 g m^{-2} Depth on surface: 0.2 – 0.5 mm Depth in voids: 0.4 – 1.5 mm	Area density: 40 – 180 g m^{-2} Depth on surface: 0.2 – 0.4 mm Depth in voids: 0.2 – 0.7 mm
	Fine (35 – 45 µm)	Area density: 45 – 80 g m^{-2} Depth on surface: trace – 0.1 mm Depth in voids: trace – 0.1 mm	Area density: 35 – 80 g m^{-2} Depth on surface: trace – 0.1 mm Depth in voids: trace – 0.1 mm	Area density: 30 – 65 g m^{-2} Depth on surface: trace – 0.1 mm Depth in voids: trace – 0.1 mm

4.4.1 Road marking type

The thickness of surface paint appears to have some influence on road marking coverage. Figure 4.4 illustrates that the lines with four coats of paint generally become covered more easily than a single coated line. This is intuitive because the greater quantity of paint acts to reduce the macrotexture of the asphalt surface, causing the voids to fill sooner with the same mass of ash.

The markings of paint that incorporate retroreflective glass beads in the mix are generally more easily obscured. This is perhaps due to the retroreflective beads adding to the overall volume of paint, thus reducing the macrotextural depth of the asphalt voids. The rougher microtexture may cause more ash to remain on the surface than for road markings without beads (caused by retroreflective beads 'trapping' individual ash particles as they fall). Crystalline ash particles will also act to reflect light, potentially reducing the effectiveness of the added retroreflective beads. Therefore, although retroreflective beads are added to paint with the overall intention of improving road safety, they act to

reduce the visibility of road markings when volcanic ash accumulates, reducing road safety in such environments.

The ranges of ash area densities and ash depths shown in Table 4.2 are mainly due to the variations in road marking characteristics. Generally, the higher values reflect conditions where there is less paint and/or where the paint mix does not contain retroreflective beads, and the lower values in the table correspond to road markings formed of multiple paint layers (with little wear) and/or where the paint incorporates retroreflective beads.

4.4.2 Ash particle size

It is evident that road marking coverage is highly dependent on the particle size distribution of volcanic ash falling on textured road surfaces such as SMA (Table 4.2). Ash depth measurements in petri dishes and on different locations of the asphalt surfaces, and through visual observations when the ash was falling, revealed that this is largely due to the behaviour of individual particles upon impact (Figure 4.5).

A mass of fine ash particles is more effective at covering road markings than the same mass of coarse particles. Indeed, for our samples the mass of the ash in petri dishes when the road markings became covered (i.e. when only 8% white line paint was visible) ranged from 0.2 g (for fine-grained particles) to 14 g (for coarse-grained particles). This is largely because coarser particles bounce into the macrotextural voids of the asphalt aggregate and initially accumulate in these spaces, with white road marking paint on the upper asphalt surface remaining uncovered and visible to drivers (Figure 4.5). Even as the ash in the void spaces accumulates to the upper surface of the asphalt, ash particles settling on the surface of the aggregate have a tendency to be displaced by further ash that falls and collect in areas immediately above the voids where the thicker existing ash limits movement. This results in very small mounds of ash immediately above the voids (with white line paint still visible in-between) before ash spreads across the entire surface of the asphalt.

Fine ash particles pack more densely wherever they settle, causing the surface to be easily covered. This process is observed on the asphalt and on the flat surfaces of our petri dish bases. It has also recently been attributed to the vulnerability of horizontally placed photovoltaic modules and power-output reduction (Zorn and Walter 2016). Furthermore, the fine ash particles appear to exhibit electrostatic properties and adhere more readily to the asphalt surface, successfully covering the line-covered aggregate at various orientations. Ash with finer particle size distributions, and sometimes more triboelectrically charged particles (Aplin et al. 2014) are relatively common in distal volcanic plumes. Therefore, our findings indicate that road marking coverage, especially in distal locations from volcanic vents, should not be overlooked.

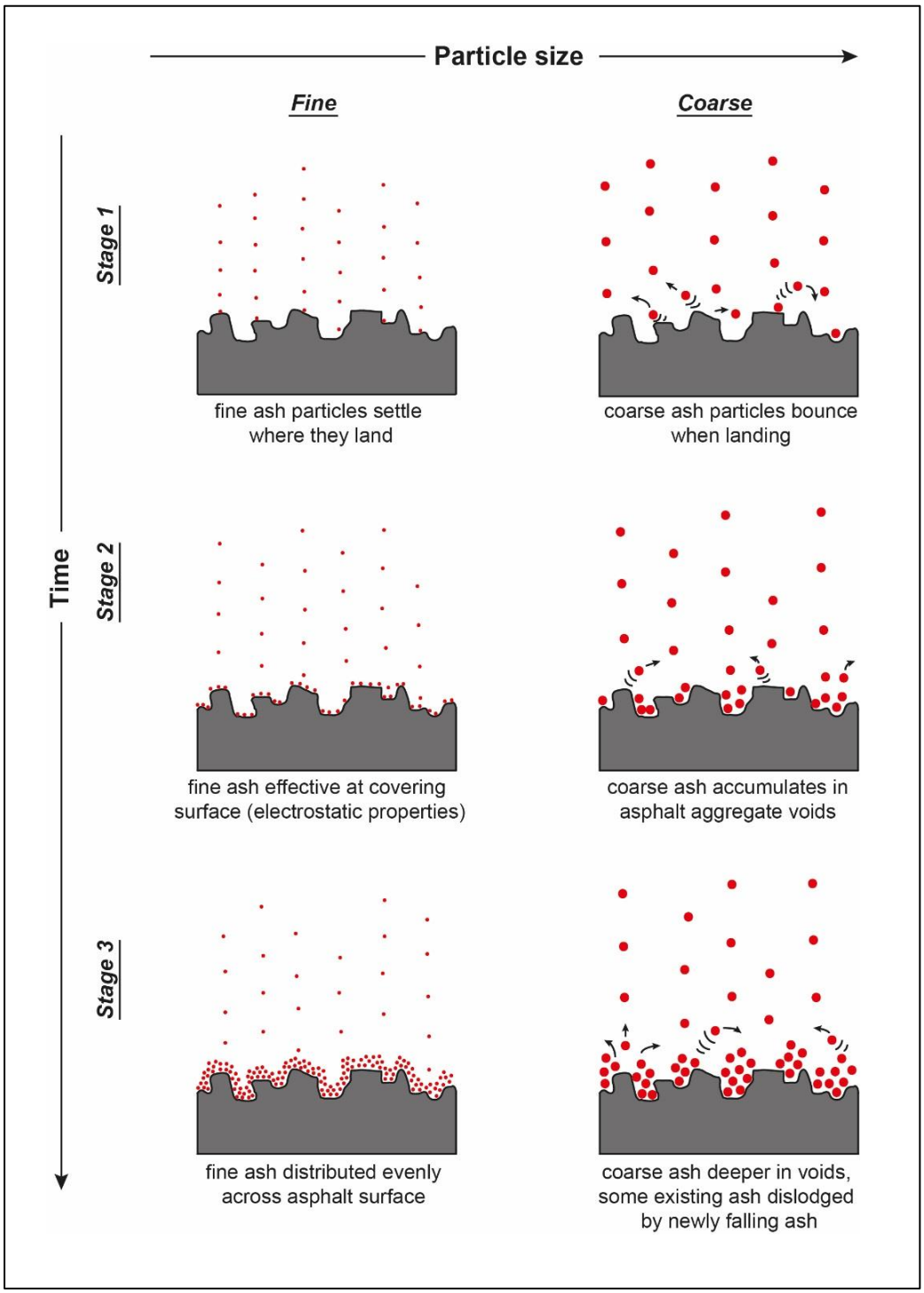

Figure 4.5 The process of ash accumulation on textured road surfaces showing the difference between ash containing predominantly fine and coarse particles.

4.4.3 Ash type and contrast

Although the mean dry bulk densities for the light-coloured ash were less than those of the darker material, less ash is required at intermediate and coarse particle sizes to cover the same percentage of road markings. For example, at intermediate particle sizes (i.e. 200-260 μm modal distributions), 8% of line paint is visible at mean asphalt surface accumulations of 0.55 mm for the basalt (dark-coloured), 0.35 mm for the andesite (mid-coloured), and 0.30 mm for the rhyolite (light-coloured) (Figure 6.4). This suggests that white road markings covered by light-coloured deposits such as the rhyolite may become obscured at smaller depths than dark-coloured deposits such as the basalt. Although the same trend is suspected for fine ash particle sizes, it is not verified here due to the very small accumulations it took for surfaces to be covered (≤ 0.1 mm) and difficulties in measuring and estimating ash depths.

Some of the difference between ash colour types may be due to errors in the image analysis process whereby the ash and markings are more difficult to classify when the ash is of lighter colour. However, the image analysis findings correspond with the visual observations recorded during experimentation in that it was more difficult to distinguish road markings when covered by light-coloured ash compared to the same depths of dark-coloured ash (Blake et al. 2016). The findings also align with the mere definition of visual contrast (i.e. the difference in colour or brightness between objects that makes them distinguishable). With light-coloured ash covering the dark asphalt either side of white road markings; the markings will be less distinguishable. Additionally, the farther an object is from a driver, the greater the contrast requirements (Gibbons et al. 2004). Therefore a driver's ability to see road markings with distance may be less for light-coloured than dark-coloured ash (Blake et al. 2016).

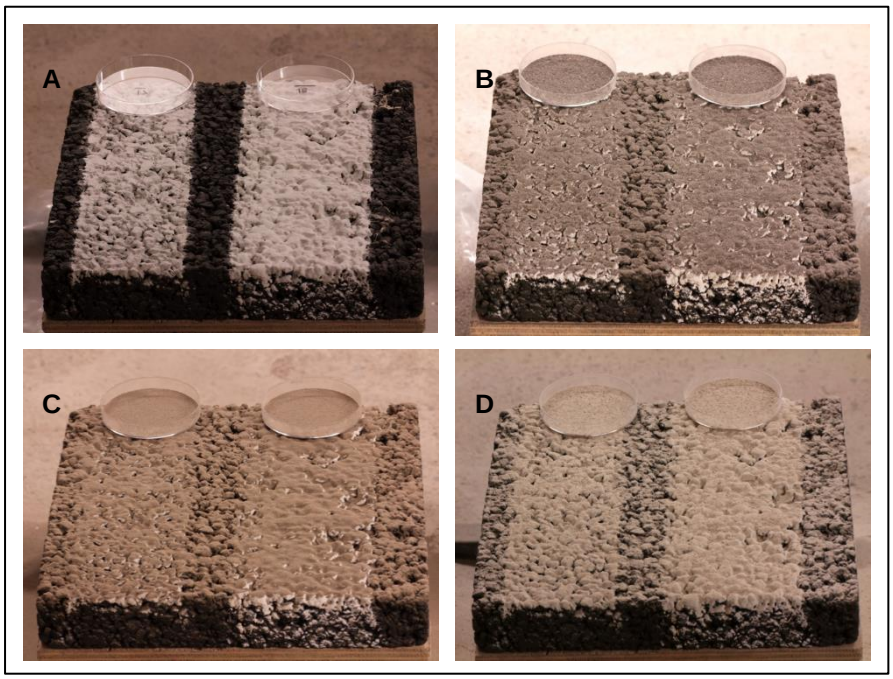

Figure 4.6 Road markings painted on a SMA slab as one coat (left lines) and four coats (right lines), both containing no retroreflective beads in the paint mix (adapted from Blake et al. 2016). a) shows the markings with no volcanic ash on the surface. b), c) and d) show when ≤ 8% of line paint is visible (i.e. when it would be difficult for drivers to see the lines) for basaltic, andesitic and rhyolitic ash of 200-260 µm modal particle size distributions respectively. This corresponds to mean thicknesses on the surface of the asphalt aggregate of 0.55 mm for the basalt, 0.35 mm for the andesite, and 0.30 mm for the rhyolite.

4.5 Conclusion

Our experimental findings demonstrate that very low levels of volcanic ash accumulation can cause substantial road marking coverage. If ash particles are predominantly fine (i.e. mode particle sizes ≤45 µm), then road markings may become obscured for drivers when ash area densities are between 30 and 80 g m^{-2}. This is equivalent to ≤0.1 mm of ash accumulation on the surface of the asphalt.

Ash particle size distribution is likely the most important characteristic for road marking coverage at small depths and a mass of fine particles is much more effective at covering a surface than the same mass of coarse particles. This is largely attributed to the ash particle behaviour upon initial impact, with coarse particles bouncing into voids between the asphalt aggregate and fine particles generally settling where they initially land. For coarse (i.e. mode particle sizes ≥600 µm) ash, depths ≥1.0 mm, measured from the surface of the aggregate, or ≥3.2 mm, measured within the asphalt voids, lead to road marking coverage. This represents ash area densities at least 13 times greater than for fine ash of the same type. These thresholds assume dry and near-pristine atmospheric conditions (i.e. no airborne ash) and further work is required to determine the extent of visual range impairment by suspended ash particles.

Road markings covered by light-coloured ash of the same thickness as dark-coloured ash are more difficult to distinguish (due to low contrast). Multiple paint layers (assuming little wear) and paint mix that incorporates retroreflective glass beads also make markings more difficult to distinguish when covered by ash. Although crucial to consider on all road networks that include line painted surfaces in volcanically active regions, our findings especially highlight the susceptibility of road markings being covered in distal areas from the vent.

We recommend thresholds for when road cleaning should occur on asphalt surfaces in order to maintain road safety and network functionality. Note that the values assume 'worse-case conditions' for volcanic ash coverage in terms of paint characteristics:

1. For fine (~30 – 45 μm mode particle size) ash of all types and felsic ash such as rhyolite up to a size dominated by ~300 μm particles, road cleaning should be conducted at or before ash area densities of 30 – 45 g m^{-2}. Depths will be extremely difficult to measure at such accumulations but will likely be around 0.1 – 0.2 mm from the surface of the upper aggregate.

2. For intermediate size (up to ~300 μm mode particle size) andesite, road cleaning should be conducted at ash area densities of ~100 g m^{-2}. For mafic ash such as basalt of the same size, it should be conducted at ~250 g m^{-2}. Surface depths will be around 0.2 – 1.0 mm at this stage.

3. For coarse (mode particle sizes up to ~800 μm) andesite and basalt, road cleaning should occur at ash area densities of ~1,000 and 1,500 g m^{-2} respectively, which is equivalent to surface depths of approximately 1.0 – 2.5 mm.

Due to road safety considerations in environments when there is no volcanic ash, it seems counterintuitive to suggest changes to road marking paint mix properties such as changes in retroreflective glass bead concentrations or design, so that visibility of road markings is maintained at a higher standard solely during ashy conditions. Therefore, we do not suggest that any major changes to physical road marking properties should be made in areas prone to volcanic ashfall. Applying new coats of paint should only be conducted if existing paint is sufficiently worn and if it is required to improve road safety in normal conditions. This is because thicker paint can lead to road markings becoming more easily obscured by ash. Changes to the physical structure of the road surface itself, such as the application of an aerodynamic profile to promote particle removal from the carriageway by wind-driven saltation (as achieved in Kuwait (Aljassar et al. 2006)), may be cost-effective in some regions frequently affected by volcanic ash. However, perhaps the simplest technique to improve road safety in all areas when road markings become covered is for all drivers to travel at a reduced speed, or to avoid driving until the ash is cleared.

4.6 Acknowledgements

We thank the University of Canterbury Mason Trust scheme, New Zealand Earthquake Commission (EQC) and Determining Volcanic Risk in Auckland (DEVORA) project for their financial support towards the study through the provision of funding for authors Daniel Blake and Thomas Wilson. We also express thanks for the support towards laboratory assistance and equipment provided by several people, whose help was vital to the success of this study. In particular we wish to thank Janet Jackson and Howard Jamison of Downer Group for coordinating the painting of the asphalt concrete slabs, and Kerry Swanson, Matt Cockcroft, Chris Grimshaw, Stephen Brown, Alec Wild, Connor Jones and Brigitt White for their assistance with sample preparation and conducting experiments at the University of Canterbury's Volcanic Ash Testing Lab. Daniel Blake would also like to thank his PhD co-supervisors, Jim Cole (University of Canterbury), Jan Lindsay (The University of Auckland) and Natalia Deligne (GNS Science) for their edits, guidance and support throughout the project.

4.7 References

ADOT (2011) Dusty roads. Arizona Department of Transportation Blog. http://www.azdot.gov/media/blog/posts/2011/04/18/dusty-roads, Accessed 13 October 2015.

Aljassar, A.H. Al-Kulaib, A. Ghoneim, A.N. Metwali, E-S. (2006) A cost effective solution to the problem of sand accumulation on a desert road in Kuwait. Third Gulf Conference on Roads, March 6-8, 2006. www.draljassar.net/text/t0026.doc, Accessed 13 October 2015.

Aplin, K. Houghton, I. Nicoll, K. Humphries, M. Tong, A. (2014) Electrical charging of volcanic ash. Proceedings ESA Annual Meeting on Electrostatics. http://www.electrostatics.org/images/ESA_2014_G_Aplin_et_al.pdf, Accessed 20 January 2016.

Babic, D. Fiolic, M. Prusa, P. (2014) Evaluation of road markings retroreflection measuring methods. European Scientific Journal, 3, pp.105-114.

Barnard, S.T. (2009) The vulnerability of New Zealand lifelines infrastructure to ashfall. Doctor of Philosophy Thesis, Department of Geological Sciences, University of Canterbury, Christchurch, New Zealand.

Becker, J. Smith, R. Johnston, D. Munro, A. (2001) Effects of the 1995-1996 Ruapehu eruptions on communities in central North Island, New Zealand, and people's perceptions of volcanic hazards after the event. The Australasian Journal of Disaster and Trauma Studies, 2001-1.

Blake, D.M. Wilson, T.M. Deligne, N.I. Lindsay, J.L. Cole, J.W. (2016) Impacts of volcanic ash on road transportation: considerations for resilience in central Auckland. Proceedings Paper for the Institute of Professional Engineers New Zealand (IPENZ) Transportation Group Conference (March 2016), Auckland, New Zealand.

Bonadonna, G.G.J. Ernst, R.S.J. Sparks, C. (1998) Thickness variations and volume estimates of tephra fall deposits: the importance of particle Reynolds number. Journal of Volcanology and Geothermal Research, 81:3-4, pp.173-187.

Brooks, J.O. Crisler, M.C. Klein, N. Goodenough, R. Beeco, R.W. Guirl, C. Tyler, P.J. Hilpert, A. Miller, Y. Grygier, J. Burroughs, B. Martin, A. Ray, R. Palmer, C. Beck, C. (2011) Speed choice and driving performance in simulated foggy conditions. Accident Analysis and Prevention, 43:3, pp.698-705.

Carlson, P. Miles, J. (2011) Nighttime visibility of in-service pavement markings, pavement markers, and guardrail delineation in Alaska (with and without continuous lighting). Alaska Department of Transportation, Statewide Research Office, Juneau, Alaska. http://www.dot.state.ak.us/stwddes/research/assets/pdf/fhwa_ak_rd_11_04.pdf, Accessed 26 September 2015.

Carnaby, B. (2005) Road marking is road safety. Conference paper by Potters Asia Pacific, presented at the New Zealand Roadmarkers Federation Conference 2005, Christchurch, New Zealand.

Cole, J.W. Sabel, C.E. Blumenthal, E. Finnis, K. Dantas, A. Barnard, B. Johnston, D.M. (2005) GIS-based emergency and evacuation planning for volcanic hazards in New Zealand. Bulletin of the New Zealand Society for Earthquake Engineering, 38:2, pp.149-164.

Dravitzki, V.K. Wood, C.W.B. Laing, J.N. Potter, S. (2003) Guidelines for performance of New Zealand markings, Opus Central Laboratories Report 03-527605. http://www.nzta.govt.nz/assets/resources/guidelines-for-performance-of-nz-road-markings/docs/guidelines-for-performance-of-nz-road-markings.pdf, Accessed 25 January 2016.

Durand, M. Gordon, K. Johnston, D. Lorden, R. Poirot, T. Scott, J. Shephard, B. (2001) Impacts and responses to ashfall in Kagoshima from Sakurajima Volcano – lessons for New Zealand. GNS Science Report 2001/30, 53 p.

Fambro, D.B. Fitzpatrick, K. Rodger, J.K. (1997) Determination of stopping sight distances. National Cooperative Highway Research Program Report 400, Transportation Research Board National Research Council, Washington D.C.

Gibbons, R.B. Hankey, J. Pashaj, I. (2004) Wet night visibility of pavement markings: executive summary. Virginia Tech Transportation Institute, Virginia Polytechnic Institute and State University, Charlottesville, Virginia. https://vtechworks.lib.vt.edu/bitstream/handle/10919/46697/05-cr4.pdf?sequence=1, Accessed 26 September 2015.

Gibbons, R.B. Williams, B.M. (2012) Assessment of the durability of wet night visible pavement markings: wet visibility project phase IV. Virginia Centre for Transportation Innovation and Research, Charlottesville, Virginia. http://www.virginiadot.org/vtrc/main/online_reports/pdf/12-r13.pdf, Accessed 26 September 2015.

Hill, D.J. (2014) Filtering out the ash: mitigating volcanic ash ingestion for generator sets. Master of Science Thesis, Department of Geological Sciences, University of Canterbury, Christchurch, New Zealand.

Jenkins, S.F. Wilson, T.M. Magill, C.R. Miller, V. Stewart, C. Marzocchi, W. Boulton, M. (2014) Volcanic ash fall hazard and risk: technical background paper for the UN-ISDR 2015 Global Assessment Report on Disaster Risk Reduction. Global Volcano Model and IAVCEI. www.preventionweb.net/english/hyogo/gar Accessed 08 January 2016.

Leonard, G.S. Johnston, D.M. Williams, S. Cole, J.W. Finnis, K. Barnard, S. (2005) Impacts and management of recent volcanic eruptions in Ecuador: lessons for New Zealand. GNS Science Report 2005/20, 52 p.

Loughlin, S.C. Sparks, R.S.J. Brown, S.K. Jenkins, S.F. Vye-Brown C. (2015) Global Volcanic Hazards and Risk, Cambridge University Press, UK.

Matsumoto, A. Nakagawa, M. Amma-Miyasaka, Iguchi, M. (2013) Temporal variations of the petrological features of the juvenile materials during 2006 to 2010 from Showa crater, Sakurajima volcano, Kyushu, Japan. Bulletin of Volcanology, 58:1, pp.191-212.

Miwa, T. Shimano, T. Nishimura, T. (2015) Characterization of the luminance and shape of ash particles at Sakurajima volcano, Japan, using CCD camera images. Bulletin of Volcanology, 77:5, 13p.

Magill, C. Wilson, T. Okada, T. (2013) Observations of tephra fall impacts from the 2011 Shinmoedake eruption, Japan. Earth Planets Space, 65, pp.677-698.

Nanayama, F. Furukawa, R. Ishizuka, Y. Yamamoto, T. Geshi, N. Oishi, M. (2013) Chracterization of fine volcanic ash from explosive eruption from Sakurajima volcano, South Japan, American Geophysical Union Fall Meeting 2013, December 2013.

Sommer, C. Strähle, C. Köthe, U. Hamprecht, F.A. (2011) Ilastik: interactive learning and segmentation toolkit. BibTex file, Technical Report, In: Eighth IEEE International Symposium on Biomedical Imaging Proceedings, pp.230-233.

USGS (2013) Volcanic ash: effects and mitigation strategies. United States Geological Survey. http://volcanoes.usgs.gov/ash/trans/, Accessed 21 September 2015.

Wilson, G. Wilson, T. Cole, J. Oze, C. (2012) Vulnerability of laptop computers to volcanic ash and gas. Natural Hazards, 63:2, pp.711-736.

Wilson, G. Wilson, T.M. Deligne, N.I. Cole, J.W. (2014) Volcanic hazard impacts to critical infrastructure: a review. Journal of Volcanology and Geothermal Research, 286, pp.148-182.

Wilson, T.M. Cole, J.W. Stewart, C. Cronin, S.J. Johnston, D.J. (2011) Ash storms: impacts of wind-remobilised volcanic ash on rural communities and agriculture following the 1991 Hudson eruption, southern Patagonia, Chile. Bulletin of Volcanology, 73, pp.223-239.

Wilson, T.M. Stewart, C. Sword-Daniels, V. Leonard, G.S. Johnston, D.J. Cole, J.W. Wardman, J. Wilson, G. Barnard, S.T. (2012) Volcanic ash impacts on critical infrastructure. Physics and Chemistry of the Earth, 45-46, pp.5-23.

Wolshon, B. (2009) Transportation's role in emergency evacuation and re-entry: a synthesis of highway practice. National Cooperative Highway Research Program, Transportation Research Board Synthesis 392, Washington D.C.

Wicander, R. Monroe, J. (2006) Essentials of Geology: fourth edition. Thomson Brooks/Cole, United States of America.

Woo, G. (2009) A new era of volcano risk management: RMS special report. Risk Management Solutions, Inc. London, UK.

Yamanoi, Y. Takeuchi, S. Okumura, S. Nakashima, S. Yokoyama, T. (2008) Color measurements of volcanic ash deposits from three different styles of summit activity at Sakurajima volcano, Japan: conduit processes recorded in color of volcanic ash. Journal of Volcanology and Geothermal Research, 178, pp.81-93.

Zorn, E. Walter, T.R. (2016) Influence of volcanic tephra on photovoltaic (PV)-modules: an experimental study with application to the 2010 Eyjafjallajökull eruption, Iceland. Journal of Applied Volcanology, 5:2, pp.1-14.

5. VISIBILITY IN AIRBORNE VOLCANIC ASH: CONSIDERATIONS FOR SURFACE TRANSPORTATION USING A LABORATORY-BASED METHOD

Daniel M Blake[1], Thomas M Wilson[1], Carol Stewart[2]

[1] Department of Geological Sciences, University of Canterbury, Private Bag 4800, Christchurch, New Zealand

[2] Joint Centre for Disaster Research, Massey University/GNS Science, Massey University Wellington Campus, PO Box 756, Wellington 6140, New Zealand

Journal: Natural Hazards

Received: 22 June 2016

Current Status: In Review

5.1 Abstract

All modes of surface transportation can be disrupted by visibility degradation caused by airborne volcanic ash. Despite much qualitative evidence of low visibility on roads following historical eruptions worldwide, there have been few detailed studies that have attempted to quantify relationships between visibility conditions and observed impacts on network functionality and safety. In the absence of detailed field observations, such gaps in knowledge can be filled by developing empirical data sets through laboratory investigations. Here, we use historical eruption data to estimate a plausible range of ash-settling rates and ash particle characteristics for Auckland City. However, given the wide-ranging ash characteristics possible in Auckland, many of our findings are applicable worldwide. We then propose and implement a new experimental set-up in controlled laboratory conditions, which incorporates a dual-pass transmissometer and solid aerosol generator, to reproduce these ash-settling rates and calculate associated visual ranges through the airborne volcanic ash.

Our findings demonstrate that visibility is most impaired for large ash-settling rates (i.e. >500 g m^{-2} h^{-1}) and particle size is deemed the most influential ash characteristic for visual range. For the samples tested (all <320 μm particle diameter), visual ranges were as low as ~1-2 m when ash settling was replicated for the largest expected rate for Auckland (i.e. ~4,000 g m^{-2} h^{-1}), and were especially low when ash particles were fine-grained, more irregular in shape and lighter in colour. Finally, we consider potential implications for disruption to surface transportation in Auckland through comparisons with existing research which investigates the consequences of visual range reduction for other atmospheric hazards such as fog. This includes discussing how our approach might be utilised in emergency and transport management planning. Various possible mitigation strategies to improve visibility in environments contaminated with volcanic ash are also summarised herein.

5.2 Introduction

Reduced visibility may occur during primary volcanic ashfall or through the remobilisation and resuspension of existing fall deposits (Sparks et al. 1997, USGS 2013, Folch et al. 2014) into the atmosphere by wind, vehicle movement, cleaning processes or other human activities. Both primary and remobilised ash may produce potential issues for transportation (Barsotti et al. 2010, Folch 2012, Wilson et al. 2014, Blake et al. 2016, Blake et al. in review 1, 2). There have been many cases where reduced visibility following volcanic eruptions has impacted surface transportation function, particularly road (Table 5.1), but also rail, maritime and at airports, sometimes to near-total darkness (Blong 1982, Guffanti et al. 2009). For example, following the Mount St Helens eruption in 1980, “zero visibility” (p. 19) caused traffic to come to a standstill in several places including on Interstate 90 near Ellensburg in Washington, with visibility so poor that authorities used flares to guide motorists to nearby schools and churches (Warrick 1981). Once the initial ashfall was over, it became imperative to control traffic movement through speed restrictions, spacing vehicles on roads, and road closures to avoid vehicles creating “great clouds of ash” (p. 20) and again reducing visibility on the roads

(Warrick 1981). Hundreds of accidents in the affected areas were attributed to the billowing of ash behind vehicles and associated loss in visibility (Blong 1984). More recently, following the eruption of Cordón Caulle, Chile, in 2011, visibility in neighbouring Argentina, where ash fell, was so low that several main roads including Route 40 (linking Bariloche city and the Neuquén province) were subsequently closed. This affected the transportation of persons and goods at a national level (Folch et al. 2014). Vehicle headlights and brake lights are often reported to be ineffective in such conditions and barely visible to other drivers (Cole and Blumenthal 2004, Wilson et al. 2012a, USGS 2013). In addition to general disruption on network functionality and effects of safety hazards, accounts indicate that access to critical infrastructure is an important consideration during ashfall. For example, Wilson et al. (2012a) reported that thick falling fine-grained rhyolitic ash from the Chaitén volcano, Chile, in May 2008 “reduced visibility to nil” (p. 16) in places. Staff access to the impacted Fuataleufú dam site (Chubut province, Argentina) was inhibited by thick accumulations of ash.

Disruption to rail and maritime transportation during ashfall, caused by poor visibility resulting in safety and navigational issues, has also been documented (Johnston 1997, Wilson et al. 2012a). For example, rail operations were shut down during the initial Mount St Helens 1980 ashfall due to reduced visibility (as well as health concerns), with substantial speed restrictions and inspections necessary in the following days (Warrick 1981, Blong 1984).

Despite the many impacts to surface transportation that have been described (Table 5.1), there has been little quantitative analysis into the effects of airborne volcanic ash on reducing visibility and the subsequent consequences for network functionality and safety. Contemporary critical infrastructure management increasingly aims to optimise network performance during natural hazards, especially for non-damaging events, such as for small ash accumulations (Wilson et al. 2014). However, ash thickness has usually been the key measure of hazard intensity adopted in the past (Table 5.1), which is likely to be of little relevance when assessing visibility impacts; airborne ash concentration and ash-settling rates are more important for such impacts. This lack of an evidence base means that surface transportation operators typically can only make crude management decisions of either taking a precautionary approach of shutting systems down in the presence of ash (or in the event of forecasted ash), or a reactive approach if airborne ash causes problems for a surface transportation system. However, several contemporary ash dispersion and fallout forecasting models can provide outputs that include atmospheric concentrations and settling rates (e.g. FLEXPART – Stohl et al. 1998, Stohl et al. 2005; VOL-CALPUFF – Barsotti et al. 2008; FALL3D – Costa et al. 2006, Folch et al. 2009). Folch 2012 outlines these in more detail. Therefore, the capacity now exists for surface transportation vulnerability assessments to adopt these metrics. Furthermore, settling-rate and airborne concentration are important metrics to consider for other impacts to transportation. For example, it has been determined that concentrations as low as $1x10^{-4}$ g m^{-3} can cause substantial damage to aircraft (Witham et al. 2007, Folch and Sulpizio 2010).

Ash thickness is clearly important for certain impact types such as loss of skid resistance and road marking coverage (Blake et al. 2016, Blake et al. in review 1,2). However, other characteristics, which

influence or even control the level of damage or function, are often overlooked (Wilson et al. 2012) and it is somewhat illogical to associate visibility-induced impacts on surface transportation networks with a ground-based measurement. Although ash thickness can clearly influence the duration of deposits and subsequent recovery time (e.g. Warrick 1981, Searl et al. 2002, Hincks et al. 2006, Wilson et al. 2011), the effect of fall depth on airborne ash concentration and, consequent, impacts on surface transportation networks through visibility reduction is debatable, especially since airborne concentration of ash will increase before any accumulation on the ground. A review of literature suggests that thickness plays a minimal role in controlling airborne ash concentration and initial levels of visibility degradation and associated impact to transportation (e.g. Warrick 1981, Blong 1982). Others however, indicate that thickness may have a more substantial role (e.g. Thorarinsson 1971, Johnston 1997, Searl et al. 2002), most likely for when un-compacted ash becomes resuspended. We propose that ash-settling rate (especially for direct ashfall) and airborne particle concentration[5] (for both direct and resuspended ash) are more appropriate metrics to adopt when assessing visibility impairment in environments containing volcanic ash. Therefore, the thicknesses outlined in Table 5.1 (with additional information in Appendix C1) have little direct link to the visibility observations and should only be used as a loose proxy for airborne ash concentration and duration of exposure.

[5] Many countries have well-established networks to monitor airborne particle concentrations in relation to legal standards on ambient air quality. Historically, the main parameter measured was total suspended particulates (TSP), which includes all airborne particles (typically 0-40 µm). More recently, regulatory standards are based on PM_{10} (the concentration in µg m^{-3} of particles with a diameter of 10 µm or less), and $PM_{2.5}$, with the latter being considered of greater relevance to public health (WHO 2013). Air quality monitoring networks have been used to track volcanic ash plumes (Elliott et al. 2010, Leonard et al. 2014).

Table 5.1 Historical records of visibility impacts on roads following volcanic eruptions. Other occurrences described as general impacts to transportation, where impacts on visibility may have occurred but are not specified in literature, are not shown.

Volcano	Year	Ash thickness (mm)	Initial ashfall visibility observations	Re-suspended ash visibility observations	Mitigation measures	Reference
Ruapehu	1945	"few mm"	• Reduced visibility on roads was common • Ash made streetlights hazy.	• Bus headlamps blacked out by thick ash • Recently deposited ash easily lifted by passing vehicles • Re-suspended ash similar to dust produced on unsealed roads.	• Road closures • Drivers reduced speeds (to as low as ~25 km h^{-1} • Ash removal • Rain improved visibility.	Johnston 1997.
St Helens	1980	<50	• Traffic reduced to a virtual standstill because of zero visibility • Gravel and sealed roads had similar visibility problems • Flares had to be used to guide people.	• Ash billowing up behind fast-moving vehicles reduced visibility and likely caused hundreds of accidents • Bus services shut down and then limited services.	• Road closures • Stricter speed limits • Convoys • Restrictions on vehicle type and numbers • Advice not to drive except in emergencies • Speed bumps constructed from ash • Ash removal with some dampening first.	Sarkinen and Wiitala 1981, Warrick 1981, Blong 1984, Johnston 1997.
Hudson	1991	20-50		• ~1 m visual range a week after eruption ("transport virtually closed down") • Poor visibility on main coastal highway for up to a month.	• Road closures • Rainfall contributed to ash hazards diminishing • People avoided going outside • Cleaning of streets prioritised.	Wilson et al. 2009, Wilson 2009 (unpublished field notes).
		200-300	• People couldn't drive partly due to visibility • Ashfall blocked sun and visibility was as low as 1 m in daytime.			
Spurr	1992	3	• Ash limited visibility on roads.	• Bus services shut down and then limited service.	• City trimmed bus schedules and sent 40% of workforce home • Rain alleviated issues.	Johnston 1997, Barnard 2009.
Unzen	1992		• Visibility reduced on roads by suspended ash.			Yanagi et al. 1992, Barnard 2009.
Ruapehu	1995-96	"thin"	• Reduced visibility.	• Visibility on roads commonly reduced after ashfalls.	• Nearby state highway closed 3 times • Diversions • Ash removal.	Johnston 1997, Barnard 2009.
Etna	2002	<2		• Ash remobilisation by traffic and wind caused reduced visibility.		Barnard 2009

Chaitén	2008		• Reduced visibility "to nil" meant that maintenance crews were unable to traverse the access road to a hydroelectric dam	• Visibility issues from vehicles travelling too fast (~50 m visual range in places).	• Roads restricted by army to emergency vehicle use only • Some roads made one-way to reduce accidents • Permanent crew at dam for 1 month (rather than shifts) to reduce remobilisation • Drivers reduced speeds • Headlights used • Rain alleviated issues.	Wilson et al. 2012b, Wilson 2008 (unpublished field notes).
		~300	• 10-15 m visibility			
Pacaya	2011	20-30	• Difficult to drive due to impaired visibility.		• Ash removal • Rain helped consolidate tephra.	Wardman et al. 2012.
Cordón Caulle	2011			• Low visibility led to difficult driving conditions for 2 weeks and accidents • Visibility reduction meant no urban clean-up for a week in places.	• Road closures • Lower speed enforcement & recommendations (some 20 km h^{-1}) • Ash dampened with water • Ash removal.	Wilson et al. 2013, Folch et al. 2014, Craig et al. 2016.
		>100	• "No visibility" – decreased visibility.			
Shinmoedake	2011		• Reduced visibility.	• Visibility problems lasted for some time.	• Roads closed • Rapid clean-up operation.	Magill et al. 2013.
San Cristóbal	2013		• Visibility greatly reduced ~15 km from vent.		• Headlights used.	GVP 2013.
Kelud	2014		• Reduced visibility.	• Accident rates increased up to 220 km from vent • Bus services shut down and then limited service.	• Advice to not drive if possible • Headlights used • Drivers reduced speeds • Ash removal • Rain improved visibility.	Blake et al. 2015.
Calbuco	2015	~50	• Visibility reduced to 500 m ~100 km from vent.			AccuWeather 2015.

Fog, smoke from wildfires, airborne mineral dust, pollen, sea spray, vog (a visible haze comprised of sulphur dioxide emitted from volcanoes plus sulphuric acid and sulphate aerosol), and particulate emissions attributed to domestic heating and industrial, agricultural and vehicular emissions are other atmospheric hazards that can compromise the visibility for surface transportation. Darkness also has an understandably adverse effect on road safety, especially when combined with fog, smoke or dust (Cova and Conger 2003). Although smoke, particularly from wildfires, routinely disrupts road networks and inhibits operations at airports each summer, it is, like volcanic ash, a relatively under-researched topic in transportation hazards (Cova and Conger 2003, Abdel-Aty et al. 2011). The same can be said for particulate emissions although research in this field is growing, particularly as cases of very high air pollution in some populous Asian cities become more frequent. However, there have been many studies into the impacts of fog and mineral dust on visibility (e.g. Codling 1971, Moore and Cooper 1972, Hagen and Skidmore 1977, Summer et al. 1977, Perry 1981, Musk 1991, Taylor and Moogan 2010, Abdel-Aty et al. 2011, Weinzierl et al. 2012, USDOT 2013, Ashley et al. 2015). High concentrations of fog droplets and mineral dust particulates are required to cause low visibilities. For example, Hagen and Skidmore (1977) highlight that mineral dust concentrations exceeding 50 to 100 mg m^{-3} seriously reduce visibility during daylight, with lower concentrations hazardous at night. However, the atmospheric occurrence and properties of volcanic ash and other aerosols differ due to different source locations and different mobilisation mechanisms (Weinzierl et al. 2012) (discussed further in Section 5.3). General consequences for surface transportation are similar for all atmospheric hazards though, due to the common effect on visibility degradation. Suggested consequences for road transportation include an overall reduction in speed and more demanding and relatively dangerous driving conditions (OECD 1986, Musk 1991). Specifically, previous studies document that the presence of thick fog or dust influences roads by:

1. Reducing the volume of traffic.
2. Increasing the risk of accidents (despite lower traffic volumes).

Furthermore, accidents in low visibility are more likely to involve multiple vehicles and generally cause a higher percentage of severe injuries (Ashley et al. 2015). If a leading vehicle experiences low visibility, it may either stop or drive off the road with other vehicles closely following. Head-on and rear-end crashes are two of the most frequent crash types in terms of crash risk and severity (Abdel-Aty et al. 2011). For example, in September 2013, a 150-vehicle crash in fog (with visual range of ~23 m) on the Sheppey Crossing in the UK led to 69 casualties, 37 of which required hospital treatment, and the bridge being closed for several hours (BBC 2013, Hardy 2015), and in June 2015, two people died and four others were injured in a multi-vehicle accident during a dust storm in Colorado (Ibrahim 2015). Rear-end crashes have also been reported during volcanic ashfall (e.g. Bartley 1980, Folch et al. 2014, Blake et al. 2015).

Mitigation measures for managing reduced visibility due to airborne volcanic ash may comprise a variety of techniques. Observations and reports from road managers suggest that these vary in effectiveness and are dependent on the occurrence of further ashfall and remobilisation of ash deposits, which is typically influenced by meteorological conditions and vehicle traffic (Wilson et al. 2012a). Besides the complete removal of ash deposits, which may not be possible or cost-effective due to accessibility, spatial extent of the ashfall, or recurring ashfall, common mitigation measures include reducing vehicle speed (including the implementation of lower-than-usual speed limits), restricting the number, type and/or spacing of vehicles on the network, dampening surfaces with water to minimise the resuspension of ash, and closing selected roads through heavily contaminated areas (Table 5.1).

In this paper, we simulate volcanic ashfall in a laboratory setting to investigate the effect of ash characteristics and settling rate on visual range. Precise and consistent ash-generation rates (g h^{-1}) are produced in a purpose-built container using a Solid Aerosol Generator *(Topas SAG 410).* We also use a dual-pass transmissometer *(Dynoptic DSL-460 MkII)*, an instrument often used within factory smoke stacks for the measurement of opacity as a proxy for particulate emissions. We use datasets containing ash characteristic and locational information from literature available following worldwide historical eruptions to test our methodology. Specifically, we replicate ash types/colour, particle sizes and settling rates that can be expected in Auckland City given a future volcanic eruption in the Auckland Volcanic Field (AVF) or from the larger volcanoes of the Taupo Volcanic Zone (TVZ) in New Zealand (Figure 5.1) as an example of how our methods can be applied. We then suggest evidence-based, semi-quantitative mitigation strategies that could be implemented in operational environments where driving in volcanic ash may be necessary.

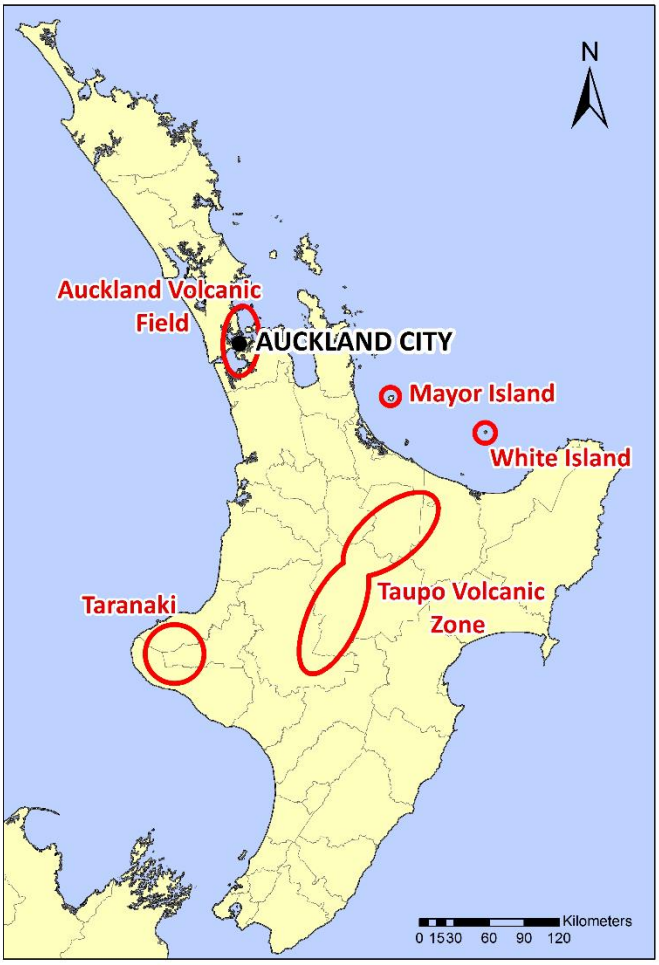

Figure 5.1 Potential sources of volcanic ash in New Zealand that could affect Auckland City (adapted from Blake et al. 2016). Fine grey lines indicate territorial authority boundaries.

5.3 Visibility in Airborne Volcanic Ash

5.3.1 Airborne volcanic ash considerations

To successfully implement our methodology, an estimation of near-ground atmospheric particle concentration and/or ash-settling rate with respect to eruption size and distance from the vent is required, allowing the reproduction of realistic conditions in the laboratory. Two processes affect airborne volcanic ash concentrations near ground level:

1. Primary ashfall from the eruptive vent, which is the result of explosive volcanic eruptions causing the disintegration of magma or vent material and production of rock fragments (Jenkins et al. 2014) (Figure 5.2, Appendix C2).

2. The remobilisation and resuspension of existing ash into the atmosphere from entrainment by meteorological winds or from small-scale atmospheric turbulence caused by vehicle movement, cleaning processes or other human activities (Figure 5.2, Appendix C2).

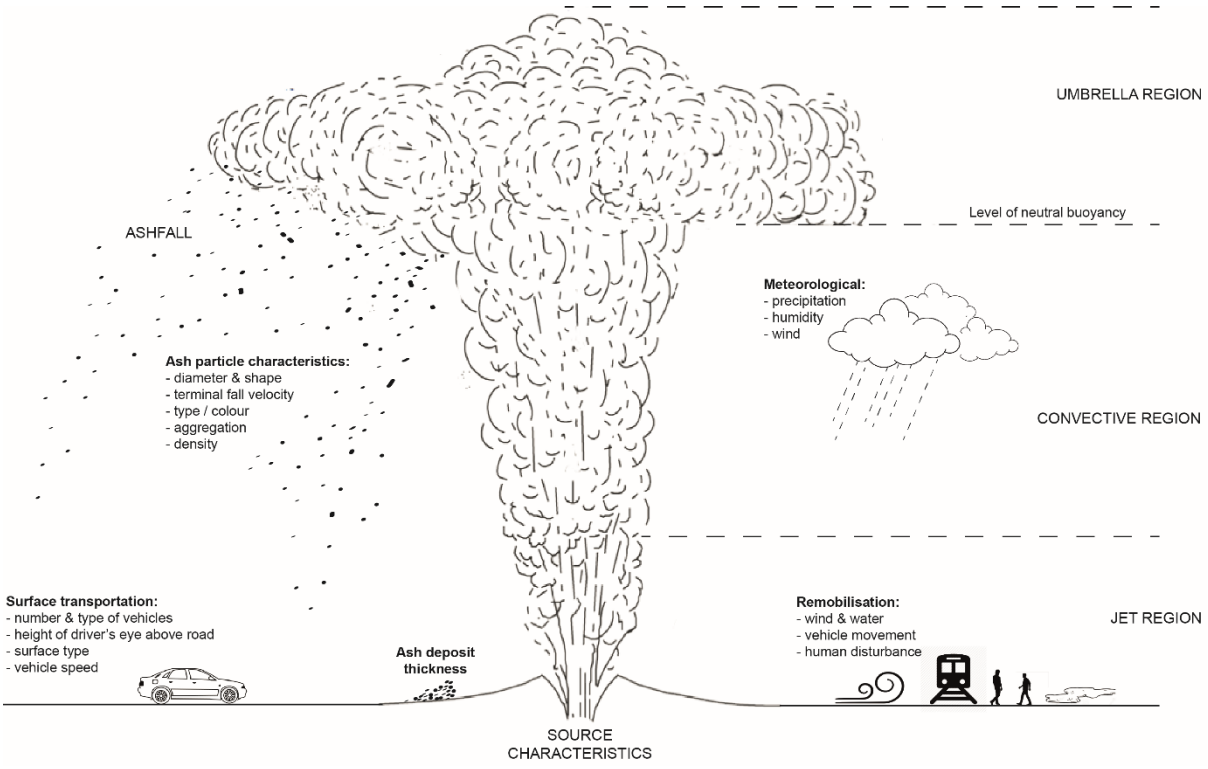

Figure 5.2 Eruption and environmental characteristics that influence airborne volcanic ash concentrations (eruption column characteristics modified from Carey and Bursik 2015). Note that additional information related to this figure can be found in Appendix C2.

The most important ash particles (see Appendix C3) in terms of impact to infrastructure including transportation, is generally fine-grained ash (e.g. Wilson et al. 2012a, Blake et al. in review 1) (i.e. <500 μm and especially ash <250 μm). Fine ash can disperse for up to hundreds of kilometres from the vent before settling due to gravity and therefore generally settles over extensive areas. The proportions of ash in these fine fractions (see Appendix C1) increase with increasing eruption explosivity (White et al. 2011) and fine ash is more susceptible to remobilisation by the processes described in point 2 above (Wilson et al. 2011, see Appendix C2).

Auckland can experience ashfall from a range of volcanic sources and of a variety of types. Basaltic ash may originate from new eruptions in the AVF, on which the city is built (Figure 5.1). Andesite can be deposited from eruptions within the Tongariro volcanic centre and from Taranaki volcano, with ash from Taranaki being most likely due to the relative frequency of eruptions (Magill and Blong 2005,

Molloy et al. 2009) and predominant south-westerly winds in New Zealand. Rhyolite may be deposited in Auckland from eruptions within the Taupo and Okataina volcanic centres in the central North Island with rhyolitic ash from Mayor Island also possible. As such, given new eruptions, Auckland is exposed to ashfall with a relatively wide range of airborne concentrations, settling rates, as well as particle sizes, densities and shapes.

Settling rate[6], defined here as the mass of particles falling onto a surface over time (g m^{-2} h^{-1}), is an important aspect in many geological phenomena (Komer and Reimers 1978). At present, there is limited primary empirical data available for volcanic ash-settling rates, largely due to the absence of direct measurement or record of ashfall duration associated with field measurements of ash thickness or loading. Due to the limited temporal information for most data, some settling rates are estimated based on the total ashfall duration (e.g. Hill 2014 – see Appendix C4), although it is possible that pulses of ashfall with periods of quiescence occur during that time. Furthermore, complications from plume and atmospheric turbulence, particle-particle interaction, and atmospheric conditions (Bonadonna et al. 2011) mean that accurate correlations between total ash thicknesses and settling rates are difficult to produce. As accurate source data is somewhat limited, it is hoped that recent developments of automated ash sampling instrumentation (e.g. Shimano et al. 2013, Weber et al. 2013, Andò et al. 2014, Tajima et al. 2015) will soon improve our understanding of settling rates.

5.3.2 Visual range derivation

Visibility involves human perception of the environment and thus, no instrument truly measures visibility (Malm 1979). Aerosols in the atmosphere, including volcanic ash, interact with light waves leading to absorption and scattering. The amount of light energy redirected from its original path is referred to as the extinction coefficient (b_{ext}) and is equal to the sum of four interactions (Robinson 1968, Hyslop 2009):

$$b_{ext} = b_{scat,p} + b_{scat,g} + b_{abs,p} + b_{asb,g} \quad (1)$$

where $b_{scat,p}$ is the light scattering by particles, $b_{scat,g}$ is that by gases, $b_{asb,p}$ is the light absorption by particles and $b_{asb,g}$ is that by gases.

The extinction coefficient is thus the optical parameter which is the best proxy for visibility assessment. It is commonly used to measure air quality in environmental health studies and, combined with the optical effects of the object and illumination, it determines the apparent contrast of an object against a background (EPA 2001). Light scattering by particles is the dominant cause of reduced visibility in most areas because particles scatter light more efficiently than gases (van de Hulst 1957, White 1990, Hyslop 2009). Measurements in non-urban areas suggest that light scattering accounts for around 90% of the extinction coefficient (EPA 2001). Once the extinction coefficient is calculated, the corresponding visual range (VR) in meters can be estimated, defined as

[6] We refer to *ash-settling rate* in this paper for the mass of ash particles settling onto a surface over time. However, it may also be referred to as *ash-deposition rate* or *ash accumulation rate* in other literature.

the longest distance that a large, black object can be seen against the sky at the horizon with the unaided eye (Binkowski et al. 2002, Seinfeld and Pandis 2006, Hyslop 2009, Blake et al. 2016):

$$VR = 3.912 / (b_{ext}) \quad (2)$$

where the value at the numerator is constant.

Visual range is often used to quantify visibility, as it is effectively an idealised measure of how far one can see through the atmosphere. Sometimes, a Rayleigh coefficient of 0.01 is added to the extinction coefficient in Equation 2 to correspond to "pristine" conditions (i.e. atmospheric conditions at an elevation of about 1500-1800 m) (Barsotti et al 2010). In a Rayleigh atmosphere (i.e. an imaginary "pure" atmosphere composed only of gases and devoid of any visible light reflection), visual range is 391 km (APTI 2000). At sea level, the visual range in a Rayleigh atmosphere is limited to about 296 km (Seinfeld and Pandis 2006). However, 70 km has historically been taken as representing almost perfect visibility as few people are able to distinguish between 296 km and 70 km (MFE 2001). As the visibility results in this paper are applied at ground level and in an urban context, we omit the Rayleigh coefficient value and use the 70 km visual range as a comparative value for 'typical' conditions. VR and b_{ext} are inversely related by the Koschmieder equation (Koschmieder 1925, MFE 2001, Seinfeld and Pandis 2006, Hyslop 2009):

$$VR = -In (C_L) / b_{ext} \quad (3)$$

where C_L is the minimum observable contrast (contrast being the ratio of the difference in brightness of the black object and the horizon to the brightness of the horizon, and is equal to 0.02 – 0.05 for most observers).

Relative humidity is not considered in the above equations and they thus correspond to dry conditions. Observational data concerning the humidity-dependent effect of volcanic ash particles on light attenuation is lacking. However, visibility in mineral dust storms is known to decrease if the relative humidity is high, particularly if more than 70% (Hagen and Skidmore 1977). It is therefore very likely that for volcanic ash, the higher the relative humidity, the greater the light scattering of particles and lower the visual range, especially due to the hygroscopic properties that the particles exhibit (Malm et al. 2003, Barsotti et al. 2010). Therefore, the equations may produce results, which underestimate visibility reduction.

Although some studies assess the optical properties of volcanic ash at high altitude using remote sensing techniques for the purposes of flying aircraft operability (e.g. Weinzierl et al. 2012), to the best of our knowledge, there is no existing quantitative analysis of visual range during ashfall near ground level. However, if visibility characteristics associated with volcanic ash can be determined near the ground, then comparisons with other, more studied hazards such as fog and dust storms can be made, and impacts on surface transportation and vehicle mobility estimated. Critically, comparisons should only occur when the visual range has been determined, or otherwise be viewed

in a broad sense, as the characteristics of certain particles and subsequent effect on light attenuation may be different.

5.3.3 Particulate characteristics

Monitoring of particulate matter concentrations in smoke stacks started during the 1960s (EPA 2000). Particulate matter concentrations are a useful adjunct to optical measurements and permit assessment of the contribution of anthropogenic and natural sources to visibility degradation (EPA 2001). Opacity is often used as a surrogate for particulate emissions. For example, in the United States it provides qualitative information on the operation and maintenance of particulate control equipment for the Environmental Protection Agency's (EPA's) emission regulations (EPA 2000). Opacity (OP) and extinction coefficient (b_{ext}), and thus visual range, are interchangeable as they all relate to transmission (T), the fundamental unit of measurement:

$$OP\ (\%) = 100(1-\sqrt{T}) \quad (4)$$

$$b_{ext}\ (m^{-1}) = -ln(T) / 2L \quad (5)$$

where L (in meters) is the path length of transmission (developed from DynOptic 2014).

Thus: $b_{ext} = -ln(1-0.01*OP)/L$ (6)

Particles smaller than the light wavelength (particle diameter <0.05 μm in white light) have little effect on opacity. Larger particles (particle diameter >2 μm in white light) however, have a much greater effect with characteristics such as size, shape and composition being much more influential (Connor 1974, EPA 2000). Fog droplets generally have particle diameters of 2-70 μm and are thus relatively inefficient at scattering light individually. However, poor visibility may result in fog as droplets often occur at very high concentrations.

A departure of a particle from a spherical shape causes a decrease in its settling rate (Komar and Reimers 1978, Wilson and Huang 1979). Volcanic ash particles are often more elongated in shape than other particulates. Indeed, Walker et al. (1971) show that it is better to consider volcanic particles >5 mm as cylinders than as spheres (Scollo et al. 2005). More recently, Weinzierl et al. (2012) compared the physical properties of volcanic ash and mineral dust by using samples from Eyjafjallajökull volcano, Iceland and the Sahara Desert. They demonstrate that the median aspect ratio of mineral dust is lower than that for volcanic ash (1.6 rather than 2.0 for their samples).

Transmissometers have been established as reliably measuring opacity as a proxy for particle concentration in industrial pollution monitoring. For example, Connor (1974) demonstrates strong linear relationships between concentration and opacity for three different sources: a kraft pulp mill recovery furnace, a cement plant kiln, and a coal-fired boiler. Tests to correlate opacity and particulate matter have also been conducted at Portland cement plants and oil-fired power stations (e.g. Conner et al. 1979, Uthe 1980). These show that opacity-concentration relationships depend not only on

physical characteristics of particulates such as size or shape, but chemical characteristics including water content. Indeed, some particles are hygroscopic, particularly those containing nitrate and sulphate which may include volcanic ash. Thus, as relative humidity increases, their ability to scatter light increases (Tang 1996, Hyslop 2009), resulting in lower opacity (Malm et al. 2003, Barsotti et al. 2010).

5.4 Methodology

5.4.1 Experimental set-up

The purpose of our set-up is to simulate conditions in volcanic ashfalls in a controlled laboratory environment so that visual range through ash of different settling rates and physical characteristics can be calculated. The key equipment used for this are a transmissometer and solid aerosol generator, both selected specifically for the purpose and incorporated into a custom-made experimental set-up.

We use a dual-pass transmissometer (Dynoptic DSL-460 MkII) for our experiments, an instrument often incorporated within smoke stacks for the measurement of opacity as a proxy for particulate emissions. The transmissometer is adopted to measure the optical characteristics over a pre-set path length of 1.4 m. It measures a specific amount of green light transmitted from the source/transceiver securely mounted to the side of a container, to a reflector mounted opposite, and back to the same transceiver (Figure 5.3). This allows the direct and continuous (1 second interval) calculation of the extinction coefficient of the air along the path length for light with a wavelength of what the human eye observes. A small amount of dust accumulates on the optics of the transmissometer during each test. However, following trial tests, this was substantially limited by extracting purge air (which the instrument uses to clean the optics during operation) through ducting from an adjacent clean room. Following the extraction of purge air from a cleaner source, the accumulation of ash on the optics accounted for only ~ 1.0×10^{-6} % of the maximum values recorded which is deemed insufficient to affect results. The transceiver and reflector are simply cleaned with compressed air between each experiment and results corrected so as to always start with zero values for the extinction coefficient and avoid drift.

Precise and consistent ash-generation rates (g h^{-1}) are produced using a solid aerosol generator (Topas SAG 410) (named *ash disperser* from herein) into the top and centre of a purpose-built stainless-steel cylindrical container (Figure 5.3), shaped as such to encourage evenly distributed flow because trial tests suggested that cylinders were preferential to cuboids where ash-settling rate varied in corners. Two simultaneous methods for calibration of the ash disperser for each ash type of particular particle diameter size distribution were used to determine the machine settings required for different generation rates and estimated ash-settling rates in the container; a gain-in-weight technique

where ash dispersed from the instrument is collected in filter bags, and a loss-in-weight technique where the whole instrument weight is recorded.

When the ash enters the container, a purpose-built nozzle on the end of the tube causes the ash to be dispersed in all directions before settling under gravity. The height of the container (1.3 m total, with a 1 m fall distance to the light beam of the transmissometer) was chosen by considering formulas derived from Bonadonna et al. (1998) (Appendix C2), which suggest that the majority of ash particles dispersed reach terminal velocity before passing through the measurement level. However, the set-up was also constrained by workspace limitations and accessibility requirements to the hopper of the ash disperser, which had to be positioned above. Beneath the measurement level of the transmissometer, the ash settles at the base of the container (0.75 m^2 in area). Half of the area (i.e. 0.375 m^2) at the centre of the base is dedicated to a board on top of an automated mass balance set to poll and record the weight of ash every 10 seconds. The other half around the edge consists of foam, which allows the air to evenly escape from the base of the container but the vast majority of ash to be deposited and remain static. Trial tests suggested that the solid board at the centre had little influence on ash flow currents towards the base of the container and that there was minimal remobilisation of ash that would affect results.

Some radial differences in ash-settling rates were identified for samples, both for individual experiments and between experiments. However, the consistent airflow within the container, along with the light beam traversing the entire diameter, means that there is negligible effect on the transmissometer readings and that the entire transect would appropriately represent a steady ashfall. To account for the radial differences in settled ash at the base (i.e. because the board does not cover the whole area), a series of 10 petri dishes are equally positioned (5 on the central board and 5 on the foam edge). These are weighed after each experiment to analyse the distribution profile for the settling ash in our experiments. The results from the petri dishes, in conjunction with the centred mass balance weights are used to calculate and record mean ‘actual’ (rather than estimated) ash-settling rates (g m^{-2} h^{-1}) at the base (Section 5.5.2).

Preliminary test runs revealed that equilibriums between ash generation into the container and ash settling at the base occurred within 15 minutes for all ash types. Therefore, every experiment for each ash type at a specific generation rate and distribution for particle diameter size is run for a total of 1 hour where possible (some high generation rates caused ash supply to be exhausted within 45 minutes). This allows at least 30 minutes of continuous measurement at equilibrium conditions, which is sufficient time for a mean value of the extinction coefficient and visual range for each sample and ash-generation rate to be calculated. The transmissometer is then left operating for at least a further 15 minutes after the disperser is switched off to allow continued monitoring whilst all the ash settles out. Ash is cleaned from the board, foam and container edges between each experiment and a thorough clean of all equipment is conducted, and ash disperser tube disposed of and replaced, at the end of testing with each ash sample.

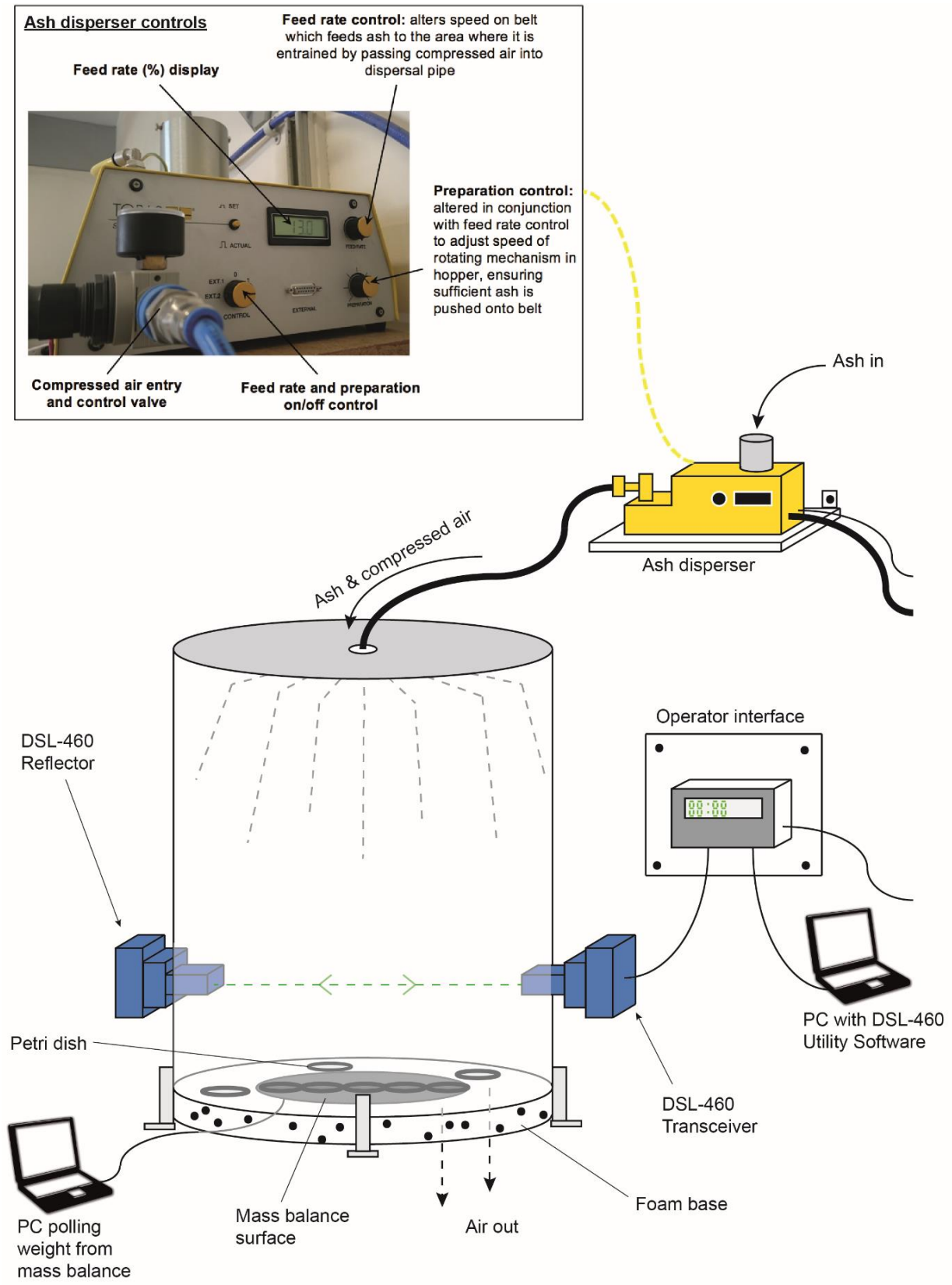

Figure 5.3 Experimental set-up developed and implemented for visibility testing (adapted from Blake et al. 2016).

5.4.2 Ash sample selection

We use Auckland as a case study location to test our methodology due to the relatively large population (>1.4 million people (Statistics New Zealand 2013)) and extensive transport networks, as well as potential exposure to volcanic ash from a variety of sources. We attempt to replicate ash types (Section 5.4.2.1), particle sizes (Section 5.4.2.2) and settling rates (Section 5.4.2.3) that can be expected in the city given a future volcanic eruption in the AVF or from the larger volcanoes of the central North Island of New Zealand. However, given the range of eruption styles and distances from vents, anticipated conditions in Auckland are wide-ranging, with many of our results being applicable worldwide.

5.4.2.1 Ash type

Basaltic, andesitic and rhyolitic ashfall is possible in Auckland and we conduct experiments with all three types; a dark-coloured basalt derived from a deposit of Pupuke Volcano in the AVF, a mid-coloured andesite sourced from a deposit from the Poutu eruption of Tongariro Volcano, and a light-coloured rhyolite from the Kaharoa eruption of Tarawera Volcano, in New Zealand (Table 5.2).

Table 5.2 Characteristics of the four ash types used for experimentation.

	Pupuke, Auckland Volcanic Field, New Zealand			**Poutu, Tongariro, New Zealand**	**Kaharoa, Tarawera, New Zealand**	**Chaitén, Chile**
Year of eruption	~200,000 BP			~11,000 - 12,000 BP	1314	2008
Ash type	Basalt			Andesite	Rhyolite	Rhyolite
Colour *(determined from Munsell Rock Colour Chart)*	N4: Medium Dark Grey			5Y 6/1: Light Olive Grey	5YR 5/2: Pale Brown	5Y 8/1: Yellowish Grey
SiO_2 content *(determined by Philips PW2400 XRF analysis)*	44% (mafic)			52% (intermediate)	75% (felsic)	75% (felsic)
Dominant minerals *(determined by Philips XRD analysis)*	Diopside, Forsterite, Anorthite			Albite, Augite	Albite, Quartz	Albite
Particle size group	a	b	c	b	b	b
Mode particle size (µm) (see Figure 5.5)	12	40	105	22	30	21
Dry bulk density (g cm^{-3})	0.92	1.12	1.28	0.89	0.87	0.83

The raw samples were largely selected from sources outside of the AVF, as many of those within the AVF have been weathered, contaminated by organic material, and/or disturbed or removed by human

activity (e.g. Alloway et al. 2004, Cassidy and Lock 2004, Howe et al. 2011, Adams 2013). Our samples were modified through pulverisation to achieve a range of particle diameter size distributions possible in Auckland and thus likely contain a higher than natural proportion of particles that are blocky in nature with a high degree of angularity due to the milling process (Broom 2010). Therefore an additional fine-grained sample (sourced from the 2008 eruption of Chaitén in Chile – Table 5.2) is also tested to investigate the effects of particle shape on visual range. This sample was not altered through pulverisation and only sieved to remove the larger particles that can cause clogging of the ash disperser. All samples were dried at 65°C for >48 hours prior to testing.

5.4.2.2 Particle size

Following a detailed literature review, we further developed work by Hill (2014) (see Appendix C4) to estimate ash particle sizes that can be expected in Auckland from volcanic sources in New Zealand (Figure 5.4). Unlike Hill (2014) however, who focussed solely on median data, we incorporate all available data for particle size, including individual data or median size recorded at specific locations from a vent (shown as points), modes (bold points or bold ranges), full distributions (vertical 'error bars') and distributions in spatial extent (horizontal 'error bars'). Triangles in Figure 5.4 denote maximum clast sizes of blocks, and black data points show particle sizes and distances from vents determined from recent analysis of deposits in six Auckland maars from historical AVF eruptions of One Tree Hill, Three Kings and Mt Eden volcanoes (Jenni Hopkins, Victoria University of Wellington, pers comm, 19 July 2014).

Due to the maximum particle size constraints of the ash disperser and likely clogging when particle diameters exceed ~300 μm, our experiments focus on samples defined as *fine ash* by Folch et al. (2009) (see Appendix C3), in that mode particle diameters for most samples are <64 μm. All mode particle diameters are <110 μm (Figure 5.5). However, we subdivide our samples into three categories of mode particle diameter size for ease of interpretation; a. <20 μm, b. 20-50 μm, and c. >50 μm (Table 5.2). For the basalt sample we test ash for all three categories to investigate the effect of particle diameter size on visual range. For the andesite and rhyolite samples however, we only test for the category b range due to ash sample availability. Specific ash particle sizes were achieved by means of a trial and error process using a rock pulveriser with different disc separation distance and sieves with different mesh aperture sizes, followed by laser sizing to determine the particle diameter size distributions. Total particle diameters for all samples used are ~1 – 320 μm (Figure 5.5) which corresponds with the mid- to lower-grain sizes of ash particles that can be expected in Auckland given a future eruption in New Zealand (Figure 5.4).

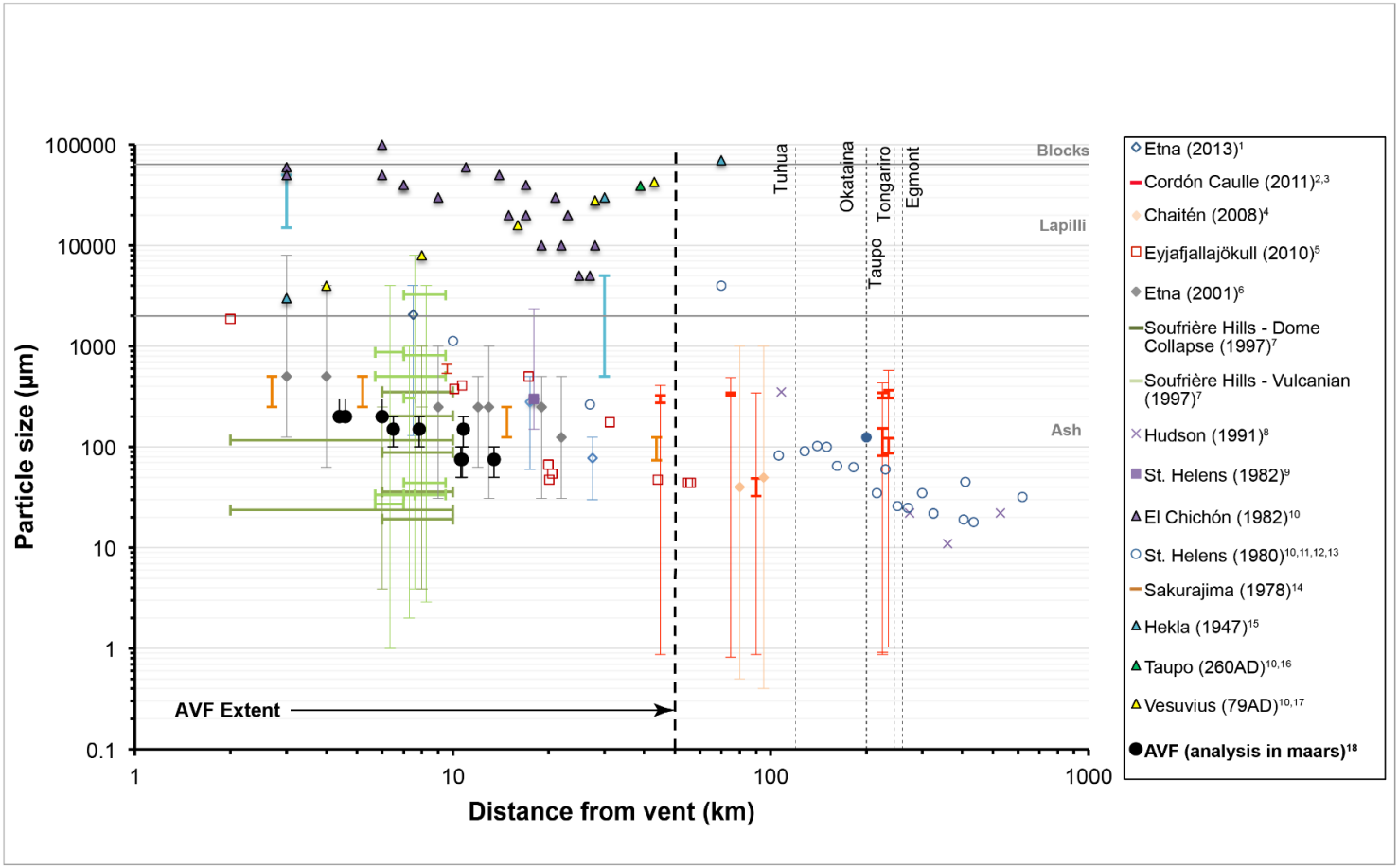

Figure 5.4 Particle sizes of ash deposits and their associated distances from 15 worldwide eruptive vents and analysis from maars in the AVF. The distances from central Auckland (depicted as 0 km) to New Zealand volcanic ash sources are identified by a series of dashed vertical lines, and approximate maximum axial extent of the AVF deposits by a bold dashed vertical line. Solid horizontal grey lines denote the boundaries between ash and lapilli (2 mm) and lapilli and block (64 mm) particle diameters.

(Data from: [1]Andò 2014, [2]Wilson et al. 2013, [3]Heather Craig, University of Canterbury, pers comm, 17 July 2014, [4]Watt et al. 2009, [5]Bonadonna et al. 2011, [6]Scollo et al. 2007, [7]Bonadonna et al. 2002, [8]Scasso et al. 1994, [9]Harris and Rose 1983, [10]Carey and Sigurdsson 1986, [11]Scheidegger and Federman 1982, [12]Sarna-Wojcicki et al. 1981, [13]Carey and Sigurdsson 1982, [14]Eto 2001, [15]Wilcox 1959, [16]Walker 1981, [17]Sigurdsson et al. 1985, [18]Jenni Hopkins, Victoria University of Wellington, pers comm, 19 July 2014).

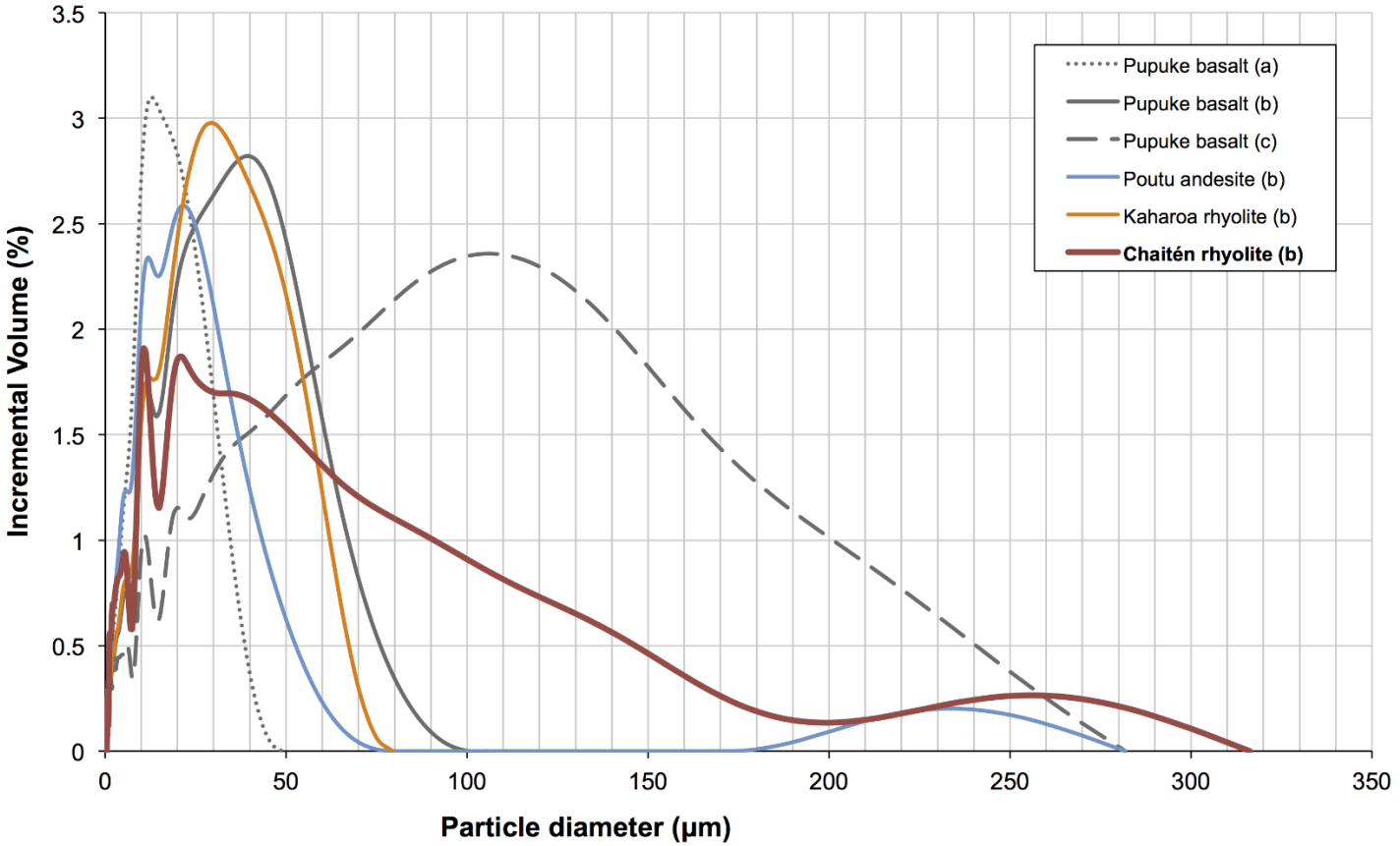

Figure 5.5 Particle diameter size distribution plots for the ash used in experimentation, derived from three tests per sample using a Micromeritics Saturn DigiSizer II laser sizer instrument. a-c refers to the mode size categories shown in Table 5.2. All ash samples used generally have a normal distribution for particle sizes, with the exception of the rhyolite sample from Chaitén, where particle sizes have a distinctive positive skew.

5.4.2.3 Estimated ash-settling rates for Auckland

It is necessary to obtain estimates of ash-settling rates that can be expected in Auckland to inform the experimental set-up. As the generation rate of each ash type and particle size is determined as part of the instrument calibration, estimations of settling rate can be made given the known volume of the container where the ash is dispersed and replicated under controlled conditions. A detailed literature review revealed relatively limited data available for settling rate measurements following worldwide volcanic eruptions. As with particle sizes however, all available data was plotted to show a generally decreasing settling rate with distance from vent (Figure 5.6).

Based on the settling rates in Figure 5.6, and the particle sizes adopted for experimentation (Table 5.2), which represent ashfall in Auckland from distal eruptions or mid to lower particle sizes expected from an AVF eruption, we attempt to replicate ash-settling rates between 50 and 1,000 g m^{-2} h^{-1} (four specific ash-settling rates within this range per sample) for all six of the samples. However, we also attempt to replicate settling rates towards the upper limit of what can be expected in Auckland (i.e. around 2,000 and 10,000 g m^{-2} h^{-1}) for the Pupuke basalt and Chaitén rhyolite (category b) samples, where more material was available, to determine expected absolute minimum visual ranges from direct ashfall in the AVF. Thus, in addition to multiple trial tests, a total of 28 experiments are conducted as part of this study.

We highlight that the ash-settling rates determined at this stage are those forecast using the ash disperser calibration results. Actual ash-settling rates at the base of the container are lower; particularly for high ash-generation conditions, due to several factors, particularly:

- Adherence of some ash to the container side and top reducing the airborne concentration and settling rate.
- An increase in pressure within the container acting against more ash entering as compressed air continues to enter at the top of the container but the foam at the base becomes clogged.
- Leakage of some ash from the container altogether, either through the foam or small gaps, especially when the air pressure inside is very high.

Actual ash-settling rates are determined from the centred mass balance and petri dish procedure outlined in Section 5.4.1.

Although the transmissometer records regular measurements of airborne particle concentration, these readings are viewed with caution in our experiments, as precise values would require the density correction factor (set as 1.00 for our tests) to be adjusted between each sample. In the absence of complex isokinetic sampling of the airborne ash in the container, this cannot be achieved (DynOptic 2014).

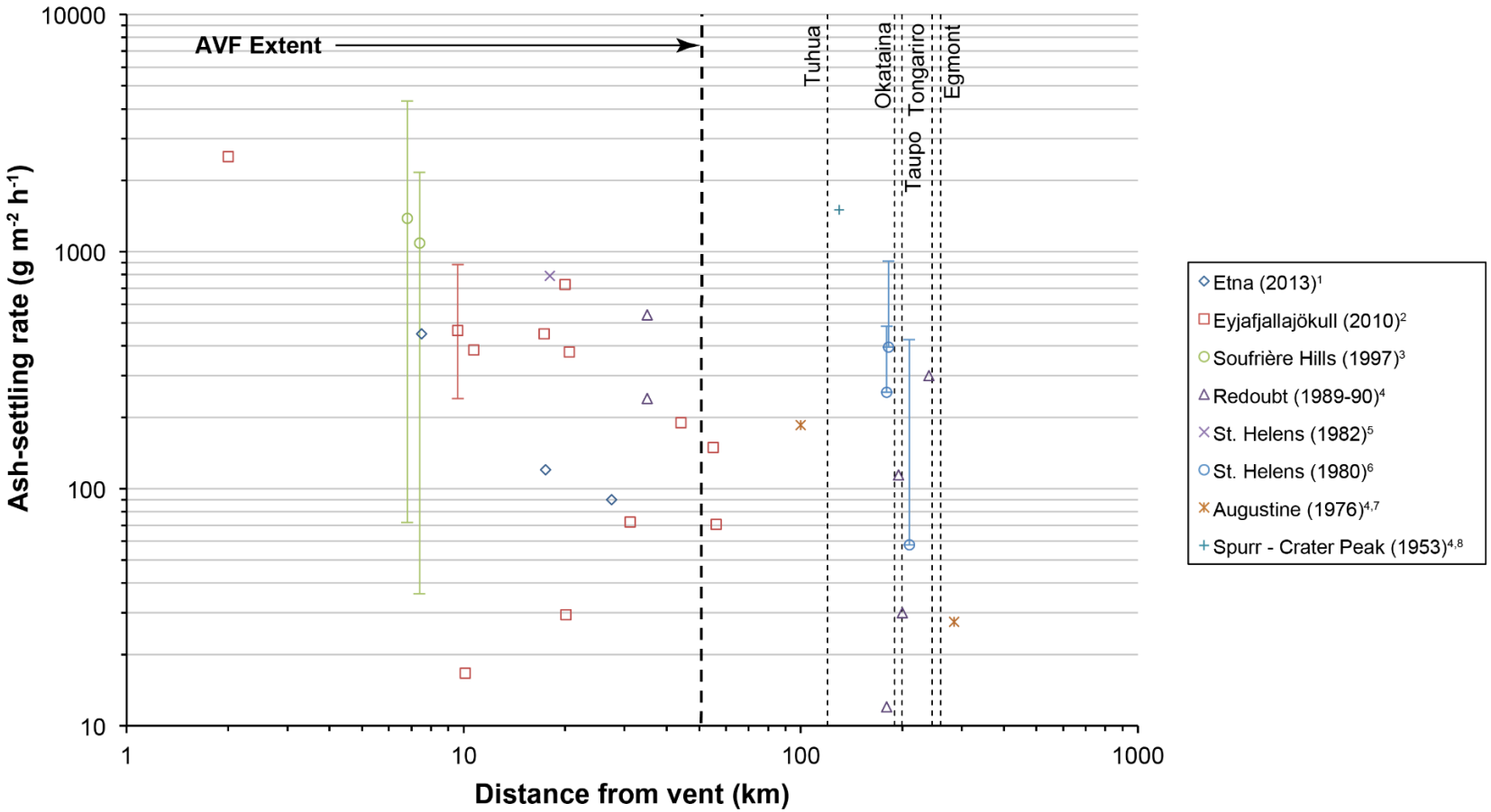

Figure 5.6 Ash-settling rates and their associated distances from 8 worldwide eruptive vents. The distances from central Auckland (depicted as 0 km) to New Zealand volcanic ash sources are identified by a series of dashed vertical lines, and approximate maximum axial extent of the AVF deposits by a bold dashed vertical line.

(Data from: [1]Andò 2014, [2]Bonadonna et al. 2011, [3]Bonadonna et al. 2002, [4]Scott and McGimsey 1994, [5]Harris and Rose 1983, [6]Scheidegger and Federman 1982, [7]Kienle and Swanson 1985, [8]Wilcox 1959).

5.5 Results and Discussion

5.5.1 Airborne concentration

Measurements of airborne ash concentration taken directly from the transmissometer were ~40 – 1,600 mg m^{-3} for all experiments, with higher values corresponding to the highest ash-settling rates and lowest visual ranges. However, these values should be viewed with caution due to limitations of the approach (Section 5.4.2.3), which is why we adopt ash-settling rate as the key unit of measurement. The time taken for the airborne concentration to fall to zero upon cessation of ash dispersal at the top of the container is of particular interest. It provides an indication of how long remobilised ash would take to settle from a 1-meter height above the ground given no on-going disturbances such as wind or traffic and in the absence of rainfall. Such information can be used to inform transportation management strategies such as the spacing of trains or road vehicles to allow sufficient time for ash to settle and reduce impairment to drivers caused by visual range reduction. There were no distinct differences between airborne particle concentration reductions for the different ash samples or ash-generation rates we used in experimentation. It took 11 minutes (± 2 minutes) for airborne concentrations to return to original levels. However, given the exponential decay in airborne particle concentration following the cessation of new ash entering the container, values decreased to <10% of their maximum values in less than 5 minutes.

5.5.2 Ash dispersal and actual settling rate

For the relatively coarse-grained ash samples (particularly size category c, and to some extent b), a greater weight of ash and more ash of larger particle size fell towards the centre of the container base, with ash becoming more fine-grained towards the edge. Fine-grained ash adhered to the edge and top of the container (Figure 5.7). Adherence was prevalent for the ash samples with the finest particle sizes (i.e. category a, and to some extent b), and especially so for the Chaitén rhyolite sample, causing sometimes large decreases in ash-settling rates towards the extreme edge of the base. This is likely explained by the electrostatic charging of ash particles (Bonadonna and Phillips 2003, Folch 2012). However, as the light beam of the tranmissometer passes the width of the container (1.4 m path length) and because inconsistencies occur in a radial pattern, this allowed the accurate calculation of mean ash-settling rates.

It was evident that the Chaitén sample became highly electrostatically charged with many electrostatic discharges occurring when touching the container both during experimentation and subsequent cleaning. More specifically, we suggest that the process of triboelectrification, described in relation to volcanic ash by Aplin et al. (2014) and Aplin et al. (2015), occurred frequently for the Chaitén sample. Triboelectrification is the type of contact electrification that occurs when two materials make contact with each other. Some electrical charge transfers from one material to the other with one gaining an excess of electrons (i.e. becoming negatively charged) and the other losing electrons (i.e. becoming positively charged) (Electrostatic Solutions Ltd. 2000). This process can occur readily in volcanic ash

with a polydisperse particle size distribution but which exhibits predominantly very fine particle sizes (Aplin et al. 2014), such as our Chaitén sample (Figure 5.5). When the particles become more separated (as they do following dispersal in the container), they can take the charge with them. The charge will try to recombine, or dissipate to earth, which explains the sudden electrostatic discharges observed.

Due to the inconsistencies across the container base, results displayed for ash-settling rates are in the form of three values, corrected for a 1-hour period over 1 m^2:

1. A minimum value calculated from the weight recorded on the centred mass balance board at the container base multiplied by a correction factor determined by the weight difference between ash in the petri dishes on the board and on the foam edges for that particular sample.
2. A maximum value calculated by doubling the weight recorded on the central mass balance board at the container base for that sample to assume the same weight falls on the foam edge.
3. The midpoint between points 1 and 2 above, which is deemed the value most likely to represent the true ash-settling rate.

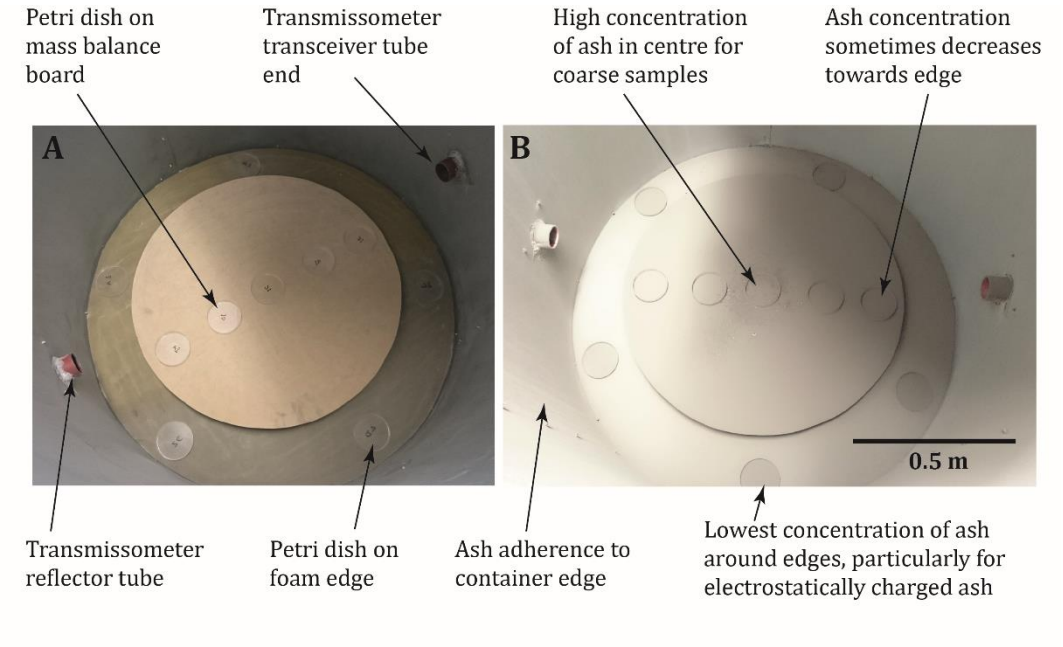

Figure 5.7 Annotated plan-view photos taken looking down into the container showing (a) petri dishes on the central mass balance board and foam edge, and (b) describing general ash accumulation patterns across the container base (determined from the mass of ash on the centred board and in petri dishes, and through visual observations after each experiment).

Based on these values, although ash-settling rates forecast from the ash disperser calibration were ~50 – 10,000 g m^{-2} h^{-1} (Section 5.4.2.3), the actual ash-settling rates for our results are calculated at 28 – 4,800 g m^{-2} h^{-1}. The results sufficiently cover the range of settling rates that can be expected in Auckland given a future eruption in New Zealand based on correlation with the limited dataset available from worldwide eruptions (Figure 5.6).

5.5.3 Visual range and particle size

The visual range fluctuates between readings (Figure 5.8), depending on the quantity and characteristics of particles between the light beam of the transmissometer at the precise time of measurement. However, as values are recorded at one-second intervals and because we calculate each mean visual range result from at least 30 minutes of experimentation (Figure 5.8), i.e. >1,800 data points, our results are deemed reliable. Nevertheless, we display maximum and minimum values recorded by the transmissometer, which have greater deviation from the mean for the lowest airborne concentrations and ash-settling rates.

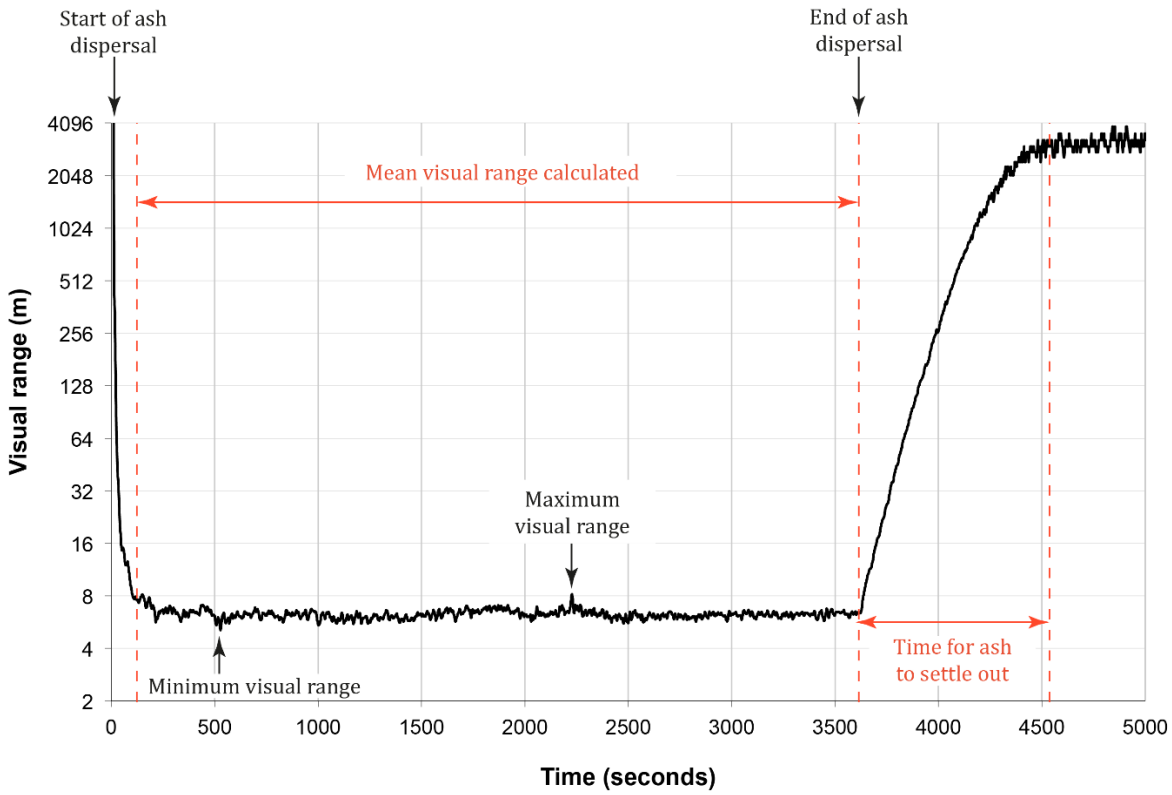

Figure 5.8 Unprocessed transmissometer results for the Kaharoa rhyolite sample when ash was dispersed at the highest generation rate tested. Annotations show how the mean, maximum and minimum visual ranges were determined, as well as time taken for all ash to settle out and airborne concentration and visual range to return to original conditions

The clearest trends that emerged from our results were between particle size and visual range (Figure 5.9). For the Pupuke basalt, which had the highest bulk density of the four ash types used, testing

was conducted using three distinct particle diameter size distributions. It is evident that for a given ash-settling rate, visual range is less for ash predominantly containing finer particles. This corresponds to the findings by Connor (1974), in that the mass scattering efficiency of light decreases as particle size increases. Lines of best fit followed inverse power relationships (Figure 5.9) with the following formulae:

$$y = 4589.1\ x^{-0.893} \quad \textit{(for Pupuke basalt with 105 µm mode particle size)} \quad (7)$$

$$y = 1031.2\ x^{-0.732} \quad \textit{(for Pupuke basalt with 40 µm mode particle size)} \quad (8)$$

$$y = 740.84\ x^{-0.779} \quad \textit{(for Pupuke basalt with 12 µm mode particle size)} \quad (9)$$

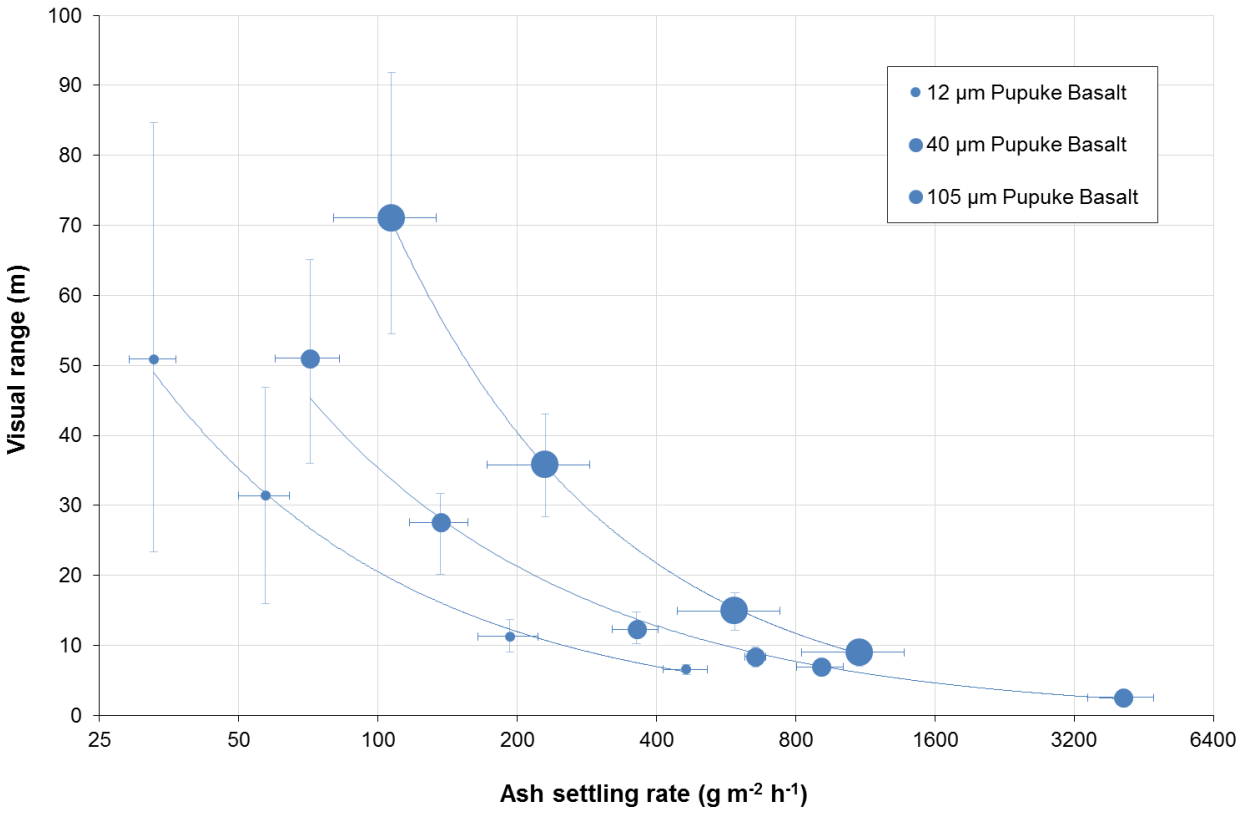

Figure 5.9 Visual ranges for the three Pupuke basalt particle diameter size distributions. Each point is for the mean visual range when ash flow into the container was at equilibrium with ash-settling rate at the base for each experiment. Horizontal minimum and maximum error bar values and the point values correspond to points 1-3 in Section 5.5.2 respectively. Vertical error bars show the maximum and minimum values recorded by the transmissometer during the periods of equilibrium (Figure 5.8).

For Auckland, small ash particle diameter sizes are possible from eruptions in both the AVF and TVZ of New Zealand (given appropriate wind directions). Although recurrence rates for AVF eruptions estimated from existing tephra layers are highly variable, return periods >2,000 years characterise most of the record (Molloy et al. 2009). Similarly, eruptions from the rhyolitic Taupo and Okataina

volcanic centres (corresponding to eruption volumes of 1 km^3 and 0.5-5 km^3 respectively) have a return period of ~2,500 years (Stirling and Wilson 2002). Ash-settling rates of ~1,000 g m^{-2} h^{-1}, possibly up to ~4000 g m^{-2} h^{-1}, may occur in Auckland from any of these eruption locations (Figure 5.6), and extrapolation of the line of best-fit for the finest grained ash we tested (12 μm mode particle diameter) to these settling rates suggest that visual ranges as low as ~1-2 m can occur under such conditions. However, ash-settling rates are likely to be higher (resulting in shorter visual ranges) for explosive eruptions, which generally also produce a relatively large proportion of fine-grained ash (White et al. 2011).

5.5.4 Visual range and ash type

Visual range for excellent conditions is typically taken to be >70 km (MFE 2001). Indeed, the mean visual range taken over a three year period (from 2001 to 2003) from nephelometer readings over Auckland City (Dr Gerda Kuschel, Auckland Council, pers comm, 21 June 2016) is similar, calculated at 66.5 km with 95% CI [65.1, 67.8]; the slightly shorter visual range is unsurprising given the city environment with likely higher background particulate concentrations than 'typical excellent' conditions. Even the smallest estimated ash-settling rates in Auckland (~10 g m^{-2} h^{-1}) during an eruption would cause a visibility reduction of over two hundred times from typical baseline visual range for ash with characteristics in the range we tested.

As with the Pupuke basalt, the relationships between visual range and ash settling rates are best described by inverse power law relationships for rhyolitic and andesitic ash types (Figure 5.10):

$y = 1843.2\ x^{-0.822}$ *(for Chaitén rhyolite with 21 μm mode particle size)* (10)

$y = 749.55\ x^{-0.739}$ *(for Kaharoa rhyolite with 30 μm mode particle size)* (11)

$y = 874.22\ x^{-0.875}$ *(for Poutu andesite with 22 μm mode particle size)* (12)

It appears that, despite lying within the same particle size category, differences are somewhat attributable to particle size distribution within the categories. Comparing the Pupuke basalt and Kaharoa rhyolite, which were pulverised and sieved with the same dimension controls, results suggest that the light-coloured rhyolite causes lower visual ranges than the dark-coloured basalt. This makes intuitive sense, as there is more reflection from light-coloured surfaces. Low visual ranges for the andesite sample are perhaps explained by augite being one of the dominant minerals (constituting ~20% of the sample). With two prominent cleavages, meeting at angles near 90 degrees for augite, light scattering may be relatively high. Furthermore, the particle sizes for the andesitic ash are low compared to the basalt and Kaharoa rhyolite, and fallout of the andesite may be slowed by relatively irregular particle shapes (Riley et al. 2003, Pardini et al. 2016).

The Chaitén sample produced unexpected results with greater visual ranges than all other types in the same particle size category, despite being the lightest-coloured ash we tested. The most likely explanation is due to the larger positive particle size distribution from the mode than the other

samples (Figure 5.5), and thus higher proportions of relatively large diameter particles. Additionally, the comparatively low processing undertaken when producing this sample led to particles that are relatively spherical in shape (Figure 5.11). As such, they reflect less light than the irregular-shaped particles of the other samples we tested. In fact, the Chaitén ash is more representative of fresh volcanic ash samples and our results for the other samples, which were all mechanically pulverised, thus provide a worst-case situation for visual range reduction during intial ashfall in this regard. However, as our experiments were conducted using oven-dried samples, they do not fully account for potential hygroscopic properties that are encountered outside due to relative humidity effects, which would increase light scattering and reduce visual range, thus counteracting the effect of increased irregularity to some degree.

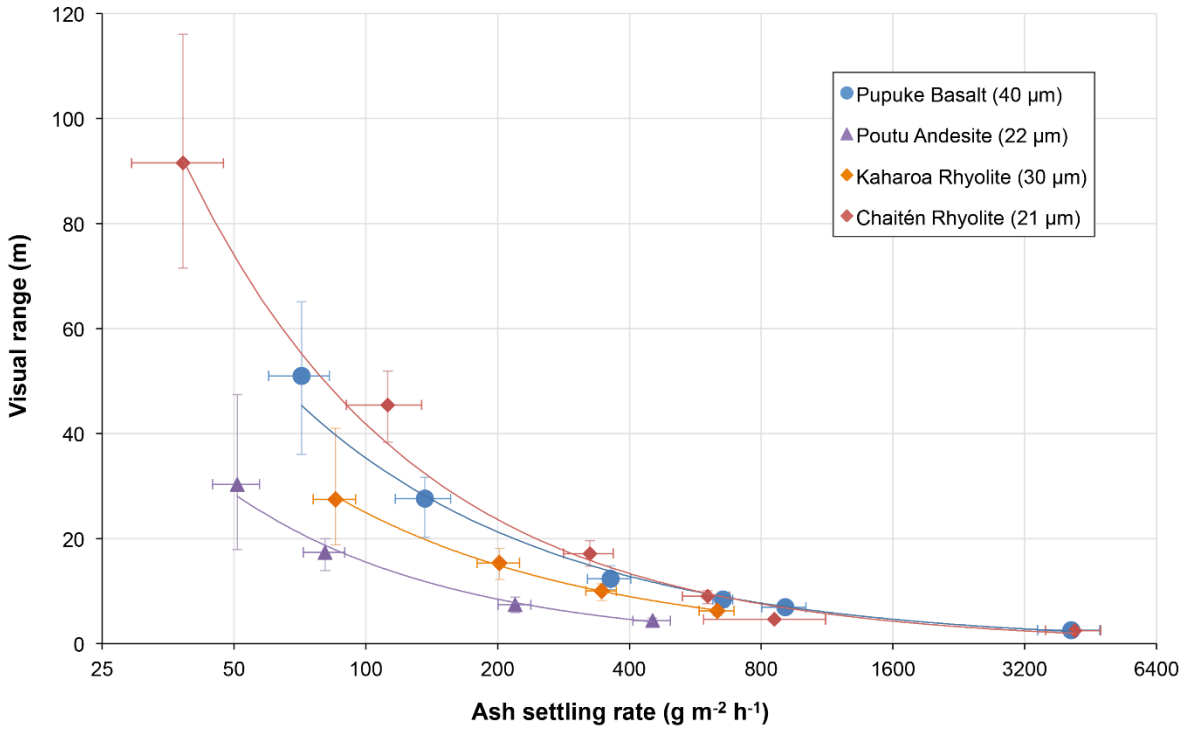

Figure 5.10 Visual ranges for the four ash samples in particle diameter size distribution category b (i.e. 20-50 µm mode diameters). Each point is for the mean visual range when ash flow into the container was at equilibrium with ash-settling rate at the base for each experiment. Horizontal minimum and maximum error bar values and the point values correspond to bullet points 1-3 in Section 5.5.2 respectively. Vertical error bars show the maximum and minimum values recorded by the transmissometer during the periods of equilibrium (Figure 5.8).

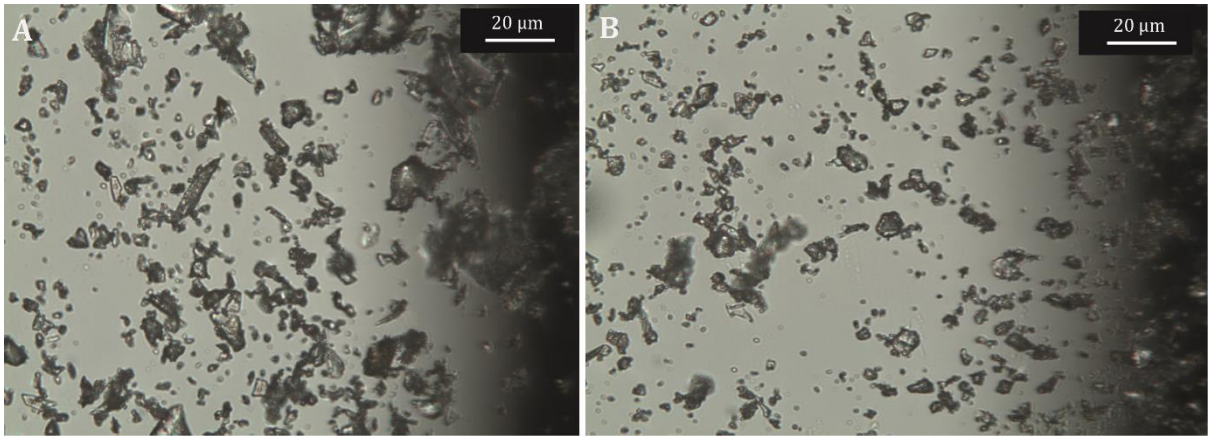

Figure 5.11 Microscope images for (a) Kaharoa rhyolite sample, (b) Chaitén rhyolite sample, both in particle size group b. The individual particles of the Chaitén sample are generally more spherical in shape. A Leica DM2500P microscope (with 40x zoom) and Leica DFC295 camera attachment was used to capture the images.

5.5.5 Ash remobilisation considerations

We recognise the importance of ash remobilisation and that correlations perhaps exist between ash depth and other characteristics on the ground, and airborne ash concentration (Thorarinsson 1971, Johnston 1997, Searl et al. 2002). However, given that ash deposits are often characterised across transects or accessible lines rather than across grids (Folch 2012), and given the number and complexity of variables associated with the remobilisation and resuspension of ash (e.g. meteorological conditions, ash wetness, particle characteristics, road surface specifics and vehicle type), we do not investigate the conditions for resuspended ash in detail. Rather, our calculations of visibility impairment largely represent conditions that can be expected during initial ashfall when ash accumulation on the ground is minimal. Current developments in resuspension modelling (e.g. Folch et al. 2014) will likely aid the future understanding of interactions between ash remobilisation and visibility effects. Our results are presently most reliable for road transportation where surfaces are wet and for maritime transportation, as atmospheric remobilisation will be minimal due to ash settling on water. For on-going eruptions however, our results should be treated as highly conservative for most land-based transportation types where cleaning has not occurred.

5.5.6 Considerations for transportation and emergency management authorities

Road transportation may be disrupted by reduced visibility from ashfall, with potential effects on the volume of traffic, average speed of vehicles and accident rate. Speed restrictions and road closures may be implemented as a result, although these are often at the discretion of road authorities and local transportation management procedures. As with other atmospheric hazards, in most circumstances it is likely that reduced visual range from airborne volcanic ash during initial ashfall will have the effect of reducing the volume of traffic and increasing the accident rate. Management actions

by authorities may also contribute towards reduced traffic volumes, for example if the public are advised to remain indoors because of health concerns (Blake et al. 2015).

Brooks et al. (2011) used a driver-simulation method to determine how drivers react when driving in varying levels of fog and to assess whether drivers are willing to drive at speeds where their lane keeping performance is degraded due to the reduced visibility. All participants were instructed to stay in lane and drive the speed limit of 55 miles per hour (88.6 km h^{-1}). The visual range for the simulator on the straight road ranged from 496 m in the clear condition to 178, 70, 31, 18 and 6m as the level of fog increased. Observed speed reductions were as follows (Brooks et al. 2011):

- For visual ranges of 496-31 m, average speeds decreased from 91.3 to 89.1 km h^{-1}
- For 18 m visual range, speeds decreased further to 82.9 km h^{-1}
- In the foggiest condition tested (6 m visual range) speeds decreased to 71.7 km h^{-1}, representing a decrease of ~20 km h^{-1} from clear conditions.

Despite the speed reductions for the most reduced visibility however, it was calculated that drivers would likely be incapable of stopping to avoid obstacles in the roadway (Brooks et al. 2011, Blake et al. 2016), a situation that corresponds to what has been recorded on actual roads in inclement weather (Edwards 1999). Additionally, lane-keeping ability was reduced when fog resulted in visibility distances <30 m (Brooks et al. 2011). Mueller and Trick (2012) also used a driver-simulation method and investigated average speeds for young drivers in clear and reduced visibility. Each scenario encompassed 6.8 km of road with speed limits of 80 km h^{-1}, with one practice scenario, one scenario with clear visibility and one with a fog density causing 600 m visual range (a relatively long distance when compared with Brooks et al's (2011) study). All drivers in this study reduced their speed in fog compared to clear visibility with an average speed reduction of 6.4 km h^{-1} (Mueller and Trick 2012).

From these studies, it is evident that even the lowest ash-settling rates expected in Auckland and the largest particle diameter sizes (<110 μm mode) used in our research would cause disruption to road transportation from speed reduction due to visibility degradation (<600 m visual ranges). Speed reduction in volcanic ashfall may be even greater than for fog due to additional transportation impacts such as road marking coverage by ash and reduced skid resistance (Wilson et al. 2012, Wilson et al. 2014, Blake et al. in review 1, 2). In the absence of key research on driver behaviour in volcanic ashfall and assuming no speed restrictions, based on data available for other atmospheric hazards we estimate an average free-flow speed of 30 km h^{-1} for a visual range of 5 m, with an increased chance of accidents due to lack of lane-keeping ability and obstructions hidden from view. With 20 m visual range, 50 km h^{-1} may be possible, but for the lowest expected visual ranges in Auckland (~1-2 m), driving is likely to become highly impractical and dangerous.

In an operational environment, roading and emergency management officials may use such knowledge of anticipated driver behaviour, along with information on previous mitigation measures following historical eruptions (Table 5.1), to appropriately deal with reduced visibility (in addition to other impact types) from volcanic ash. We suggest a range of mitigation options in addition to clean-

up for where it may be necessary to keep roads open in ash-contaminated environments, especially relevant in dry conditions or during prolonged eruptions with recurring ashfalls:

- Ash dispersion and fall models should be used for eruption scenarios to provide estimates of ash-settling rates and ash particle characteristics in different locations. Expected visual ranges can then be calculated, allowing predictions of free-flow vehicle speeds and transportation route 'hot-spots' where increased accident rates would be more likely.

- During eruptions, depending on the road type and existing restrictions, lower speed limits can be implemented to minimise the resuspension of ash behind vehicles and reduce accident rates. If driving is still possible and the environment is heavily contaminated with ash, speeds as low as 20 km h^{-1} may be necessary in urban locations. This aligns well with speeds that have either been enforced or recommended following some historical eruptions worldwide (e.g. Ruapehu 1945, Cordón Caulle 2011 – Table 5.1).

- Implementing one-way systems, particularly on roads with no median barrier to separate traffic, may be beneficial to reduce impacts from airborne ash and minimise accidents.

- Organised spacing of vehicles and slow-moving convoys are other operational techniques that should be considered. However, vehicle spacing would have to be substantial to allow the majority of resuspended ash to settle between vehicles (typically ~5 minute spacing for ~90% of ash to settle, assuming no wind or other disturbances). Such spacing aligns well with the spacing of vehicles implemented on major routes following the Mount St Helens (1980) eruption; as Warrick (1981) states, "although the highways were officially closed, [vehicles] were allowed to proceed westward on I-90 and northward on U.S.-97 at a rate of one vehicle every 5 minutes and a maximum speed of 25 mph" (p.21). A 5-minute spacing may also be important to consider for rail transportation.

- Regularly dampening road surfaces with water can be highly effective in reducing ash resuspension and improving visibility. It should be noted that this may have the undesired effects of depleting water supplies and reducing skid resistance, although the skid resistance effects will unlikely be substantial as dry ash is often nearly as slippery (Blake et al. in review 2). Additionally, care should be taken not to wash ash into drains as it may lead to blockage and costly clean-up operations (Hayes 2014).

- If operational, existing roadside infrastructure such as mobile signage, variable message signs and monitoring cameras may be useful to provide guidance to motorists encountering airborne volcanic ash.

Besides road, all other forms of surface transportation may be disrupted by reduced visibility from ash with local regulations and transportation management policies potentially affecting the level of disruption:

- **Rail transportation:** KiwiRail's heat management procedures specify a 40 km h^{-1} speed restriction, which is also typically introduced during other adverse weather conditions including strong wind and dense fog, as well as following earthquakes with large shaking intensity (Steel and O'Connell 2011, Peter Ramsay and Mark Goodman, KiwiRail, pers comm, 03 August 2015). During initial ashfall, we suggest that such a policy (with a 40 km h^{-1} speed restriction) should be enacted when visual range is ~10 m or less; a slightly higher speed than the estimated free-flow speed on roads due to the different infrastructure for rail, such as more automated controls and fixed paths of travel. However, as for road, rail operations are likely to become highly impractical and dangerous when visual range is very low (~1 m).

- For **maritime** transportation near Auckland City, a "restricted visibility routine" for the area/s affected may come into effect when visibility of less than 1 nautical mile from a vessel's bridge is encountered (AC 2014). Under such conditions, vessels with automatic identification systems can continue to operate with increased communication between the harbourmaster and restrictions on the number of vessels in certain areas. In accordance with Maritime Rule 22.6, speed reduction may be required so that "a vessel can be stopped within a distance appropriate to the prevailing circumstances and conditions" (MNZ 2015, p.4), taking into account the state of visibility (AC 2014, MNZ 2015). Stopping at such distances will likely be very difficult for some vessels during low visual ranges in ashfall and we anticipate that the movement of some vessels may cease until visibility improves.

- For **airport** operations at Auckland Airport, assuming no preceding closure due to other factors such as potential damage to aircraft engines, the visual ranges expected from most initial ashfalls mean that low visibility procedures would be initiated (triggered by <1,500 m visual range) (CAA 2008). Only essential ground support traffic directly involved with the arrival or departure of an aircraft will be allowed to operate in the manoeuvring area during such conditions. As the runway is equipped with a Category III B Instrument Landing System, aircraft and pilots with the appropriate ratings can land if the visual range is >50 m (Auckland Airport 2008), with a maximum of six aircraft take-off and landing movements per hour (CAA 2008). With lower visual ranges, operations at the airport would cease, although closure would likely be necessary due to other factors by this stage.

5.6 Conclusions

We have developed and implemented a laboratory-based approach to allow the calculation of visual range from given ash-settling rates for a range of different volcanic ash samples with different particle size and compositional characteristics. Our experiments incorporated only fine-grained ash (all particle diameters <320 μm with mode sizes <110 μm) due to limitations of the ash dispersal equipment. Compared to most other airborne particulate matter, ash particles are relatively large in

size. However, their occurrence in large concentrations, like fog droplets, can cause substantial reductions in visibility, although they generally fall to the ground and out of suspension more quickly. Our results demonstrate that visibility decreases with increasing ash-settling rate (and thus also increasing airborne concentration). Just a ~10 g m^{-2} h^{-1} settling rate of fine-grained ash, which could occur >200 km from a vent (Figure 5.6), can cause visibility degradation of over two hundred times from the typical baseline visual range (i.e. <300 m rather than 70 km visual ranges).

Of all the ash characteristics, ash particle size has the greatest effect on visual range. For a given settling rate, fine-grained ash causes a shorter visual range than coarse-grained ash, a finding that aligns with existing research involving other particulate types. For settling rates of ~4,000 g m^{-2} h^{-1}, the largest that can be expected in Auckland based on limited worldwide data, with predominantly fine-grained ash, visual ranges as low as ~1-2 m may result. We suggest that such large settling rates with predominantly fine-grained ash are most likely from either highly explosive eruptions in the TVZ, or local and relatively explosive eruptions within the AVF.

The influence of ash type, colour and shape on visual range reduction is not as clear-cut as for particle size. From our experiments, we conclude that samples with a higher proportion of irregular-shaped particles cause a greater reduction in visual range than those with more spherical shapes. Light-coloured ash such as rhyolite appears to result in lower visual ranges than dark-coloured ash such as basalt; a trend that makes intuitive sense given increased reflection off light-coloured surfaces. However, further laboratory or field-based studies are required to confirm the true extent that particle colouration and shape impacts visual range.

Based on comparisons with other atmospheric hazards, we suggest several implications for surface transportation during initial ashfall.

- Drivers of road vehicles will likely reduce their speeds during ashfall with ash-settling rates of 10-4,000 g m^{-2} h^{-1} and particle size distributions of 1-320 μm:
    - Although based on limited comparative data, speeds of 50 km h^{-1} for a visual range of 20 m and 30 km h^{-1} for a visual range of 5 m may occur without restriction during initial ashfall.
    - Stopping in time to avoid obstacles at such speeds may be difficult and the implementation of lower-than-usual speed restrictions may be required to reduce accidents and ensure network functionality is maintained.

- For very short visual ranges (i.e. 1-2 m), driving would be extremely dangerous and road closures would likely be necessary.

- Operations at airports and on rail and maritime transportation networks would be affected by the ash-settling rates investigated:
    - Reduced capacity is likely due to lower-than-usual speed restrictions and stricter limits on the numbers of aircraft or vessels operating.

- Some operations may cease altogether due to visual range reduction alone, perhaps for ash-settling rates of ~30 g m^{-2} h^{-1} or more.

We emphasise that our conclusions are for initial volcanic ashfall only and that any remobilised and resuspended ash from the ground could result in lower visual ranges for extended periods of time post-eruption, exacerbating any transportation impacts. The effect of ash remobilisation was not directly investigated as part of this study. However, our experiments provide insights on the length of time required for ash to settle out of the atmosphere. It took an average of ~11 minutes for airborne concentrations of ash and associated visual ranges to return to their original pre-experiment levels and ash-settling rate to decrease to zero from a height of 1 meter. However, given the exponential increase in visual range upon cessation of ash dispersal, values returned to 90% of their maximum within ~5 minutes with no clear differences observed between samples. Various mitigation measures may be implemented by transportation and emergency management authorities to improve visibility and/or reduce accident rates during primary volcanic ashfall and times of ash remobilisation, including stricter-than-usual speed restrictions, increased vehicle spacing, dampening of surfaces with water, and road closures.

Importantly, our study emphasises the need for rapid syn-eruptive and reliable measurements or calculations of visual range and the consideration of different ash characteristic metrics besides ash thickness in volcanic eruptions, including particle size distribution. Additionally, contemporary ash dispersion and fallout models, which provide outputs of airborne ash concentration and/or ash-settling rate given particular eruptions, can be used to produce scenarios of transportation disruption from reduced visibility, as well as other assessments including for human and animal health hazards. In conjunction with scenarios for other impact types (e.g. reduced skid resistance and marking coverage by ash), this would allow the improvement of transportation management strategies during and following future volcanic ashfall.

5.7 Acknowledgments

We acknowledge the support of the University of Canterbury Department of Geological Sciences, which allowed us to purchase both the *TOPAS SAG-410 solid aerosol generator* (ash disperser) and *DynOptic DSL-460 MkII transmissometer* required for experimentation. Additionally, we thank the Chartered Institute of Logistics and Transport (CILT) for their financial contribution towards equipment costs. The support for the authors from the New Zealand Earthquake Commission (EQC), Determining Volcanic Risk in Auckland (DEVORA) project, Natural Hazards Research Platform (NHRP) and University of Canterbury Mason Trust scheme is also greatly appreciated. Peter Jones, Rob Spiers, Chris Grimshaw, Matt Cockcroft, Sacha Baldwin-Cunningham, Cathy Higgins, Sarah Pope, Connor Jones and Stephen Brown, who we gratefully thank, supported technical laboratory work. We also acknowledge and appreciate the technical support provided by Stephan Große of TOPAS GmbH and Jozua Taljaard and Andrew Blair of Ecotech NZ Environmental for the operation

and adaptations of the ash disperser and transmissometer respectively. Daniel Blake would also like to thank his other PhD supervisors, Natalia Deligne (GNS Science), Jan Lindsay (The University of Auckland) and Jim Cole (University of Canterbury), for their edits, guidance and advice throughout the project. To all these persons and organisations, we express our sincere thanks.

5.8 References

Abdel-Aty, M. Akram, A. Huang, H. Choi, K. (2011) A study on crashes related to visibility obstruction due to fog and smoke. Accident Analysis and Prevention, 43:5, pp.1730-1737.

AC (2014) Harbourmaster's Office Operation of Vessels During Periods of Restricted Visibility: Navigation Safety Operating Requirements. Auckland Council, Auckland, New Zealand.

AccuWeather (2015) First Calbuco eruption in 42 years suspends flights in Buenos Aires. AccuWeather.com. http://www.accuweather.com/en/weather-news/more-than-4000-evacuated-after/46042985, Accessed 23 November 2015.

Adams, C. (2013) Identification of tuff rings in the Auckland Volcanic Field using LiDAR and ground penetrating radar. New Zealand Journal of Geology and Geophysics. http://frontiersabroad.com/wp-content/uploads/2014/03/Cameron-Adams.pdf, Accessed 08 June 2016.

Alloway, B. Westgate, J. Pillans, B. Pearce, N. Newnham, R. Byrami, M. Aarburg, S. (2004) Stratigraphy, age and correlation of middle Pleistocene silicic tephras in the Auckland region, New Zealand: a prolific distal record of Taupo Volcanic Zone volcanism. New Zealand Journal of Geology and Geophysics, 47, pp.447–479.

Andò, B. Baglio, S. Marletta, V. (2014) Selective measurement of volcanic ash flow-rate. IEEE Transactions of Instrumentation and Measurement, 63:5, pp.1356-1363.

Aplin, K. Houghton, I. Nicoll, K. Humphries, M. Tong, A. (2014) Electrical charging of volcanic ash. Proceedings of the ESA Annual Meeting on Electrostatics. http://www.electrostatics.org/images/ESA_2014_G_Aplin_et_al.pdf, Accessed 10 March 2016.

Aplin, K. Nicoll, K. Houghton, I. (2015) Electrical charging of volcanic ash from Eyjafjallajökull. Geophysical Research Abstracts, 17, EGU Gneral Assembly 2015.

APTI (2000) OS 411: Computational atmospheric sciences. Air Pollution Training Institute, Shodor Education Foundation Inc., US EPA. https://www.shodor.org/os411/index.html, Accessed 27 February 2016

Ashley, W.S. Strader, S. Dziubla, D.C. Haberlie, A. (2015) Driving blind: weather-related vision hazards and fatal motor vehicle crashes. American Meteorology Society, Northern Illinois University. http://journals.ametsoc.org/doi/pdf/10.1175/BAMS-D-14-00026.1, Accessed 07 April 2016.

Auckland Airport (2008) Newsroom: Fog at Auckland Airport and Category IIIB, 19 November 2008, Auckland Airport. http://www.aucklandairport.co.nz/~/media/3FF843AAFCBB4C23B941EAA7406EAB7B.ashx?sc_database=web, Accessed 19 March 2016.

Barnard, S. (2009) The vulnerability of New Zealand lifelines infrastructure to ashfall. PhD Thesis, Hazard and Disaster Management, University of Canterbury, Christchurch, New Zealand.

Barsotti, S. Neri, A. Scire, J.S. (2008) The VOL-CALPUFF model for atmospheric ash dispersal: 1. approach and physical formation. Journal of Geophysical Research, 113, 12p.

Barsotti, S. Andronico, D. Neri, A. Del Carlo, P. Baxter, P.J. Aspinall, W.P. Hincks, T. (2010) Quantitative assessment of volcanic ash hazards for health and infrastructure at Mt. Etna (Italy) by numerical simulation. Journal of Volcanology and Geothermal Research, 192, pp.85-96.

Bartney, B. (1980) Showers of muddy ash fall from fresh eruption. The Lawrence Daily: Journal – World, Kansas, 26 May 1980, 122:147, 20p.

BBC (2013) Sheppy crossing crash: dozens hurt as 130 vehicles crash, 05 September 2013. http://www.bbc.com/news/uk-england-kent-23970047, Accessed 10 October 2015.

Becker, J. Smith, R. Johnston, D. Munro, A. (2001) Effects of the 1995-1996 Ruapehu eruptions on communities in central North Island, New Zealand, and people's perceptions of volcanic hazards after the event. The Australian Journal of Disaster and Trauma Studies, 2001-1.

Binkowski, F.S. Roselle, S.J. Mebest, M.R. Eder, B.K. (2002) Modeling atmospheric particulate matter in an air quality modelling system using a modal method, IN: Chock, D.P. Carmichael, G.R. (Eds.) Atmospheric modelling. The IMA Volumes in Mathematics and its Applications, 130.

Blake, D.M. Wilson, G. Stewart, C. Craig, H.M. Hayes, J.L. Jenkins, S.F. Wilson, T.M. Horwell, C.J. Andreastuti, S. Daniswara, R. Ferdiwijaya, D. Leonard, G.S. Hendrasto, M. Cronin, S. (2015) The 2014 eruption of Kelud volcano, Indonesia: impacts on infrastructure, utilities, agriculture and health. GNS Science Report 2015/15, 139p. *[APPENDIX A OF THIS THESIS]*

Blake, D.M. Wilson, T.M. Deligne, N.I. Lindsay, J.L. Cole, J.W. (2016) Impacts of volcanic ash on road transportation: considerations for resilience in central Auckland. Proceedings Paper for the Institute of Professional Engineers New Zealand (IPENZ) Transportation Group Conference, March 2016. Auckland, New Zealand.

Blake, D.M. Wilson, T.W. Gomez, C. (in review 1) Road marking coverage by volcanic ash: an experimental approach. Environmental Earth Sciences. *[CHAPTER 4 OF THIS THESIS]*

Blake, D.M. Wilson, T.M. Cole, J.W. Deligne, N.I. Lindsay, J.M. (in review 2) Impact of volcanic ash on road and airfield surface skid resistance. Journal of Transportation Research Part D: Transport and Environment. *[CHAPTER 3 OF THIS THESIS]*

Blong, R.J. (1982) The time of darkness: local legends and volcanic reality in Papua New Guinea. Australian National University Press, Canberra, Australia.

Blong, R.J. (1984) Volcanic hazards: a sourcebook on the effects of eruptions. Academic Press, Sydney, Australia.

Bonadonna, C. Ernst, G.G.J. Sparks, R.S.J. (1998) Thickness variations and volume estimates of tephra fall deposits: the importance of particle Reynolds number. Journal of Volcanology and Geothermal Research, 81, pp.173-187.

Bonadonna, C. Mayberry, G.C. Calder, E.S. Sparks, R.S.J. Choux, C. Jackson, P. Lejeune, A.M. Loughlin, S.C. Norton, G.E. Rose, W.I. Ryan, G. Young, S.R. (2002) Tephra fallout in the eruption of Soufrière Hills Volcano, Montserrat. IN: Druitt, T.H. Kokelaar, B.P. (Eds.) The eruption of Soufrière Hills Volcano, Montserrat, from 1995 to 1999. Geological Society, London, Memoirs, 21, pp.483-516.

Bonadonna, C. Phillips, J. (2003) Sedimentation from strong volcanic plumes. Journal of Geophysical Research: Solid Earth, 108, B7.

Bonadonna, C. Houghton, B. (2005) Total grain-size distribution and volume of tephra-fall deposits. Bulletin of Volcanology, 67, pp.441-456.

Bonadonna, C. Genco, R. Gouhier, M. Pistolesi, M. Cioni, R. Alfano, F. Hoskuldsson, A. Ripepe, M. (2011) Tephra sedimentation during the 2010 Eyjafjallajökull eruption (Iceland) from deposit, radar, and satellite observations. Journal of Geophysical Research, 116, B12202.

Bonadonna, C. Costa, A. (2012) Estimating volume of tephra deposits: a new simple strategy. Geology 40,5, pp.415–418.

Bonasia, R. Costa, A. Folch, A. Capra, L. Macedonio, G. (2012) Numerical simulation of tephra transport and deposition of the 1982 El Chichon eruption and implications for hazard assessment. Journal of Volcanology and Geothermal Research, 231–232, pp.39–49.

Brooks, J.O. Crisler, M.C. Klein, N. Goodenough, R. Beeco, R.W. Guirl, C. Tyler, P.J. Hilpert, A. Miller, Y. Grygier, J. Burroughs, B. Martin, A. Ray, R. Palmer, C. Beck, C. (2011) Speed choice and driving performance in simulated foggy conditions. Accident Analysis and Prevention, 43, 3, pp.698-705.

Broom, S.J. (2010) Characterisation of “pseudo-ash” for quantitative testing of critical infrastructure components with a focus on roofing fragility. BSc (Hons) Thesis, Hazard and Disaster Management, University of Canterbury, Christchurch, New Zealand.

CAA (2008) Low Visibility Operations at Auckland Airport. Vector: Pointing to Safer Aviation, Issue 4, Civil Aviation Authority of New Zealand. https://www.caa.govt.nz/Publications/.../Vector_2007_Issue4_JulAug.pdf. Accessed 19 March 2016

Carey, S. Sigurdsson, H. (1982) Influence of particle aggregation on deposition of distal tephra from the May 18, 1980 eruption of Mount St. Helens Volcano. Journal of Geophysical Research, 87, B8, pp.7061-7072.

Carey, S. Sigurdsson, H. (1986) The 1982 eruptions of El Chichon volcano, Mexico (2): Observations and numerical modelling of tephra-fall distribution. Bulletin of Volcanology, 48, pp.127-141.

Carey, S. Sparks, R.S.J. (1986) Quantitative models of the fallout and dispersal of tephra from volcanic eruption columns. Bulletin of Volcanology, 48, pp.109-125.

Carey, S. Bursik, M. (2015) Volcanic plumes. IN: Sigurdsson, H. (Ed). Encyclopedia of Volcanoes, Academic Press, pp.571-585.

Cassidy, J. Locke, C. (2004) Temporally linked volcanic centres in the Auckland Volcanic Field. New Zealand Journal of Geology and Geophysics, 47, pp.287–290.

Codling, J.P. (1971) Thick fog and its effect on traffic flow and accidents. Transport and Road Research Laboratory. TRRL Report LR 397, TRRL, Crowthorne.

Cole, J. Blumenthal, E. (2004) Evacuate!: what an evacuation order given because of a pending volcanic eruption could mean to residents of the Bay of Plenty. Tephra, June 2004. Natural Hazards Research Centre, University of Canterbury.

Conner, W.D. (1974) Measurement of opacity and mass concentration of particulate emissions by transmissometry, EPA 650/2-74-128. United States Environmental Protection Agency.

Conner, W.D. Knapp, K.T. Nader, J.S. (1979) Applicability of transmissometers to opacity measurement of emissions – oil-fired power plants and Portland cement plants, EPA 600/2-79-188. United States Environmental Protection Agency.

Costa, A. Macedonio, G. Folch, A. (2006) A three-dimensional Eulerian model for transport and deposition of volcani ashes. Earth Planet Science Letters, 241;3-4, pp.634-647.

Costa, A. Dell'Erba, F. Di Vito, M.A. Isaia, R. Macedonio, G. Orsi, G. Pfeiffer, T. (2009) Tephra fallout hazard assessment at the Campi Flegrei caldera (Italy). Bulletin of Volcanology, 71:3, pp.259–73.

Costa, A. Folch, A. Macedonio, G. (2013) Density-driven transport in the umbrella region of volcanic clouds: implications for tephra dispersion models. Geophysical Research Letters, 40, pp.4823-4827.

Cova, T.J. Conger, S. (2003) Transportation hazards. IN: Kutz, M. (Ed.) Handbook of Transportation Engineering, McGraw-Hill Handbook.

Craig, H. Wilson, T. Stewart, C. Outes, V. Villarosa, G. Baxter, P. (2016) Impacts to agriculture and critical infrastructure in Argentina after ashfall from the 2011 eruption of the Cordón Caulle volcanic complex: an assessment of published damage and function thresholds. Journal of Applied Volcanology, 5:7, 31p.

Dobran, F. Neri, A. Macedonio, G. (1993) Numerical-simulation of collapsing volcanic columns. Journal of Geophysical Research, 98, pp.4231-4259.

Durant, A.J. Rose, W.I. Sarna-Wojcicki, A.M. Carey, S. Volentik, A.C. (2009) Hydrometeor-enhanced tephra sedimentation from the 18 May 1980 Mount St. Helens (USA) volcanic cloud. Journal of Geophysical Research, 114.

DynOptic (2014) DSL-460 double pass opacity/dust monitor: operators manual v1.4. DynOptic Systems Ltd. Brackley, Northamptonshire, UK

Edwards, J.B. (1999) Speed adjustment of motorway commuter traffic to inclement weather. Transportation Research Part F2, pp.1-14.

Electrostatic Solutions Ltd. (2000) Electrostatic Solutions Technical Brief No. 6: triboelectrification – how materials charge by contact. Hampshire, UK. http://www.electrostatics.net/pdf/TB6-triboelectrification.pdf, Accessed 15 May 2016.

Elliot, A.J. Singh, N. Loveridge, P. Harcourt, S. Smith, S. Pnaiser, R. Kavanagh, K. Robertson, C. Ramsay, C.N. McMenamin, J. Kibble, A. Murray, V. Ibbotson, S. Catchpole, M. McCloskey, B. Smith, G.E. (2010) Syndromic surveillance to assess the potential public health impact of the Icelandic volcanic ash plume across the United Kingdom, April 2010. Eurosurveillance 15:23.

EPA (2000) Current knowledge of particulate matter (PM) continuous emission monitoring: final report. United States Environmental Protection Agency. https://www3.epa.gov/ttnemc01/cem/pmcemsknowfinalrep.pdf, Accessed 14 March 2016.

EPA (2001) Protecting visibility: an EPA report to congress, chapter 3. United States Environmental Protection Agency. http://www.epa.gov/nscep, Accessed 06 March 2016.

Eto, T. (2001) Estimation of amount and dispersal volcanic ash-fall deposits ejected by vulcanian type eruption. Reports of the Faculty of Science, Kagoshima University, 34, pp.35-46.

Folch, A. Costa, A. Macedonia, G. (2009) FALL3D: A computational model for transport and deposition of volcanic ash. Computers and Geosciences, 35, pp.1334-1342.

Folch, A. Sulpizio, R. (2010) Evaluating long-range volcanic ash hazard using supercomputing facilities: application to Somma-Vesuvius (Italy), and consequences for civil aviation over the Central Mediterranean area. Bulletin of Volcanology, 72, pp.1039-1059.

Folch, A. (2012) A review of tephra transport and dispersal models: evolution, current status, and future perspectives. Journal of Volcanology and Geothermal Research, 235-236, pp.96-115.

Folch, A. Mingari, L. Osores, M.S. Collini, E. (2014) Modeling volcanic ash resuspension – application to the 14-18 October 2011 outbreak episode in central Patagonia, Argentina. Natural Hazards and Earth System Sciences, 14, pp.119-133.

Fowler, W.B. Lopushinsky, W. (1986) Wind-blown volcanic ash in forest and agricultural locations as related to meteorological conditions. Atmospheric Environment, 20:3, pp.421-425.

Guffanti, M. Mayberry, G.C. Casadevall, T.J. Wanderman, R. (2009) Volcanic hazards to airports. Natural Hazards, 51, pp.287-302.

GVP (2013) Report on San Cristobal (Nicaragua): January 2013. Global Volcanism Program. http://volcano.si.edu/showreport.cfm?doi=10.5479/si.GVP.BGVN201301-344020, Accessed 23 November 2015.

Hagen, L.J. Skidmore, E.L. (1977) Wind erosion and visibility problems. Transactions of the American Society of Agricultural Engineers, 20:5, pp.898-903.

Hardy, S.E.J. (2015) Major incident in Kent: a case report. Scandinavian Journal of Trauma, Resuscitation and Emergency Medicine, 23,:71.

Harris, D.M. Rose, W.I. (1983) Estimating particle sizes, concentrations, and total mass of ash in volcanic clouds using weather radar. Journal of Geophysical Research, 88:C15, pp.10969-10983.

Hayes, J. (2014) Tephra clean-up in Auckland City, New Zealand: quantitative impact assessment and response planning. Masters Thesis. Hazard and Disaster Management, University of Canterbury, Christchurch, New Zealand.

Hill D.J. (2014) Filtering out the ash: mitigating volcanic ash ingestion for generator sets. Masters Thesis. Hazard and Disaster Management, University of Canterbury, Christchurch, New Zealand.

Hincks, T.K. Aspinall, W.P. Baxter, P.J. Searl, A. Sparks, R.S.J. Woo, G. (2006) Long term exposure to respirable volcanic ash on Montserrat: a time series simulation. Bulletin of Volcanology, 68, pp.266-284.

Horwell, C.J. (2007) Grain-size analysis of volcanic ash for the rapid assessment of respiratory health hazards. Journal of Environmental Monitoring, 9, pp.1107-1115.

Howe, T. Lindsay, J.M. Mortimer, N. Leonard, G. (2011) DEVORA borehole database: status update and manual, IESE Report 1-2011.03. Institute of Earth Science and Engineering, Auckland, New Zealand.

van de Hulst, H.C. (1957) Light scattering by small particles, John Wiley & Sons, Inc, New York.

Hyslop, N. (2009) Impaired visibility: the air pollution people see. Atmospheric Environment, 43:1, pp.182-195.

Ibrahim, D. (2015) Massive dust storm triggers deadly pileup in Colarado. The Weather Network. http://www.theweathernetwork.com/us/news/articles/massive-dust-storm-triggers-deadly-pileup-in-colorado/52592/, Accessed 18 January 2016.

Johnston, D.M. (1997) Physical and social impacts of past and future volcanic eruptions in New Zealand. PhD Thesis. Earth Science, Massey University, Palmerston North, New Zealand.

Kieffer, S. (1984) Factors governing the structure of volcanic jets. Explosive volcanism: inception, evolution and hazards, National Academy Press, Washington D.C, pp.143-157.

Kienle, J. Swanson, S.E. (1985) Volcanic hazards from future eruptions of Augustine Volcano, Alaska. University of Alaska Geophysical Institute, 122p.

Komer, P.D. Reimers, C.E. (1978) Grain shape effects on settling rates. Journal of Geology, 86, pp.193-209.

Koschmieder, H. (1925) Theorie de horizontalen Sichtweite, Keim and Nemnich.

Leonard, G.S. Stewart, C. Wilson, T.M. Proctor, J.N. Scott, B.J. Keys, H.J. Jolly, G.E. Wardman, J.B. Cronin, S.J. McBride, S.K. (2014) Integrating multidisciplinary science, modelling and impact data into evolving, syn-event volcanic hazard mapping and communication: A case study from the 2012 Tongariro eruption crisis, New Zealand. Journal of Volcanology and Geothermal Research, 286, pp.208-232.

Macedonio, G. Costa, A. Scollo, S. Neri, A. (2016) Effects of eruption source parameter variation and meteorological dataset on tephra fallout hazard assessment: example from Vesuvius (Italy). Journal of Applied Volcanology, 5:5.

Magill, C. Blong, R. (2005) Volcanic risk ranking for Auckland, New Zealand II: Hazard consequences and risk calculation. Bulletin of Volcanology, 67, pp.340-349.

Magill, C. Wilson, T. Okada, T. (2013) Observations of tephra fall impacts from the 2011 Shinmoedake eruption, Japan. Earths Planets and Space, 65, pp.677-698.

Malm, W. (1979) Visibility: a physical perspective. IN: Fox, D. Loomis, R.J. Greene, T.C. Proceedings of the workshop in visibility values. U.S. Department of Agriculture, Fort Collins, Colorado, pp.56-68.

Malm, C.W. Day, D.E. Kreidenweis, S.M. Collett, J.L. Lee, T. (2003) Humidity-dependent optical properties of fine particles during the Big Bend Regional Aerosol and Visibility Observational Study. Journal of Geophysical Research, 108:D9.

MFE (2001) Good practice guide for monitoring and management of visibility in New Zealand. Ministry for the Environment Report, Wellington, New Zealand.

MNZ (2015) Maritime Rules Part 22: Collision Prevention. Maritime New Zealand, Wellington, New Zealand. https://www.maritimenz.govt.nz/Rules/Rule-documents/Part22-maritime-rule.pdf, Accessed 19 March 2016.

Moen, W.S. (1981) Physical and chemical properties of ash from the May 18, 1980, eruption of Mount St. Helens, In: Moen, W.S. McLucas, G.B. Mount St. Helens Ash – Properties and Possible Uses, Report of Investigations 24. Washington Department of Natural Resources, Division of Geology and Earth Resources.

Molloy, C. Shane, P. Augustinus, P. (2009) Eruption recurrence rates in a basaltic volcanic field based on tephra layers in maar sediments: implications for hazards in the Auckland volcanic field. Geological Society of America Bulletin, 121:11/12, pp.1666-1677.

Moore, R.L. Cooper, L. (1972) Fog and road traffic. Transport and Road Research Laboratory, TRRL Report LR 446. TRRL, Crowthorne.

Morton, B. Taylor, G. Turner, J. (1956) Turbulent gravitational convection from maintained and instantaneous sources. Proceedings of the Royal Society of London: A, 234, pp.1-23.

Mueller, A.S. Trick, L.M. (2012) Driving in fog: the effects of driving experience and visibility on speed compensation and hazard avoidance. Accident Analysis and Prevention, 48, pp.472-479.

Musk, L. (1991) Climate as a factor in the planning and design of new roads and motorways. IN: Perry, A.H. Symons, L.J. (Eds.) Highway Meteorology, E. & F.N. Spon, London.

OECD (1986) Road Safety Research 1986, Paris, OECD, 106p.

Pardini, F. Spanu, A. Vitturi, M.M. Salvetti, M.V. Neri, A. (2016) Grain size distribution uncertainty quantification in volcanic ash dispersal and deposition from weak plumes. Journal of Geophysical Research: Solid Earth, 121.

Parfitt, L. Wilson, L. (2009) Fundamentals of Physical Volcanology. IN: Sigurdsson, H. (Ed.) Encyclopedia of Volcanoes, Academic Press.

Perry, A.H. (1981) Environmental hazards in the British Isles, George Allen and Unwin, London.

Pyle, D.M. (1989) The thickness, volume and grainsize of tephra fall deposits. Bulletin of Volcanology, 51, pp.1-15.

Riley, C.M. Rose, W.I. Bluth, G.J.S. (2003) Quantitative shape measurements of distal volcanic ash. Journal of Geophysical Research, 108:B10.

Robinson, E. (1968) Effect on the physical properties of the atmosphere. IN: Stern, A.C. (Ed.) Air Pollution, 1:2. Academic Press, New York, pp.349-400.

Rose, W.I. Durant, A.J. (2009) Fine ash content of explosive eruptions. Journal of Volcanology and Geothermal Research, 186, pp.32-39.

Sarkinen, C.F. Wiitala, J.T. (1981) Investigation of volcanic ash on transmission facilities in the Pacific Northwest. IEEE Transactions on Power Apparatus and Systems PAS-100, 5, pp.2278-2286.

Sarna-Wojcicki, A.M. Shipley, S. Waitt, R.B. Dzurisin, D. Wood, S.H. (1981) Areal distribution, thickness, mass, volume, and grain size of air-fall ash from six major eruptions of 1980. IN: Lipman, P.W. Mullineaux, D.R. (Eds.) The 1980 eruptions of Mount St. Helens, Washington, USGS Professional Paper, 1250, pp.577-600.

Scasso, R.A. Corbella, H. Tiberi, P. (1994) Sedimentological analysis of the tephra from the 12-15 August 1991 eruption of Hudson volcano. Bulletin of Volcanology, 56, pp.121-132.

Scheidegger, K.F. Federman, A.N. (1982) Compositional heterogeneity of tephras from the 1980 eruptions of Mount St. Helens. Journal of Geophysical Research, 87:B13, pp.10861-10881.

Scollo, S. Coltelli, M. Prodi, F. Folegani, M. Natali, S. (2005) Terminal settling velocity measurements of volcanic ash during the 2002-2003 Etna eruption by an X-band microwave rain gauge disdrometer. Geophysical Research Letters, 32:10.

Scollo, S. Del Carlo, P. Coltelli, M. (2007) Tephra fallout of 2001 Etna flank eruption: analysis of the deposit and plume dispersion. Journal of Volcanology and Geothermal Research, 160, pp.147-164.

Scollo, S. Folch, A. Costa, A. (2008) A parametric and comparative study of different tephra fallout models. Journal of Volcanology and Geothermal Research, 176:2, pp.199–211.

Scott, W.E. McGimsey, R.G. (1994) Character, mass, distribution, and origin of tephra-fall deposits of the 1989-1990 eruption of Redoubt Volcano, south-central Alaska. Journal of Volcanology and Geothermal Research 62, pp.251-272.

Searl, A. Nicholl, A. Baxter, P.J. (2002) Assessment of the exposure of islanders to ash from the Soufriere Hills volcano, Montserrat, British West Indies. Occupational and Environmental Medicine, 59, pp.523-531.

Seinfeld, J.H. Pandis, S.N. (2006) Atmospheric chemistry and physics: from air pollution to climate change. John Wiley & Sons Inc, Hobeken, New Jersey.

Shimano, T. Nishimura, T. Nobuyuki, C. Shibasaki, Y. Iguchi, M. Miki, D. Yokoo, A. (2013) Development of an automatic volcanic ash sampling apparatus for active volcanoes. Bulletin of Volcanology, 75:773.

Sigurdsson, H. Carey, S. Cornell, W. Pescatore, T. (1985) The eruption of Vesuvius in AD 79. National Geographic Research, 1, pp.332-387.

Sivakumar, M.V.K. (2005) Impacts of sand stroms/dust storms on agriculture. IN: Sivakumar, M.V.K. Motha, R.P. Das, H.P. (Eds.) Natural disasters and extreme events in agriculture. Springer Berlin, pp.159-177.

Sparks, R. (1986) The dimensions and dynamics of volcanic eruption columns. Bulletin of Volcanology, 48, pp.3-15.

Sparks, R.S.J. Bursik, M.I. Ablay, G.J. Thomas, R.M.E. Carey, S.N. (1992) Sedimentation of tephra by volcanic plumes. Part 2: controls on thickness and grain-size variations of tephra fall deposits. Bulletin of Volcanology, 54, pp.685-695.

Sparks, R.S.J. Bursik, M.I. Carey, S.N. Gilbert, J.S. Glaze, L.S. Sigurdsson, H. Woods, A.W. (1997) Volcanic plumes, John Wiley and Sons.

Statistics New Zealand (2013) 2013 Census QuickStats about a place: Auckland Region. http://www.stats.govt.nz/Census/2013-census/profile-and-summary-reports/quickstats-about-a-place.aspx?request_value=13170&tabname, Accessed 16 June 2016.

Steel, P. O'Connell, P. (2011) Managing rail resources and infrastructure to restore and maintain operations in the aftermath of major earthquakes. International Railway Safety Conference, 16-21 October 2011. Melbourne, Australia.

Stirling, M.W. Wilson, C.J.N. (2002) Development of a volcanic hazard model for New Zealand: first approaches from the methods of probabilistic seismic hazard analysis. Bulletin of the New Zealand Society for Earthquake Engineering, 35:4, pp.266-277.

Stohl, A. Hittenberger, M. Wotawa, G. (1998) Validation of the Lagrangian particle dispersion model FLEXPART against large scale tracer experiments. Atmospheric Environment, 32, pp.4245–4264.

Stohl, A. Forster, C. Frank, A. Siebert, P. Wotawa, G. (2005) Technical note: the Langrangian particle dispersion model FLEXPART version 6.2. Atmospheric Chemistry and Physics, 5, pp.2461-2474.

Summer, R. Baguley, C. Burton, J. (1977) Driving in fog on the M4. Transport and Road Research Laboratory TRRL Report LR 281. TRRL, Crowthorne.

Tang, I.N. (1966) Chemical and size effects of hygroscopic aerosols on light scattering coefficients. Journal of Geophysical Research, 101, pp.19245-19250.

Tajima, Y. Ohara, D. Fukuda, K. Shimomura, S. (2015) Development of automatic tephrometer for monitoring of volcano. https://www.n-koei.co.jp/business/technology/library/thesis/pdf/forum23_005.pdf, Accessed 17 June 2016.

Taylor, J.R. Moogan, J.C. (2010) Determination of visual range during fog and mist using digital camera images. IOP Conference Series: Earth and Environmental Science, 11. 17th National Confeence of the Australian Meteorological and Oceanographic Society.

Thorarinsson, S. (1971) Damage caused by tephra fall in some big Icelandic eruptions and its relation to the thickness of tephra layers. Acta of the First International Science Congress on the Volcano of Thera, Greece, 1969, pp.15-23.

USDOT (2013) How do weather events impact roads? Weather Management Program. www.ops.fhwa.dot.gov/weather/q1_roadimpact.htm, Accessed 07 April 2016.

USGS (2013) Volcanic ash: effects and mitigation strategies. United States Geological Survey. http://volcanoes.usgs.gov/ash/trans/, Accessed 21 September 2015.

Uthe, E.E. (1980) Evaluation of an infrared transmissometer for monitoring particulate mass concentrations of emissions from stationary sources. Journal of Air Pollution Control Association, 30, pp.382-386.

Walker, G.P.L. Wilson, L. Bowel, E.L.G. (1971) 1, Explosive volcanic eruptions-I: the rate of fall of pyroclasts. Geophysical Journal of the Royal Astronomical Society, 22, pp.377-383.

Walker, G.P.L. (1981) The Waimihia and Hatepe plinian deposits from the rhyolitic Taupo Volcanic Centre. New Zealand Journal of Geology and Geophysics, 24:3, pp.305-324.

Wardman, J. Sword-Daniels, V. Stewart, C. Wilson, T. (2012) Impact assessment of the May 2010 eruption of Pacaya volcano, Guatemala. GNS Science Report 2012/09, 90p.

Warrick, R.A. (1981) Four communities under ash. Institute of Behavioural Science, University of Colorado, Boulder, U.S.

Watt, S.F.L. Pyle, D.M. Mather, T.A. Martin, R.S. Matthews, N.E. (2009) Fallout and distribution of volcanic ash over Argentina following the May 2008 explosive eruption of Chaitén, Chile. Journal of Geophysical Research, 114:B04207.

Weber, K. Fischer, C. Vogel, A. Pohl, T. Böhlke, C. (2013) First results of an airborne release of volcanic ash for testing of volcanic ash plume measurement instruments. Proceedings of Energy and Environment, pp.169-172.

Weinzierl, B. Sauer, D. Minikin, A. Reitebuch, O. Dahlkötter, F. Mayer, B. Emde, C. Tegen, I. Gasteiger, J. Petzold, A. Veira, A. Kueppers, U. Schumann, U. (2012) On the visibility of airborne volcanic ash and mineral dust from the pilot's perspective in flight. Physics and Chemistry of the Earth, 45-46, pp.87-102.

White, J. Stewart, C. Wareham, D. Wilson, T. (2011) Treatment of volcanic ash-contaminated surface waters through the optimisation of physical and chemical processes. GNS Science Report 2011/35, 34p.

White, W.H. (1990) The components of atmospheric light extinction: a survey of ground-level budgets. Atmospheric Environment, 24A, pp.2673-2679.

WHO (2013) Review of evidence on health aspects of air pollution – REVIHAAP project: final technical report. World Health Organisation European Centre for Environment and Health, Bonn.

Wilcox, R.E. (1959) Some Effects of Recent Volcanic Ash Falls With Especial Reference to Alaska. Geological Survey Bulletin, 1028-N.

Wilson, G. Wilson, T.M. Deligne, N.I. Cole, J.W. (2014) Volcanic hazard to critical infrastructure: a review. Journal of Volcanology and Geothermal Research, 286, pp.148-182.

Wilson, L. (1976) Explosive volcanic eruptions III. Plinian eruption columns. Geophysical Journal of the Royal Astronomical Society, 45, pp.543 – 556.

Wilson, L. Huang, T.C. (1979) The influence of shape on the atmospheric settling velocity of volcanic ash particles. Earth and Planetary Science Letters, 44, pp.311-324.

Wilson, T.M. (2008) Unpublished field notes from the Chaitén eruption field visit. University of Canterbury, Christchurch, New Zealand.

Wilson, T.M. (2009) Unpublished field notes from the Hudson eruption field visit. University of Canterbury, Christchurch, New Zealand.

Wilson, T.M. Stewart, C. Cole, J.W. Dewar, D.J. Johnston, D.M. Cronin, S.J. (2009) The 1991 eruption of Volcan Hudson, Chile: impacts on agriculture and rural communities and long-term recovery. GNS Science Report 2009/66, 99p.

Wilson, T.M. Cole, J.W. Stewart, C. Cronin, S.J. Johnston, D.M. (2011) Ash storms: impacts of wind-remobilised volcanic ash on rural communities and agriculture following the 1991 Hudson eruption, southern Patagonia, Chile. Bulletin of Volcanology, 73, pp.223-239.

Wilson, T.M. Stewart, C. Sword-Daniels, V. Leonard, G.S. Johnston, D.M. Cole, J.W. Wardman, J. Wilson, G. Barnard, S.T. (2012a) Volcanic ash impacts on critical infrastructure. Physics and Chemistry of the Earth, 45-46, pp.5-23.

Wilson, T. Cole, J. Johnston, D. Cronin, S. Stewart, C. Dantas, A. (2012b) Short- and long-term evacuation of people and livestock during a volcanic crisis: lessons from the 1991 eruption of Volcan Hudson, Chile. Journal of Applied Volcanology, 1:2.

Wilson, T. Stewart, C. Bickerton, H. Baxter, P. Outes, V. Villarosa, G. Rovere, E. (2013) Impacts of the June 2011 Puyehue-Cordon Caulle volcanic complex eruption on urban infrastructure, agriculture and public health. GNS Science Report 2012/20, 88p.

Witham, C. Hort, M. Potts, R. Servranckx, R. Husson, P. Bonnardot, F. (2007) Comparison of VAAC atmospheric dispersion models using the 1 November 2004 Grimsvotn eruption. Meteorological Applications, 14, pp.27-38.

Yanagi, T. Okada, H. Ohta, K. (1992) Unzen volcano, the 1990-1992 eruption. The Nishinippon and Kyushu University Press, Fukuoka, 137p.

6. IMPROVING VOLCANIC ASH FRAGILITY FUNCTIONS THROUGH LABORATORY STUDIES: EXAMPLE OF SURFACE TRANSPORTATION NETWORKS

Daniel M Blake[1], Natalia I Deligne[2], Thomas M Wilson[1] Grant Wilson[1,3]

[1] Department of Geological Sciences, University of Canterbury, Private Bag 4800, Christchurch, New Zealand.

[2] GNS Science, PO Box 30-368, Lower Hutt 5040, New Zealand.

[3] State Emergency Management Committee Secretariat, 20 Southport Street, West Leederville, WA, Australia.

Journal: Journal of Applied Volcanology

Received: 23 June 2016

Current Status: In Review

6.1 Abstract

Surface transportation networks are a frequently affected critical infrastructure following volcanic eruptions. Disruption to surface transportation from volcanic ash is often complex with the severity of impacts influenced by a vast array of parameters including, among others, ash properties such as particle size and deposit thickness, meteorological conditions, pavement characteristics, and mitigation actions. Fragility functions are used in volcanic risk assessments to express the probability of impact (in the form of damage or functional loss) given a range of hazard intensities. Most existing fragility functions for volcanic ash adopt ash thickness as the sole metric to assess impact, forming the basis of thresholds for functional loss. However, the selection of appropriate hazard intensity metrics has been highlighted as a crucial factor for fragility function development and recent empirical evidence suggests that ash thickness is not always the most appropriate metric to consider. To refine existing thresholds of functional loss for ash thickness, we apply results from a series of recent laboratory experiments, which investigate the impacts of volcanic ash on surface transportation (i.e. road, rail, maritime and airport). We also establish new fragility thresholds and functions, which adopt ash-settling rate as a second core hazard intensity metric. The relative importance of alternative hazard intensity metrics to surface transportation disruption is assessed with a suggested approach to account for these in existing fragility functions. Our work demonstrates the importance of considering ash-settling rate, in addition to ash thickness, as critical measures of hazard intensity for surface transportation, but highlights that other metrics, especially particle size, are also important for transportation. Future datasets, obtained from both post-eruption field studies and additional laboratory experimentation, will provide fresh opportunities to further refine fragility functions. Our findings also justify the need for rapid and active monitoring and modelling of various ash characteristics (i.e. not ash thickness alone) during volcanic eruptions, particularly as potential disruption to surface transportation can occur with only ~0.1 mm of ash accumulation.

6.2 Introduction

Surface transportation including road, rail and maritime networks (see Table 6.1 for terminology) is critical for society, particularly in urban environments with dense populations. Disruption to surface transportation can affect commuter travel, access for emergency services, and the distribution and provision of goods and services, and may result in cascading consequences for interdependent sectors (e.g. electricity systems, water and fuel supplies, tourism) and the economy. Damage and loss of function to surface transportation during historical volcanic eruptions worldwide has been qualitatively and semi-quantitatively well recorded for roads and airports (e.g. Blong 1984, Nairn 2002, Barnard 2009, Guffanti et al. 2009, Wilson et al. 2014). Until recently however, quantitative empirical data sourced from historical eruptions or controlled laboratory experimentation has been lacking, meaning that there have been limited hybrid datasets to provide robust relationships between hazard intensity and impact (damage and disruption) (Wilson et al. in review – Appendix D).

Table 6.1 Definitions and context of key terminology used within this paper.

Term	Definition	Paper specifics	References
Airport	Surface transportation site consisting of airfield and facilities used to service aircraft.	Surface and near-surface (<10 m above ground) environmental conditions at airfields are considered when referring to airports.	
Exposure	People, property, systems, or other elements present in hazard zones that are thereby subject to potential losses.		UNISDR 2009, Craig et al. 2016a.
Fragility function	Probabilistic vulnerability models that describe the probability that a damage or functional state will be reached or exceeded for a given hazard intensity.	Only fragility functions for volcanic ash are discussed in detail.	Singhal and Kiremidjian 1996, Choi et al. 2004, Rossetto et al. 2013, Tarbotton et al. 2015.
Hazard	A phenomenon that may cause loss of life, injury or other health impacts, property damage, loss of livelihoods and services, social and economic disruption, or environmental damage.	Hazard is referred to in the context of a dangerous phenomenon from volcanoes (i.e. volcanic tephra, pyroclastic density currents, lava flows, lahars).	UNISDR 2009.
Hazard Intensity Metric (HIM)	A measure used to describe the intensity of a volcanic hazard at a particular site, which is the independent variable of vulnerability and fragility functions.	Ash thickness is often used as the HIM for volcanic ash fragility functions. Alternative HIMs are explored here including ash-settling rate and particle size.	Wilson 2015, Wilson et al. in review.
Impact	The effect a hazardous event has on an exposed system. Defined as a function of the hazard, and the vulnerability and exposure of a system (I = H*V*E).	Multiple impact types are inferred when discussing impact.	Jenkins et al. 2014a, Craig et al. 2016a.
Impact State (IS)	States of damage or disruption defined by qualitative impact descriptions.	These are numbered numerically with 0 being "no damage or disruption", and increasing numbers referring to an increasing level of damage or disruption.	Blong 2003, Wilson et al. in review.
Impact type	An individual feature of an infrastructure system that can be affected by the function of hazard, vulnerability and exposure.	Surface transportation impact types include skid resistance reduction, visibility impairment, road marking coverage and engine air inlet filter blockage.	
Maritime	Surface transportation connected with the sea.	Covers trade shipping, recreational boating and ferry services.	
Mitigation	The lessening or limitation of the adverse impacts of hazards and related disasters.		UNISDR 2009.
Rail	Surface transportation on wheeled vehicles running on rails.	Covers electric and diesel modes on conventional tracks.	
Risk	The combination of the probability of an event and its negative consequences.	A volcanic hazard is implied to be the "event".	UNISDR 2009.
Road	Surface transportation on dedicated sealed or unsealed routes.	We generally refer to paved surfaces, particularly asphalt concrete.	
Skid resistance	The force developed when a tyre that is prevented from rotating slides along a pavement surface.	(Often referred to as traction in post-eruption literature.)	Highway research board 1972, Blake et al. in review a.
Surface	Transportation types on land or	Road, rail and maritime	

transportation	water used to convey passengers and/or goods.	transport are covered, as well as transport that occurs on the ground at airports.	
Visual range	The longest distance that a large, black object can be seen against the sky at the horizon with the unaided eye.	Used as a measure of visibility.	Hyslop 2009, Binkowski et al. 2012, Blake et al. in prep.
Vulnerability	The characteristics and circumstances of a community, system or asset that make it susceptible to the damaging effects of a hazard.	Largely transportation systems or assets are referred to.	UNISDR 2009.
Vulnerability function	A correlation of hazard intensity to a component's damage or function loss as a value relative to total impact or as an economic cost.	We generally refer to fragility functions instead, which incorporate probability.	Wilson 2015.

Figure 6.1 summarises recorded impacts, caused by various volcanic hazards with a focus on tephra, following historical eruptions since 1980 for road, rail and airports. Impacts to transportation can be complex, particularly with the potential for multiple volcanic hazards during eruptions and due to different impact states resulting for the different hazards. Furthermore, volcanic ash (i.e. the component of tephra with particle size <2 mm) is often widespread (Blong 1984) and generally has complex interactions with surface transportation. Other volcanic hazards however (shown in the top sections of the charts in Figure 6.1) such as pyroclastic density currents (PDCs) and lava flows, are generally more geographically constrained. Studies since the 1980 Mount St Helens eruption (e.g. Blong 1984, Johnston 1997, Guffanti et al. 2009, Horwell et al. 2010, Wilson et al. 2011, Dunn 2012, Wardman et al. 2012, Wilson et al. 2012, Stewart et al. 2013, Wilson et al. 2014, Blake et al. in review a & b) demonstrate that volcanic ash frequently reduces skid resistance and covers markings on paved surfaces. Reduced visibility caused by airborne ash and the abrasion or cracking of vehicle windscreens are also common, and engine failure may result if vehicle air intake filters are not adequately maintained. All of these impacts can affect transportation functionality, whether it is by reduced vehicle volumes and speed, an increase in accident rates and congestion, or network closures. As such, we focus on the impacts associated with volcanic ash in this paper.

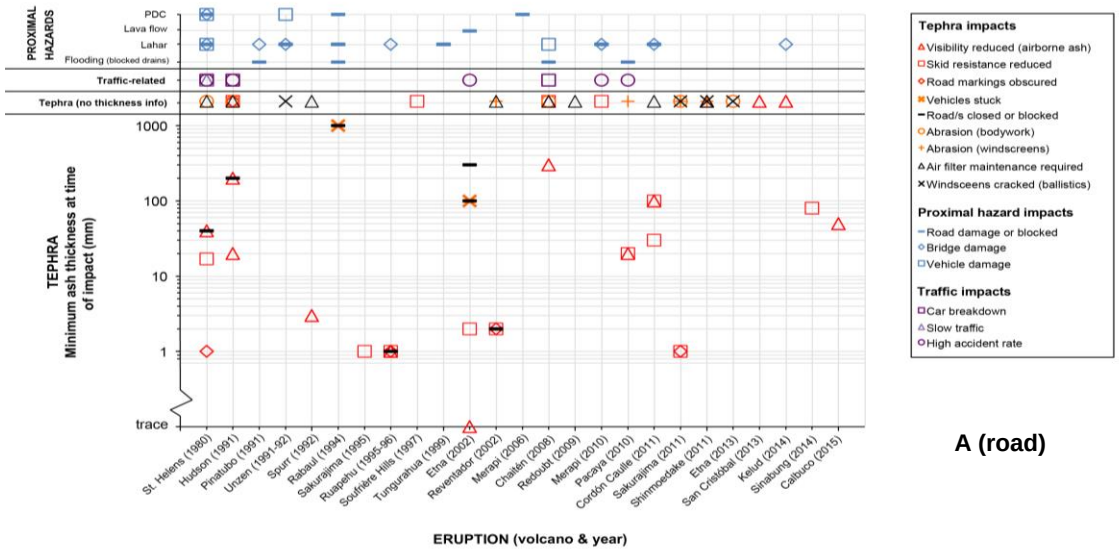

A (road)

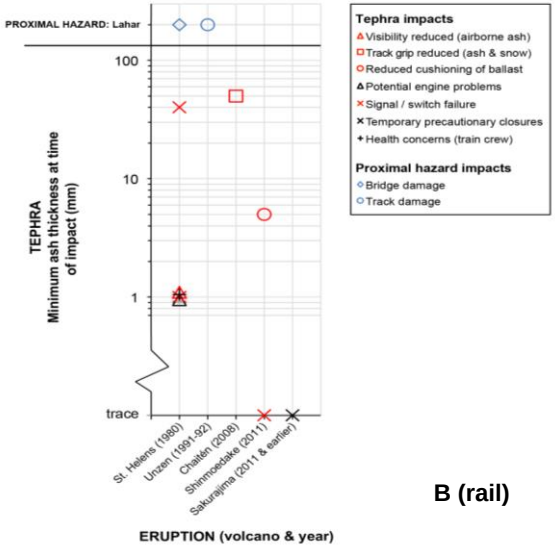

B (rail)

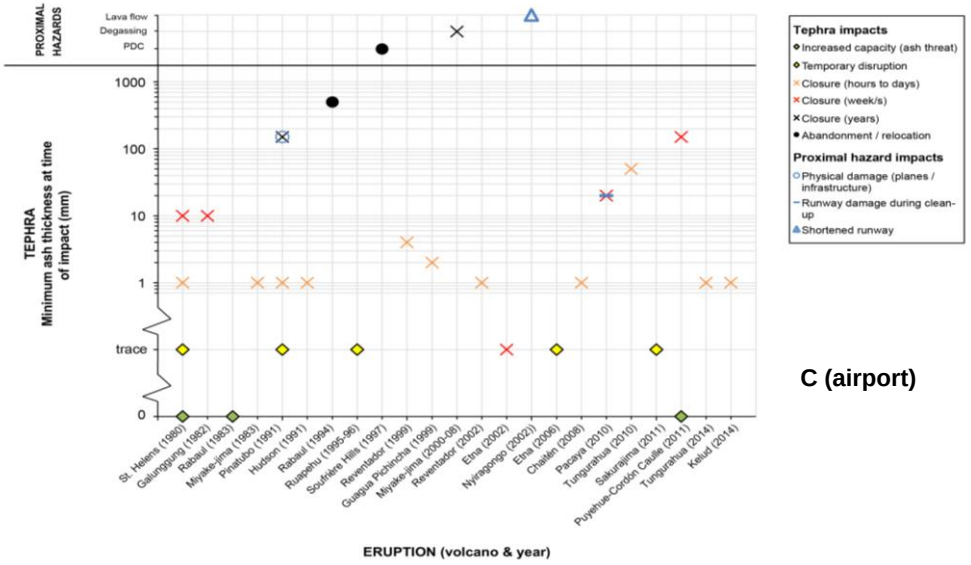

C (airport)

Figure 6.1 Post-1980 reports of (a) road, (b) rail and (c) airport impacts following volcanic eruptions worldwide.

There are few recorded impacts to transportation from tephra before 1980. Note that the only known reported impacts to maritime transportation since 1980 are from pumice rafts causing abrasion to vessels and obstruction to navigation. These are not shown graphically as they cannot be associated with thickness measurements.

There has previously been limited quantitative data for the impact of ash on surface transportation; experimental data is sparse due to the complexities of replicating infrastructural components and volcanic ash properties in laboratories (Jenkins et al. 2014b, Wilson et al. 2014). Where quantitative data exist, impacts on transportation, as well as other critical infrastructure, have generally been related to the thicknesses of ash on the ground. For example, Wilson et al. (in review – Appendix D) use the ash thickness variable (defined as a *Hazard Intensity Metric* (HIM) – Table 6.1) to produce a series of volcanic ash fragility functions for different infrastructure types. Although adopting ash thickness as a HIM has distinct advantages, particularly in that it is a frequently modelled and often relatively readily measured variable following eruptions, it is not always appropriate to consider this metric alone. Characteristics such as ash particle size, ash type, the quantity of soluble components, wetness and airborne concentration or ash-settling rate may have large effects on overall impact intensity and subsequent loss of functionality in some cases. Recent work by Blake et al. (in review a, b & c) has focused on investigating common surface transportation impact types for volcanic ash under controlled laboratory conditions through a series of targeted experiments. New quantitative data available from these studies enables analysis of HIM importance and appropriateness, the refinement of thresholds for functional loss (termed *Impact State* (IS)), and opportunities to improve fragility and vulnerability functions. Such approaches, whereby the vulnerability of infrastructure is assessed using laboratory studies to supplement field-based empirical observations, has been proven in other disciplines including earthquake engineering and for structural loading in tsunami (e.g. Rossetto et al. 2013, Nanayakkara and Dias 2016).

In this paper, we summarise existing IS thresholds for surface transportation from previous, largely qualitative, post-eruption literature, and using ash thickness on the ground as the HIM. Next we adopt the empirical results from Blake et al's (in review a, b & c) (see Table 6.2 for key findings summary) suite of targeted laboratory experiments to refine these established thresholds for thickness, and to develop new IS options for visibility impairment based on ash-settling rate as the HIM. The importance of additional HIMs (such as ash particle size and colour) as measures of functional loss for specific impact types is investigated through relative comparisons to one another. This allows us to propose a credible strategy to enhance fragility functions, by means of incorporating related uncertainty. We only consider discrete and direct ash fall events and not effects that may occur from remobilised ash. Our focus is on road disruption as most garnered data is directly related to road infrastructure. However, disruption to airports and rail and maritime transportation are also discussed, particularly as recent empirical studies of visibility reduction apply to all surface transportation modes.

Table 6.2 Summary of key findings from recent laboratory experiments to investigate impacts of volcanic ash on surface transportation.

Manuscript title	Key findings	Reference
Impact of volcanic ash on road and airfield surface skid resistance	Especially reduced skid resistance caused by: • Thin (~1 mm thick) coarse-grained ash (on road asphalt) • Thicker (~5 mm thick) hard ash • Ash with high degree of soluble components • Line-painted surfaces covered by thin layers of ash.	Blake et al. (in review a – Chapter 3)
Road marking coverage by volcanic ash: an experimental approach	• 0.1 - 2.5 mm ash thickness obscures road markings • Road markings more easily hidden by fine-grained, light-coloured ash • Multiple road marking paint layers and paint containing retroreflective glass beads makes markings more difficult to distinguish • Ash initially accumulates in ashphalt aggregate voids when coarse.	Blake et al. (in review b – Chapter 4)
Visibility in airborne volcanic ash: considerations for surface transport using a laboratory-based method	• ~10 g m^{-2} h^{-1} settling rate enough to disrupt transport on roads • Fine-grained ash causes lower visual ranges than coarse-grained • Lower visual ranges when ash more irregular in shape and light-coloured • Rail 'more resilient' than road due to automated systems and fixed paths • Maritime transport heavily influenced by vessel type and local policies • ~4,000 g m-2 h-1 would make most travel very difficult • Airport closure likely for relatively low ash-settling rates.	Blake et al. (in review c – Chapter 5)

6.3 Background: Quantitative Volcanic Impact Assessments

Risk assessments may incorporate vulnerability functions to describe the likelihood that infrastructure / an asset will sustain varying degrees of loss over a range of hazard intensities (Rosetto et al. 2013). The ‘loss’ may be expressed as economic cost, damage (e.g. physical damage of a sealed road surface from ballistics) and/or functionality (e.g. reduced speeds on roads from volcanic ash). However, vulnerability functions are less common in volcanic risk assessments than they are in risk assessments for many other disciplines such as seismic engineering due to the variety of volcanic hazards and associated complexities (Jenkins et al. 2014b).

Sometimes, stories and qualitative data obtained following eruptions are sufficient to establish and communicate necessary information relating to expected impacts during future events. For example, exclusion zones may be implemented in the immediate vicinity of the vent due to knowledge about the high likelihood of severe damage from proximal hazards such as pyroclastic density currents (PDCs) and lahars, and advice can be issued to avoid travel in relatively short-lived and localised ashfall events until ash has been cleared. Residents often heed this kind of advice due to health concerns

(Stewart et al. 2013) and to avoid potential damage to their vehicles (e.g. Blake et al. 2015). However, the volcanic ash hazard can have complex impacts on infrastructure networks causing widespread disruption (Johnston and Daly 1997), potentially affecting thousands of kilometres of surface transportation routes. Loss of functionality can also be prolonged due to on-going volcanic activity and the remobilisation, re-suspension and secondary deposition of ash (sometimes for months to years after an eruption has ceased) by wind, fluvial processes, and/or anthropogenic disturbance. As such, it is beneficial to establish thresholds from semi-quantitative and/or quantitative data (e.g. ash thickness measurements) to indicate when specific impact types (e.g. road marking coverage or visibility impairment), and of what severity, occur. These impact thresholds can, in turn, inform damage ratios which express the economic cost required to restore infrastructure (i.e. absolute damage) by indicating the damaged proportion of the infrastructure (i.e. relative loss) (Reese and Ramsay 2010, Tarbotton et al. 2015). Impact thresholds and damage ratios can be adopted by emergency management officials and in transportation maintenance guidelines such as for informing when to commence road sweeping or implement road closures following volcanic ashfall (Hayes et al. 2015). Sometimes however, a more gradational approach to assess the vulnerability of infrastructure to volcanic ash is required and fragility functions can be used in such situations.

Fragility functions are probabilistic vulnerability models that describe the probability that a damage or functional state will be reached or exceeded for a given hazard intensity (Singhal and Kiremidjian 1996, Choi et al. 2004, Rossetto et al. 2013, Tarbotton et al. 2015). They allow the quantification of risk and provide a basis for cost-benefit analysis of mitigation strategies (Jenkins et al. 2014b, Wilson et al. 2014). To date, most volcanic fragility functions have focused on damage, particularly the physical damage to buildings and roofs. However, the functionality of infrastructure may be as, if not more, important than damage in some cases. The loss of infrastructure functionality can have potentially large implications for governments and local authorities (e.g. deciding whether to shut down parts of a network) and cause substantial, sometimes unexpected, effects on end-users of critical infrastructure such as drivers and residents through a reduced 'level of service'. It is important to note that there are often many impact types, along with factors such as infrastructure characteristics and decision-making by authorities, which influence whether networks remain open. For example, in New Zealand a main state highway was closed following <3 mm of ash accumulation from the 2012 Tongariro eruption (Jolly et al. 2014, Leonard et al. 2014), but in Argentina after the 2011 Cordón Caulle eruption, many key roads remained open despite receiving up to 50 mm of ash (Craig et al. 2016b). Such differences are likely due to duration of disruption, threat of future ashfall, criticality of the road, previous experiences with volcanic ash and different tolerance levels in different regions (Craig et al. 2016b).

It is difficult to incorporate all factors which contribute to surface transportation closure (Table 6.3) into volcanic fragility functions. However, these variations in damage and disruption can be accounted for by introducing estimates of uncertainty within fragility functions. Uncertainties include aleatory uncertainties such as natural variations between volcanic eruptions and infrastructure response, and epistemic uncertainties such as *those associated with limited data or* choosing appropriate HIMs and

ISs (Rossetto et al. 2014, Wilson et al. in review – Appendix D). These uncertainties are outlined more fully by Wilson et al. (in review – Appendix D). Sometimes, HIMs cannot be measured in the field in real time (Jenkins et al. 2013, Wilson et al. in review – Appendix D); for example, it may be dangerous to measure ash characteristics due to the ash or other volcanic hazards potentially impacting health. Laboratory experimentation can be used to reduce epistemic uncertainty through the provision of larger impact data sets. Additionally, the controlled nature of laboratory experimentation means that particular conditions can be assessed, and uncertainty can often be reduced in this respect as well. However, the introduction of new data that differs from previous data may reflect either aleatory or epistemic uncertainty. As was conducted by Wilson et al. (in review – Appendix D), where possible, we account for uncertainties by calculating the probability that the surface transportation mode could be in each IS at each HIM value. Binning the HIM values and adopting the median HIMs on each chart accounts for the variation in values (Wilson et al. in review – Appendix D). It is important that uncertainties are subsequently transferred across to plans and strategies that utilise fragility functions, ideally using probabilistic techniques to ensure that different outcomes are considered (Jenkins et al. 2014b). However, as new qualitative field data and quantitative data from further laboratory experiments becomes available, existing datasets can be reviewed and fragility functions adjusted accordingly, thus reducing overall uncertainty.

Table 6.3 Factors that can contribute to surface transportation closure during ashfall. This excludes interdependencies from impacts to other infrastructure, as it is difficult to consider all factors when producing fragility functions.

			Details for surface transportation mode			
			Road	**Rail**	**Airport**	**Maritime**
Factors that contribute to closure	**Hazard**	**Ash characteristics**	Thickness, density on ground, settling rate / airborne concentration, particle size, shape / irregularity, colour, wetness, soluble components, hardness, friability.			
		Meteorological conditions	Precipitation (rain, snow, hail, sleet), humidity, temperature, fog, ice, wind speed and direction.			
	Asset	**Static infrastructure type and condition**	Priority of infrastructure, requirement for emergency operations (e.g. evacuation, transport of goods), users, capacity, critical infrastructure interdependencies.			
			Sealed or unsealed surfaces and properties, slope of road, road marking properties, drainage.	Track and ballast properties, overhead line and pylon properties (if electric), gradient, station facilities, track-locomotive communications, collision avoidance systems.	Sealed or unsealed surfaces and properties, length of runway/s, terminal facilities, landing system technology.	Port facilities and technology.
		Mobile infrastructure type and condition	Fuel supply, extent of autonomous operation, requirement for emergency operations (e.g. evacuation, transport of goods).			
			Petroleum or electric, drive of vehicles (e.g. four-wheel drive, rear wheel drive), tyres, weight, power and torque, ground clearance, differential, traction control, transmission.	Electric or diesel locomotives and interchangability, locomotive-track communications, collision avoidance systems.	Aircraft type (e.g. turboprop, turbine engine, helicopter), on-board technology (e.g. volcanic ash avoidance systems).	Vessel type and method of mobility (e.g. cargo ship, ferry, yacht), size and weight, on-board technology (e.g. GPS and automatic identification systems).
	Impact	**Impact type**	Visibility impairment, signage and lighting covered, air filter blockage, engine failure due to ash ingestion, abrasion (bodywork and windscreens), cracked windscreens, health concerns.			
			Skid resistance reduction, road marking coverage, vehicles stuck, traffic light and variable message sign failures.	Track grip reduced, ballast contamination (potential for reduced cushioning), signal/switch failure, trains stuck.	Skid resistance reduction, light and airfield marking coverage, airspace closure.	Pumice raft obstruction to navigation, sedimentation in channels, accumulation of tephra on vessels.

	Preparedness / Mitigation	**Population attributes**	Frequency of ashfall events in area, prior vehicle operation in environments containing ash, knowledge sharing and traditions.			
		Organisational involvement	Infrastructure providers, local authorities, regional government, emergency management, national government, scientific research and monitoring organisations, goods and service logistic companies, other businesses, aid agencies, cleaning and disposal organisations.			
			Motoring associations, residents.	Rail companies.	Airport operators, Civil Aviation Authority, Volcanic Ash Advisory Centres.	Maritime bodies, harbourmasters.
		Physical measures	Cleaning of static and mobile infrastructure, drainage system changes, air filter maintenance and replacement, light and signage alterations, diversions.			
			Bridge strengthening, road surface and marking alterations, vehicle alterations, driving advice.	Bridge strengthening, ballast and track alterations, locomotive alterations, locomotive driver training changes.	Airfield surface and marking alterations, terminal facility changes, aircraft adaptations, pilot training changes.	Port facility changes, vessel adaptations, captain / helmsman training changes.

Selection of appropriate HIMs and establishment of representative IS thresholds are crucial to produce robust fragility functions (Rossetto et al. 2013). Wilson et al. (2014) and Wilson et al. (in review – Appendix D) highlight that fragility functions in volcanology are poorly developed compared to those from other natural hazard disciplines. They also outline that the range of intrinsic volcanic hazard properties, such as the particle size of ash, can cause different impacts, leading to difficulties in deriving functions. Additionally, much of the data that has informed volcanic fragility functions is qualitative or semi-quantitative with limited quantitative empirical, analytical or theoretical data from field studies or laboratory experiments.

To date, the most common HIM for volcanic ash fragility functions to assess surface transportation disruption is the thickness of ash on the ground (Wilson et al. 2014), largely due to its extensive use in existing impact datasets and applicability to hazard model outputs at the time. Previous IS thresholds that have been defined using thickness as the HIM (Wilson et al. in review - Appendix D) are shown in our results (Section 6.5.1) for comparative purposes. Of particular note is that IS_1 (reduced visibility, loss of traction, covering of road markings and/or road closures) was previously identified as occurring with thicknesses of ~1 mm or more, due to reduced traction (technically known as *skid resistance*) and impaired visibility disrupting most transportation types. Impacts to maritime transportation have not been considered in detail in relation to thickness, as most ash types (with the exception on pumiceous material, which can form pumice rafts) do not accumulate, or are readily dispersed, on water and are thus difficult to monitor. The majority of data used to inform previous ISs was from qualitative post-eruption impact assessments and media reports. Observations from Barnard (2009), who conducted a number of semi-quantitative field experiments on Mt Etna, Italy, also informed ISs for road transportation where thicknesses exceed 50 mm.

Blake et al. (in review a, b & c) conducted targeted experiments under controlled laboratory conditions to investigate the most frequent surface transportation impact types identified from post-eruption assessments: skid resistance reduction, visibility impairment and road marking coverage (see Table 6.2 for key findings summary). The studies assessed the effect of key HIMs (Table 6.4) on functionality and we refer the reader to each of the corresponding papers for detailed information on the methodologies adopted for the experiments including different approaches used to measure HIMs.

Table 6.4 Summary of hazard intensity metrics considered during experimental work ([1]Blake et al. (in review a), [2]Blake et al. (in review b), [3]Blake et al. (in review c)).

Hazard intensity metric	Skid resistance reduction[1]	Road marking coverage[2]	Visibility impairment[3]
Thickness (mm) – related to area density / loading (kg/m2) in some cases	✓	✓	
Ash-settling rate (g m^{-2} h^{-1})			✓
Particle size (μm)	✓	✓	✓
Colour		✓	✓
Wetness	✓		
Soluble content	✓		
Hardness (proxy: ash type)	✓	✓	✓
Shape (proxy: ash generation method)	✓	✓	✓

The studies by Blake et al. (in review a, b & c) suggest that ash thickness and ash-settling rate are the most critical HIMs for the assessment of surface transportation functionality during initial volcanic ashfall events, particularly as they are two of the most readily measured variables in the field. There would rarely be impacts to transportation when there is no ground accumulation of ash and no suspended ash in the atmosphere, which further emphasises the importance of these two HIMs. However, recent laboratory work has also revealed that alternative HIMs to ash thickness and settling rate (Table 6.4) should not be underestimated.

6.4 Methodology

Figure 6.2 summarises previous and current developments to volcanic ash fragility functions for surface transportation. Most steps in the diagram indicate anticipated improvements to data accuracy. However, as fragility functions are developed, requirements for more impact data are often introduced to test and improve new findings and reduce uncertainty.

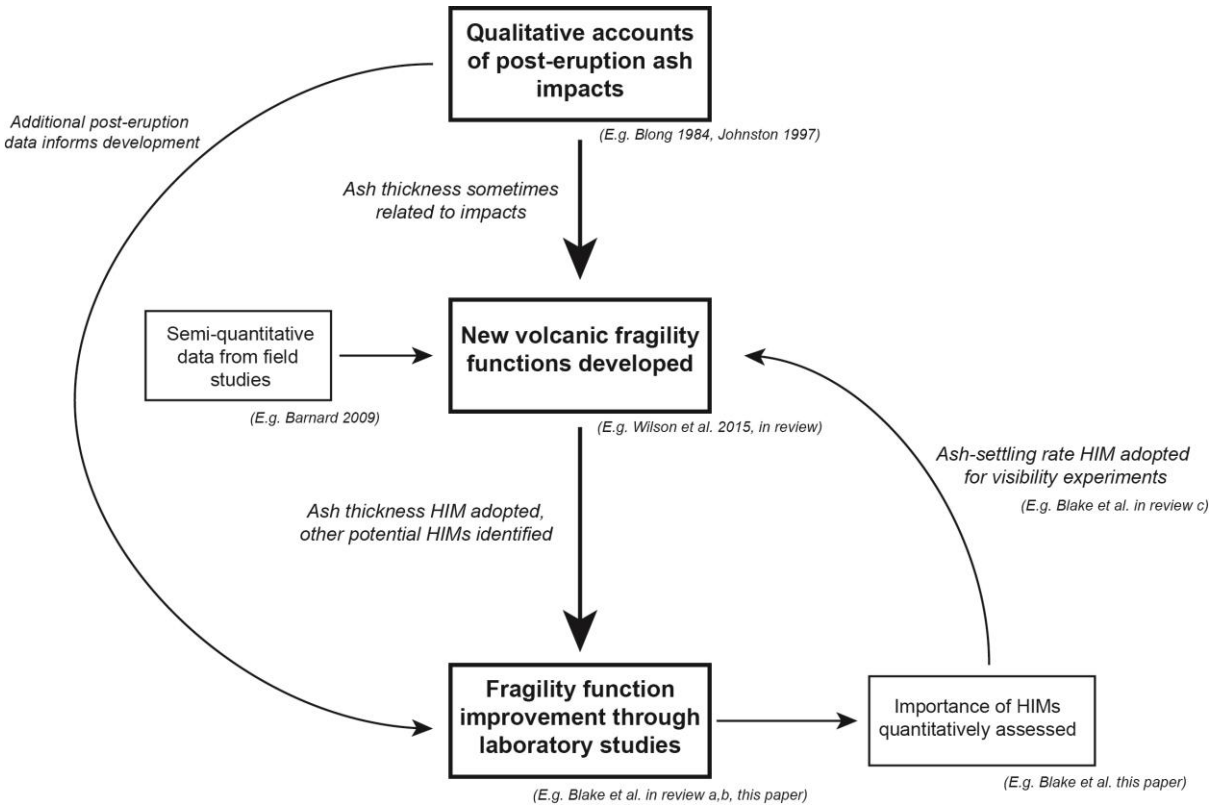

Figure 6.2 Previous and current developments to volcanic ash fragility functions for surface transportation.

6.4.1 Impact state thresholds

Using the key findings of the skid resistance and road marking coverage laboratory studies, we refine the IS thresholds for surface transportation established by Wilson et al. (in review - Appendix D) which adopt ash thickness as the HIM (Figure 6.2). New thresholds are applied directly from laboratory study analysis results but some require rounding to the nearest order of magnitude using expert judgement to account for uncertainties such as those associated with the variation in results between individual tests and lack of extensive datasets in some cases. We remove previously suggested correlations between visibility and ash thickness because, as stated by Blake et al. (in review c), it is "illogical to associate an atmospheric-related impact to a ground-based measurement", especially as we do not consider effects from remobilised ash in this paper. Laboratory work using ash thickness as the core HIM considered paved surfaces on roads and at airports. Railway tracks were not considered in detail, partly because there has been only one recorded instance of track-wheel adhesion loss following ashfall (Figure 6.1b) and the effects were complicated by snowfall at the time. As such, we do not provide any refinements for rail transportation ISs in relation to ash thickness and the previously established thresholds for rail transportation are therefore unchanged by our study. For maritime transportation, a challenge for fragility function development is that due to ash dispersing in water, impact mechanisms from tephra cannot easily be linked to deposition thickness as they can for road, rail and airports. However, as with other forms of transportation, and as occurs in dense fog, it is

likely that navigation by sea can be disrupted or even temporarily halted by visibility impairment during ashfall. Therefore, maritime transportation impacts are segregated from the ash thickness HIM and assessed solely in relation to visibility impairment.

As ash deposit thickness has a debatable impact on visibility impairment, and due to recent developments in both field monitoring equipment, and ash dispersion and fallout models which provide settling-rate outputs (Blake et al. in review c), we consider ash-settling rate as an alternative HIM (Figure 6.2) and propose new IS thresholds. Our settling rate IS thresholds are informed by (a) direct empirical laboratory results, adjusted using expert judgement and rounding, (b) literature for shipping in Auckland's Waitemata Harbour (e.g. Harbourmaster and Maritime New Zealand information for maritime impacts (Auckland Council 2014, MNZ 2015)) and Auckland Airport and CAA guidelines for airport impacts (Auckland Airport 2008, CAA 2008), and (c) expert consultation with critical infrastructure managers (Deligne et al. 2015). We establish IS thresholds for all modes of surface transportation related to visibility impairment. This is achieved by means of comparison with guideline information and impact states expected for corresponding visual ranges in foggy conditions, the data sources of which are discussed in Blake et al. (in review c):

- IS thresholds for roads are largely based on comparisons with empirical studies involving driver simulations in fog.
- Comparisons with operational procedures for fog in Auckland are used to establish thresholds for airports and maritime transportation, and thus these thresholds should be treated as more area-dependent than for road.
- IS thresholds for rail are the most subjective of the four transportation modes: we implement higher threshold values than for road due to the often automated controls for the spacing of locomotives along the network and additional technological safety systems which visibility impairment does not affect.

6.4.2 Hazard intensity metric analysis

We conduct a comparative analysis of additional HIMs by assessing their relative importance to surface transportation disruption. Without extensive datasets for all HIMs, this is achieved by applying simple rank values to each HIM for the core HIMs of ash settling rate and at different ash thicknesses. HIMs are ordered by relative importance to one another and given a rank value of between 1 and 6. Although somewhat subjective, the lower the rank value applied, the greater the influence of that HIM on surface transportation disruption. HIMs of similar importance are given the same rank value.

6.4.3 Fragility function development

We use procedures described by Wilson et al. (in review - Appendix D) for volcanic fragility function development, the basic methodological principles of which are summarised as follows:

- Assign each data point a HIM value and IS value;

- Order data set by increasing HIM value;
- Group into HIM bins, such that each bin has approximately the same number of data points;
- Calculate probability of being greater than, or equal to, each IS of interest;
- Obtain discrete HIM values by taking the median of each HIM bin.

New road and airport fragility functions for ash thickness are established through modification of those proposed by Wilson et al. (in review - Appendix D). All points representing median thickness within the HIM bins obtained from post-eruption data are retained as the number of post-eruption records remains unchanged. New points are added to the chart to appropriately display the new findings from IS threshold adjustment following laboratory work, with a focus on improving functions for relatively thin deposits (the focus of laboratory work). More substantial updates are made to airport fragility functions as we also incorporated the duration of airport closure. However, we stress that some points have been corrected using best judgement in order to fit with guidelines outlined by Wilson et al. (in review - Appendix D).

The IS thresholds for ash-settling rate are used to establish separate fragility functions for road, rail and maritime transportation, and at airports. Without reliable field data it is difficult to follow Wilson et al's (in review - Appendix D) methodology for fragility function production, especially to accurately calculate probabilities of ash-settling rate values equalling or exceeding each IS. However, we produce functions using empirical laboratory studies and comparisons to research for fog, to indicate expected impact on visibility and vehicles at near-ground level. This is achieved through adopting the basic principles and rules outlined by Wilson et al. (in review - Appendix D). As we cannot group data into HIM bins and obtain discrete HIM values, specific ash-settling rates are chosen based on key changes in impact states instead. We use best judgement to assign probabilities and these are open to revision in future.

6.4.4 Limitations of methodology

Besides the general limitations outlined by Wilson et al. (in review - Appendix D) for fragility function production, our methodology for fragility function improvement through empirically informed data contains several additional limitations which may also introduce uncertainty:

- The laboratory experiments used to inform fragility functions were based on the assessment of key impact types previously identified from post-eruption observations. However, observations of volcanic ash impacts to transportation are relatively limited (at least compared to impacts from other hazards such as earthquake damage to buildings) with an apparent increase in frequency of events after 1980. We suggest that this increase is due to heightened awareness and land-monitoring of volcanic hazards following the 1980 Mount St Helens eruption, and recent increases in the number of motor vehicles and general population growth and infrastructure development in volcanically active areas worldwide (TRB 1996, Woo & Grossi 2009). Additionally, there is a higher frequency of impacts recorded for roads than for other modes of surface transportation, likely due to more road networks in the areas

affected by volcanic activity. Therefore, the relevance of further impact types may be underestimated by our study, and future observations and additional laboratory testing will verify the extent of this.

- The empirical datasets we use are constrained by the equipment and set-ups that were adopted in the laboratory studies. For example, the skid resistance testing used a Pendulum Skid Resistance Tester, which was restricted to investigating small (<10 mm) ash thicknesses (Blake et al. in review a). Furthermore, it was unfeasible to investigate all possible ash characteristics (e.g. every soluble component option, all moisture regimes) during laboratory testing, so our results are limited to those characteristics that we did investigate.
- Laboratory experiments are generally time and resource intensive. As the experiments by Blake et al. (in review a,b,c) were the first to be developed and conducted to specifically assess ash impacts on individual transportation components, the datasets are currently relatively small. The repetition of laboratory experiments will help to reduce uncertainty in the future but our results are limited to those characteristics investigated to date.

6.5 Results and Discussion

6.5.1 Ash thickness fragility function improvements

Figure 6.3 shows IS thresholds for surface transportation, which were defined using ash deposit thickness as the HIM. It includes thresholds for rail that were unmodified from Wilson et al. (in review - Appendix D), and original (grey) and newly revised (red) thresholds for roads and airports; the revised thresholds were informed by key findings from recent laboratory experiments that can be directly related to ash accumulation (i.e. skid resistance reduction and road marking coverage (Blake et al. in review, a, b)), in addition to new post-eruption data where available. Figure 6.3 illustrates that some disruption to roads and airports can occur with an ash thickness of ~0.1 mm, an order of magnitude less than previously suggested by most anecdotal data. Figure 6.3 also suggests that larger thicknesses of ash may not always result in greater disruption. For example, an ash thickness of ~10 mm on roads could potentially lead to less disruption than a thickness of ~5 mm as skid resistance reduction is more likely at 5 mm. Although the impacts of reduced visibility (accounted for separately) may mask such effects overall, we suggest particularly elevated disruption to road transportation from ash thicknesses between ~2.5 and 5.0 mm. At this range, all road markings are covered and especially reduced skid resistance occurs. Although limited, the post-eruption data available (Blake et al. in review a,b,c) indicates that fewer impacts are identified when ash is ~5-20 mm thick, supporting the hypothesis of elevated disruption regions on the thickness scale. Fluctuating intensities of road transportation disruption with thickness have not been identified in the past, highlighting the importance of laboratory testing and the complexities that can be involved in determining accurate IS thresholds.

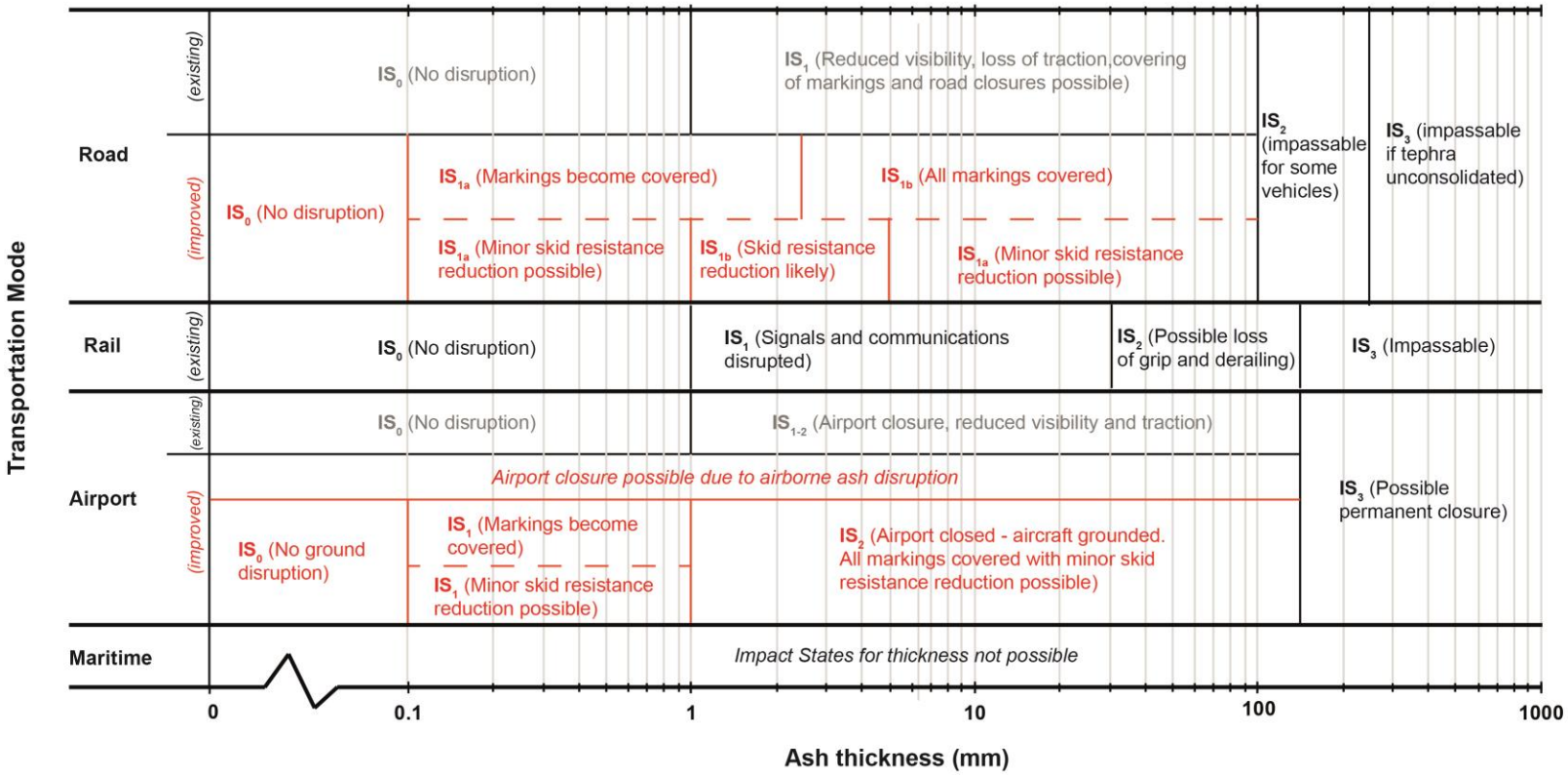

Figure 6.3 Impact states for expected ground-related disruption to transportation as a function of ash thickness. The existing impact states (shown in black) were derived from qualitative post-eruption impact assessments and limited semi-quantitative field studies (adapted from Wilson et al. in review - Appendix D). Impact states that were improved in this study are shown in red.

Figure 6.4 shows corresponding fragility functions for roads, updated from Wilson et al. (in review - Appendix D). Two new points (at 0.1 and 5.0 mm ash thickness) have been added to appropriately account for new findings from laboratory work for IS_1 (i.e. disruption in the form of skid resistance reduction (Blake et al. in review a) and road marking coverage (Blake et al. in review b)). The decrease in function observed for IS_1 when ash thickness exceeds 5.0 mm is due to the potential increase in skid resistance; it is largely informed by recent laboratory findings (which do have limitations – Section 6.4.4) but is somewhat supported by semi-quantitative field observations. A decreasing fragility function breaks one of the core guidelines established by Wilson et al. (in review - Appendix D), which states that "functions should not decrease as the HIM value increases". However, this guideline was established for damage rather than functional loss, and for when there is limited data to base vulnerability estimates on (i.e. not accounting for detailed empirical studies).

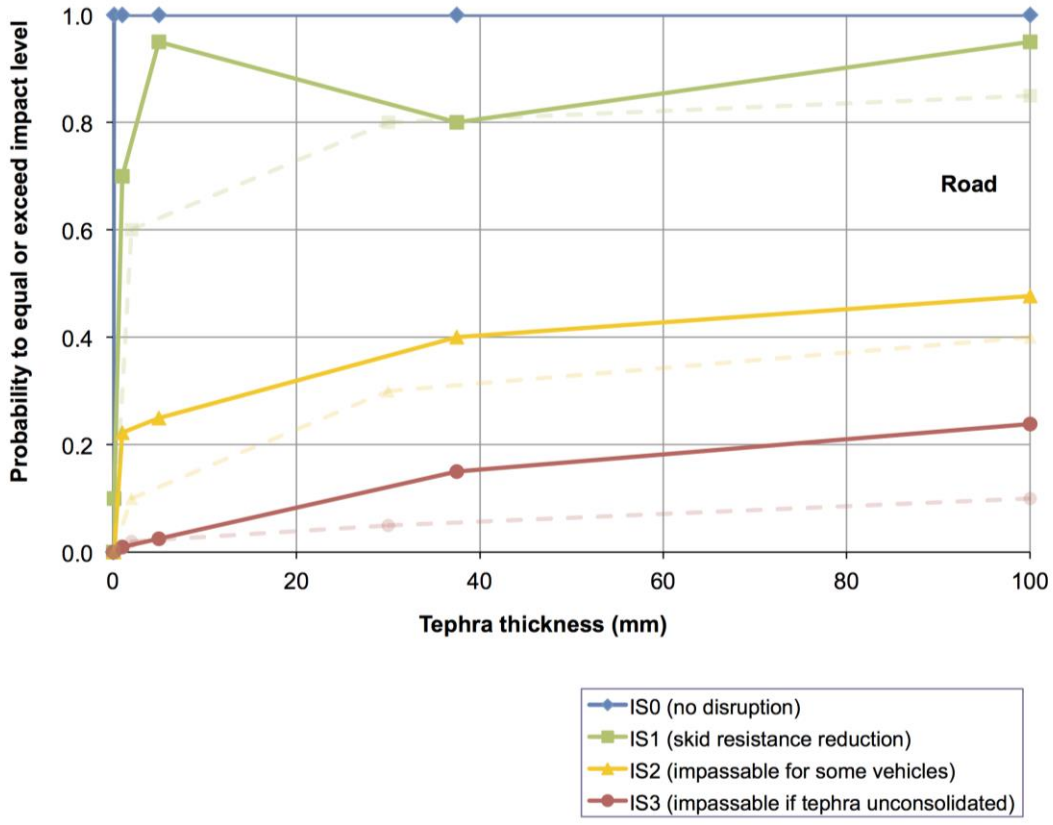

Figure 6.4 Fragility functions for road transportation (solid lines) updated from Wilson et al. in review - Appendix D (dashed lines). These have been updated with empirical data from skid resistance and road marking coverage laboratory experiments.

Airports can be closed due to ash in nearby airspace, without any ground accumulation of ash (Guffanti et al. 2009). Indeed, the International Civil Aviation Organisation (ICAO) advise that “aircraft should avoid volcanic ash encounters” (p.1-1), although “the operator is responsible for the safety of its operations” (p.2-1) and is required to complete a risk assessment as part of its safety management system, and have satisfied the relevant national (or supra-national) CAA before initiating operations into airspace forecast to be, or at airports known to be, contaminated with volcanic ash (ICAO 2012). Aircraft will likely become grounded due to a reduced runway friction coefficient when ash deposits exceed 1 mm (ICAO 2001, Wilson et al. in review - Appendix D). Furthermore, severe deterioration in local visibility can result when engine exhausts from aircraft taxiing, landing and taking off disturb ash on the runway (ICAO 2001).

We assess functionality loss of airfields by applying the key findings from skid resistance and road marking coverage experiments for airfield concrete surfaces covered by ash (Figure 6.1). It is important to consider such impact types, as aircraft operation may be possible when airborne ash concentrations are below aviation authority, and airline and airport guideline values. Although vehicle operation on airfields by ground staff could occur, even when aircraft are grounded, we focus on aircraft operations for the fragility function chart (Figure 6.5). These fragility functions estimate the temporal duration of airport function assuming that the surrounding airspace is open and prior to any clean-up. Some functionality loss of the airport surface is possible between 0.1 and 1.0 mm due to markings becoming covered and reduced skid resistance (Blake et al. in review a,b) before the airport is likely closed if ash accumulates to >1 mm thickness. We display the temporal component for airport closure graphically as separate ISs (Figure 6.5) as such information may be beneficial for end-users of fragility functions.

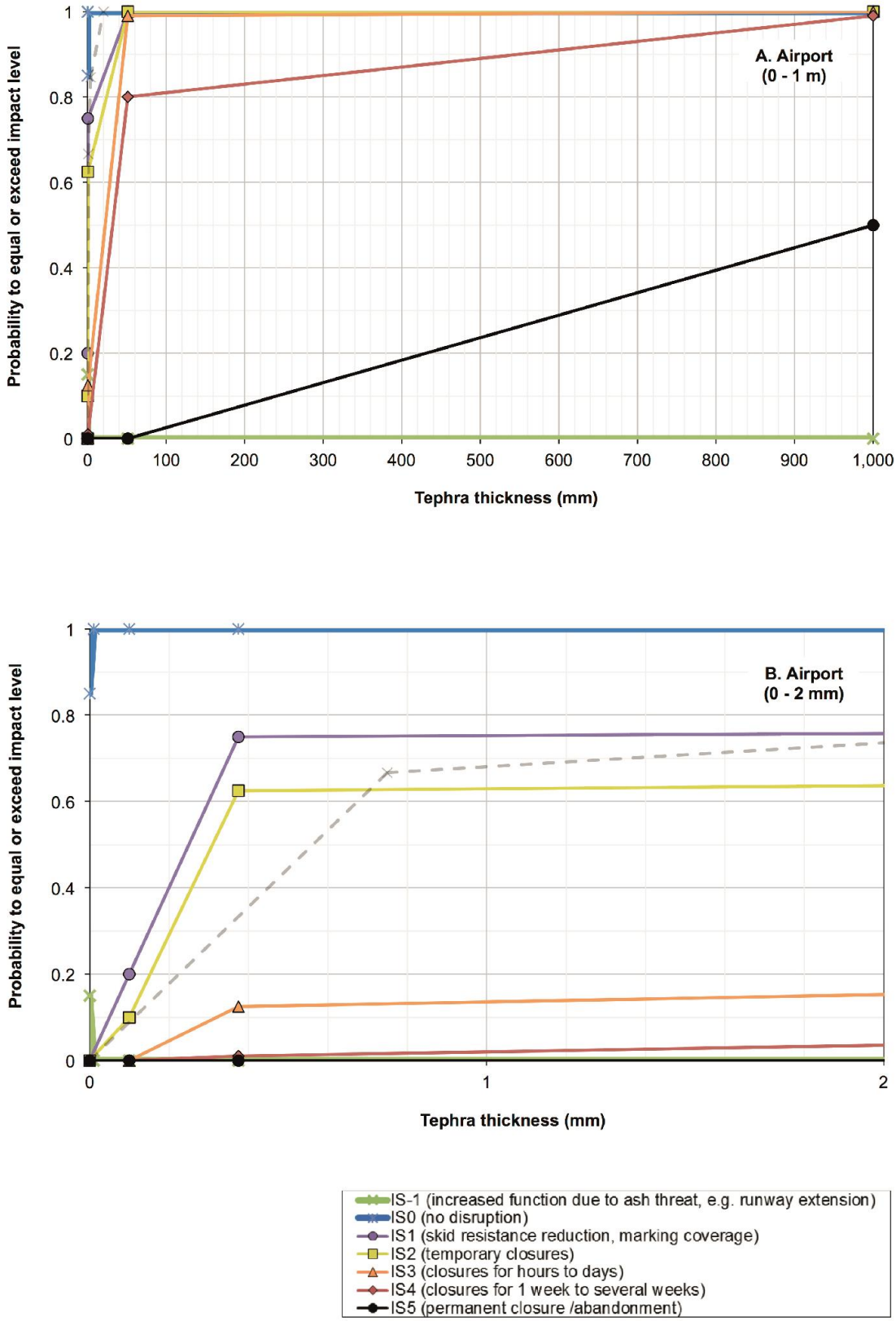

Figure 6.5 New fragility functions for airport surfaces developed from post-eruption and laboratory experimental data. The previous function for "airport closure" developed by Wilson et al. (in review - Appendix D) is shown by the grey dashed lines. Note that some points have been corrected using best judgement in order to fit with guidelines outlined by Wilson et al. (in review - Appendix D).

6.5.2 New ash-settling rate fragility functions

Figure 6.6 shows IS thresholds for visibility with ash-settling rate adopted as the HIM. Forecasts for visibility disruption are particularly useful for areas where there is minimal ash accumulation on the ground (i.e. during initial ashfall events or subsequent events following thorough clean-up), as well as for maritime transportation and where surfaces are wet due to any re-suspension of ash into the atmosphere being minimised by water. Many of the thresholds established in Figure 6.6, and depicted in new fragility function charts in Figure 6.7, are particularly influenced by decisions made by local transportation authorities and we stress that our established thresholds are preliminary and open for improvement. We use best judgement to determine some thresholds. For example, IS1 starts at 10 g m^{-2} h^{-1} for road, but at 20 g m^{-2} h^{-1} for rail, due to the relative resilience of rail to airborne ash, which results from more automated controls and fixed paths of travel (Blake et al. in review c). IS thresholds may require adaptation to be compatible in other areas, especially where infrastructure types and associated technology differ. Thresholds are established for visibility only and do not consider other potential disruption caused by airborne volcanic ash such as ingestion into engines or the abrasion of windscreens.

A literature search revealed no quantitative or semi-quantitative data for visual ranges at specified ash-settling rates following previous eruptions worldwide. Figure 6.7 shows fragility functions for the ash-settling rate HIM, based entirely on empirical laboratory studies and comparisons to research for fog, to indicate expected impact on visibility and vehicles at near-ground level. Further extensive laboratory testing, in addition to syn- and post-eruption field surveys, will help to refine probabilities. Studies of ash remobilisation and re-suspension will likely improve our understanding of potential links between ash thickness and settling rate.

We emphasise that our studies were carried out in the context of transportation infrastructure found in New Zealand (e.g. ash characteristics and pavement properties found in the country) and that fragility functions may vary in different parts of the world. However, we suspect the trends will remain similar.

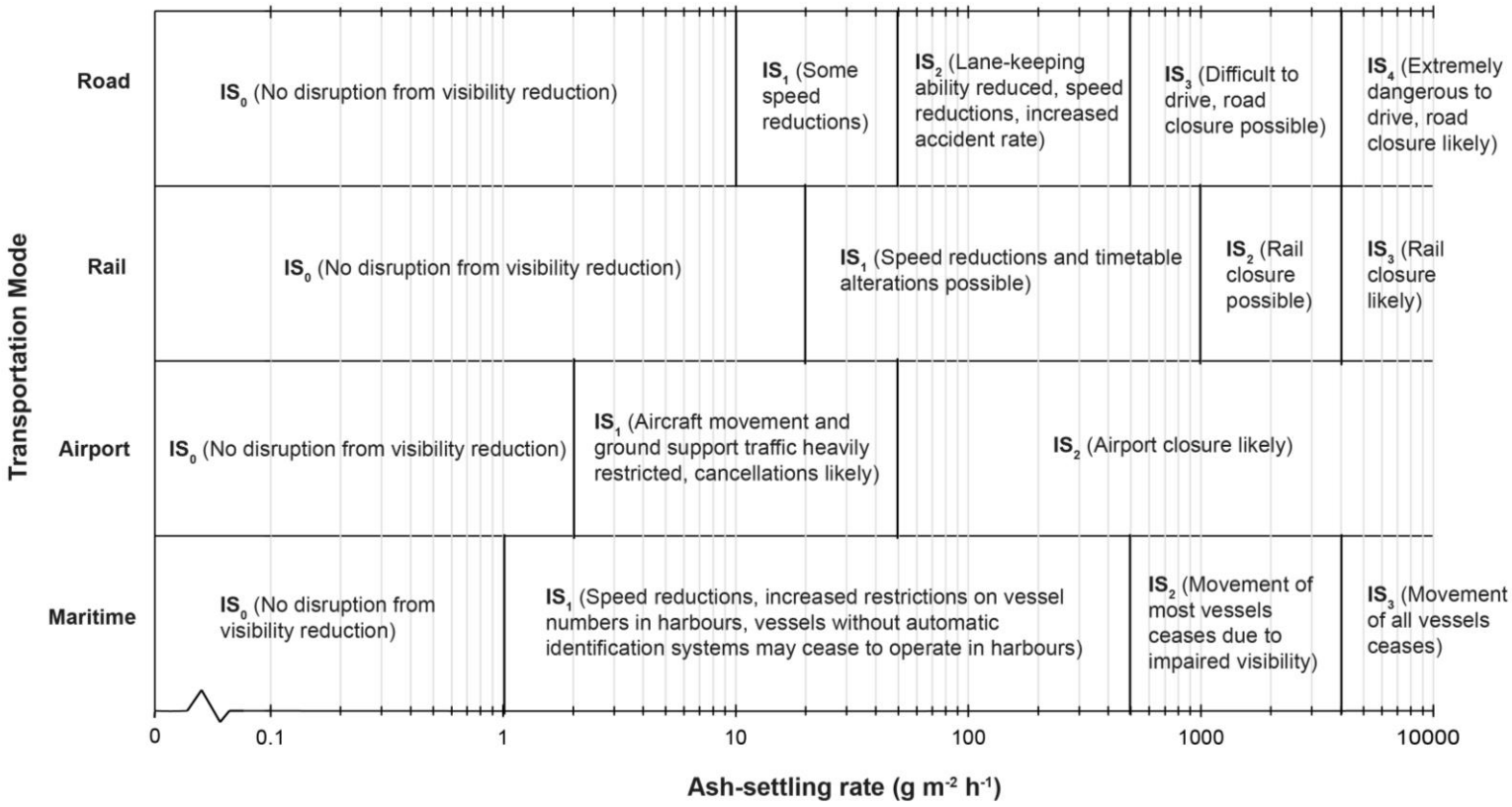

Figure 6.6 Impact states for expected visibility-related disruption to surface transportation as a function of ash-settling rate. These are determined from quantitative laboratory experiments by Blake et al. (in review c), and comparisons to visual range and driver behaviour in fog. Thresholds have been derived in the context of transportation in New Zealand.

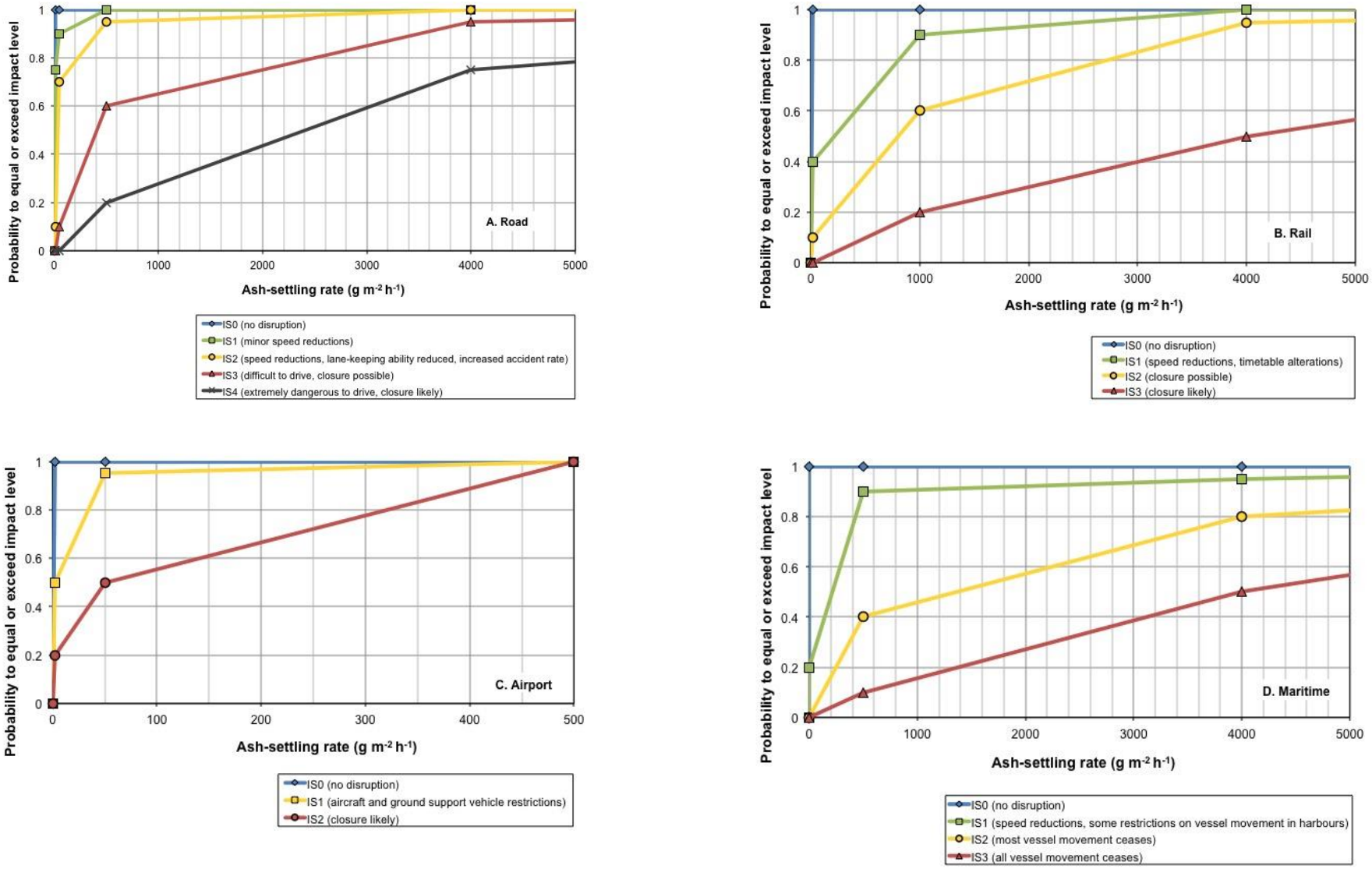

Figure 6.7 Fragility function charts for transportation-visibility impacts, with ash-settling rate as the HIM.

6.5.3 Multiple hazard intensity metrics

Figure 6.8 presents the results of comparative analysis of six additional HIMs identified during laboratory experimentation as having effects on surface skid resistance and road marking coverage. This was achieved by using best judgement considering recent laboratory experiments to apply simple rank values to each HIM. The core HIM of ash thickness was used with the values of alternative HIMs dependent on relative importance to one another. It is clear from Figure 6.8 that as ash increases in thickness on the ground, the effect of different HIMs on surface transportation functionality changes. For example, particle size and colour play an important role below ~1.0 mm thickness due to the effect of fine-grained and light-coloured ash on road marking coverage, but less of a role when ash thickness exceeds ~1.0 mm. However, the wetness of ash is important compared to other HIMs when ash thicknesses are >10 mm because it influences how readily ash binds together, in turn affecting how easily vehicles can drive through thicker deposits.

Arguably even more relevant for fragility functions is the relative importance of additional HIMs for visibility impairment (Figure 6.9). Unlike ash thickness, there is no evidence to suggest that the importance of different HIMs relative to one another changes as settling rate changes. However, results from Blake et al (in review c) indicate that, as for thickness, the effect of additional HIMs has a lesser effect on functionality loss for greater ash-settling rates. This is likely due to the more dominant effect of there simply being more ash particles in the atmosphere. The HIM characteristics responsible for greater disruption are largely the same as for ash thickness (Figure 6.8), with the exception of ash particle shape; irregular-shaped ash particles may lead to greater disruption when airborne due to more light reflectance and subsequently lower visual range, whereas spherical-shaped ash particles can lead to greater disruption when on paved surfaces as a result of lower skid resistance. Particle size is clearly a crucial ash characteristic to consider when assessing surface transportation disruption, especially for <10 mm thicknesses.

Further repeated laboratory experiments to investigate the effect of each ash characteristic on every surface transportation impact type, along with detailed post-eruption field sampling and analysis, and subsequent computational probabilistic modelling will assist to fill this gap in knowledge. In the meantime, and in the absence of extensive datasets, it is difficult to evaluate the precise quantitative effect of alternative HIMs (i.e. those other than ash thickness and settling rate) on surface transportation disruption from volcanic ash and perform meaningful statistical analysis. However, we suggest that the importance of multiple HIMs can be accounted for by considering ‘error boundaries’ that illustrate uncertainty around existing functions for ash thickness and settling rate (Figure 6.10) (although other uncertainties also exist). The conceptual diagram (Figure 6.10) shows that with thicker ash or greater ash-settling rates, alternative HIMs (e.g. particle size, colour, shape) become less important with it being more beneficial to solely consider the core HIMs of ash thickness or ash-settling rate when forecasting impact levels.

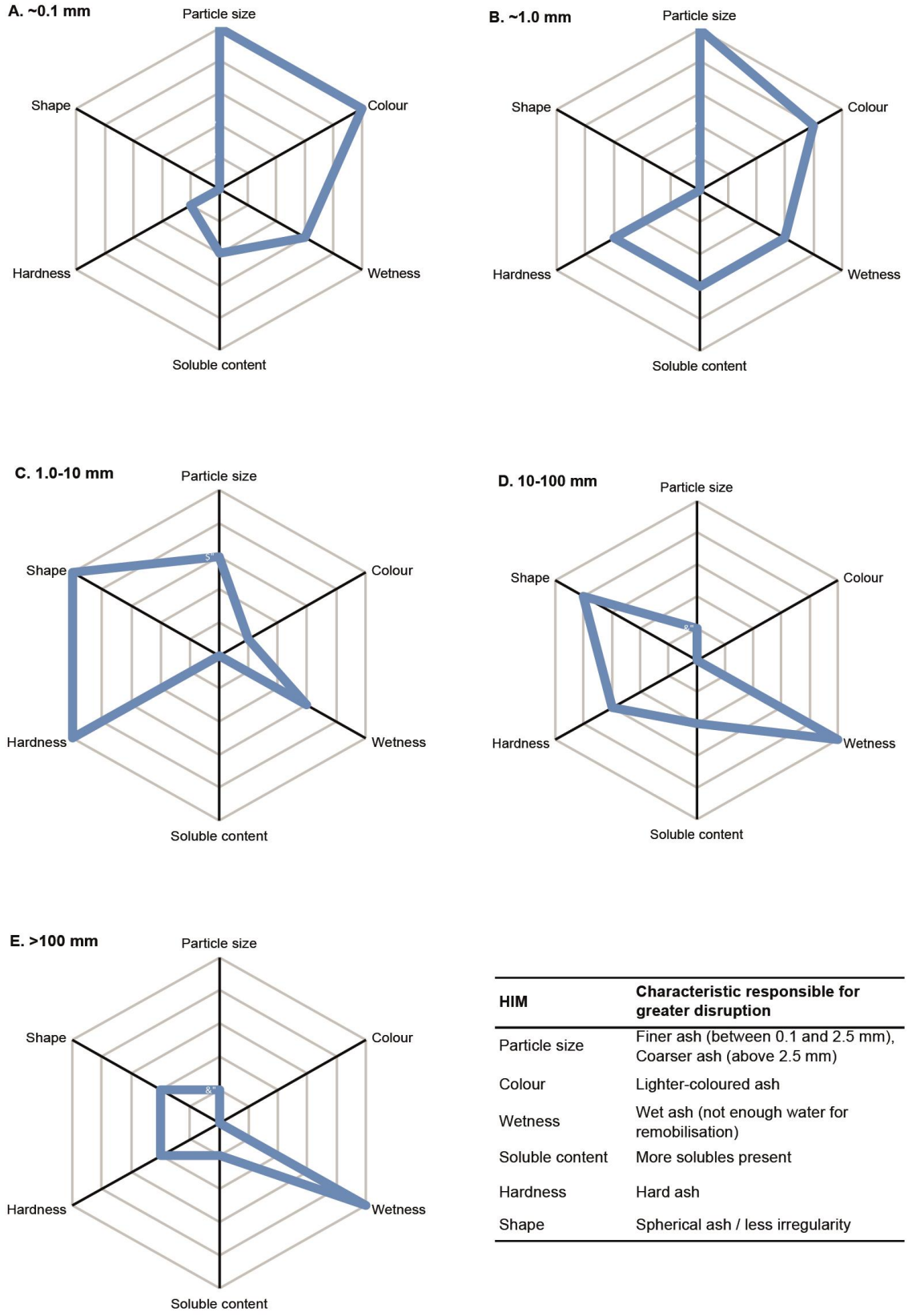

HIM	Characteristic responsible for greater disruption
Particle size	Finer ash (between 0.1 and 2.5 mm), Coarser ash (above 2.5 mm)
Colour	Lighter-coloured ash
Wetness	Wet ash (not enough water for remobilisation)
Soluble content	More solubles present
Hardness	Hard ash
Shape	Spherical ash / less irregularity

Figure 6.8 Relative importance of additional HIMs at key ash thickness intervals (A-E). The charts consider the impact types of skid resistance reduction and road marking coverage in combination. Values towards the outside of the radar charts indicate lower rank values / greater importance for surface transportation disruption. The key shows the particular characteristic of each HIM responsible for greater disruption.

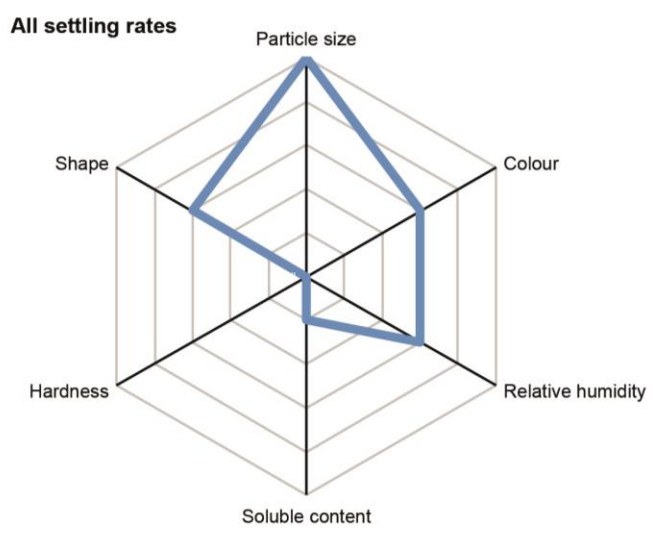

HIM	Characteristic responsible for greater disruption
Particle size	Finer-grained ash
Colour	Lighter-coloured ash
Relative humidity	Greater relative humidity
Soluble content	More solubles present
Hardness	Unknown / no effect
Shape	More irregular / less sphericity

Figure 6.9 Relative importance of additional HIMs for the impact type of visibility impairment. The key shows the characteristic of each HIM responsible for greater disruption to surface transportation. Note that there is no evidence at present to suggest that the importance of HIMs change relative to one another as ash-settling rate changes.

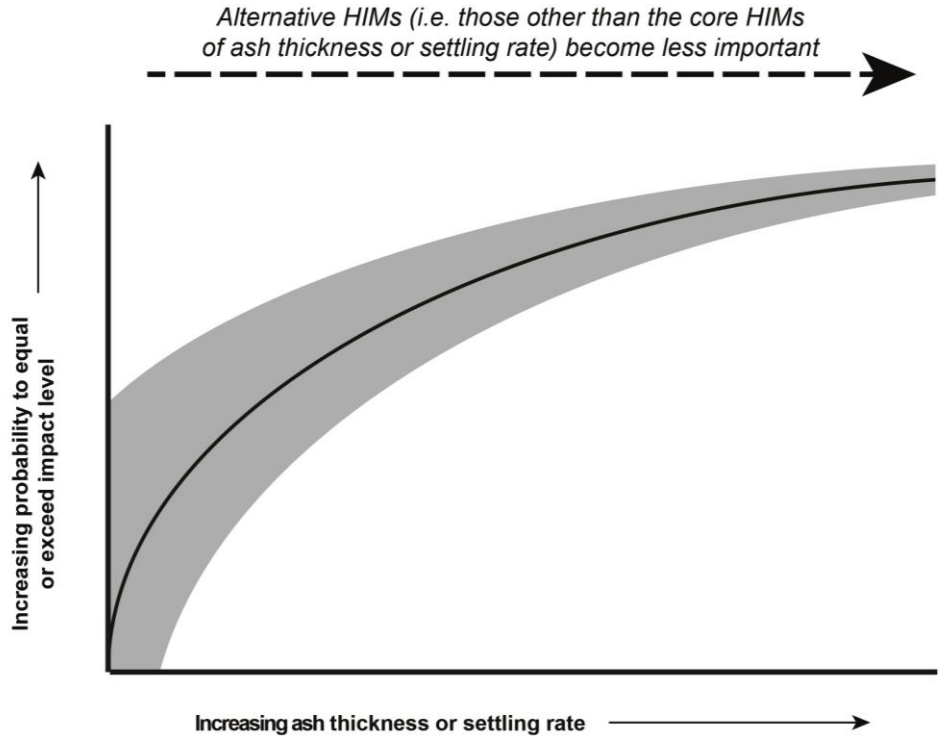

Figure 6.10 Example of fragility function to show the relative importance of 'alternative HIMs' to 'core HIMs'. The importance of 'alternative HIMs' is depicted by the light shading. Used in conjunction with the radar charts in Figure 6.9 (which were derived from laboratory experimentation), probabilities (shown on the y-axis) can be better estimated using such fragility functions. However, we note that the 'error extents' displayed here are arbitrary at this stage.

6.6 Conclusion

We conclude that ash thickness and settling rate are the critical HIMs for the assessment of surface transportation functionality during volcanic ashfall events. However, due to current difficulties in quantifying the impact that ash thickness has on visibility impairment (the key impact type relatable to ash-settling rate and relevant for all modes of surface transportation), the two HIMs are not directly comparable and should be considered separately. For the ash thickness HIM, we identify the potential for fluctuating intensities of road transportation disruption as thickness increases, a feature that has not been identified in the past from empirical studies and is a product of experimental data obtained from targeted laboratory testing for specific impact types. We highlight that disruption can occur at an order of magnitude less than previously indicated (i.e. for thicknesses of ~0.1 mm rather than 1.0 mm) due to the potential for surface marking coverage; fragility functions for road and airports have been updated accordingly. Although highly subjective, preliminary fragility functions for visibility with ash-settling rate adopted as the HIM have been established using empirical data alone and by making comparisons to impacts previously identified in fog.

Our analysis of alternative HIMs (i.e. other than the critical HIMs of ash thickness and settling rate) and their effect on volcanic ash fragility function development for surface transportation leads to several key findings:

- Although ash thickness and settling rate should be treated as core HIMs for the assessment of surface transportation disruption, alternative HIMs should not be overlooked.
- Ash particle size is identified as the next most important HIM for functionality loss, especially when airborne concentrations and accumulations of ash on the ground are relatively small.
- For different ash thicknesses, the relative importance of alternative HIMs may be different. However, for different ash-settling rates there is no evidence to suggest that alternative HIMs change in their relative importance to one another.
- As ash thickness and ash-settling rates increase, alternative HIMs have less of an influence on surface transportation functionality loss. This confirms that it is indeed appropriate to consider ash thickness and settling rate as core HIMs for surface transportation impact assessments.
- Without extensive datasets, it is difficult to accurately model the effect of alternative HIMs on disruption. However, we suggest that they could be incorporated into fragility functions by implementing ‘error boundaries’, alongside descriptors for the specific ash characteristic features responsible for increased probabilities of impact states being reached or exceeded.

Our findings support the need to provide forecasts and actively monitor a range of ash characteristics in areas that may be affected by volcanic ashfall, especially the thickness of deposits on the ground and ash-settling rate, but also other ash properties including particle size distributions, colour, and shape. This should be prioritised where there are abundant exposed surface transportation networks

and populations: potential disruption can occur with ~0.1 mm ash thickness on the ground, depending on the ash characteristics present. Additional (particularly quantitative) datasets derived from new eruptions and laboratory tests will assist with the advancement of volcanic ash fragility functions for surface transportation, thus allowing further improvements in risk assessments and contingency planning in volcanically active regions.

6.7 Acknowledgements

We acknowledge all the technical and financial support received to conduct the extensive laboratory experimentation on surface transportation impacts from volcanic ash. Although the results were not directly covered in this paper (they are covered in separate publications), many of the key findings would not have been possible without these initial studies. Particular thanks are expressed to the New Zealand Earthquake Commission (EQC), Determining Volcanic Risk in Auckland (DEVORA) project, Natural Hazards Research Platform (NHRP), University of Canterbury Mason Trust, and GNS Science Core Programme funding scheme for their recent support to the authors. Also, the financial support from the University of Canterbury Department of Geological Sciences is greatly appreciated, which allowed the purchase of key laboratory equipment. Daniel Blake would like to thank his additional PhD co-supervisors, Jan Lindsay (The University of Auckland) and Jim Cole (University of Canterbury), for their edits, guidance and advice throughout this study.

6.8 References

Auckland Council (2014) Harbourmaster's Office Operation of Vessels During Periods of Restricted Visibility: Navigation Safety Operating Requirements. Auckland Council, Auckland, New Zealand.

Auckland Airport (2008) Newsroom: Fog at Auckland Airport and Category IIIB. 19 November 2008, Auckland Airport. http://www.aucklandairport.co.nz/~/media/3FF843AAFCBB4C23B941EAA7406EAB7B.ashx?sc_database=web. Accessed 19 March 2016.

Barnard, S. (2009) The vulnerability of New Zealand lifelines infrastructure to ashfall. PhD Thesis, Hazard and Disaster Management. University of Canterbury, Christchurch, New Zealand.

Binkowski, F.S. Roselle S.J. Mebest M.R. Eder B.K. (2002) Modeling atmospheric particulate matter in an air quality modelling system using a modal method. IN: Chock, D.P. Carmichael, G.R. (Eds.) Atmospheric modelling. The IMA Volumes in Mathematics and its Applications, 130.

Blake, D.M. Wilson, G. Stewart, C. Craig, H.M. Hayes, J.L. Jenkins, S.F. Wilson, T.M. Horwell, C.J. Andreastuti, S. Daniswara, R. Ferdiwijaya, D. Leonard, G.S. Hendrasto, M. Cronin, S. (2015) The 2014 eruption of Kelud volcano, Indonesia: impacts on infrastructure, utilities, agriculture and health. GNS Science Report 2015/15, 139p. *[APPENDIX A OF THIS THESIS]*

Blake, D.M. Wilson, T.M. Cole, J.W. Deligne, N.I. Lindsay, J.M. (in review a) Impact of volcanic ash on road and airfield surface skid resistance. Journal of Transportation Research Part D: Transport and Environment. *[CHAPTER 3 OF THIS THESIS]*

Blake, D.M. Wilson, T.W. Gomez, C. (in review b) Road marking coverage by volcanic ash: an experimental approach. Environmental Earth Sciences. *[CHAPTER 4 OF THIS THESIS]*

Blake, D.M. Wilson, T.M. Stewart, C. (in review c) Visibility in airborne volcanic ash: considerations for surface transport using a laboratory-based method. Natural Hazards. *[CHAPTER 5 OF THIS THESIS]*

Blong, R.J. (1984) Volcanic hazards: a sourcebook on the effects of eruptions. New South Wales, Australia.

Blong, R. (2003) A new damage index. Natural Hazards, 30, pp.1–23.

CAA (2008) Low Visibility Operations at Auckland Airport. Vector: Pointing to Safer Aviation, Issue 4. Civil Aviation Authority of New Zealand. https://www.caa.govt.nz/Publications/.../Vector_2007_Issue4_JulAug.pdf, Accessed 19 March 2016.

Choi, E. DesRoches, R. Nielson, B. (2004) Seismic fragility of typical bridges in moderate seismic zones. Engineering Structures, 26, pp.187-199.

Craig, H. Wilson, T. Stewart, C. Villarosa, G. Outes, V. Cronin, S. Jenkins, S. (2016a) Agricultural impact assessment and management after three widespread tephra falls in Patagonia, South America. Natural Hazards, pp.1-63.

Craig, H. Wilson, T. Stewart, C. Outes, V. Villarosa, G. Baxter, P. (2016b) Impacts to agriculture and critical infrastructure in Argentina after ashfall from the 2011 eruption of the Cordón Caulle volcanic complex: an assessment of published damage and function thresholds. Journal of Applied Volcanology, 5:7, 31p.

Deligne, N.I. Blake, D.M. Davies, A.J. Grace, E.S. Hayes, J. Potter, S. Stewart, C. Wilson, G. Wilson, T.M. (2015) Economics of Resilient Infrastructure Auckland Volcanic Field scenario. ERI Research Report 2015/03, 151p. *[APPENDIX E2 OF THIS THESIS]*

Dunn, M.G. (2012) Operation of gas turbine engines in an environment contaminated with volcanic ash. Journal of Turbomachinery, 134:5, 18p.

Guffanti, M. Mayberry, G.C. Casadevall, T.J. Wunderman, R. (2009) Volcanic hazards to airports. Natural Hazards, 51, pp.287-302.

Hayes, J.L. Wilson, T.M. Magill, C. (2015) Tephra fall clean-up in urban environments. Journal of Volcanology and Geothermal Research, 304, pp.359–377.

Highway Research Board (1972) National Cooperative Highway Research Program Synthesis of Highway Practice 14: skid resistance. Highway Research Board, National Academy of Sciences, Washington D.C.

Horwell, C.J. Baxter, P.J. Hillman, S.E. Damby, D.E. Delmelle, P. Donaldson, K. Dunster C, Calkins, J.A. Fubini, B. Hoskuldsson, A. Kelly, F.J. Larsen, G. Le Blond, J.S. Livi, K.J.T. Mendis, B. Murphy, F. Sweeney, S. Tetley, T.D. Thordarson, T. Tomatis, M. (2010) Respiratory health hazard assessment of ash from the 2010 eruption of

Eyjafjallajökull volcano, Iceland: a summary of initial findings from a multi-centre laboratory study. IVHHN and Durham University, Durham, UK.

Hyslop, N. (2009) Impaired visibility: the air pollution people see. Atmospheric Environment, 43:1, pp.182-195.

ICAO (2001) Manual on volcanic ash, radioactive material and toxic chemical clouds. http://www3.alpa.org/portals/alpa/volcanicash/12_Doc9691ManualICAOVolAshRadioactiveMaterial.pdf, Accessed 16 June 2016.

ICAO (2012) Flight safety and volcanic ash: risk management of flight operations with known or forecast volcanic ash contamination. International Civil Aviation Organisation. http://www.icao.int/publications/Documents/9974_en.pdf, Accessed 16 June 2016.

Jenkins, S. Komorowski, J-C. Baxter, P. Spence, R. Picquout, A. Lavigne, F. (2013) The Merapi 2010 eruption: an interdisciplinary impact assessment methodology for studying pyroclastic density current dynamics. Journal of Volcanology and Geothermal Research, 261, pp.316–329.

Jenkins, S.F. Wilson, T.M. Magill, C.R. Miller, V. Stewart, C. (2014a) Volcanic ash fall hazard and risk: technical background paper for the UN-ISDR Global Assessment Report on Disaster Risk Reduction 2015. http://www.preventionweb.net/english/hyogo/gar/2015/en/home/documents.html, Accessed 19 April 2016.

Jenkins, S.F. Spence, R.J.S. Fonseca, J.F.B.D. Solidum, R.U. Wilson, T.M. (2014b) Volcanic risk assessment: quantifying physical vulnerability in the built environment. Journal of Volcanology and Geothermal Research, 276, pp.105-120.

Johnston, D.M. (1997) Physical and social impacts of past and future volcanic eruptions in New Zealand. PhD Thesis. Earth Science, Massey University, Palmerston North, New Zealand.

Johnston, D.M. Daly, M. (1997) Auckland erupts!! New Zealand Science Monthly, 8:10, pp.6-7.

Jolly, G.E. Keys, H.J.R. Procter, J.N. Deligne, N.I. (2014) Overview of the co-ordinated risk-based approach to science and management response and recovery for the 2012 eruptions of Tongariro volcano, New Zealand. Journal of Volcanology and Geothermal Research, 286, pp.184-207.

Leonard GS, Stewart C, Wilson TM, Procter JN, Scott BJ, Keys HJ, Jolly GE, Wardman JB, Cronin SJ, McBride SK (2014) Integrating multidisciplinary science, modelling and impact data into evolving, syn-event volcanic hazard mapping and communication: A case study from the 2012 Tongariro eruption crisis, New Zealand. Journal of Volcanology and Geothermal Research 286:208–232.

MNZ (2015) Maritime Rules Part 22: Collision Prevention. Maritime New Zealand, Wellington, New Zealand. https://www.maritimenz.govt.nz/Rules/Rule-documents/Part22-maritime-rule.pdf, Accessed 19 March 2016.

Nairn, I.A. (2002) The effects of volcanic ash fall (tephra) on road and airport surfaces. GNS Science Report 2002/13, 32p.

Nanayakkara, K.I.U. Dias, W.P.S. (2016) Fragility curves for structures under tsunami loading. Natural Hazards, 80:1, pp.471–486.

Reese, S. Ramsay, D. (2010) RiskScape: flood fragility methodology. NIWA Technical Report WLG2010-45, 42 p.

Rossetto, T. Ioannou, I. Grant, D.N. (2013) Existing empirical vulnerability and fragility functions: compendium and guide for selection. GEM Technical Report 2013-X, GEM Foundation, Pavia, Italy.

Rossetto, T. D'Ayala, D. Ioannou, I. Meslem, A. (2014) Evaluation of existing fragility curves. IN: Pitilakis, K. Crowley, H. Kaynia, A.M. (Eds.) SYNER-G: typology definition and fragility functions for physical elements at seismic risk. Springer Dordrecht.

Singhal, A. Kiremidjian, A.S. (1996) Method for probabilistic evaluation of seismic structural damage. Journal of Structural Engineering, 122, pp.1459–1467.

Stewart, C. Horwell, C. Plumlee, G. Cronin, S. Delmelle, P. Baxter, P. Calkins, J. Damby, D. Mormon, S. Oppenheimer, C. (2013) Protocol for analysis of volcanic ash samples for assessment of hazards from leachable elements. IAVCEI, IVHHN, Cities on Volcanoes Commission, USGS, GNS Science.

Tarbotton, C. Dall'Osso, F. Dominey-Howes, D. Goff, J. (2015) The use of empirical vulnerability functions to assess the response of buildings to tsunami impact: comparative review and summary of best practice. Earth-Science Reviews, 142, pp.120-134.

TRB (1996) Transportation options for megacities in the developing world: a working paper, Transport Research Board. IN: NRC (1996) Meeting the challenges of megacities in the developing world: a collection of working papers. National Research Council, National Academy Press, Washington DC, United States.

UNISDR (2009) UNISDR terminology on disaster risk reduction. United Nations International Strategy for Disaster Reduction, Geneva, Switzerland. http://www.unisdr.org/files/7817_UNISDRTerminologyEnglish.pdf, Accessed 21 April 2016.

Wardman, J. Sword-Daniels, V. Stewart, C. Wilson, T. (2012) Impact assessment of the May 2010 eruption of Pacaya volcano, Guatemala. GNS Science Report 2012/09, 90p.

Wilson, G. Wilson, T.M. Deligne, N.I. Cole, J.W. (2014) Volcanic hazard impacts to critical infrastructure: a review. Journal of Volcanology and Geothermal Research, 286, pp.148-182.

Wilson, G. (2015) Vulnerability of critical infrastructure to volcanic hazards. PhD Thesis in Hazards and Disaster Management. Department of Geological Sciences, University of Canterbury, Christchurch, New Zealand.

Wilson, G. Wilson, T.M. Deligne, N.I. Blake, D.M. Cole, J.W. (in review) Framework for developing volcanic fragility functions for critical infrastructure. Journal of Applied Volcanology. *[APPENDIX D OF THIS THESIS]*

Wilson, T.W. Stewart, C. Cole, J.W. Dewar, D.J. Johnston, D.M. Cronin, S.J. (2011) The 1991 eruption of Volcán Hudson, Chile: impacts on agriculture and rural communities and long-term recovery. GNS Science Report 2009/66, 99p.

Wilson, T.M. Stewart, C. Sword-Daniels, V. Leonard, G.S. Johnston, D.M. Cole, J.W. Wardman, J. Wilson, G. Barnard, S.T. (2012a) Volcanic ash impacts to critical infrastructure. Physics and Chemistry of the Earth, 45-46, pp.5-23.

Woo, G. Grossi, P. (2009) A new era of volcano risk management. Stanford, CA, Risk Management Solutions Inc. https://support.rms.com/publications/Volcano_Risk_Management.pdf, Accessed 20 June 2013.

7. INVESTIGATING THE CONSEQUENCES OF URBAN VOLCANISM USING A SCENARIO APPROACH: INSIGHTS INTO TRANSPORTATION NETWORK DAMAGE AND FUNCTIONALITY

Daniel M Blake[1], Natalia I Deligne[2], Thomas M Wilson[1], Jan M Lindsay[3], Richard Woods[2]

[1] Department of Geological Sciences, University of Canterbury, Private Bag 4800, Christchurch, New Zealand.

[2] GNS Science, 1 Fairway Drive, Avalon 5010, PO Box 30-368, Lower Hutt 5040, New Zealand.

[3] School of Environment, The University of Auckland, Private Bag 92019, Auckland, New Zealand.

Journal: Journal of Volcanology and Geothermal Research

Received: 20 October 2016

Current Status: In Review

7.1 Abstract

Transportation networks are critical infrastructure in urban environments. Before, during and following volcanic activity, these networks can incur direct and indirect impacts, which subsequently reduces the *Level-of-Service* available to transportation end-users. Additionally, reductions in service can arise from management strategies including evacuation zoning, causing additional complications for transportation end-users and operators. Here, we develop metrics that incorporate Level-of-Service for transportation end-users as the key measure of vulnerability for multi-hazard volcanic impact and risk assessments.

A hypothetical eruption scenario recently developed for the Auckland Volcanic Field, New Zealand, is adopted to describe potential impacts of a small basaltic eruption on different transportation modes, namely road, rail, aviation and activities at ports. We demonstrate how the new metrics can be applied at specific locations worldwide by considering the geophysical hazard sequence and evacuation zones in this scenario, a process that was strongly informed by consultation with transportation infrastructure providers and emergency management officials. We also discuss the potential implications of modified hazard sequences (e.g. different wind profiles during the scenario, and unrest with no resulting eruption) on transportation vulnerability and population displacement.

The vent area selected for the eruption scenario used in our study is located to the north of the Māngere Bridge suburb of Auckland, and the volcanic activity progresses from seismic unrest, through phreatomagmatic explosions generating pyroclastic surges to a magmatic phase generating a scoria cone and lava flows. Our results show that most physical damage to transportation networks occurs from pyroclastic surges during the initial stages of the eruption. However, the most extensive service reduction across all networks in fact occurs ~6 days prior to the eruption onset, largely attributed to the implementation of evacuation zones; these disrupt crucial north-south links through the south Auckland isthmus, and at times cause up to ~435,000 residents and many businesses to be displaced. Ash deposition on road and rail following tephra-producing eruptive phases causes widespread Level-of-Service reduction, and a degree of disruption continues for >1 month following the end of the eruption until clean-up and re-entry to most evacuated zones is complete. Different tephra dispersal and deposition patterns can result in substantial variations to Level-of-Service and consequences for transportation management. Additional complexities may also arise during times of unrest with no eruption, particularly as residents are potentially displaced for longer periods of time due to extended uncertainties on potential vent location. We believe the Level-of-Service metrics developed here effectively highlight the importance of considering transportation end-users when developing volcanic impact and risk assessments. We suggest that the metrics are universally applicable in similar environments.

7.2 Introduction

Efficient transportation networks are a prerequisite for future growth of top performing economies (NEC 2014), and vital for societies worldwide. However, volcanic activity can cause substantial cumulative disruption to transportation, causing a reduction in the ability of networks to convey goods and people. This is particularly relevant in urban areas with complex transportation systems, high demand and/or little network redundancy. Even before eruptions commence, pro-active strategies to reduce exposure such as evacuation zoning can cause transportation disruption through access restrictions (Jenkins et al. 2014). Potentially widespread cascading consequences caused by changes in demand across the network may also result (Woo 2008, Wolshon 2009). If a volcanic eruption ensues, further complexities for transportation end-users may be introduced by damage or disruption resulting from proximal volcanic hazards such as pyroclastic density currents and lava flows, and distal hazards such as tephra fall which can affect areas up to hundreds of kilometers from the vent itself (Wilson et al. 2012a, Wilson et al. 2014). Table 7.1 illustrates the multitude of damage and disruption that has occurred on transportation networks in the past due to proximal and distal volcanic hazards.

Roads are particularly important for the movement of people and freight in urban areas due to many interdependencies with other critical infrastructure types and often-widespread public use (Daly and Johnston 2015). However, rail, aviation and maritime transportation may also have crucial roles during volcanic activity in some locations, with all modes potentially affected by volcanic hazards. For example, ash from the 2010 eruption of Eyjafjallajökull volcano in Iceland caused serious disruption to aviation across the North Atlantic and Europe, with global economic losses of around US$5 billion (Ragona et al. 2011, Louglin et al. 2015). Once direct volcanic threats have subsided and any exclusion zones are lifted, transportation plays a crucial role in both immediate and long-term recovery, including the provision of access for clean-up operations and facilitating the restoration of other critical infrastructure and businesses in affected areas (Cova and Conger 2003, Hayes et al. 2015, Hayes et al. in review).

Table 7.1 Examples of damage and disruption to transportation from volcanic hazards associated with infamous worldwide eruptions. x = road, o = rail, Δ = maritime, ◊ = airport. (Adapted from Blake et al., in review a,b,c,d). Note that only transportation activities on land or sea are considered (aircraft in flight are excluded).

Volcano and country	Year	Physical damage from proximal hazards					Disruption from volcanic ash					
		Pyroclastic density current	Lava flow	Lahar	Tsunami	Deformation or degassing	Reduced skid resistance	Visibility issues	Marking coverage	Closure or obstruction	Vehicle or engine issues	Derailment (tram)
Komagatake, Japan	1640				Δ							
Garachico, Spain	1706		Δ									
Oshima, Japan	1741				Δ							
Sakurajima, Japan	1779									Δ		
Tambora, Indonesia	1815				Δ					Δ		
Cotopaxi, Ecuador	1877			x								
Vulcan, Papua New Guinea	1878									Δ		
Krakatau, Indonesia	1883				xoΔ			Δ		Δ	Δ	
Sagir, Indonesia	1891									Δ		
La Soufrière, St. Vincent and the Grenadines	1902											o
Matavanu, Samoa	1905-07		x		x							
Vesuvius, Italy	1906		o	o								
Matavanu, Samoa	1907				Δ							
Novaruputa, U.S.A	1912									Δ	Δ	
Sakurajima, Japan	1914		xΔ									
San Salvador, El Salvador	1917		o									
Deception Island, (Antarctic Treaty administration)	1921										Δ	
Kilauea, U.S.A	1924					o						
Etna, Italy	1928		o									
Deception Island, (Antarctic Treaty administration)	1930									Δ	Δ	
Tavurvur, Papua New Guinea	1937			x	Δ					Δ	Δ	
Vesuvius, Italy	1944		o								Δ	
Usu, Japan	1944					xo						
Ruapehu, New Zealand	1945			o				x			x	
Lamington, Papua New Guinea	1951			x								
Bayonnaise Rocks (submarine), Japan	1952										Δ	
Iwo-Jima, Japan	1957					◊						
South Sandwich Islands, U.K (overseas territory)	1960s									Δ	Δ	
Calbuco, Chile	1961			x								
Agung, Indonesia	1963			x								
Irazu, Japan	1964			x								
Kilauea, U.S.A	1968					x						
Mayon, Philippines	1968			o								
Villarrica, Chile	1971			x								
Heimaey, Iceland	1973		Δ									
Ruapehu, New Zealand	1975			x								
Piton de la Fournaise, France (overseas territory)	1977		x									
Nyiragongo, Democratic	1977		x									

Republic of Congo												
Etna, Italy	1979		x								x	
Lamington, Papua New Guinea	1979	x										
Mount St Helens, U.S.A	1980	x		xo			x	xo	x	xoΔ◊	xo	
Galunggung, Indonesia	1982									◊		
Miyakejima, Japan	1983									◊		
(Unknown, South China Sea)	1986									Δ		
Redoubt, U.S.A	1989-90									◊		
Hudson, Chile	1991						x	x	x	xΔ◊	x	
Pinatubo, Philippines	1991			x						◊	◊	
Spurr, U.S.A	1992							x			x	
Unzen, Japan	1991-92	x		xo				x			x	
Tavurvur and Vulcan, Papua New Guinea	1994	x		x			x			x Δ◊	x	
Sakurajima, Japan	1995						x		x			
Ruapehu, New Zealand	1995-96			x			x	x	x	x◊		
Popocatepetl, Mexico	1997									◊		
Soufrière Hills, U.K (overseas territory)	1997	◊					x					
Reventador, Ecuador	1999									◊		
Pichincha, Ecuador	1999									◊		
Miyakejima, Japan	2000-08					◊						
Etna, Italy	2002-03		x				x	x		x◊		
Reventador, Ecuador	2002						x		x	x◊	x	
Nyiragongo, Democratic Republic of Congo	2002		◊									
Popocatepetl, Mexico	2003									◊		
Anatahan, Mariana Islands	2003-05									◊		
Merapi, Indonesia	2006	x										
Home Reef, Tonga (submarine)	2006									Δ	Δ	
Etna, Italy	2006									◊		
Chaitén, Chile	2008			x			xo	x		xΔ◊	xΔ	
Okmok, U.S.A	2008										Δ	
Redoubt, U.S.A	2009										x	
Merapi, Indonesia	2010			x			x					
Pacaya, Guatemala	2010						x	x	◊	◊	x	
Tungurahua, Ecuador	2010									◊		
Cordón Caulle, Chile	2011			x			x	x		Δ◊	x	
Sakurajima, Japan	2011						x		x	o◊	x	
Shinmoedake, Japan	2011						x	x		o	xo	
Etna, Italy	2013									◊	x	
San Cristóbal, Nicaragua	2013							x				
Kelud, Indonesia	2014			x			◊	x◊		◊	◊	
Sakurajima, Japan	2014								x			
Sinabung, Indonesia	2014						x					
Tungurahua, Ecuador	2014									◊		
Calbuco, Chile	2015							x				
Villarrica, Chile	2015			x								

(Information from: Hurlbut and Verbeek 1887, Corwin and Foster 1959, Tazieff 1977, Sarniken and Wiitala 1981, Tyler and Reynertson 1981, Warrick et al. 1981, Labadie 1983, Blong 1984, Hirano et al. 1992, Yanagi et al. 1992, Bitschene and Fernández 1995, Blong and McKee 1995, Johnston 1997, Casadevall et al. 1999, Nakada et al. 1999, Stammers 2000, Anna-Barradas 2001, Becker et al. 2001, Durand et al. 2001, Nairn 2002, Oppenheimer 2003, Barnard 2004, Cole and Blumenthal 2004, Cole et al. 2005, Kagoshima City Office 2005 (pers comm), Leonard et al. 2006, Wilson et al. 2007, Guffanti et al. 2009, Barnard 2009, USGS 2009, Wilson 2008, Wilson 2009, Wilson et al. 2009a, Wilson et al. 2009b, Barsotti et al. 2010, Jamaludin 2010, Sword-Daniels et al. 2011, Surono et al. 2012, Wardman et al. 2012, Wilson et al. 2012b, GVP 2013, Jenkins et al. 2013, Magill et al. 2013, USGS 2013, Wilson et al. 2013, Folch et al. 2014, Volcano Discovery 2014, AccuWeather 2015, Blake et al. 2015, Craig et al. 2016, Cubellis et al. 2016, Blake et al. in review a,b,c,d.)

Vulnerability assessments can be used as part of volcanic risk assessments to describe the likelihood that assets will incur loss for a range of hazard intensities (Rossetto et al. 2013). In the past, the majority of volcanic vulnerability assessments have focused on direct physical damage to infrastructure, especially concerning the structural components of buildings, and associated loss of life (e.g. Spence et al. 1999, Magill and Blong 2005, Zuccaro et al. 2008, Jenkins et al. 2013, Hampton et al. 2015). However, disruption through the loss of critical infrastructure functionality from volcanic hazards may be equally, if not more, important to consider than direct damage in many situations (Wilson et al. 2014, Blake et al. in review d). Loss of functionality can cause widespread and cumulative effects on society (Jenkins et al. 2015) and subsequent complexities for governments and local authorities (Mei et al. 2013). For example, if a pyroclastic surge crosses (or is forecast to cross) a section of road, authorities may quickly decide that the affected section should be closed due to life-safety considerations. However, deciding whether to close the same road section if it is affected by light volcanic ash fall may be riddled with complexities; it may be that it remains open, albeit with reduced functionality. Importantly, the functional loss of transportation networks during volcanic activity, results in the end-users of the system experiencing a degree of disruption to service (Deligne et al. companion paper – Appendix E1), such as reduced speeds, temporary traffic management systems, congestion, or increased accident rates (Blake et al. in review d). Such disruption can be described by the overall usability of the network section or facility of interest, which we term *Level-of-Service (LoS)*. Many transportation authorities are increasingly focusing on LoS measures, with a general shift from maintaining networks primarily through technical solutions to maintenance approaches which particularly address end-user needs (e.g. the ‘One Network Road Classification’ performance measures implemented by the New Zealand Transport Agency, which “places the customer at the heart of every investment decision”; NZTA 2013, p.3). LoS can be expressed descriptively as a series of general qualitative metrics, and/or as quantitative metric values that take into account site-specific details (e.g. Robinson et al. 2015). However, studies focusing on detailed assessments of transportation LoS are rare, especially during and after volcanic activity, despite the many multi-hazard impacts that can occur (e.g. Table 7.1).

The aim of this paper is to design and develop a universally-applicable but location-adaptable impact assessment model that incorporates LoS as a key measure of transportation vulnerability. We develop LoS metrics by considering the consequences of damage from geophysical hazards and evacuations during volcanic activity for the end-users of key transportation modes (road, rail, aviation and infrastructure at ports). This contributes to the volcanic risk assessment discipline by considering the impact of volcanic hazards on transportation end-users, whether it be from disruption caused by the effects of management strategies that act to reduce population and infrastructure exposure (such as evacuation zoning or volcanic deposit clean-up), or that from physical damage caused by volcanic hazards directly impacting transportation networks.

We adopt the “Māngere Bridge” scenario of the Auckland Volcanic Field (AVF), New Zealand, described by Deligne et al. (companion paper – Appendix E1), as a basis to demonstrate the application of LoS metrics. LoS metrics are implemented at key times during the course of the

hypothetical eruption and its aftermath. In our application, the conceptual approach for impact assessment model development is guided by official emergency management policies, the latest data for transportation impacts from post-eruption and laboratory studies, and direct consultation with officials from transportation and emergency management authorities. We also consider two geophysical adaptations to the established Māngere Bridge scenario – a sequence of volcanic unrest, similar to that in the original scenario but with no resultant eruption, and a sequence of events the same as the original scenario but with a predominant south-westerly wind direction (the dominant wind direction for Auckland; Chappell 2014). This allows us to explore the effects that potential alterations in the geophysical hazard sequence may have on evacuations, displaced populations, transportation damage and, importantly, LoS. Interdependencies with other critical infrastructure are briefly discussed but not analysed in detail.

7.3 Transportation in Auckland

In Auckland, New Zealand's largest and most populous city (population ~1.6 million; Statistics New Zealand 2015), functional transportation networks are important for the regional and national economy (AELP-1 1999). However, Auckland's geography poses some major challenges as it generally acts to constrain transportation networks on the ground; the Waitemata and Manukau Harbours act as major obstacles (Figure 7.1), constricting routes through narrow stretches of land. There are two main isthmus' which lie around 10 km from Auckland City; one to the south east (~2.3 km wide), and one to the south west (~5.2 km wide) (Tomsen 2010). Additionally, Auckland City is built directly on top of the 360 km^2 basaltic AVF (Louglin et al. 2015), and as transportation routes service highly populated areas, the consequences of disruption caused by volcanic activity could be substantial and widespread. There are four key transportation modes in Auckland, all of which are vulnerable to future volcanic activity in the field:

7.3.1 Road

The road network in Auckland is extensive, with multiple highways, arterial (Figure 7.1) and local routes, spanning over 8,000 km across the region (NZTA 2008). The majority of trips are made by car (Auckland Council 2013a) and the bus network provides the bulk of public transport (ARTA 2009, Tomsen 2010). Walking mostly takes place within a transport system that must work for a range of road users (NZTA 2009). As Auckland's geography acts to constrain the road transportation network (Figure 7.1), generally one of four highway bridges must be crossed in order to enter or leave the city area by highway.

7.3.2 Rail

Most rail in the central and suburban areas is electrified (Figure 7.1), with the electric system supplied by two connections to the national grid, at Southdown and Penrose substations (Deligne et al. companion paper – Appendix E1). At the time of writing, a diesel shuttle service runs between

Papakura and Pukekohe on the Southern Line (Figure 7.1). Diesel freight services also operate on the rail network through Auckland (Auckland Transport 2013a). In many instances rail routes consist of two or three tracks, but their close proximity means that if one is damaged the others are likely to be too (AELP-2 2014).

7.3.3 Aviation

The main aviation hub (passenger and cargo) is Auckland Airport (Figure 7.1), the largest and busiest passenger airport in New Zealand. It is one of only two civilian airports in New Zealand capable of handling the largest of passenger aircraft. In the Auckland region there is also an aerodrome at Ardmore and Royal New Zealand Air Force (RNZAF) base at Whenuapai, both of which have active airfields (Beca Planning 2003).

7.3.4 Maritime

There are three key port sites in Auckland (Figure 7.1): the Port of Auckland (the main seaport located in the Waitemata Harbour with cargo and cruise services), the Port of Onehunga (in the Manukau Harbour with a limited cargo service), and the Wiri Intermodal Freight Hub (in Wiri, South Auckland). Many ferry terminals, marinas and boat ramps also serve the region.

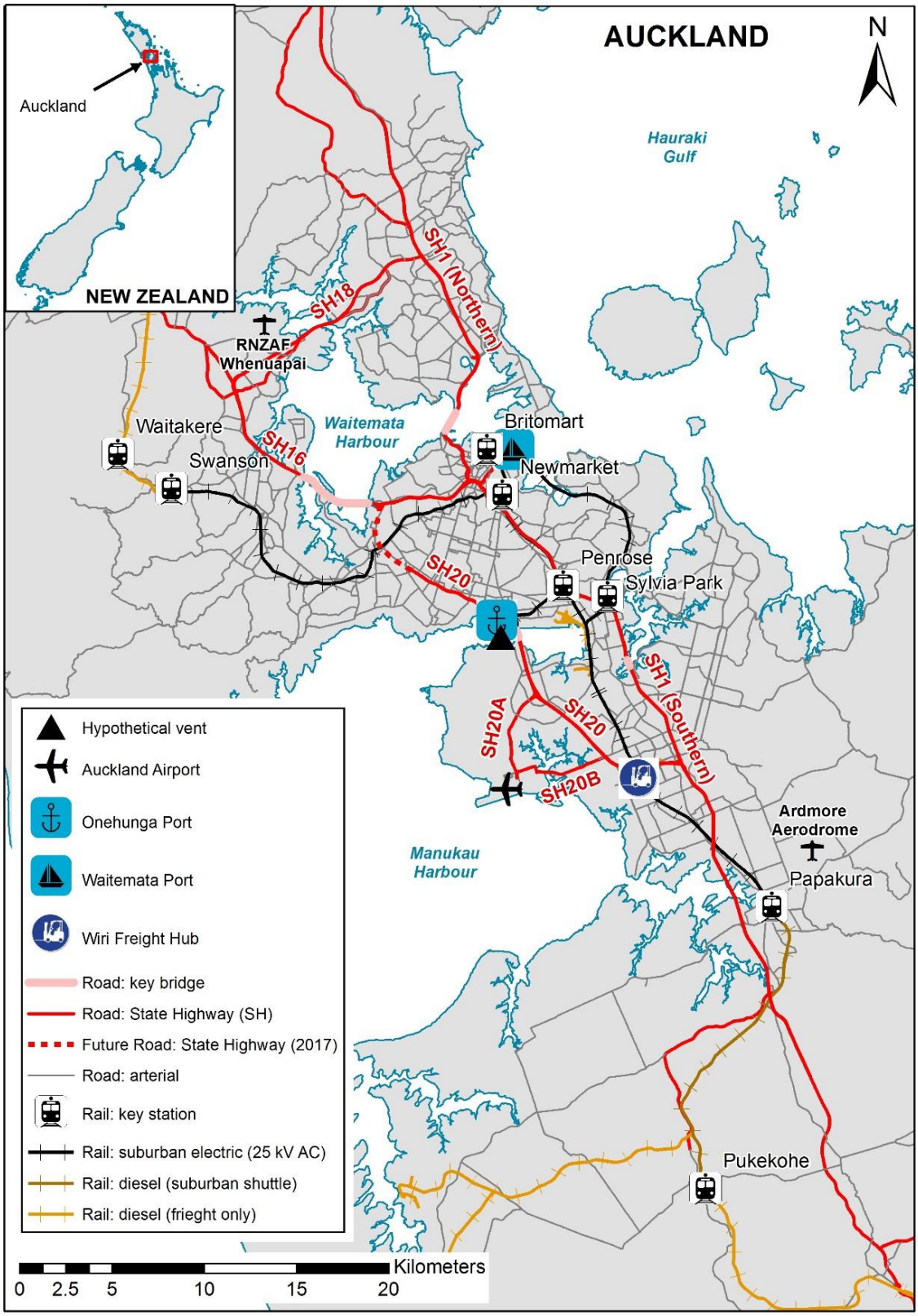

Figure 7.1 Major transportation routes and facilities in the Auckland City area. Inset shows location of Auckland City study area within New Zealand.

7.4 Methodology and Application

The approach used to assess transportation LoS and produce time series maps is shown in Figure 7.2. In our methodology, we first consider the geophysical hazards (Section 7.4.1), using hazards in the Māngere Bridge scenario (Deligne et al. companion paper – Appendix E1) as a basis, to consider the effect on direct damage to the transportation network (Section 7.4.2). This is required to inform the core vulnerability component of our model: LoS metric development for transportation (Section 7.4.3). We then consider the latest emergency and transportation management policies for Auckland to demonstrate how LoS metrics can be applied in a particular location (Section 7.4.4).

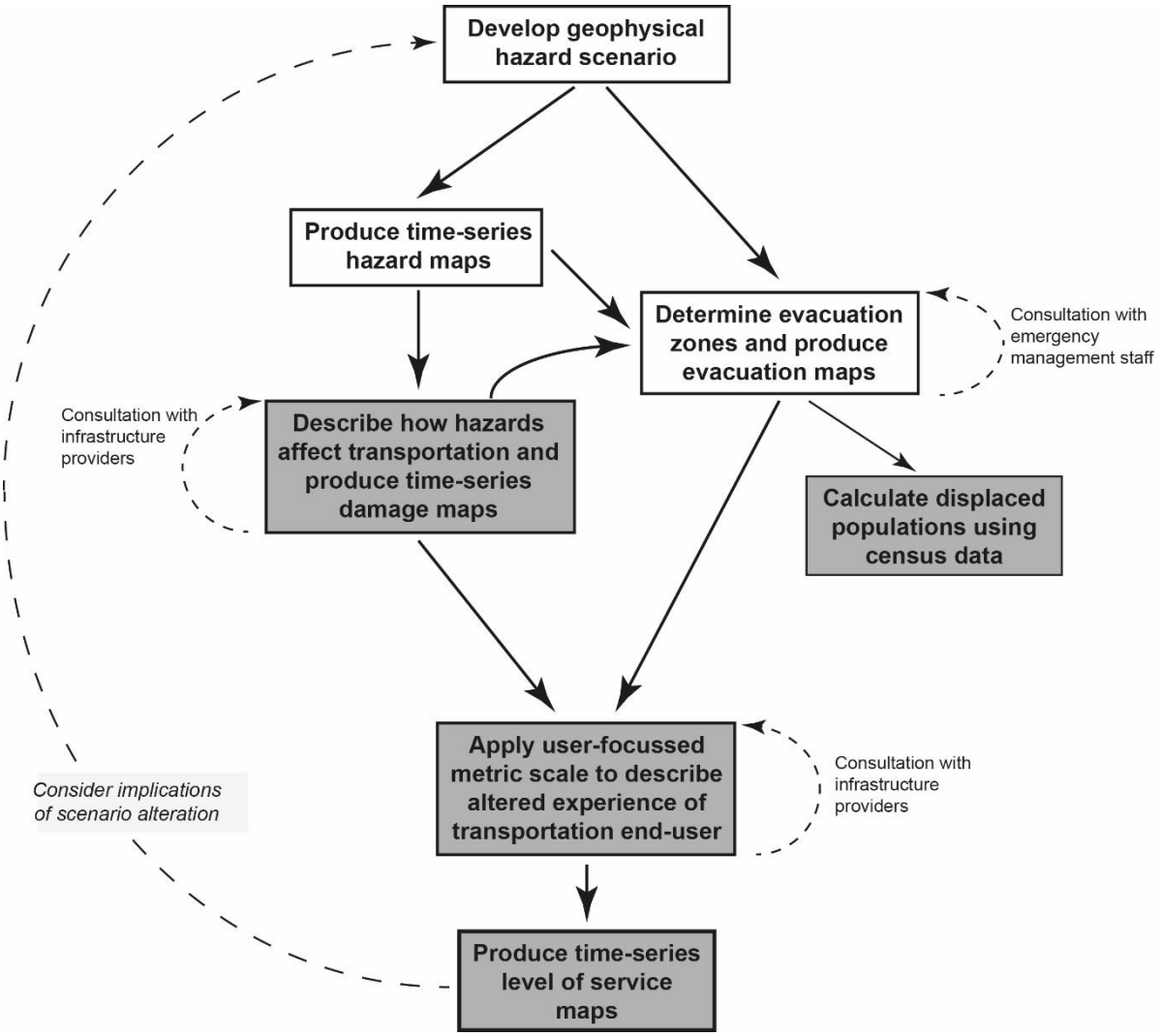

Figure 7.2 Summary of methodological approach and processes used to assess transportation Level-of-Service. White-filled boxes indicate work outlined in Deligne et al. (companion paper – Appendix E1). Grey-filled boxes indicate work explored in this paper.

7.4.1 Geophysical hazards

The Māngere Bridge scenario includes an unrest sequence with earthquakes, gas emission and ground deformation, followed by an eruption sequence which includes the six volcanic hazards of edifice, pyroclastic surges, tephra, ballistics, lava flows, and tsunami – all are described in Deligne et al. (companion paper – Appendix E1). Potential secondary hazards such as fire and flooding are beyond the scope of this study due to uncertainties in their location and extent. We build upon the extent and severity of hazards in the original scenario by also considering the implications on transportation of different (south-westerly) wind profiles on tephra deposition (Section 7.4.1.1) and a sequence of activity involving unrest with no eruption (Section 7.4.1.2). These additions to the original scenario are later used to demonstrate how LoS metrics can be applied in different situations.

7.4.1.1 Predominant south-westerly wind

As discussed in Deligne et al. (companion paper – Appendix E1), in the Māngere Bridge scenario the tephra dispersal event with the largest hazard footprint has an unusual wind direction for Auckland; the scenario adopted wind profiles for specific dates in March 2014 which may be seasonally constrained and atypical for the city. Therefore, we consider an additional option to the original Māngere Bridge scenario – new wind profiles which represent the predominant wind direction in Auckland, south-westerly winds. We perform additional modelling using the TEPHRA2 program (Bonadonna et al. 2005, Connor et al. 2011) to model ash deposition from the existing eruptive sequence with south-westerly winds prevalent throughout to make comparisons with the previously modelled ash deposition (Deligne et al. companion paper – Appendix E1) and discuss potential consequences for transportation.

The first south-westerly wind profile was chosen from the New Zealand National Climate Database (NIWA CliFlo) from a random selection of 6-hourly profiles at Auckland Airport within a 10 year period between 01 January 1975 and 31 December 1984 – a similar method to that used by Magill et al. (2006). The date and time of the wind profile selected was 24 January 1976 (12:00) (Appendix E3). This wind profile was adopted for TEPHRA2 modelling for the first tephra plume of the scenario (i.e. 14 March PM), with subsequent tephra plumes modelled using corresponding dates between the scenario timeframe and days following the first wind profile; a random time was selected from the 4 NIWA CliFlo wind profile options on each day (Appendix E3). Minor adjustments were made to other TEPHRA2 input parameters to those used in the original Māngere Bridge scenario modelling to most appropriately reflect current knowledge of volcanic ash characteristics that could occur in the AVF (often using analogue worldwide eruptions). The new suite of tephra parameters (Appendix E4) was adopted for modelling our south-westerly wind addition. The input mass for each eruptive phase was kept consistent with the original scenario and all thicknesses below 0.1 mm converted to 0 mm as before.

7.4.1.2 Unrest with no eruption

For the purpose of exploring the consequences of volcanic unrest with no eruption, we adopt the same unrest sequence that occurred during the original Māngere Bridge scenario from 19 February (when small swarms of high frequency non-volcanic earthquakes are detected), through to early on 14 March (where tremor earthquakes and acceleration of deformation occurs). Although this is accompanied by visual observation of cracking near Māngere and an increase in volcanic gases, no phreatic eruption follows the sequence. From there onwards, we adopt the general sequence of events described in Pallister et al. (2010) for the series of earthquakes that occurred in the Harrat lava province of Saudi Arabia (April-June 2009), attributed to a magmatic dyke intrusion. There is currently no evidence for shallow dyke intrusions or surface ruptures without subsequent eruptions in the AVF. However, we cannot rule out the possibility of this occurring in the future and thus such a scenario is important to consider for emergency planning purposes.

For the unrest scenario, we consider policy outlined in the AVF Contingency Plan (Auckland Council, 2015) and Auckland Evacuation Plan (Auckland Council, 2014) regarding the establishment of Primary Evacuation Zones (PEZs) and Secondary Evacuation Zones (SEZs).

7.4.2 Physical damage to transportation

We consider the six volcanic hazards in the hypothetical Māngere Bridge eruption and earthquakes associated with prior unrest activity by producing time-series maps that display the physical damage to transportation through the scenario. Each transportation mode is considered separately, as is damage from proximal volcanic hazards and volcanic ash. Deligne et al. (companion paper – Appendix E1) adopted the ‘worst-case’ and ‘average-case’ scenarios for pyroclastic surges, originally proposed by Brand et al. (2014) who provide guidance on the physical impact to buildings through the consideration of previous studies, but here used for transportation infrastructure. We use expert judgment to consider transportation buildings (e.g. rail stations, port facilities) and linear components of the network (e.g. rail lines, roads) separately. We classify the physical damage from pyroclastic surges using radial distance thresholds (established from dynamic pressures) using expert judgment from transportation infrastructure managers.

For earthquakes, we assume minimal direct damage to infrastructure given the relatively modest magnitudes (up to M_L4.8) for the Māngere Bridge scenario, and considering that the New Zealand building code is deemed adequate at a worldwide scale (Daniell et al, 2014). However, some minor blockages from landslides and other debris, and damage to specific components, may occur on the ground transportation network during earthquakes which are shallow and with epicenters nearby. As such, we take a conservative approach and apply the same damage category (“minor damage and blockage possible”) to all roads and rail lines that fall within an area ~5 km from earthquake zone boundaries in the scenario, also including all of the central Auckland area between the two isthmus’.

In areas beyond the zones affected by the edifice, pyroclastic surges and earthquakes, we apply findings from Blake et al. (a,b,c) and Wilson et al. (2014) to evaluate physical damage from tephra fall. We designate the same 'possible damage' category (Section 7.6.1) adopted for the outer extent of surges (i.e. radial extents with relatively low dynamic pressures) to electric rail lines in these areas. We do not anticipate any direct physical damage to road networks in this area. However, we allocate a distinct category termed 'minor accumulations of deposits' to road sections affected by this tephra layer, to highlight areas where potential knock-on consequences may exist (for example, subsequent physical damage caused by accidents or blockage of stormwater networks). In scenarios elsewhere, where tephra accumulation is more extensive in distal areas, additional physical damage categories should be considered for tephra fall based on laboratory and observational data.

Following an eruption, clean-up of the transportation network is required for it to return to full functionality, and also for key site access to maintain or restore other critical infrastructure. In this study, we adopt the volcanic tephra clean-up model and timeframe examined in Hayes et al. (2015).

7.4.3 Level-of-service metric development for transportation

To develop the metric series, we consider the expected disruption resulting from physical damage caused by hazards (Section 7.4.2) and operational activities such as evacuation zoning and area exclusions outlined in the Māngere Bridge scenario. Expert knowledge from transportation infrastructure managers informed the development of metrics. Specifically, LoS metrics for road and rail include the consideration of:

- Destruction of the network by geophysical hazards
- Deposits on the network from geophysical hazards
- Inspection and maintenance requirements (e.g. due to ground shaking)
- Access (e.g. due to evacuation zones or blockage)
- Use of infrastructure for alternative purposes (e.g. rail stations used as welfare facilities).

For road transportation, a single suite of LoS metrics is developed to consider the linear part of the network (i.e. components such as bridges and traffic signals are not considered separately). For the purpose of this study we assume that all road surfaces are sealed, although we recognise that a small proportion may be unsealed in reality with potential variations in impact and clean-up characteristics (Nairn 2002). LoS metrics are developed around similar principles for the rail line network (i.e. rail tracks and overhead lines which are both equally important to end-users and considered as one in this study). However, rail stations are also critical components, as stations and lines may be impacted and restored differently, and ultimately could affect end-users of rail transportation in different ways; we thus develop separate LoS metrics for rail stations.

We developed LoS metrics for aviation in consultation with the Auckland Airport Compliance and Quality Assurance Manager. The aim was to best describe possible partial or complete closure scenarios for an international airport. We assumed that the location of the arrival / destination city

(e.g. whether it is a domestic or international flight) is correlated with the type of aircraft used and scheduling complexities, and that the quantity of flights departing / arriving relative to a benchmark is an appropriate proxy for how well the aviation sector is delivering service. In other words, the metric had to reflect that different operations at an airport have different response capabilities (e.g. international flights will often require more time to change schedules than domestic flights), and that different aircraft types have different airfield requirements.

7.4.4 Level-of-service metric application

We illustrate how the LoS metrics can be applied using the Māngere Bridge scenario by considering the spatial and temporal extents of evacuation zones, damage from geophysical hazards, operational priorities, and clean-up that has occurred on sections of the network. LoS metrics in each area are informed by expert judgment, with guidance from local infrastructure managers and emergency management officials taking priority as they often have the best knowledge of the system. Sometimes, overlaying the spatial extent of particular evacuation zones and/or physical damage layer is sufficient to designate a specific LoS metric to sections of the network. However, a more manual approach is sometimes required – for example, where particular routes and facilities are prioritised for reopening to restore vital connections.

We use the Māngere Bridge scenario to display the LoS for end-users of the Auckland transportation network at key stages throughout the hypothetical eruption and its aftermath. We also suggest metric values for Auckland Airport as the percentage proportion of 'typical capacity' can be estimated.

7.4.4.1 Road and rail

Due to the relatively large spatial distribution of road and rail networks, we display maps of LoS for these modes of transportation. Road sections are defined as the segments between intersections or highway on/off ramps, and therefore differ in length. Where hazard or evacuation zone boundaries cross road boundaries, the same LoS calculated within the boundary is often extended outside of the zone to the nearest intersection. A similar method is used for rail lines, where the same LoS from within zones is extended out to the nearest station. In comparison, LoS for Auckland Airport, the Port of Auckland and Port of Onehunga, which are single point sources, are only described in text and tables. Following consultation with transportation and emergency management officials in Auckland we make the following assumptions when applying LoS metrics and developing maps:

- Highways and critical arterial roads are prioritised for reopening, especially when restoring a north-south link through the southern isthmus is required.
- Only volcanic hazards are responsible for the destruction, damage or functional loss of transportation networks. In reality, particularly for rapid-onset eruptions, substantial human-induced modification may also occur (e.g. the intentional blockage or destruction of some state highway on/off ramps to facilitate contraflow).

- All roads and rail networks may be used for the purposes of evacuating residents when an evacuation zone is first implemented (rail services would only collect passengers and not allow disembarkation from stations within the evacuation zones).
- In some cases, critical road routes may be opened to allow travel through an evacuation zone (with no stopping or exit allowed from the critical routes within the evacuation zone itself).
- The spatial extent of areas affected by direct tephra fall and pyroclastic surge deposits is not extended due to the re-suspension and secondary deposition of deposits (although this is discussed in places).
- Congestion and accidents do not cause any impact on subsequent LoS designations.
- There are no major cascading effects resulting from other critical infrastructure failure or disruption.

7.4.4.2 Aviation

To determine aviation LoS metrics, we applied New Zealand Civil Aviation Authority (CAA) policy for airspace management during a volcanic crisis (Lechner 2015) to determine airspace restrictions over the course of the Māngere Bridge scenario (Figure 7.3). We then assigned LoS metrics in consultation with the Auckland Airport Compliance and Quality Assurance Manager, making the following assumptions:

- There is progressive closure of Auckland Airport during the unrest sequence.
- Airports are closed when within evacuated zones on the ground (although prioritised reinstatement may occur when they lie close to boundaries of these zones).
- There is minimal aircraft operation within Volcanic Hazard Zones (VHZs), which are established in response to VALs of 1 or greater, and corresponding Notices to Airmen (NOTAMs)[7].
- Airfields at RNZAF Whenuapai base and Ardmore Aerodrome can accommodate limited domestic, trans-Tasman and Pacific island traffic, primarily cargo.

Our results were then vetted and approved by an Air New Zealand Senior Business Continuity Management Advisor to check that they were realistic. We stress that our work should not be taken as policy endorsement or an indication of how individual airlines would respond in a similar situation.

[7] Although aircraft are permitted to operate within VHZs during daylight hours and in visual meteorological conditions, this only occurs at the specific request of pilots. Otherwise, air traffic control will not clear an aircraft to operate on any route or procedure that infringes VHZs, and aircraft under radar control will be vectored clear of VHZ boundaries (AIP NZ, 2016).

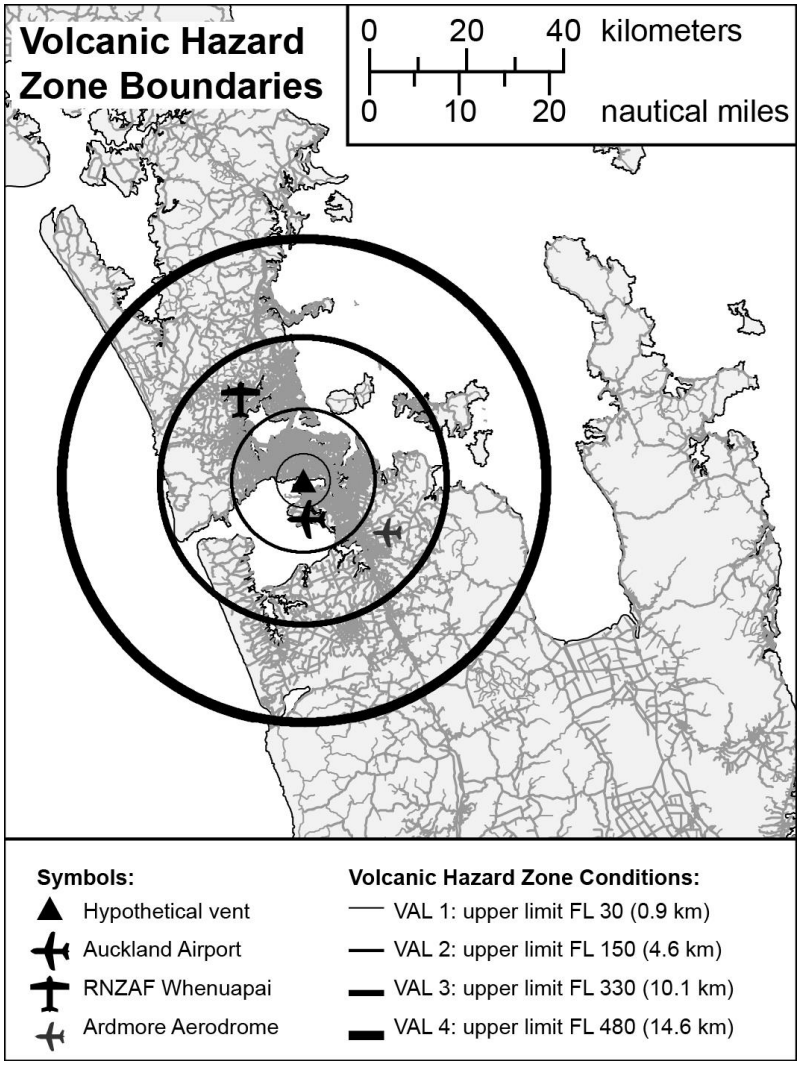

Figure 7.3 Hypothetical Volcanic Hazard Zone boundaries for the original Māngere Bridge scenario based on VALs (using zone radii of 3, 8, 16, and 27 nautical miles for VAL 0 and 1, 2, 3, and 4 respectively; Lechner 2015). The legend indicates the Flight Level (FL) below which pilots require specific permission to enter VHZs. For example, at VAL 0 or 1, pilots require permission to enter areas below FL 30 within 3 nautical miles of the volcanic vent.

7.4.4.3 Maritime

Although we consider the impacts to both port infrastructure and the navigation of ships in harbour areas for the development of LoS metrics, the operation of ports themselves is the main focus for the Māngere Bridge scenario. This was undertaken using best judgment taking into account post-eruption impacts observed elsewhere. Marinas and boat ramps are not considered in this paper. Similar to our approach for applying LoS metrics for Auckland Airport, we only describe LoS for the Port of Auckland and Port of Onehunga in text and tables (rather than on maps) as they are point sources.

7.4.4.4 Evacuation and displaced populations

As transportation LoS is strongly influenced by the establishment and alteration of evacuation zones, we consider the consequences of the evacuations summarised in Deligne et al. (companion paper – Appendix E1) with regard to the number of residents impacted and considerations for transportation demand. Consultation with emergency management staff in Auckland confirmed that throughout eruptions such as in our scenario, the national emergency management body in New Zealand (Ministry of Civil Defence and Emergency Management; MCDEM) and Auckland CDEM would work alongside infrastructure providers to assess when cordoned areas can be entered for clean-up, repair and maintenance (Auckland Council 2015). CDEM, through the provisions of the CDEM Act (2002), can grant concessions for staff to access evacuation areas to expedite reinstatement of critical services. Thus, while evacuated areas are off limits to residents and businesses, infrastructure providers such as transportation management authorities will sometimes be able to temporarily enter during lulls in volcanic activity, especially since activity in the AVF could continue for months to years. Consultation with transportation infrastructure providers in Auckland highlighted that the Southern Motorway (SH1) would remain open whenever possible, albeit at limited capacity with access restrictions, even when it is within officially evacuated zones.

The number or residents displaced by evacuation and exclusion zones is calculated using night-time resident population data. For the Māngere Bridge scenario, we use data collected in the 2013 New Zealand Census (Statistics New Zealand 2013). Rather than an estimate of those who reside within the exact extent of the evacuation zones, we adopt census meshblock[8] values using all meshblocks that fall within and intersect the zone boundaries and round values to the nearest hundred (Figure 7.4). This is deemed to be a more accurate representation as the true extent of any evacuation zone will likely reach beyond the initially designated extent in places due to features on the ground such as roads, potentially isolated neighbourhoods, and large property boundaries. Accounting for the number of businesses displaced by evacuation zones is beyond the scope of this study.

[8] A meshblock is the smallest geographic unit for which statistical data is collected and processed by Statistics New Zealand. Meshblocks in Auckland have a median land area of 0.039 km^2.

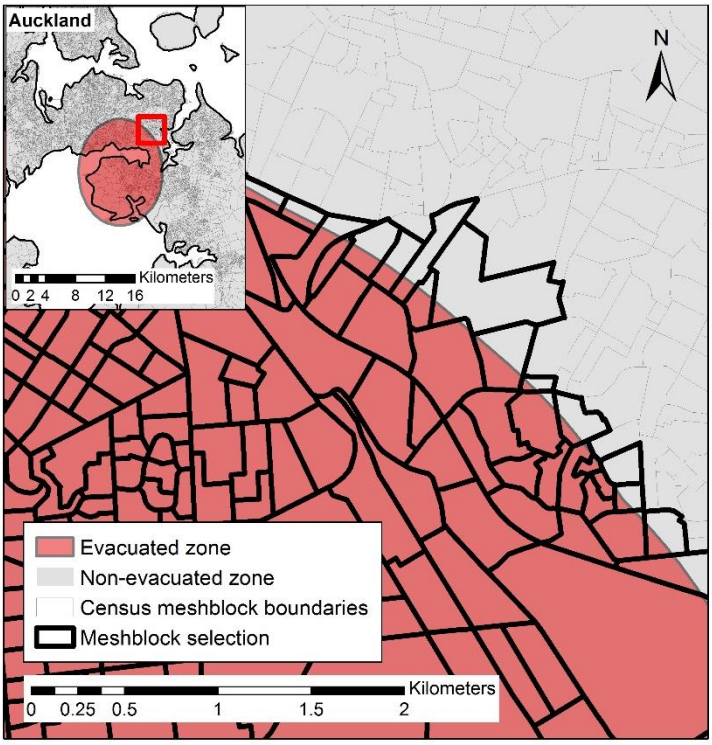

Figure 7.4 Example calculation of displaced populations using census meshblocks (using the Primary Evacuation Zone on 21-30 April for the scenario involving unrest but no eruption). In this case, the thick boundaries indicate the census meshblocks which would be used to calculate the population displaced by the evacuation zone (i.e. night-time resident populations in the meshblocks either completely inside the evacuation zone or which intersect the evacuation zone boundary).

7.5 Level-of-Service Metrics

The suites of LoS metrics developed for road, rail stations, rail lines and ports are shown in Table 7.2, Table 7.3, Table 7.4 and Table 7.5 respectively.

Table 7.2 Road network Level-of-Service metrics. Metrics are descriptive, and the codes are simply used as references and do not necessarily indicate incremental differences in network availability.

Metric code	Road Level-of-Service	Example situations that could lead to LoS
I	Full service – road fully open	
IIa	Reduced service with no direct deposits (no access restrictions)	• Inspection requirements following ground shaking. • Preparatory road maintenance or traffic control measures.
IIb	Reduced service due to direct deposits (no access restrictions)	• Minor tephra accumulations (0.1 – 5.0 mm).
IIIa	Access restrictions with no direct deposits	• New evacuation zones being implemented (e.g. one-way travel to outside of zone) • *Critical routes through evacuation zones (with hazard thresholds for immediate re-closure).*
IIIb	Access restrictions due to direct deposits	• Moderate to severe tephra accumulations

		(>5.0 mm) • Pyroclastic surge, lava flow and lahars
IV	Critical infrastructure and maintenance staff access only	• Lulls in volcanic activity before or during an eruption (within evacuation zones).
V	No service – road closed to all	• Road infrastructure destroyed or severely damaged beyond repair • Road closed due to being in evacuated area.

Consultation with transportation infrastructure managers suggested that lower speed restrictions may be imposed for LoS metric codes II and III, with temporary traffic management measures such as additional signage, cones and/or barriers. Metric codes IV and V would require major traffic management with well signed diversions and potential presence of officials, such as Police or Military staff, and/or physical measures, to ensure compliance. We note that there might be occasional overlaps between metrics. For example, as indicated by the italic text for metric IIIa (Table 7.2), critical routes may be restored through evacuation zones with access restricted (due to operational purposes rather than any deposits) onto and off these routes through the zones themselves. However, deposits may also reduce the LoS somewhat in such areas (e.g. tephra may remain from previous falls or accumulate through secondary deposition from remobilised material – i.e. metric code IIb). Where such overlaps occur, we suggest that the routes of interest be allocated the metric with the largest overall LoS reduction.

Table 7.3 Rail station Level-of-Service metrics.

Metric code	Rail station Level-of-Service	Example situations that could lead to LoS
I	Full service - station fully open	
II	Partial service	• Evacuations - no exit from stopping trains, i.e. entry-only • Limited station facilities due to volcanic hazard damage (e.g. shelter, ticketing, retail).
III	Only used for different purpose	• Line damage renders station inoperable for rail network *(other purposes may include shelter from tephra fall, evacuation welfare facility, and temporary bus stop).*
IV	No service - station closed	• Station destroyed or severely damaged beyond repair • Station closed due to being in evacuated area.

Table 7.4 Rail line Level-of-Service metrics.

Metric code	Rail line Level-of-Service	Example situations that could lead to LoS
I	Full service – line fully open	
II	Restricted service	• New timetabling with fewer services • Speed restrictions due to minor airborne ash.
III	Rolling / temporary outage	• Temporary damage to components due to ground shaking or deposits • Inspection requirements • Re-distribution of fleet.

IV	No stopping service	• Evacuations require transportation of people through evacuated areas • Severe damage to stations and surrounding infrastructure but lines operable.
V	Evacuation service only	• Evacuations require special service to transport residents from newly established evacuation zones.
VI	No service – line closed	• Line destroyed or severely damaged beyond repair • Line closed due to being in evacuated area.

Different suites of metrics are presented for rail stations and lines as the separate components of the rail system could affect end-users in different ways. As with roads, there may be slight overlaps between LoS metrics. For example, evacuation services may also be non-stopping when travelling through much of the evacuation zone. Again, best judgment should be used to determine the largest impact on service and most appropriate LoS metric chosen.

Table 7.5 Port Level-of-Service metrics.

Value	Port Level-of-Service	Example situations that could lead to LoS
I	Full service – port fully open	
II	Partial service	• Volcanic deposits affect operations at the port or navigation of vessels • Evacuation zones affect some navigation routes. • Staff unable to access port facilities.
III	No service – port closed	• Port destroyed or severely damaged beyond repair • Severe sedimentation in shipping channels means vessels cannot operate • Port closed due to being in evacuated area.

For aviation, the LoS is described slightly differently. We consider domestic and international destinations separately. As we focus our studies in New Zealand, we also consider 'trans-Tasman and Pacific island routes' which refers to flights between New Zealand and eastern Australia and some South Pacific island nations. For each market, the LoS is the percent capacity of flights relative to normal airport operations for the time of year. Thus, a LoS metric for aviation could be 50% capacity in the domestic market – this means that half of domestic flights that are normally scheduled to land and depart from the airport are able to do so.

The effects of congestion, accidents and breakdowns on traffic flow are not directly considered for the LoS metrics provided in this study. Although we recognise that such impacts could be substantial at times, further work is required to more accurately understand travel behavior during ashfall to make estimations of traffic demand and flow. Various other constraints will be required to make such estimations including the time of day or day of the week (Tomsen et al. 2014), and considerations of new transportation projects in the area of interest.

7.6 Results and Discussion – Māngere Bridge Scenario

7.6.1 Physical damage

The physical damage to road and rail networks from volcanic hazards which occur in the original Māngere Bridge scenario is summarised in Table 7.6, with maps to illustrate the damage in Figure 7.5 (roads) and Figure 7.6 (rail).

Table 7.6 Physical damage to road and rail networks from geophysical hazards examined in Deligne et al. (companion paper – Appendix E1). A more detailed version of the table, showing network specifics to Auckland can be found in Appendix E5.

Scenario Date	Event Specifics	Road Physical Damage	Rail Physical Damage
22 February	VAL increases from 0 to 1	None	None
08 March	08 March Primary Evacuation Zone (PEZ)		
11 March	11 March PEZ		
12 March	12 March Secondary Evacuation Zone (SEZ)		
13 March	Volcanic gases detected. Shallow earthquakes (up to M_L4.5).	• Potential minor damage and blockages possible (inspections may be required). *Length of road in impacted area ~2,900 km*	<u>Rail stations:</u> • None <u>Rail lines:</u> • Potential damage and blockage on suburban electric network (inspections required). *Southern part more susceptible to ground-shaking due to peat and ash geology.*
14 March AM	Pyroclastic surge causes complete destruction 0-4 km from vent and some damage 4-6 km from vent. Shallow earthquakes (up to M_L4.5).	• Road infrastructure destroyed or severely damaged 0-4 km from vent. • Some road infrastructure damaged with major blockages 4-6 km from vent. • Additional damage/blockage the same as 13 March. *115 km destroyed.* *202 km severely damaged with complete blockage.* *457 km some damage and major blockages*	<u>Rail stations:</u> • Two stations close to vent destroyed or severely damaged beyond repair. • Possible damage to stations 4- 6 km from vent. <u>Rail lines:</u> • Lines up to 4 km from vent destroyed or severely damaged • Possible damage to lines 4-6 km from vent. • Potential damage and blockage on suburban electric network (inspections required).
14 March PM	Tephra fallout to west. Shallow earthquakes (up to M_L4.8).	(Also see Figure 7.5a) • Tephra deposition on some minor roads to west of vent. • Additional damage/blockage the same as 13 March. *163 km outside of the initial surge area experiences direct tephra deposition.*	(Also see Figure 7.6a) <u>Rail stations:</u> (same as 14 March AM) <u>Rail lines:</u> (same as 14 March AM) *Tephra fall to west does not directly fall on the rail network. Remobilised ash may reach some lines but no impacts are anticipated.*

		Remobilised ash may extend to roads beyond the area mentioned but no substantial impacts are anticipated.	
16 March	11 March PEZ and 12 March SEZ lifted. 16 March PEZ and 16 March SEZ implemented	• Minor accumulation of deposits remain on cleaned sections including critical routes through SEZ. • Other sections within initial surge area remain destroyed, damaged or blocked. • Tephra deposition is cleaned-up or removed by rainfall beyond the SEZ extent. *Any minor damage from previous earthquakes has been repaired with no further impacts to the road network at this stage.*	Rail stations: (same as 14 March AM) Rail lines: • Damage within 6 km from vent remains same as 14 March AM *Any damage to components from previous earthquakes is repaired with no impact to the rail network beyond 6 km from the vent at this stage.*
21 March	Tephra fallout to north west. Pyroclastic surge.	(Also see Figure 7.5b) • Some further accumulation of surge and tephra deposits up to 6 km from vent. • Tephra deposition on roads to north west of SEZ *984 km road beyond the initial surge area experiences tephra accumulation. Thus, a total of 1,758 km of road is impacted at this stage* ***(the largest extent throughout the scenario).***	(Also see Figure 7.5b) Rail stations: (same as 14 March AM) Rail lines: • Damage within 6 km from vent remains same as 14 March AM. • Possible damage to rail components on lines affected by tephra fall to north west of SEZ. *Initial damage from ash accumulation beyond the SEZ is fixed by late on 22 March. However, some failures may continue due to ash remobilisation on the network.*
30 March	Tephra fallout to south east.	• Only minor accumulation of deposits on cleaned critical routes. *All other roads within initial surge area remain destroyed, damaged or blocked to some degree.*	Rail stations: (same as 14 March AM) Rail lines: (same as 16 March, before tephra fall)
05 April	Lava flows. 16 March SEZ lifted.	(Also see Figure 7.5c) • Continued clean-up of remobilised tephra, means only minor accumulation of deposits remains on many critical routes. *All other roads within initial surge area remain destroyed, damaged or blocked to some degree, although are widely accessible from this date for clean-up following the lifting of the SEZ.*	(Also see Figure 7.6c) Rail stations: • Two stations closest to vent remain destroyed by initial surge. *Previous damage to other stations within 6 km of vent is repaired.* Rail lines: (same as 16 March, before tephra fall) *Possible damage from tephra continues 4-6 km from vent until clean-up prevents further remobilisation and infiltration.*
01 May	16 March PEZ lifted. **Permanent exclusion zone implemented.**	• Restoration has occurred beyond the extent of the severe damage / complete blockage zone caused by the initial surge (0-4 km from the vent). *The road length in this area at the start of the scenario was 305 km.*	Rail stations: (same as 05 April) Rail lines: • Lines remain destroyed up to 4 km from vent *Demand to reconstruct the infrastructure required to reopen this line is expected to be low. The stations and line may be decommissioned or relocated based on rebuild activities.*

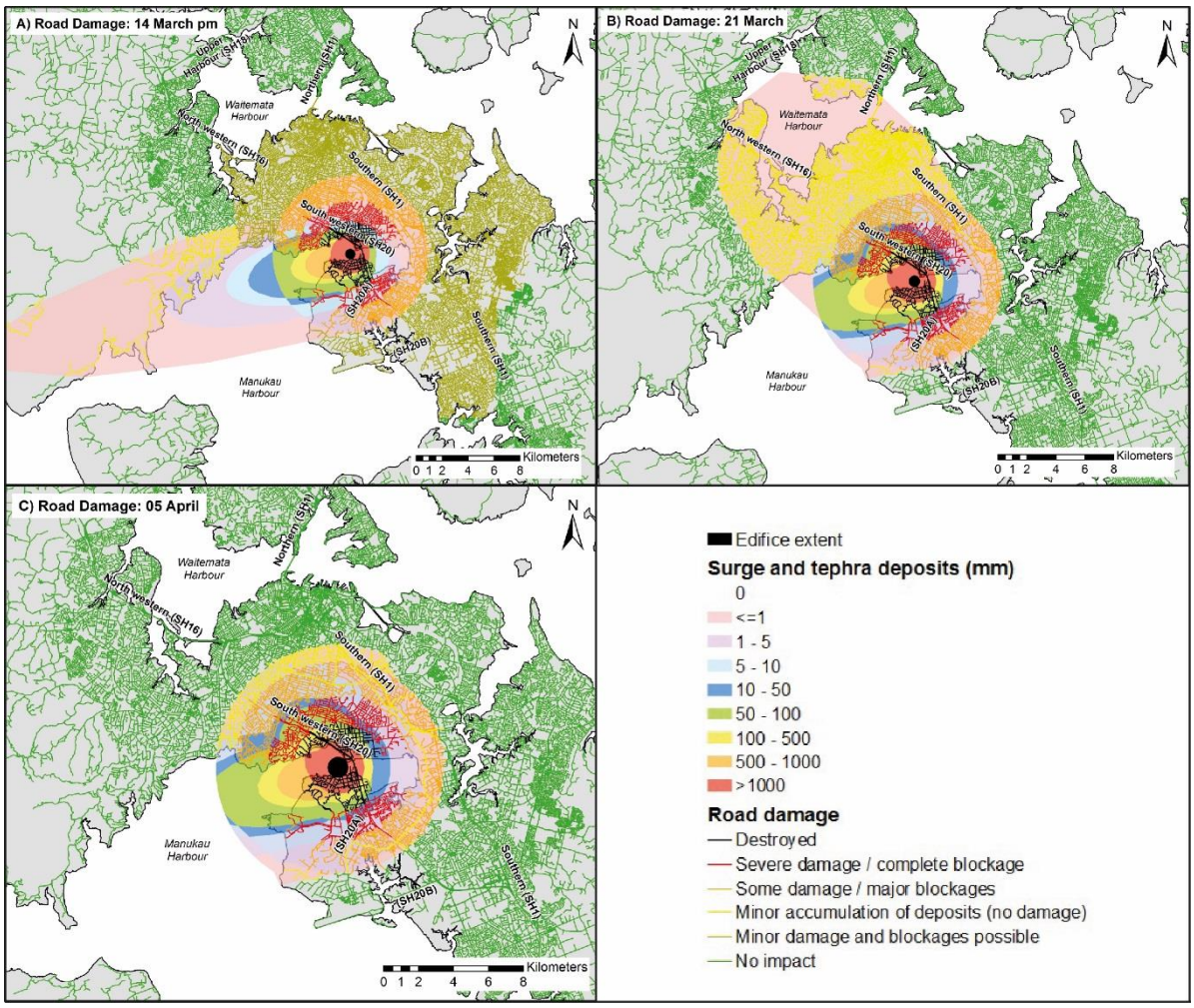

Figure 7.5 Physical damage to the road network at a selection of key times during the scenario. Note that the full series of physical damage road maps can be seen in Appendix E6.

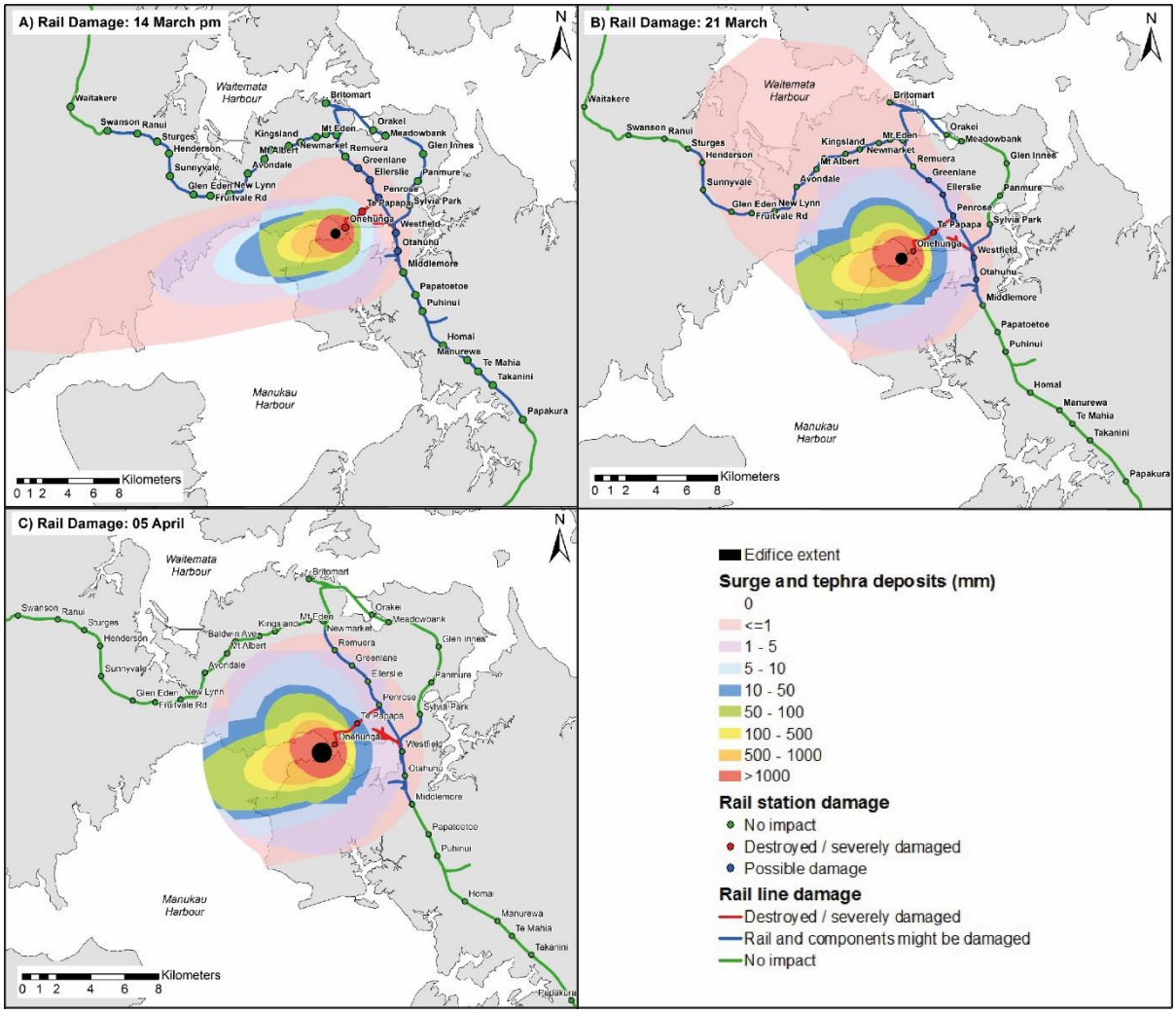

Figure 7.6 Physical damage to the rail network at a selection of key times during the scenario. Note that the full series of physical damage rail maps can be seen in Appendix E7.

Most physical damage to road and rail transportation results from the initial pyroclastic surge on 14 March in the scenario, which was derived from the following radial damage thresholds:

- Destroyed: <0.5 km (average-case), <2.5 km (worst-case)
- Severe damage / complete blockage: 0.5 – 2 km (average-case), 2.5 – 4 km (worst-case)
- Some damage / minor blockages: 2 – 4 km (average-case), 4 – 6 km (worst-case).

We note that surges in other locations may require the modification of radial distance thresholds, considering the dynamic pressures expected from different eruption styles, and specific infrastructure types.

Other damage and potential blockage of networks in our scenario result from ground shaking due to earthquakes and tephra fall. These effects are generally more temporary with road-cleaning and inspections occurring soon after each hazard where possible to restore functionality. The general priority is to repair and maintain critical north-south links through the southern isthmus. However, the effects of ash remobilisation on transportation could be substantial and extend the temporal and spatial extent of impacts. Detailed ash resuspension modelling, such as that conducted by Reckziegel et al. (2016), would be required to investigate these impacts more fully.

Auckland Airport does not encounter any direct physical damage from any volcanic hazards over the course of the scenario. However, it is indirectly impacted by restricted access (due to evacuation zoning, and volcanic hazards affecting roads nearby), airspace restrictions, and physical damage to other critical infrastructure such as the wastewater system (Stewart et al. companion paper).

Only one of the ports in Auckland, the Port of Onehunga, the smallest and arguably least important of the facilities, is directly impacted by geophysical hazards in the original Māngere Bridge scenario. However, the facilities at the port are closed due to the effects of evacuation zoning (on 08 March) before being destroyed by pyroclastic surges (on 14 March), which results in permanent closure. The eruption changes the landscape where the Port of Onehunga used to be and also devastates the local built environment. A rebuild would not be practical at the same site as the area becomes landlocked. However, it is possible that another port elsewhere in the Manukau Harbour, or indeed somewhere else in the Auckland region, would be built.

The Port of Auckland at Waitemata Harbour is not directly impacted in the original Māngere Bridge scenario. No major damage or substantial LoS reduction is expected from earthquakes, and tephra accumulation over much of the Port of Auckland on 21 March is <1 mm thick, which is not deemed substantial enough to close port operations (although indirect impacts such as access restrictions may have cascading implications for port operations). However, different wind directional profiles may have consequences for tephra thicknesses at the port and subsequent LoS (Section 7.6.4.1).

7.6.2 Level-of-Service

Table 7.7 details the considerations for assigning LoS metrics to the road and rail (station and line) network, and to Auckland Airport over the course of the scenario. This is followed by a selection of associated time-series maps for road (Figure 7.7) and rail (Figure 7.8) to illustrate LoS metrics at key stages in the scenario, in addition to a table to show specific LoS metric values (based on capacity and guided by policy) for Auckland Airport (Table 7.8).

Table 7.7 Level-of-Service descriptions for Auckland's road, rail and airport transportation networks over the course of the Māngere Bridge scenario. A more detailed version of the table, showing network specifics to Auckland can be found in Appendix E8.

Scenario Date	Event Specifics	Road Level-of-Service	Rail Level-of-Service	Airport Level-of-Service
22 February	VAL increases from 0 to 1	Full service. *Note. Some self-evacuation and preparation for evacuation may lead to increase in traffic congestion.*	Full service. *Some self-evacuation may lead to increase in passengers and delays at stations.*	Auckland Airport starts making plans for a potential closure.
08 March	08 March PEZ implemented	• Evacuations occur from the PEZ. Access becomes restricted for most entering the zone. Some critical lifelines staff can still enter. • All road transport between north and south Auckland is disrupted. *All other infrastructure remains fully operational, although some measures may be implemented to control evacuation flow.* *784 km road affected by 08 March PEZ.*	Rail stations: • Partial service within PEZ Rail lines: • Evacuation service only on lines within and intersecting PEZ (with speed restrictions) *Restricted service may occur on the remaining suburban electric rail network from now onwards due to timetable changes and redistribution of fleet.*	Auckland Airport issues NOTAM indicating airport closure. Minor domestic traffic at other airfields. Most domestic traffic possibly diverted outside of region.
11 March	11 March PEZ implemented	• No access to roads affected by the initial PEZ on 08 March except critical lifelines staff. • Evacuations occur from a new PEZ section in the Māngere area. Access is restricted for most. *1019 km road is now affected by the new wider (11 March) PEZ.*	Rail stations: • Stations within 08 March PEZ now closed. • Partial service within newly established PEZ area. Rail lines: • Lines affected by 08 March PEZ now closed. • Evacuation service only on lines affected by new PEZ area *Diesel freight through-traffic ceases.*	Auckland Airport issues NOTAM indicating that the airport is within evacuation zone.
12 March	12 March SEZ implemented	• No service (roads closed) in area covered by 11 March PEZ. • Evacuations occur from SEZ with restricted access for most. • Some measures may be implemented elsewhere to control evacuation flow. *1415 km road is now affected by evacuation*	Rail stations: • Stations affected by 08 and 11 March PEZ now closed. • Partial service within newly established SEZ. Rail lines: • Lines affected by 08 and 11 March PEZ now closed.	

		zones (11 March PEZ and 12 March SEZ).	• Evacuation service only on lines affected by new SEZ.	
13 March	Volcanic gases detected. Shallow earthquakes (up to M_L4.5).	• No service (roads closed) in area covered by 11 March PEZ and 12 March SEZ. • Reduced service possible on roads impacted by ground shaking from earthquakes.	<u>Rail stations:</u> • Stations within evacuation zones closed. <u>Rail lines:</u> • Lines directly affected by evacuation zones closed. • Rolling outages on remainder of suburban network.	
14 March AM	Pyroclastic surge causes complete destruction 0-4 km from vent and some damage 4-6 km from vent. Shallow earthquakes (up to M_L4.8). VAL increases from 2 to 3.	• LoS in morning remains the same as 13 March. *Impact on electricity transmission and distribution may affect road LoS for the entire Auckland region.*	• LoS remains the same as 13 March.	No air traffic in or out of Auckland Airport.
14 March PM	Tephra fallout to west. VAL increases from 3 to 4. Clean-up outside of SEZ begins (for ~1 day). Some critical routes also cleaned through SEZ.	• Tephra in afternoon causes reduced LoS on some arterial and minor roads to west of vent.		
16 March	11 March PEZ and 12 March SEZ lifted. 16 March PEZ and 16 March SEZ implemented. VAL 2 (after reducing to 3 on 15 March).	• Road service restored on roads beyond new 16 March PEZ and SEZ extents. • Partial road service on some critical routes through evacuation zones during daytime. • No service on all other roads within PEZ and SEZ.	<u>Rail stations:</u> • Station within new evacuation zones closed. <u>Rail lines:</u> • Lines within or intersecting new PEZ closed. • No stopping (with speed restrictions) occurs through new SEZ. *Some diesel freight services restored with restrictions due to operational infrastructure damage.* *New timetabling may be implemented on remainder of suburban rail network.*	Auckland Airport issues NOTAM indicating it is no longer in evacuation zone but that airport remains closed.
21 March	Tephra fallout to north west. Pyroclastic surge. VAL 4 (after increasing to 3 on 18 March).	• No service (roads closed again) through PEZ and SEZ due to threat from surge and tephra fall. • Tephra deposition causes reduced service on many roads to north west of SEZ.	<u>Rail stations:</u> • (same as 16 March) <u>Rail lines:</u> • Same as 16 March except for rolling outages and	Volcanic eruption resumes. No air traffic in or out of Auckland Airport.

22 March	Tephra. VAL reduces to 3. Clean-up outside of PEZ and SEZ begins (for ~1 week). Some critical routes also cleaned through PEZ and SEZ.	• LoS remains the same on roads to north west affected by 21 March tephra. • Partial service restored on major critical routes through SEZ from north to south. • Some critical lifelines staff can enter SEZ. • No service elsewhere within PEZ and SEZ.	speed restrictions on lines affected by new tephra. *Rolling outages are expected to be short-lived (until late on 22 March). However, further outages are possible due to ash remobilisation.*	
30 March	Tephra fallout to south east.	• Full service restored to roads beyond SEZ affected by 21 March tephra fall. • Service within PEZ and SEZ remains same as 22 March except some further critical routes which are reopened during daytime.	<u>Rail stations:</u> • (same as 16 March) <u>Rail lines:</u> • Same as 21 March except restoration of service when recent tephra fall occurred outside SEZ.	
05 April	Lava flows. 16 March SEZ lifted. Major clean-up operation within lifted SEZ begins (for ~1 month).	• Further critical routes through the now lifted SEZ are re-established with partial service. • Only reduced service due to tephra deposits remain on some roads beyond the outer initial surge. • Very limited access occurs on roads affected by the initial surge deposit up to the extent of the previous PEZ. • No service (roads closed) within PEZ.	<u>Rail stations:</u> • Only stations within PEZ remain closed. <u>Rail lines:</u> • Lines within or intersecting PEZ remain closed. • Speed restrictions on lines affected by previous SEZ. *All diesel freight services restored.*	Auckland Airport issues a NOTAM indicating it remains outside of the evacuation zone with new evacuation orders in place. Airport is re-opened with minimal service.
08 April				Auckland Airport resumes full operations.
16 April	VAL reduces to 2.			Auckland Airport issues a NOTAM that VAL has decreased.
01 May	16 March PEZ lifted. Permanent exclusion zone implemented. VAL reduces to 1. Major clean-up operation within lifted PEZ begins (for ~1 month).	• Full service restored to all roads beyond 4 km from the vent. • Very limited access 2-4 km from the vent. • No service (remaining roads closed indefinitely) 0-2 km from the vent.	<u>Rail stations:</u> • Stations closed on 05 April remain closed for coming months. <u>Rail lines:</u> • Some lines closed on 05 April remain closed for coming months.	Auckland Airport partially re-opened.
01 June	VAL reduces to 0.			Auckland Airport re-opens.

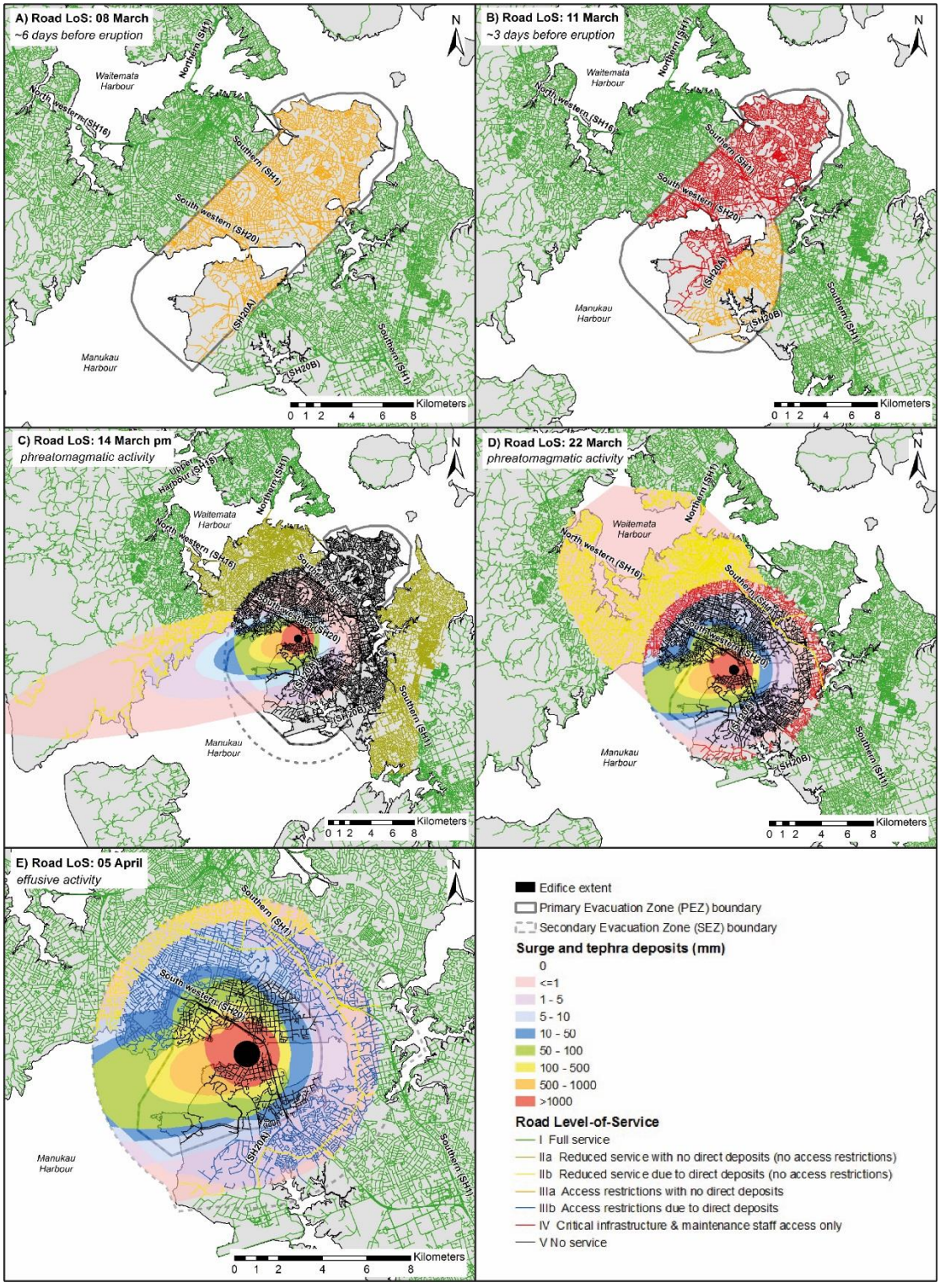

Figure 7.7 Level-of-Service metrics for the road network at a selection of key times during the scenario. Note that the full series of Level-of-Service road maps can be seen in Appendix E9.

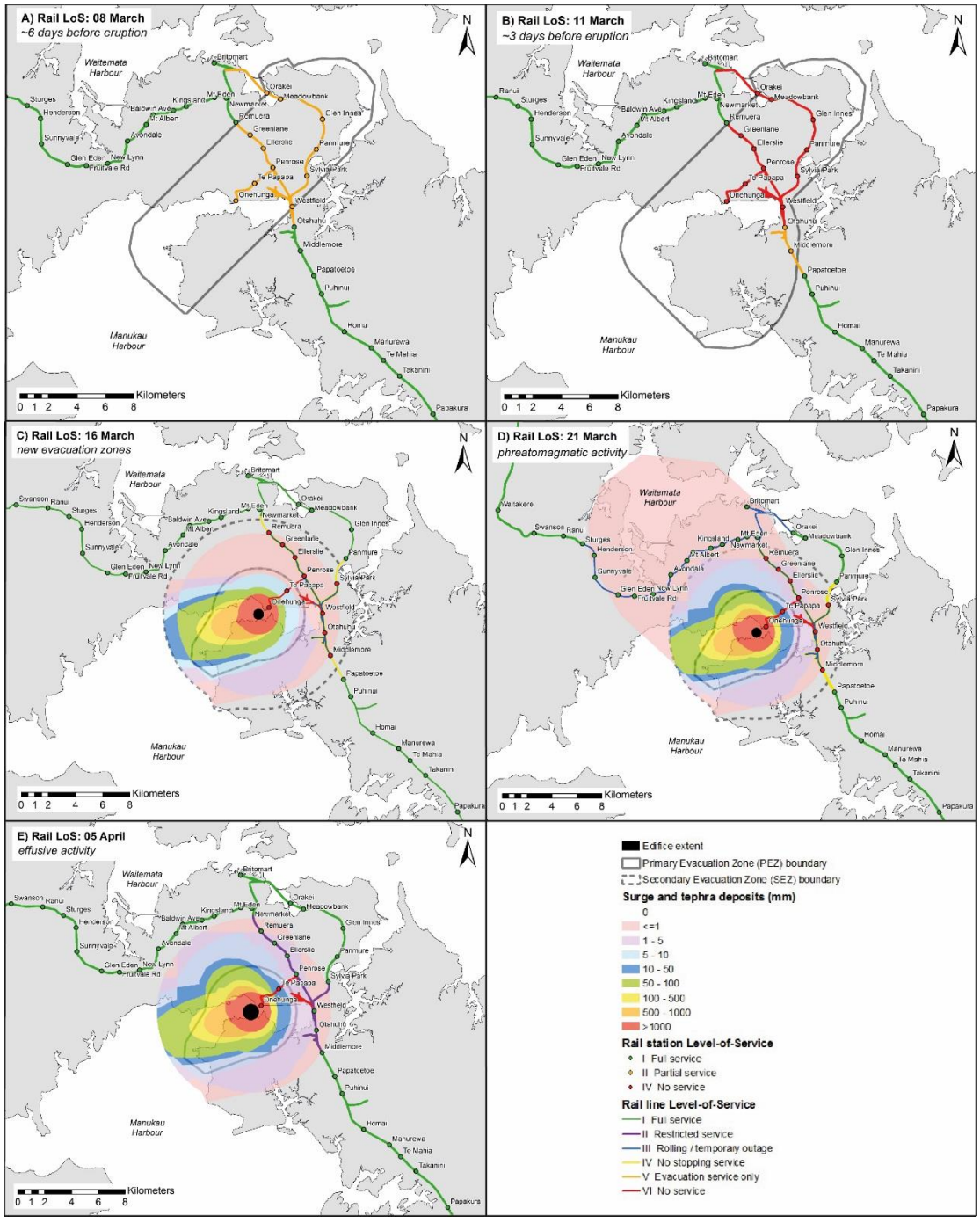

Figure 7.8 Level-of-Service metrics for the rail network at a selection of key times during the scenario. Note that the full series of Level-of-Service rail maps can be seen in Appendix E10.

Table 7.8 Changes in Level-of-Service metric percentage values for Auckland Airport for the Māngere Bridge scenario. Percentage values indicate the capacity with 100% = 'typical' operating capacity and 0% = no capacity.

Scenario Date	Domestic	Trans-Tasman and Pacific Islands	International
22 February	100	100	100
08 March	80	50	50
11 March	5	0	0
14 March	0	0	0
16 March	5	0	0
21 March	0	0	0
05 April	10	0	0
08 April	80	25	10
16 April	80	30	10
01 May	80	50	10
01 June	80	80	25
15 June	100	100	100

Importantly, the LoS for all transportation modes is affected by evacuation zoning before the modes are impacted by geophysical hazards and experience any physical damage. LoS reductions occur from 08 March onwards for all modes, the scenario date when the first PEZ is implemented. This includes the closure of a major highway (SH20), which is expected to lead to increased traffic on alternative arterial and highway routes. In the Māngere Bridge scenario road and rail encounter the greatest overall LoS loss on 13 and 14 March, and all north-south ground transportation links across the southern isthmus are blocked at this time. Some service is restored on 16 March, although subsequent tephra fall and threat of surges on 21 March causes secondary temporary disruption. The strength and direction of wind on 22 March in the Māngere Bridge scenario mean that the impact of tephra fall then is minimal, and restoration is possible again from this date forward. However, full restoration takes several weeks for most road and rail transportation networks in the area extending 4 km radially from the vent, even following the end of effusive activity. Some infrastructure within 2 km of the vent is permanently destroyed.

LoS reduction also starts on 08 March at Auckland Airport. From 08 March to 01 May, VALs determine the volume of airspace affected by volcanic ash, described by NOTAMs that invoke VHZs. During this time, air traffic control will not clear aircraft to operate on routes that infringe a VHZ, unless specifically requested by the pilot during daylight hours only (AIP NZ, 2016). Auckland Airport is only within evacuated areas on the ground from 11-15 March. Ardmore and Whenuapai airfields are outside evacuated areas for the duration of the scenario and are within VHZs for shorter periods than Auckland Airport; they may be used for some aircraft diversions from Auckland Airport at times. As the Auckland Airport runway is roughly oriented east-west and the Māngere Bridge scenario vent location is to the north, the flight approach shouldn't be substantially compromised by the VHZ implemented at VAL 1. However, airport officials indicated that it would take a few days for international airlines to

start flying into Auckland again once they are allowed to land, in part due to the time it would take to reorganise schedules and redistribute aircraft.

Onehunga Port closes on 08 March when it falls within evacuation zones, and all vessels are diverted elsewhere (i.e. LoS metric code III). No LoS is restored in the same location as the port is subsequently destroyed by pyroclastic surges from 14 March onwards.

We do not apply metric code III ("only used for a different purpose") for rail stations for any of the timesteps in the scenario. This is because stations that are inoperable for rail operations often fall within evacuated areas and would thus not be suitable for any other purpose. Additionally, the detailed information required to allocate this metric is beyond the scope of this paper. Similarly, metric code II for rail lines ("restricted service") has only been allocated where speed restrictions are expected due to minor airborne deposits; consultation with rail network managers suggested that speeds of 40 km h^{-1} would be typical in such situations on Auckland's network. Restrictions are likely on other sections of the network during this scenario. However, often the more severe LoS reduction of "rolling outages" (i.e. metric code III) occurs at the same time and we adopted this metric where the two exist simultaneously. Timetabling restrictions may occur at times across other parts of the suburban network. However, as we do not consider knock-on consequences in detail in this study and as rail demand is unknown, the potential for new timetabling is simply noted in Table 7.7 and the associated LoS metric (i.e. metric code IV for rail lines) is not displayed on Figure 7.8. In future scenarios involving a predominantly diesel fleet, which is impacted by minor tephra fall, metric code II should be considered over code III in some situations due to the potentially higher resilience of diesel locomotives (over electric alternatives) in such conditions. However, observational data of such impacts is limited and we suggest a conservative approach be taken (adopting the more severe of the two LoS metrics) in situations where epistemic uncertainty is high.

Specific LoS metric values are not calculated for road or rail networks for the Māngere Bridge scenario. Although we do make calculations for the expected numbers of displaced residents due to evacuation zones with potential implications for transportation (Section 7.6.3), further work is required to more accurately understand the impacts on traffic demand and flow and thus allow estimations of proportional network availability from what is typical in Auckland. Furthermore, new transportation projects in the city (e.g. Waterview Connection (NZTA 2016a), City Rail Link (Auckland Transport 2016), East West Link (NZTA 2016b)) may have substantial impacts on network capacity with knock-on implications for traffic demand and flow. Nonetheless, the allocation of LoS metric descriptors using a scenario approach as demonstrated in this study is an important contribution in representing the disruption encountered by transportation end-users.

7.6.3 Displaced populations and consequences for transportation

Displaced population numbers during the Māngere Bridge scenario resulting from the evacuation zones of Deligne et al. (companion paper – Appendix E1) are shown in Table 7.9. We expect some residents beyond official evacuation zone boundaries will also evacuate, causing a *shadow evacuation* effect. The concept of shadow evacuation in Auckland aligns with discussions in Tomsen et al. 2014 and with findings from a recent risk perception survey conducted in the city (Coomer et al. 2015). As indicated in Deligne et al. (companion paper – Appendix E1), there may also be self-evacuations before official evacuation zones are established and different evacuation conditions for some patients in major hospitals. However, the numbers of self-evacuees and relevant patients is unknown and not shown in Table 7.9.

Table 7.9 Displaced populations during the Māngere Bridge scenario. Note that shadow evacuees are calculated as the total number of residents within 1 km from the outer evacuation zone boundaries to align with the findings in Coomer et al. (2015) where relevant.

Scenario Date	Total Evacuees
21 February	0
22 February – 07 March	*(potential for self-evacuation – number unknown)*
08 – 10 March	199,200
11 March	253,700
12 – 15 March	434,300 (incl. 72,300 shadow evacuees)
16 March – 04 April	275,900
05 - 30 April	57,300
01 May onwards	8,700

During volcanic activity in the Māngere Bridge scenario, large populations are evacuated, with the highest displacement totals on 12-15 March. Emergency management officials may try to encourage evacuations in a progressive manner in some eruptive situations, particularly to minimise traffic disruption. Auckland road network operators indicated that during evacuations from city areas in Auckland, on-ramp signals to highways will likely be set to operate on typical peak weekday evening settings with the aim of assisting traffic flow along highways but potentially causing additional congestion along arterial routes that lead to highways. Evacuation zone boundaries would usually be managed so that residents are prevented access to their homes. Business owners and workers would also be prevented from accessing their properties, which can have cascading impacts on other businesses due to disruptions in the supply chain. Transportation may be impacted in such situations through having to relocate headquarters or operation centres, and from disruption to the supply of materials or components required for transportation maintenance or repair. Additionally, businesses can suffer when staff members are displaced or have uncertainty in their living

situation, an important consideration for all transportation operators and highlighted several times through consultation. For example, further transportation disruption would result if there are shortages of pilots, train drivers, rail maintenance crew or officials that control traffic flow and manage accidents.

7.6.4 Alternative scenario considerations

We applied our methods for determining damage and LoS to assess the consequences of modifications to the geophysical hazard sequence in the original Māngere Bridge scenario, specifically different wind directions and unrest with no eruption. This allows us to assess differences in societal outcomes, particularly related to transportation.

7.6.4.1 Predominant south-westerly wind

Tephra deposits from the same individual eruptions as in the original Māngere Bridge scenario (Deligne et al., companion paper – Appendix E1), but modelled in TEPHRA2 using the south-westerly wind profiles (Appendix E3), are shown in Figure 7.9. No change to impact or LoS at Auckland Airport is expected from the different tephra deposition, with most disruption still resulting from evacuation zoning, VAL changes and VHZ areas (which would remain the same). However, the disruption to road and rail networks, as well as operations at ports is expected to be more severe, especially because of greater tephra accumulation on Auckland City and critical routes. Expected consequences from the revised tephra deposits include:

- Greater physical damage and LoS reduction on 14 March; tephra covers most of the central city area rather than being deposited towards the west. This coincides with the timing and spatial extent of the largest evacuation zone and area potentially affected by earthquakes.
    - Complications managing evacuations and inspecting road and rail networks for physical damage from the earthquakes are expected due to the additional tephra hazard (up to 50 mm in places outside of the PEZ).
    - A decision may be made to extend the extent and/or duration of evacuation zones established on 12 March to reflect increased LoS reduction on transportation networks.
    - Critical north-south links through the southern isthmus would likely take longer to restore.
    - Substantially more resources will be required for clean-up of tephra in this urban area once access to the PEZ is permitted.
    - Unlike the original Māngere Bridge scenario, the Port of Auckland at Waitemata Harbour may be affected (by up to 5 mm of tephra). Both the port itself and maritime navigation in the Waitemata Harbour may encounter reduced LoS due to tephra fall and associated visibility impairment (Blake et al. in review c).

- With tephra being dispersed further east on 21 March, the central city area is less affected by this event than in the original scenario. However, disruption to road and rail is expected to be as, if not more, severe due to critical north-south links receiving greater accumulation of tephra. The restoration of any links through the evacuation zones would be unlikely before new tephra deposition on 22 March.
- The new wind profiles on 22 and 29-30 March cause substantially different tephra deposition patterns to the original scenario with much more widespread effects.
    - As on 14 March, LoS reduction would occur on transportation routes through the city area, again including the Port of Auckland, which may receive up to 5 mm ash on 22 March.
    - Further tephra accumulation on north-south links through the southern isthmus also occurs.
    - The spatial extent and duration of evacuation zones may be increased and clean-up activities would take longer than in the original scenario.

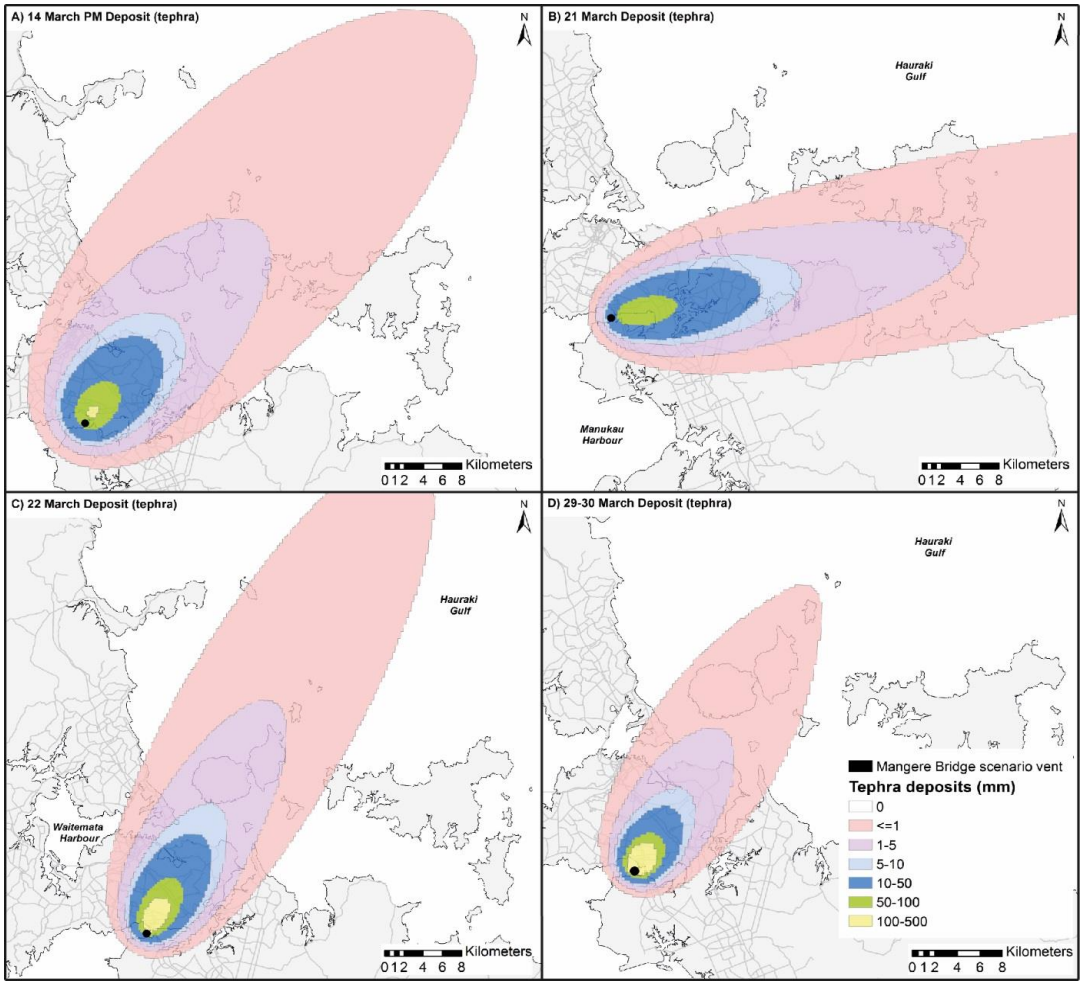

Figure 7.9 Tephra deposits for the four tephra plume-producing eruptions during the Māngere Bridge scenario, modelled using south-westerly wind profiles.

During this scenario modification, it is expected that north-south ground transportation routes will be completely blocked (or only partially accessible at best) for a total period of ~2 weeks. There may also be a higher number of displaced residents due to the more persistent nature of tephra fall over highly populated areas and different evacuation zones. Therefore, in addition to expected disruption on maritime and aviation transportation, the provision of sufficient accommodation, food and other resources in Auckland City should be carefully considered.

7.6.4.2 Unrest with no eruption

The geophysical hazard sequence for the alternative to the Māngere Bridge scenario involving an unrest sequence with no eruption is shown in Table 7.10.

Table 7.10 Geophysical hazard sequence for the unrest sequence with no eruption. Italicised text indicates where the geophysical hazard and monitoring sequence remains consistent with the original Māngere Bridge scenario (i.e. Deligne et al. companion paper – Appendix E1).

Scenario Day	Geophysical Hazards and Monitoring "Observations"
19 February	*Small swarms of high-frequency (non-volcanic) earthquakes.*
22 February	*Swarm of low frequency earthquakes at 39–45 km depth (*M_L*1.8–2.2).*
01-05 March	*125 mostly low frequency earthquakes at 34–45 km depth (*M_L*1.8–2.2).*
07-10 March	*Some high frequency earthquakes, increasing in magnitude and shallowing. Swarms with up to 300 quakes per day. Ground deformation detected.*
11 March	*Seismic activity becomes focussed in the Māngere area.*
12-13 March	*Volcanic gases detected. Some high frequency earthquakes, increasing in magnitude and shallowing. Swarms with up to 300 quakes per day.*
14 March (early)	*Tremor earthquakes, acceleration of deformation. Visual observation of cracking near Māngere, Volcanic gases increase.*
14 March (late) – 19 March	Number and magnitude of earthquakes decreases. Deformation and gas level reduction.
20-31 March	Swarm of ~3,000 earthquakes at 5-10 km depth. Most are <M_L3.5, but during peak of activity on 29 March, 8 earthquakes of M_L4.0 or greater occur, including a M_L5.3 event (some structural damage from the larger earthquakes). ENE-trending 8 km long surface rupture accompanies largest earthquakes (with the direction determined from the direction of the inferred Manukau fault in the area (Kenny et al., 2012)). Gas levels increase slightly.
01 April	Number and magnitude of earthquakes decreases dramatically.
02-13 April	Seismicity remains at relatively constant low level, except for a few increases in event rate, which last less than 6 hrs. No gas emissions detected.
14 April	Seismicity diminishes to typical background levels.

Damage from the geophysical hazard sequence would thus be very different to that in the original scenario, the majority of which would occur due to ground shaking and surface rupture. As with the evacuations in the original Māngere Bridge scenario (Deligne et al.

companion paper – Appendix E1), we develop evacuation zones for the alternative sequence through information derived from the AVF Contingency Plan (Auckland Council 2015) and Auckland Evacuation Plan (Auckland Council 2014):

- The same evacuation zones are used up until and including 15 March.
- On 16 March, evacuation zones are revised due to continued unrest focused on the Māngere area and overall decrease in seismicity, deformation and gas levels.
    - The PEZ consists of a 3 km buffer from the extent of the probable vent location area determined on 12 March.
    - Unlike the original scenario, the SEZ now remains the same as on 12 March (5 km from the probable vent location area) (Figure 7.10d).
- On 21 April, one week after the decrease in seismicity to around background levels, the SEZ is removed (Figure 7.10e).
- Following seismic inactivity, the size of the PEZ is reduced on 01 May so that previously included 1 km buffer is removed (the PEZ now covers the same area as the 12 March probable vent location) (Figure 7.10f).
- One month later on 01 June, the PEZ is removed, allowing the return of residents to all areas and use of all transportation routes and facilities.

We note that some areas where PEZs and SEZs are removed may temporarily transition to *restricted recovery zones* or similar due to the potential effects of previous volcanic activity on re-habitation such as inspection and service restoration requirements. These are not displayed on Figure 7.10 but may occur on 16 March – 20 April (in the area to the north east of the vent) and on 21 – 30 April (in the area where the SEZ is removed).

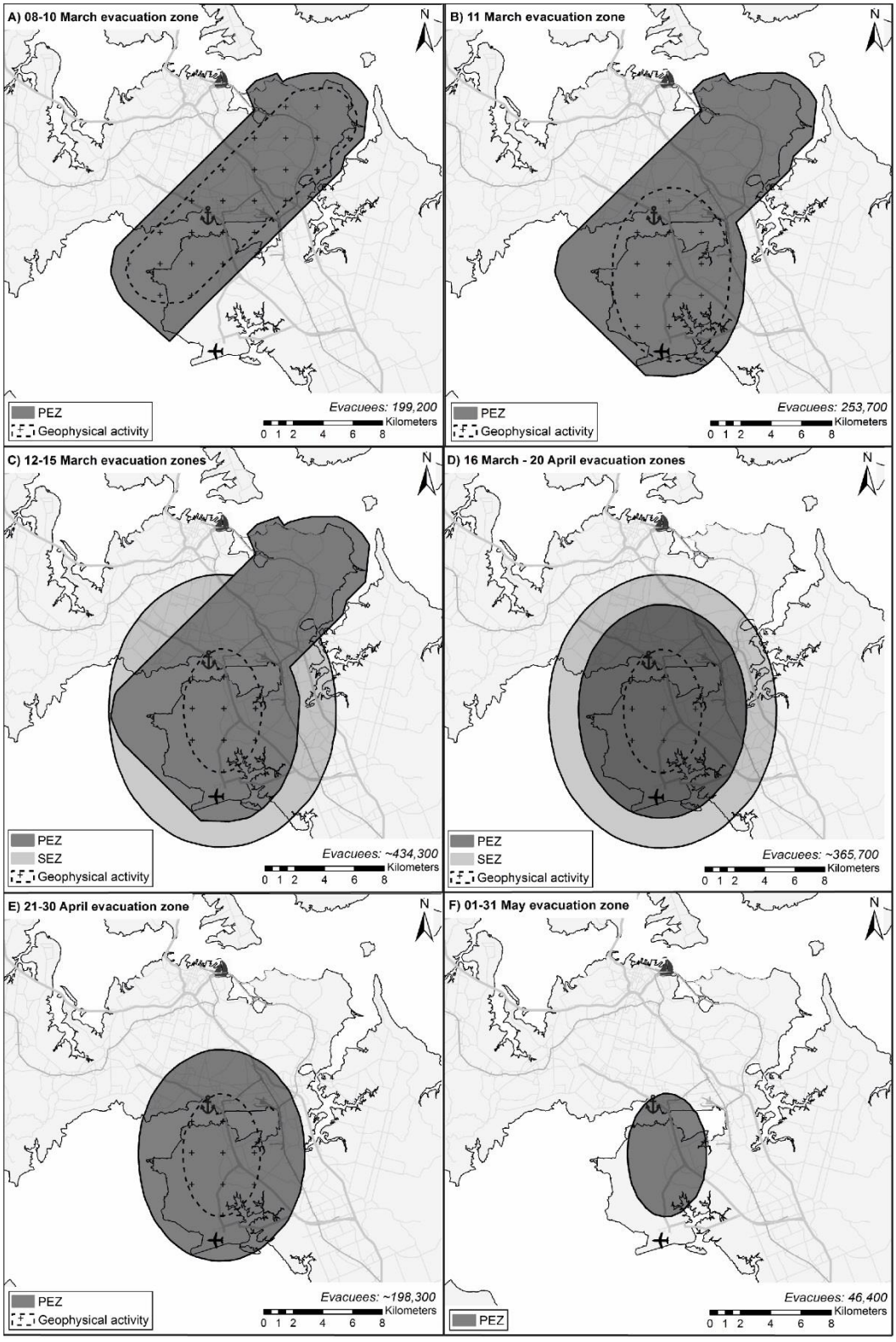

Figure 7.10 New Primary and Secondary Evacuation Zones established for the modified scenario involving unrest but no eruption. Note that the same evacuation zones established for the original Māngere Bridge scenario are used up until and including 15 March (7.10a-7.10c – adapted from Deligne et al., companion paper – Appendix E1).

Figure 7.11 shows the expected population displaced by the original Māngere Bridge scenario compared to the modified scenario. We suggest that up to 434,300 residents would seek alternative accommodation at times during the eruptive sequence of the original Māngere Bridge scenario (accounting for the shadow evacuation effect). However, business activities would also be affected and forced to relocate (e.g. Seville et al. 2014). An estimated 8,700 residents are permanently displaced by the eruption. In the alternative scenario involving unrest but no eruption, the maximum number of displaced residents is the same as for the original scenario (both on 12 March). However, from 16 March until 01 June, there is a higher number of displaced people overall despite fewer geophysical hazards and less damage.

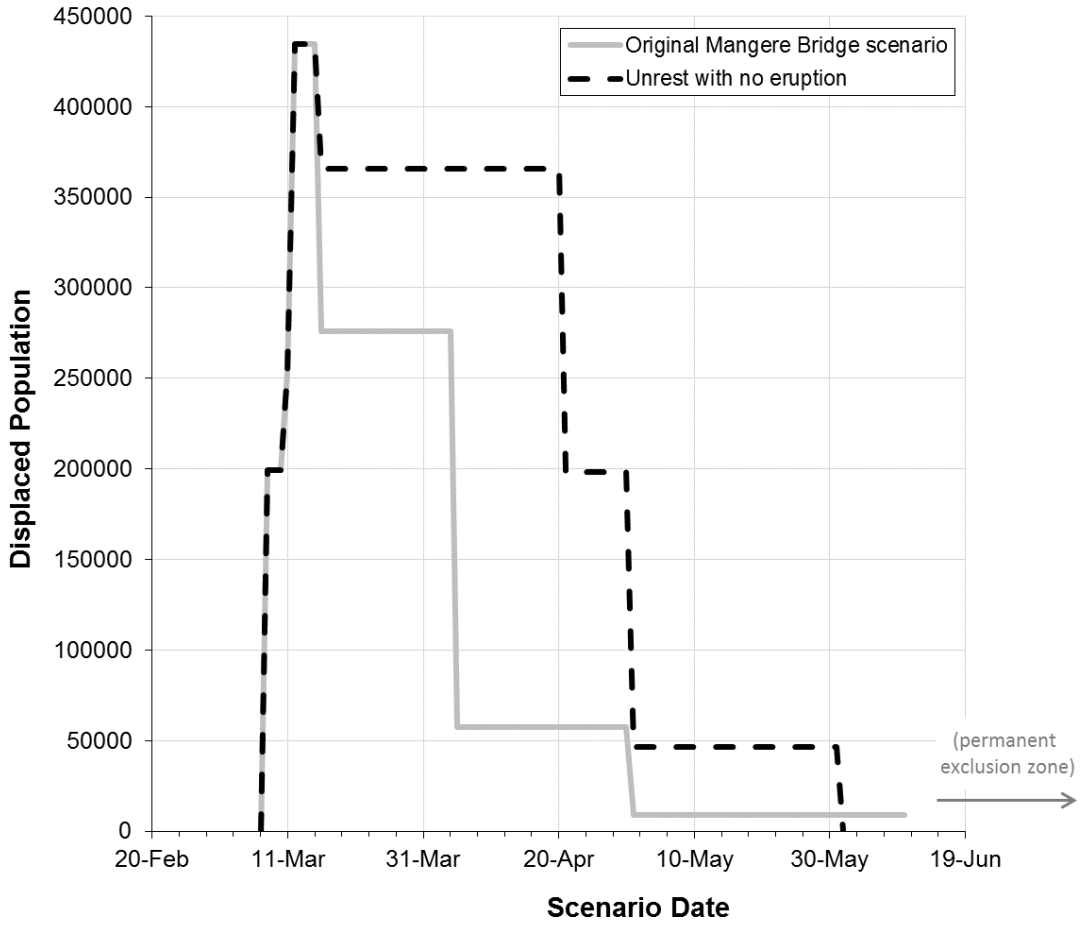

Figure 7.11 Displaced populations during the original Māngere Bridge scenario (grey line) and alternative (unrest with no eruption) option to the scenario (black-dashed line).

The large number of evacuees during the revised sequence highlights the substantial influence that evacuation zoning may have on society during volcanic unrest, even if there was no substantial damage from surficial volcanic hazards. In Auckland, the longer duration

of larger evacuation zones would have substantial implications for transportation, particularly as more of the Southern Motorway (SH1) and north-south rail line are covered by evacuation zones for longer. Furthermore, the greater number and magnitude of earthquakes may lead to structural damage of some critical infrastructure. Inspections of key transportation routes, components and facilities will be required in areas that experienced the greatest shaking, and closures may be necessary due to inspections, physical damage and/or blockage. If possible, a decision to open some critical transportation routes that lie within the evacuation zones close to the boundaries would be likely, especially to maintain crucial north-south links through Auckland (albeit with restricted entry/exit points and hazard thresholds for immediate re-closure). Most critical routes through Auckland are accessible from 01 May for the alternative scenario. However, part of the South western Motorway (SH20) remains firmly within the PEZ (since 08 March), which will likely cause greater than usual congestion across the Auckland road network, especially with the return of previously displaced residents.

During the scenario involving unrest with no eruption, according to existing policy (Section 7.4.4.2) Auckland Airport falls within the PEZ for ~6 weeks, in contrast to 5 days in the original Māngere Bridge scenario. However, due to the major LoS implications that would result from such a closure, we speculate that social, political and economic pressure may result in amendments to the PEZ boundary. This would mean that Auckland Airport and some access routes lie outside of the boundary allowing services to be partially reinstated, albeit with established hazard thresholds for immediate re-closure.

7.6.5 Transportation network interdependencies

Failure or disruption of electricity supply is arguably one of the most important infrastructure interdependencies for ground transportation. For roads, traffic signal and variable message sign failure may occur (Hughes and Healy 2014), with police support required at major intersections and traffic congestion expected as a result. In Auckland, electricity is also crucial for the suburban rail network, although there is a limited diesel fleet that could be distributed across the network (although not sufficient to maintain typical capacity). Effective business continuity measures where electricity is crucial could include the use of emergency generators and stockpiles of diesel fuel, as occurs at Auckland Airport. Conversely, the electricity sector also depends on functional transportation for access to sites damaged or in need of maintenance and for material delivery. In the Māngere Bridge scenario, transmission towers will need to be installed when new transmission lines are required (Deligne et al. companion paper – Appendix E1), and the restoration of electricity may be required before evacuation zones are lifted (Auckland Council 2014).

Fuel supply is also recognised as a particularly important interdependency for transportation, and disruption to critical routes such as in the Māngere Bridge scenario will affect supply to fuel stations by tanker, even within non-evacuated areas. We also note that the Refinery Auckland Pipeline would be directly impacted by deformation and other hazards in the

Māngere Bridge scenario, with severe impacts on aviation and road fuel supply likely for weeks (Auckland Council 2013b, Deligne et al. 2015 – Appendix E2). Large changes in demand may occur, whether it be due to evacuations or the relocation of residents and businesses from impacted areas. Operationally, the aviation sector and ports are reliant on fuel. In Auckland, the ports and associated operations account for nearly a quarter of diesel fuel used daily by critical consumers in the region (Auckland Council 2013b). Tephra clean-up operations will require the mobilisation of a large number of trucks, sweepers, bulldozers, and graders (Hayes et al. 2015, Hayes et al. in review), all of which require fuel. Fuel supply restrictions could increase the time it takes to clean up, which could have cascading impacts on health, infrastructure and economic activities. Additionally, increased demand for water for clean-up and potential water restrictions due to eruption impacts (Stewart et al. companion paper) may affect the ability to clean ground transportation networks. Without water for firefighting capabilities and sewerage, airports may be effectively shut (Stewart et al. companion paper).

Changes in road demand may result from impacts on other transportation infrastructure. For example, when rail services cease to operate, some passengers may revert to road transport and the diversion of flights from airports will likely increase demand and traffic on roads elsewhere. Similarly, rail, aviation and maritime transportation may be affected by impacts to roads as they all require staff to operate. Maintaining a roster of additional staff that can be called in when required and having alternative sites with suitable capabilities (e.g. immigration facilities for international flights diverted to alternative airports) will aid business continuity and improve transportation end-user LoS. In some situations following volcanic activity, it may be that certain features of all transportation modes are adjusted or react in such a way, that overall transportation LoS incurs only minimal reduction, or even improves. However, detailed modelling of interdependency relationships is required to more accurately explore impacts on overall LoS.

7.7 Summary and Conclusions

The LoS metrics developed in this paper account for the various disruptive events through considering damage from geophysical hazards and operational activities such as evacuation and exclusion zoning. The LoS metric development process was heavily informed by consultation with transportation infrastructure providers and emergency management officials who generally have expert knowledge of particular transportation systems and their operation. Although the LoS metrics were formed using an eruption scenario in the AVF as a basis, many of the considerations in their compilation are universal and we thus suggest that the metrics can be applied in other locations affected by volcanic activity worldwide. We believe them to be particularly relevant in urban areas containing relatively advanced transportation networks and established emergency and transportation management policies.

We have demonstrated how small-scale explosive and effusive basaltic volcanic activity within an urban area can result in substantial disruption to transportation networks. Even in the absence of surficial volcanic hazards, the implementation of evacuation zones can have severe consequences on LoS for transportation end-users. Indeed, activity involving unrest episodes but with no, or few, surficial volcanic hazards may lead to equally, if not more, disruption for transportation end-users than activity with surficial hazards. This is largely due to uncertainties associated with potential vent areas and possibly large evacuation zones which could remain for longer durations. Critical routes and transportation hubs may be closed as a result with possible cascading consequences on other critical infrastructure which rely on transportation, whether it be through staff unable to access key sites or the breakdown of supply chains affecting the delivery of resources for maintenance and repair. Additionally, there may be large societal implications with normally resident and working populations displaced by evacuation zones and forced to find accommodation elsewhere and relocate business activities. Such potentially large consequences for LoS based on operational decisions such as evacuation boundary delineation highlight the importance of robust policy and guidance that can be applied during events.

We considered multiple volcanic hazards for impact assessment and LoS analysis. Although physical damage to transportation networks from proximal volcanic hazards such as pyroclastic density currents can be severe, other damage and potential blockage of transportation networks may also occur from volcanic hazards that extend further from the vent; this includes earthquakes accompanying volcanic activity and tephra accumulation which could be substantial in places, especially during highly explosive eruptions and/or with consistent wind direction. The impact of tephra fall is generally considered more temporary and easily remedied through clean-up operations. However, evacuation zones and ash remobilisation may complicate clean-up and repair, and extend the duration and spatial extent of LoS reduction. Importantly, even if there is minimal physical damage from hazards such as tephra and earthquakes, widespread disruption to end-users can occur due to required inspections of networks and components.

Specifically for the Māngere Bridge scenario, all modes of transportation encounter disruption and a reduced LoS before being impacted by geophysical hazards. No service exists on some critical north-south road and rail routes across the south Auckland isthmus at times due to the restrictions from evacuation zones, and Auckland Airport and the Port of Onehunga experience closure. Most LoS reduction for transportation networks starts ~6 days before the eruption due to the first PEZ being implemented, although some earlier self-evacuations may occur. Overall, LoS experiences fluctuations throughout the scenario due to different eruptive episodes and revisions to the extent of evacuation zones. Up to ~435,000 residents, as well as many businesses are displaced at times. A degree of LoS reduction continues for several weeks after the eruption itself due to clean-up and repair requirements, and 8,700 residents are permanently displaced due to the final exclusion zone.

For the modified Māngere Bridge scenario involving unrest but no eruption, the estimated maximum displaced population is the same as for the original scenario but residents and businesses are generally displaced for longer. Auckland Airport and critical transportation links are severely affected in this version of the scenario due to the large spatial extent and duration of evacuation zones. Relatively minor alterations to the geophysical hazard sequence such as different wind profiles can also have major consequences for LoS. Different wind profiles for the Māngere Bridge scenario demonstrate potential changes to:

- Evacuation zone management and network restoration due to different tephra accumulation patterns.
- Spatial and temporal extents of evacuation zones and networks impacted by geophysical hazards.
- The quantity of resources required to manage clean-up and recovery.

Our findings demonstrate the importance of considering transportation end-users when assessing the vulnerability of transportation networks to volcanic activity. LoS metrics account for all disruption that may be encountered by transportation end-users and ultimately aid the development of robust impact and risk assessments for transportation networks.

7.8 Acknowledgements

We express our sincere thanks to all of the officials from transportation authorities in New Zealand that were involved in the consultation process, and heavily informed the findings of this study. In particular, we thank Roy Robertson (Auckland Airport), Peter Halliwell (Air New Zealand), Peter Lechner (CAA, New Zealand), Murray Parker (NZTA), Peter Scott and Paul Jenkinson (Auckland Transport), David Murphy (Auckland Transport Operations Centre; ATOC), and Peter Ramsay and Mark Goodman (KiwiRail). Although this paper focuses on transportation impacts, other critical infrastructure impacts have been assessed to some extent, and our paper has benefitted from this work, especially through the brief consideration of interdependencies. We would thus like to thank Josh Hayes and Alistair Davies (University of Canterbury, New Zealand), Grant Wilson (State Emergency Management Committee Secretariat, WA, Australia), and Carol Stewart (Massey University, New Zealand). Daniel Blake would also like to thank his co-supervisor, Jim Cole, for his guidance and edits.

We acknowledge support from the Economics of Resilient Infrastructure (ERI) and Determining Volcanic Risk in Auckland (DEVORA) research programmes; ERI is funded by the New Zealand Ministry of Business, Innovation, and Employment (MBIE) and DEVORA is funded by the New Zealand Earthquake Commission (EQC) and Auckland Council. The authors were also supported through Natural Hazards Research Management Platform (NHRP) funding (contract C05X0804), University of Canterbury Mason Trust grants (Daniel

Blake), additional EQC and DEVORA funds (Daniel Blake), and the GNS Science Core Research Programme (Natalia Deligne).

7.9 References

AccuWeather, (2015) First Calbuco eruption in 42 years suspends flights in Buenos Aires, AccuWeather.com. http://www.accuweather.com/en/weather-news/more-than-4000-evacuated-after/46042985, Accessed 23 November 2015.

AELP-1 (1999) Final report: stage 1. Auckland Engineering Lifelines Project Technical Publication No. 112, November 1999. Auckland Regional Council, Auckland, New Zealand.

AELP-2 (2014) Auckland Engineering Lifelines Project stage 2: assessing Auckland's infrastructure vulnerability to natural and man-made hazards and developing measures to reduce our region's vulnerability. Auckland Engineering Lifelines Group Report Version 1.1. http://www.aelg.org.nz/document-library/critical-infrastructure-reports/, Accessed 01 August 2016.

AIP NZ (2016) ENR 5.3, Aeronautical Information Publication New Zealand: other hazardous airspace, Civil Aviation Authority of New Zealand. http://www.aip.net.nz/pdf/ENR_5.3.pdf, Accessed 20 September 2016.

Arana-Barradas, A. (2001) Out of the ashes after Mount Pinatubo. Airman, November 2001.

ARTA (2009) Auckland report narrative 2009/10: What we do. Auckland Regional Transport Authority, New Zealand. https://at.govt.nz/media/imported/4468/AT-ARTA-Report-AnnualReportNarrative2009-2010.pdf, Accessed 24 August 2015.

Auckland Council (2013a) The Auckland Plan: Chapter 13. Auckland Council. http://theplan.theaucklandplan.govt.nz/aucklands-transport/, Accessed 20 August 2015.

Auckland Council (2013b) Auckland CDEM Fuel Contingency Plan, version 3.1. http://www.aucklandcivildefence.org.nz/media/30013/Final%20Auckland%20Fuel%20Plan%20V3.1%20October%202013.pdf, Accessed 20 August 2015.

Auckland Council (2014) Auckland Evacuation Plan. Civil Defence and Emergency Management. http://www.aucklandcivildefence.org.nz/about-us/document-library/supporting-plans/, Accessed 09 September 2015.

Auckland Council (2015) Auckland Volcanic Field Contingency Plan. Civil Defence and Emergency Management. http://www.aucklandcivildefence.org.nz/about-us/document-library/supporting-plans/, Accessed 09 September 2015.

Auckland Transport (2013) Electric trains. Auckland Transport. https://at.govt.nz/projects-roadworks/auckland-rail-upgrade/electric-trains/, Accessed 09 September 2015.

Auckland Transport (2016) City Rail Link: project overview. Auckland Transport. https://at.govt.nz/projects-roadworks/city-rail-link/, Accessed 01 August 2016.

Barnard, S. (2004) Results of a reconnaissance trip to Mt. Etna, Italy: the effects of the 2002 eruption of Etna on the province of Catania. Bulletin of the New Zealand Society for Earthquake Engineering, 37:2, pp.47–61.

Barnard, S. (2009) The vulnerability of New Zealand lifelines infrastructure to ashfall. PhD Thesis, Hazard and Disaster Management. University of Canterbury, Christchurch, New Zealand.

Barsotti, S. Andronico, D. Neri, A. Del Carlo, P. Baxter, P.J. Aspinall, W.P. Hincks, T. (2010) Quantitative assessment of volcanic ash hazards for health and infrastructure at Mt. Etna (Italy) by numerical simulation. Journal of Volcanology and Geothermal Research, 192, pp.85–96.

Beca Planning (2003) Whenuapai Air Base: planning issues and constraints. New Zealand Defence Force. http://www.nzdf.mil.nz/downloads/pdf/whenuapai/whenuapaiairbase.pdf, Accessed 10 September 2015.

Becker, J. Smith, R. Johnston, D. Munro, A. (2001) Effects of the 1995-1996 Ruapehu eruptions on communities in central North Island, New Zealand, and people's perceptions of volcanic hazards after the event. The Australasian Journal of Disaster and Trauma Studies, 2001-1.

Bitschene, P.R. Fernández, M.I. (1995) Volcanology and petrology of fallout ashes from the August 1991 eruption of Volcán Hudson (Patagonian Andes). IN: Bitschene P.R. Mendia J. (Eds.) The August 1991 eruption of Volcán Hudson (Patagonian Andes): a thousand days after. Cuvillier, Göttingen. 27-54.

Blake, D.M. Wilson, G. Stewart, C. Craig, H.M. Hayes, J.L. Jenkins, S.F. Wilson, T.M. Horwell, C.J. Andreastuti, S. Daniswara, R. Ferdiwijaya, D. Leonard, G.S. Hendrasto, M. Cronin, S. (2015) The 2014 eruption of Kelud volcano, Indonesia: impacts on infrastructure, utilities, agriculture and health. GNS Science Report 2015/15, 139p. *[APPENDIX A OF THIS THESIS]*

Blake, D.M. Wilson, T.M. Cole, J.W. Deligne, N.I. Lindsay, J.M. (in review a) Impact of volcanic ash on road and airfield surface skid resistance. Journal of Transportation Research Part D: Transport and Environment. *[CHAPTER 3 OF THIS THESIS]*

Blake, D.M. Wilson, T.W. Gomez, C. (in review b) Road marking coverage by volcanic ash: an experimental approach. Environmental Earth Sciences. *[CHAPTER 4 OF THIS THESIS]*

Blake, D.M. Wilson, T.M. Stewart, C. (in review c) Visibility in airborne volcanic ash: considerations for surface transport using a laboratory-based method. Natural Hazards. *[CHAPTER 5 OF THIS THESIS]*

Blake, D.M. Deligne, N.I. Wilson, T.M. Wilson, G. (in review d) Improving volcanic ash fragility functions through laboratory studies: example of surface transportation networks. Journal of Applied Volcanology. *[CHAPTER 6 OF THIS THESIS]*

Blong, R.J. (1984) Volcanic hazards: a sourcebook on the effects of eruptions. New South Wales, Australia.

Blong, R.J. McKee, C. (1995) The Rabaul eruption 1994: destruction of a town. Natural Hazards Research Centre, Macquarie University, Australia, 52p.

Bonadonna, C. Connor, C.B. Houghton, B.F. Connor, L. Byrne, M. Laing, A. Hincks, T.K. (2005) Probabilistic modeling of tephra dispersal: hazard assessment of a multiphase rhyolitic eruption at Tarawera, New Zealand. Journal of Geophysical Research, 110.

Brand, B.D. Gravley, D. Clarke, A. Lindsay, J. Boomberg, S.H. Agustin-Flores, J. Németh, K. (2014) Combined field and numerical approach to understanding dilute pyroclastic density current dynamics and hazard potential: Auckland Volcanic Field, New Zealand. Journal of Volcanology and Geothermal Research, 276, pp.215–232.

Casadevall, T.J. Reyes, P.J.D. Schneider, D.J. (1999) The 1991 Pinatubo eruptions and their effects on aircraft operations. http://pubs.usgs.gov/pinatubo/casa/, Accessed 03 June 2014.

Chappell, P.R. (2014) The climate and weather of Auckland, 2nd edition. NIWA Science and Technology Series Number 60. NIWA Taihoro Nukurangi, New Zealand.

Cole, J.W. Blumenthal, E. (2004) Evacuate! What an evacuation order given because of a pending volcanic eruption could mean to residents of the Bay of Plenty. Natural Hazards Research Centre, University of Canterbury, New Zealand.

Cole, J.W. Sabel, C.E. Blumenthal, E. Finnis, K. Dantas, A. Barnard, B. Johnston, D.M. (2005) GIS-based emergency and evacuation planning for volcanic hazards in New Zealand. Bulletin of the New Zealand Society for Earthquake Engineering, 38:2, pp.149-164.

Connor, L. Connor, C. Courtland, L. Saballos, A. (2011) Tephra2 Users Manual, Spring 2011, University of South Florida, Tampa. https://vhub.org/resources/756/download/Tephra2_Users_Manual.pdf, Accessed 01 August 2016.

Coomer, M.A. Lambie, E.S. Wilson, T. Potter, S.H. Leonard, G.S. Maxwell, K. Bates, A. Keith, H. (2015) DEVORA volcanic survey: people's panel. GNS Science Report 2015/39, 60p.

Corwin, G. Foster, H.L. (1959) The 1957 explosive eruption on Iwo Jima, Volcano Islands. American Journal of Science, 257, pp.161–171.

Cova, T.J. Conger, S. (2003) Transportation hazards. IN: Kutz, M. (Ed.) Handbook of Transportation Engineering, McGraw-Hill Handbook.

Craig, H. Wilson, T. Stewart, C. Outes, V. Villarosa, G. Baxter, P. (2016) Impacts to agriculture and critical infrastructure in Argentina after ashfall from the 2011 eruption of the Cordón Caulle volcanic complex: an assessment of published damage and function thresholds. Journal of Applied Volcanology, 5:7, 31p.

Cubellis, E. Marturano, A. Pappalardo, L. (2016) The last Vesuvius eruption in March 1944: reconstruction of the eruptive dynamic and its impact on the environment and people through witness reports and volcanological evidence. Natural Hazards, 82:1, pp.95–121.

Daly, M. Johnston, D. (2015) The genesis of volcanic risk assessment for the Auckland engineering lifelines project: 1996–2000. Journal of Applied Volcanology, 4:7.

Daniell, J.E. Wenzel, F. Khazai, B. Santiago, J.G. Schaefer, A. (2014) A worldwide seismic code index, country-by-country global building practice factor and socioeconomic vulnerability indices for use in earthquake loss estimation. Second European Conference on Earthquake Engineering and Seismology, Istanbul, August 25-29. http://www.eaee.org/Media/Default/2ECCES/2ecces_eaee/1400.pdf, Accessed 09 September 2016.

De la Cruz-Reyna, S. Yokoyama, I. (2011) A geophysical characterization of monogenetic volcanism. Geofisica Internacional. 50:4, pp.465–484.

Deligne, N.I. Blake, D.M. Davies, A.J. Grace, E.S. Hayes, J. Potter, S. Stewart, C. Wilson, G. Wilson, T.M. (2015) Economics of Resilient Infrastructure Auckland Volcanic Field scenario. ERI Research Report 2015/03. 151p. *[APPENDIX E2 OF THIS THESIS]*

Deligne, N.I. Fitzgerald, R. Blake, D.M. Davies, A.J. Hayes, J.L. Kennedy, B. Stewart, C. Wilson, G. Wilson, T.M. Carneiro, R. Muspratt, S. Woods, R. (companion paper). Investigating the consequences of urban volcanism using a scenario approach I: development and application of a hypothetical eruption in the Auckland Volcanic Field, New Zealand. Journal of Volcanology and Geothermal Research. *[APPENDIX E1 OF THIS THESIS]*

Durand, M. Gordon, K. Johnston, D. Lorden, R. Poirot, T. Scott, J. Shephard, B. (2001) Impacts and responses to ashfall in Kagoshima from Sakurajima Volcano – lessons for New Zealand. GNS Science Report 2001/30, 53p.

Fitzgerald, R.H. Dohaney, J. Hill, D. Wilson, T.M. Kennedy, B. Lindsay, J. (2015) Teaching volcanic monitoring and hazard mitigation within an urban area: a volcanic hazards simulation of the Auckland Volcanic Field. GNS Science Report 2014/70, 53p.

Folch, A. Mingari, L. Osores, M.S. Collini, E. (2014) Modeling volcanic ash resuspension – application to the 14-18 October 2011 outbreak episode in central Patagonia, Argentina. Natural Hazards and Earth System Sciences, 14, pp.119-133.

Fries, Jr. C. (1953) Volumes and weights of pyroclastic material, lava, and water erupted by Parícutin volcano, Michoacan, Mexico. Transactions – American Geophysical Union. 34, pp.603-616.

Guffanti, M. Mayberry, G.C. Casadevall, T.J. Wanderman, R. (2009) Volcanic hazards to airports. Natural Hazards, 51, pp.287-302.

GVP (2013) Report on San Cristobal (Nicaragua): January 2013. Global Volcanism Program. http://volcano.si.edu/showreport.cfm?doi=10.5479/si.GVP.BGVN201301-344020, Accessed 23 November 2015.

Hampton, S.J. Cole, J.W. Wilson, G. Wilson, T.M. Broom, S. (2015) Volcanic ashfall accumulation and loading on gutters and pitched roofs from laboratory empirical experiments: Implications for risk assessment. Journal of Volcanology and Geothermal Research. 304, pp.237–252.

Hayes, J.L. Wilson, T.M. Magill, C. (2015) Tephra fall clean-up in urban environments. Journal of Volcanology and Geothermal Research, 304, pp.359–377.

Hayes, J.L. Wilson, T.M. Deligne, N.I. Cole, J. Hughes, M. (in review) A model to assess tephra clean-up requirements in urban environments. Journal of Applied Volcanology.

Hirano, M. Hashimoto, H. Moriyama, T. (1992) Debris Flows in Mt. Fugen. IN: Yanagi, T. Okada, H. Ohta, K. (Eds.) Unzen volcano: the 1990-1992 Eruption. 67–73. Fukuoka, Japan: Nishinippon Co., Ltd.

Hopkins, J.L. Millet, M.-A. Timm, C. Wilson, C.J.N. Leonard, G.S. Palin, J.M. Neil, H. (2015) Tools and techniques for developing tephra stratigraphies in lake cores: a case study from the basaltic Auckland Volcanic Field, New Zealand. Quaternary Science Reviews, 123, pp.58–75.

Houghton, B.F. Bonadonna, C. Gregg, C.E. Johnston, D.M. Cousins, W.J. Cole, J.W. Del Carlo, P. (2006) Proximal tephra hazards: recent eruption studies applied to volcanic risk in the Auckland volcanic field, New Zealand. Journal of Volcanology and Geothermal Research, 155, pp.138–149.

Hughes, J.F. Healy, K. (2014) Measuring the resilience of transport infrastructure. New Zealand Transport Agency Research Report 546. New Zealand Transport Agency, Wellington, New Zealand.

Hurlbut, G.C. Verbeek, R.D. (1887) Krakatau. Journal of the American Geographical Society of New York, 19, pp.233–253.

Hurst, A.W. (1994) ASHFALL – A computer program for estimating volcanic ash fallout, report and users guide. Kelburn, Wellington, New Zealand.

Jamaludin, D. (2010) BORDA respond to Merapi Disaster. Bremen Overseas Research and Development Association, Indonesia. http://www.borda-sea.org/news/borda-sea-news/article/borda-respond-to-merapi-disaster.html, Accessed 23 November 2015.

Jenkins, S. Komorowski, J.-C. Baxter, P.J. Spence,R. Picquout, A. Lavigne, F. (2013) The Merapi 2010 eruption: An interdisciplinary impact assessment methodology for studying pyroclastic density current dynamics. Journal of Volcanology and Geothermal Research, 261, pp.316–329.

Jenkins, S. Wilson, T.M. Magill, C.R. Miller, V. Stewart, C. (2014) Volcanic ash fall hazard and risk: technical background paper for the UN-ISDR Global Assessment Report on Disaster Risk Reduction 2015. Global Volcano Model and IAVCEI. www.preventionweb.net/english/hyogo/gar, Accessed 09 August 2016.

Jenkins, S.F. Wilson, T. Magill, C. Miller, V. Stewart, C. Blong, R. Marzocchi, W. Boulton, M. Bonadonna, C. Costa, A. (2015) Volcanic ash fall hazard and risk. IN: Loughlin, S.C. Sparks, R.S.J. Brown, S.K. Jenkins, S.F. Vye-Brown, C. (Eds.) Global Volcanic Hazards and Risk. Cambridge University Press, United Kingdom.

Johnson, P.J. Valentine, G.A. Cortés, J.A. Tadini, A. (2014) Basaltic tephra from monogenetic Marcath Volcano, central Nevada. Journal of Volcanology and Geothermal Research, 281, pp.27–33.

Johnston, D.M. Daly, M. (1997) Auckland erupts!! New Zealand Science Monthly, 8:10, pp.6-7.

Kagoshima City Office (2015) Discussion with staff at the Kagoshima City Office, Kagoshima, Japan. Personal Communication, 08 June 2015.

Kenny, J.A. Lindsay, J.M. Howe, T.M. (2012) Post-Miocene faults in Auckland: insights from borehole and topographic analysis. New Zealand Journal of Geology and Geophysics, 55:4, pp.323-343.

Labadie, J.R. (1983) Volcanic ash effects and mitigation. Air Force Office of Scientific Research and the Defence Advanced Research Projects Agency, U.S. 17p.

Lechner, P. (2015) Living with volcanic ash episodes in civil aviation: The New Zealand Volcanic Ash Advisory System (VAAS) and The International Airways Volcano Watch (IAVW), version 13, November 2015. Civil Aviation Authority of New Zealand. https://www.caa.govt.nz/Meteorology/Living_with_Volcanic_Ash.pdf, Accessed 20 September 2016.

Leonard, G.S. Johnston, D.M. Williams, S. Cole, J.W. Finnis, K. Barnard, S. (2006) Impacts and management of recent volcanic eruptions in Ecuador: lessons for New Zealand. GNS Science Report 2005/20, 52p.

Loughlin, S.C. Sparks, S. Brown, S.K. Jenkins, S.F. Vye-Brown, C. (2015) Global Volcanic Hazards and Risk. GVM, IAVCEI and UNISDR. Cambridge University Press, United Kingdom.

Magill, C.R. Blong, R.J. (2005) Volcanic risk ranking for Auckland, New Zealand. II. Hazard consequences and risk calculation. Bulletin of Volcanology, 67, pp.340–349.

Magill, C.R. Hurst, A.W. Hunter, L.J. Blong, R.J. (2006) Probabilistic tephra fall simulation for the Auckland Region, New Zealand. Journal of Volcanology and Geothermal Research. 153, pp.370–386.

Magill, C. Wilson, T. Okada, T. (2013) Observations of tephra fall impacts from the 2011 Shinmoedake eruption, Japan. Earths Planets and Space, 65, pp.677-698.

Mei, E.T.W. Lavigne, F. Picquout, A. de Bélizal, E. Brunstein, D. Grancher, D. Sartohadi, J. Cholik, N. Vidal, C. (2013) Lessons learned from the 2010 evacuations at Merapi volcano. Journal of Volcanology and Geothermal Research, 261, pp.348–365.

Morrissey, M. Zimanowski, B. Wohletz, K. Buettner, R. (2000) Phreatomagmatic fragmentation. IN: Sigurdsson, H. Houghton, B. McNutt, S.R. Rymer,H. Stix, J. (Eds.) Encyclopedia of Volcanoes. Academic Press, London, pp.431-445.

Nairn, I.A. (2002) The effects of volcanic ash fall (tephra) on road and airport surfaces. Institute of Geological and Nuclear Sciences Science Report 2002/13, 32p.

Nakada, S. (1999) Overview of the 1990 – 1995 eruption at Unzen Volcano. Journal of Volcanology and Geothermal Research, 89, pp.1–22.

NEC (2014) An economic analysis of transportation infrastructure investment. National Economic Council and the President's Council of Economic Advisors. The White House, Washington. https://www.whitehouse.gov/sites/default/files/docs/economic_analysis_of_transportation_investments.pdf, Accessed 08 August 2016.

NIWA CliFlo. National Climate Database on the Web. http://cliflo.niwa.co.nz, National Institute of Water and Atmospheric Research. Accessed 1 August 2015.

NZTA (2008) Regional summary: Auckland. New Zealand Transport Agency, December 2008. http://www.nzta.govt.nz/assets/resources/regional-summaries/auckland/docs/auckland-regional-summary.pdf, Accessed 25 July 2016.

NZTA (2009) Pedestrian planning and design guide. New Zealand Transport Agency, October 2009, Wellington, New Zealand. https://www.nzta.govt.nz/resources/pedestrian-planning-guide/, Accessed 24 August 2015.

NZTA (2013) One Network Road Classification. Road Efficiency Group, New Zealand Transport Agency, New Zealand. https://www.nzta.govt.nz/roads-and-rail/road-efficiency-group/onrc/, Accessed 24 August 2016.

NZTA (2016a) Waterview Connection: project overview. New Zealand Transport Agency. http://www.nzta.govt.nz/projects/the-western-ring-route/waterview-connection/, Accessed 01 August 2016.

NZTA (2016b) East West Link: project overview. New Zealand Transport Agency. http://www.nzta.govt.nz/projects/east-west-link/, Accessed 01 August 2016.

Oppenheimer, C. (2003) Climatic, environmental and human consequences of the largest known historic eruption: Tambora volcano (Indonesia) 1815. Progress in Physical Geography, 27:2, pp.230–259.

Pallister, J.S. McCausland, W.A. Jónsson, S. Lu, Z. Zahran, H.M. Hadidy, S.E. Aburukbah, A. Stewart, I.C.F. Lundgren, P.R. White, R.A. Moufti, M.R.H. (2010) Broad accommodation of rift-related extension recorded by dyke intrusion in Saudi Arabia. Nature Geoscience, 3:10, pp.705–712.

Ragona, M. Hannstein, F. Mazzocchi, M. (2011) The impact of volcanic ash crisis on the European airline industry. IN: Alemannio, A. (Ed.) Governing disasters: the challenges of Emergency risk regulations. Edward Elgar Publishing.

Reckziegel, F. Bustos, E. Mingari, L. Báez, W. Villarosa, G. Folch, A. Collini, E. Viramonte, J. Romero, J. Osores, S. (2016) Forecasting volcanic ash dispersal and coeval resuspension during the April–May 2015 Calbuco eruption. Journal of Volcanology and Geothermal Research, 321, pp.44–57.

Robinson, T.R. Buxton, R. Wilson, T.M. Cousins, W.J. Christophersen, A.M. (2015) Multiple infrastructure failures and restoration estimates from an Alpine Fault earthquake: capturing modelling information for MERIT. ERI Research Report 2015/04, 80p.

Rossetto, T. Ioannou, I. Grant, D.N. (2013) Exisiting empirical vulnerability and fragility functions: compendium and guide for selection. GEM Technical Report 2013-X. GEM Foundation, Pavia, Italy.

Rowland, S.K. Jurado-Chichay, Z. Ernst, G. Walker, G.P.L. (2009) Pyroclastic deposits and lava flows from the 1759-1774 eruption of El Jorullo, México: aspects of “violent Strombolian” activity and comparison with Parícutin. Special Publications of IAVCEI. 2, pp.105–128.

Sarkinen, C.F. Wiitala, J.T. (1981) Investigation of volcanic ash on transmission facilities in the Pacific Northwest. IEEE Transactions on Power Apparatus and Systems, PAS-100:5, pp.2278-2286.

Segerstrom, K. (1950) Erosion studies. IN: Luhr, J.F. Simkin, T. (1993) Parícutin: the volcano born in a Mexican cornfield. Smithsonian Institution, Geoscience Press, Arizona, U.S.A.

Self, S. Sparks, R.S.J. Booth, B. Walker, G.P.L. (1974) The 1973 Heimaey Strombolian Scoria deposit, Iceland. Geological Magazine, 111:6, pp.539–548.

Seville, E. Stevenson, J. Brown, C. Giovinazzi, S. Vargo, J. (2014) Disruption and resilience: how organisations coped with the Canterbury earthquakes. ERI Research Report 2014/002, 45p.

Spence, R.J.S. Pomonis, A. Baxter, P.J. Coburn, A.W. White, M. Dayrit, M. (1999) Building damage caused by the Mount Pinatubo eruption of June 15, 1991. http://pubs.usgs.gov/pinatubo/spence/, Accessed 08 August 2016.

Stammers, S.A.A. (2000) The effects of major eruptions of Mt Pinatubo, Philippines and Rabaul Caldera, Papua New Guinea, and the subsequent social disruption and urban recovery: lessons for the future. University of Canterbury, New Zealand.

Statistics New Zealand (2013) 2013 Census meshblock dataset. http://www.stats.govt.nz/Census/2013-census/data-tables/meshblock-dataset.aspx, Accessed 15 July 2015.

Statistics New Zealand, 2015. Subnational population estimates. http://nzdotstat.stats.govt.nz/wbos/Index.aspx?DataSetCode=TABLECODE7502, Accessed 31 August 2016.

Stewart, C.S. Deligne, N.I. Davies, A. Grace, E. Wilson, T.M. (companion paper – in prep) Investigating the consequences of urban volcanism using a scenario approach III: contrasting implications for water supply, wastewater, and stormwater networks. Journal of Volcanology and Geothermal Research.

Surono, Jousset, P. Pallister, J. Boichu, M. Buongiorno, M.F. Budi-Santoso, A. Costa, F. Andreastutti, S. Prata, F. Schneider, D. Lieven, C. Humaida, H. Sumarti, S. Bignami, C. Griswold, J. Carn, S. Oppenheimer, C. Lavigne, F. (2012) The 2010 explosive eruption of Java's Merapi volcano – a '100-year' event. Journal of Volcanology and Geothermal Research, 241–242, pp.121–135.

Sword-Daniels, V. Stewart, C. Johnston, D. Wardman, J. Wilson, T. Rossetto, T. (2011) Infrastructure impacts, management and adaptations to eruptions at Volcán Tungurahua, Ecuador, 1999-2010. GNS Science Report 2011/24, 73p.

Tazieff, H. (1977) An exceptional eruption: Mt. Niragongo, Jan. 10th, 1977. Bulletin Volcanologique, 40:3, pp.189–200.

Tomsen, E. (2010) GIS-based mass evacuation planning for the Auckland Volcanic Field. Master's Thesis. School of Environment, University of Auckland, Auckland, New Zealand.

Tomsen, E. Lindsay, J. Gahegan, M. Wilson, T. Blake, D.M. (2014) Auckland Volcanic Field evacuation planning: a spatio-temporal approach for emergency management and transportation network decisions. Journal of Applied Volcanology, 3:6.

Tyler, J.L. Reynertson, K.D. (1981) A pain in the ash: the effort of the men and women of Fairchild AFB overcame the neighborhood nuisance, Mt. St. Helens. Engineering and Services Quarterly, 16-19.

USGS (2009) Small explosion produces light ash fall at Soufriere Hills volcano, Montserrat. United States Geological Survey. https://volcanoes.usgs.gov/ash/ashfall.html#eyewitness, Accessed 20 October 2015.

USGS (2013) Volcanic ash: effects and mitigation strategies. United States Geological Survey. http://volcanoes.usgs.gov/ash/trans/, Accessed 21 September 2015.

Volcano Discovery (2014) Sinabung eruption update: 13 January 2014. Volcano Discovery. http://www.volcanodiscovery.com/sinabung-eruptions.html, Accessed 16 January 2014.

Walker, G.P.L. Croasdale, R. (1971) Two plinian-type eruptions in the Azores. Journal of the Geological Society of London, 127, pp.17-55.

Walker, G.P.L. (1973) Explosive volcanic eruptions: a new classification scheme. Geologische Rundschau, 62, pp.431-446.

Wardman, J. Sword-Daniels, V. Stewart, C. Wilson, T. (2012) Impact assessment of the May 2010 eruption of Pacaya volcano, Guatemala. GNS Science Report 2012/09, 90p.

Warrick, R.A. (1981) Four communities under ash after Mount St. Helens. Institute of Behavioral Science, Boulder, Colorado, U.S.

Wilson, G. Wilson, T.M. Deligne, N.I. Cole, J.W. (2014) Volcanic hazard impacts to critical infrastructure: a review. Journal of Volcanology and Geothermal Research, 286, pp.148–182.

Wilson, T. Kaye, G. Stewart, C. Cole, J. (2007) Impacts of the 2006 eruption of Merapi volcano, Indonesia, on agriculture and infrastructure. GNS Science Report 2007/07, 69p.

Wilson, T.M. (2008) Unpublished field notes from the Chaiten eruption field visit. University of Canterbury, Christchurch, New Zealand.

Wilson, T.M. (2009) Unpublished field notes from the Hudson eruption field visit. University of Canterbury, Christchurch, New Zealand.

Wilson, T. Daly, M. Johnston, D. (2009a) Review of impacts of volcanic ash on electricity distribution systems, broadcasting and communication networks. Auckland Regional Council Technical Publication No. 051. Auckland Engineering Lifelines Group, Auckland, New Zealand.

Wilson, T.M. Stewart, C. Cole, J.W. Dewar, D.J. Johnston, D.M. Cronin, S.J. (2009b) The 1991 eruption of Volcan Hudson, Chile: impacts on agriculture and rural communities and long-term recovery. GNS Science Report 2009/66, 99p.

Wilson, T.M. Stewart, C. Sword-Daniels, V. Leonard, G.S. Johnston, D.M. Cole, J.W. Wardman, J. Wilson, G. Barnard, S. (2012a) Volcanic ash impacts on critical infrastructure. Physics and Chemistry of the Earth, 45–46, pp.5–23.

Wilson, T.M. Cole, J. Johnston, D. Cronin, S. Stewart, C. Dantas, A. (2012b) Short- and long-term evacuation of people and livestock during a volcanic crisis: lessons from the 1991 eruption of Volcán Hudson, Chile. Journal of Applied Volcanology, 1:1, pp.1-11.

Wilson, T. Outes, V. Stewart, C. Villarosa, G. Bickerton, H. Rovere, E. Baxter, P. (2013) Impacts of the June 2011 Puyehue-Cordón Caulle volcanic complex eruption on urban infrastructure, agriculture and public health. GNS Science Report 2012/20, 88p.

Wolshon, B. (2009) Transportation's role in emergency evacuation and reentry: a synthesis of highway practice. National Cooperative Highway Research Program, Synthesis 392, Transportation Research Board, Washington D.C.

Woo, G. (2008) Probabilistic criteria for volcano evacuation decisions. Natural Hazards, 45, pp.87-97.

Yanagi, T. Okada, H. Ohta, K. (1992) Unzen volcano, the 1990-1992 eruption. The Nishinippon and Kyushu University Press, Fukuoka. 137p.

Zuccaro, G. Cacace, F. Spence, R.J.S. Baxter, P.J. (2008) Impact of explosive eruption scenarios at Vesuvius. Journal of Volcanology and Geothermal Research, 178:3, pp.416–453.

8. SYNTHESIS

8.1 Thesis Overview

The primary aim of this thesis has been to improve volcanic risk assessments for surface transportation networks. It achieves this by primarily investigating and quantifying the impacts of volcanic ash on individual components of surface transportation systems. The findings help inform volcanic Disaster Risk Reduction (DRR) measures to reduce damage and disruption of critical infrastructure services through developing surface transportation resilience. In the initial stages of the project it became apparent that there is a lack of data: (a) quantifying surface transportation vulnerability from volcanic ash hazards; (b) analysing the influence of different hazard intensity metrics (HIMs) on surface transportation function and damage; and (c) assessing multi-volcanic hazard transportation vulnerability in spatial and temporal contexts. The thesis addresses these gaps by:

1. **Investigating key unknown or uncertain consequences of volcanic ash impacts on surface transportation by analysing existing and new post-eruption observations.** This includes findings from field studies and interviews on an impact assessment trip to areas affected by the 2014 Kelud volcanic eruption, Indonesia (Chapter 2). Three key areas with knowledge gaps have been identified from post-eruption observations worldwide, all of which relate to the functionality of surface transportation networks during ashfall as opposed to physical damage. Experiments in these three areas (listed below) were designed and conducted to fill the knowledge gaps:
    - Skid resistance on ash-covered road and airfield surfaces (Chapter 3)
    - Road marking coverage by volcanic ash (Chapter 4)
    - Visibility in airborne volcanic ash (Chapter 5).

2. **Developing vulnerability models for surface transportation functional loss and clean-up during ashfall.** This study establishes or refines hazard intensity thresholds related to specific surface transportation impact types (i.e. the effects of different ash characteristics on skid resistance, road marking coverage and visibility – Chapters 3-5 respectively).

    Fragility functions have been developed using all available quantitative and qualitative impact data to describe the probability of damage or functional states for surface transportation being reached or exceeded for given hazard intensities (Chapter 6). This includes improving existing fragility functions (from Wilson et al. in review), which adopt ash thickness as the HIM, and the development of new functions with ash-settling rate as the primary HIM. The new fragility functions are a particularly important advancement because qualitative post-eruption observations have indicated that ash-settling rate is a more appropriate measure for

visibility impairment than ash thickness, and contemporary ash dispersion and fallout models can incorporate such atmospheric metrics.

3. **Applying the newly developed vulnerability models to a case study area (Auckland City) through the implementation of a scenario involving a hypothetical volcanic eruption in the Auckland Volcanic Field (AVF), New Zealand** (Chapter 7). The focus here is to consider both the physical damage and functional loss expected from multiple volcanic hazards during an eruption – physical damage from proximal volcanic hazards such as pyroclastic density currents (PDCs) and edifice formation, in addition to the impacts associated with ashfall and other distal hazards.

   The scenario approach enables consideration of spatial and temporal aspects through the assessment of impacts at key stages in the eruption sequence across the entire Auckland metropolitan area. Physical damage and functionality are assessed from the perspective of transportation end-users by means of Level-of-Service (LoS) assessment for each transportation mode – a highly topical consideration as transportation authorities are increasingly approaching network maintenance through the needs of end-users (e.g. SAP AG 2006, NZTA 2013).

8.2 Research Summary

8.2.1 Characterisation: surface transportation vulnerability to volcanic ash

As set out in Section 1.2, hazard, exposure, and vulnerability need to be considered in combination to determine the true nature and extent of risk. Prior to this thesis, there was a scarcity of quantitative vulnerability data to determine the likely impacts to surface transportation from volcanic hazards. This thesis identifies the requirement for a greater understanding of volcanic ashfall impacts to surface transportation due to their widespread, multifaceted, and long-lasting effects, and range of intensities. It improves our understanding of vulnerability to ashfall for all surface transportation, including maritime transport, which has received little attention in the past. It also contributes to a better understanding of wider societal volcanic impacts, as surface transportation is a vital component of most modern integrated systems.

As multiple volcanic hazards occur during eruptions, risk assessments are challenging, especially when individual hazards interact with one another and/or result in cascading secondary hazards. There are often a variety of impact states for volcanic flow hazards (e.g. Jenkins et al. 2013, Jenkins et al. 2015) and tephra fall (e.g. T.M.Wilson et al. 2012, Wilson et al. 2014), which complicates vulnerability assessments. Although proximal hazards can result in higher numbers of fatalities and casualties than ash, they are often more spatially confined than ashfall (Auker et al. 2015), and are commonly associated with more clear-cut and decisive actions in terms of life-safety and critical infrastructure protection.

The adopted approaches for developing vulnerability assessments are largely inter-disciplinary, involving contemporary practices and procedures from Earth science, engineering, chemistry and physics. Obtaining and applying quantitative empirical data relating to volcanic ash vulnerability by means of controlled laboratory experimentation forms a core component of this thesis. However, other (qualitative and semi-quantitative) data sources, including post-eruption and theoretical information, are also used, as a variety of data types are optimal for compiling contemporary risk assessments (Petrazzuoli and Zuccaro 2004, Jenkins et al. 2014). The detailed analysis of ash particle sizes and settling-rates at distances from volcanic vents (Chapter 5) is one such example.

8.2.2 Core research findings from the laboratory

Detailed and inter-disciplinary laboratory experiments have been developed and conducted to investigate specific surface transportation impacts from volcanic ash (i.e. skid resistance on road and airfield surfaces, road marking coverage, and visibility). The amalgamation of results from the individual laboratory studies and post-eruptive data leads to several over-arching findings that are important considerations for future volcanic risk assessments for surface transportation:

- Thin volcanic ash deposits are important when making vulnerability assessments – laboratory experiments indicate that ash <1 mm thick, sometimes even as thin as ~0.1 mm, can lead to reduced functionality. Such low thresholds have rarely been reported in post-eruption records (although thicknesses are rarely accurately measured). This emphasises the need to consider impacts in distal areas where deposits are often thinner than proximal settings.

- It is inappropriate to directly relate all impacts to ash thickness on the ground. Visibility is better associated with ash-settling rate or airborne ash concentration.

- Different ash particle size distributions, keeping deposit thickness or airborne concentration constant, can result in very different impacts to surface transportation. This is especially true when deposits are thin or airborne concentrations are low. Although fine-grained ash generally causes more severe impacts on functionality, this is not the case for all impact types (e.g. skid resistance reduction). However, distal areas are considered more prone to reduced functionality from volcanic ashfall than proximal areas because of the predominantly fine-grained particles in the former.

- Alternative HIMs (besides ash thickness, airborne concentration and particle size) are also important to consider. For example, the wetness of ash and soluble components have an effect on skid resistance. However, further laboratory experimentation is required to test these effects in detail in some cases – the visibility and road marking coverage tests were only conducted using dry ash, for example.

- Physical parameters for surface transportation are important when considering impacts from ashfall. For example, the macro- and micro-texture features of paved surfaces are crucial

properties when assessing skid resistance and road marking coverage by thin ash deposits, as well as implications for road-cleaning to mitigate such impacts. Also, road marking properties can influence how slippery surfaces become and to what extent road markings are visible to drivers during ashfall.

This thesis has integrated quantitative data from laboratory experimentation with qualitative and semi-quantitative post-eruption data to develop vulnerability models. It builds on previous laboratory studies that examine volcanic ash impacts to infrastructure and components (e.g. Dunn 2012, Wardman et al. 2012a, G.Wilson et al. 2012, Hill 2014), and provides more appropriate and refined fragility functions (Chapter 6) that can be incorporated into future volcanic risk assessments, thus assisting DRR strategies.

8.2.3 Multi-hazard and operational considerations

An important and innovative part of this thesis is the development of LoS metrics for surface transportation that account for operational activities such as the implementation of evacuation zones and multi-hazard impacts (Chapter 7). A multi-hazard approach is important for many risk assessments as critical infrastructure networks may experience several impacts of different intensities from different hazards during volcanic eruptions. Such an approach can lead to improved land-use planning, better response capacity, greater risk awareness, and increased ability to set priorities for mitigation actions. LoS metrics enable more robust risk assessments by accounting for disruption associated with multiple hazards including ashfall. Crucially, LoS metrics also consider transportation end-user requirements, which is important for many contemporary infrastructure management strategies and for analysing the wide societal effects of volcanic eruptions (e.g. displacement of residents; accommodation needs).

Applying LoS metrics to surface transportation networks is successfully demonstrated by developing a hypothetical volcanic eruption sequence in the AVF and examining the effects on Auckland City, New Zealand. This demonstrates how small-scale basaltic volcanic activity within an urban area can severely disrupt transportation networks. The scenario is a particularly useful approach because spatio-temporal hazard, vulnerability, capacity and exposure associated with critical infrastructure functionality loss are all considered – an important conceptual mechanism to achieving more resilient systems (UNISDR 2015). Even in the absence of any volcanic hazards, severe disruption to surface transportation can result from the establishment of evacuation zones simply in response to volcanic unrest. LoS reduction also results from proximal and distal volcanic hazards with values fluctuating due to different eruptive episodes, revisions to evacuation zone extents, and network inspection requirements, among other factors. The vulnerability of surface transportation functionality to volcanic ashfall, as examined through the laboratory studies, forms an important component of the scenario. LoS reduction can also continue for some time after the eruption has ceased due to exclusion zones, permanent physical modification to networks, clean-up requirements and ash remobilisation in the environment. This part of the study highlights the importance of consulting with staff of critical infrastructure and emergency management authorities as they have expert knowledge of particular

systems and procedures, and LoS can be strongly affected by the decisions that they make during adverse events.

8.2.4 Limitations of laboratory testing

The interdisciplinary and novel features of the laboratory work have led to some practical methodological challenges. Experts with different disciplinary backgrounds have been consulted wherever possible to assist with methodological development, but challenges remain, leading to some compromises and limitations:

- Decisions on the physical location of experiments have been required. Ideally, testing would be conducted in the field (i.e. on real transportation networks) to replicate realistic conditions where volcanic ash would fall, but environmental and safety concerns restrict this option. Additionally, there are issues with obtaining and delivering sufficient quantities of ash (or pseudo ash) for full scale testing. Therefore, studies are conducted in the Volcanic Ash Testing Laboratory (VAT Lab) at the University of Canterbury. The laboratory focus places limits on some of the methodological approaches available (e.g. equipment and set-ups appropriate for the room dimensions), but this is also an advantage in that it assists with narrowing down different methodological options.

- There are some obstacles associated with the samples required for laboratory experimentation, particularly:
    - New asphalt and concrete slabs are constructed specifically for experimental studies. The new slabs have different properties to worn surfaces (e.g. reflectivity and skid resistance characteristics), but this is accounted for by assessing temporal changes during experimentation.
    - Relatively large quantities of volcanic ash are required and pseudo ash (often with some different characteristics to real ash) is thus created and used (Chapter 3). However, some real ash samples are incorporated into testing to provide comparative results.

- Replicating precise and consistent flow rates for the visibility experiments (Chapter 5) is required with new high-tech equipment adopted. There are few previous examples of the equipment being used specifically for volcanic ash testing and several modifications are required. For example, the plastic piping to deliver the ash abraded rapidly (due to the sharp nature of ash particles) and required frequent replacement (Chapter 5). The methodology is limited to relatively fine-grained ash because coarse-grained ash can not be dispersed due to the design of the machine.

- There have been difficulties identifying and sourcing suitable equipment for the studies including that required for measuring:
    - Skid resistance on ash-covered surfaces (Chapter 3) – The majority of equipment available is not designed for use with thick lose contaminants such as volcanic ash. The pendulum skid tester is deemed the most suitable equipment and has extensive comparative results from previous studies (in environments excluding ash), and

standardised methodologies for its use. Only bare surfaces or those covered by relatively thin ash deposits are tested with the equipment.

- Airborne volcanic ash in order to calculate visual range (Chapter 5) – Most equipment is designed for relatively low concentrations of airborne particulates over large distances. The opacity meter adopted required some adaptations for use with ash as it is typically used for monitoring the effects of smoke particles.

- Some limitations are evident during the laboratory experiments themselves. For example, the thickness value of ash on asphalt surfaces depends on what part of the asphalt aggregate it is measured. Standardised ad-hoc measuring techniques were developed to account for this (Chapter 3 and 5) and caution is required when taking similar measurements in the future.

8.2.5 Limitations of risk assessment approach

- The importance of ash remobilisation is discussed, but the detailed quantitative analysis of its effects is beyond the scope of this thesis. It is likely that any remobilisation would amplify the spatial and temporal effects of disruption (e.g. Wilson et al. 2011, Reckziegal et al. 2016, Craig et al. 2016). Additionally, spatial and temporal effects of disruption may be amplified by long-duration eruptions. Eruptions at volcanic fields (e.g. Jorollo and Parícutin volcanoes in the Michoacan Guanajuato volcanic field, Mexico) suggest that single eruptions could continue for around a decade (Sherburn et al. 2007), and episodic eruptions from individual volcanic vents may occasionally occur (e.g. Shane et al. 2013, Linnell et al. 2016). Thus, many of the findings in this thesis should be treated as conservative in this respect.

- There may be previously unidentified or uncommon impacts to surface transportation that occur during future eruptions and this research is thus constrained by what has been observed in the past, as well as by findings from laboratory experimentation. An example of this is the impacts of volcanic ash on electric rail – there is only one well-recorded case study from post eruption observations, that of rail near the Kirishima volcanic complex, Japan, that was impacted following the 2011 Shinmoedake eruption (Magill et al. 2013). Complete network functionality loss occurred following trace ash deposits in this case. However, until similar infrastructure is exposed in future ashfall, it will remain unclear as to whether an unusual set of circumstances led to functionality loss or if such impacts are likely elsewhere.

- Care should be taken if applying research outputs to other locations (besides Auckland) because physical infrastructure parameters can vary across geographical boundaries, and the spatial extent of specific impacts should thus be considered with caution. Additionally, for the purpose of analysis, it was assumed that environmental conditions were pristine besides the effects from volcanic ash (e.g. clean paved surfaces, no additional atmospheric particulates such as smoke, fog, sea-spray) so key findings may require modification before use in some impact and risk assessments.

- Interdependencies between surface transportation networks and other critical infrastructure influence vulnerability because cascading failures can cause disruption (Rinaldi et al. 2001, Wilson 2015). The importance of interdependencies is highlighted throughout this thesis, but not analysed in detail. The complexities involved with assessing all interdependencies are vast, and it was deemed most beneficial to gain a better understanding of how vulnerability to single critical infrastructure networks (surface transportation in this research) is affected by multiple volcanic hazards before introducing interdependencies between different critical infrastructure types into the mix.

Despite the limitations, the thesis expands and improves quantitative empirical information related to surface transportation functionality, and the findings are considered robust and highly applicable for future volcanic risk assessments and DRR strategies.

8.3 Future Research

8.3.1 Applicability

Although Auckland, New Zealand, is used as a case study location for much of the research, many of the findings are internationally applicable due to the wide range of ash characteristics possible in the city. The research is particularly applicable in developed countries and urban areas where surface transportation infrastructure is broadly similar to Auckland (e.g. sealed roads with road markings, electronic traffic signals and/or VMS). The research outputs from this project are relevant to many sectors including transportation and emergency management, and insurance, especially in other developed countries worldwide.

Advances in volcanic risk management can result from the work, particularly through improved volcanic impact and risk assessments. Long-term surface transportation network design improvements could include:

- Land-use and transportation construction project planning, such as the incorporation of sufficient network redundancy in areas exposed to proximal and/or distal volcanic hazards. This will aid in assessing the vulnerability of both current and planned critical infrastructure to volcanic hazards.
- Transportation response planning activities such as identifying when cleaning of pyroclastic material from surface transportation surfaces should commence.
- Emergency management policy development, including spatial and temporal considerations of volcanic exclusion zones in evacuation and recovery plans and resource allocation including water and equipment for efficient cleaning of transportation networks.
- Engineering-focused mitigation strategies such as specific surface line-painting guidelines and water sprinkler systems for routes that frequently encounter volcanic ashfall.

This research provides opportunities for the development of operational activities during volcanic eruptions, including improved:

- Monitoring of ashfall, including the rapid assessment of multiple HIMs during volcanic crises using different equipment such as transmissometers. This will likely prove useful where impact forecast maps have large associated uncertainties.
- Transportation management mitigation strategies, including the delivery of appropriate advice for end-users travelling during ashfall, and prompt implementation of appropriate clean-up practices.
- Near-real time ashfall impact forecast maps to be used operationally, and incorporation of contemporary fallout and dispersion models (with multiple HIMs).
- Traffic predictions during volcanic eruptions (e.g. forecast accident rates and speeds) through the integration of results from near-real time ashfall and impact models (above) with live traffic observations, particularly through monitoring at transport operation centres.
- Information displayed on hazard/risk maps and signs, especially in areas with extensive surface transportation networks.

In addition, the studies enable better estimations of hazard intensity thresholds for past eruptions through knowledge of impacts for those same eruptions. For example, if road markings were known to be covered and particle size information is available following a particular eruption in the past, a minimum ash thickness can be estimated.

Such tools and strategies will enable improved network operations during volcanic activity. This is important, as resources and staff availability can be limited in a crisis, and strict prioritisation may be required. Comparative infrastructure issues may result from other natural hazards such as earthquakes and flooding, so inter-disciplinary links can be identified and overall infrastructure resilience strengthened. Importantly, the thesis raises awareness of the risk from multiple volcanic hazards and impacts to surface transportation functionality, which will lead to better response capacity and increased ability to set priorities for mitigation actions (GFDRR 2014).

8.3.2 Experimental vulnerability data

This work demonstrates the importance of quantitative empirical data obtained from laboratory experimentation to improve our understanding of surface transportation vulnerability and assist with volcanic risk assessment and reduction. Due to the wide array of impacts to surface transportation, there are many opportunities for further experimental studies including:

- **Vehicle engine air inlet filter testing**: Although air filters can be cleaned and replaced to minimise engine damage, constraining the thresholds at which they reduce function (e.g. become blocked) by volcanic ash would be useful. This would allow more specific advice for motorists, avoid unnecessary replacement cost and inconvenience, and help ensure that enough resources are available given future eruptions.

- **Vehicle bodywork and windscreen testing**: Post-eruption records suggest that vehicle bodywork can be dented, scratched and corroded by tephra fall, and windscreens may crack when impacted by material of large lapilli size or greater. Although less of a concern for network functionality (as vehicles will remain operational in most cases), determining thresholds for such impacts would be particularly useful from an insurance perspective, providing financial information on loss/repair. Such information would be especially beneficial for urban areas where high numbers of vehicles are exposed.

- **Rail lines:** There are few cases where rail has been impacted by volcanic ash, particularly modern electric rail. Electric rail networks appear vulnerable to volcanic ash and laboratory work would help explore these impacts in detail. Loss of adhesion between a railway wheel and track has implications for braking and traction (Gallardo-Hernandez and Lewis 2008). Although there appears to be minimal negative effect on adhesion due to the lack of post-eruption reports, laboratory testing would help confirm this too.

- **Signage and signals:** Post-eruption observations suggest that surface transportation signs and signals can become covered by volcanic ash, affecting the amount of information communicated to end-users and potentially reducing overall network safety. However, the properties of volcanic ash and transportation infrastructure that promote or inhibit coverage by ash have not been studied. Such knowledge would be useful to transportation and emergency management authorities to understand appropriate mechanisms to communicate information to end-users travelling during ashfall, in addition to non-crisis safety information.

- **In-flight aircraft**: This thesis focuses on surface transportation but the impacts of volcanic ash on flying aircraft clearly warrants further investigation (e.g. Guffanti et al. 2009, ICAO 2012, Carey and Bursik 2015), and is important for surface transportation networks due to the interconnectedness of all transportation systems. Laboratory and field testing has been – and is continuing to be – conducted by various companies who have the available resources required to determine safe operating thresholds of aircraft through volcanic ash (e.g. Airbus 2013, EasyJet 2013, NASA 2015). The findings from many of these studies have implications for aircraft operations on the ground too, and should thus be applied in airfield volcanic risk assessments.

- **Combined impacts**: The laboratory studies in this thesis focus on the impacts of reduced skid resistance, road marking coverage and visibility impairment independently from one another (before the findings are considered in combination for the scenario). However, some impacts may be affected by other impacts occurring simultaneously. For example, the effects on road skid resistance and visibility may be affected by road marking coverage if average speed of vehicles reduces due to driver disorientation. Experimental studies on driving behaviour that investigate differences between individual and combined impacts could assist – either conducted using simulators or on proving grounds.

- **Indirect impacts**: In addition to interdependent effects from other critical infrastructure on transportation, a particular area of concern highlighted by transportation operators through this thesis was the potential requirement of staff (e.g. train drivers, maintenance and repair crews) to work in ash-contaminated environments and associated health and safety implications. Laboratory-based experimentation is actively being conducted in this field of research (e.g. Horwell 2007), which will assist decision-making and improve volcanic risk assessments. Longitudinal studies on the health effects of volcanic ash will also help (Bernstein et al. 1986, Horwell and Baxter 2006, Sword-Daniels et al. 2014).

Data from future laboratory studies, along with that from new post-eruption observations and modelling, will help to further refine impact thresholds and fragility functions for surface transportation, and improve vulnerability assessments. For example, if thresholds for airborne ash concentrations are determined for road vehicle engine air inlet filter blockage, they could be compared to the new fragility functions for visibility impairment to better-forecast overall impacts on road network functionality. Even repeated laboratory testing using the methodologies developed in this thesis on the same impact types investigated (i.e. skid resistance, marking coverage, visibility impairment) would enhance the current dataset, reduce epistemic uncertainties, and potentially refine fragility functions.

8.3.3 Field impact assessment data

This thesis has emphasised the need for detailed impact assessments following volcanic eruptions. Where possible, future impact assessments should incorporate the measurement of multiple HIMs, not just ash thickness. For example, there is a current lack of knowledge on ash-settling rates or airborne ash concentrations near ground level during volcanic ashfalls, and further field information on this HIM could help refine vulnerability assessments related to visibility. Sophisticated equipment such as the transmissometer/opacity meter used in this study would be beneficial to collect a range of readings in situ, especially for long-lasting eruptions. However, the sudden and short-lived nature of some eruptions, as well as other labour demands in the field at the time, may mean that comparatively basic hand-held devices such as particle counters are more practical and preferable at times. Simultaneous collection of ash samples would then allow correlations between recorded impacts (or indeed no impacts) and other HIMs to be estimated at a later date.

8.3.4 Volcanic impact and surface transportation network models

The scenario approach adopted is deemed successful to consider both the spatial and temporal components of multiple volcanic hazards from a full eruption sequence, and importantly help analyse the consequences of physical damage and operational decisions on transportation end-users. It is also useful to engage with various stakeholders and receive input from transportation infrastructure providers, emergency management authorities, and other volcanic risk specialists, who all assist the scenario development process. The scenario is site-specific. In order to investigate the impacts in Auckland more fully, further hazard and impact scenarios should be developed in different locations across the AVF, which incorporate a broader range of eruption styles and consider multiple HIMs. A

suite of different scenarios would also allow for surface transportation (and other critical infrastructure) hotspots to be identified if impacts were modelled probabilistically across the entirety of the AVF – such scenarios are currently being developed for Auckland. Such an approach could be applied in other volcanically active areas worldwide, as long as care is taken to appropriately reflect the eruptive and infrastructural characteristics at new sites, as well as local operational policies and practices in the areas studied; consultation with experts who have detailed and interdisciplinary knowledge of systems in the areas of interest is crucial for the development of realistic scenarios.

There are opportunities to develop near-real time ashfall impact models that incorporate ash dispersion forecasts. With increased knowledge on the importance of different HIMs for surface transportation functionality, this would provide many opportunities to use existing research in an operational setting during volcanic eruptions. For example, if the airborne concentration and particle size distribution of ash is forecast for a section of state highway, VMS signs leading to the area could be illuminated to provide advice to motorists (e.g. speed restrictions or recommended diversions) based on the expected visual range and ash accumulation rate. Temporary signage or traffic management crews could be deployed to the relevant areas and clean-up equipment and staff could be put on stand-by. If models suggest that impacts will be particularly severe (e.g. prime conditions for reduced skid resistance, road marking coverage and/or severely impaired visibility), an early decision could be made to close affected (or soon to be affected) sections of transportation routes, thus preventing exposure of infrastructure to ash and minimising vehicle damage and accident rates. Detailed modelling could also account for the effects of ash re-suspension and re-deposition on transportation impacts in different environments.

There are also opportunities for detailed transportation analysis such as macro- and micro-scale simulation modelling. Such work has the potential to further inform policies such as evacuation and recovery planning and can be integrated with key findings from laboratory studies. It is particularly important in locations such as Auckland where population growth and geographical constraints continue to place challenges on transportation management and end-users. The results from detailed modelling can assist with increasing transportation resilience both during emergencies and on a daily basis. Dynamic properties of risk must be considered to assist future volcanic risk assessments. For example, it is important to account for changes in exposure such as from population growth and infrastructure expansion, and to consider vulnerability changes such as from the implementation of new mitigation strategies, including those suggested in this thesis. Network models that can incorporate alterations to transportation infrastructure and impacts from volcanic hazards can provide insights for the implications of dynamic risk properties on end-users.

There are difficulties when it comes to predicting how people will behave during a volcanic crisis. In Auckland, with high rates of immigration and no known volcanic activity having occurred within the AVF for several generations, it would be particularly beneficial to better understand likely responses of the local population given heightened volcanic activity. General surveys that assess risk perception to volcanic hazards provide a benchmark for further work (e.g. MCDEM 2008, Coomer et al. 2016).

However, these attempt to cover a wide range of topics, and more specific surveys (e.g. targeting travel / evacuation behaviour) could assist future risk assessments and DRR strategies. Knowledge gained from societies with similar characteristics and infrastructure overseas when they experience volcanic eruptions could also be applied in Auckland and elsewhere.

8.3.5 Multi-hazard advancements

Multiple volcanic hazards are considered in the scenario in this thesis – an approach that leads to more thorough risk assessments and prevents maladaptation to individual hazards (GFDRR 2014). However, little attention is paid to secondary hazards such as fire triggered by lava flows, PDCs and/or hot ballistics. New studies could account for such secondary volcanic hazards, which would further enhance risk assessments. Additionally, simultaneous natural hazard events may have knock-on effects on the volcanological risk already considered. For example, heavy rainfall from storms could wash minor ashfall from roads and airfields, increasing skid resistance and clearing road markings – effectively decreasing vulnerability. However, rainfall could also create additional issues such as flooding if it occurs over thick ash deposits, which can become dislodged and block stormwater systems (e.g. Pacaya volcanic eruption, Guatemala; Wardman et al. 2012b). Lahars (although likely small-scale in Auckland) created by stormwater runoff mixing with ash could cause additional impacts to critical infrastructure. Further research is required to more fully understand such multi-hazard impacts on critical infrastructure and society.

8.3.6 Interdependencies

To account for all possible interdependencies would require highly complex modelling. However, the probabilistic scenario-based approach suggested in Section 8.3.4 could allow the identification of critical infrastructure pinchpoints where disruption to different infrastructure types could cause cascading failures across networks (Sword-Daniels et al. 2015). The consequences of the hypothetical AVF eruption on other critical infrastructure besides transportation (e.g. electricity, fuel, water supply) allows various interdependent links to be suggested and provides a platform for detailed interdependency modelling. Such work could lead to the identification of a wide range of further potential infrastructure failure modes and the emergence of previously unidentified hazards that can cause failure (Hughes and Healy 2014).

It may be appropriate to direct vulnerability research that attempts to incorporate interdependent effects towards fully understanding the bi-directional effects between two common interconnected systems before additional systems are introduced into mix. For example, electricity and surface transportation have many interconnected properties; their interdependent effects could be modelled in detail before other critical infrastructure systems such as fuel and water supply are introduced. Resilience could result from the improved understanding of bi-directional relationships between two infrastructure types alone, perhaps inadvertently improving resilience between other infrastructure types too.

8.3.7 New and emerging infrastructure

Relatively new, and emerging infrastructure, such as electric vehicles, autonomous vehicles, and advances in intelligent transportation systems, may be susceptible to the effects of volcanic hazards. For example, solar powered traffic lights in Yogyakarta, Indonesia, were found to be vulnerable following ashfall from the 2014 Kelud eruption (Blake et al. 2015), and variable message signs (VMS) that incorporate solar technology may also be affected in certain latitudes (Zorn and Walter 2016). Conversely, new and emerging infrastructure may also exhibit resilient properties that reduce infrastructure vulnerability and assist risk management strategies. For example, car-to-car communication may assist with transferring knowledge on areas affected by volcanic ash, thus enabling the majority of vehicles to avoid such areas (reducing exposure), and providing rapid advice to transportation and emergency management authorities to assist recovery.

There are also many opportunities to explore the direct and indirect economic consequences of surface transportation damage and disruption. Such information would assist DRR strategies and improve resilience, such as through cost-benefit analyses and the improved prioritisation of mitigation measures (UNISDR 2004, GFDRR 2014, UNISDR 2015).

8.4 References

Airbus (2013) Airbus partnership aims to help aircraft “avoid” volcanic ash dangers, 12 November 2013. http://www.airbus.com/newsevents/news-events-single/detail/airbus-partnership-aims-to-help-aircraft-avoid-volcanic-ash-dangers/, Accessed 15 December 2013.

Auker, M.R. Sparks, R.S.J. Jenkins, S.F. Aspinall, W. Brown, S.K. Deligne, N.I. Jolly, G. Loughlin, S.C. Marzocchi, W. Newhall, C.G. Palma, J.L. (2015) Development of a new global Volcanic Hazard Index (VHI). IN: Loughlin, S.C. Sparks, R.S.J. Brown, S.K. Jenkins, S.F. Vye-Brown, C. (Eds.) Global volcanic hazards and risk. Cambridge University Press, Cambridge, U.K.

Bernstein, R.S. Baxter, P.J. Falk, H. Ing, R. Foster, L. Frost, F. (1986) Immediate public health concerns and actions in volcanic eruptions: lessons from the Mount St. Helens eruptions, May 18-October 18, 1980. American Journal of Public Health, 76, pp.25–38.

Blake, D.M. Wilson, G. Stewart, C. Craig, H.M. Hayes, J.L. Jenkins, S.F. Wilson, T.M. Horwell, C.J. Andreastuti, S. Daniswara, R. Ferdiwijaya, D. Leonard, G.S. Hendrasto, M. Cronin, S. (2015) The 2014 eruption of Kelud volcano, Indonesia: impacts on infrastructure, utilities, agriculture and health. GNS Science Report 2015/15, 139p. *[APPENDIX A OF THIS THESIS]*

Carey, S. Bursik, M. (2015) Chapter 5: volcanic plumes. IN: Sigurdsson, H. Houghton, B. McNutt, S. Rymer, H. Stix, J. (2015) The encyclopaedia of volcanoes (second edition), pp.571-585.

Coomer, M.A. Lambie, E.S. Wilson, T. Potter, S.H. Leonard, G.S. Maxwell, K. Bates, A. Keith, H. (2015) DEVORA volcanic survey: people’s panel. GNS Science Report 2015/39, 60p.

Craig, H.M. Wilson, T.M. Stewart, C. Villarosa, G. Outes, V. Cronin, S. Jenkins, S. (2016) Agricultural impact assessment and management after three widespread tephra falls in Patagonia, South America. Natural Hazards.

Dunn, M.G. (2012) Operation of gas turbine engines in an environment contaminated with volcanic ash. Journal of Turbomachinery, 134:5.

easyJet (2013) AVOID volcanic ash detection: detecting volcanic ash clouds with AVOID, October 2013. http://corporate.easyjet.com/corporate-responsibility/avoid-volcanic-ash-detection.aspx?sc_lang=en, Accessed 15 December 2013.

Gallardo-Hernandez, E.A. Lewis, R. (2008) Twin disc assessment of wheel/rail adhesion. Wear, 265:9–10, pp.1309–1316. Academic Press.

GFDRR (2014) Understanding risk in an evolving world: emerging best practices in natural disaster risk assessment. Global Facility for Disaster Reduction and Recovery, The World Bank, Washington. https://www.gfdrr.org/sites/gfdrr/files/publication/Understanding_Risk-Web_Version-rev_1.8.0.pdf, Accessed 23 September 2016.

Guffanti, M. Mayberry, G.C. Casadevall, T.J. Wanderman, R. (2009) Volcanic hazards to airports. Natural Hazards, 51, pp.287-302.

Hill (2014) Filtering out the ash: mitigating volcanic ash ingestion for generator sets. PhD Thesis. Department of Geological Sciences, University of Canterbury, New Zealand.

Horwell, C.J. Baxter, P.J. (2006) The respiratory health hazards of volcanic ash: a review for volcanic risk mitigation. Bulletin of Volcanology, 69:1, pp.1–24.

Horwell, C.J. (2007) Grain-size analysis of volcanic ash for the rapid assessment of respiratory health hazard. Journal of Environmental Monitoring, 9:10, pp.1107–1115.

Hughes, J.F. Healy, K. (2014) Measuring the resilience of transport infrastructure, February 2014. New Zealand Transport Agency Research Report 546, Wellington, New Zealand, 82 p.

ICAO (2012) Flight safety and volcanic ash: risk management of flight operations with known or forecast volcanic ash contamination. International Civil Aviation Organisation. http://www.icao.int/publications/Documents/9974_en.pdf, Accessed 16 June 2016.

Jenkins, S. Komorowski, J.-C. Baxter, P.J. Spence, R. Picquout, A. Lavigne, F. (2013) The Merapi 2010 eruption: An interdisciplinary impact assessment methodology for studying pyroclastic density current dynamics. Journal of Volcanology and Geothermal Research, 261, pp.316–329.

Jenkins, S.F. Spence, R.J.S. Fonseca, J.F.B.D. Solidum, R.U. Wilson, T.M. (2014) Volcanic risk assessment: quantifying physical vulnerability in the built environment. Journal of Volcanology and Geothermal Research, 276, pp.105-120.

Jenkins, S.F. Phillips, J.C. Price, R. Feloy, K. Baxter, P.J. Hadmoko, D.S. de Belizal, E. (2015) Developing building-damage scales for lahars: application to Merapi volcano, Indonesia. Bulletin of Volcanology, 77:75.

Linnell, T. Shane, P. Smith, I. Augustinus, P. Cronin, S. Lindsay, J. Maas, R. (2016) Long-lived shield volcanism within a monogenetic basaltic field: the conundrum of Rangitoto volcano, New Zealand. Geological Society of America Bulletin, B31392.1.

Magill, C. Wilson, T. Okada, T. (2013) Observations of tephra fall impacts from the 2011 Shinmoedake eruption, Japan. Earths Planets and Space, 65, pp.677-698.

MCDEM (2008) Exercise Ruaumoko '08 final exercise report. Ministry of Civil Defence and Emergency Management, Wellington, New Zealand.

NASA (2015) NASA studying volcanic ash engine test results, 20 November 2015. http://www.nasa.gov/feature/langley/nasa-studying-volcanic-ash-engine-test-results, Accessed 03 June 2016.

NZTA (2013) One Network Road Classification. Road Efficiency Group, New Zealand Transport Agency, New Zealand. https://www.nzta.govt.nz/roads-and-rail/road-efficiency-group/onrc/, Accessed 24 August 2016.

Petrazzuoli, S.M. Zuccaro, G. (2004) Structural resistance of reinforced concrete buildings under pyroclastic flows: a study of the Vesuvian area. Journal of Volcanology and Geothermal Research, 133:1–4, pp.353–367.

Reckziegel, F. Bustos, E. Mingari, L. Báez, W. Villarosa, G. Folch, A. Collini, E. Viramonte, J. Romero, J. Osores, S. (2016) Forecasting volcanic ash dispersal and coeval resuspension during the April–May 2015 Calbuco eruption. Journal of Volcanology and Geothermal Research, 321, pp.44–57.

Rinaldi, B.S.M. Peerenboom, J.P. Kelly, T.K. (2001) Complex networks: identifying, understanding, and analyzing critical infrastructure interdependencies. IEEE Control Systems Magazine, U.S.A., December 2001, pp.11–25.

SAG AG (2006) Transportation management and the adaptive supply chain network: keeping pace with innovation and globalization. SAP White Paper, SAP Group. http://www.scdigest.com/assets/Reps/Transportation_Mngt_and_the_Adaptive_Supply_Chain.pdf?cid=862, Accessed 07 October 2016.

Shane, P. Gehrels, M. Zawalna-Geer, A. Augustinus, P. Lindsay, J. Chaillou, I. (2013) Longevity of a small shield volcano revealed by crypto-tephra studies (Rangitoto volcano, New Zealand): Change in eruptive behavior of a basaltic field. Journal of Volcanology and Geothermal Research, 257, pp.174–183.

Sherburn, S. Scott, B.J. Olsen, J. Miller, C. (2007) Monitoring seismic precursors to an eruption from the Auckland Volcanic Field, New Zealand. New Zealand Journal of Geology and Geophysics, 50, pp.1–11.

Sword-Daniels, V. Wilson, T.M. Sargeant, S. Rossetto, T. Twigg, J. Johnston, D.M., Loughlin, S.C. Cole, P.D. (2014) Chapter 26, consequences of long-term volcanic activity for essential services in Montserrat: challenges, adaptations and resilience. Geological Society, London, Memoirs, 39:1, pp.471–488.

Sword-Daniels, V.L. Rossetto, T. Wilson, T.M. Sargeant, S. (2015) Interdependence and dynamics of essential services in an extensive risk context: a case study in Montserrat, West Indies. Natural Hazards Earth Systems Science, 15, pp.947-961.

UNISDR (2004) Living with risk: a global review of disaster reduction initiatives. United Nations International Strategy for Disaster Reduction, Geneva, Switzerland, 429 p. http://www.unisdr.org/we/inform/publications/657, Accessed 10 September 2016.

UNISDR (2015) Sendai Framework for Disaster Risk Reduction (2015-2030). United Nations International Strategy for Disaster Reduction, Geneva, Switzerland. http://www.unisdr.org/we/coordinate/sendai-framework, Accessed 15 June 2016.

Wardman, J.B. Wilson, T.M. Bodger, P.S. Cole, J.W. Johnston, D.M. (2012a) Investigating the electrical conductivity of volcanic ash and its effect on HV power systems. Physics and Chemistry of the Earth, 45–46, pp.128–145.

Wardman, J. Stewart, C. Sword-Daniels, V. Wilson, T. (2012b) Impact assessment of the May 2010 eruption of Pacaya volcano, Guatemala. GNS Science Report 2012/09, 90p.

Wilson, G. Wilson, T. Cole, J. Oze, C. (2012) Vulnerability of laptop computers to volcanic ash and gas. Natural Hazards, 63:2, pp.711–736.

Wilson, G. (2015) Vulnerability of critical infrastructure to volcanic hazards. PhD Thesis. Hazards and Disaster Management, Department of Geological Sciences, University of Canterbury, Christchurch, New Zealand.

Wilson, G. Wilson, T.M. Deligne, N.I. Blake, D.M. Cole, J.W. (in review) Framework for developing volcanic fragility functions for critical infrastructure. Journal of Applied Volcanology. *[APPENDIX D OF THIS THESIS]*

Wilson, T.M. Cole, J.W. Stewart, C. Cronin, S.J. Johnston, D.M. (2011) Ash storms: impacts of wind-remobilised volcanic ash on rural communities and agriculture following the 1991 Hudson eruption, southern Patagonia, Chile. Bulletin of Volcanology, 73:3, pp.223–239.

Wilson, T.M. Stewart, C. Sword-Daniels, V. Leonard, G.S. Johnston, D.M. Cole, J.W. Wardman, J. Wilson, G. Barnard, S.T. (2012) Volcanic ash impacts to critical infrastructure. Physics and Chemistry of the Earth, 45-46, pp.5-23.

Zorn, E. Walter, T.R. (2016) Influence of volcanic tephra on photovoltaic (PV)-modules: an experimental study with application to the 2010 Eyjafjallajökull eruption, Iceland. Journal of Applied Volcanology, 5:1.

APPENDIX A. THE 2014 ERUPTION OF KELUD VOLCANO, INDONESIA: IMPACTS ON INFRASTRUCTURE, UTILITIES, AGRICULTURE AND HEALTH

PUBLICATION DETAILS:

Daniel M Blake[1], Grant Wilson[1,2], Carol Stewart[3], Heather M Craig[1,4], Josh L Hayes[1], Susanna F Jenkins[5], Thomas M Wilson[1], Claire J Horwell[6], Supriyati Andreastuti[7], Riswanda Daniswara[8], Djoni Ferdiwijaya[9], Graham S Leonard[10], Muhammad Hendrasto[7], Shane Cronin[11]

[1] Department of Geological Sciences, University of Canterbury, Private Bag 4800, Christchurch 8140, New Zealand

[2] State Emergency Management Committee Secretariat, 20 Southport Street, West Leederville, WA, Australia

[3] Joint Centre for Disaster Research, Massey University/GNS Science, Massey University Wellington Campus, PO Box 756, Wellington 6140, New Zealand

[4] Waikato Regional Council, 401 Grey Street, Private Bag 3038, Waikato Mail Centre, Hamilton 3240, New Zealand

[5] School of Earth Sciences, University of Bristol, Wills Memorial Building, Queen's Road, Clifton BS8 1RJ, United Kingdom

[6] Institute of Hazard, Risk and Resilience, Department of Earth Sciences, Durham University Science Labs, South Road, Durham DH1 3LE, United Kingdom

[7] Centre for Volcanology and Geological Hazard Mitigation (CVGHM), Jl. Diponegoro No. 57, Bandung 40122, West Java, Indonesia

[8] Disaster Management Study Centre UPN, Veteran Campus, Perumahan Pendowo Asri F-2 RT08/RW50, Pendowoharjo Sewon, Bantul, Yogyakarta 55185, Indonesia

[9] Independent Disaster Risk Reduction Practitioner, Yogyakarta, Indonesia

[10] GNS Science, PO Box 30368, Lower Hutt 5040, New Zealand

[11] School of Environment, University of Auckland, Private Bag 92019, Auckland 1142, New Zealand.

Publication: GNS Science Report ***(SEE SEPARATE ELECTRONIC APPENDIX)***

Status: Published

Report Reference: 2015/15

Date: November 2015

Available from: http://shop.gns.cri.nz/the-2014-eruption-of-kelud-volcano-indonesia-impacts-on-infrastructure-utilities-agriculture-and-health/

APPENDIX B. SUPPLEMENTARY MATERIAL TO CHAPTER 3. IMPACT OF VOLCANIC ASH ON ROAD AND AIRFIELD SURFACE SKID RESISTANCE

Appendix B1. Concentration of elements in the Ruapehu and White Island crater lake fluids at the strength used to dose the ash (after Broom 2010, Wilson 2012)

Element	Concentration (mg/L)	
	Ruapehu Crater Lake (100% strength)	White Island Crater Lake (20% strength)
Aluminium (Al)	370	965
Boron (B)	17.2	28.6
Bromine (Br)	10.8	44.2
Calcium (Ca)	909	823
Chlorine (Cl)	5,568	19,452
Fluorine (F)	133	1,518
Iron (Fe)	424	179
Potassium (K)	90	686
Lithium (Li)	0.77	5.60
Magnesium (Mg)	1,067	1,325
Sodium (Na)	660	3,372
Ammonia (NH_3)	13.0	24.8
Sulfate (SO_4^{2-})	7,988	4,952
pH	**1.13**	**0.07**

Appendix B2. Water leachate results showing relative soluble components (expressed as Electrical Conductivity (EC) and Total Dissolved Solids (TDS)), and pH. A) 1:100 ash to de-ionised water, B) 1:20 ash to de-ionised water

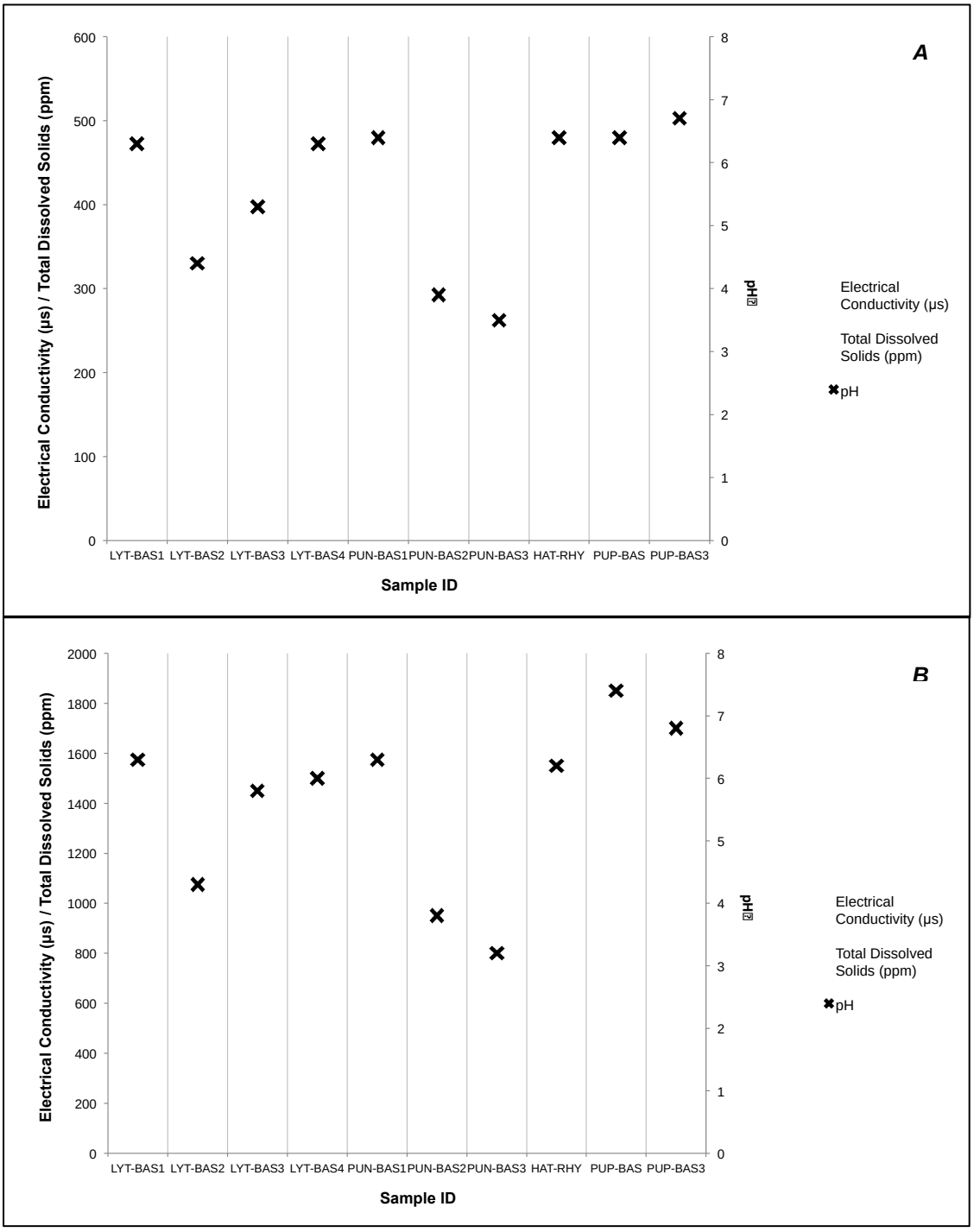

Appendix B3. Ash characteristics analysed during experimentation and illustrations to show production of each characteristic

Chracteristic	Variables	Method Summary
Ash type	Hard basalt, scoriaceous basalt, pumiceous rhyolite	Different volcano source locations in New Zealand (see figure 3)
Ash grain size	<1000 µm, <106 µm	Rock splitting, crushing and pulverisation (as required), then sieving

Hydraulic press (Hill 2014) → *Jaw crusher (Hill 2014)* → *Disk pulverisor (Hill 2014)* → *Rock sieves*

Ash thickness	1-2 mm, 5 mm	Manual sprinkling (1-2 mm), Metal spacer across ash surface (5 mm)

1-2 mm

5 mm

Soluble components	Non-dosed, dosed with Ruapehu Crater Lake fluid, dosed with White Island Crater Lake fluid	Established laboratory dosing technique (see section 2.1.1)

Wetness	Wetted to saturation, dry (no added moisture)	Hand-held water sprayer (water at room temperature)

Dry

Wet

Appendix B4. Summary of sand patch volumetric technique used to calculate the average pavement macrotexture depth (adapted from ASTM E965 2006)

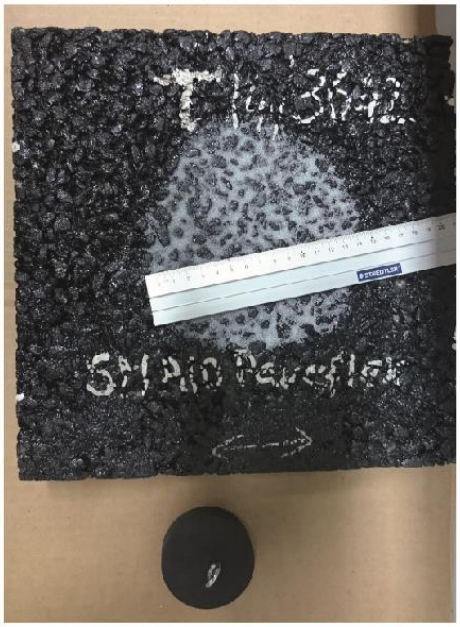

1. Pour glass beads (600-850 µm diameter and minimum 65% true spheres) up to a level on the cylinder which has a known volume.

2. Gently tap base of cylinder several times and add more glass beads to level.

3. Determine mass of material in cylinder (which is used for each measurement).

4. Pour measured volume and weight of material onto asphalt concrete surface.

5. Carefully spread material into circular patch with the rubber disk tool, filling the surface voids flush with the aggregate particle tips.

6. Measure and record the diameter of the circular area covered by the material at four equally spaced locations around the sample circumference.

7. Compute and record the average diameter.

8. Calculate average pavement macrotexture depth using equation (2).

Appendix B5. Image capture using stereo-microscope to analyse asphalt at a microtextural scale. Note that the grid squares (left) are spaced at 10 mm intervals

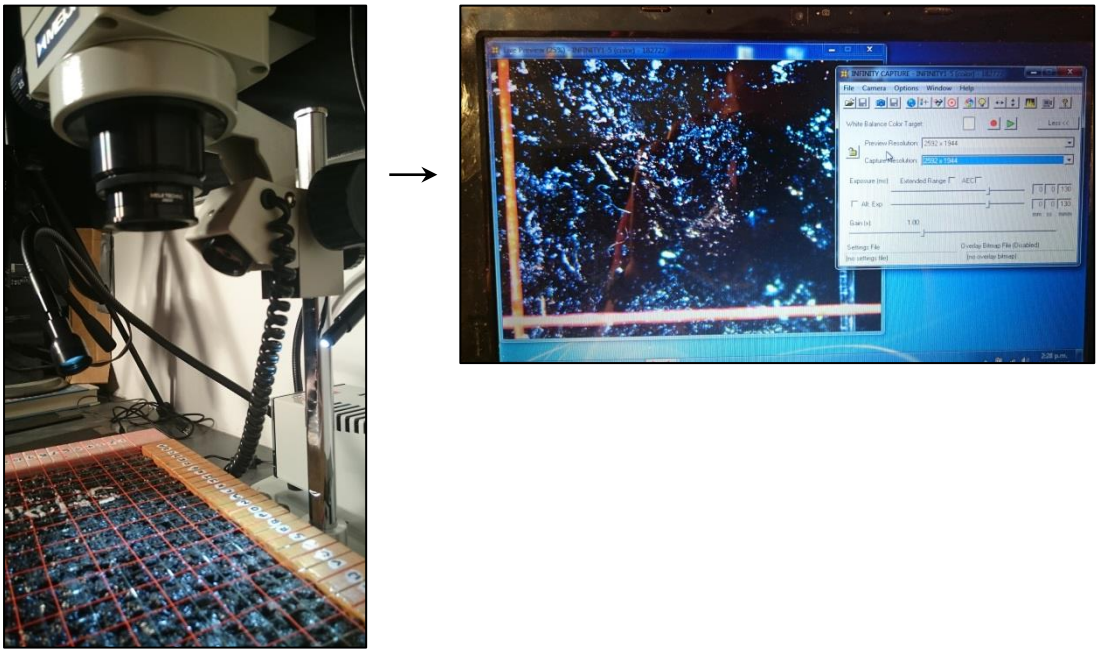

APPENDIX C. SUPPLEMENTARY MATERIAL TO CHAPTER 5. VISIBILITY IN AIRBORNE VOLCANIC ASH: CONSIDERATIONS FOR SURFACE TRANSPORTATION USING A LABORATORY-BASED METHOD

Appendix C1. Volcanic Ash Deposit Considerations

As Macedonio et al (2016) discuss, the total erupted mass of ash is often estimated from field data analysis (Pyle 1989, Bonadonna and Houghton 2005, Bonadonna and Costa 2012) or a procedure involving best-fit (Scollo et al. 2008, Costa et al 2009, Bonasia et al 2012). The relationship between total erupted mass and surface density (g m-2) at ground level would be linear if it were not for other parameters such as particle size, aggregation and wind (Macedonio et al. 2016).

Put simply, the total accumulated thickness of a volcanic ash deposit progressively decreases with distance from the vent. However, there are several factors that may lead to spatial variations in thickness:

- There is often a proximal region where fallout from the plume margins results in a more rapid decrease in thickness so that a deposit shows two segments on a thickness versus distance plot (Sparks et al. 1992).
- Situations may occur where the downwind thickness of deposits increases away from the vent in places. For example, if there is an unusually large proportion of medium sized particles erupted relative to larger and smaller sizes, these will fall mainly at intermediate distances resulting in an increase in thickness at the respective location (Parfitt and Wilson 2009).
- Sometimes, additional segments on a thickness versus distance plot can be observed at a distance further from the vent than the region of column margin to umbrella cloud transition, such as for the 1980 Mount St Helens deposit. This has been attributed to the aggregation of fine ash (predominantly <100 μm) (Carey and Sigurdsson 1982, Scasso et al. 1994, Bonadonna et al. 1998). Particle aggregation strongly depends on the initial particle sizes and can significantly affect deposit thinning, with secondary maxima of mass accumulation possible due to small aggregates sedimenting in a wind field (Bonadonna and Phillips 2003).
    - In wet conditions, aggregation may occur as a result of water film formation on the surface of particles causing them to adhere to one another (Parfitt and Wilson 2009).
    - In dry conditions, particles may become electrostatically charged, largely through triboelectrification resulting in aggregation.

Appendix C2. Primary Ashfall and Resuspended Ash Considerations

Upon leaving the eruptive vent, volcanic ash, along with coarser material and magmatic gases, is erupted upwards into the atmosphere to form the jet region of an eruption column (Figure 5.2). The ash-gas mixture continues to rise under convection due to buoyancy forces acting on the hot eruptive gases and heated entrained air (Morton et al. 1956, Wilson 1976, Kieffer 1984, Carey and Sparks 1986, Sparks 1986, Dobran et al. 1993, Costa et al. 2006, Carey and Bursik 2015). Once the particles reach a level of neutral buoyancy and enter the umbrella region (Figure 5.2), they may be dispersed and transported under the effects of wind and atmospheric turbulence to form ash clouds. The ash falls out of suspension with larger, heavier fragments typically deposited closer to the vent and smaller, lighter fragments dispersed farther downwind (Jenkins et al. 2014). Ash particles released from an umbrella cloud accelerate downward until the air drag retarding them is balanced by their gravitational weight, at which point they reach a steady final speed, or *terminal fall velocity* (Parfitt and Wilson 2009, Rose and Durant 2009). The terminal fall velocity of sedimenting particles affects airborne concentration near ground level and is mainly dependent on their diameter, densities and, to some extent, their shape, which if not spherical, complicates and slows fallout (Riley et al. 2003, Pardini et al. 2016).

Historical experiments have demonstrated that the normal rules of fluid mechanics apply to volcanic particles provided due account is taken of their often very irregular shapes. The airflow past falling fine ash particles is laminar, and under these conditions, the drag coefficient is inversely proportional to a dimensionless number called the *Reynolds number*. The Reynolds number represents the ratio between inertial forces and the viscous forces acting on the particle and is defined by (Parfitt and Wilson 2009):

$$Re = (d\ U\ \rho_a)/\eta_a) \qquad (13)$$

where Re is the Reynolds number, d is the average particle diameter, U is the speed of the particle through the air, ρ_a is the density of the atmospheric air and η_a is the viscosity of the gas.

Equations derived from Bonadonna et al. (1998) describe the terminal fall velocity of ash, depending on whether Re is <0.4 where Stokes Law applies (Equation 14), 0.4 – 500 (Equation 15), or >500 (Equation 16) (Bonadonna et al. 1998, Hill 2014, Blake et al. in review 1):

$$V_t \approx (g\ \rho\ d^2 / 18\ \mu) \qquad (14)$$

$$V_t \approx d\ (4\rho^2\ g^2 / 225\ \mu\ \sigma)^{1/3} \qquad (15)$$

$$V_t \approx (3.1\ g\ \rho\ d / \sigma)^{½} \qquad (16)$$

where V_t is the terminal velocity, g is the acceleration due to gravity (9.81 m s^{-2}), ρ is the density of the particles, d is the particle diameter, σ is the density of the air and μ is the dynamic viscosity of the medium

The quantity of volcanic ash which becomes resuspended is dependent on the particle size, density, shape, roughness of the ground material on which it has settled, and the degree of binding and compaction (Sivakumar 2005, Wilson et al. 2011). When wind forces above the settled ash exceed the static threshold forces of the least stable ground surface particles, some particles begin to vibrate and increasing wind speed causes some of them to be ejected into the atmosphere (Fowler and Lopushinsky 1986, Wilson et al. 2011). Unconsolidated, fine and low-density ash such as pumice deposited after particularly explosive volcanic eruptions are more prone to remobilisation and resuspension (Wilson et al. 2011). Water however, either from rainfall or from the intentional dampening of ash deposits, acts to suppress atmospheric remobilisation, as do other techniques such as reducing vehicle speeds or limiting the number of vehicles on roads or rail networks (Table 5.1).

Appendix C3. Volcanic Ash Particle Size Considerations

Airborne mineral dust often has a homogeneous internal structure, especially when advected with the wind across mountains or from land to sea over cool oceanic air (Weinzierl et al. 2012). In contrast, volcanic ash is generally inhomogeneous: the size of erupted material may vary by several orders of magnitude in one plume, ranging from very fine sub-micron ash to blocks exceeding one meter in diameter. The largest material leaves the eruption column at low levels, falling to the ground on ballistic trajectories, whereas the finest particles may become entrapped in the atmosphere for several months to years (Costa et al. 2006, Folch et al. 2009, Parfitt and Wilson 2009, Folch 2012). However, the most important group of material in terms of impact to infrastructure including transportation is generally ash of intermediate size range, defined here as fine ash (i.e ash with particle diameters <64 μm (Folch et al. 2009)). Fine ash can disperse for up to hundreds of kilometres from the vent before settling due to gravity and therefore generally settles over extensive areas. The proportions of ash in these fine fractions increase with increasing eruption explosivity (White et al. 2011). Indeed, for the infamous Mount St Helens (1980) eruption, although higher than expected amounts of coarse ash fell in some locations, the majority of the deposit consisted of fine ash, with >90% of the fallout in eastern Washington finer than 100 μm (Moen 1981, Durant et al. 2009) and ~25% finer than 10 μm in diameter (Horwell 2007).

Ash particles will only settle to the ground after they are carried to the edge of the eruption column, whereby they are then carried in the direction of the wind. The smaller the particle, the greater the height to which it is carried above the vent, and because the column expands with height, the greater the cross-wind distance that it will land from the vent. Additionally, greater windspeeds cause ash to be transported further downwind, suggesting that there should be a unique relationship between particle size and position in the final deposit (Parfitt and Wilson 2009). Complexities arise however, because at a given height, a range of particle sizes is released from the eruption column due to turbulence. Thus, at every location on the ground, an ash deposit will contain a range of particle sizes (Parfitt and Wilson 2009). There may also be eruptive pulses or changes in eruption style, which can result in alternating fine-grained and coarse-grained ashfall in the same location (Scasso et al. 1994).

Particle size distributions of volcanic deposits are poorly constrained due to sparse data, variations in wind conditions and dimensions of eruption columns, and inconsistencies in the methods of measurement. Many particle size analyses carried out for ash deposits are incomplete, lacking data below 63 μm (Bonadonna and Houghton 2005). However, given a single eruptive episode and weak or negligible cross-wind, particle size distributions generally exhibit patterns of exponentially decreasing median diameter with distance from the vent (Sparks et al. 1992) with the square root of the area enclosed by an isopach or isopleth contour (Pyle 1989).

Appendix C4. Hill (2014) Particle Size and Settling Rate Analysis Summary

Hill (2014) obtained median ash particle size and settling rate data from eight historical worldwide eruptions where field measurement sites were known. Analysis by Hill (2014) demonstrated that median particle size and ash-settling rate generally decreases with distance from the vent. Distal eruptions were found to cause ash deposits with predominant ash particle sizes of 20 – 250 μm, whereas deposits from proximal eruptions can occupy a much greater range of particle sizes (30 – 2,000 μm). Ash-settling rates were up to ~900 g m-2 h-1 (Hill 2014). Hill (2014) also derived estimates of median particle sizes and settling rates for Auckland based on a correlation of distance between the city and known eruptive centres in New Zealand.

APPENDIX D. FRAMEWORK FOR DEVELOPING VOLCANIC FRAGILITY AND VULNERABILITY FUNCTIONS FOR CRITICAL INFRASTRUCTURE

PUBLICATION DETAILS:

Grant Wilson[1,2], Thomas M Wilson[2], Natalia I Deligne[3], Daniel M Blake[2], Jim W Cole[2]

[1] State Emergency Management Committee Secretariat, 20 Southport Street, West Leederville, WA, Australia

[2] Department of Geological Sciences, University of Canterbury, Private Bag 4800, Christchurch 8140, New Zealand

[3] GNS Science, PO Box 30368, Lower Hutt 5040, New Zealand

Journal: Journal of Applied Volcanology

Received: 09 February 2016

Status: In Review

(SEE SEPARATE ELECTRONIC APPENDIX)

APPENDIX E. ADDITIONAL PUBLICATIONS AND SUPPLEMENTARY MATERIAL FOR CHAPTER 7. INVESTIGATING THE CONSEQUENCES OF URBAN VOLCANISM USING A SCENARIO APPROACH: INSIGHTS INTO TRANSPORTATION NETWORK DAMAGE AND FUNCTIONALITY

Appendix E1. Investigating the Consequences of Urban Volcanism Using a Scenario Approach I: Development and Application of a Hypothetical Eruption in the Auckland Volcanic Field, New Zealand

PUBLICATION DETAILS:

Natalia I Deligne[1], Rebecca Fitzgerald[2], Daniel M Blake[2], Alistair J Davies[2], Josh L Hayes[2], Carol Stewart[3], Grant Wilson[2,4], Thomas M Wilson[2], Ben Kennedy[2], Ranella Carneiro[5], Scott Muspratt[5], Richard Woods[1]

[1] GNS Science, PO Box 30368, Lower Hutt 5040, New Zealand

[2] Department of Geological Sciences, University of Canterbury, Private Bag 4800, Christchurch 8140, New Zealand

[3] Joint Centre for Disaster Research, GNS Science/Massey University, PO Box 756, Wellington 8140, New Zealand

[4] State Emergency Management Committee Secretariat, 20 Southport Street, West Leederville, WA, Australia

[5] Vector Limited, PO Box 99882, Newmarket, Auckland, New Zealand

Journal: Journal of Volcanology and Geothermal Research

Received: 20 October 2016

Status: In Review

(SEE SEPARATE ELECTRONIC APPENDIX)

Appendix E2. Economics of Resilient Infrastructure Auckland Volcanic Field Scenario

PUBLICATION DETAILS:

Natalia I Deligne[1], Daniel M Blake[2], Alistair J Davies[2], Emily S Grace[1], Josh Hayes[2], Sally Potter[1], Carol Stewart[3], Grant Wilson[2,4], Thomas M Wilson[2]

[1] GNS Science, PO Box 30368, Lower Hutt 5040, New Zealand

[2] Department of Geological Sciences, University of Canterbury, Private Bag 4800, Christchurch 8140, New Zealand

[3] Joint Centre for Disaster Research, GNS Science/Massey University, PO Box 756, Wellington 8140, New Zealand

[4] State Emergency Management Committee Secretariat, 20 Southport Street, West Leederville, WA, Australia

Publication: Economics of Resilient Infrastructure Research Report ***(SEE SEPARATE ELECTRONIC APPENDIX)***

Status: Published

Report Reference: 2015/03

Available from: http://www.gns.cri.nz/static/download/ERI_2015-03__AVF_scenario_.pdf

Appendix E3. Wind Profiles Selected for Modelling the Four Tephra Plumes in the South-Westerly Wind Scenario Addition in TEPHRA2 (14 March PM, 21 March, 22 March, 29-30 March)

Wind profile from:
24/01/1976 (12:00)

SCEANRIO PLUME 1
(14 MARCH PM)

Height (m)	Wind speed (km/h)	Wind direction (degrees away)	Wind direction (degrees towards)
33	15.1	225	45
1022	14.8	194	14
1502	32	207	27
2009	36	233	53
3116	38.9	248	68
4369	58.7	259	79
5808	65.5	279	99
7520	109.1	262	82
9638	124.2	260	80
10886	136.4	258	78
11033	136.8	259	79

Wind profile from:
31/01/1976 (06:00)

SCEANRIO PLUME 2
(21 MARCH)

Height (m)	Wind speed (km/h)	Wind direction (degrees away)	Wind direction (degrees towards)
0	22.7	252	72
998	51.5	258	78
1460	55.1	259	79
1973	50	249	69
3016	61.6	249	69
4230	90.4	275	95
5607	126.4	275	95
7220	139	280	100
9181	172.4	293	113
10402	163.8	289	109
10800	180	283	103

Wind profile from:
01/02/1976 (00:00)

SCEANRIO PLUME 3
(22 MARCH)

Height (m)	Wind speed (km/h)	Wind direction (degrees away)	Wind direction (degrees towards)
33	34.2	198	18
1056	46.8	212	32
1523	41	218	38
2011	43.9	215	35

3065	63	211	31
4256	92.2	231	51
5638	135	226	46
7271	175.7	227	47
8133	194.4	228	48
9262	172.1	233	53
10457	163.1	239	59
11914	141.1	251	71
13774	95	245	65
16319	68	238	58
18534	33.8	212	32
20002	19.4	112	292
20645	16.2	117	297
23925	47.5	99	279
24946	50.8	98	278
26600	61.2	90	270
30067	72.4	96	276
31305	79.6	85	265
33800	90	102	282

Wind profile from:
8/02/1976 (00:00)

SCEANRIO PLUME 4
(29-30 MARCH)

Height (m)	**Wind speed (km/h)**	**Wind direction (degrees away)**	**Wind direction (degrees towards)**
33	45	209	29
967	42.1	211	31
1439	40.7	225	45
1937	33.8	238	58
3020	27.4	337	157
4244	83.9	335	155
5653	109.8	337	157
7308	118.4	340	160
9341	163.1	338	158
10333	180	336	156
10565	180.7	337	157
12064	149.8	336	156
13916	121	330	150
16444	55.8	345	165
18651	40.3	10	190
20120	31	54	234
20762	34.2	72	252
24027	39.6	95	275
25035	46.8	94	274
26666	47.5	99	279
30097	75.6	90	270

31320	76	95	275
35000	90	90	270
35900	97.2	99	279

Appendix E4. TEPHRA2 Tephra Characteristic Input Parameters Used for Modelling Ash Deposition from the Predominant South-Westerly Wind Profiles in the Scenario

Parameter	Value	Informing References
Maximum grain size (ϕ)	-4.5	Segurstrom 1950, Walker and Croasdale 1971, Self et al. 1974, Magill et al. 2006, Rowland et al. 2009, Jenni Hopkins, Victoria University of Wellington, pers comm, 19 July 2014, Johnson et al. 2014, Hopkins et al. 2015.
Minimum grain size (ϕ)	6	
Median grain size (ϕ)	-1	
Standard deviation grain size (ϕ)	2	
Eddy constant	0.04	Bonadonna et al. 2005, Connor et al. 2011.
Diffusion coefficient (m^2 s^{-1})	12,000	Hurst 1994, Magill et al. 2006.
Fall time threshold (s)	100,000	Bonadonna et al. 2005, Connor et al. 2011.
Lithic density (kg m^{-3})	2,200	Fries 1953, Bonadonna et al. 2005, Houghton et al. 2006, De la Cruz-Reyna and Yokoyama 2011, Johnson et al. 2014, Blake et al. in review a,b,c.
Pumice density (kg m^{-3})	1,200	
Column steps	100	Bonadonna et al. 2005, Connor et al. 2011.
Plume model	0.2	
Plume ratio	0.2	

Appendix E5. Physical Damage Descriptions with Auckland Specifics for Road and Rail Networks from Geophysical Hazards in the Māngere Bridge Scenario

Scenario Date	Event specifics	Road Physical Damage	Rail Physical Damage
22 February	VAL increases from 0 to 1	None	None
08 March	08 March PEZ implemented	None	None
11 March	11 March PEZ implemented	None	None
12 March	12 March SEZ implemented	None	None
13 March	Volcanic gases detected. Shallow earthquakes (up to M4.5).	Potential minor damage to some bridges and roadside equipment in areas proximal to earthquake epicentres (inspections may be required). • Potential for minor blockage by landslides from steep slopes onto roads. *Length of road in impacted area ~2,900 km*	Rail stations: • No physical impact expected. Rail lines: • Potential damage to rail and components across the suburban electric network from earthquakes and ground deformation (inspections required).*Note. Southern part of network is perhaps more susceptible due to geology (peat and ash).* • Potential for blockage by landslides from steep slopes onto tracks and tunnel entrances (e.g. Newmarket).
14 March AM	Base surge causes complete destruction 0-4 km from vent and some damage 4-6 km from vent. Shallow earthquakes (up to M4.5).	Road infrastructure destroyed or severely damaged 0-4 km from vent including sections of: • South western Motorway (SH20) • George Bolt Memorial Drive (SH20A) • Arterial and minor roads to north and south of Mangere Inlet. Some road infrastructure damaged with major blockages 4-6 km from vent including sections of: • Southern motorway (SH1) • Ellerslie-Panmure Highway and South-Eastern Highway • Arterial and minor roads surrounding Mangere Inlet. Potential further minor damage to some bridges and roadside equipment in areas proximal to earthquake epicentres (inspections may be required). • Potential for minor blockage by landslides from steep slopes onto roads. *115 km road destroyed.* *202 km road severely damaged with complete blockage.* *457 km road with some damage and major blockages*	Rail stations: • Onehunga and Te Papapa stations destroyed or severely damaged beyond reasonable repair by base surge • Possible damage to stations on line between Greenlane and Otahuhu (inclusive) by outer surge (<5 KPa). Rail lines: • Line between Penrose and Onehunga, and nearby branch destroyed or severely damaged by base surge • Possible damage to line between Remuera and Middlemore, and sidings from Westfield by initial outer surge (<5 KPa). • Potential damage to rail and components across the suburban electric network from further earthquakes and ground deformation (inspections required).
14 March PM	Tephra fallout to west.	Tephra deposition on some minor roads to west of scenario vent.	Rail stations: • Onehunga and Te Papapa stations

	Shallow earthquakes (up to M4.8).	*Note. Remobilised ash may extend to roads beyond the area mentioned but no substantial impacts are anticipated.* Potential further minor damage to some bridges and roadside equipment in areas proximal to earthquake epicentres (inspections may be required). • Potential for minor blockage by landslides from steep slopes onto roads. *163 km road outside of the initial surge area experiences direct tephra deposition.*	remain destroyed or severely damaged • Possible damage remains to stations on line between Greenlane and Otahuhu (inclusive) by initial outer surge (<5 KPa). Rail lines: • Line between Penrose and Onehunga, and nearby branch remain destroyed or severely damaged by initial base surge • Possible damage remains to line between Remuera and Middlemore, and sidings from Westfield by initial outer surge (<5 KPa) and associated deposits. • Potential damage to rail and components across the suburban electric network from further earthquakes and ground deformation (inspections required). *Note. Tephra fall to west does not directly fall on the rail network. Remobilised ash may reach the line between Glen Eden and New Lynn but no impacts are anticipated.*
16 March	11 March PEZ and 12 March SEZ lifted. 16 March PEZ and 16 March SEZ implemented	Following clean-up and any necessary repair or removal of blockages, including on critical routes through evacuation zones, only minor accumulation of deposits remain on section of: • Southern motorway (SH1) • Ellerslie-Panmure Highway east of SH1. All other roads within initial surge area remain destroyed, damaged or blocked to some degree. Tephra deposition is cleaned-up or removed by rainfall beyond the SEZ extent – no further impact. *Note. Any minor damage from previous earthquakes has been repaired with no further impacts to the road network at this stage.*	Rail stations: • Onehunga and Te Papapa stations remain destroyed or severely damaged • Possible damage remains to stations on line between Greenlane and Otahuhu (inclusive) by initial outer surge (<5 KPa). Rail lines: • Line between Penrose and Onehunga, and nearby branch remain destroyed or severely damaged by initial base surge • Possible damage remains to line between Remuera and Middlemore, line from Westfield to Sylvia Park and Britomart to Orakei, and sidings from Westfield by initial outer surge (<5 KPa) and associated deposits. *Note. Any damage to components from previous earthquakes is repaired with no impact to the rail network beyond 6 km from the vent at this stage.*
21 March	Tephra fallout to north west. Base surge.	Physical impact to the roads within 0-6 km from the vent remains, similar to that on 16 March with some further accumulation of surge and tephra deposits. Tephra deposition also occurs on roads to north west of SEZ including sections of: • Southern Motorway (SH1) extending onto the Northern	Rail stations: • Onehunga and Te Papapa stations remain destroyed or severely damaged • Possible damage remains to stations on line between Greenlane and Otahuhu (inclusive) by initial outer surge (<5 KPa). Rail lines: • Line between Penrose and

		Motorway (SH1) over the Auckland Harbour Bridge • Northern section of South western Motorway (SH20) • North-Western Motorway (SH16) • Arterial and minor roads in central Auckland, to the immediate west, and north of the Auckland Harbour Bridge. *984 km road beyond the initial base surge area experiences tephra accumulation. Thus, a total of 1,758 km of road is impacted at this stage* ***(the largest extent throughout the scenario).***	Onehunga, and Southdown branch remain destroyed or severely damaged by initial base surge • Possible damage remains to line between Remuera and Middlemore, line from Westfield to Sylvia Park and Britomart to Orakei, and sidings from Westfield by initial outer surge (<5 KPa) and associated deposits • Possible damage to rail components on line between Britomart and Otahuhu, and line between Britomart and Sturges from ash deposition and infiltration to components. *Note. Initial component failures from ash accumulation beyond the SEZ are fixed by late on 22 March. However, some failures may continue due to ash remobilisation on the network.*
30 March	Tephra fallout to south east.	Following clean-up, there is no further impact from the previous tephra accumulation beyond the SEZ. Continued clean-up of remobilised tephra on critical routes means only minor accumulation of deposits remains on the previously affected sections of: • Southern motorway (SH1) • Ellerslie-Panmure Highway east of SH1. New clean-up activity and any necessary repair or removal of blockages, means only minor accumulation of deposits remains on the previously affected sections of: • South-eastern Highway east of SH1 • Arterial and minor roads in a zone ~6 km north west of the vent. *All other roads within initial surge area remain destroyed, damaged or blocked to some degree.*	Rail stations: • Onehunga and Te Papapa stations remain destroyed or severely damaged • Possible damage remains to stations on line between Greenlane and Otahuhu (inclusive) by initial outer surge (<5 KPa). Rail lines: • Line between Penrose and Onehunga, and nearby branch remain destroyed or severely damaged by initial base surge • Possible damage remains to line between Newmarket and Middlemore, line from Westfield to Sylvia Park, and sidings from Westfield by initial outer surge (<5 KPa) and accumulating tephra deposits.
05 April	Lava flows. 16 March SEZ lifted.	Continued clean-up of remobilised tephra, means only minor accumulation of deposits remains on sections of the: • Southern motorway (SH1) • Ellerslie-Panmure Highway east of SH1 • South-eastern Highway east of SH1 • Arterial and minor roads in a zone ~6 km north west of the vent. New clean-up activity and any necessary repair or removal of	Rail stations: • Onehunga and Te Papapa stations remain destroyed or severely damaged. *Note. Previous damage to stations on line between Greenlane and Otahuhu (inclusive) by initial outer surge (<5 KPa) has been repaired.* Rail lines: • Line between Penrose and Onehunga, and Southdown branch remain destroyed or severely damaged by initial base surge

		blockages along further critical routes means only minor accumulation of deposits remains on previously affected sections of: • SH20 (to south) • Critical routes extending circularly around the east through the initial 4-6 km base surge area from the airport to Newmarket. *All other roads within initial surge area remain destroyed, damaged or blocked to some degree, although are widely accessible from this date for clean-up following the lifting of the SEZ.*	• Possible damage from tephra continues to line between Newmarket and Middlemore, line from Westfield to Sylvia Park, and sidings from Westfield until clean-up prevents further remobilisation and infiltration to components.
01 May	16 March PEZ lifted. **Permanent exclusion zone implemented.**	Following clean-up, repair of damage and removal of blockages, roads are restored beyond the extent of the severe damage / complete blockage zone caused by the initial surge (0-4 km from the vent). *The previous total road length in this area was 305 km.*	Rail stations: • Onehunga and Te Papapa stations remain destroyed or severely damaged. Rail lines: • Line between Penrose and Onehunga remains destroyed or severely damaged by initial base surge. *Note. Demand to reconstruct the infrastructure required to reopen the above section of the line is expected to be low. The stations and line may be decommissioned or relocated based on rebuild activities.* *Although the nearby branch is now deemed to be restored at this time, demand may be too low for this to occur with the previous damage incurred, and possible closure of storage and distribution facilities in this area could occur.*

Appendix E6. Full Time-Series Maps Showing Physical Damage to the Road Network During the Original Māngere Bridge Scenario

Map Legend:

Edifice extent

Surge and tephra deposits (mm)

0
<=1
1 - 5
5 - 10
10 - 50
50 - 100
100 - 500
500 - 1000
>1000

Road damage

Destroyed
Severe damage / complete blockage
Some damage / major blockages
Minor accumulation of deposits (no damage)
Minor damage and blockages possible
No impact

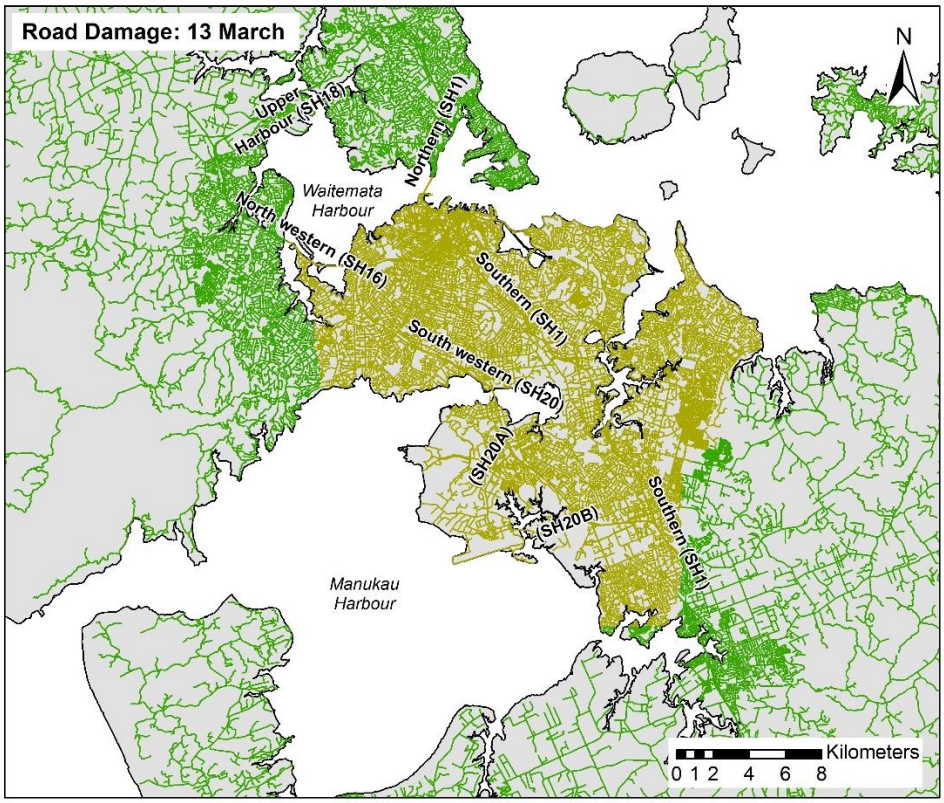

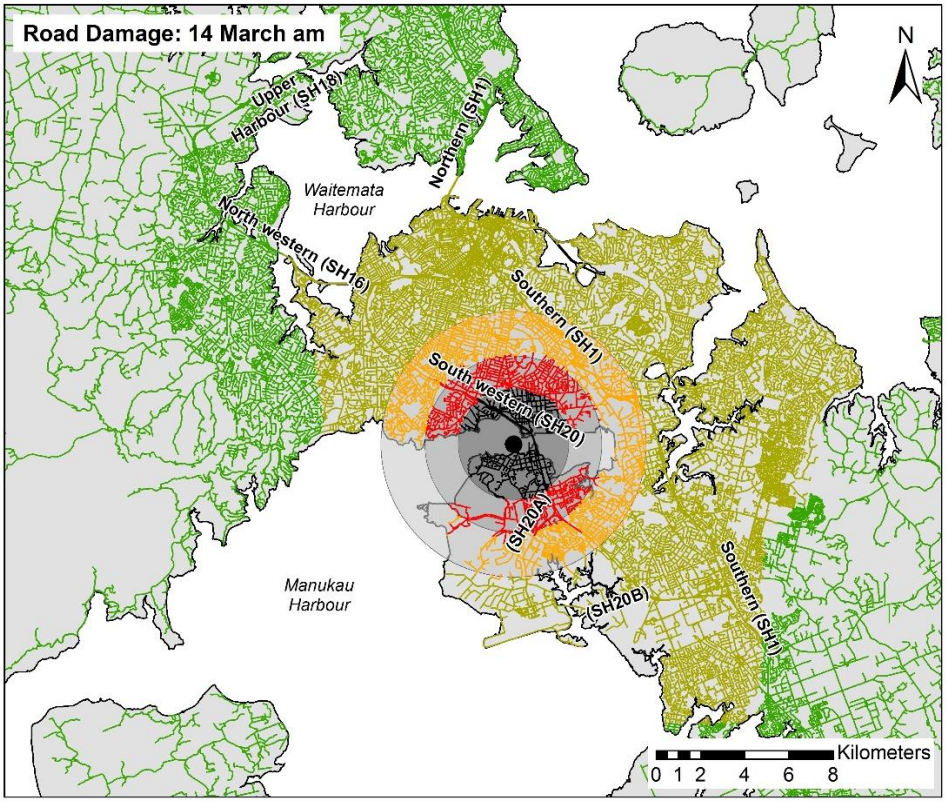
Road Damage: 14 March am
N
Upper Harbour (SH18)
Northern (SH1)
Waitemata Harbour
North western (SH16)
Southern (SH1)
South western (SH20)
(SH20A)
(SH20B)
Southern (SH1)
Manukau Harbour
Kilometers
0 1 2 4 6 8

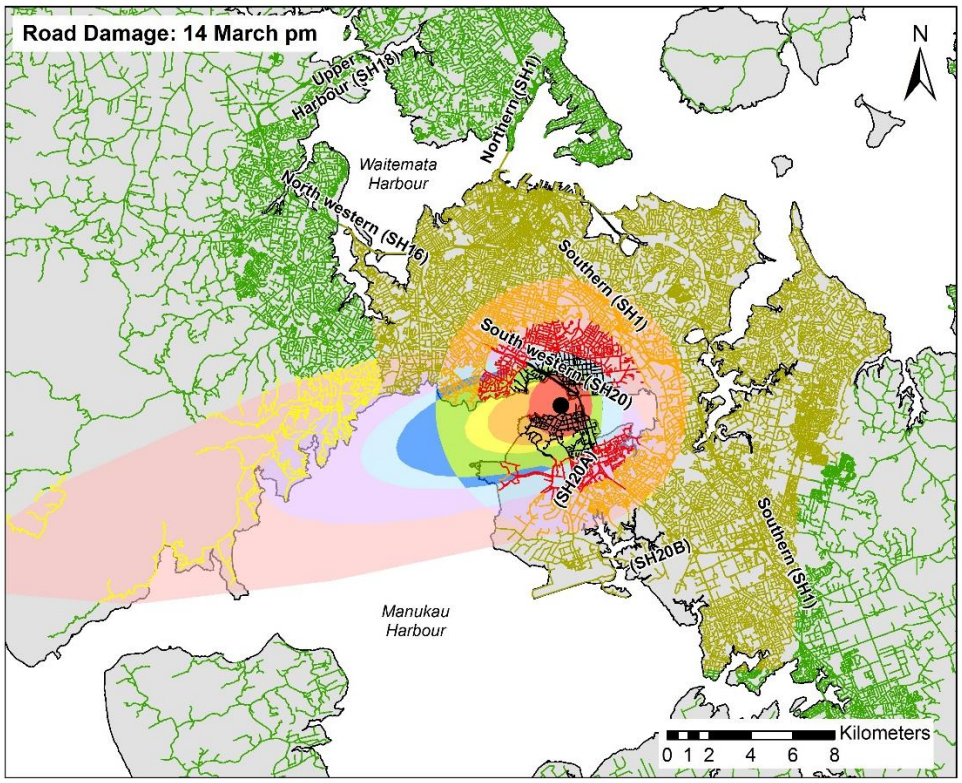
Road Damage: 14 March pm
N
Upper Harbour (SH18)
Northern (SH1)
Waitemata Harbour
North western (SH16)
Southern (SH1)
South western (SH20)
(SH20A)
(SH20B)
Southern (SH1)
Manukau Harbour
Kilometers
0 1 2 4 6 8

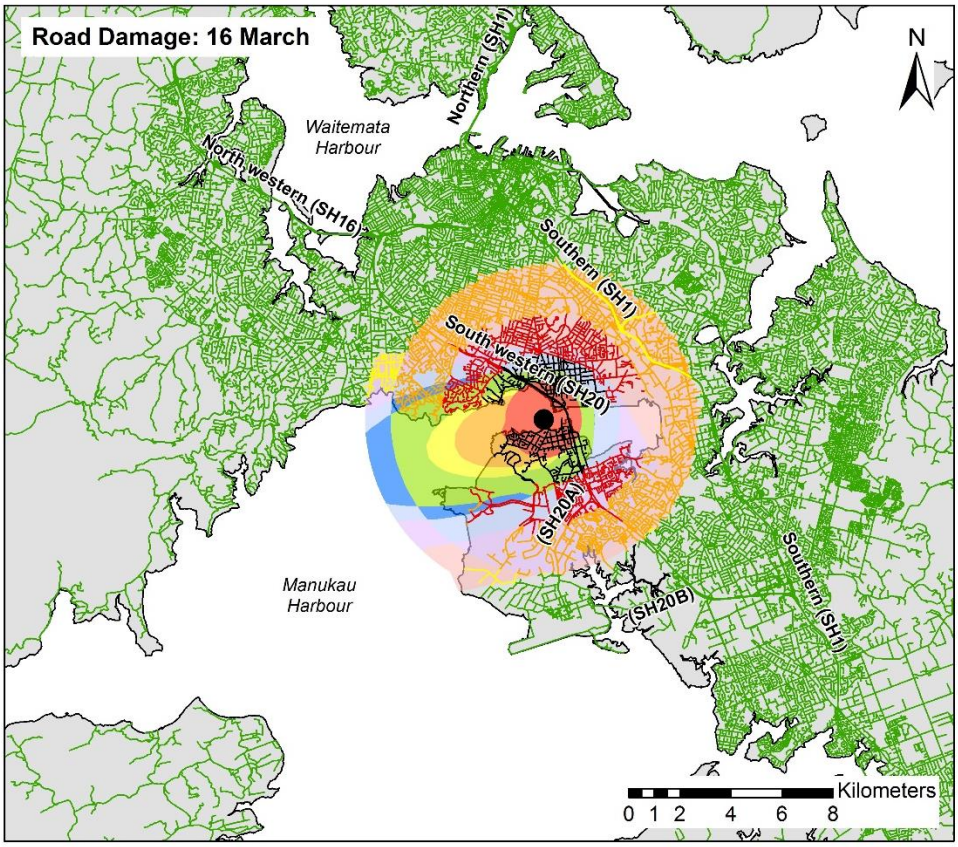
Road Damage: 16 March
N
Waitemata Harbour
Manukau Harbour
Northern (SH1)
North western (SH16)
Southern (SH1)
South western (SH20)
(SH20A)
(SH20B)
Southern (SH1)
Kilometers
0 1 2 4 6 8

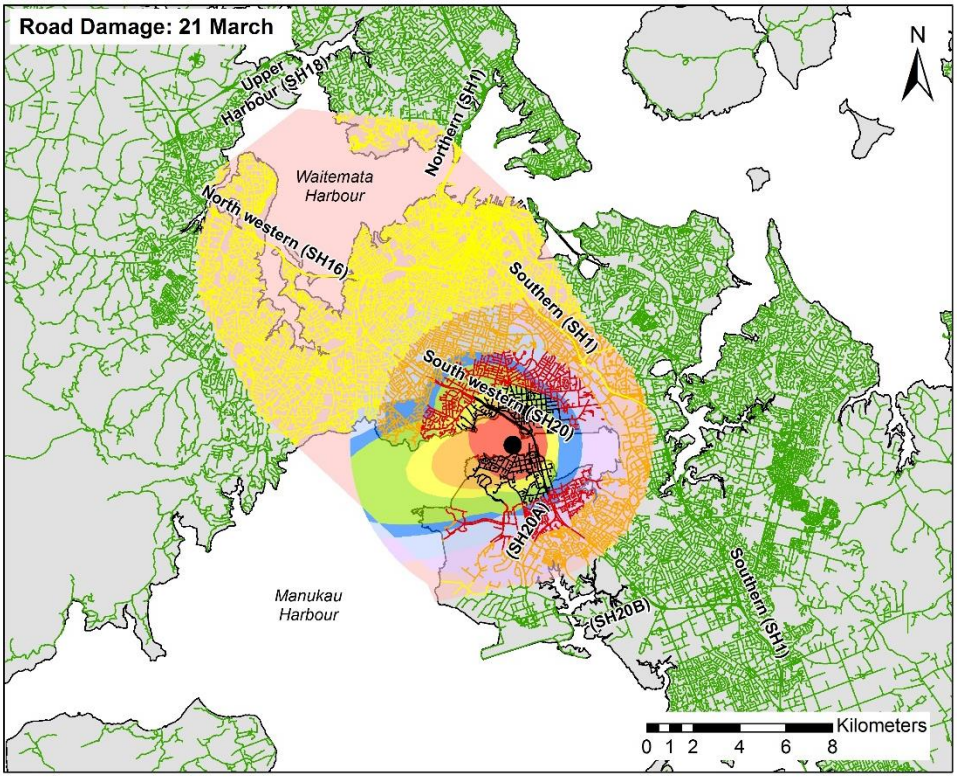
Road Damage: 21 March
N
Upper Harbour (SH18)
Waitemata Harbour
Manukau Harbour
Northern (SH1)
North western (SH16)
Southern (SH1)
South western (SH20)
(SH20A)
(SH20B)
Southern (SH1)
Kilometers
0 1 2 4 6 8

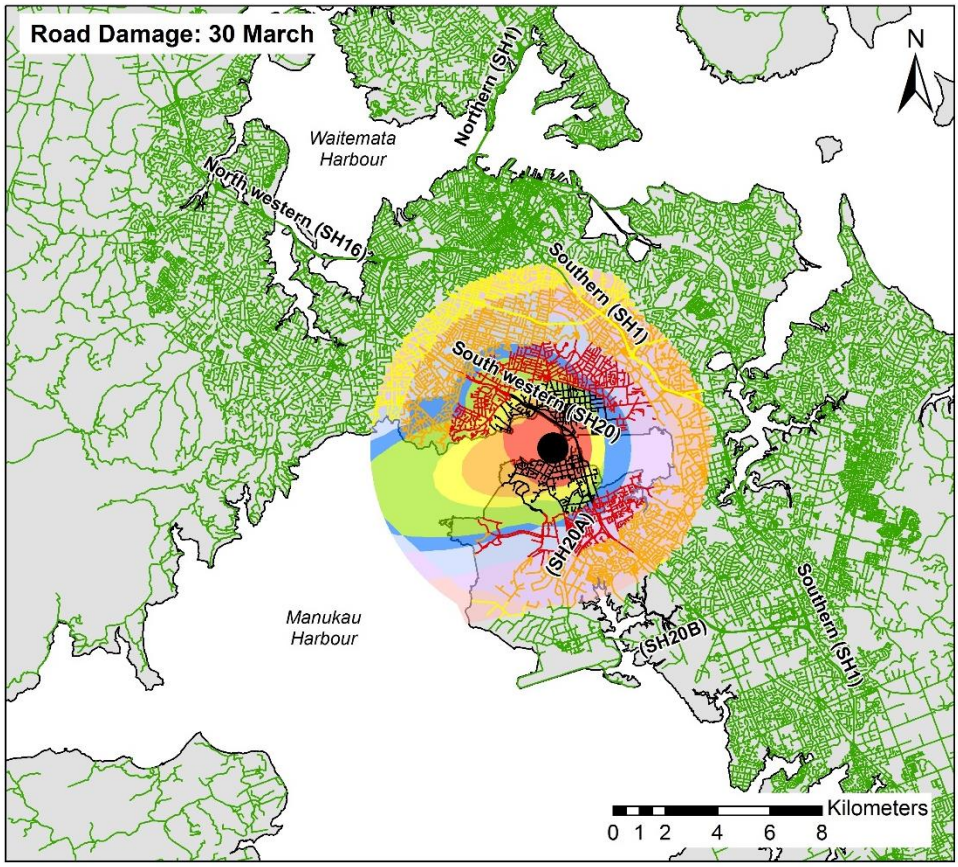
Road Damage: 30 March
N
Waitemata Harbour
Northern (SH1)
North western (SH16)
Southern (SH1)
South western (SH20)
(SH20A)
(SH20B)
Manukau Harbour
Southern (SH1)
Kilometers
0 1 2 4 6 8

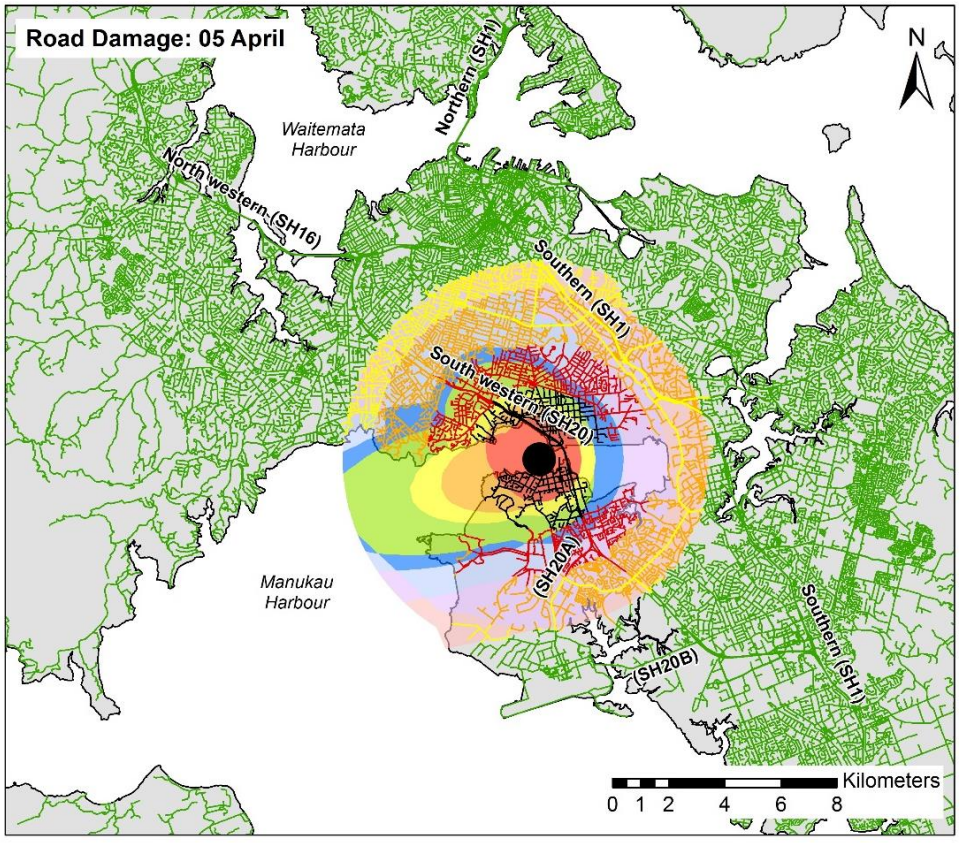
Road Damage: 05 April
N
Waitemata Harbour
Northern (SH1)
North western (SH16)
Southern (SH1)
South western (SH20)
(SH20A)
(SH20B)
Manukau Harbour
Southern (SH1)
Kilometers
0 1 2 4 6 8

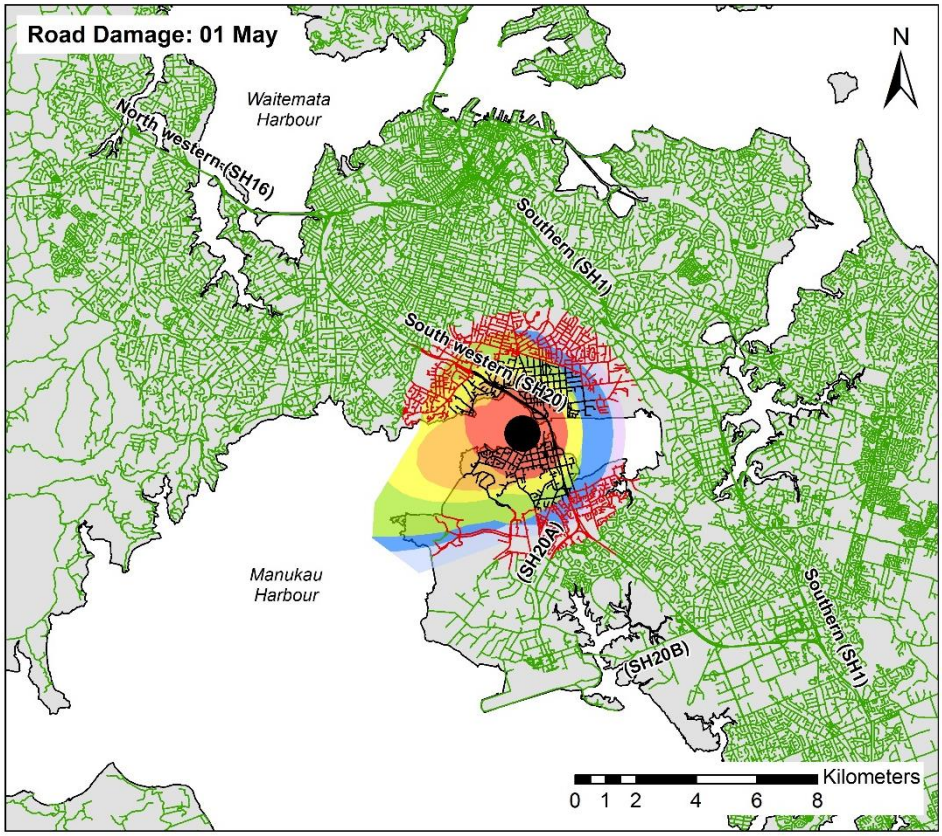
Road Damage: 01 May
N
Waitemata Harbour
North western (SH16)
Southern (SH1)
South western (SH20)
(SH20A)
Manukau Harbour
(SH20B)
Southern (SH1)
Kilometers
0 1 2 4 6 8

Appendix E7. Full Time-Series Maps Showing Physical Damage to the Rail Network During the Original Māngere Bridge Scenario

Map Legend:

Edifice extent

Surge and tephra deposits (mm)

- 0
- <=1
- 1 - 5
- 5 - 10
- 10 - 50
- 50 - 100
- 100 - 500
- 500 - 1000
- >1000

Rail station damage

- No impact
- Destroyed / severely damaged
- Possible damage

Rail line damage

- Destroyed / severely damaged
- Rail and components might be damaged
- No impact

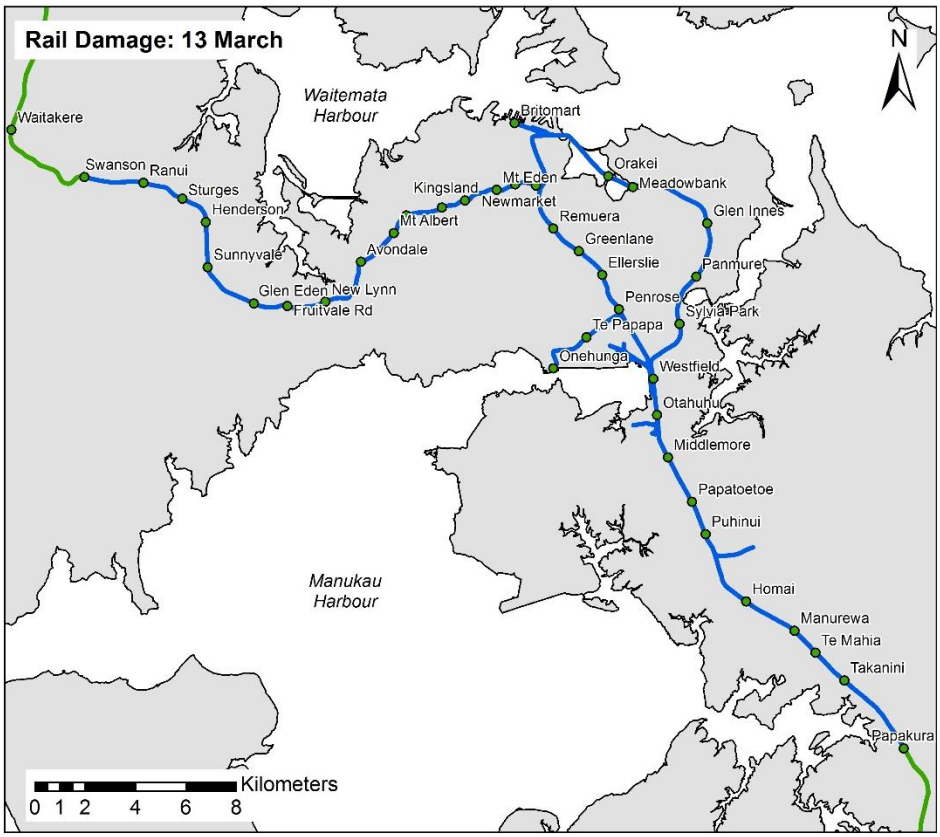

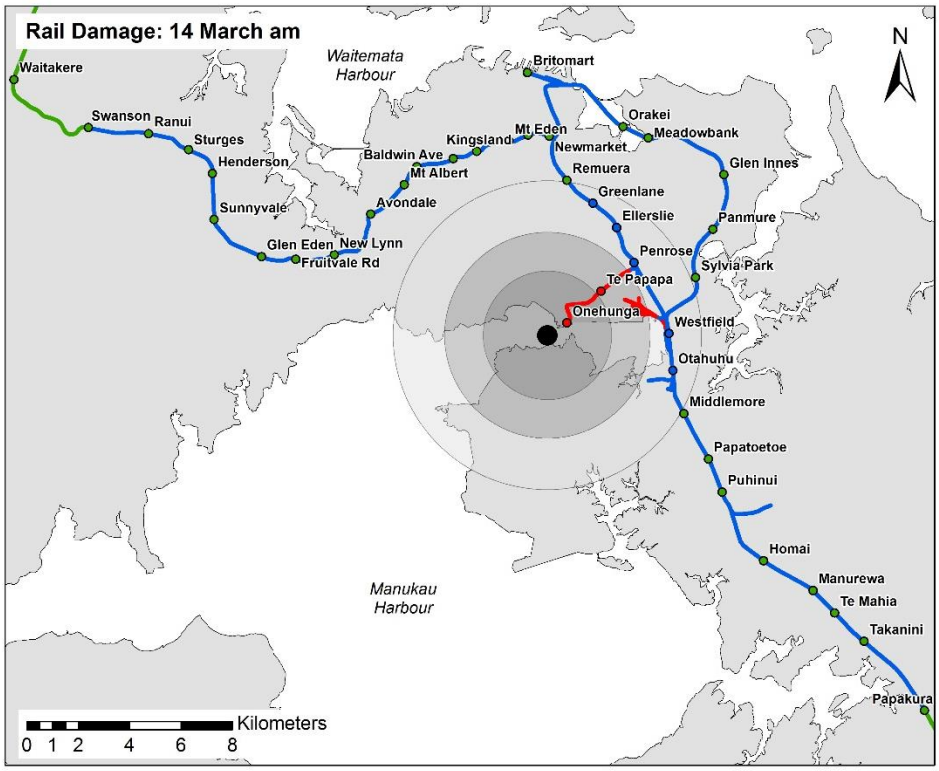
Rail Damage: 14 March am
N
Waitakere
Waitemata Harbour
Britomart
Swanson
Ranui
Sturges
Henderson
Kingsland
Mt Eden
Baldwin Ave
Mt Albert
Newmarket
Orakei
Meadowbank
Glen Innes
Remuera
Greenlane
Ellerslie
Panmure
Sunnyvale
Avondale
Glen Eden
New Lynn
Fruitvale Rd
Penrose
Sylvia Park
Te Papapa
Onehunga
Westfield
Otahuhu
Middlemore
Papatoetoe
Puhinui
Homai
Manurewa
Te Mahia
Takanini
Papakura
Manukau Harbour
Kilometers
0 1 2 4 6 8

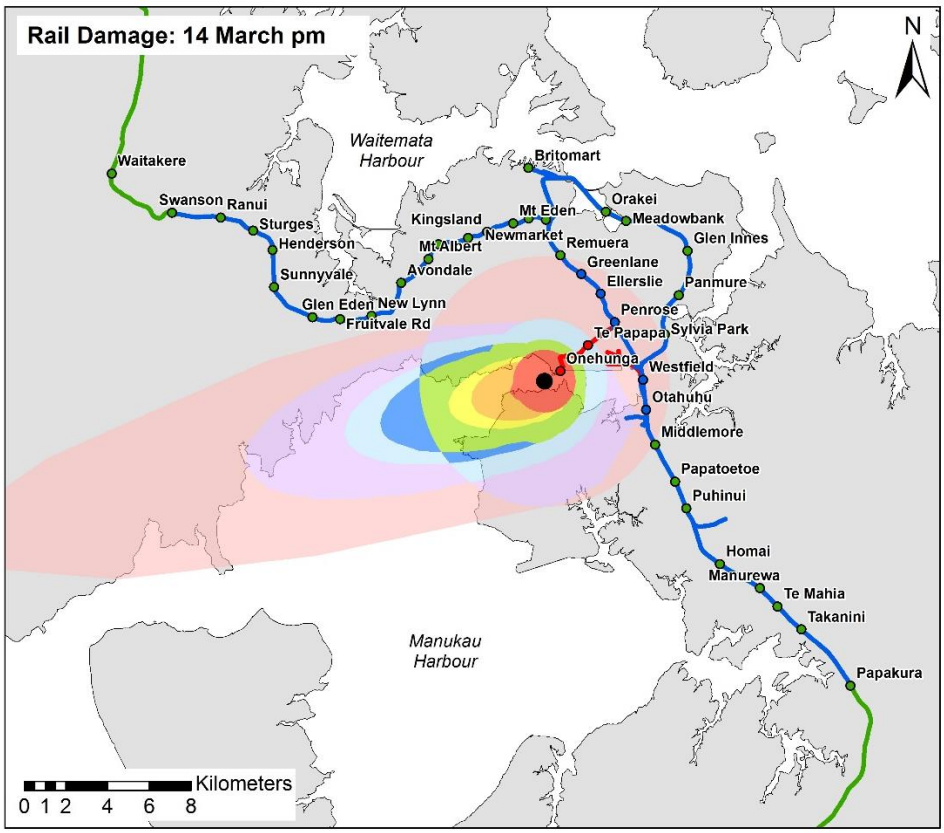
Rail Damage: 14 March pm
N
Waitakere
Waitemata Harbour
Britomart
Swanson
Ranui
Sturges
Henderson
Kingsland
Mt Eden
Newmarket
Orakei
Meadowbank
Glen Innes
Mt Albert
Remuera
Greenlane
Ellerslie
Panmure
Sunnyvale
Avondale
Glen Eden
New Lynn
Fruitvale Rd
Penrose
Sylvia Park
Te Papapa
Onehunga
Westfield
Otahuhu
Middlemore
Papatoetoe
Puhinui
Homai
Manurewa
Te Mahia
Takanini
Papakura
Manukau Harbour
Kilometers
0 1 2 4 6 8

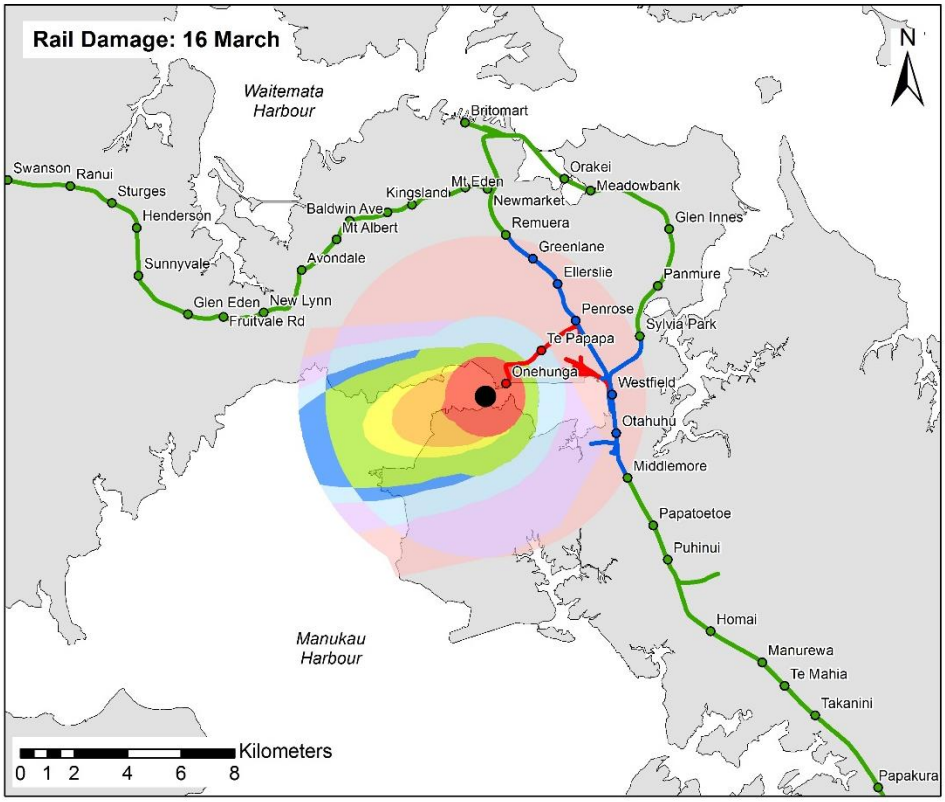
Rail Damage: 16 March
N
Waitemata Harbour
Britomart
Swanson
Ranui
Sturges
Henderson
Sunnyvale
Glen Eden
New Lynn
Fruitvale Rd
Kingsland
Mt Eden
Baldwin Ave
Mt Albert
Avondale
Newmarket
Orakei
Meadowbank
Glen Innes
Remuera
Greenlane
Ellerslie
Panmure
Penrose
Sylvia Park
Te Papapa
Onehunga
Westfield
Otahuhu
Middlemore
Papatoetoe
Puhinui
Homai
Manurewa
Te Mahia
Takanini
Papakura
Manukau Harbour
Kilometers
0 1 2 4 6 8

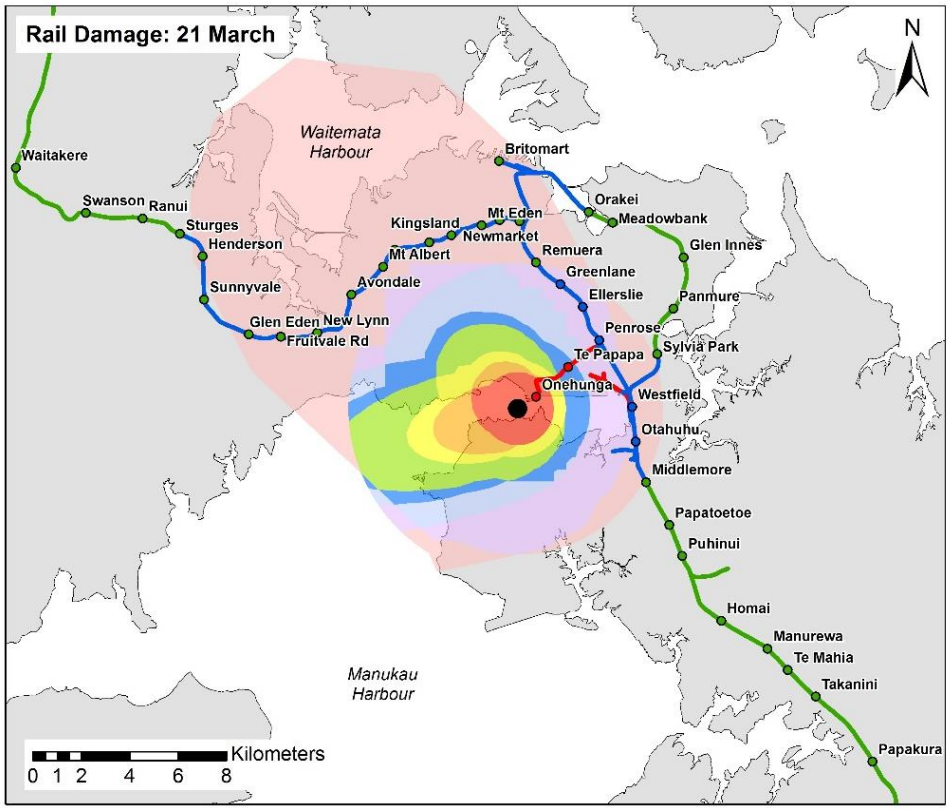
Rail Damage: 21 March
N
Waitemata Harbour
Waitakere
Britomart
Swanson
Ranui
Sturges
Henderson
Sunnyvale
Glen Eden
New Lynn
Fruitvale Rd
Kingsland
Mt Eden
Mt Albert
Avondale
Newmarket
Orakei
Meadowbank
Glen Innes
Remuera
Greenlane
Ellerslie
Panmure
Penrose
Sylvia Park
Te Papapa
Onehunga
Westfield
Otahuhu
Middlemore
Papatoetoe
Puhinui
Homai
Manurewa
Te Mahia
Takanini
Papakura
Manukau Harbour
Kilometers
0 1 2 4 6 8

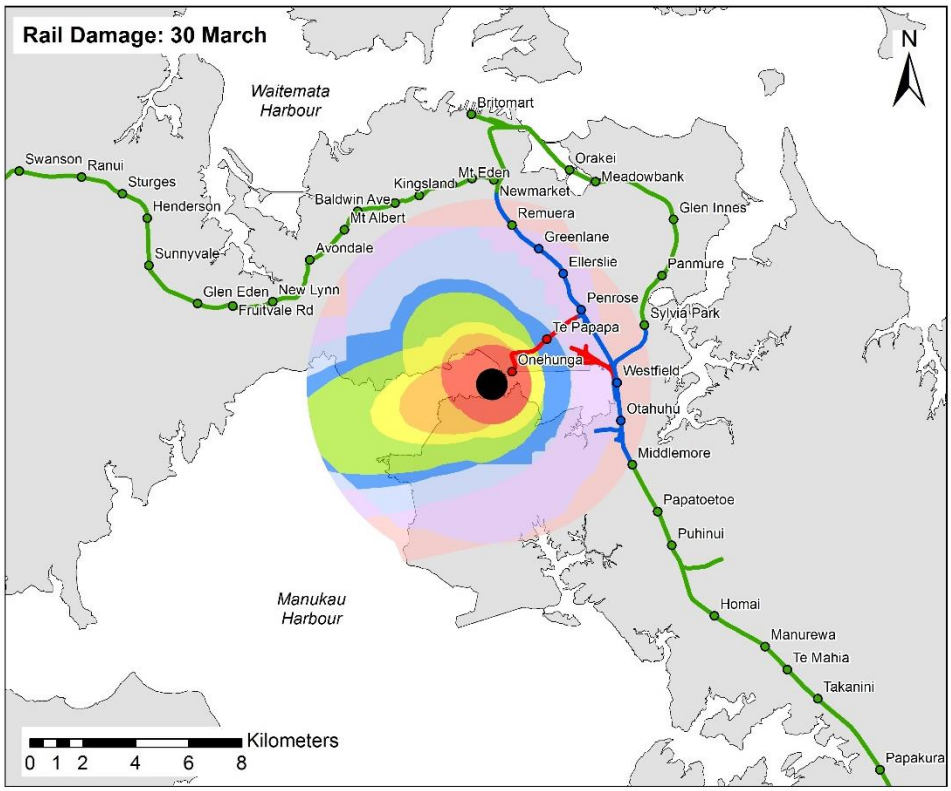
Rail Damage: 30 March
N
Waitemata Harbour
Britomart
Orakei
Meadowbank
Mt Eden
Kingsland
Newmarket
Baldwin Ave
Mt Albert
Remuera
Glen Innes
Greenlane
Avondale
Sunnyvale
Ellerslie
Panmure
Penrose
Glen Eden
New Lynn
Fruitvale Rd
Sylvia Park
Te Papapa
Onehunga
Westfield
Otahuhu
Middlemore
Papatoetoe
Puhinui
Manukau Harbour
Homai
Manurewa
Te Mahia
Takanini
Papakura
Swanson
Ranui
Sturges
Henderson
Kilometers
0 1 2 4 6 8

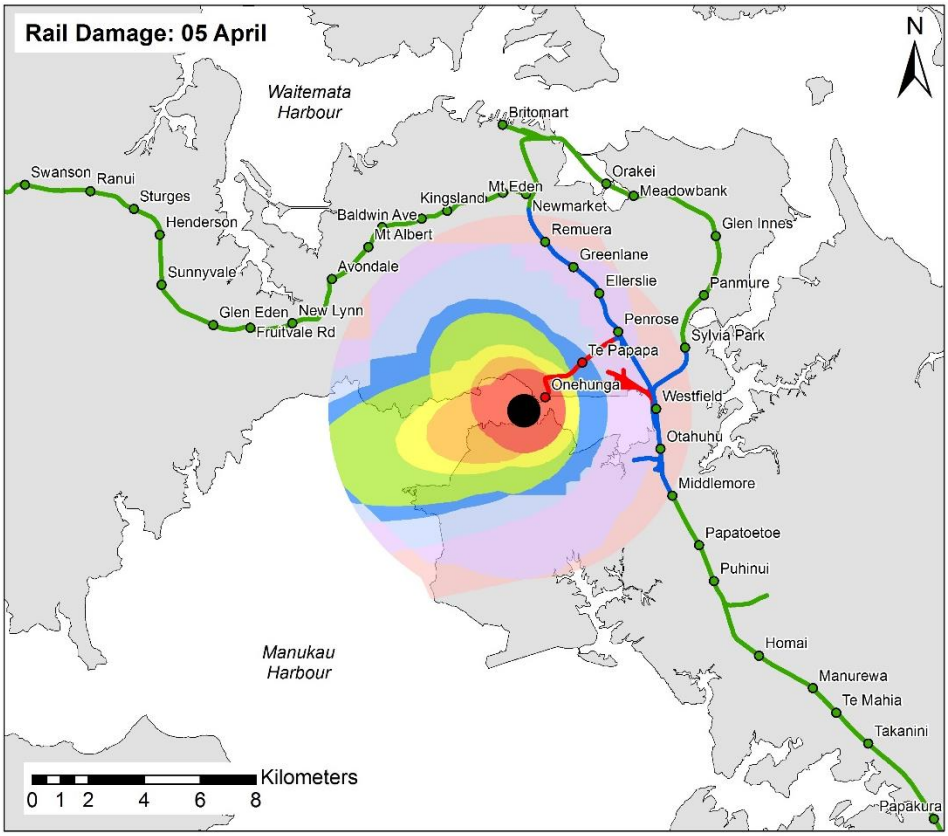
Rail Damage: 05 April
N
Waitemata Harbour
Britomart
Orakei
Meadowbank
Mt Eden
Kingsland
Newmarket
Baldwin Ave
Mt Albert
Remuera
Glen Innes
Greenlane
Avondale
Sunnyvale
Ellerslie
Panmure
Penrose
Glen Eden
New Lynn
Fruitvale Rd
Sylvia Park
Te Papapa
Onehunga
Westfield
Otahuhu
Middlemore
Papatoetoe
Puhinui
Manukau Harbour
Homai
Manurewa
Te Mahia
Takanini
Papakura
Swanson
Ranui
Sturges
Henderson
Kilometers
0 1 2 4 6 8

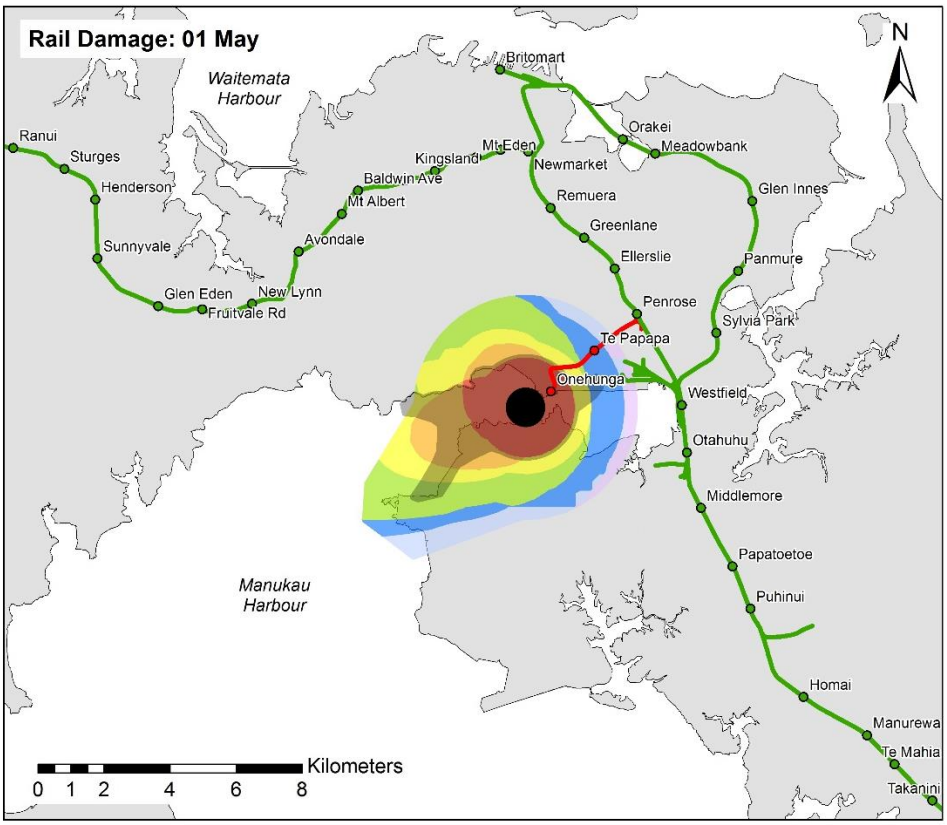
Rail Damage: 01 May
N
Waitemata Harbour
Manukau Harbour
Britomart
Orakei
Meadowbank
Mt Eden
Newmarket
Kingsland
Baldwin Ave
Mt Albert
Ranui
Sturges
Henderson
Sunnyvale
Avondale
Glen Eden
New Lynn
Fruitvale Rd
Remuera
Greenlane
Ellerslie
Glen Innes
Panmure
Penrose
Sylvia Park
Te Papapa
Onehunga
Westfield
Otahuhu
Middlemore
Papatoetoe
Puhinui
Homai
Manurewa
Te Mahia
Takanini
Kilometers
0 1 2 4 6 8

Appendix E8. Detailed Level-of-Service Descriptions for Auckland's Road, Rail and Airport Transportation over the Course of the Māngere Bridge Scenario

Scenario Date	Event Specifics	Road Level of Service	Rail Level of Service	Airport Level of Service
22 February	VAL increases from 0 to 1	Full service. *Note. Some self-evacuation and preparation for evacuation may lead to increase in traffic congestion (due to increased vehicle journeys) but the implications are considered minor on overall service.*	Full service. *Note. Some self-evacuation may lead to increase in passengers and delays at stations (due to increased boarding time) but the implications are considered minor on overall service.*	Auckland Airport starts making plans for a potential closure and issues a Notice to Airmen (NOTAM) notifying pilots of hazards and conditions on the airfield.
08 March	08 March PEZ implemented	Evacuations occur from the PEZ. Access becomes restricted for most entering the zone. However, some people such as those assisting with evacuation, critical infrastructure staff, hospital staff, emergency workers, and those assisting with distribution of critical resources, can still enter. All road transport between north and south Auckland is disrupted including sections of: • South western Motorway (SH20) including Manukau Harbour Crossing • Southern Motorway (SH1) between Mt Wellington and Ellerslie • Ellerslie-Panmure Highway including Panmure Bridge • South-Eastern Highway including Waipuna Bridge • Arterial and minor roads to east and south of Auckland City area. *Note. As the eruption has not started and no volcanic hazards are occurring, all other*	Rail stations: • Stations from Onehunga to Penrose, Greenlane to Westfield, and Westfield to Orakei become entry only (no exit from stopping trains due to evacuation zone). Rail lines: • Lines between Onehunga and Penrose, Remuera and Otahuhu, and line to east of city only operate as an evacuation service • 40 km/h limit is introduced on these lines due to the threat of earthquakes and complications such as increased chance of obstructions at level crossings due to road evacuations. *Note. Cascading effects on the operability of the remainder of the suburban electric rail network are expected and new timetabling is anticipated for much of the scenario from this date. However, this is not displayed on the figures.* *Some trains are out-stabled from Wiri to Henderson*	Auckland Airport issues NOTAM indicating airport closure. Minor domestic traffic at Ardmore Aerodrome. Most domestic traffic possibly diverted to Hamilton or Rotorua.

		infrastructure remains fully operational. Traffic signals, Variable Message Signs (VMS) and Police are used to optimise evacuation flow. Re-configuration of some motorway lanes may occur to increase capacity out of the PEZ, particularly on the Southern Motorway travelling south from the PEZ. *784 km road affected by 08 March PEZ.*	*and Swanson to allow continued operation on the line to the west of the city (including some diesel fleet from the Papakura to Pukekoe shuttle service).* *Relocation of KiwiRail operations and services.*	
11 March	11 March PEZ implemented	No access to roads affected by the initial PEZ on 08 March except emergency workers and critical infrastructure maintenance staff. Evacuations occur from a new PEZ section in the Mangere area. Access is restricted for most entering this zone. However, some people such as those assisting with evacuation, critical infrastructure staff, hospital staff, emergency workers, and those assisting with distribution of critical resources, can still enter. New roads affected include: • South western Motorway (SH20) south to Puhinui Road (SH20B) • George Bolt Memorial Drive (SH20A) • Puhinui Road (SH20B). *Note. Traffic signals, VMS, Police, and lane re-configuration are used to optimise evacuation flow where necessary.* *1019 km road is now affected by the new wider (11 March) PEZ.*	Rail stations: • Stations from Onehunga to Penrose, Greenlane to Westfield, and Westfield to Orakei are now closed following evacuations • Otahuhu and Middlemore stations on the become entry only (no exit from stopping trains due to new evacuation zone). Rail lines: • Lines between Onehunga and Penrose, Remuera and Otahuhu, and line to east of city are now closed to all rail services • Branch and sidings near Westfield are closed • Line between Otahuhu and Papatoetoe only operates as an evacuation service (with 40 km/h limit). *Notes.* *Diesel freight through-traffic ceases. Increased shipping between Port of Tauranga and Ports of Auckland Waitemata seaport is expected in response. Also unloading of some freight at Wiri depot ready for distribution by road.* *New timetabling comes into effect on lines not affected by evacuation or closure.*	Auckland Airport issues NOTAM indicating that the airport is within evacuation zone.
12 March	12 March SEZ implemented	No service (roads closed) in area covered by 11 March PEZ.	Rail stations:	

		Evacuations occur from SEZ, based on the probable vent location and extending up to 2 km from the 11 March PEZ in places. Access becomes restricted for most entering this zone. However, some people such as those assisting with evacuation, critical infrastructure staff, hospital staff, emergency workers, and those assisting with distribution of critical resources, can still enter. New roads affected include: • Southern Motorway (SH1) through narrowest point of Auckland isthmus • South western Motorway (SH20) section to north west of already affected section. *Although no critical infrastructure staff are allowed in the PEZ, it is expected that other infrastructure remains operational. VMS and traffic signals remain functional to optimise evacuation flow from the SEZ.* *1415 km road is now affected by evacuation zones (11 March PEZ and 12 March SEZ).*	• Stations from Onehunga to Penrose, Greenlane to Middlemore, and Westfield to Orakei are closed following evacuations • Remuera, Papatoetoe and Puhinui stations become entry only (no exit from stopping trains due to evacuation zone). Rail lines: • Lines between Onehunga and Penrose, Remuera and Papatoetoe, and line to east of city are closed to all rail services • Branch and sidings near Westfield remain closed • Line between Papatoetoe and Homai, and Remuera and Newmarket, only operate as an evacuation services (with 40 km/h limit). *Notes.* *No diesel freight through-traffic remains.* *New timetabling continues on lines not affected by evacuations or closure.*	
13 March	Volcanic gases detected. Shallow earthquakes (up to M4.5).	No service (roads closed) in area covered by 11 March PEZ and 12 March SEZ. Minor reduction in service is possible on roads impacted by ground shaking from earthquakes. This may include roads in: • Auckland City • Northern Motorway (SH1) between city and Auckland Harbour Bridge • North western Motorway (SH16) west of city • South Auckland ~5 km from PEZ and SEZ	Rail stations: • Stations from Remuera to Puhinui, and all those on lines to Onehunga and east of city are closed. Rail lines: • Onehunga Line, Eastern Line, and Southern Line between Newmarket and Homai are closed to all rail services. • Southdown branch and Westfield sidings remain closed. • Remainder of electric suburban electric rail network experiences rolling outages (for hours) due to earthquakes and required inspections. *Notes.*	

			No diesel freight through-traffic remains. *New timetabling continues on lines not affected by evacuations or closure between outages due to earthquakes / inspections.*	
14 March AM	Base surge causes complete destruction 0-4 km from vent and some damage 4-6 km from vent. Shallow earthquakes (up to M4.8). VAL increases from 2 to 3.	LoS in morning remains the same as 13 March due to the same evacuation zones and continuing earthquakes. (Damage to parts of the network occurs due to base surge but closures are already in effect.) – *NO MAP* *Note. Impact on electricity transmission and distribution may affect road LoS for the entire Auckland region, particularly due to potential traffic signal and VMS failure, and fuel station pump failure.*	Service remains the same as on 13 March due to the same evacuation zones and continuing earthquakes. – *NO MAP* *Damage to parts of the network occurs due to base surge but closures are already in effect. Tephra does not cause additional LoS reduction at this stage.*	No air traffic in or out of Auckland.
14 March PM	Tephra fallout to west. VAL increases from 3 to 4. Clean-up outside of SEZ begins (for ~1 day). Some critical routes also cleaned through SEZ.	Tephra in afternoon causes reduced LoS (due to reduced traction, impaired visibility and covered road markings affecting driving) on some arterial and minor roads to west of vent.		
16 March	11 March PEZ and 12 March SEZ lifted. 16 March PEZ and 16 March	Road service restored on roads beyond new 16 March PEZ and SEZ extents. Southern (SH1) Motorway and Ellerslie-Panmure Highway to east are reopened through PEZ and SEZ during daytime to restore critical road links	Rail stations: • Sylvia Park Station, stations from Remuera to Middlemore and those on Onehunga Line remain closed.	Auckland Airport issues NOTAM indicating it is no longer in evacuation zone but that airport remains closed.

	SEZ implemented. VAL 2 (after reducing to 3 on 15 March).	between north and south with hazard thresholds established for immediate re-closure: • 50 km/h advisory speed limit is implemented • Regular road sweeping occurs on this road to keep tephra deposits to a minimum. However, reduced traction, impaired visibility and road marking coverage is expected from remobilised ash • Exit ramps from SH1 within evacuation zone are purposefully blocked (other than Ellerslie-Panmure Highway). No service on all other roads within PEZ and SEZ.	Rail lines: • Onehunga Line and branch near Westfield remains closed • A non-stopping service between Newmarket and Papatoetoe through the new SEZ comes into effect restoring the north-south link on the rail network (with hazard thresholds for immediate re-closure established). As this route passes through outer surge deposits (between Remuera and Middlemore), a 40 km/h limit is in effect and rolling outages occur due to ash infiltration, associated component failure and required inspections. *Notes.* *Limited diesel freight services are restored from Wiri to north of Auckland and from Wiri to Waitemata Port. However, there are restrictions due to the relocation of railhead (and lifting equipment capacity) from Westfield. Some freight at Wiri is distributed to the north by road.* *New timetabling occurs on line to west and line south of Papatoetoe. A limited service may be restored from Britomart to Panmure although low demand may deem this unnecessary at this stage.*	
21 March	Tephra fallout to north west. Base surge. VAL 4 (after increasing to 3 on 18 March).	No service (roads closed again) through PEZ and SEZ due to threat from surge and tephra fall. Tephra deposition causes reduced service on roads to north west of SEZ including sections of: • Southern Motorway (SH1), extending onto the Northern Motorway (SH1) over the Auckland Harbour Bridge • Northern section of South western Motorway (SH20) • North-Western Motorway (SH16) west from Auckland city	Rail stations: • Sylvia Park Station, stations from Remuera to Middlemore, and those on Onehunga Line remain closed. Rail lines: • Onehunga Line and branch near Westfield remain closed. • A non-stopping service between Newmarket and Papatoetoe through the new SEZ (with rolling outages due to surge and accumulating tephra,	Volcanic eruption resumes. No air traffic in or out of Auckland.

		• Arterial and minor roads in Auckland City and to the west and north.	and 40 km/h limit) continues. • Rolling outages occur from Britomart to Sturges due to tephra deposition and possible ash infiltration into components (40 km/h limit is introduced). *Notes.* *Limited diesel freight services continue from Wiri to north of Auckland and from Wiri to Waitemata Port.* *New timetabling remains on the line to west of city, and line south of Papatoetoe. A limited service remains possible between Orakei and Panmure.* *Initial outages on line to west are expected to be short-lived (until late on 22 March). However, further outages are possible due to ash remobilisation.*	
22 March	Tephra. VAL reduces to 3. Clean-up outside of PEZ and SEZ begins (for ~1 week). Some critical routes also cleaned through PEZ and SEZ.	LoS remains the same on roads to north west affected by 21 March tephra fall with ash remobilisation. Road sweeping recommences on SH1 and Ellerslie-Panmure Highway to re-established critical routes from north to south (same restrictions as 16 March). Only critical infrastructure staff are permitted access within the SEZ (up to the extent of the outer initial surge deposit) to attempt infrastructure repairs. No service elsewhere within the PEZ and SEZ.		
30 March	Tephra fallout to south east.	Full service is restored to roads beyond SEZ that were affected by 21 March tephra fall. Service within PEZ and SEZ remains the same as 22 March except on two east-west critical routes which are reopened through the zones during daytime (with hazard thresholds established for immediate re-closure). Therefore, four critical routes have been partly re-established through the evacuation zones (with same restrictions as 16 March).	LoS is the same as 21 March except services (with new timetabling) are restored on the line to west following ash clean-up outside of the SEZ.	
05 April	Lava flows. 16 March SEZ lifted. Major clean-up operation within	In addition to the critical routes re-established on 30 March, others are restored (with same restrictions and reduced service due to reduced traction, visibility impairment and road marking coverage). This includes sections of: • South western Motorway (SH20) • Route extending circularly around the east through the initial 4-6 km base surge area from	Rail stations: • Onehunga and Te Papapa stations remain closed. Rail lines: • Onehunga Line and branch near Westfield remain closed • Some service is restored on all other lines (with 40	Auckland Airport issues a NOTAM indicating it remains outside of the evacuation zone with new evacuation orders in place. Airport is re-opened with minimal service. Some airlines request

	lifted SEZ begins (for ~1 month).	the airport to Newmarket • Other arterial roads to north. Only reduced service due to tephra deposits remain on some roads beyond the outer initial surge. Very limited access occurs on roads affected by the initial surge deposit up to the extent of the PEZ. No service (roads closed) within PEZ.	km/h limit between Newmarkert and Middlemore until minimal remobilisation of ash occurs). *Notes.* *Diesel freight services, including the railhead at Wiri are restored with some delays.* *New timetabling remains across much of the suburban electric rail network.* *Out-stabling of trains and relocation of KiwiRail staff is reconsidered.*	daytime access into the no-fly zone.
				Auckland Airport resumes full operations.
	VAL reduces to 2.			Auckland Airport issues a NOTAM that VAL has decreased.
01 May	16 March PEZ lifted. Permanent exclusion zone implemented. VAL reduces to 1. Major clean-up operation within lifted PEZ begins (for ~1 month).	Full service is restored to all roads beyond 4 km from the vent. Very limited access occurs 2-4 km from the vent. No service (roads closed indefinitely) 0-2 km from the vent including the Manukau Harbour Crossing and a section of the South western Motorway (SH20), which are permanently destroyed / buried.	Full service is restored to all stations and rail, with the exception of the Onehunga Line and Onehunga and Te Papapa stations which remain closed for the coming months.	Auckland Airport partially re-opened.
01 June	VAL reduces to 0.			Auckland Airport re-opens.
15 June				Auckland Airport fully open, although some airlines and/or routes may take a while to re-establish.

Appendix E9. Full Time-Series Maps Showing Level-of-Service for the Road Network During the Original Māngere Bridge Scenario

Map Legend:

Edifice extent
Primary Evacuation Zone (PEZ) boundary
Secondary Evacuation Zone (SEZ) boundary

Surge and tephra deposits (mm)

0
<=1
1 - 5
5 - 10
10 - 50
50 - 100
100 - 500
500 - 1000
>1000

Road Level-of-Service

I Full service
IIa Reduced service with no direct deposits (no access restrictions)
IIb Reduced service due to direct deposits (no access restrictions)
IIIa Access restrictions with no direct deposits
IIIb Access restrictions due to direct deposits
IV Critical infrastructure & maintenance staff access only
V No service

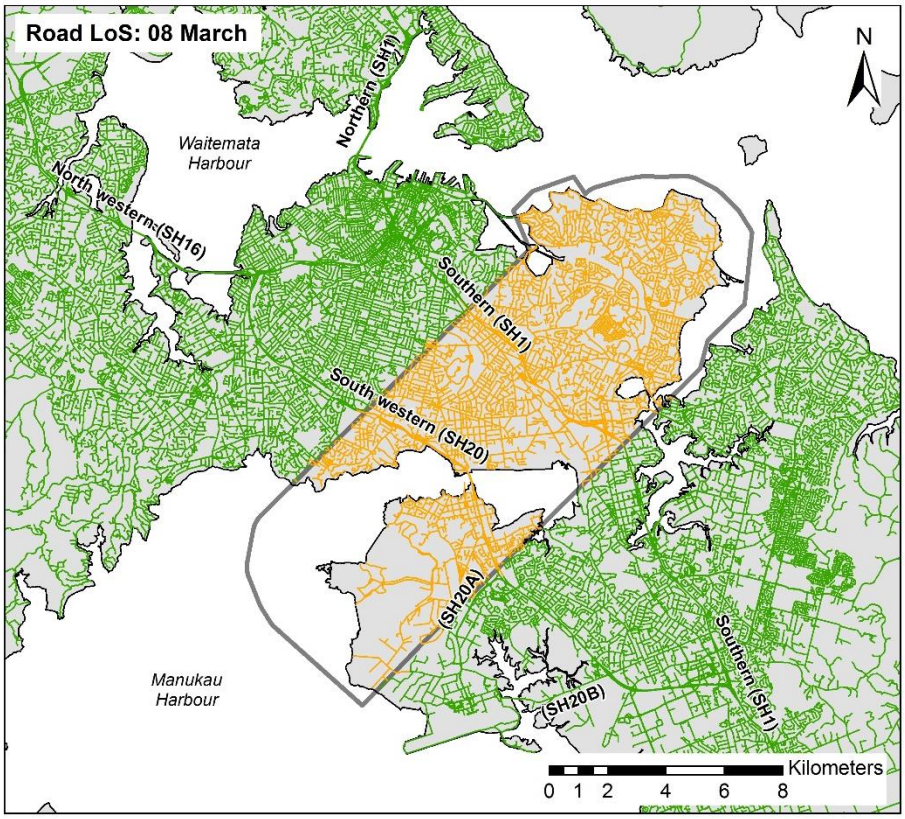

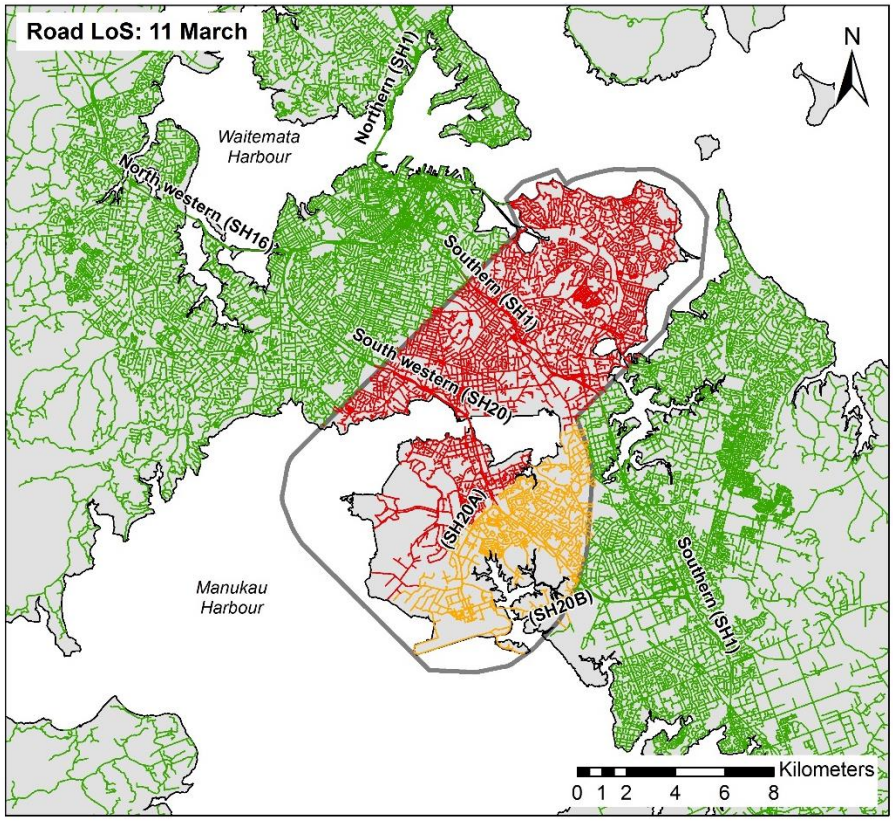
Road LoS: 11 March
N
Waitemata Harbour
Northern (SH1)
North western (SH16)
Southern (SH1)
South western (SH20)
(SH20A)
(SH20B)
Manukau Harbour
Southern (SH1)
Kilometers
0 1 2 4 6 8

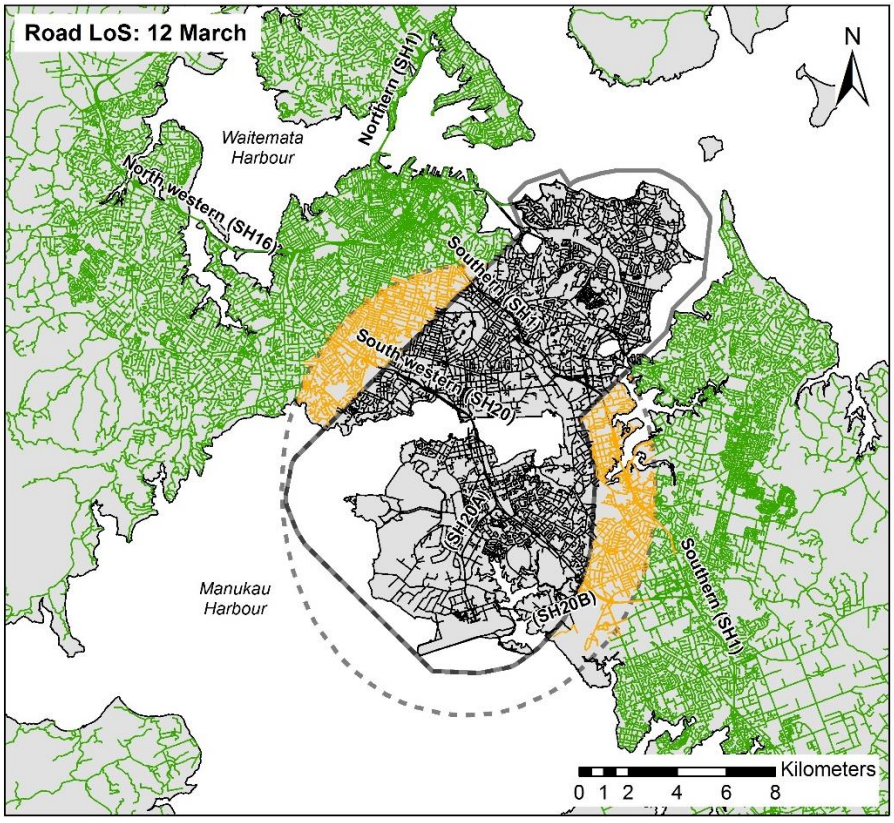
Road LoS: 12 March
N
Waitemata Harbour
Northern (SH1)
North western (SH16)
Southern (SH1)
South western (SH20)
(SH20A)
(SH20B)
Manukau Harbour
Southern (SH1)
Kilometers
0 1 2 4 6 8

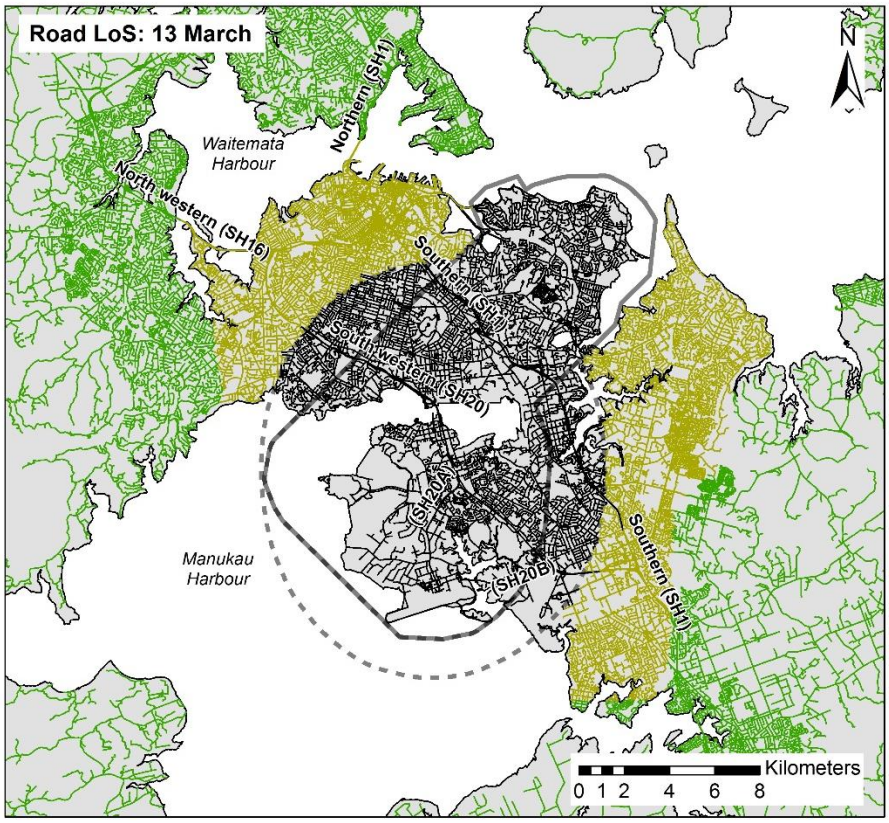
Road LoS: 13 March
N
Waitemata Harbour
Northern (SH1)
North western (SH16)
Southern (SH1)
South western (SH20)
(SH20A)
(SH20B)
Southern (SH1)
Manukau Harbour
Kilometers
0 1 2 4 6 8

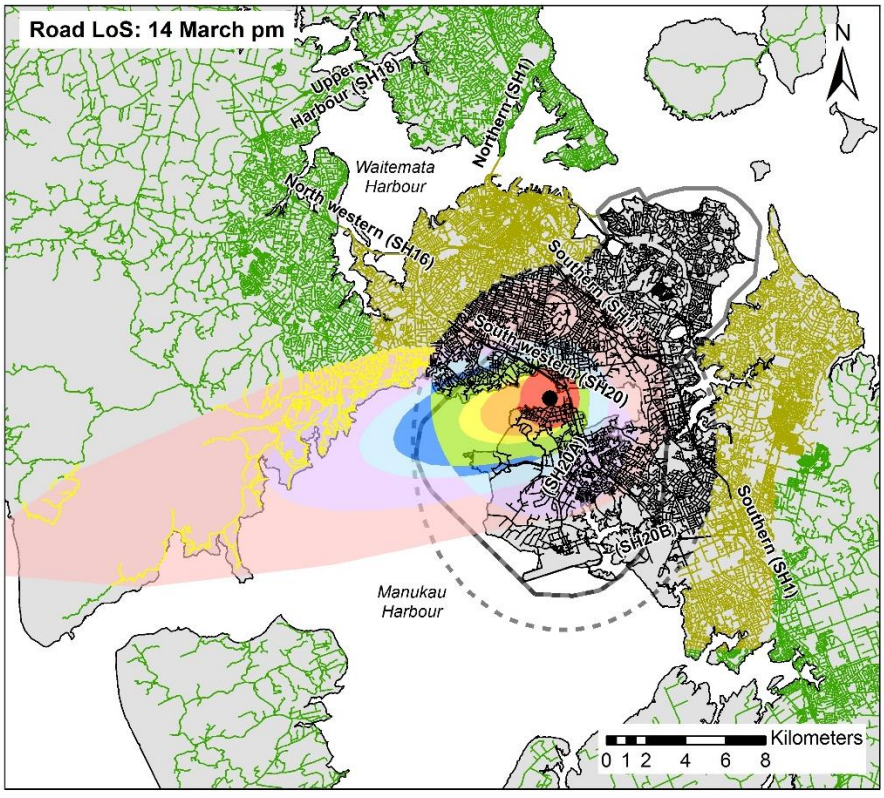
Road LoS: 14 March pm
N
Upper Harbour (SH18)
Northern (SH1)
Waitemata Harbour
North western (SH16)
Southern (SH1)
South western (SH20)
(SH20A)
(SH20B)
Southern (SH1)
Manukau Harbour
Kilometers
0 1 2 4 6 8

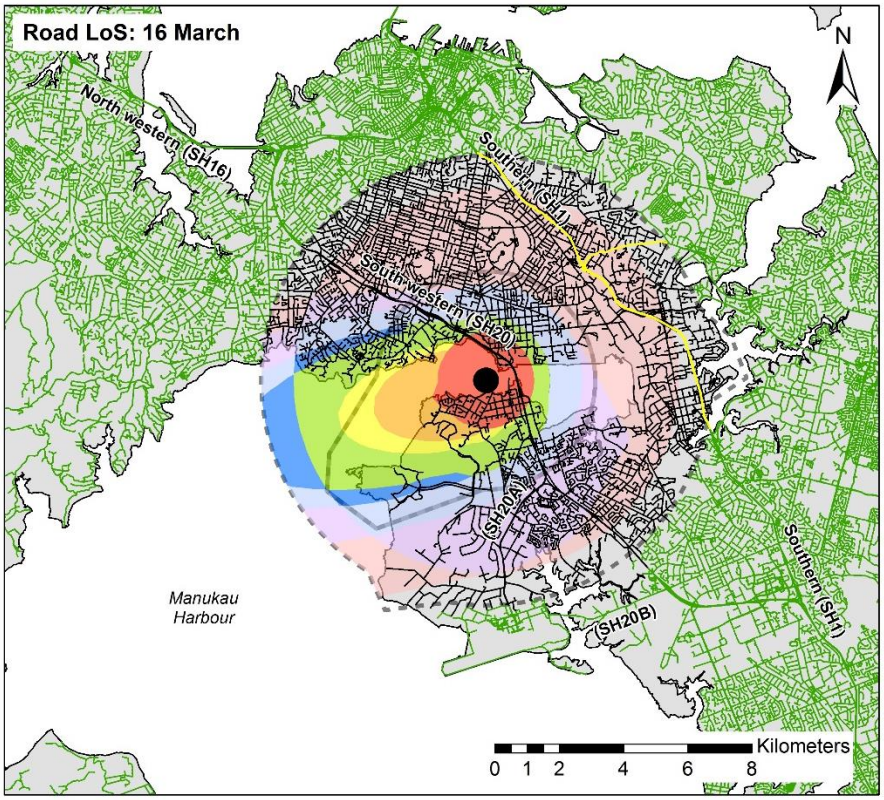
Road LoS: 16 March
N
North western (SH16)
Southern (SH1)
South western (SH20)
(SH20A)
(SH20B)
Southern (SH1)
Manukau
Harbour
Kilometers
0 1 2 4 6 8

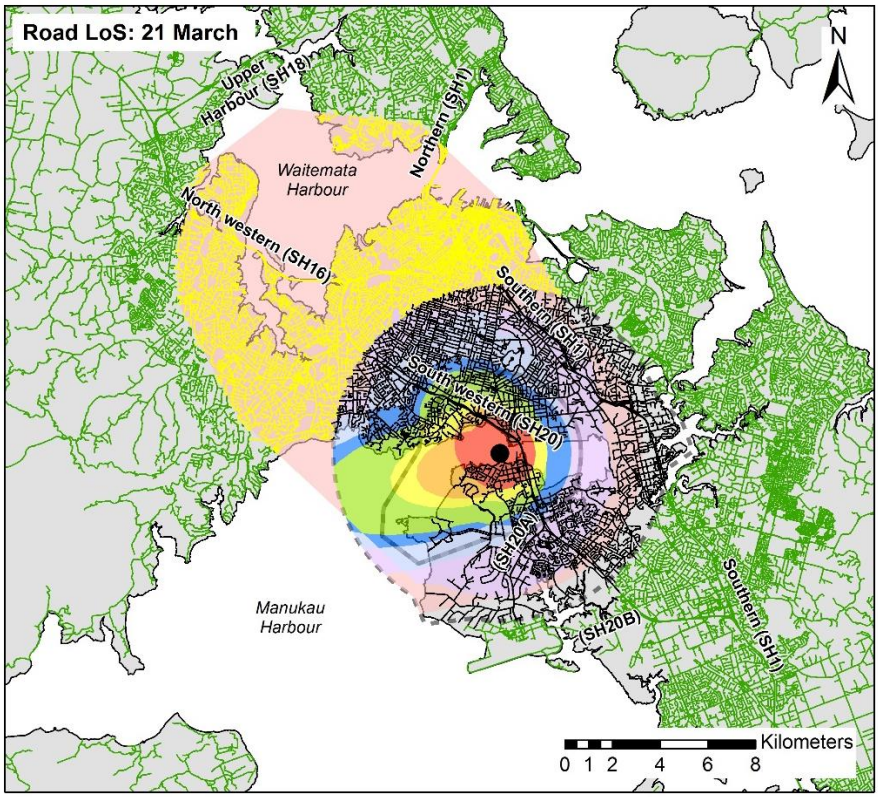
Road LoS: 21 March
N
Upper
Harbour (SH18)
Northern (SH1)
Waitemata
Harbour
North western (SH16)
Southern (SH1)
South western (SH20)
(SH20A)
(SH20B)
Southern (SH1)
Manukau
Harbour
Kilometers
0 1 2 4 6 8

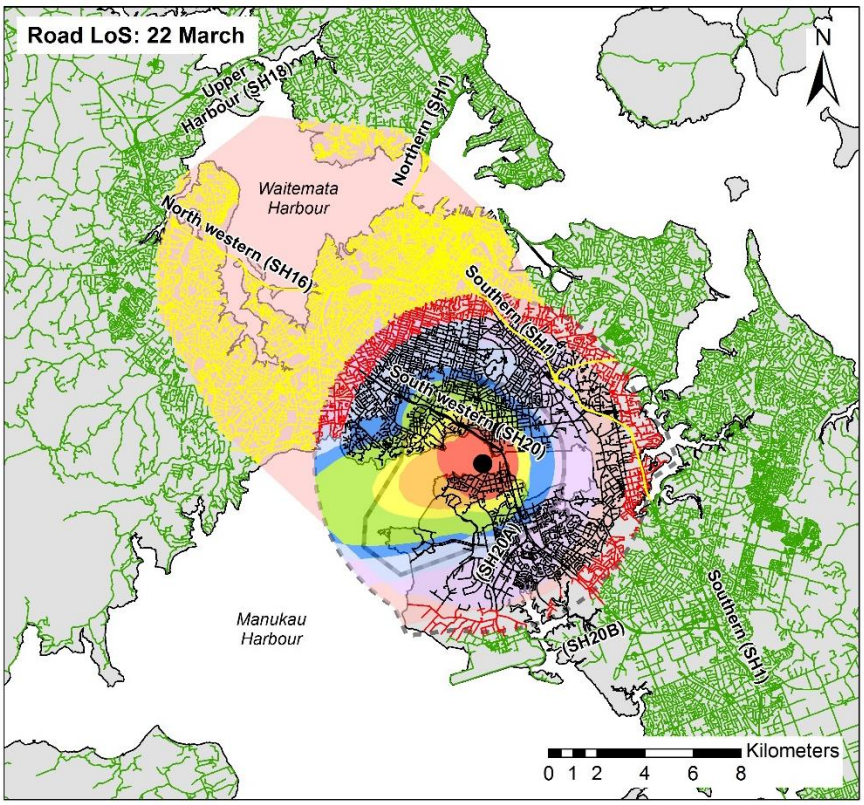
Road LoS: 22 March
N
Upper Harbour (SH18)
Northern (SH1)
Waitemata Harbour
North western (SH16)
Southern (SH1)
Southwestern (SH20)
(SH20A)
Manukau Harbour
(SH20B)
Southern (SH1)
Kilometers
0 1 2 4 6 8

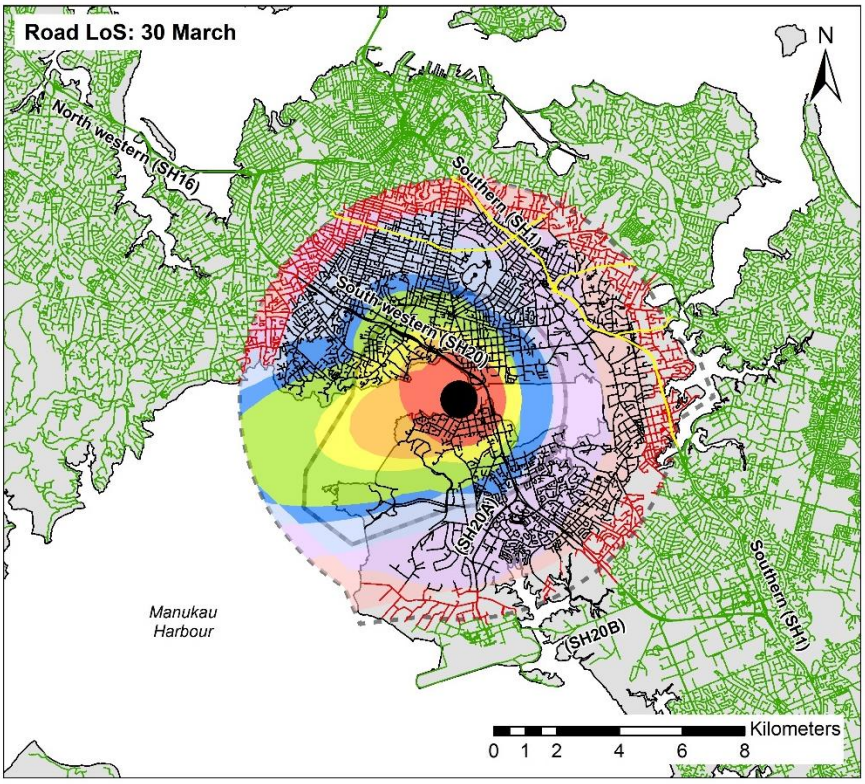
Road LoS: 30 March
N
North western (SH16)
Southern (SH1)
Southwestern (SH20)
(SH20A)
Manukau Harbour
(SH20B)
Southern (SH1)
Kilometers
0 1 2 4 6 8

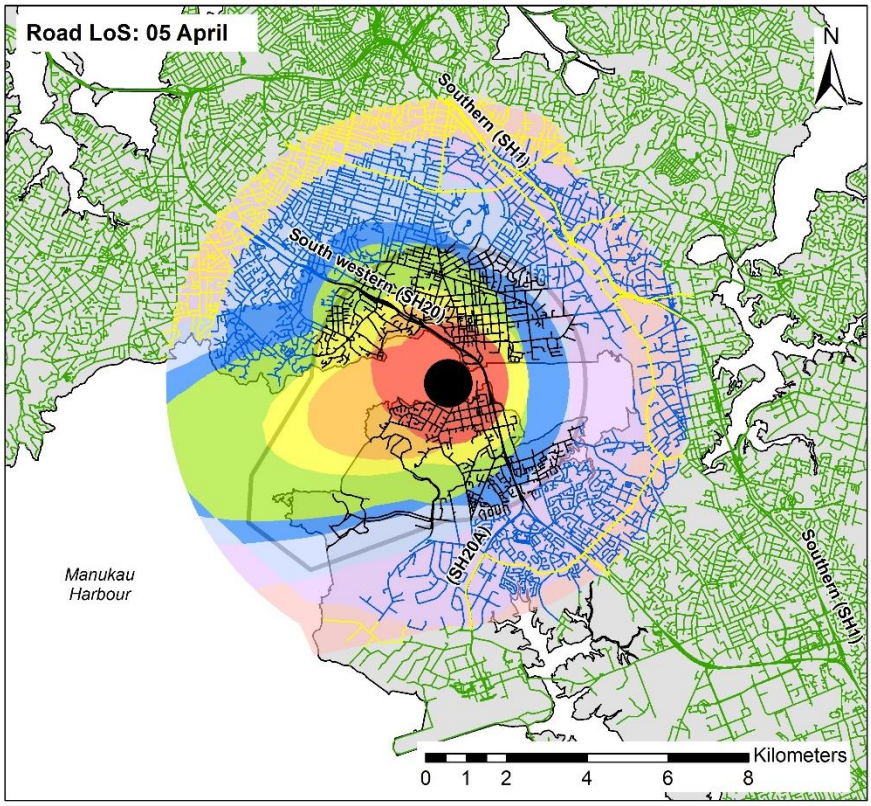
Road LoS: 05 April
N
Southern (SH1)
South western (SH20)
(SH20A)
Southern (SH1)
Manukau
Harbour
Kilometers
0 1 2 4 6 8

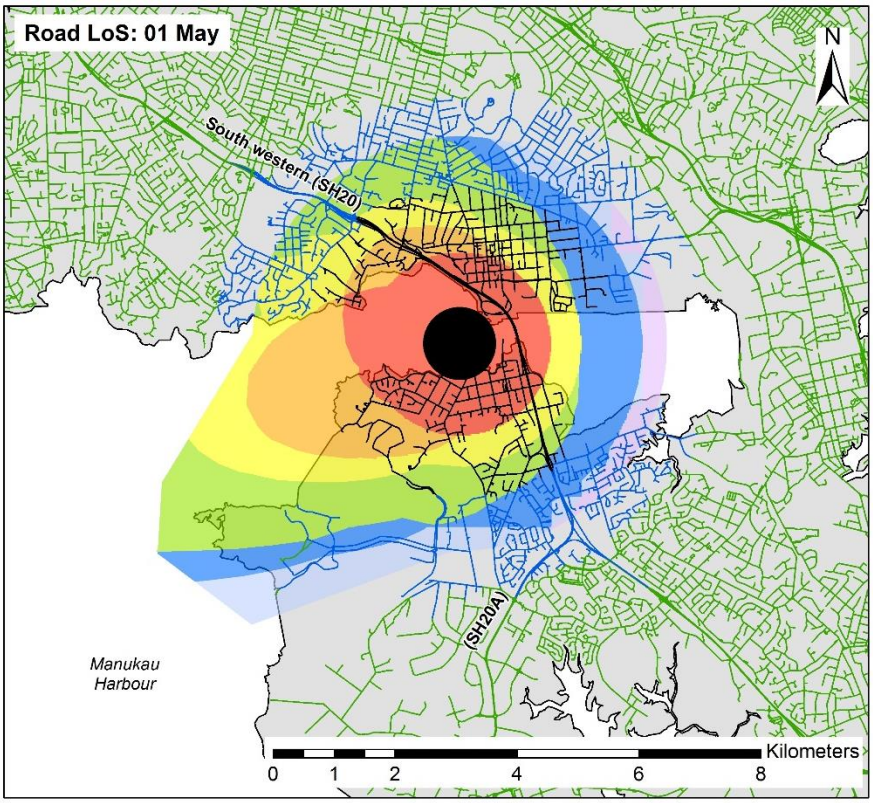
Road LoS: 01 May
N
South western (SH20)
(SH20A)
Manukau
Harbour
Kilometers
0 1 2 4 6 8

Appendix E10. Full Time-Series Maps Showing Level-of-Service for the Rail Network during the Original Māngere Bridge Scenario

Map Legend:

Edifice extent
Primary Evacuation Zone (PEZ) boundary
Secondary Evacuation Zone (SEZ) boundary

Surge and tephra deposits (mm)

0
<=1
1 - 5
5 - 10
10 - 50
50 - 100
100 - 500
500 - 1000
>1000

Rail station Level-of-Service

I Full service
II Partial service
IV No service

Rail line Level-of-Service

I Full service
II Restricted service
III Rolling / temporary outage
IV No stopping service
V Evacuation service only
VI No service

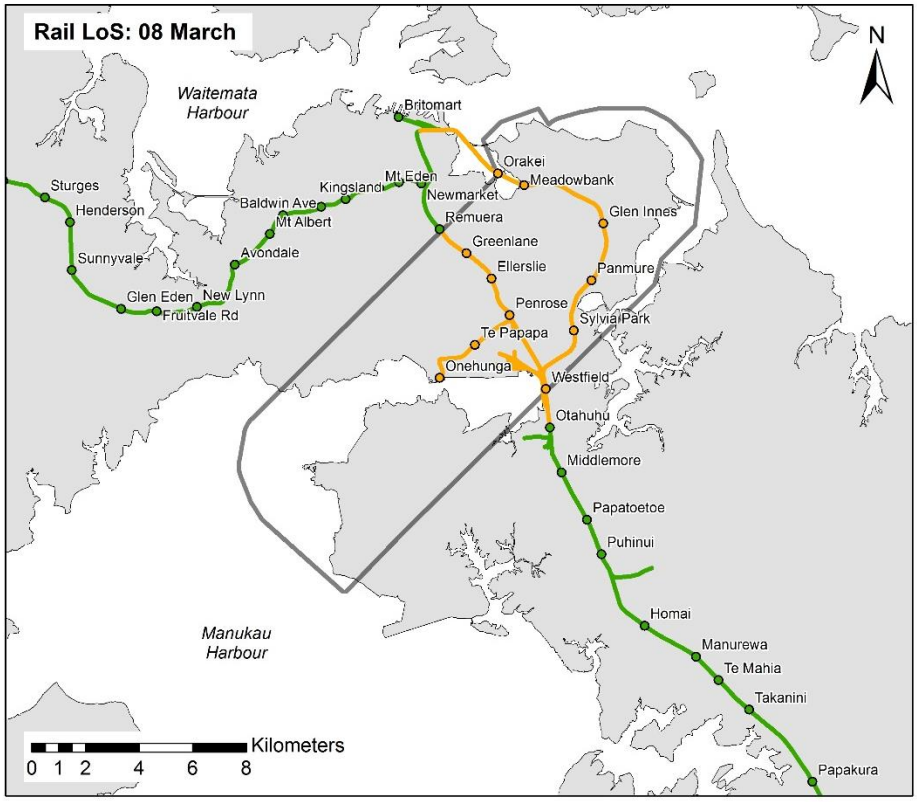

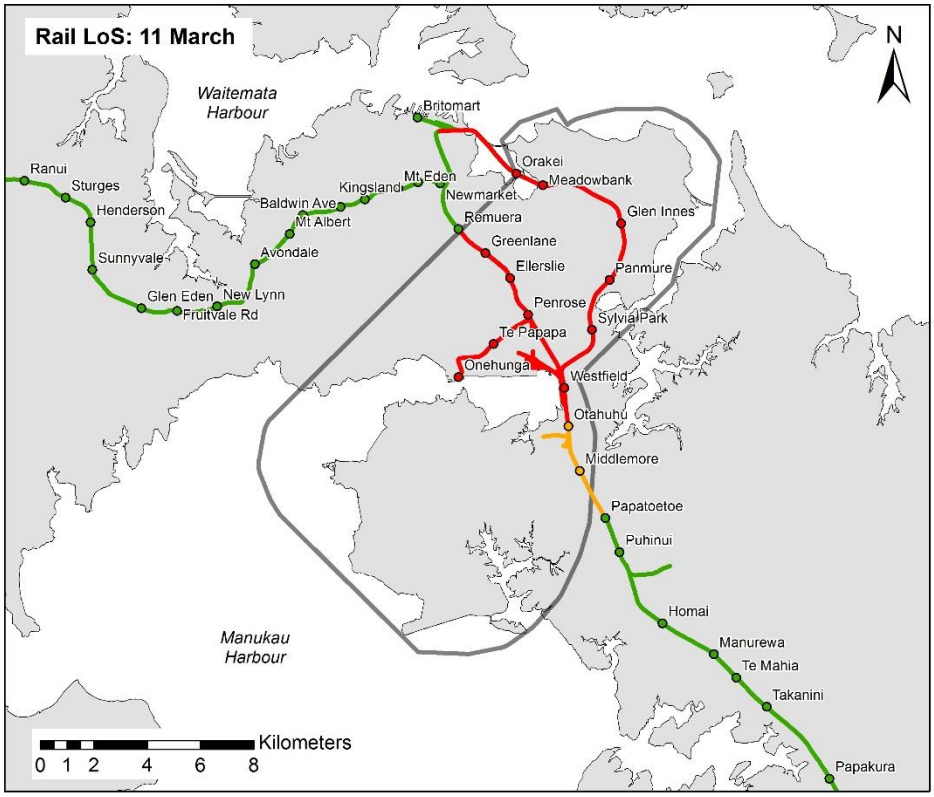
Rail LoS: 11 March
N
Waitemata Harbour
Britomart
Orakei
Meadowbank
Mt Eden
Kingsland
Newmarket
Baldwin Ave
Mt Albert
Remuera
Glen Innes
Greenlane
Ellerslie
Panmure
Penrose
Sylvia Park
Te Papapa
Onehunga
Westfield
Otahuhu
Middlemore
Papatoetoe
Puhinui
Homai
Manurewa
Te Mahia
Takanini
Papakura
Ranui
Sturges
Henderson
Sunnyvale
Avondale
Glen Eden
New Lynn
Fruitvale Rd
Manukau Harbour
Kilometers
0 1 2 4 6 8

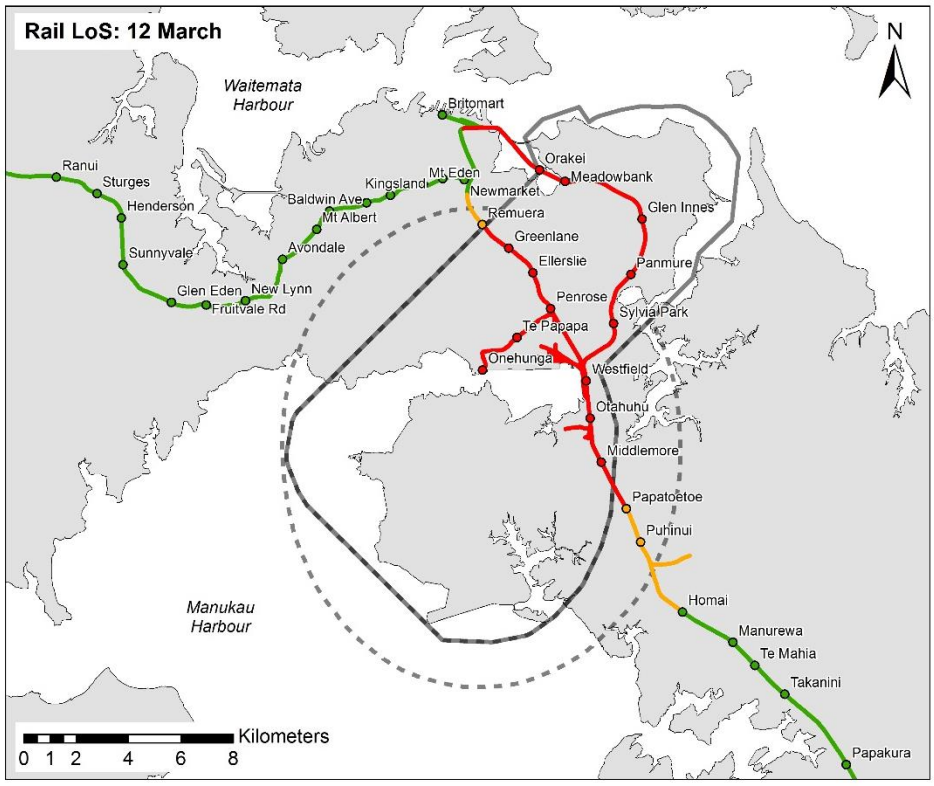
Rail LoS: 12 March
N
Waitemata Harbour
Britomart
Orakei
Meadowbank
Mt Eden
Kingsland
Newmarket
Baldwin Ave
Mt Albert
Remuera
Glen Innes
Greenlane
Ellerslie
Panmure
Penrose
Sylvia Park
Te Papapa
Onehunga
Westfield
Otahuhu
Middlemore
Papatoetoe
Puhinui
Homai
Manurewa
Te Mahia
Takanini
Papakura
Ranui
Sturges
Henderson
Sunnyvale
Avondale
Glen Eden
New Lynn
Fruitvale Rd
Manukau Harbour
Kilometers
0 1 2 4 6 8

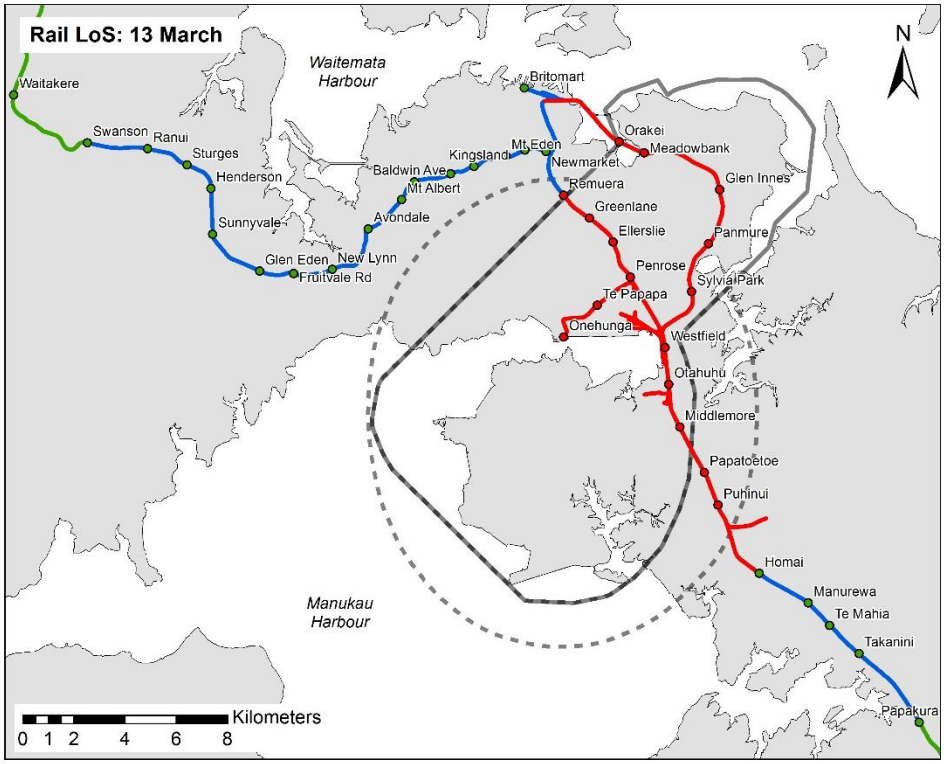
Rail LoS: 13 March
N
Waitemata Harbour
Manukau Harbour
Waitakere
Swanson
Ranui
Sturges
Henderson
Sunnyvale
Glen Eden
New Lynn
Fruitvale Rd
Baldwin Ave
Mt Albert
Avondale
Kingsland
Mt Eden
Britomart
Newmarket
Orakei
Meadowbank
Remuera
Glen Innes
Greenlane
Ellerslie
Panmure
Penrose
Sylvia Park
Te Papapa
Onehunga
Westfield
Otahuhu
Middlemore
Papatoetoe
Puhinui
Homai
Manurewa
Te Mahia
Takanini
Papakura
Kilometers
0 1 2 4 6 8

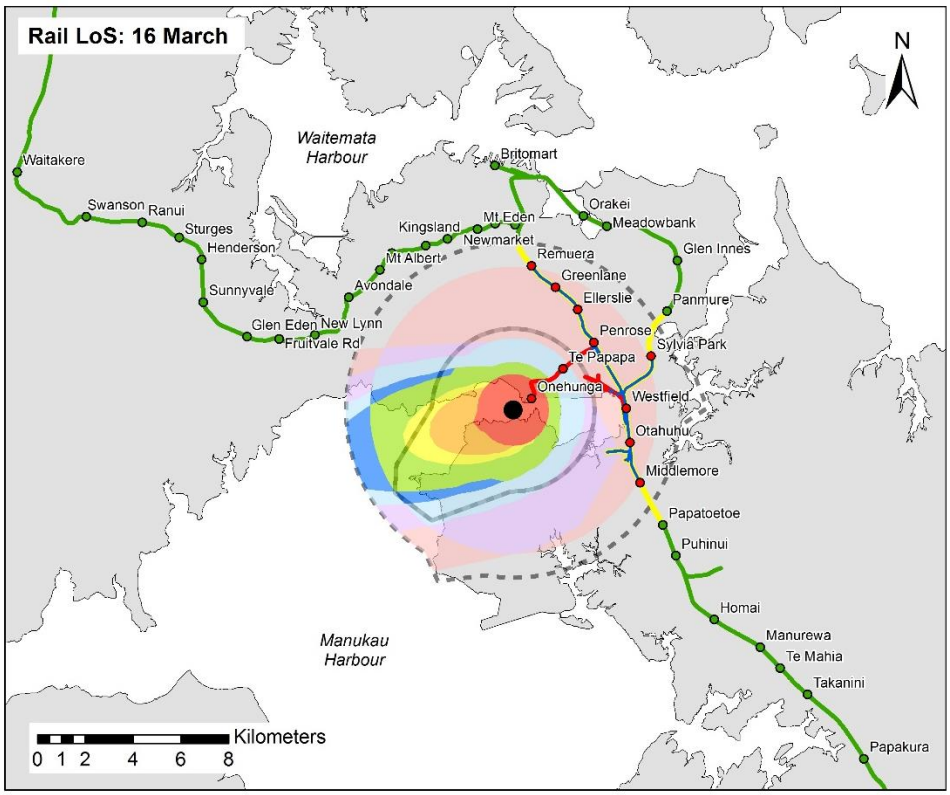
Rail LoS: 16 March
N
Waitemata Harbour
Manukau Harbour
Waitakere
Swanson
Ranui
Sturges
Henderson
Sunnyvale
Glen Eden
New Lynn
Fruitvale Rd
Mt Albert
Avondale
Kingsland
Mt Eden
Britomart
Newmarket
Orakei
Meadowbank
Remuera
Glen Innes
Greenlane
Ellerslie
Panmure
Penrose
Sylvia Park
Te Papapa
Onehunga
Westfield
Otahuhu
Middlemore
Papatoetoe
Puhinui
Homai
Manurewa
Te Mahia
Takanini
Papakura
Kilometers
0 1 2 4 6 8

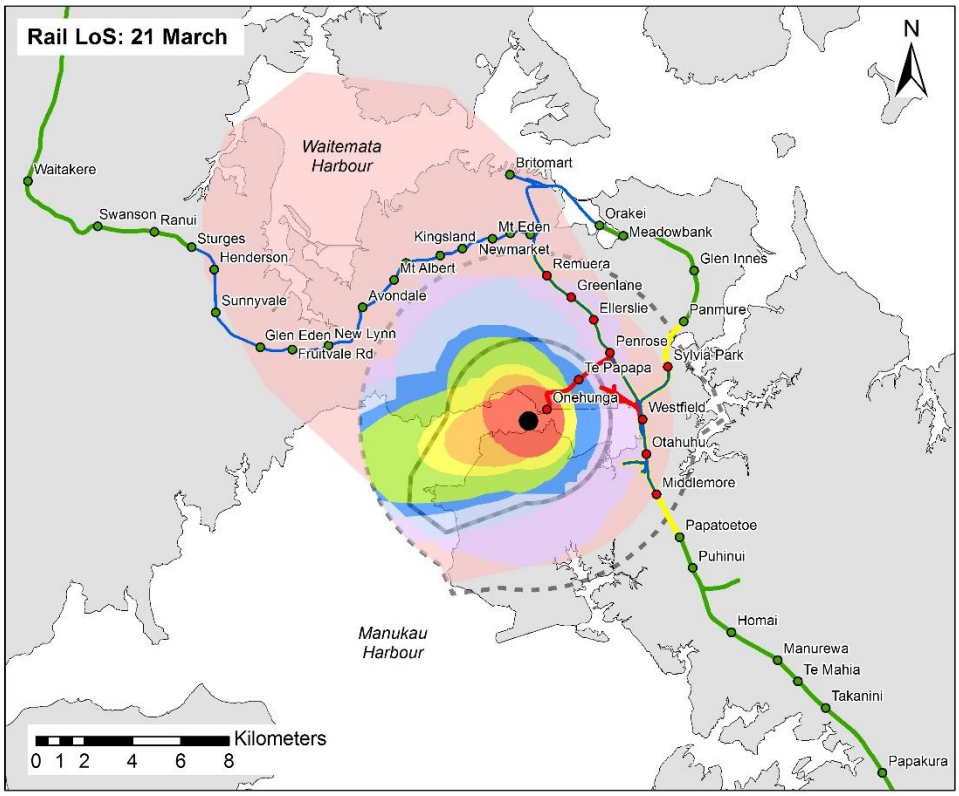
Rail LoS: 21 March
N
Waitemata Harbour
Manukau Harbour
Waitakere
Swanson
Ranui
Sturges
Henderson
Sunnyvale
Glen Eden
New Lynn
Fruitvale Rd
Avondale
Mt Albert
Kingsland
Mt Eden
Newmarket
Britomart
Orakei
Meadowbank
Glen Innes
Remuera
Greenlane
Ellerslie
Panmure
Penrose
Sylvia Park
Te Papapa
Onehunga
Westfield
Otahuhu
Middlemore
Papatoetoe
Puhinui
Homai
Manurewa
Te Mahia
Takanini
Papakura
Kilometers
0 1 2 4 6 8

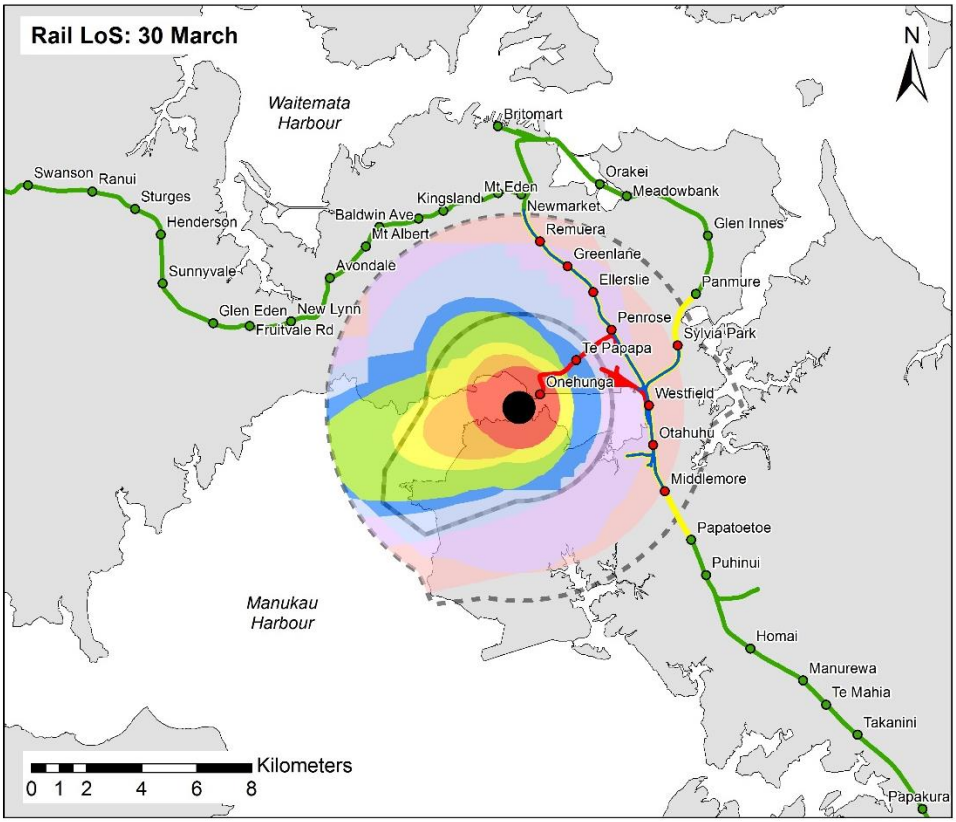
Rail LoS: 30 March
N
Waitemata Harbour
Manukau Harbour
Swanson
Ranui
Sturges
Henderson
Sunnyvale
Glen Eden
New Lynn
Fruitvale Rd
Avondale
Baldwin Ave
Mt Albert
Kingsland
Mt Eden
Newmarket
Britomart
Orakei
Meadowbank
Glen Innes
Remuera
Greenlane
Ellerslie
Panmure
Penrose
Sylvia Park
Te Papapa
Onehunga
Westfield
Otahuhu
Middlemore
Papatoetoe
Puhinui
Homai
Manurewa
Te Mahia
Takanini
Papakura
Kilometers
0 1 2 4 6 8

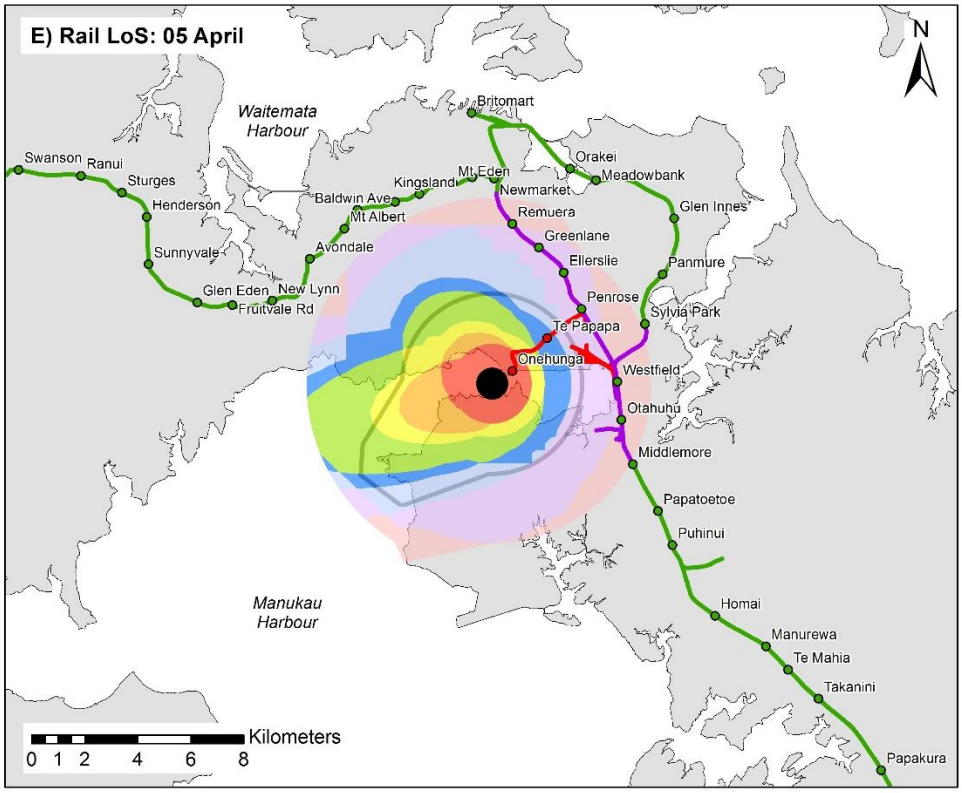
E) Rail LoS: 05 April
N
Waitemata Harbour
Britomart
Orakei
Meadowbank
Mt Eden
Newmarket
Kingsland
Swanson
Ranui
Sturges
Henderson
Baldwin Ave
Mt Albert
Glen Innes
Remuera
Greenlane
Sunnyvale
Avondale
Ellerslie
Panmure
Glen Eden
New Lynn
Fruitvale Rd
Penrose
Sylvia Park
Te Papapa
Onehunga
Westfield
Otahuhu
Middlemore
Papatoetoe
Puhinui
Manukau Harbour
Homai
Manurewa
Te Mahia
Takanini
Papakura
Kilometers
0 1 2 4 6 8

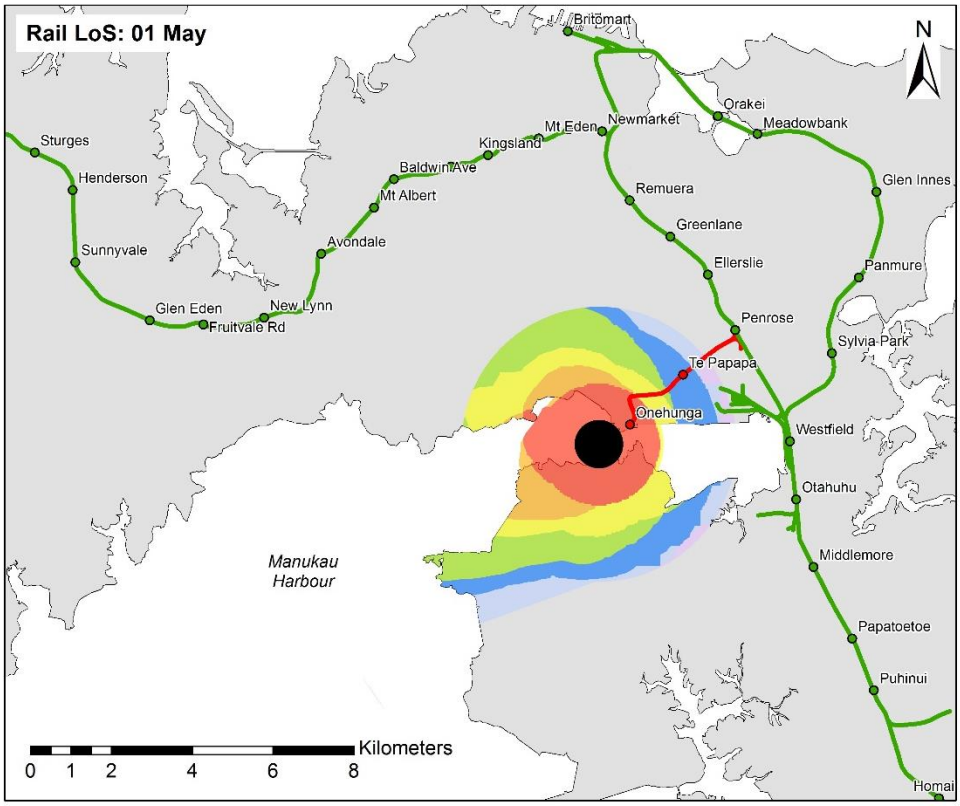
Rail LoS: 01 May
N
Britomart
Orakei
Meadowbank
Mt Eden
Newmarket
Kingsland
Sturges
Baldwin Ave
Henderson
Mt Albert
Remuera
Glen Innes
Greenlane
Sunnyvale
Avondale
Ellerslie
Panmure
Glen Eden
New Lynn
Fruitvale Rd
Penrose
Sylvia Park
Te Papapa
Onehunga
Westfield
Otahuhu
Middlemore
Manukau Harbour
Papatoetoe
Puhinui
Homai
Kilometers
0 1 2 4 6 8